NOAA Technical Memorandum NMFS-AFSC-

Model-based Essential Fish Habitat Definitions for Aleutian Islands Groundfish Species

by
Turner, K, Rooper, CN, Rooney, S, Laman, E, Cooper, D, Zimmermann, M

U.S. DEPARTMENT OF COMMERCE
National Oceanic and Atmospheric Administration National Marine Fisheries Service Alaska Fisheries Science Center
October 2015

NOAA Technical Memorandum NMFS

The National Marine Fisheries Service's Alaska Fisheries Science Center uses the NOAA Technical Memorandum series to issue informal scientific and technical publications when complete formal review and editorial processing are not appropriate or feasible. Documents within this series reflect sound professional work and may be referenced in the formal scientific and technical literature.

The NMFS-AFSC Technical Memorandum series of the Alaska Fisheries Science Center continues the NMFS-F/NWC series established in 1970 by the Northwest Fisheries Center. The NMFS-NWFSC series is currently used by the Northwest Fisheries Science Center.

This document should be cited as follows:

> Turner, K, Rooper, CN, Rooney, S, Laman, E, Cooper, D, Zimmermann, M. 2015. Model-based Essential Fish Habitat Definitions for Aleutian Island Groundfish Species. U.S. Dep. Commer., NOAA Tech. Memo. NMFS-AFSC-XXX, XXX p.

Reference in this document to trade names does not imply endorsement by the National Marine Fisheries Service, NOAA.

Model-based Essential Fish Habitat Definitions for Aleutian Islands Groundfish Species

by

Turner, K, Rooper, CN, Rooney, S, Laman, E, Cooper, D, Zimmermann, M

Alaska Fisheries Science Center
7600 Sand Point Way N.E.
Seattle, WA 98115
www.afsc.noaa.gov

U.S. DEPARTMENT OF COMMERCE
Carlos M. Gutierrez, Secretary
National Oceanic and Atmospheric Administration
Vice Admiral Conrad C. Lautenbacher, Jr., U.S. Navy (ret.), Under Secretary and Administrator
National Marine Fisheries Service
John Oliver, Acting Assistant Administrator for Fisheries
October 2015

This document is available to the public through:

National Technical Information Service
U.S. Department of Commerce 5285 Port Royal Road Springfield, VA 22161

www.ntis.gov

ABSTRACT

Defining essential habitats for fishes is important for managing groundfish in Alaska. Species distribution models have been widely used in conservation biology and terrestrial systems to define the potential habitat for organisms of interest. The models themselves can take a number of forms, from relatively simple frameworks such as generalized linear or additive models to complex modeling frameworks such as boosted regression trees, maximum entropy models, two-stage models or other formulations. We used a variety of modeling methods and data sets from scientific surveys and commercial fisheries to define the habitats for over 30 fish species in the Gulf of Alaska. Adult, juvenile, larval and egg stages were modeled in four seasons where data were available. Depth was the dominant variable determining the distribution of most adult and juvenile life history stages. Sea surface temperature was the most important variable for egg and larval stages. Using the models, maps were developed that identified local hot spots for each

species and life stage. These maps will be used for marine spatial planning and assessing impacts of anthropogenic activities in Alaska's marine environment.

CONTENTS

1.0 INTRODUCTION

The 1996 reauthorization of the Magnuson-Stevens Fishery Conservation and Management Act (MSFCMA) mandates NMFS to identify habitats essential for managed species and conserve habitats from adverse effects of fishing and other anthropogenic activities Essential Fish Habitat (EFH) is defined under the act as 'those waters and substrates necessary to fish for spawning, breeding, feeding or growth to maturity'. As part of this mandate, EFH descriptions for all species listed under a Fisheries Management Plan in Alaskan waters are needed. In addition, these descriptions are routinely revisited under a five-year cycle that reviews and updates Essential Fish Habitat information (including species descriptions) with new data and research.

Essential fish habitat descriptions consist of maps of EFH and text descriptions. In Alaska, most EFH descriptions for groundfish have been limited to qualitative statements on the distribution of adult life stages. These are useful, but could be relatively easily refined both in terms of spatial extent and life history stage using species distribution models and available data from a variety of sources. Distribution models have been widely used in conservation biology and terrestrial systems to define the potential habitat for organisms of interest (e.g. Delong and Collie 2004, Lozier et al. 2009, Elith et al. 2011, Sagarese et al. 2014). Recently species distribution models have been developed for coral and sponge species in the eastern Bering Sea, Gulf of Alaska, and Aleutian Islands (Rooper et al. 2014, Sigler et al. 2015, Rooper et al. in review).

Species distribution models themselves can take a number of forms, from relatively simple frameworks such as generalized linear or additive models to complex modeling frameworks such as boosted regression trees, maximum entropy models, two-stage models or other formulations. The models can be used to predict potential habitat, probability of presence or even abundance,

but they all have some features in common; 1) the underlying data consists of some type of independent variables (predictors) and a dependent response variable (presence, presence/absence or abundance), 2) raster maps of independent variables are used to predict a response map, 3) confidence bounds on the predictions and partitioning of the data can produce test statistics useful for evaluating the model. The outputs of species distribution models are designed to be raster maps that can show the predicted abundance of a species at each of the raster cells. This type of product is useful for EFH descriptions, as it lends itself to producing maps of areas of high abundance or hotspots of distribution and the models themselves can be used to generate the required text descriptions.

The goal of the study generating this Data Report was to produce species distribution models of EFH for all major species of groundfish and invertebrates in the Aleutian Islands. Accompanying Data Reports will be generated for Gulf of Alaska and eastern Bering Sea fishes and invertebrates. We attempted to generate models and text descriptions of EFH for each species in the Aleutian Islands where data exists for egg, larval, juvenile and adult life history stages in four seasons. From these we generated complementary distribution maps that showed the location of EFH. It is anticipated that this research could form a basis for future updates and integration of new data and studies.

2.0 METHODS

2.1 Study area and species

The Aleutian Islands area a chain of volcanic islands stretching from southwest Alaska across the North Pacific, diving the western Gulf of Alaska from the Bering Sea (Fig. 1). The continental

shelf and upper continental slope represent a diverse mosaic of benthic habitats from Unimak Pass (165°W) in the eastern Aleutian Islands to Stalemate Bank in the western Aleutian Islands (170.5°E). The Alaska Coastal Stream and Alaska Coastal Current flow westward on the GOA side of the Aleutian Islands, while on the Bering Sea side, the predominant current flows eastward. There is extensive transport to the north through passes in the island chain from the Gulf of Alaska to the Bering Sea. In the Aleutian Islands, there is a very narrow and deep continental shelf. , the continental shelf ranges in width from 20 km to greater than 200 km and the continental slope is steep and features periodic gullies and submarine canyons extending into the continental shelf (Fig. 1). The seafloor of the Aleutian Islands is diverse, with extensive areas of rocky substrate that have resulted from volcanic activity. Much of the continental shelf area is dominated by hard rocky sediments.

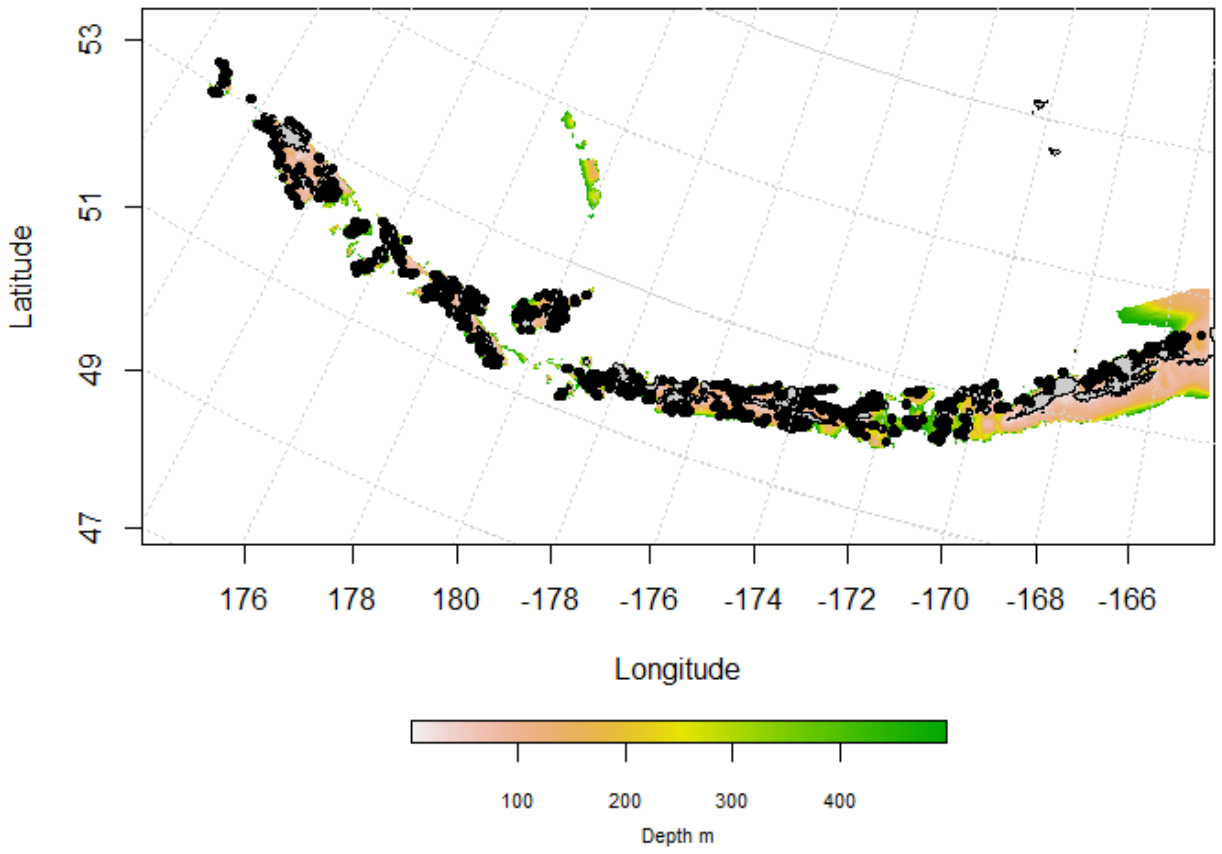

Figure 1. – Aleutian Islands from Unimak Pass to Stalemate Bank where this modeling study was carried out. Cross-hatches indicate the locations of bottom trawl hauls from the Aleutian Island biennial bottom trawl survey (1991-2014).

The species and life stages of fishes and invertebrates examined for this study are included in Table 1. The data available for early life history stages (egg, larval and early juvenile) was primarily from the FOCI ECODAAT database. The summer distributions of juvenile and adult life history stages were modeled using the RACE Aleutian Islands bottom trawl survey database (RACEBASE). The seasonal adult distributions were modeled using commercial catch data from the observer database (CIA Database). All the data was divided into four seasons for analyses: fall (October-November), winter (December-February), spring (March-May), and summer (June-September).

Table 1. Species and life stages considered in the Aleutian Islands essential fish habitat modeling exercise.

Species	Eggs	Larvae	Early juveniles	Late juveniles	Adults
Arrowtooth flounder	Atheresthes sp. as group				
Kamchatka flounder					
Northern rock sole					
Southern rock sole					
Rex sole					
Dover sole					
Flathead sole					
Greenland turbot					
Pollock					
Pacific cod					
Sablefish					
Atka mackerel					
Great sculpin					
Yellow Irish lord					
Bigmouth sculpin					
Pacific ocean perch	Sebastes sp. as group				
Northern rockfish					
Shortraker rockfish					
Dark rockfish					
Blackspotted/rougheye rockfish					
Harlequin rockfish					
Dusky rockfish					
Thornyhead rockfish					
Alaska skate					
Bering skate					
Aleutian skate					
Mud skate					
Pacific giant octopus					
Golden king crab					

2.2 Species distribution data – Recruitment processes data

FOCI's ECODAAT database contains historical catches from limited geographical locations in the Aleutian Islands (Fig. 2). The data considered includes catches from 1991 to 2013 and was

all taken from the eastern Aleutian Islands and north of Amlia Island. These catches have been collected during a number of different types of surveys with different survey objectives. As such, many different gear types have been used, including bongo and methot nets. Because of this, samples were collected from a variety of depths in the water column. Samples have been collected across all months and seasons of the year, although not all month-year combinations occurred in the database. For this reason, the data was combined across years for analysis.

Each species in the ECODAAT data was classified as either egg, larval or juvenile (we considered all juveniles to be "early" juvenile stages, as they were found in the water column rather than benthically). We used these data for presence-only models where the number of presence observations in a species-life stage combination exceeded 50. The numbers of catches for each species, season and life stage are shown in Table 2.

An important caveat to the species distribution models developed using the ECODAAT database is that these data were not collected over the entire area of the Aleutian Islands. Typically, these data were collected from a smaller regional survey grid, rather than conducted over a regular grid. The distribution of sampling effort should be considered when drawing conclusions from maps produced from these data.

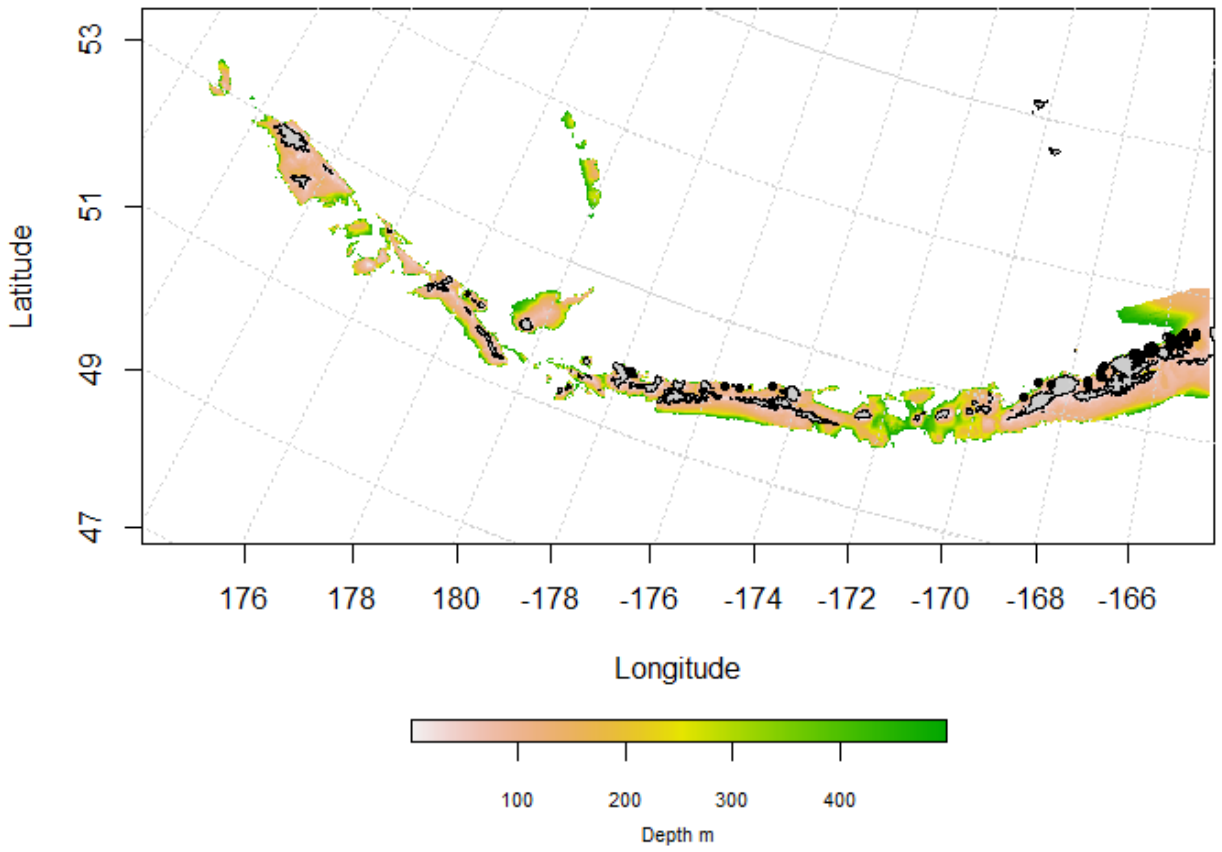

Locations (n= 606) of sampling for egg, larvae and early juvenile fish and invertebrates in the eastern Bering Sea (1991-2012) from the ECODAAT database.

Table 2. Numbers of presence records for species and life history stages available from the ECODAAT database in the Aleutian Islands. Some species were grouped by genus where the species were not individually identifiable. Maximum entropy modeling was conducted for species, season, and life history stages where the number of presence observations exceeded 50.

		Spring			Summer			Winter	
Species	Eggs	Larvae	Early juveniles	Eggs	Larvae	Early juveniles	Eggs	Larvae	Early juveniles
Atheresthes sp.	--	66	--	--	7	--	8	3	--
Atka mackerel (*Pleurogrammus monopterygius*)	106	7	--	--	--	--	--	8	--
Dover sole (*Microstomus pacificus*)	4	--	--	7	1	--	--	--	--
Greenland turbot (*Reinhardtius hippoglossoides*)	5	14	--	--	--	--	5	1	--
Cottidae sp.	--	17	1	--	--	--	--	--	--
Flathead sole (*Hippoglossoides elassodon*)	55	11	--	1	5	--	--	--	--
Pacific cod (*Gadus macrocephalus*)	1	46	--	--	2	--	--	--	--
Pollock (*Gadus chalcogramma*)	112	93	--	5	5	2	1	--	--
Rex sole (*Glyptocephalus zachirus*)	40	--	--	8	2	--	--	--	--
Sablefish (*Anoplopoma fimbria*)	4	10	--	--	1	--	--	--	--
Rockfish (*Sebastes* sp.)	--	89	--	--	13	--	--	--	--
Northern rock sole (*Lepidopsetta polyxystra*)	--	57	--	--	3	--	--	--	
Southern rock sole (*Lepidopsetta bilineatus*)	--	5	--	--	3	--	--	--	--
*egg locations were from all seasons and were taken from Lauth et al. 2007									

2.3 Species distribution data – Groundfish bottom trawl surveys

The modeling analyses also included data collected during bottom-trawl surveys of the Aleutian Islands ecosystem. These data were the most comprehensive and useful of the three types of data analyzed, as they are all from the summer season and are conducted with a rigorous statistical design. The National Marine Fisheries Service (NMFS), Alaska Fisheries Science Center (AFSC), has conducted standard bottom-trawl surveys in this ecosystems since 1980 (von Szalay et al. 2011). A stratified-random sampling design was used for the AFSC RACE Division Aleutian Islands bottom trawl survey of trawlable areas shallower than the depth of 500 m across the Aleutian archipelago (Fig. 1). The survey area extends on the north side of the Aleutian island chain from Unimak Pass in the east (165°W) to Stalemate Bank in the west (170°E); on the south side of this archipelago, the survey extends from Samalga Pass (170°E) to Stalemate Bank in the west. Strata are based on 4 depth intervals (1–100 m, 101–200 m, 201– 300 m, and 301–500 m) over the continental shelf and upper slope. The depth strata are further segregated by the North Pacific Fisheries Management Council's (NPFMC) Bering Sea Aleutian Islands regulatory area (NPFMC3) into survey districts that correspond to the NPFMC subdivisions of western, central, and eastern Aleutian districts and an additional southern Bering Sea survey district that roughly corresponds to the Bogoslof district. Trawl sample allocation in each stratum was achieved with a modified Neyman optimum allocation sampling strategy (Cochran, 1977) to provide representative samples of fishes and invertebrates occurring at each sampling location within each stratum.

The Aleutian Islands bottom trawl survey utilizes a poly Nor'Eastern high-opening bottom trawl with 24.2 m roller gear constructed with 36 cm rubber bobbins separated by 10 cm rubber disks

(Stauffer 2004). Trawl tows were conducted at a target speed of 5.6 km h–1 (3 knots) for 15 (since 1996) or 30 min (prior to 1996). Bottom contact and net dimensions were recorded throughout each trawl using net mensuration equipment. For these analyses, records were only used if trawl performance was satisfactory and if the distance fished, geographic position, average depth, and water temperature were recorded. Tows were deemed satisfactory if the net opening was within a predetermined normal range, the roller gear maintained contact with the seafloor, and the net suffered little or no damage during the tow. Data from a total of 3617 bottom-trawl tows were used for this analysis.

All fishes and invertebrates captured during a survey tow were sorted either by species or into larger taxonomic groups and the total weight in the catch was determined. Catch per unit effort (CPUE, no.*ha^{-1}) for each taxonomic group was calculated using the area swept which was computed from the net width for each tow multiplied by the distance towed recorded with the vessel's GPS. For some species both juvenile and adult sizes were captured during the bottom trawl survey. In these cases an approximate length at first maturity was used to partition the catches into juvenile and adult stages (Table 3). For some species only a subset of years was used in the modeling due to taxonomic changes that have occurred throughout the time series. For example, dusky and dark rockfishes were considered one species prior to the 1996 survey, so only data from surveys beginning in this year were used to model these two species.

Table 3. Species modeled using bottom trawl survey data. Years included in each of the modeling efforts, the percentage of positive catches (frequency of occurrence) in the bottom trawl hauls for juvenile and adult life history stages, and the maximum size considered to be the juvenile stage is shown.

Species	Years modeled	Percent positive catches - Juveniles	Percent positive catches - adults	Maximum juvenile length (cm)
Alaska skate (*Bathyraja parmifera*)	1990-	3.78	7.25	92
Aleutian skate (*Bathyraja aleutica*)	1990-	6.13	4.2	132
Arrowtooth flounder (*Atheresthes stomias*)	1993-	49.82	64.71	35
Atka mackerel (*Pleurogrammus monopterygius*)	All	14.98	41.1	27
Bering skate (*Bathyraja interrupta*)	1990-	0.7	0.45	69
Bigmouth sculpin (*Hemitripterus bolini*)	All	1.03	1.88	51
Blackspotted rockfish (*Sebastes melanostictus*)	2007-	7.1	5.23	43
Dark rockfish (*Sebastes ciliatus*)	1996-	1.75	0.28	42
Dover sole (*Microstomus pacificus*)	All	6.35	5.93	38
Dusky rockfish (*Sebastes variabilis*)	1996-	0.6	5.85	29
Flathead sole (*Hippoglossoides elassodon*)	All	16.76	29.01	29
Golden king crab (*Lithodes aequispinus*)	All	--	23.79	
Great sculpin (*Myoxocephalus polyacanthocephalus*)	All	2.3	2.35	51
Greenland turbot (*Reinhardtius hippoglossoides*)	All	3.05	8.6	65
Harlequin rockfish (*Sebastes variegatus*)	All	0.15	1.75	23
Kamchatka flounder (*Atheresthes evermanni*)	1993-	42.9	21.26	52
Mud skate (*Bathyraja taranetzi*)	1990-	10.66	3.33	62
Northern rock sole (*Lepidopsetta polyxystra*)	2001-	33.19	51.65	30
Northern rockfish (*Sebastes polyspinis*)	All	9.6	36.77	25
Octopus sp. (*Octopus dofleini*)	All	--	12.36	
Pacific cod (*Gadus macrocephalus*)	All	30.47	61.08	46
Pacific ocean perch (*Sebastes alutus*)	All	23.39	52.93	25
Pollock (*Gadus chalcogramma*)	All	17.46	51.4	29
Rex sole (*Glyptocephalus zachirus*)	All	28.09	34.72	24
Rougheye rockfish (*Sebastes aleutianus*)	2007-	0.85	1	43
Sablefish (*Anoplopoma fimbria*)	All	0.43	9.15	40
Shortraker rockfish (*Sebastes borealis*)	All	7.3	11.73	44
Shortspine thornyhead (*Sebastolobus alascanus*)	All	6.23	16.73	21
Southern rock sole (*Lepidopsetta bilineata*)	2001-	5.55	9.3	30
Yellow Irish lord (*Hemilepidotus jordani*)	All	3.88	21.61	22
	Standard GAM model			
	Hurdle GAM model			
	Maximum entropy model			

2.4 Species distribution data – Commercial catch (observer) data

Data from the catch-in-areas (CIA) observer database was used to model adult life history stages of fishes caught in commercial catches during the non-summer seasons (Table 4). The CIA data was provided by John V. Olson and Steve Lewis (AKRO). The data from observed hauls regardless of the type of fishing gear were combined across years for analysis. We used the observations of catch by species in the data for MaxEnt (presence-only) models where the number of presence observations in a species exceeded 50. The numbers of catches for each species and season are shown in Table 4. All of these fish and invertebrates were assumed to be adult life history stages. Only the fall, winter and spring seasons were considered, as the summer distributions were modeled using bottom trawl survey data.

An important caveat to the species distribution models developed using the CIA database is that for most species, the distribution of catches represent to a large extent the distribution of fishing activity. So, instead of being a regular survey conducted over a regular grid, these observations are typically clustered around areas of high catches for target species. As such, they should be viewed with some caution compared to the bottom trawl survey distribution maps.

Table 4. Numbers of presence records by species available from the CIA database in the Aleutian Islands. Maximum entropy modeling was conducted for species and season where the number of presence observations exceeded 50.

Species	Fall	Winter	Spring
Alaska skate (*Bathyraja parmifera*)	346	1004	636
Aleutian skate (*Bathyraja aleutica*)	72	484	129
Arrowtooth flounder (*Atheresthes stomias*)	428	2028	974
Atka mackerel (*Pleurogrammus monopterygius*)	1339	986	1498
Bigmouth sculpin (*Hemitripterus bolini*)	106	235	211
Blackspotted, rougheye rockfish (*Sebastes aleutianus, S. melanostictus*)	216	387	98
Dusky rockfish (*Sebastes variabilis*)	412	582	482
Flathead sole (*Hippoglossoides elassodon*)	60	736	649
Golden king crab (*Lithodes aequispinus*)	89	294	
Harlequin rockfish (*Sebastes variegatus*)		149	56
Great sculpin (*Myoxocephalus polyacanthocephalus*)	181	979	85
Greenland turbot (*Reinhardtius hippoglossoides*)	164	63	149
Kamchatka flounder (*Atheresthes evermanni*)	250	904	348
Mud skate (*Bathyraja taranetzi*)	84	282	218
Northern rock sole (*Lepidopsetta polyxystra*)	551	2385	1396
Northern rockfish (*Sebastes polyspinis*)	1296	1646	1775
Octopus sp. (*Octopus dofleini*)	88	439	271
Pacific cod (*Gadus macrocephalus*)	919	3672	2163
Pacific ocean perch (*Sebastes alutus*)	1083	793	1253
Pollock (*Gadus chalcogramma*)	654	951	1027
Rex sole (*Glyptocephalus zachirus*)	85	290	298
Sablefish (*Anoplopoma fimbria*)	155	1123	
Shortraker rockfish (*Sebastes borealis*)	113	697	54
Shortspine thornyhead (*Sebastolobus alascanus*)	120	941	
Southern rock sole (*Lepidopsetta bilineata*)		579	293
Yellow Irish lord (*Hemilepidotus jordani*)	180	533	177

2.5 Habitat-related variables

Independent variables for modeling included the standard suite of habitat variables typically collected on the bottom trawl survey as well as a few derived and modeled variables (Table 5). These variables were chosen for their availability and for their potential influence on the distribution of fishes as found from historical studies

The early life history stages of each of the fishes were generally sampled in pelagic waters. Therefore, surface water temperature, surface current speed and surface current direction were chosen as potential variables to explain early life history distributions. In addition surface current direction variability was used as well, as an indication of potential eddy vorticity or other current variability processes that might be present. These variables were derived from ROMS model runs from 1969-2005 provided by A. Hermann (Daneilson et al. 2011). The data monthly were monthly values originally on a 10 km by 10 km grid. These values were interpolated via inverse distance weighting to a 1 km by 1 km grid for modeling and summarized by season.

Additional variables used for modeling the early life history stages of fish species included the depth, slope, color and tidal current. A bathymetry raster for the entire Aleutian Islands region was from (Zimmermann et al. 2013). Bathymetric point data was derived from soundings (n > 2.1 million soundings) on NOS smooth sheets that were digitized and compiled according to the methods in Zimmermann and Benson (2013). This point data was linearly interpolated from a triangular irregular network (TIN) layer to a 100 m by 100 m raster grid. This interpolation was conducted using the Spatial Analyst package in ArcGIS software (ESRI 2009). Slope was derived from the 100 m by 100 m bathymetry raster. Slope for each raster grid cell was computed as the maximum difference between the depth at a cell and its surrounding cells. Slope was computed using the raster package in R software (R Core Development Team 2013). For the analysis of early life history data, these two layers were averaged to a 1 km by 1 km grid.

To reflect average ocean productivity (g C m-2 day-1) at each of the bottom trawl survey sites, we used MODIS ocean color data for five spring-summer months (May-September) that encompass the spring and summer phytoplankton blooms over eight years (2003-2011) for the Aleutian Islands region (Behrenfeld and Falkowski 2007). These data were downloaded from the Oregon State University Ocean Productivity website. These data were averaged by cell and by month and then averaged again by cell and by year (to account for differences in the number of samples within each cell). The averages were then interpolated to a 1 km by 1 km raster grid using inverse distance weighting.

Tidal speeds were estimated for 368 consecutive days (January 1st, 2009 to January 3rd, 2010) using a tidal inversion program parameterized for the Gulf of Alaska and Aleutian Islands on a 1 km by 1 km grid (Egbert and Erofeeva 2002). This tidal prediction model was used to produce a series of one lunar year of tidal currents for spring and neap cycles at each bottom trawl survey location. The maximum of the series of predicted tidal current was then extracted for the position of each bottom trawl survey haul. This maximum value was used as a habitat variable in the modeling. Maximum tidal current at each bottom trawl survey site were also interpolated to the entire Aleutian Islands using ordinary kriging and an exponential semi-variogram. When evaluated using leave-one-out cross-validation, the kriging model fit the observations very well ($n = 3051$, mean squared error = 407, $R2 = 0.93$). The kriging model was then used to interpolate a raster of maximum current values on a 1 km by 1 km cell size that was used for modeling early life history stages.

For modeling fish distribution from bottom trawl survey hauls, the surface data derived from the ROMS models were not used. Additionally, the rasters used for prediction was the smaller 100 m by 100 m grid for the depth, slope, maximum tidal current and ocean color variables.

Haul position and depth were collected during each bottom trawl haul. A start and end position for the vessel during the on-bottom portion of the tow were collected using the vessel-mounted GPS receiver. Vessel position was corrected for the position of the bottom trawl itself by triangulating how far the net was behind the vessel (based on the seafloor depth and the wire out) and subtracting this distance from the vessel position in the direction of the bottom trawl haul. We assumed that the bottom trawl was directly behind the vessel during the tow and that all bottom trawl tows were conducted in a straight line from the beginning point to the end point. The mid-point of the start and end positions of the net was used as the location variable in the modeling. The longitude and latitude data for each tow (and all other geographical data including the raster layers described below) were projected into Alaska Albers Equal Area Conic projection (center latitude = 50° N and center longitude = -154° W) and degrees of latitude and longitude were transformed into 100 m by 100 m square grids of eastings and northings for modeling. The location variable was used to capture any significant spatial trends across the Aleutian Islands region in bottom trawl survey catches.

The depth for each tow was estimated from a SeaBird SBE-39 microbathythermograph attached to the headrope of the net and the measured net height. Mean depth during the tow was calculated for inclusion as an explanatory variable in the modeling. A bathymetry raster for the entire Aleutian Islands region was also produced for this analysis (Zimmermann et al. 2013). This raster was used for prediction, but not for parameterizing the models. Bathymetric point data was derived from soundings ($n > 2.1$ million soundings) on NOS smooth sheets that were digitized and compiled according to the methods in Zimmermann and Benson (2013). This point data was linearly interpolated from a triangular irregular network (TIN) layer to a 100 m by 100

m raster grid. This interpolation was conducted using the Spatial Analyst package in ArcGIS software (ESRI 2009).

Slope was derived from the 100 m by 100 m bathymetry raster. Slope for each raster grid cell was computed as the maximum difference between the depth at a cell and its surrounding cells. Slope was computed using the raster package in R software (R Core Development Team 2013). The mean slope underneath each bottom trawl tow path were used as habitat variables in the modeling. The 100 m by 100 m raster layers of slope was used for prediction (Fig. 2).

The average summer temperature at each site was estimated from data collected during Aleutian Islands bottom trawl surveys from 1993-2014. Bottom temperatures are collected during each bottom trawl tow using the SBE-39 attached to the headrope of the net (Fig. 2). Mean bottom temperatures for each haul were interpolated to the 100 m by 100 m grid for the entire Aleutian Islands region. These data were interpolated using ordinary kriging (Venables & Ripley 2002) with an exponential semi-variogram model. This resulted in a single temperature raster layer that reflects the average temperature conditions in surveys from 1993-2014 (Fig. 2). When evaluated using leave-one-out cross-validation, the kriging model was a statistically significant fit to the observations ($n = 2814$, mean squared error = 0.19, $R2 = 0.38$), capturing the spatial trend in the temperature data. The temperature data used in our models were primarily designed to reflect long-term averages that could be compared spatially to the distribution of fishes and invertebrates. Mean bottom temperature underneath each bottom trawl tow path was used as a habitat variable in the modeling. The 100 m by 100 m raster layers of average temperature were used for prediction.

Two measures of water movement and its potential interaction with the seafloor were used as habitat variables in modeling and prediction. The first variable was the maximum tidal speed at

the site of each bottom trawl haul. Tidal speeds were estimated for 368 consecutive days (January 1st, 2009 to January 3rd, 2010) using a tidal inversion program parameterized for the Gulf of Alaska and Aleutian Islands on a 1 km by 1 km grid (Egbert and Erofeeva 2002). This tidal prediction model was used to produce a series of one lunar year of tidal currents for spring and neap cycles at each bottom trawl survey location. The maximum of the series of predicted tidal current was then extracted for the position of each bottom trawl survey haul. This maximum value was used as a habitat variable in the modeling. Maximum tidal current at each bottom trawl survey site were also interpolated to the entire Aleutian Islands using ordinary kriging and an exponential semi-variogram. When evaluated using leave-one-out cross-validation, the kriging model fit the observations very well (n = 3051, mean squared error = 407, R2 = 0.93). The kriging model was then used to interpolate a raster of maximum current values on a 100 m by 100 m cell size that was used for prediction (Fig. 2).

The second water movement variable was the predicted bottom water layer current speed from ROM's model runs from 1969-2005 (Danielson et al. 2011). This long-term current speed and direction were available as points on a 10 km by 10 km grid. The ROM's model was based on a three-dimensional grid with 60 depth tiers for each grid cell. For example, a point at 60 m water depth would have 60 depth bins at 1 m intervals, while a point at 120 m depth would have 60 depth bins at 2 m depth intervals, etc.). The current speed and direction for the deepest depth bin at each point (closest to the seafloor) was used in this analysis. This regularly spaced data was interpolated to a 100 m by 100 m cell size raster covering the entire Gulf of Alaska using inverse distance weighting (Fig. 2). Then the values from this raster at each of the bottom trawl survey haul locations were extracted and the mean value computed for the path of each bottom trawl survey tow. The raster was also used for prediction.

To reflect average ocean productivity (g C m-2 day-1) at each of the bottom trawl survey sites, we used MODIS ocean color data for five spring-summer months (May-September) that encompass the spring and summer phytoplankton blooms over eight years (2003-2011) for the Aleutian Islands region (Behrenfeld and Falkowski 2007). These data were downloaded from the Oregon State University Ocean Productivity website. These data were averaged by cell and by month and then averaged again by cell and by year (to account for differences in the number of samples within each cell). The averages were then interpolated to 100 m by 100 m raster grids using inverse distance weighting (Fig. 2). The mean value in this grid underlying each bottom trawl survey tow was extracted from this raster. The raster was used for prediction.

The final variables included in the modeling of bottom trawl survey data were the catches of structure forming invertebrates (corals, sponges and pennatulaceans). The presence of each of these categories of invertebrates was a binomial (presence or absence) term in the model. The prediction was accomplished by using the prediction surfaces from distribution models for each of these species (Rooper et al. 2014, Rooper unpublished data).

For commercial catch data (observer data), the same variables as were used for the bottom trawl survey models (with the exception of the structure forming invertebrate layers; Table 5).

There was some collinearity in the habitat variables included in the model (Table 6). The largest correlations were between latitude and longitude ($r = 0.60$) and slope and depth ($r = 0.53$). The remaining pairwise correlations among variables were < 0.5. Variance inflation factors were calculated using the method of Zaur et al. (2009) for each of the variables to be included in the modeling, resulting in values ranging from 1.1 to 1.7. These values were all acceptable (below 5.0) allowing inclusion of all variables in the modeling. Thus, the habitat variables were all

included in the models of habitat suitability, presence or absence and abundance of fish and invertebrates in the Aleutian Islands.

Table 5. Variables used in modeling the distributions of fishes and invertebrates in the Aleutian Islands.

Variable	Unit	Definition	Interpolation method	Source	
Position	eastings, northings	Latitude and longitude of bottom trawl hauls in Alaska Albers projection corrected for the position of the trawl net relative to the vessel	--	DGPS collected at bottom trawl hauls	
Depth	m	Bathymetry of the seafloor based on digitized and position corrected NOS charts	Linear interpolation	Mean depth of bottom trawl hauls (modeling), Zimmermann et al. 2014	
Slope	percent	Maximum difference between a depth measurement and its adjoining cells	--	Zimmermann et al. 2014	
Bottom temperature	℃	Mean summer bottom temperature for the region measured during bottom trawl surveys from 1996-2010	Ordinary kriging	Temperature data collected at bottom trawl hauls	
Surface temperature	℃	Ocean current speed predicted from the ROMS model during the years 1970-2004 and averaged on a 10 km by 10 km grid	Inverse distance weighting	Danielson et al. 2011	1
Ocean color	$Carbon*m^{-2}*day^{-1}$	Net primary production in surface waters in May to September averaged by 1080 by 2160 grid cells then averaged across years (2002-2011)	Inverse distance weighting	Behrenfeld and Falkowski 1997	
Mean bottom ocean current	$m*sec^{-1}$	Seafloor ocean current speed predicted from the ROMS model during the years 1970-2004 and averaged on a 10 km by 10 km grid	Inverse distance weighting	Danielson et al. 2011	
Maximum tidal current	$cm*sec^{-1}$	Maximum of the predicted tidal current at each bottom trawl location over a 1-year cycle	Ordinary kriging	Egbert and Erofeeva 2000	
Mean surface ocean current speed	$m*sec^{-1}$	Surface ocean current speed predicted from the ROMS model during the years 1970-2004 and averaged on a 10 km by 10 km grid	Inverse distance weighting	Danielson et al. 2011	1
Mean surface ocean current direction	angle	Surface ocean current direction predicted from the ROMS model during the years 1970-2004 and averaged on a 10 km by 10 km grid	Inverse distance weighting	Danielson et al. 2011	1
Surface ocean current direction variability	--	Variability in surface ocean current direction predicted from the ROMS model during the years 1970-2004 and averaged on a 10 km by 10 km grid	Inverse distance weighting	Danielson et al. 2011	1
Coral presence or absence	--	Coral presence or absence in bottom trawl catch and raster of predicted presence or absence of coral	--	Catch data from bottom trawl hauls (modeling), Rooper et al. (2014) (prediction)	2
Sponge presence or absence	--	Sponge presence or absence in bottom trawl catch and raster of predicted presence or absence of Sponge	--	Catch data from bottom trawl hauls (modeling), Rooper et al. (2014) (prediction)	2
Pennatulacean presence or absence	--	Pennatulacean presence or absence in bottom trawl catch and raster of predicted presence or absence of Pennatulacean	--	Catch data from bottom trawl hauls (modeling), Rooper et al. (unpublished data) (prediction)	2

[1] Used to model egg, larval and early juvenile stages only

[2] Used to model bottom trawl survey data only

Table 6. Cross-correlations among explanatory variables and variance inflation factors for Aleutian Islands data.

Variable	Variance Inflation Factor
Slope	1.31
Maximum tidal current	1.35
Ocean color	1.38
Mean bottom ocean current	1.29
Bottom temperature	1.35
Depth	1.74
Sponge presence	1.12
Coral presence	1.20
Pennatulacean presence	1.07

2.6 Modeling Methods – Recruitment processes data

The maximum entropy (MaxEnt) modeling method was used for estimating species distribution for early life history stages in the ECODAAT database (Phillips et al. 2006, Elith et al. 2011). It was implemented in R software using the dismo package. MaxEnt models use only presence observations and are based on raster grids of explanatory variables (habitat variables) and point observations of presence. The model predicts the probability of suitable habitat based on habitat related variables (i.e. given the depth, temperature, slope and current speed at each grid cell – what is the probability that this is suitable for a canary rockfish?), not probability of presence. Separate training (80%) and testing (20%) data were randomly selected for MaxEnt model developed in order to assess model performance.

2.7 Modeling Methods – Bottom trawl survey data

Three types of distribution modeling were used for the bottom trawl survey data based on the frequency of occurrence for each species in the catch. For species that occurred in > 30% of bottom trawl hauls, such as arowtooth flounder (Table 3), a standard Generalized Additive Modeling (GAM) method was used to produce maps of predicted density. Generalized additive models (Hastie & Tibshirini 1990) using the mgcv package in R (Wood 2006) were used to predict the dependent variables with the suite of untransformed habitat variables included. In each case the basis degrees of freedom used in the smoothing function was limited to ≤ 4 for univariate variables and ≤ 30 for the bivariate term (location). Insignificant terms were sequentially removed. In this case model terms were removed until there was no reduction in the Akiake Information Criterion (AIC) values (Wood 2006). For each species, the model with the lowest AIC score was deemed the best fitting model and used for further prediction and model validation. For the standard GAM's, the CPUE was fourth-root transformed prior to analyses.

For species where frequency of occurrence was between 10% and 30% a hurdle model (Cragg 1971, Potts and Elith 2006) predicting spatial distribution of fishes was used (Table 3). Hurdle models predict the spatial distribution of abundance (or in this case abundance and height) in three stages: 1) probability of presence is predicted from presence-absence data using a GAM model and binomial distribution for each species; 2) a threshold presence probability is determined that defines presence or absence of the species; 3) a separate GAM model is constructed that predicts abundance by modeling the forth-root transformed CPUE data from the bottom trawl survey where the species was present in the catch. As for the standard GAM's

above, the number of inflection points were limited and insignificant terms were sequentially removed to determine the best-fitting model.

For species with < 10% frequency of occurrence, but > 50 presence observations, the MaxEnt methodology was used to develop suitable habitat models, as for the FOCI data above.

For all models, separate training (80%) and testing (20%) data were randomly selected from the total available trawl hauls for assessing the performance of each type of modeling (Figure 3). The training and testing data sets were the same across all species for the analysis of bottom trawl survey data.

2.8 Modeling Methods – Commercial catch (observer) data

The maximum entropy (MaxEnt) modeling method was used for estimating species distribution for commercial catch data in the CIA database (Phillips et al. 2006, Elith et al. 2011). It was implemented in R software using the dismo package. MaxEnt models use only presence observations and are based on raster grids of explanatory variables (habitat variables) and point observations of presence. As with the other models, separate training (80%) and testing (20%) data were randomly selected for MaxEnt model developed in order to assess model performance.

2.9 Model validation

To test the performance of the best-fitting models, the predictions were compared to the observations. For presence and presence-absence models the area under the curve (AUC) was

computed to judge model performance. The AUC calculates the probability that a randomly chosen presence observation would have a higher probability of presence than a randomly chosen absence observation using rank data. We used the scale of Hosmer & Lemeshow (2005), where AUC value > 0.5 is estimated to be better than chance, a value > 0.7 is estimated to be acceptable, and values > 0.8 and 0.9 are excellent and outstanding, respectively. Confidence intervals for the AUC (95%) were calculated according to the methodology of DeLong et al (1988). For abundance models the performance was directly tested by correlating the predictions with the observations. Model testing was also performed on the 20% of the data withheld at random, using the same metrics. Because of space limitations, figures showing the model validation results are generally not shown. Where appropriate, deviations from model assumptions or models with very poor predictive ability relative to the testing data are highlighted. Where these occur, the results of the modeling may not be robust.

3.0 RESULTS

3.1 Flatfishes

Atheresthes spp.

Seasonal distribution of early life history stages of *Atheresthes* in the Aleutian Islands -- Arrowtooth flounder eggs, larvae and early juveniles cannot be distinguished from the other species in the genus, Kamchatka flounder (*Atheresthes evermanni*), so results from the genus *Atheresthes* are combined and presented here. There were only 4 instances of *Atheresthes* eggs observed in the FOCI database (Figure 1) from the winter season, not enough to run the model.

There were only 8 catches of *Atheresthes* larvae in winter and summer months (Figure 2), 2 in the winter and 6 in the summer (all in the eastern Aleutian Islands). There were not enough winter or summer observations for modeling. There were 51 instances of *Atheresthes* larvae in the spring, all in the eastern AI near Unalaska Island, consistent with the model prediction (Figure 3). The most important variables in the spring maxent model of *Atheresthes* larvae were sea surface temperature, ocean color, current variability, and current direction (relative importance: 26.4%, 22.4%, 17.3%, and 13.1%, respectively). The model resulted in an AUC of 99% for the training data and 90% for the testing data, indicating a good model fit.

Essential fish habitat of larval *Atheresthes* as predicted by the modeling is largely concentrated in the eastern Aleutian Islands (Figure 4). Egg EFH could not be predicted.

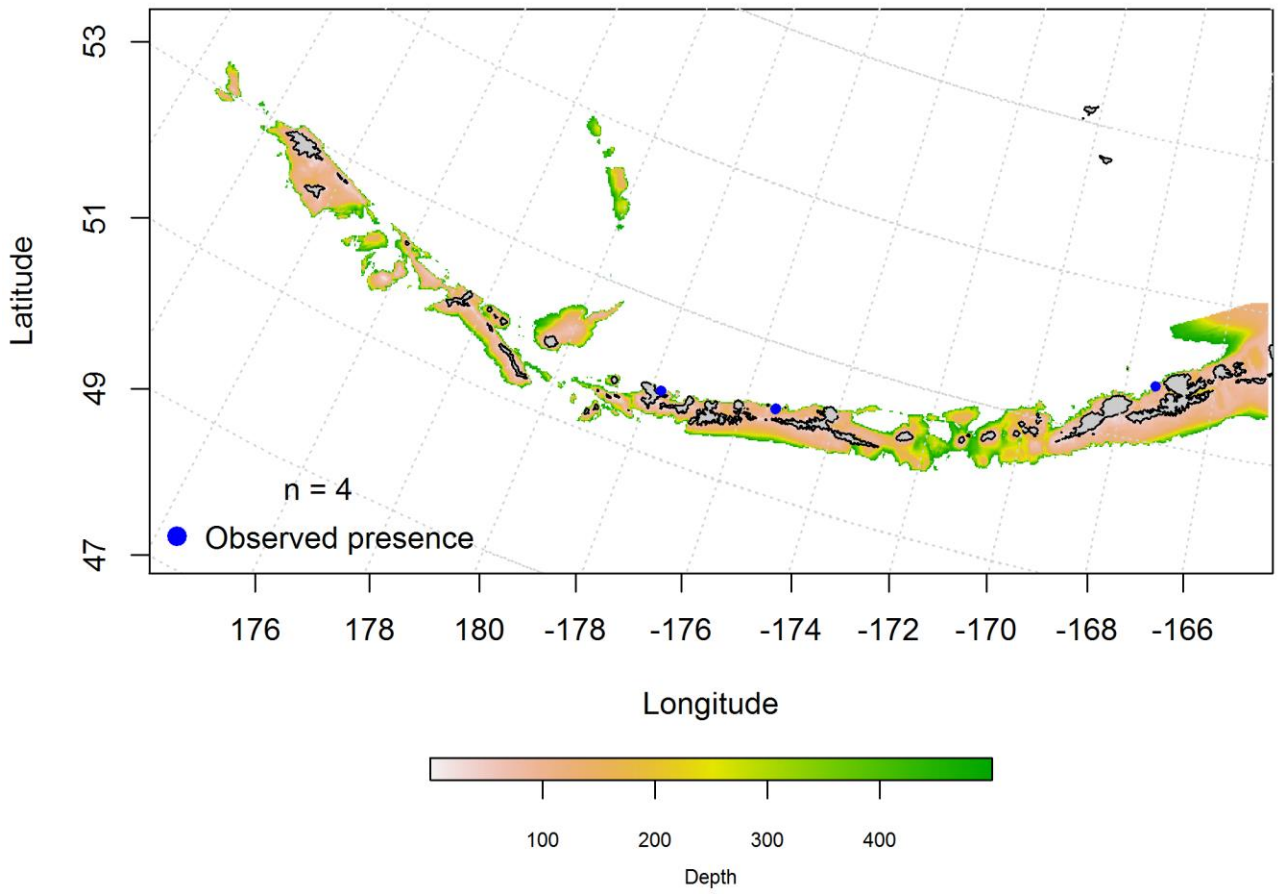

Figure 1. Winter observations of Atheresthes eggs from the Aleutian Islands.

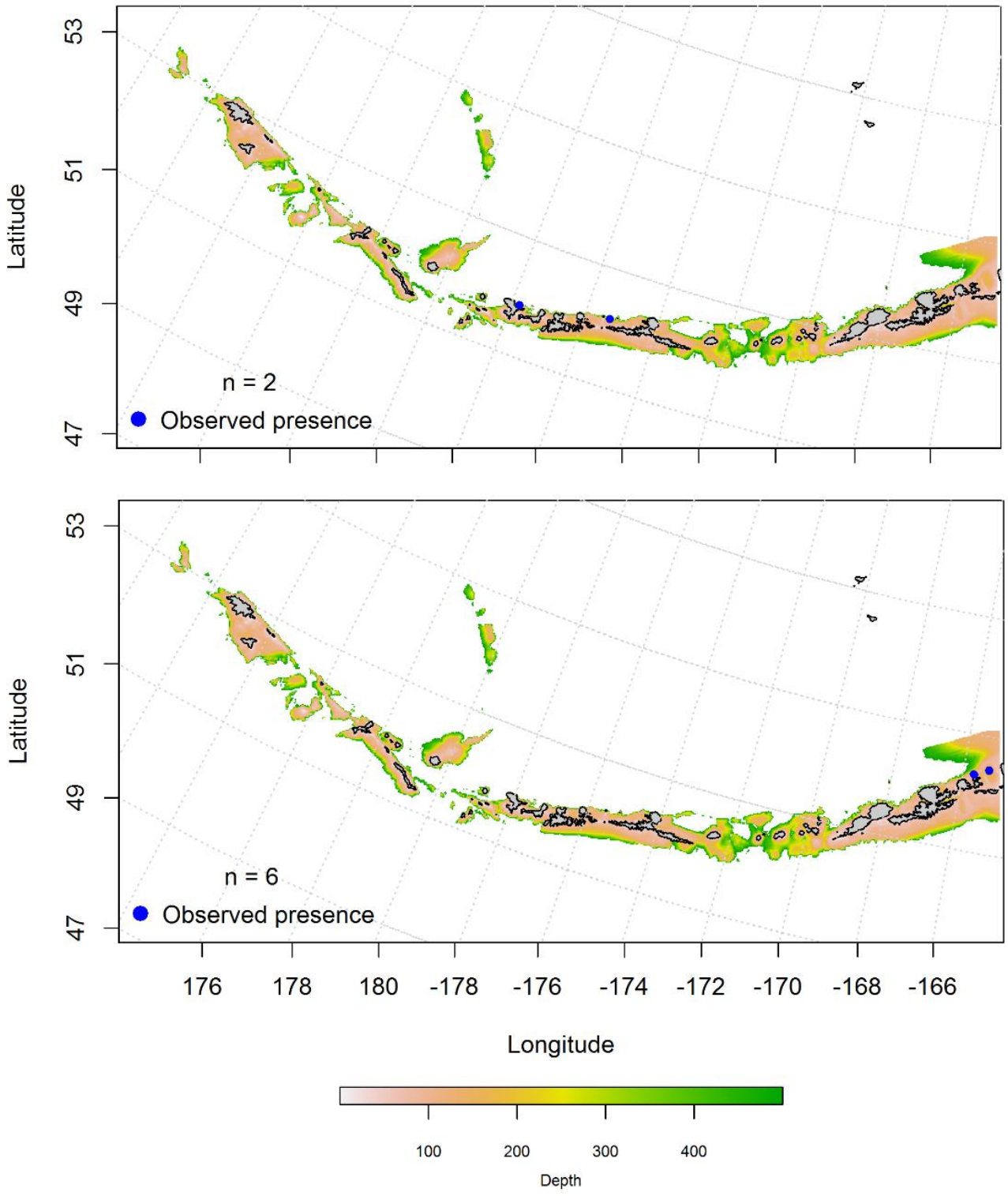

Figure 2. Winter and summer observations (top bottom panel) of larval Atheresthes from the Aleutian Islands.

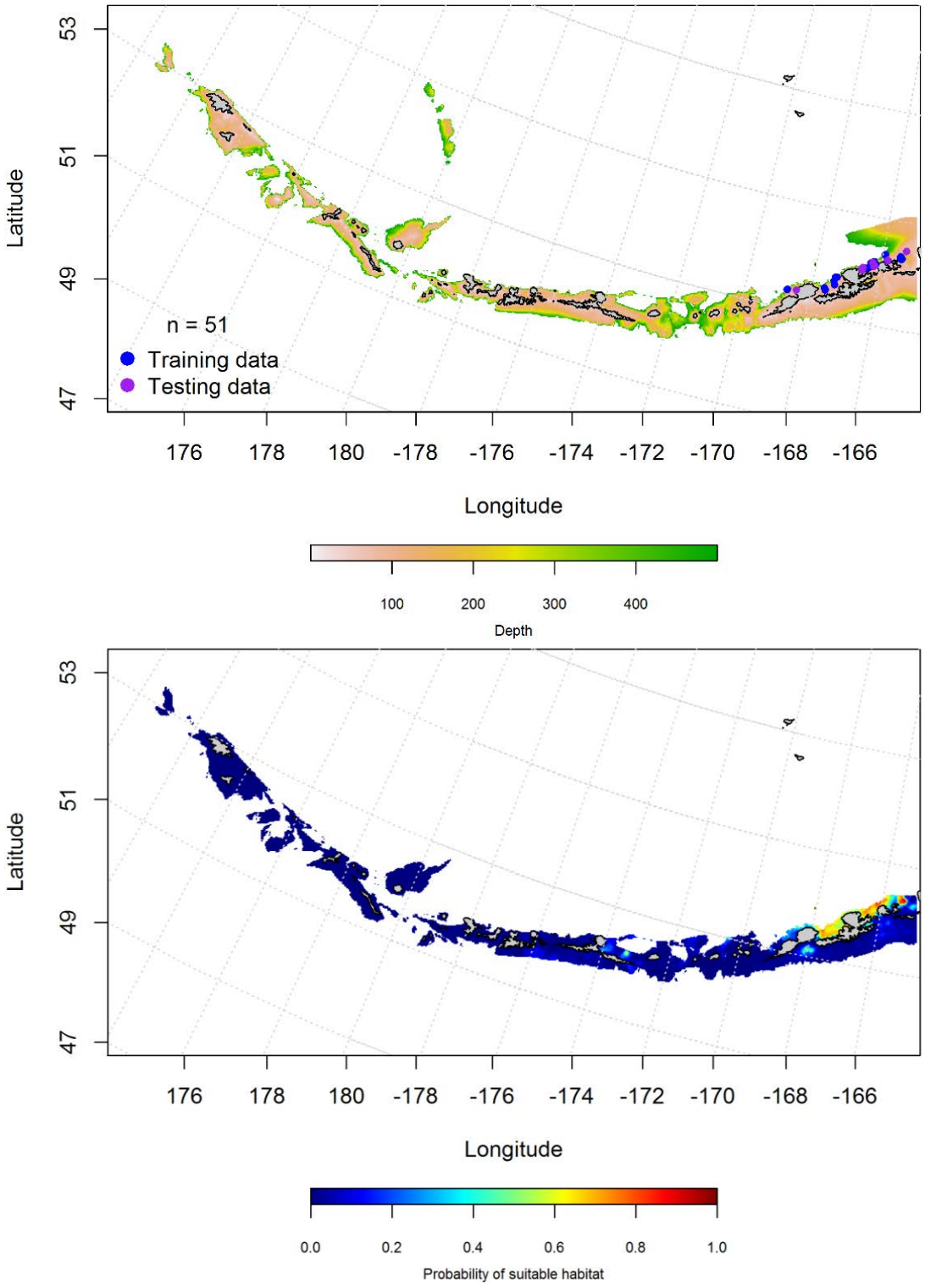

Figure 3. Locations of spring larval Atheresthes (top panel). Blue points were used to train the maximum entropy model predicting the probability of suitable spring habitat of larval Atheresthes (bottom panel) and the purple points were used to validate the model.

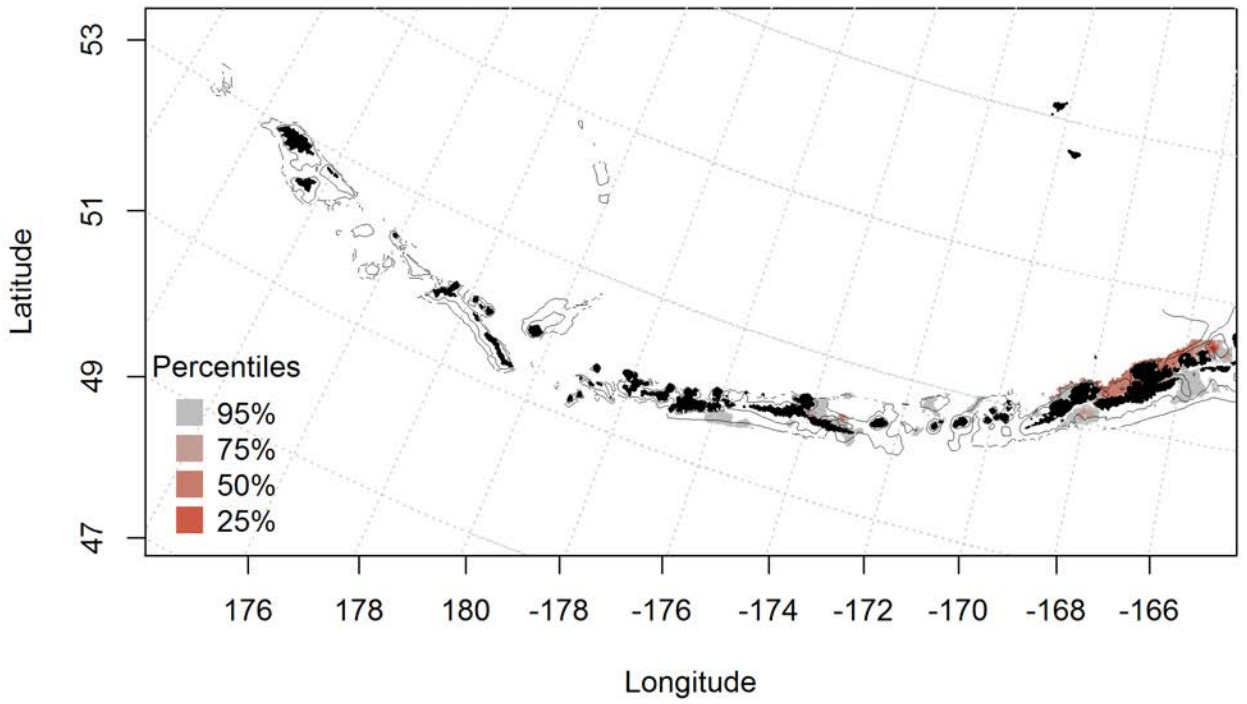

Figure 4. Spring essential fish habitat predicted for larval Atheresthes.

Arrowtooth flounder (*Atheresthes stomias*)
Species text here

Summertime distribution of juvenile and adult Arrowtooth flounder from bottom trawl surveys of the Aleutian Islands – A generalized additive model predicting the abundance of juvenile Arrowtooth flounder explained 41 % of the variability in CPUE in the bottom trawl survey. Bottom depth and geographic location were the most important variables explaining the distribution of juvenile Arrowtooth flounder. The model fit the test data set as well, explaining 40% of the variability. The model explained 40.9% of the deviance. The areas of predicted highest abundance were in the eastern and western Aleutian Islands (Figure 5).

Juvenile and adult Arrowtooth flounder were similarly distributed. As with the juveniles, the best-fitting GAM model for adult Arrowtooth flounder indicated that bottom depth and geographic location were the most important factors controlling adult Arrowtooth flounder

distribution. The model explained 32% of the deviance, 32% of the training data variability in bottom trawl CPUE, and 29% of the variability in the test data set. Adult Arrowtooth flounder were distributed across the AI but were more abundant in the eastern and western AI (Figure 6).

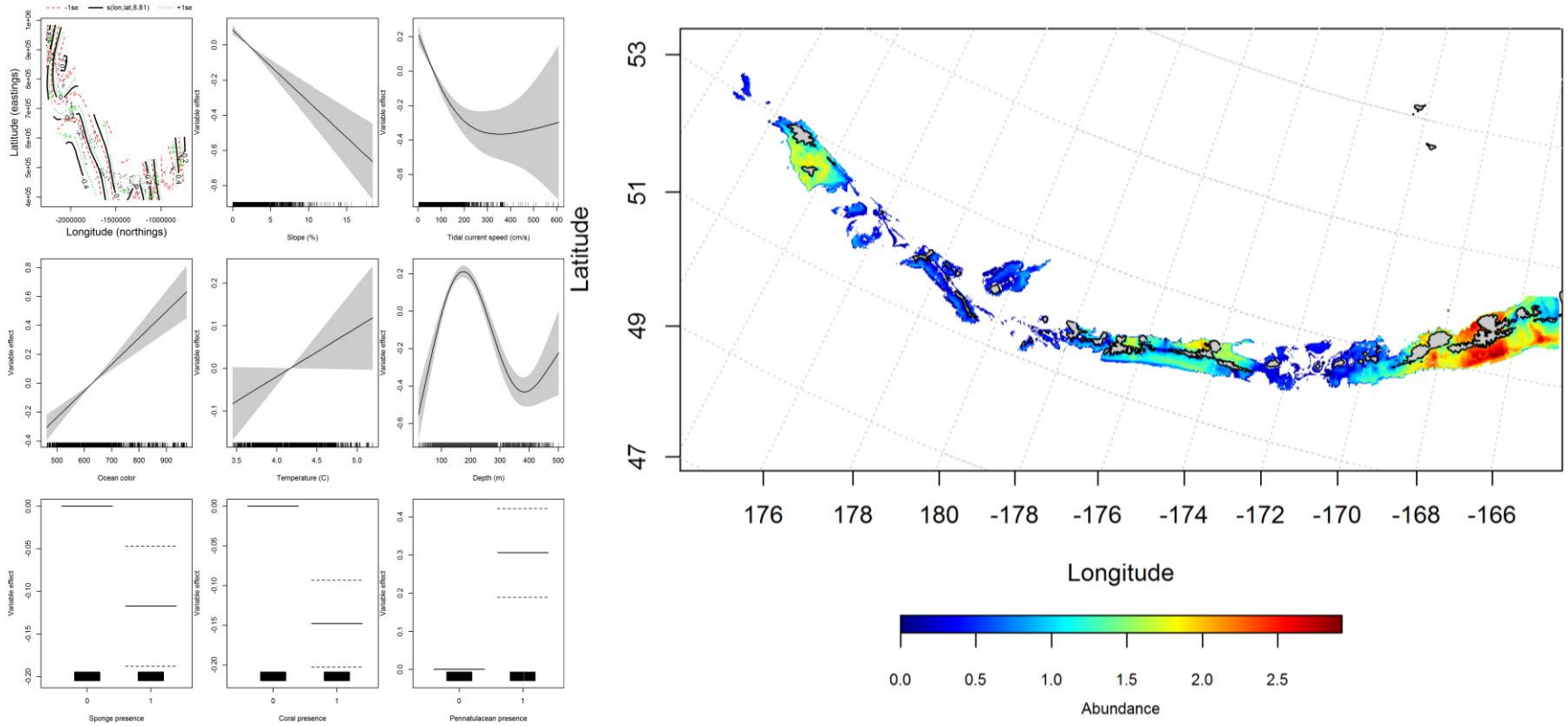

Figure 5. Best-fitting generalized additive model (GAM) effects of retained habitat variables on abundance of juvenile Arrowtooth flounder from summer bottom trawl surveys of the Aleutian Islands slope and shelf (left panel) alongside GAM-predicted juvenile Arrowtooth flounder abundance (right panel)..

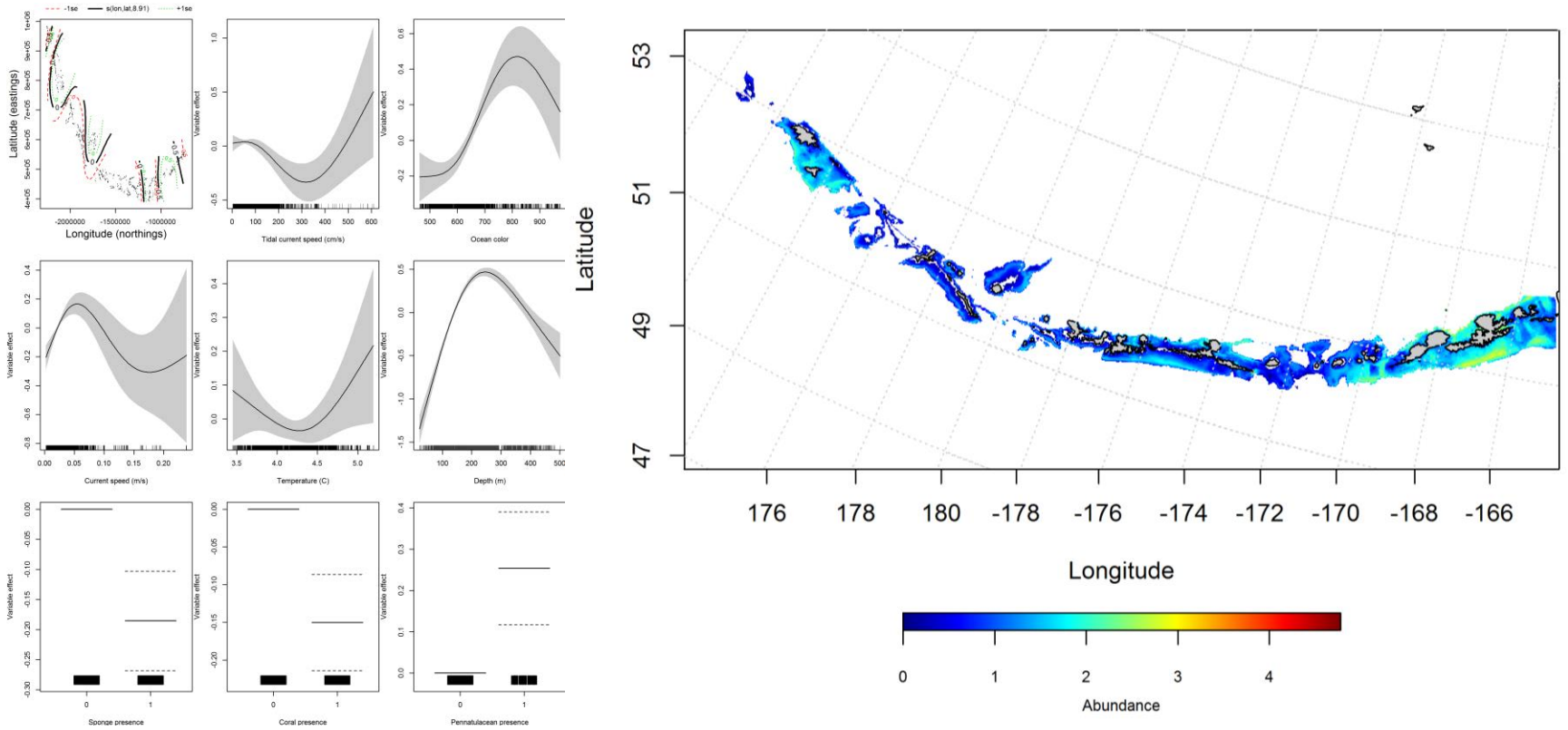

Figure 6. Best-fitting generalized additive model (GAM) effects of retained habitat variables on abundance of adult Arrowtooth flounder from summer bottom trawl surveys of the Aleutian Islands slope and shelf (left panel) alongside GAM-predicted adult Arrowtooth flounder abundance (right panel).

Seasonal distribution of commercial fisheries catches of adult Arrowtooth flounder in the Aleutian Islands – Observed instances of adult Arrowtooth flounder in the Aleutian Islands in commercial fisheries catches was generally consistent throughout all seasons. In the fall, bottom depth and surface ocean color were the most important variables determining suitable habitat of adult Arrowtooth flounder (relative importance: 41.3% and 33.4%). The AUC of the fall maxent model was 91% for the training data and 77% for the test data. The training data set correlation was 82%, and 77% in the test data set. The model predicted probable suitable habitat of Arrowtooth flounder throughout the Aleutian Islands, though slightly more probable in the east near Unalaska Islands(Figure 7).

In the winter, there were more observed instances of adult Arrowtooth flounder in the Aleutian Islands from commercial fisheries catches, and was generally consistent with fall observations. Surface chlorophyll A concentration (ocean color) and bottom depth were the most important variables determining the probability of suitable habitat of Arrowtooth flounder (relative importance: 40% and 37.7%). The AUC of the winter maxent model was 94% for the training data and 90% for the test data. 87% of the training data set, and 90% of the test data set were correctly classified. As with the fall, the model predicted probable suitable habitat of Arrowtooth flounder throughout the Aleutian Islands, though slightly more probable around Adak, Atka, Agattu, and Attu Islands (Figure 8).

In the spring, there were more observed instances of adult Arrowtooth flounder in the Aleutian Islands from commercial fisheries catches, than in the fall and winter. As with the fall and winter, bottom depth and ocean color were the most important variables determining the probability of suitable habitat of spring Arrowtooth flounder (relative importance: 51.3% and 37.7%). The AUC of the spring maxent model was 86% for the training data and 77% for the test

data. As with the fall and winter, the model predicted probable suitable habitat of Arrowtooth flounder throughout the Aleutian Islands and slightly higher near Agattu, Attu, Adak, Atka, and Unalaska Islands (Figure 9).

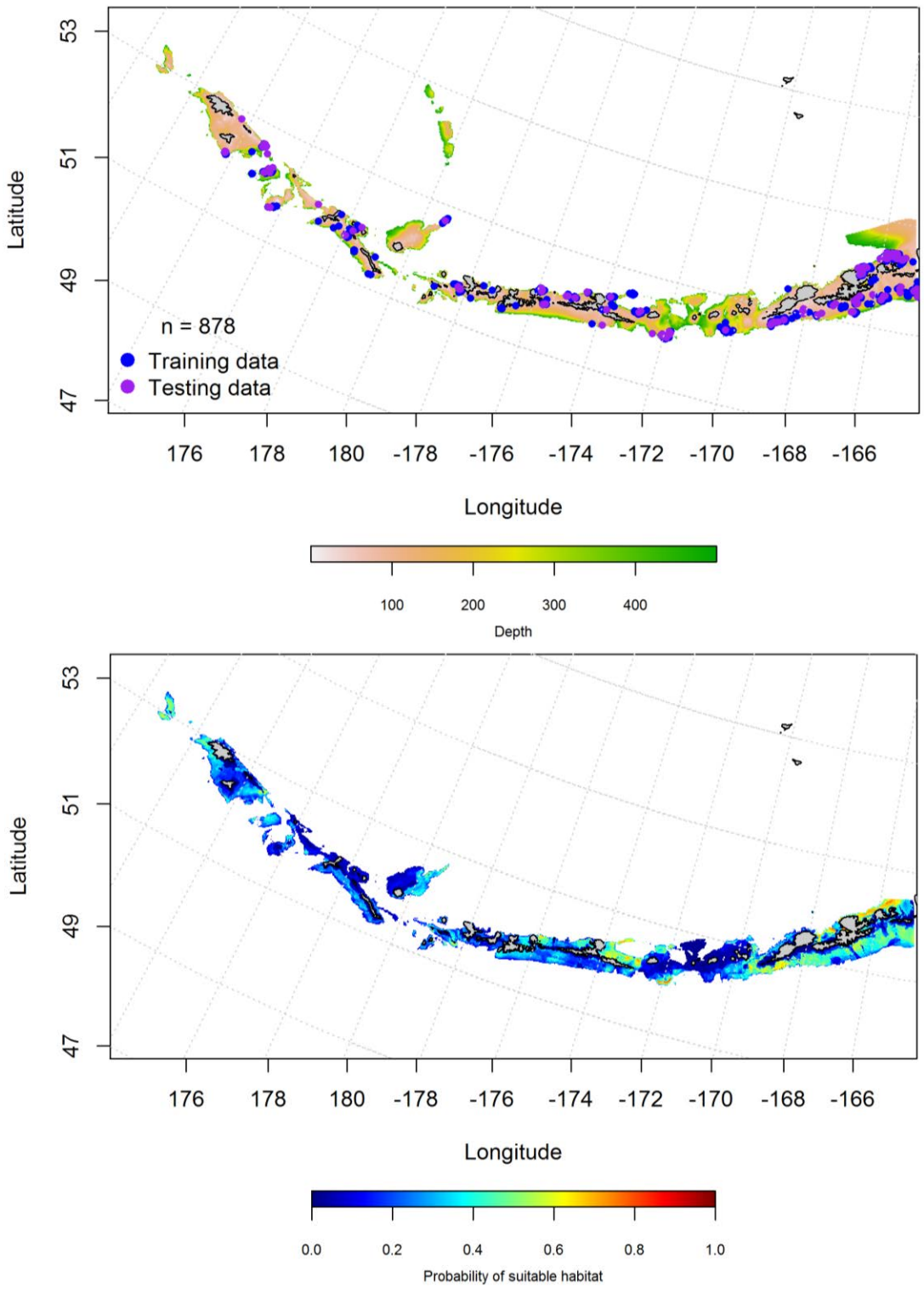

Figure 7. Locations of fall (September-November) commercial fisheries catches of Arrowtooth flounder (top panel). Blue points were used to train the maximum entropy model predicting the probability of suitable fall habitat supporting commercial catches of Arrowtooth flounder (bottom panel) and the purple points were used to validate the model.

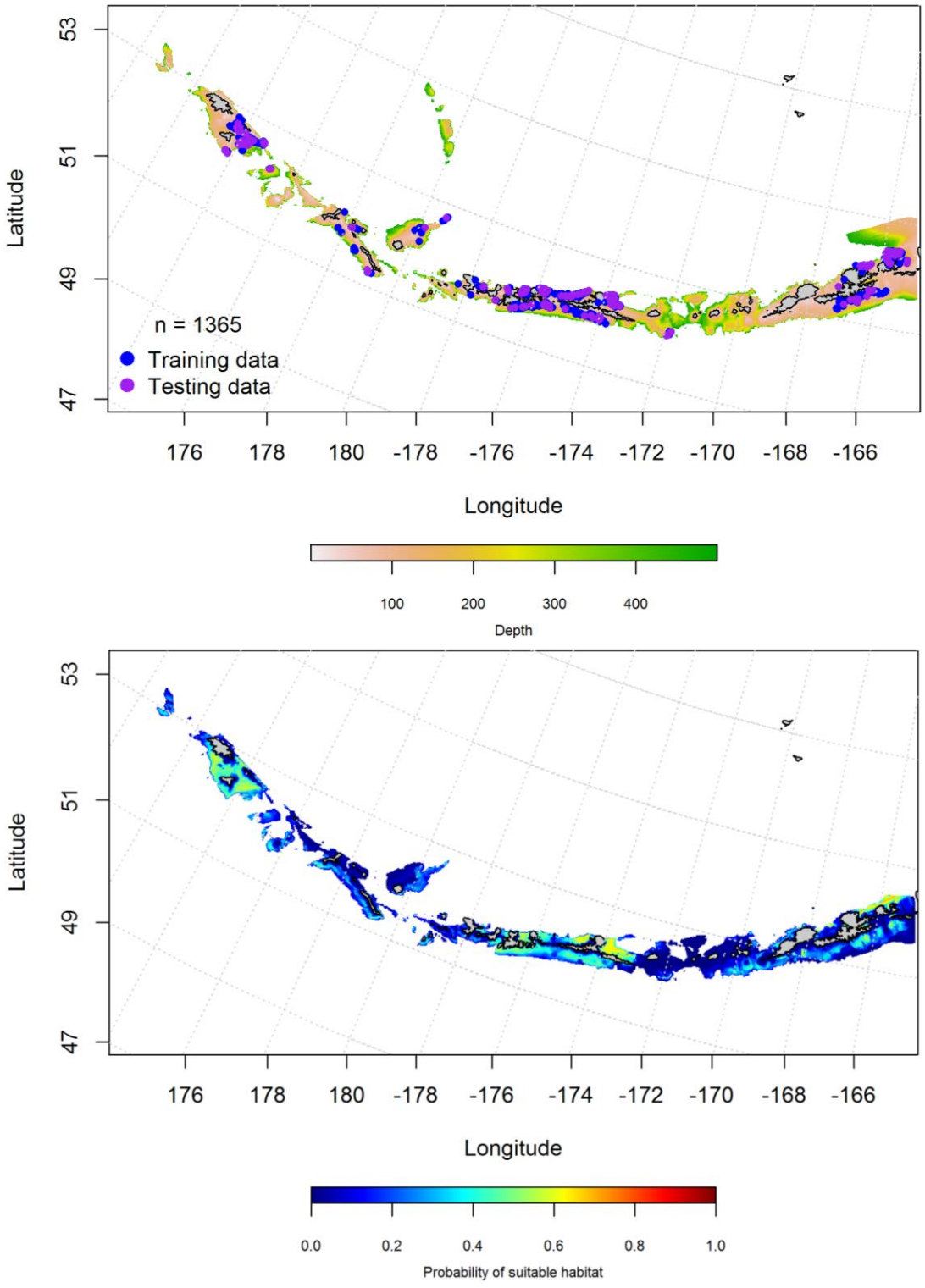

Figure 8. Locations of winter (December-February) commercial fisheries catches of Arrowtooth flounder (top panel). Blue points were used to train the maximum entropy model predicting the probability of suitable winter habitat supporting commercial catches of Arrowtooth flounder (bottom panel) and the purple points were used to validate the model.

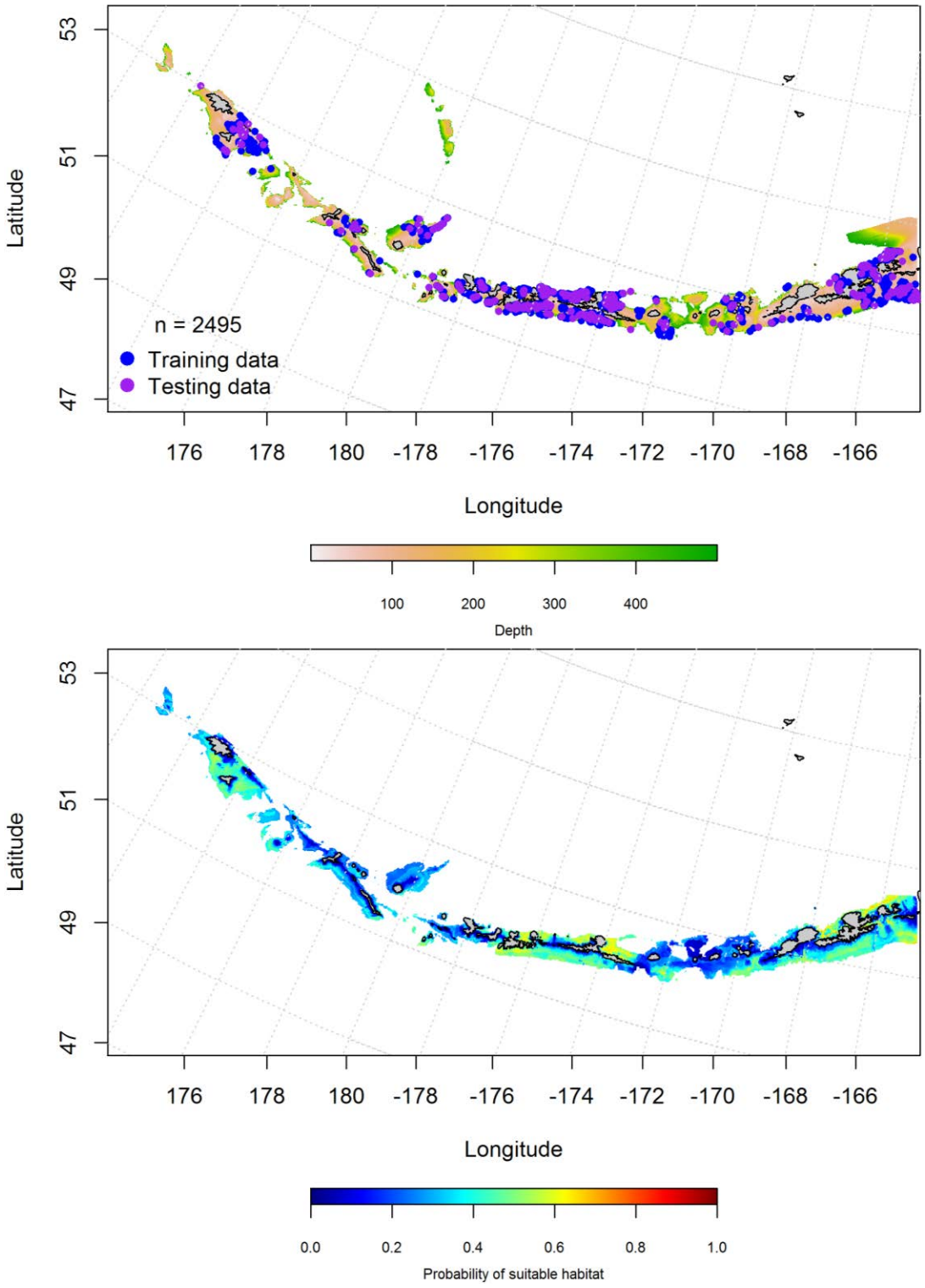

Figure 9. Locations of spring (March-May) commercial fisheries catches of Arrowtooth flounder (top panel). Blue points were used to train the maximum entropy model predicting the probability of suitable spring habitat supporting commercial catches of Arrowtooth flounder (bottom panel) and the purple points were used to validate the model.

Aleutian Islands Arrowtooth flounder Essential Fish Habitat Maps and Conclusions

-- In general, juvenile and adult ATF are widely distributed through the Aleutian Islands chain and co-occur in most places where they are found. Those collected in summertime bottom trawl surveys share similar predicted EFH distributions across the Aleutian Islands (Figure 10). These similarities can be observed in both areas of high (areas of higher CPUE exist in the eastern, central, and western Aleutians) and low abundance (e.g., large passes).

Similar to summertime bottom trawl survey data observations, the EFH predicted from commercial catches of ATF is distributed throughout the Aleutian Islands chain (Figure 11). There does not appear to be much seasonal variability to the EFH distribution and areas of high concentration are interspersed with areas of low concentration. Commercial ATF catches coincide with the same pattern EFH distribution observed from summertime bottom trawl surveys.

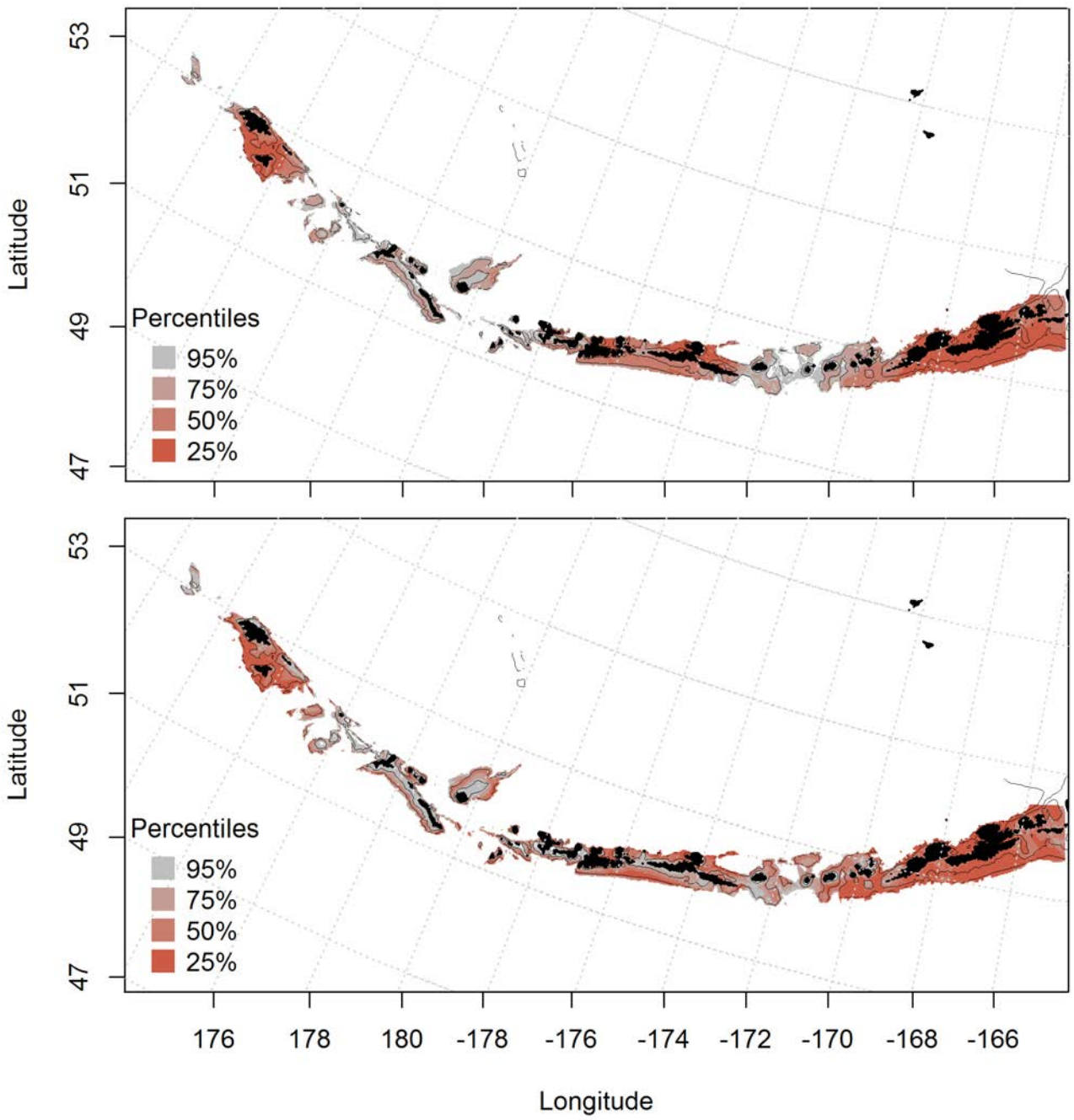

Figure 10. Predicted summer essential fish habitat for Arrowtooth flounder juveniles and adults (top and bottom panel) from summertime bottom trawl surveys.

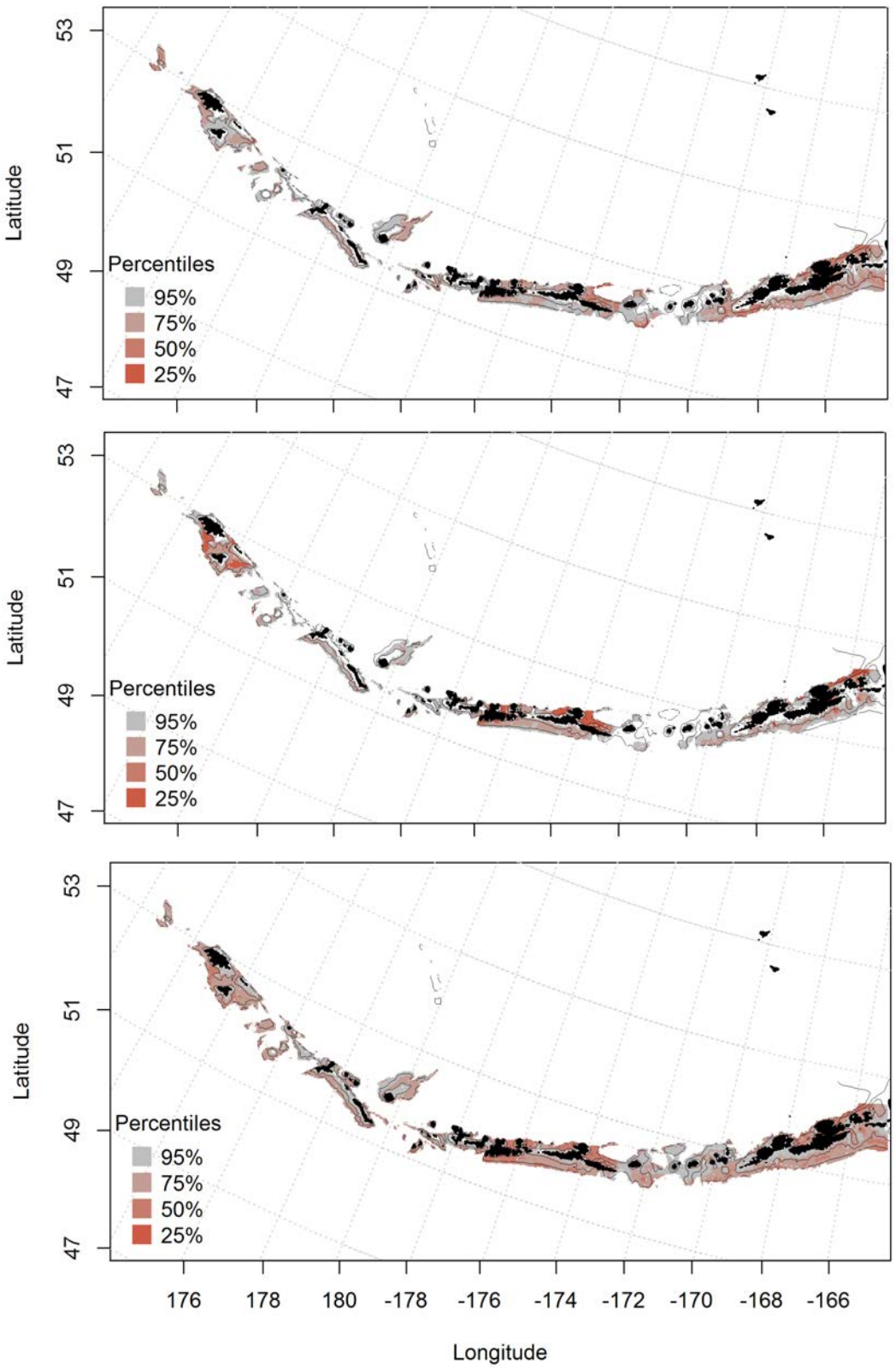

Figure 11. Essential fish habitat predicted for Arrowtooth flounder during fall (top panel), winter (middle panel) and spring (bottom panel) from summertime commercial catches.

Kamchatka flounder (*Atheresthes evermanni*)
Species text here

Summertime distribution of juvenile and adult Kamchatka flounder from bottom trawl surveys of the Aleutian Islands -- The catch of Kamchatka flounder in summer bottom trawl surveys of the Aleutian Islands indicates this species is broadly distributed. Generalized additive models predicting the abundance of juvenile Kamchatka flounder explained 25% of the training data set variability in CPUE in the bottom trawl survey, and 32% of the variability in the test data set. Geographic location and bottom depth were the most important variables explaining the distribution of juvenile Kamchatka flounder. The explained 24.7% of the deviance. The areas of predicted highest abundance were in the western Aleutian Islands (Figure 12).

Adult Kamchatka flounder were modeled using a hurdle-GAM. The presence absence GAM predicted a higher probability of presence in the western Aleutian Islands, though was fairly similar across the islands. The best-fitting PA GAM indicated that bottom depth and geographic location were the most important factors controlling adult Kamchatka flounder distribution and the model explained 89% of the training data set variability, and explained 90% of the variability in the test data set. The model also explained 36.5% of the deviance, and correctly classified 82% of the training data set and 81% of the test data set. The probability of suitable habitat for adult Kamchatka flounder was distributed across the AI, and was denser in areas with large passes (Figure 13).

The CPUE GAM model found that bottom depth and tidal current were the most important variables that explained the distribution of adult Kamchatka flounder. The model explained 34.5% of the deviance, 35% of the training set variability in CPUE in the bottom trawl survey,

16% of the variability in the test data set. The probability of suitable habitat for adult Kamchatka flounder was distributed across the AI (Figure 14).

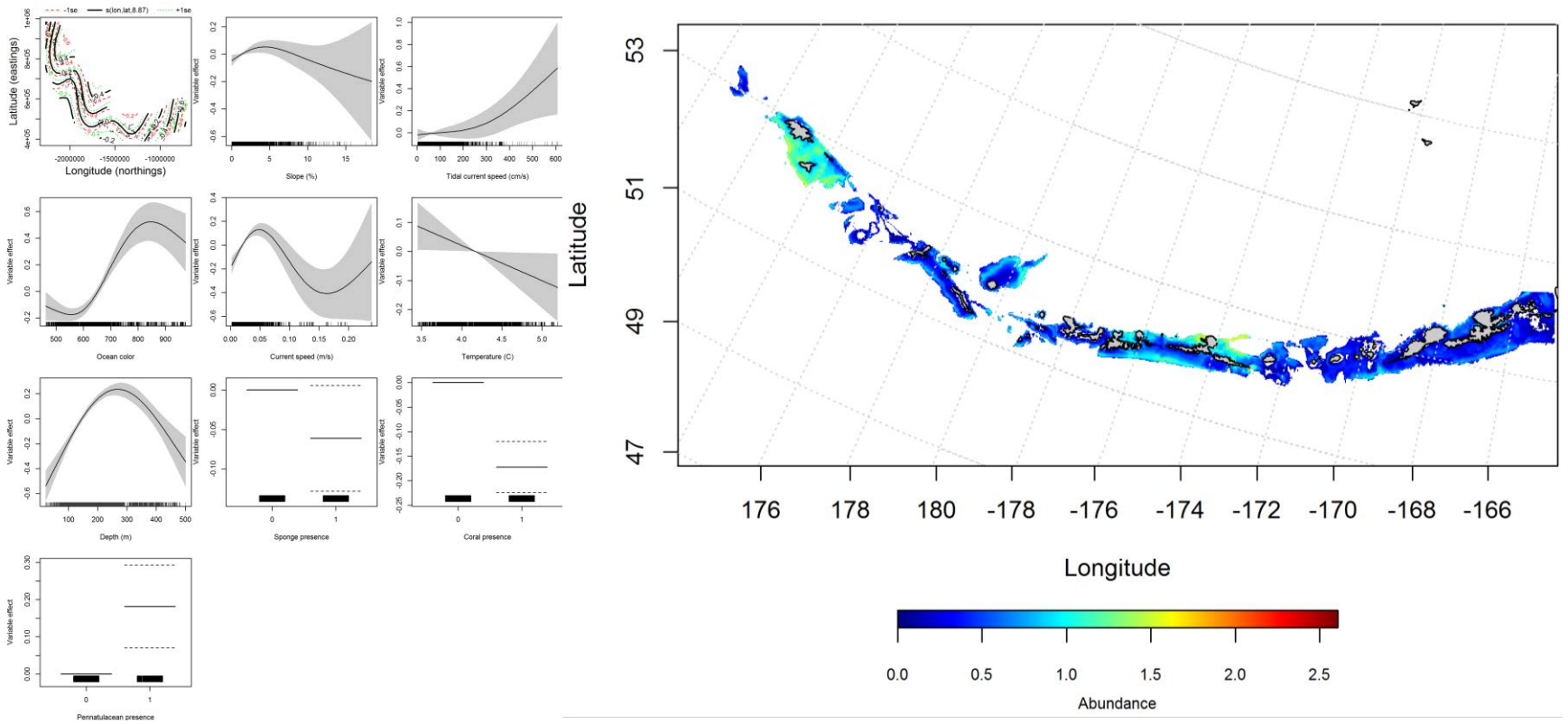

Figure 12. Best-fitting generalized additive model (GAM) effects of retained habitat variables on abundance of juvenile Kamchatka flounder from summer bottom trawl surveys of the Aleutian Islands slope and shelf (left panel) alongside GAM-predicted juvenile Kamchatka flounder abundance (right panel).

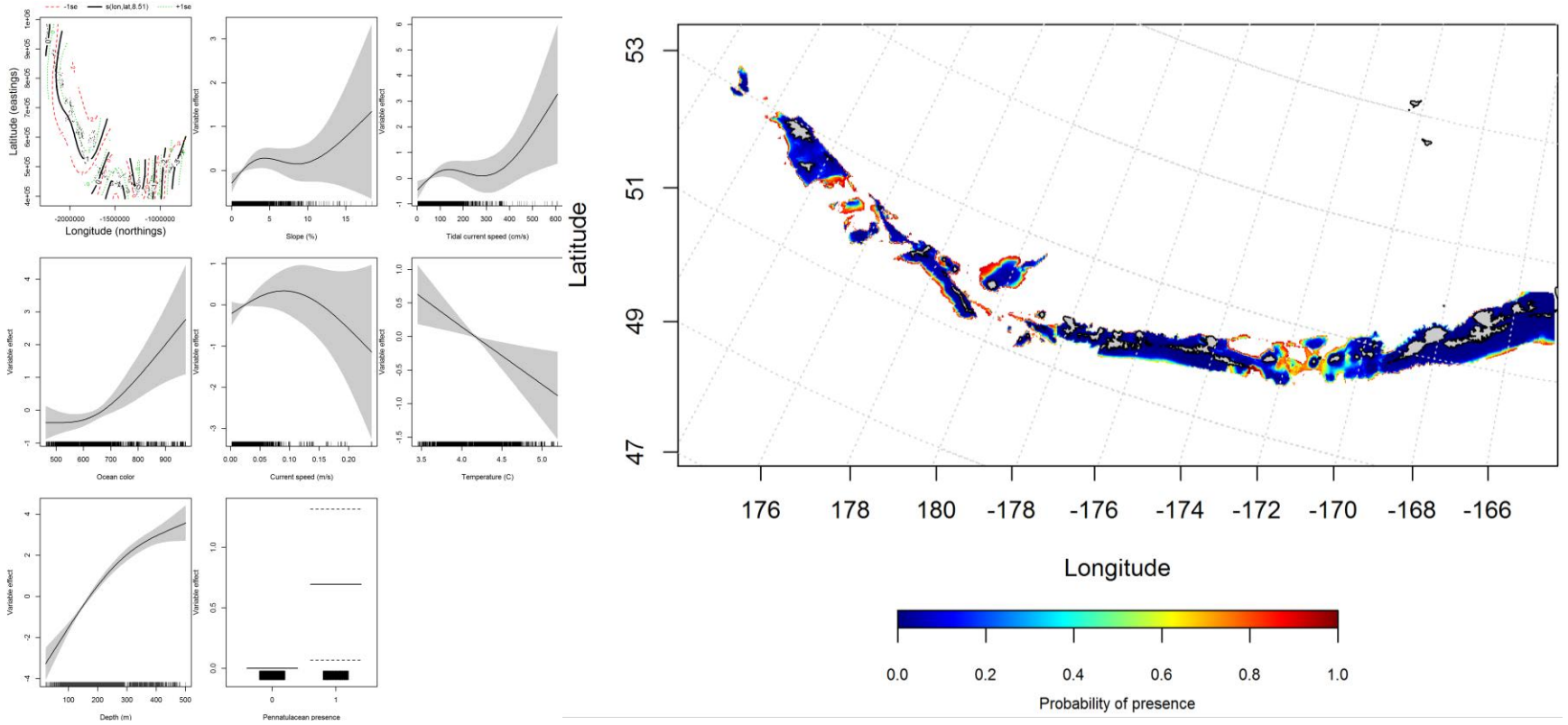

Figure 13. Best-fitting hurdle model effects of retained habitat variables on presence absence (PA) of adult Kamchatka flounder from summer bottom trawl surveys of the Aleutian Islands slope and shelf (left panel) alongside hurdle-predicted adult Kamchatka flounder PA (right panel).

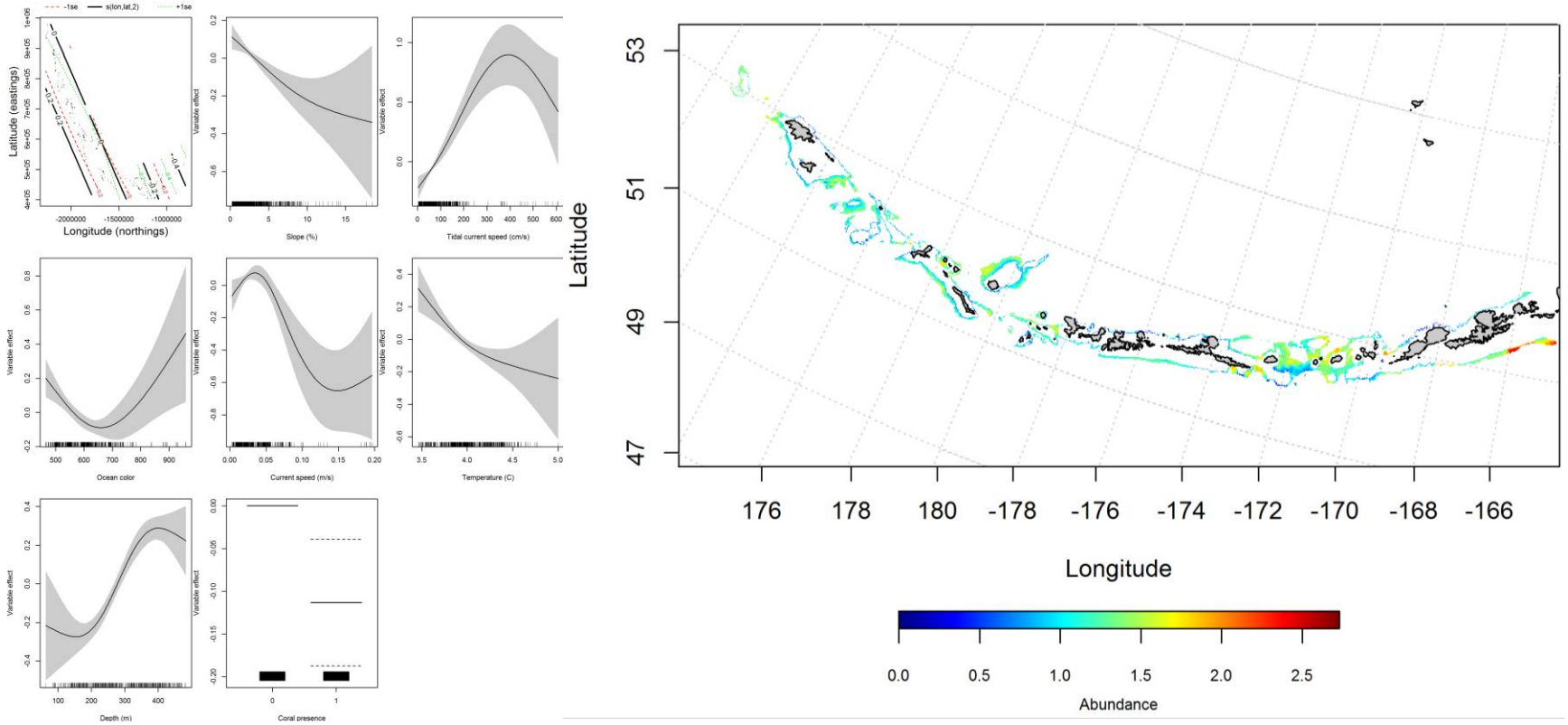

Figure 14. Best-fitting hurdle model effects of retained habitat variables on cpue of adult Kamchatka flounder from summer bottom trawl surveys of the Aleutian Islands slope and shelf (left panel) alongside hurdle-predicted adult Kamchatka flounder cpue (right panel).

Seasonal distribution of commercial fisheries catches of adult Kamchatka flounder in the Aleutian Islands -- Distribution of adult Kamchatka flounder in the Aleutian Islands in commercial fisheries catches was generally consistent throughout all seasons, though the number of observances increased from fall to spring. In the fall, bottom depth, bottom temperature and ocean color were the most important variables determining the probability of suitable habitat of Kamchatka flounder (relative importance: 34.8%, 26.9%, and 18.1%, respectively). The AUC of the fall maxent model was 91% for the training data and 79% for the test data. 72% of the cases in the training data and 73.8% of the cases in the test data were predicted correctly. The model predicted probable suitable habitat of Kamchatka flounder across the AI (Figure 15).

In the winter, ocean color, bottom depth, and tidal current were the most important variables determining the probability of suitable habitat of Kamchatka flounder (relative importance: 35.2%, 33.8%, and 17.7%, respectively). The AUC of the winter maxent model was 97% for the training data and 88% for the test data. 83.8% of the training data set and 78.4% of the testing data sets were predicted correctly. The model predicted probable suitable habitat of Kamchatka flounder catches across the AI and highest near Atka Island in the central AI (Figure 16).

In the spring, bottom depth and surface color were the most important variables determining the probability of suitable habitat of Kamchatka flounder (relative importance: 46.3% and 33%). The AUC of the fall model was 92% for the training data and 83% for the test data. 72.7% of the training data set and 71.6% of the testing data sets were predicted correctly. The model predicted probable suitable habitat of Kamchatka flounder in the central and eastern AI (Figure 17).

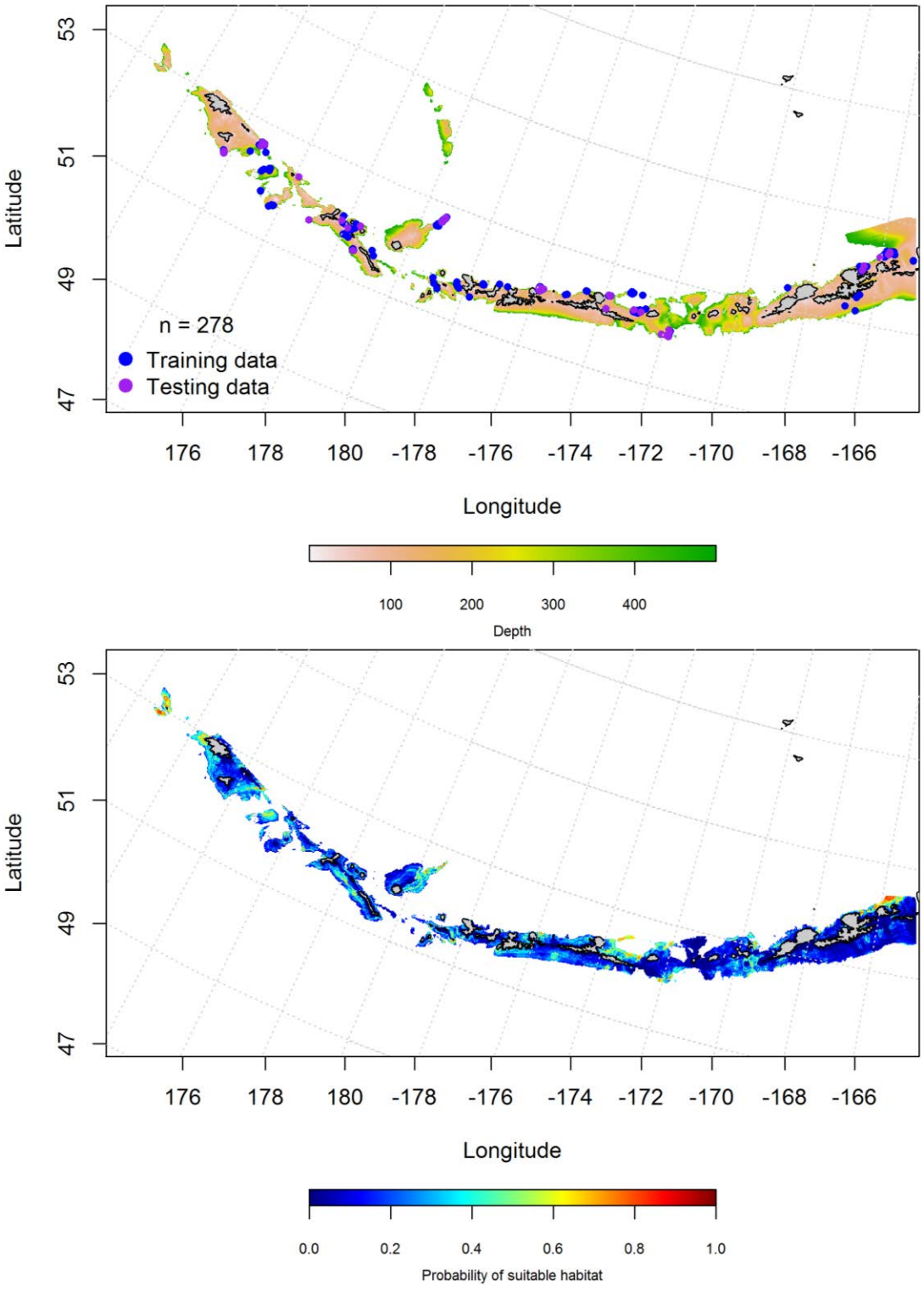

Figure 15. Locations of fall (September-November) commercial fisheries catches of Kamchatka flounder (top panel). Blue points were used to train the maximum entropy model predicting the probability of suitable fall habitat supporting commercial catches of Kamchatka flounder (bottom panel) and the purple points were used to validate the model.

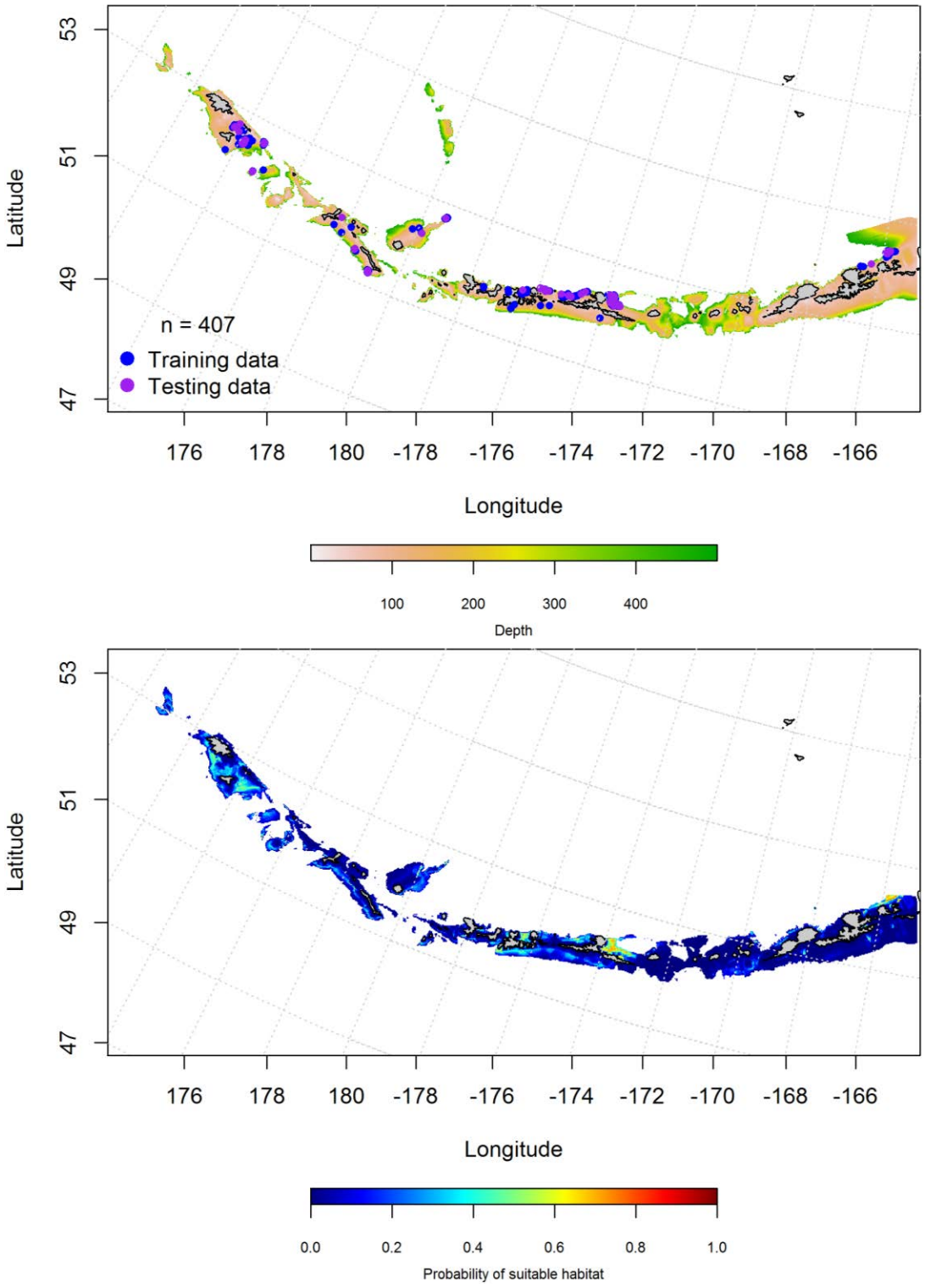

Figure 16. Locations of winter (December-February) commercial fisheries catches of Kamchatka flounder (top panel). Blue points were used to train the maximum entropy model predicting the probability of suitable winter habitat supporting commercial catches of Kamchatka flounder (bottom panel) and the purple points were used to validate the model.

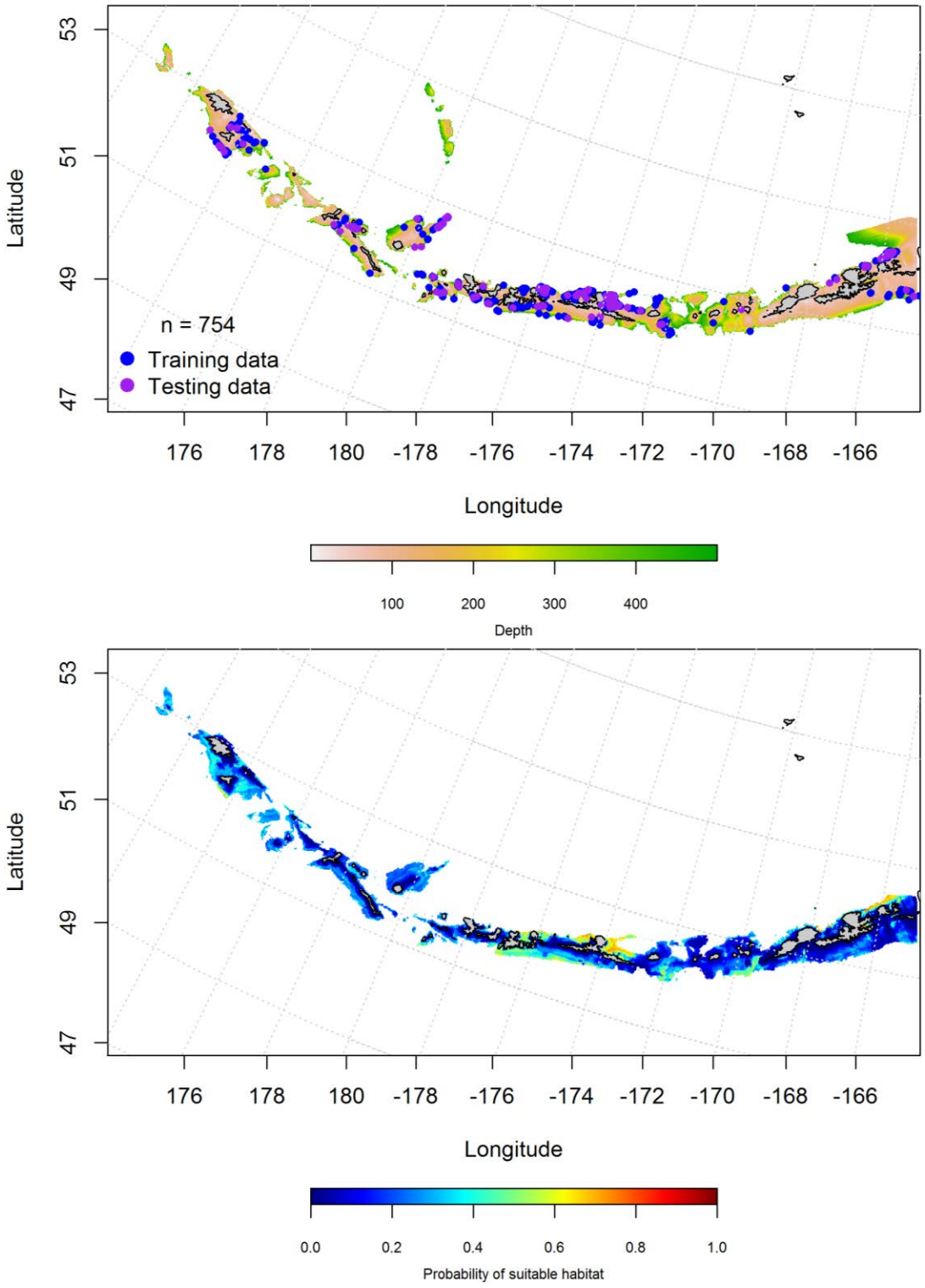

Figure 17. Locations of spring (December-February) commercial fisheries catches of Kamchatka flounder (top panel). Blue points were used to train the maximum entropy model predicting the probability of suitable spring habitat supporting commercial catches of Kamchatka flounder (bottom panel) and the purple points were used to validate the model.

Aleutian Islands Kamchatka flounder Essential Fish Habitat Maps and Conclusions –

Juvenile Kamchatka flounder are more abundant and widely distributed through the Aleutian Islands chain than adults, but co-occur in most places where they are found (Figure 18).

The EFH predicted from commercial catches of Kamchatka flounder is sparsely distributed throughout the Aleutian Islands chain (Figure 19). There does not appear to be much seasonal variability to the EFH distribution and areas of higher concentration are interspersed with areas of low concentration (i.e. large passes).

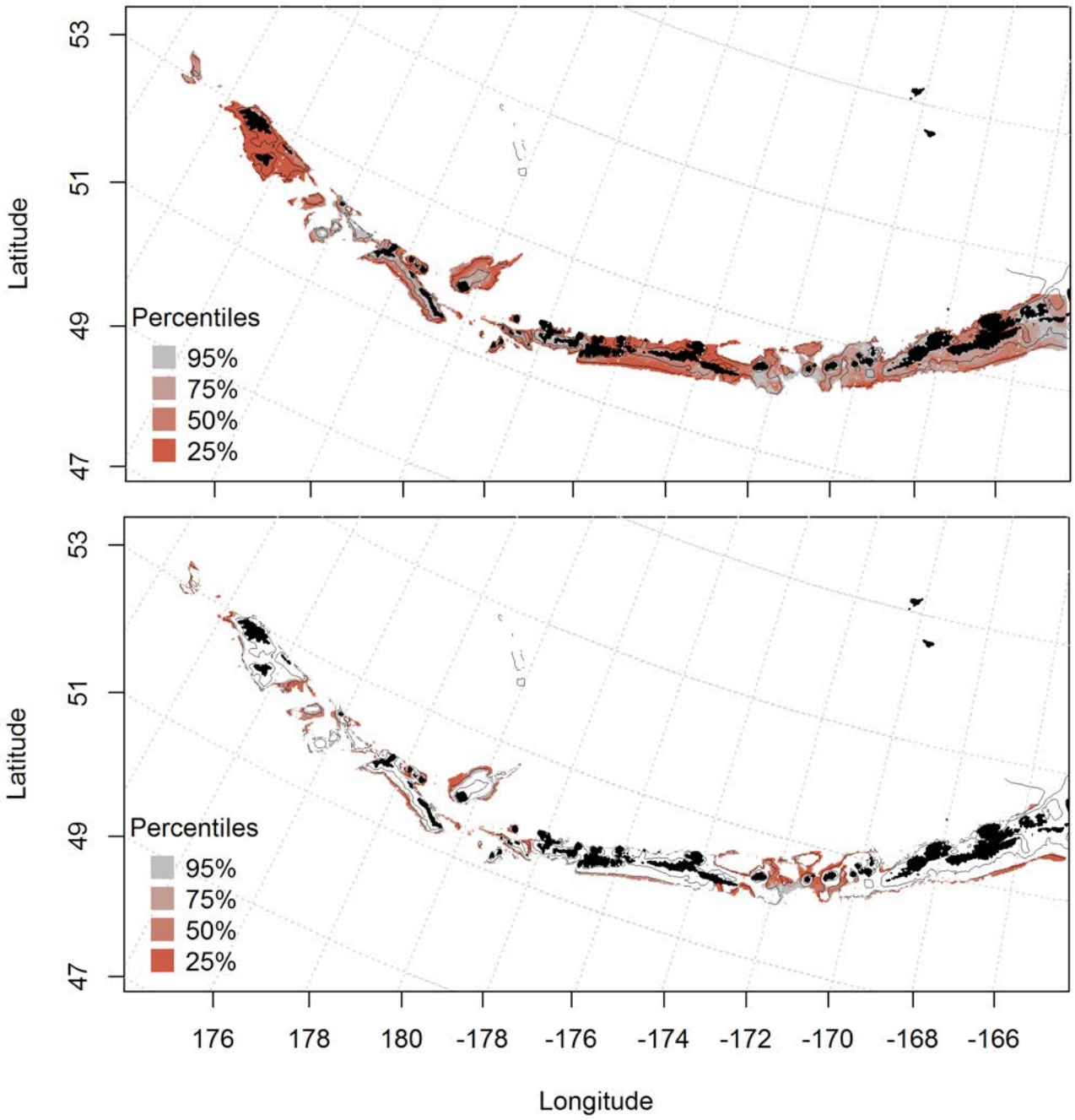

Figure 18. Predicted summer essential fish habitat for Kamchatka flounder juveniles and adults (top and bottom panel) from summertime bottom trawl surveys.

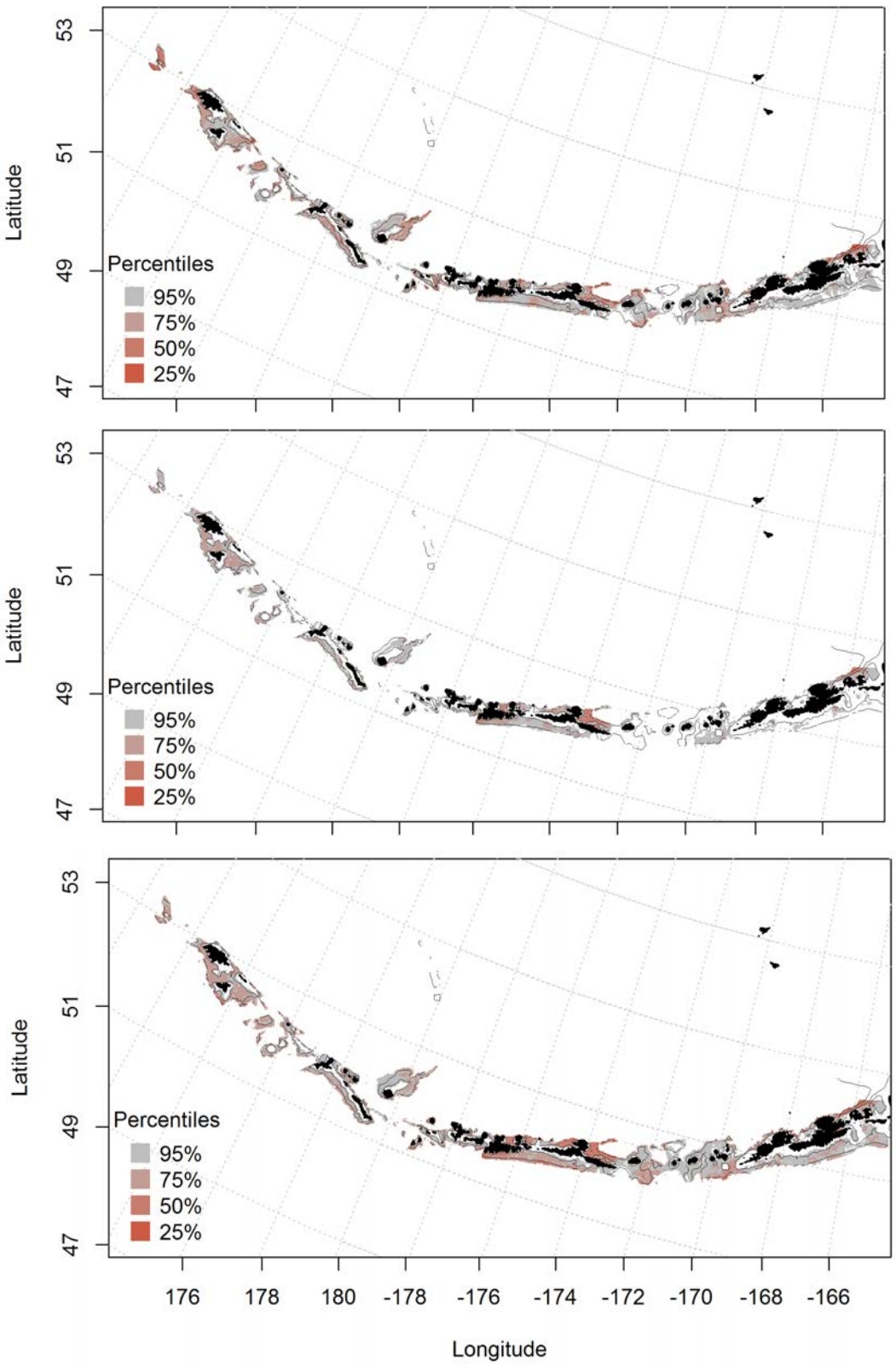

Figure 19. Essential fish habitat predicted for Kamchatka flounder during fall (top panel), winter (middle panel) and spring (bottom panel) from summertime commercial catches.

Northern rock sole (*Lepidopsetta polyxystra*)

Seasonal distribution of early life history stages of Northern rock sole in the Aleutian Islands – There were 60 instances of larval Northern rock sole (NRS) observed in the FOCI database , 57 in the spring and 3 in the summer, limited to the eastern AI. The most important variables in modeling probability of suitable habitat for spring larval Northern rock sole included surface temperature, current variability and surface ocean color (relative importance: 32.5%, 28.4%, and 18.9%, respectively). The AUC was 99% for the training data and 95% for the testing data, indicating a good model fit. The model correctly classified 98% of the training data and 95% of the test data. The model predicted probable suitable habitat of spring larval NRS across the AI and highest in areas with large passes (Figure 20).

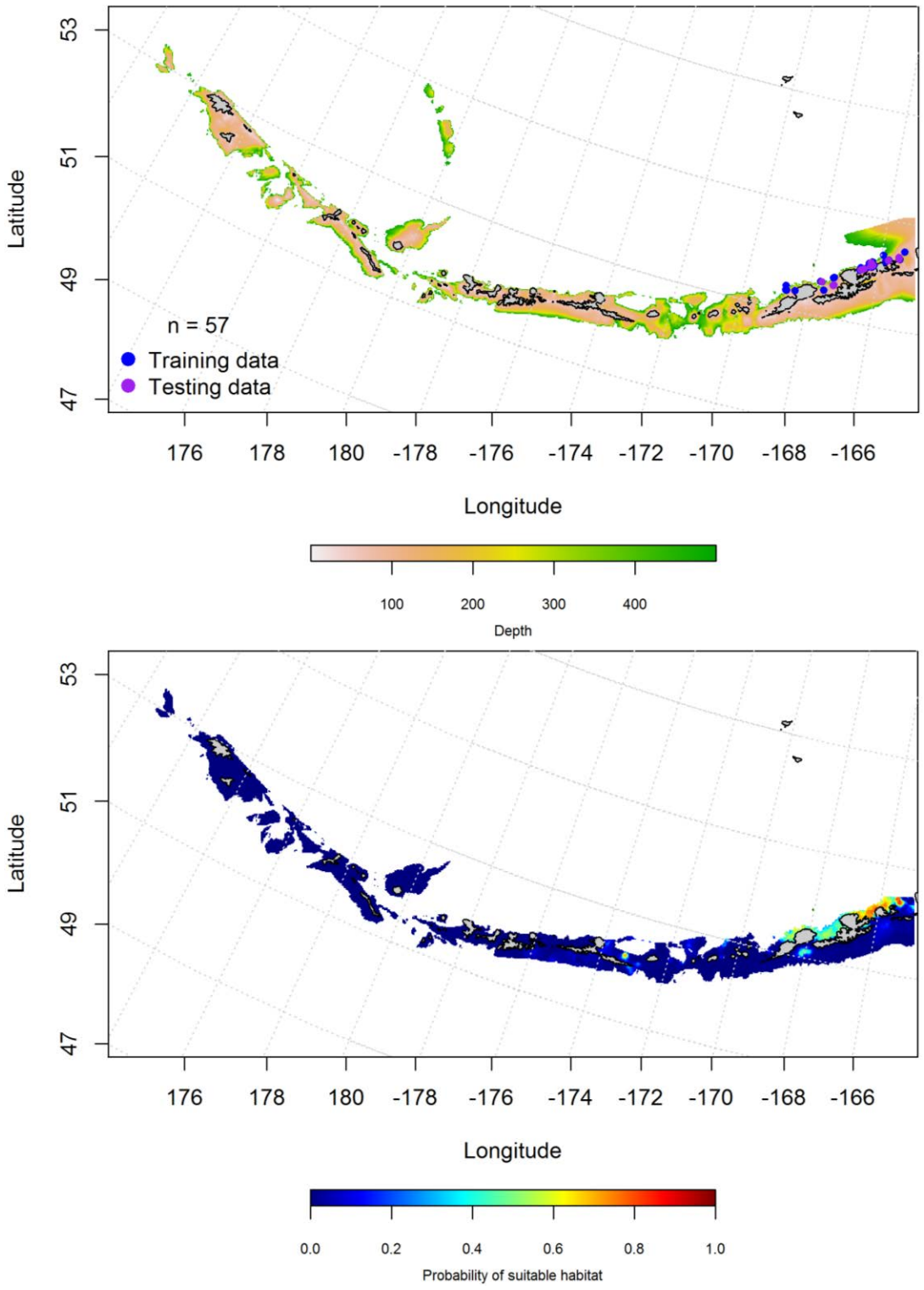

Figure 20. Locations of spring (June-August) commercial fisheries catches of larval Northern rock sole (top panel). Blue points were used to train the maximum entropy model predicting the probability of suitable spring habitat supporting commercial catches of NRS (bottom catches) and the purple points were used to validate the model.

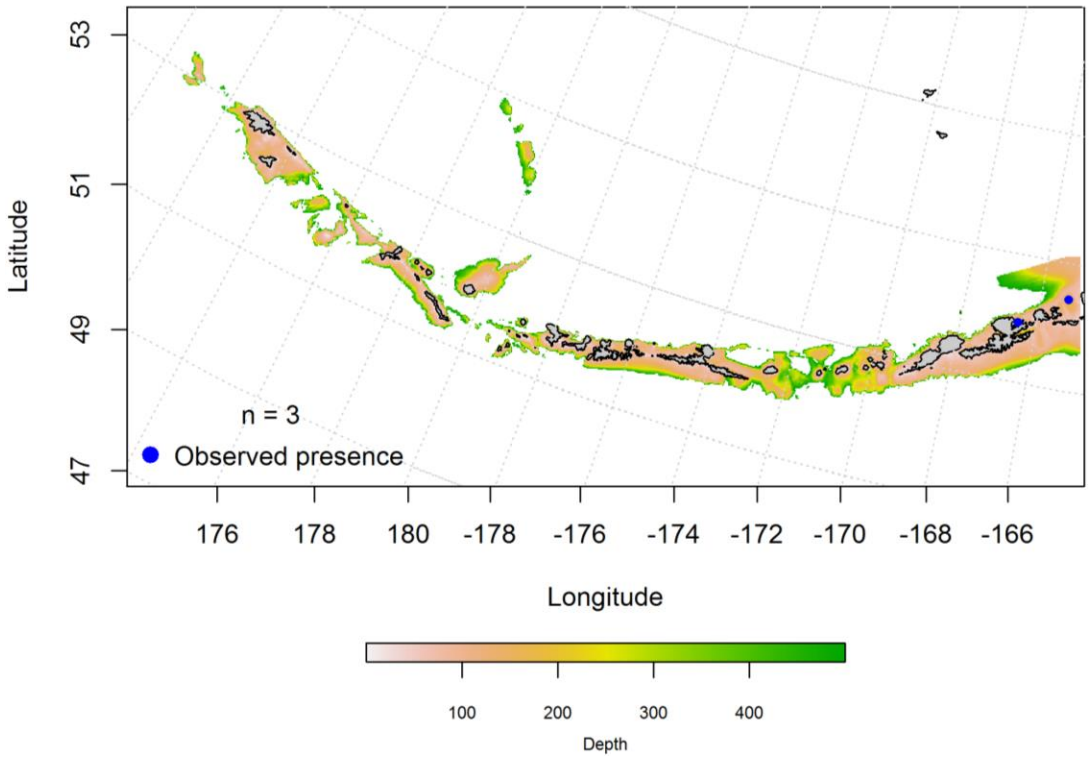

Figure 21. Locations of summer (June-August) commercial fisheries catches of NRS..

Summertime distribution of juvenile and adult Northern rock sole from bottom trawl surveys of the Aleutian Islands -- The catch of Northern rock sole in summer bottom trawl surveys of the Aleutian Islands indicates this species is broadly distributed. Generalized additive models predicting the abundance of juvenile Northern rock sole explained 55% of the variability in CPUE in the bottom trawl survey using training data, 49% of the variability in the test data, and 54.8% of the deviance. Bottom depth, geographic location, and bottom temperature were the most important variables explaining probable suitable habitat of juvenile Northern rock sole. The model predicted probable summer suitable habitat of juvenile Northern rock sole across the AI (Figure 22).

The best-fitting GAM model for adult Northern rock sole indicated that bottom depth and geographic location were the most important factors controlling the probability of suitable habitat. The model explained 38% of the variability of the training and test data sets for the bottom trawl CPUE, and 38% of the deviance. Adult Northern rock sole were distributed similarly to the juveniles, across the AI (Figure 23).

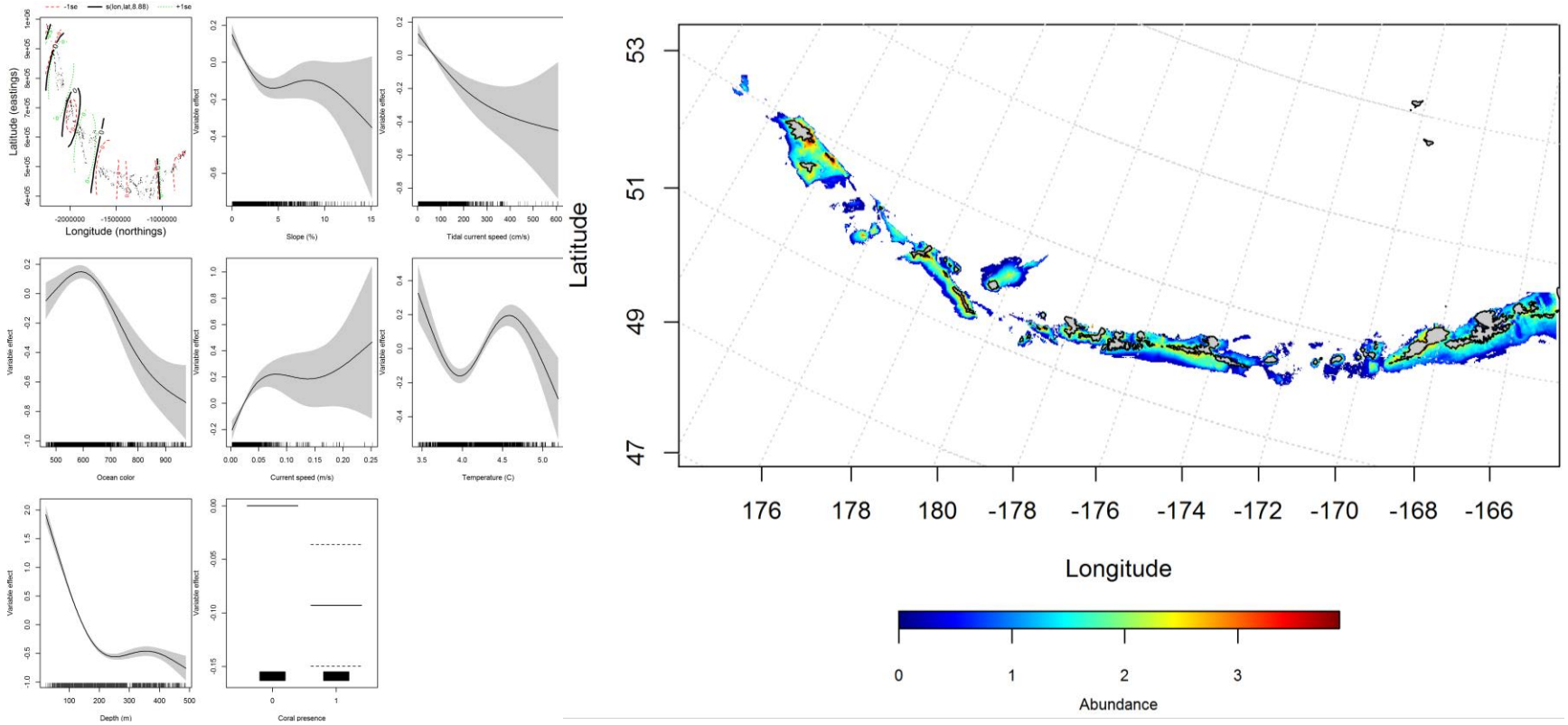

Figure 22. Best-fitting generalized additive model (GAM) effects of retained habitat variables on abundance of juvenile Northern rock sole from summer bottom trawl surveys of the Aleutian Islands (left panel) alongside GAM-predicted juvenile Northern rock sole abundance (right panel).

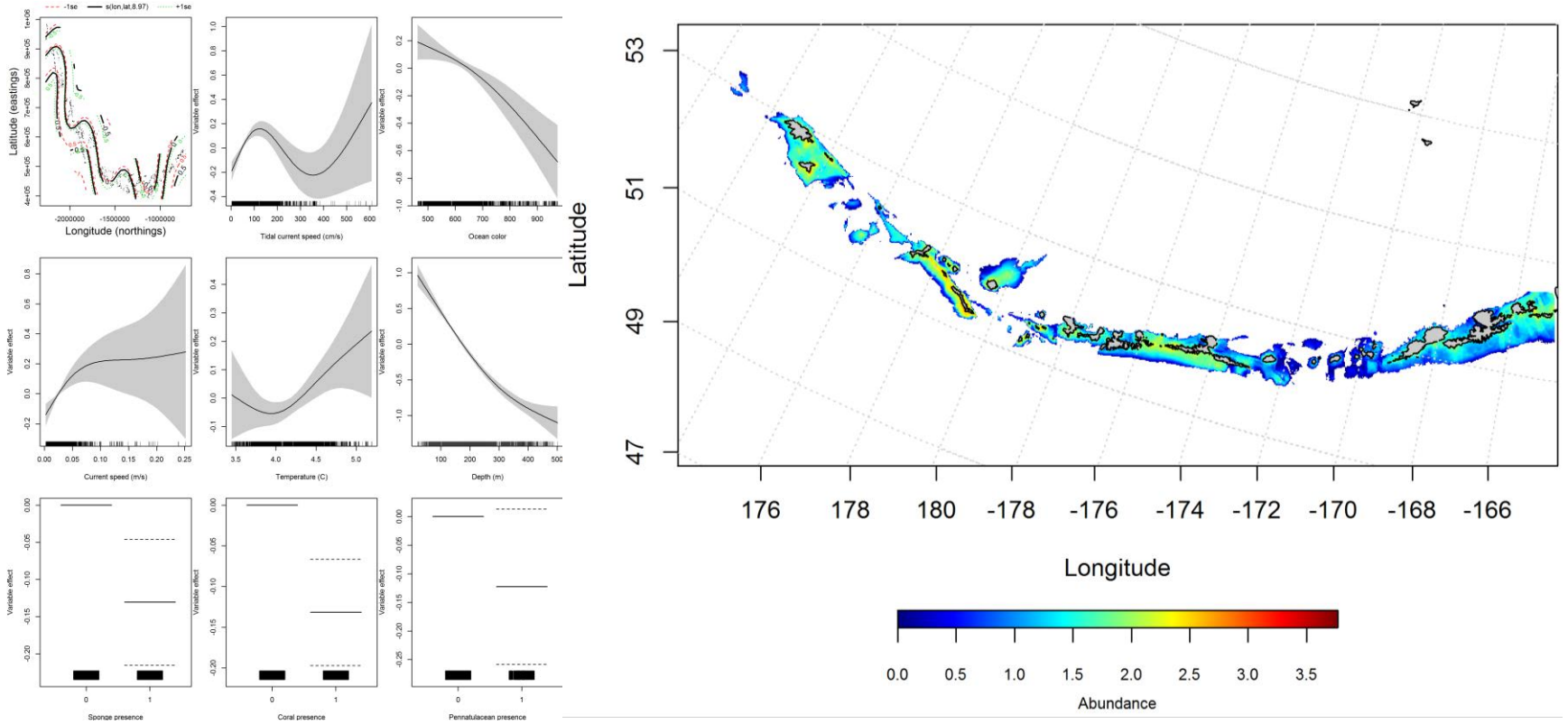

Figure 23. Best-fitting generalized additive model (GAM) effects of retained habitat variables on abundance of adult Northern rock sole from summer bottom trawl surveys of the Aleutian Islands (left panel) alongside GAM-predicted adult Northern rock sole abundance (right panel).

Aleutian Islands Northern rock sole Essential Fish Habitat Maps and Conclusions –

Spring and summer EFH for Northern rock sole larvae was distributed in the eastern AI around Unalaska Island (Figure 24).

Juvenile and adult Northern rock sole are widely distributed through the Aleutian Islands chain and co-occur in most places where they are found. Those collected in summertime bottom trawl surveys share similar predicted EFH distributions across the Aleutian Islands (Figure 25). These similarities can also be observed in areas of low abundance (e.g., large passes).

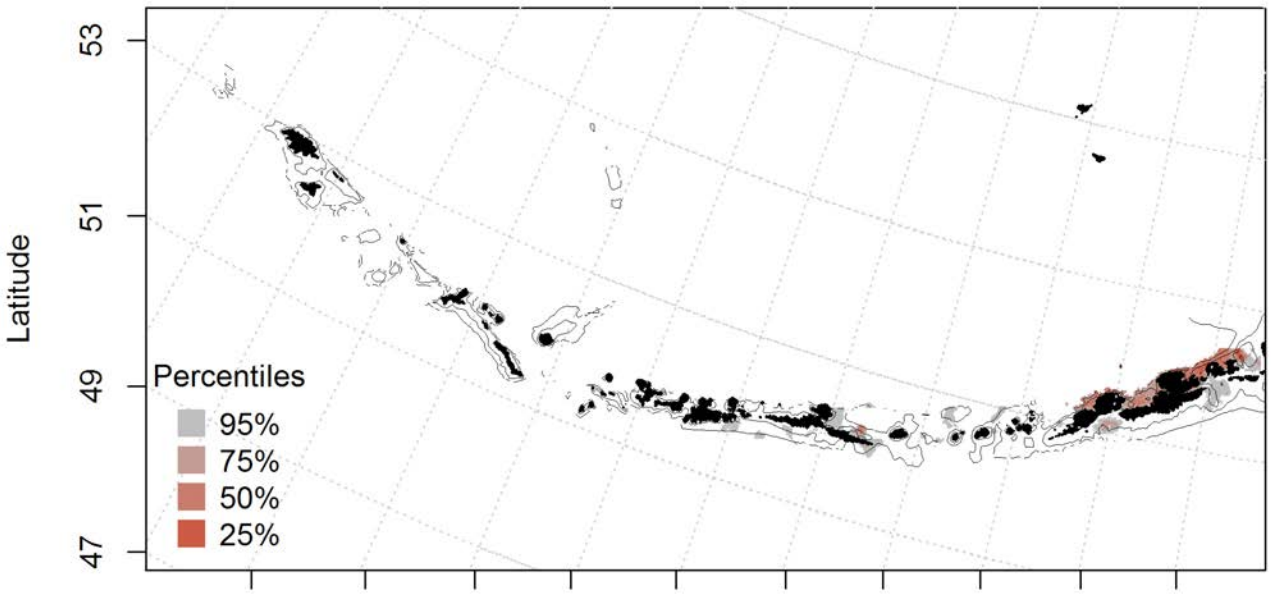

Figure 24. Spring essential fish habitat predicted for larval Northern rock sole (top and bottom panel).

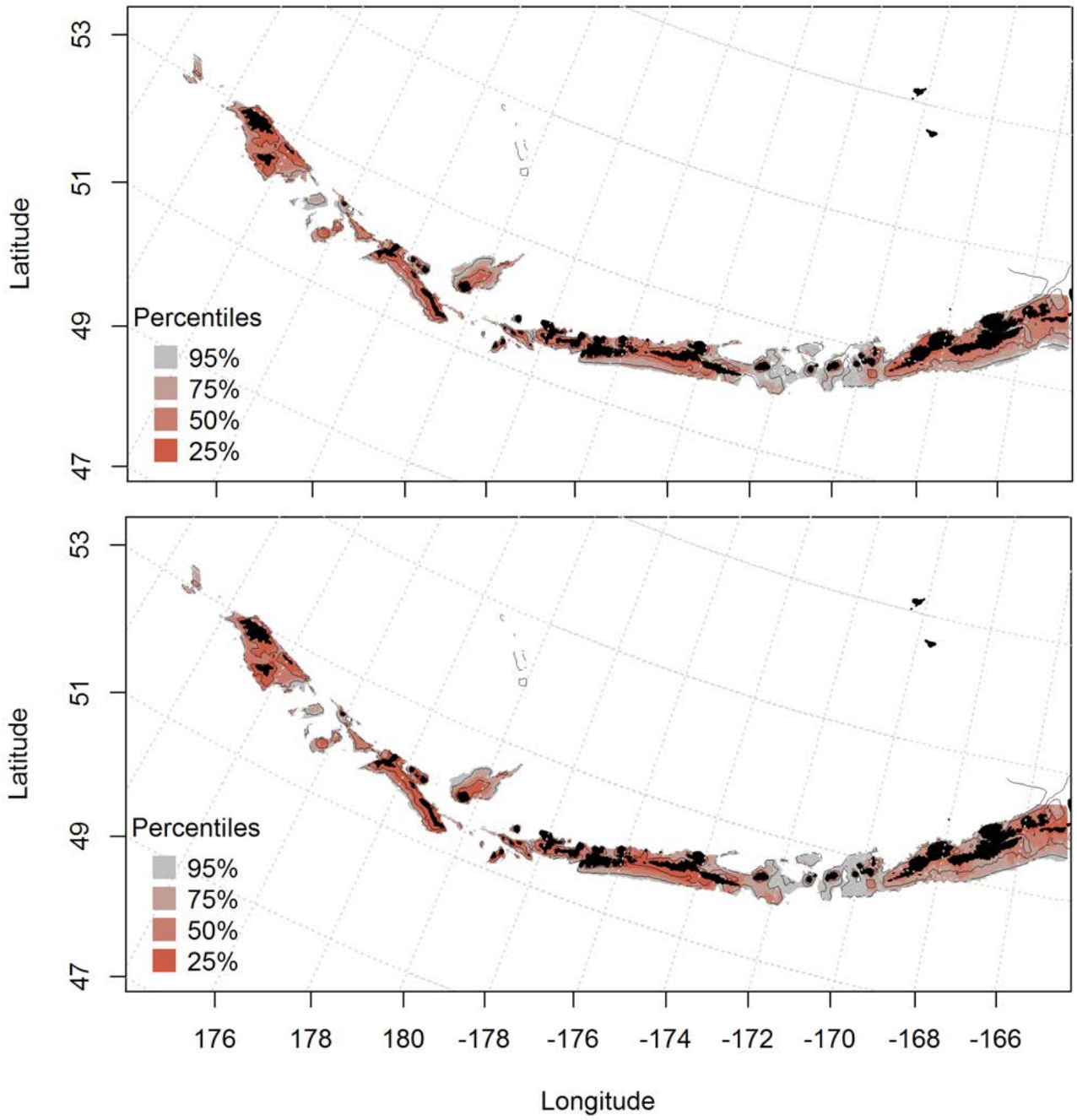

Figure 25. Predicted summer essential fish habitat for Northern rock sole juveniles and adults (top and bottom panel) from summertime bottom trawl surveys.

Southern rock sole (*Lepidopsetta bilineata*)

Seasonal distribution of early life history stages of Southern rock sole in the Aleutian Islands-- There were only 8 instances of Southern rock sole (SRS) larvae in the FOCI database (Figure 26), 5 in the spring and 3 in the summer. All observations were found in the eastern AI. No models were run for the spring or summer due to limited data.

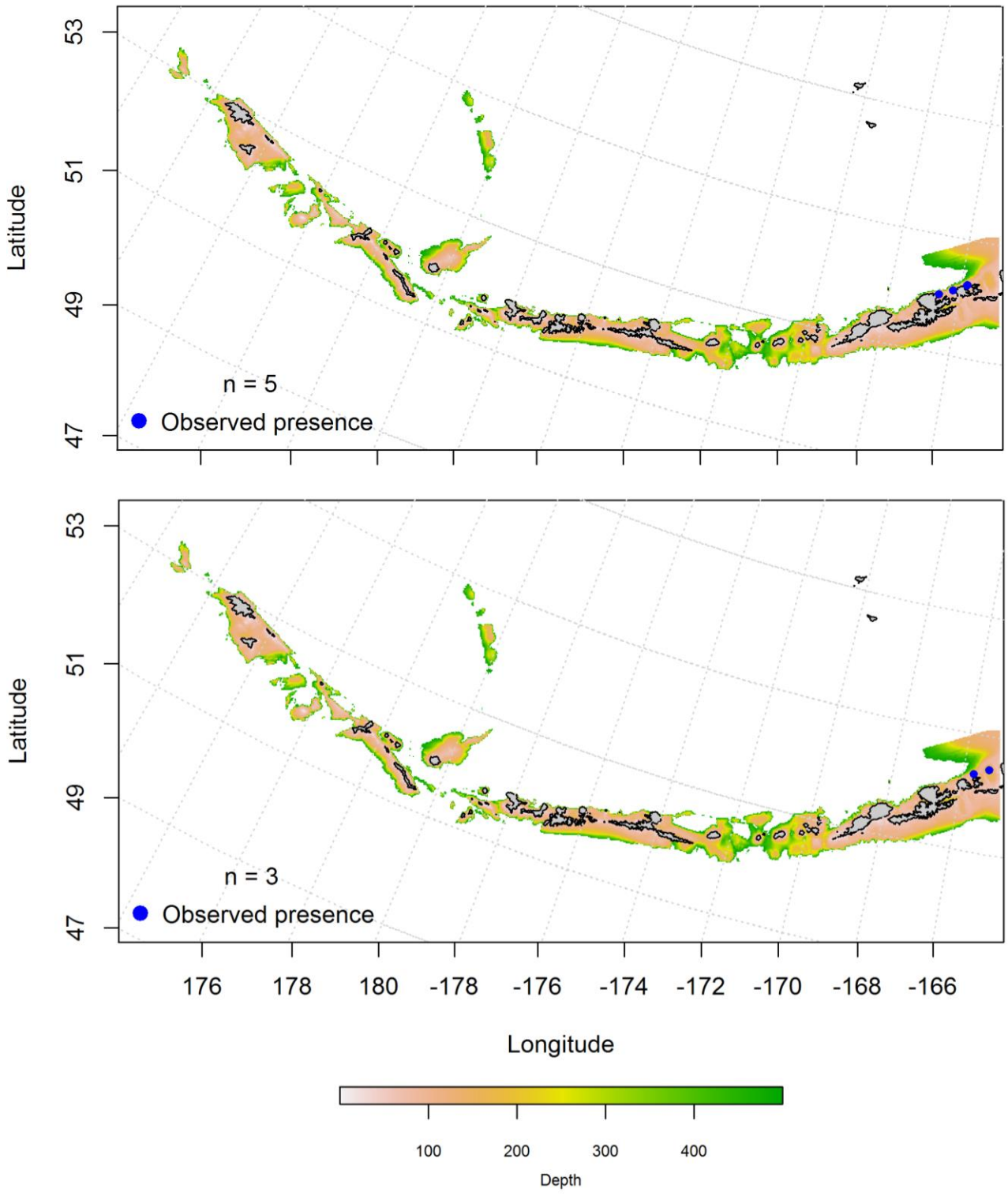

Figure 26. Spring and summer observations (top and bottom panel) of larval Southern rock sole from the Aleutian Islands.

Summertime distribution of juvenile and adult Southern rock sole from bottom trawl surveys of the Aleutian Islands – A two-step hurdle-generalized additive model was used to predict the presence and absence (PA GAM) of juvenile Southern rock sole. The model explained 98% of the variability in CPUE in the bottom trawl survey using training data and 94% of the variability using test data. Bottom depth and geographic location were the most important variables explaining the distribution of juvenile Southern rock sole. The model correctly classified 95% of the training data, 94% of the test data, and 66.9% of the deviance. The areas of predicted highest abundance were in the eastern Aleutian Islands (Figure 27).

The second step of the hurdle-GAM was used to predict the CPUE juvenile Southern rock sole. The model explained 41% of the variability in CPUE in the bottom trawl survey using training data, 39% of the variability using test data, and 40.7% of the deviance. Bottom depth was the most important variable explaining the distribution of juvenile Southern rock sole. The areas of predicted highest abundance were in the eastern Aleutian Islands (Figure 28).

A two-step hurdle-generalized additive model was used to predict the presence and absence (PA GAM) of adult Southern rock sole. The model explained 89% of the variability in CPUE in the bottom trawl survey using training data and 86% of the variability using test data. Bottom depth and geographic location were the most important variables explaining the distribution of adult Southern rock sole. The model correctly classified 80% of the training data, 79% of the test data, and 34.2% of the deviance. Predicted abundance was consistent throughout the Aleutian Islands (Figure 29Figure 27).

The second step of the hurdle-GAM was used to predict the CPUE adult Southern rock sole. The model explained 25% of the variability in CPUE in the bottom trawl survey using training data, 30% of the variability using test data, and 24.9% of the deviance. Geographic location and coral presence were the most important variables explaining the distribution of adult Southern rock sole. The areas of predicted abundance were concentrated in the western and central Aleutian Islands (Figure 30).

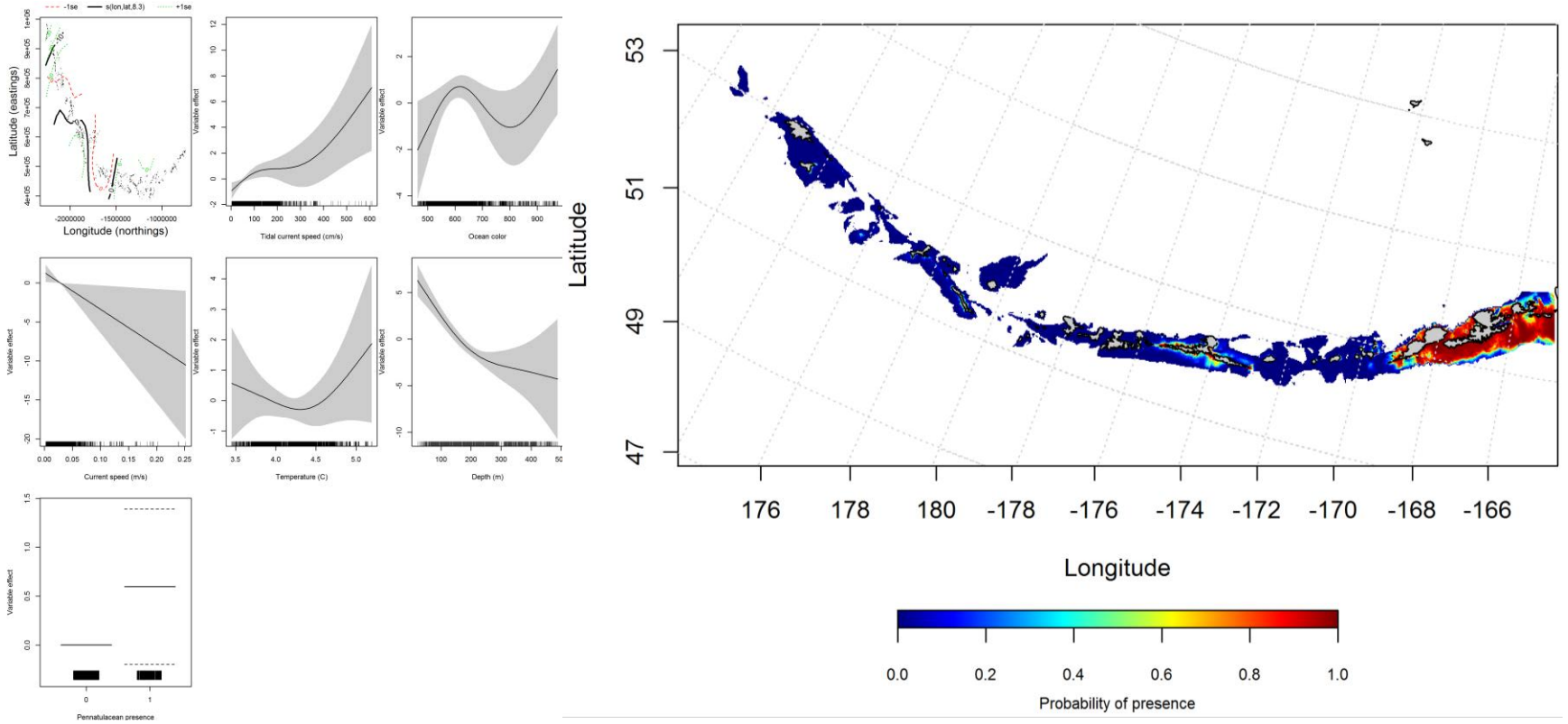

Figure 27. Best-fitting hurdle model effects of retained habitat variables on presence absence (PA) of juvenile Southern rock sole from summer bottom trawl surveys of the Aleutian Islands (left panel) alongside hurdle-predicted juvenile Southern rock sole PA (right panel).

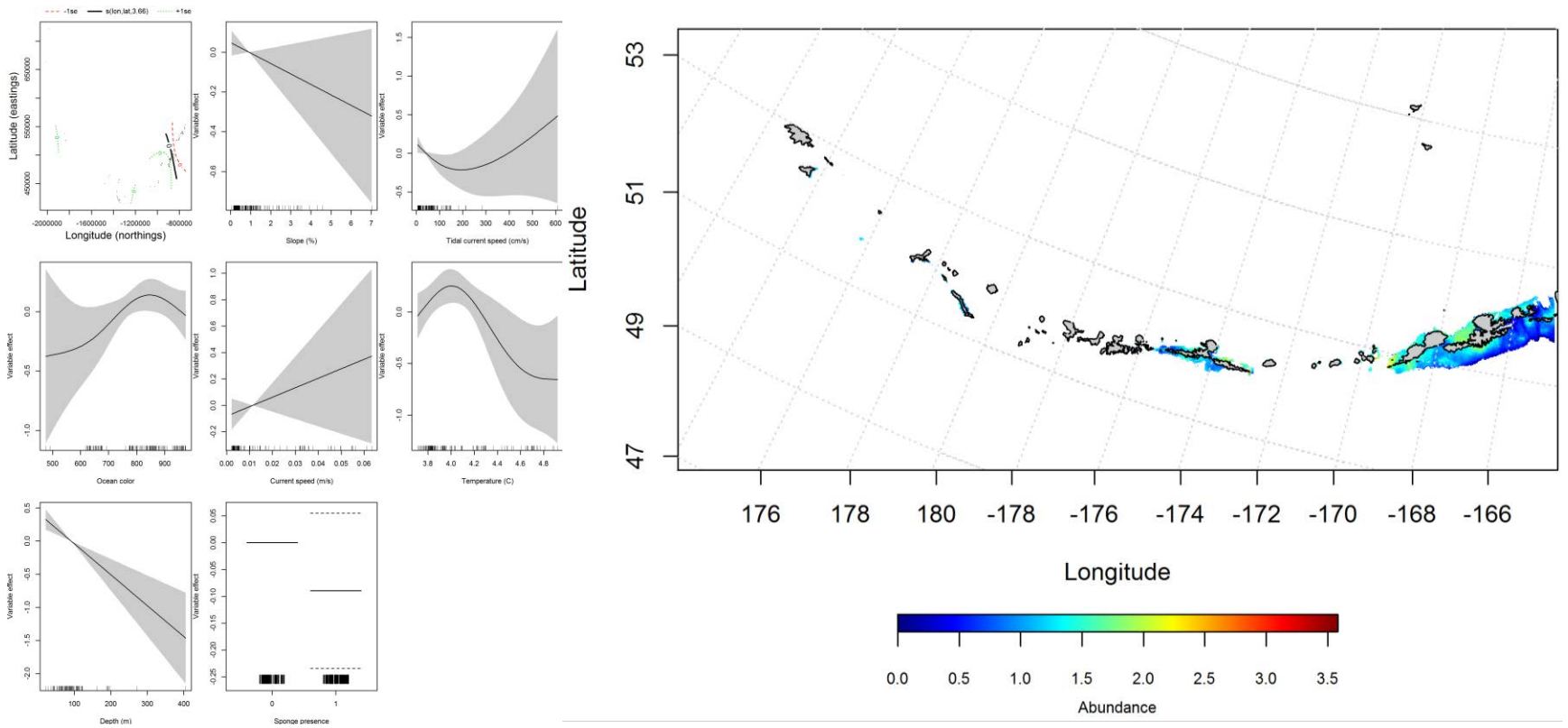

Figure 28. Best-fitting hurdle model effects of retained habitat variables on cpue of juvenile Southern rock sole from summer bottom trawl surveys of the Aleutian Islands (left panel) alongside hurdle-predicted juvenile Southern rock sole cpue (right panel)..

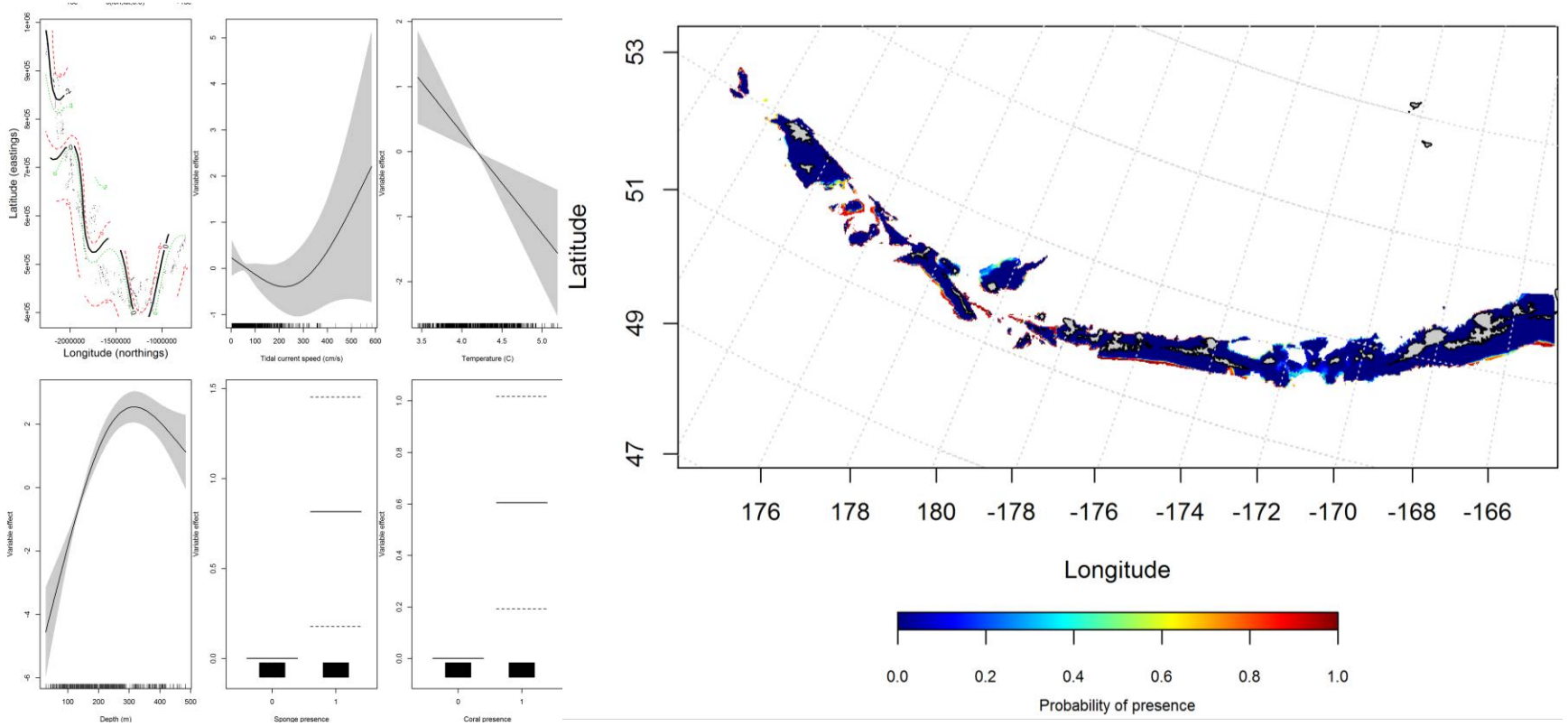

Figure 29. Best-fitting hurdle model effects of retained habitat variables on presence absence (PA) of adult Southern rock sole from summer bottom trawl surveys of the Aleutian Islands (left panel) alongside hurdle-predicted adult Southern rock sole PA (right panel).

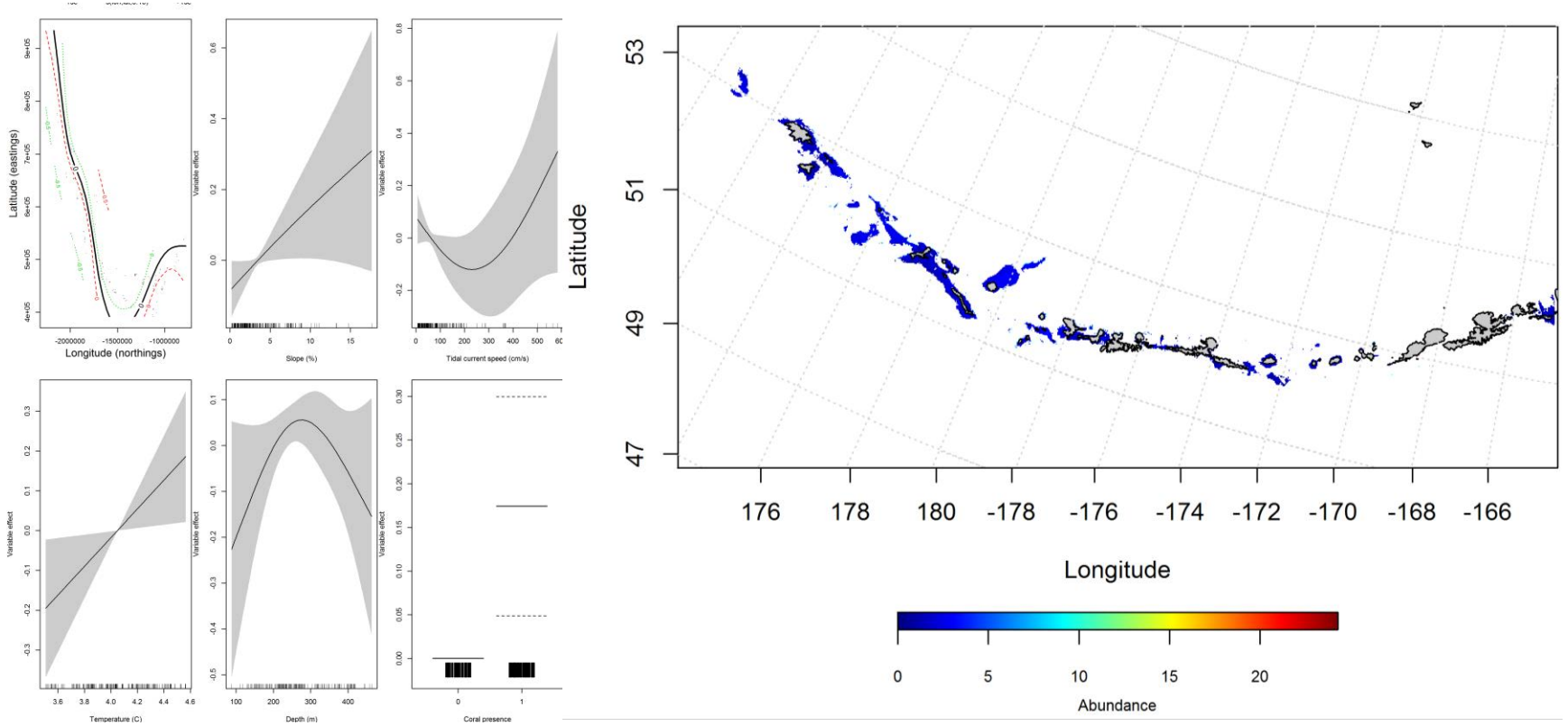

Figure 30. Best-fitting hurdle model effects of retained habitat variables on cpue of adult Southern rock sole from summer bottom trawl surveys of the Aleutian Islands (left panel) alongside hurdle-predicted adult Southern rock sole cpue (right panel).

Aleutian Islands Southern rock sole Essential Fish Habitat Maps and Conclusions

Larval Southern rock sole essential fish habitat predicted by the model during the summer is concentrated in the eastern AI north of Unalaska Island (Figure 31).

Summertime EFH of Southern rock sole varied by life stage (Figure 32). Juveniles were more concentrated in the eastern AI around Nikolski and Unalaska Islands, whereas the adults were distributed in the western AI, north of Semisopochnoi Island and in the large passes.

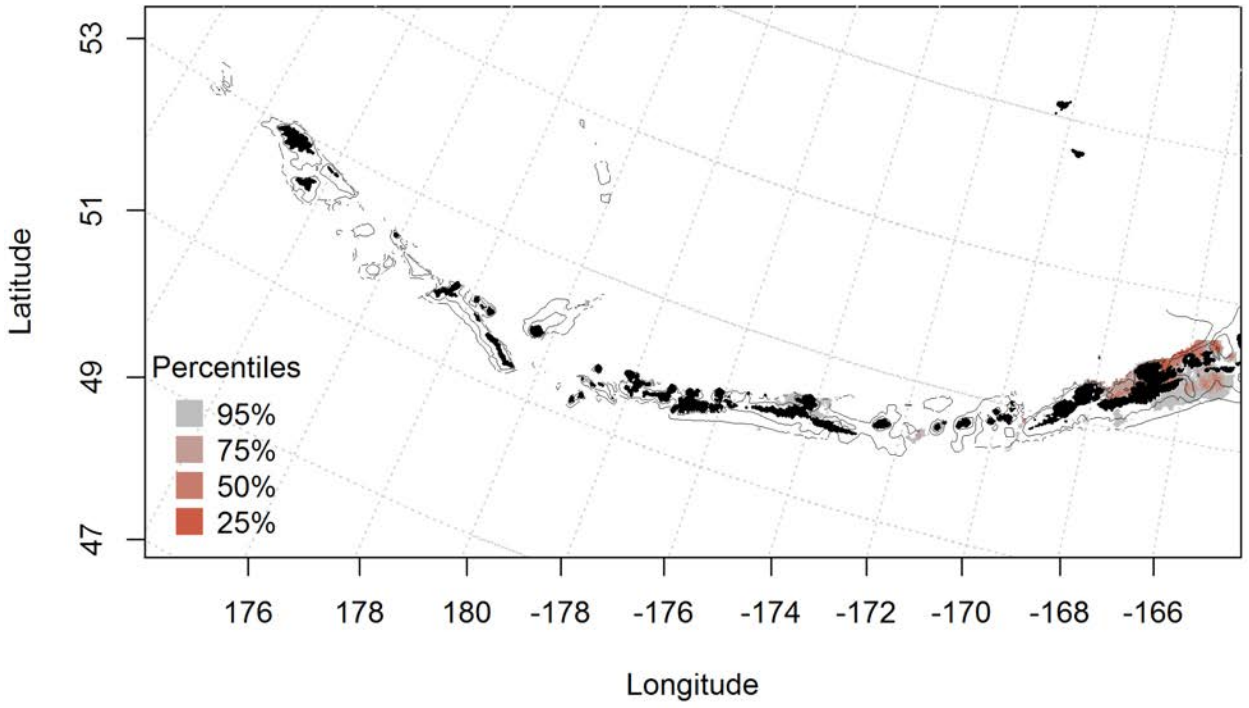

Figure 31. Summer essential fish habitat predicted for larval Southern rock sole.

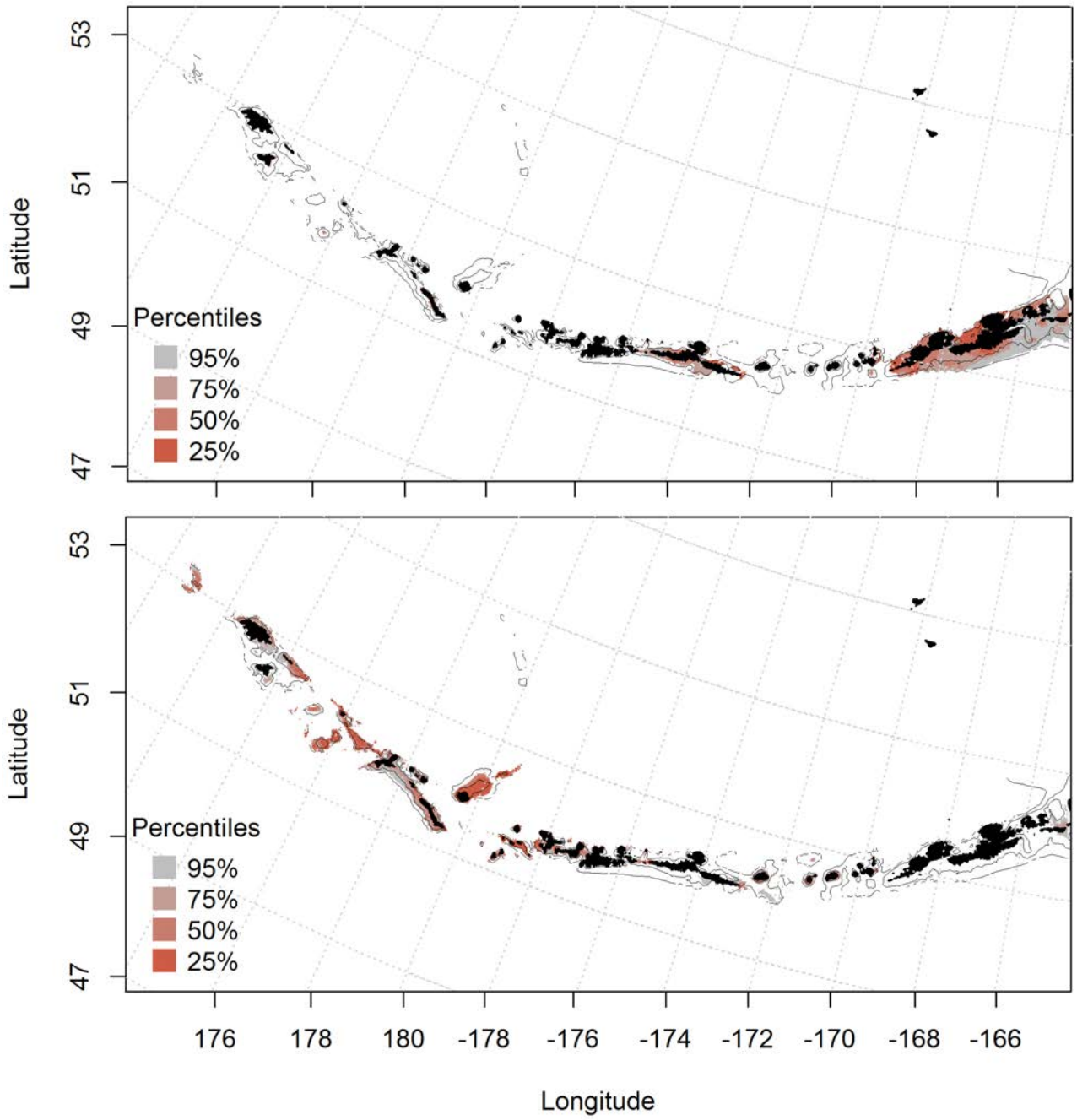

Figure 32. Predicted summer essential fish habitat for Southern rock sole juveniles and adults (top and bottom panel) from summertime bottom trawl surveys.

Greenland turbot (*Reinhardtius hippoglossoides*)

Seasonal distribution of early life history stages of Greenland turbot in the Aleutian Islands –There were only 3 instances of Greenland turbot eggs observed in the FOCI database (Figure 33), 2 in the winter and 1 in the spring. All observations, except one were found in eastern Aleutian Islands. There were not enough observations to run the model.

There were 9 instances of Greenland turbot larvae in the spring (Figure 34). The distribution of larvae was limited to the eastern Aleutian Islands, and there were not enough cases for modeling.

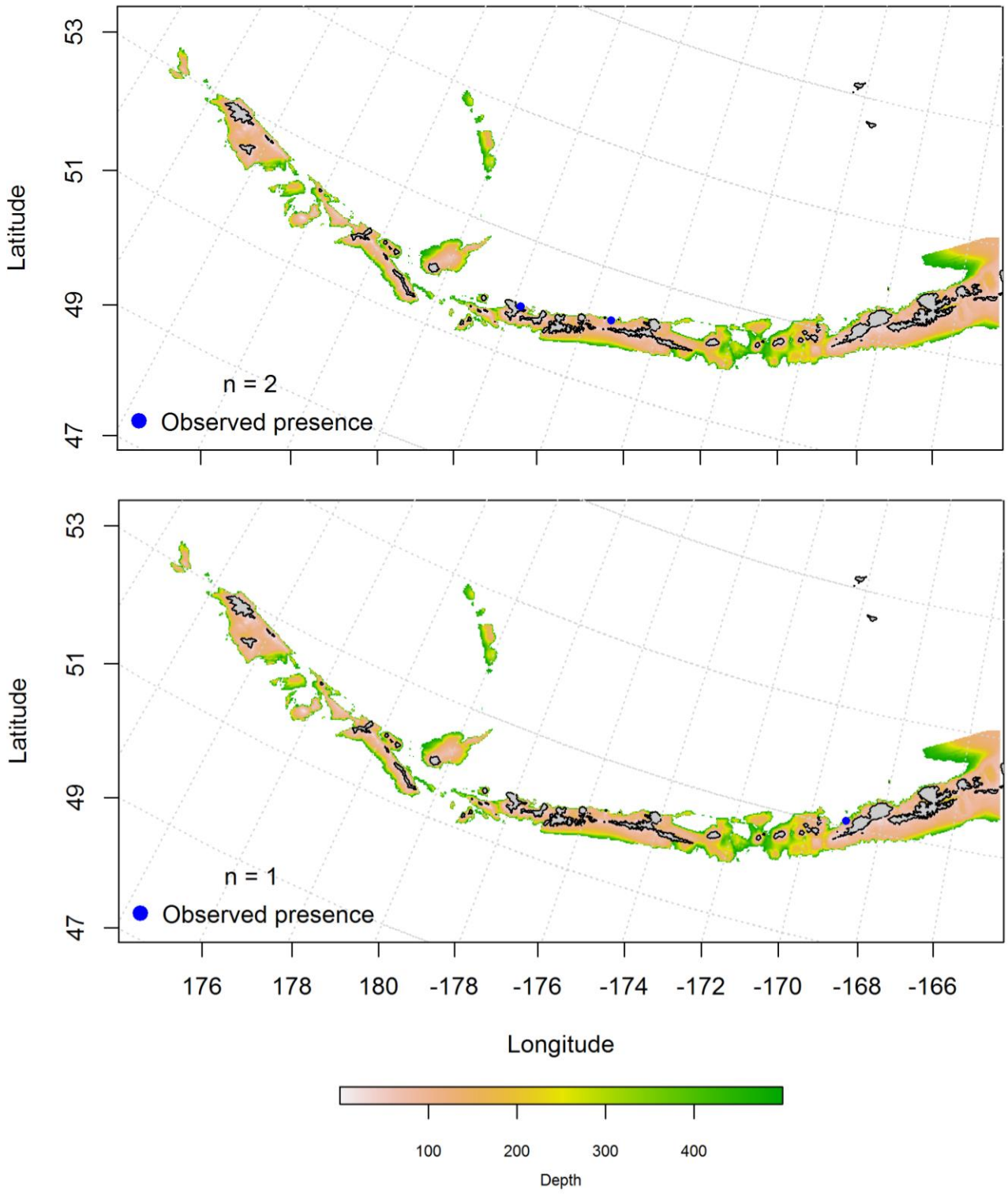

Figure 33. -- Winter and spring observations (top and bottom panel) of Greenland turbot eggs from the Aleutian Islands.

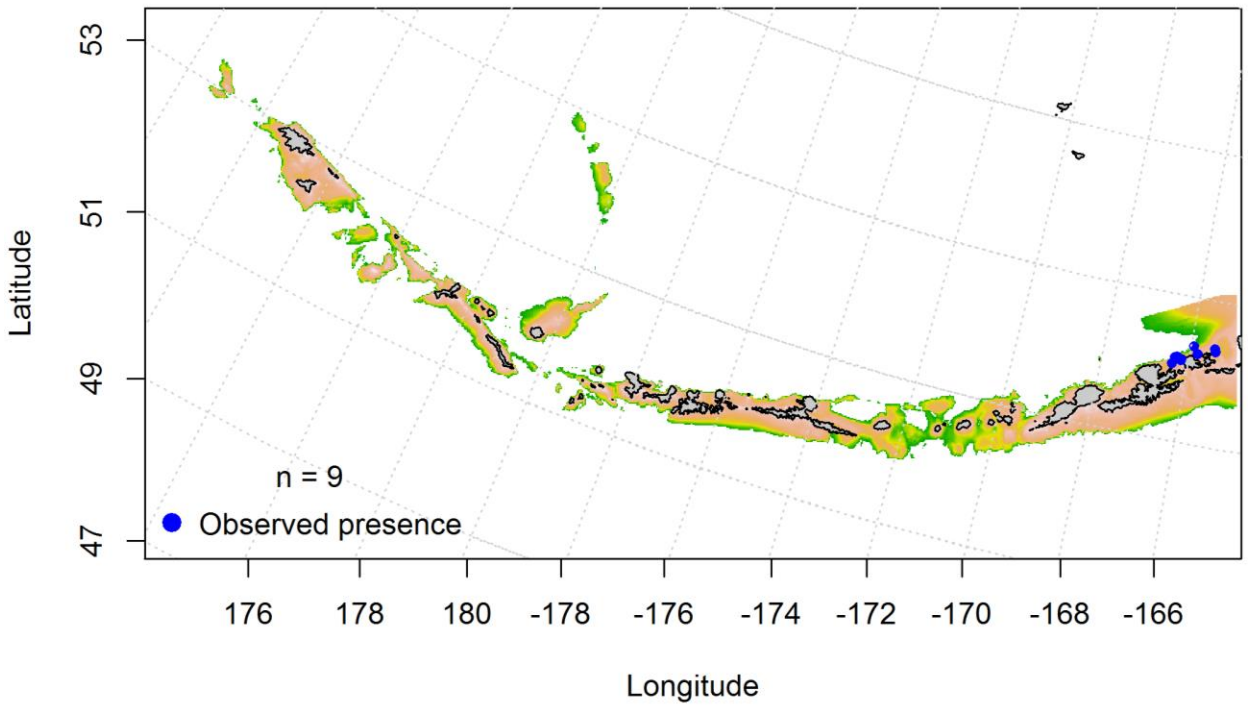

Figure 34. -- Spring observations of larval Greenland turbot from the Aleutian Islands.

Summertime distribution of juvenile and adult Greenland turbot from bottom trawl surveys of the Aleutian Islands -- A maximum entropy model predicting the probable habitat of juvenile Greenland turbot explained 98% of the variability in CPUE in the bottom trawl survey. Bottom depth and temperature were the most important variables explaining the distribution of juvenile Greenland turbot (relative importance: 56.4% and 31.9%). The model fit the data set well, explaining 94% of the variability. 93% of the training data and 94% of the test data were correctly classified. The model predicted probable suitable habitat of juvenile Greenland turbot across the AI (Figure 35).

Adult Greenland turbot were distributed similarly to the juveniles. The hurdle-GAM predicted presence absence of adult Greenland turbot throughout the AI, although there were higher concentrations around Semisopochnoi Island, and in the far eastern AI (Figure 36). In this model,

the most important variables explaining the distribution were bottom depth, geographic location, and tidal current. The model fit 95% of the training and test data sets, explained 53.3% of the deviance, and correctly classified 89% of the training data and 89% of the test data.

The best-fitting hurdle-GAM model indicated that tidal current was the most important factor controlling adult Greenland turbot CPUE. The model explained 34% of the variability in bottom trawl CPUE using the training set data, 15% of the variability using the test data set, and 33.9% of the deviance. Greenland turbot had a tighter range, although still distributed throughout the AI chain (Figure 37).

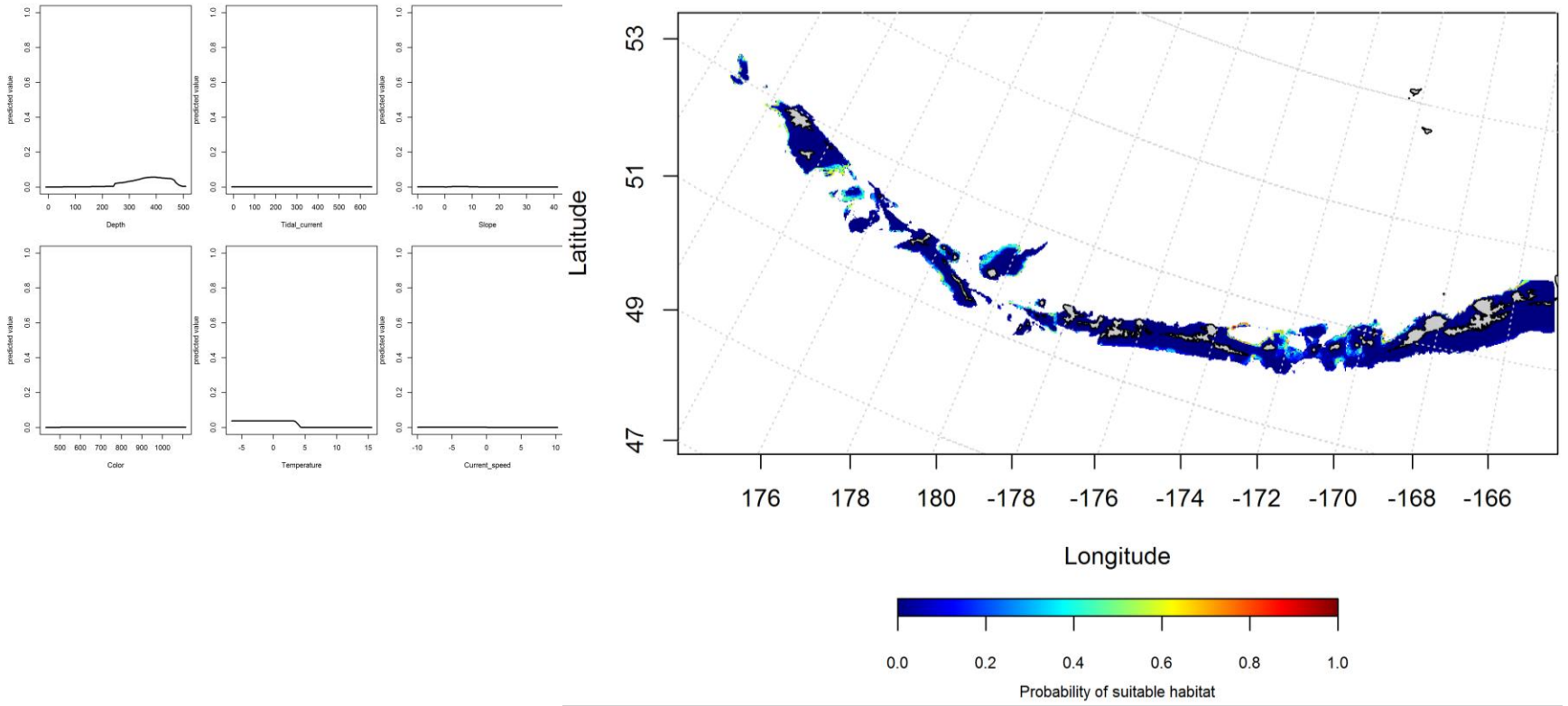

Figure 35. -- Best-fitting maximum entropy model effects of retained habitat variables on abundance of juvenile Greenland turbot from summer bottom trawl surveys of the Aleutian Islands (left panel) alongside maxent-predicted juvenile Greenland turbot probable suitable habitat (right panel).

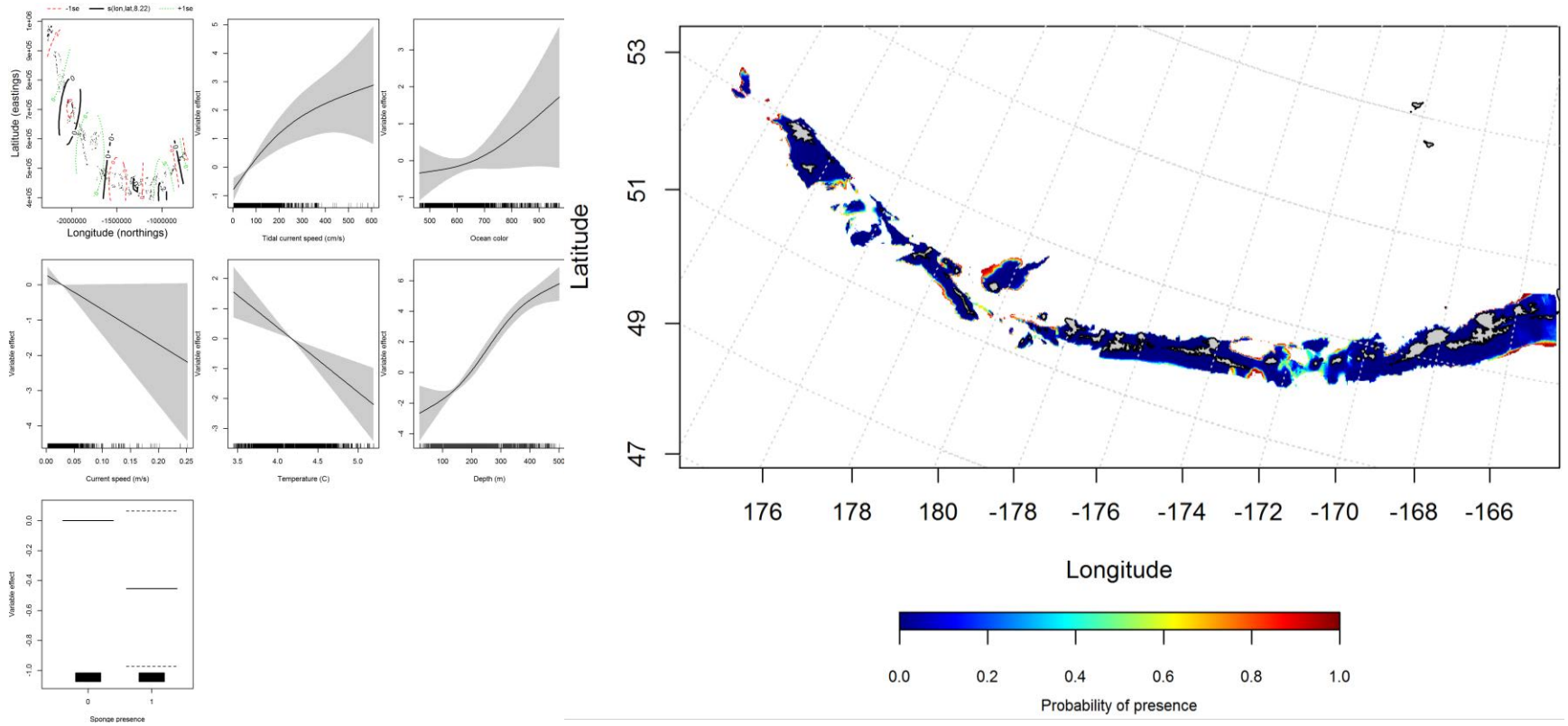

Figure 36. -- Best-fitting hurdle model effects of retained habitat variables on presence absence (PA)of adult Greenland turbot from summer bottom trawl surveys of the Aleutian Islands (left panel) alongside hurdle-predicted juvenile Greenland turbot PA (right panel).

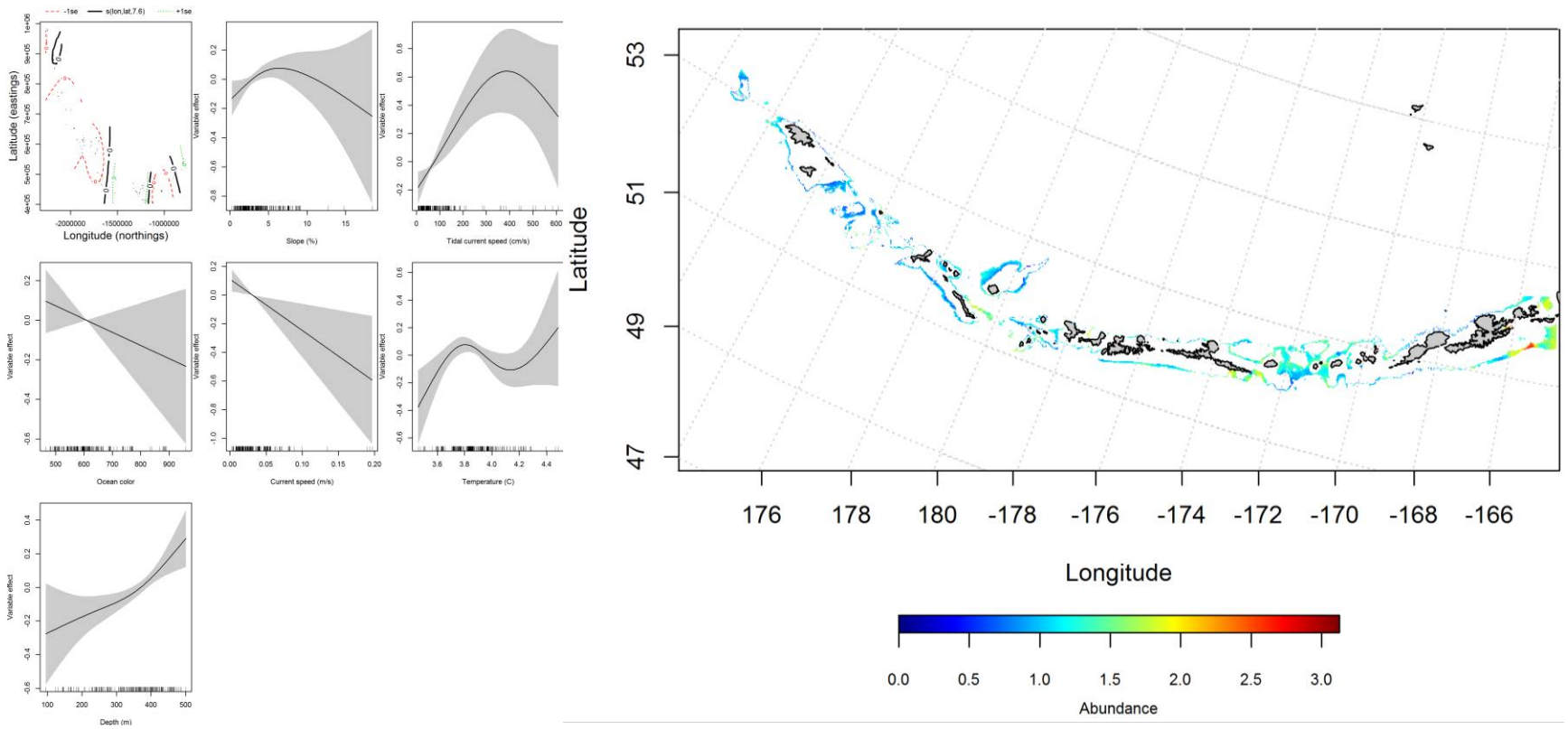

Figure 37. -- Best-fitting hurdle model effects of retained habitat variables on cpue of adult Greenland turbot from summer bottom trawl surveys of Aleutian Islands (left panel) alongside hurdle-predicted adult Greenland turbot cpue (right panel).

Seasonal distribution of commercial fisheries catches of adult Greenland turbot in the Aleutian Islands -- Distribution of adult Greenland turbot in the Aleutian Islands in commercial fisheries catches was generally consistent throughout all seasons. In the fall, bottom temperature, ocean color and bottom depth were the most important variables determining probable suitable habitat of Greenland turbot (relative importance: 27.3%, 26.3%, and 23.2%, respectively). The AUC of the fall maxent model was 95% for the training data and 82% for the test data and 88% of the cases in the training data and 82% of the test data sets were predicted correctly. The model predicted probable suitable habitat of adult Greenland turbot catches were spread throughout the AI (Figure 38).

In the winter, ocean color, bottom depth, and bottom temperature were the most important variables determining probable suitable habitat of Greenland turbot (relative importance: 44.1%, 21.3%, and 17.5%, respectively). The AUC of the winter maxent model was 97% for the training data and 83% for the test data and 92% of the cases in the training data and 83% of the test data sets were predicted correctly. As with the fall, the model predicted probable suitable habitat of adult Greenland turbot catches were spread throughout the AI (Figure 39).

In the spring, bottom depth, slope and ocean color were the most important variables determining probable suitable habitat of Greenland turbot (relative importance: 50.1%, 16.9%, and 15.5%, respectively). The AUC of the spring maxent model was 94% for the training data and 86% for the test data. 86% of the cases in the training and test data sets were predicted correctly. As with the fall and winter, the model predicted probable suitable habitat of Greenland turbot catches were distributed spread throughout the AI (Figure 40).

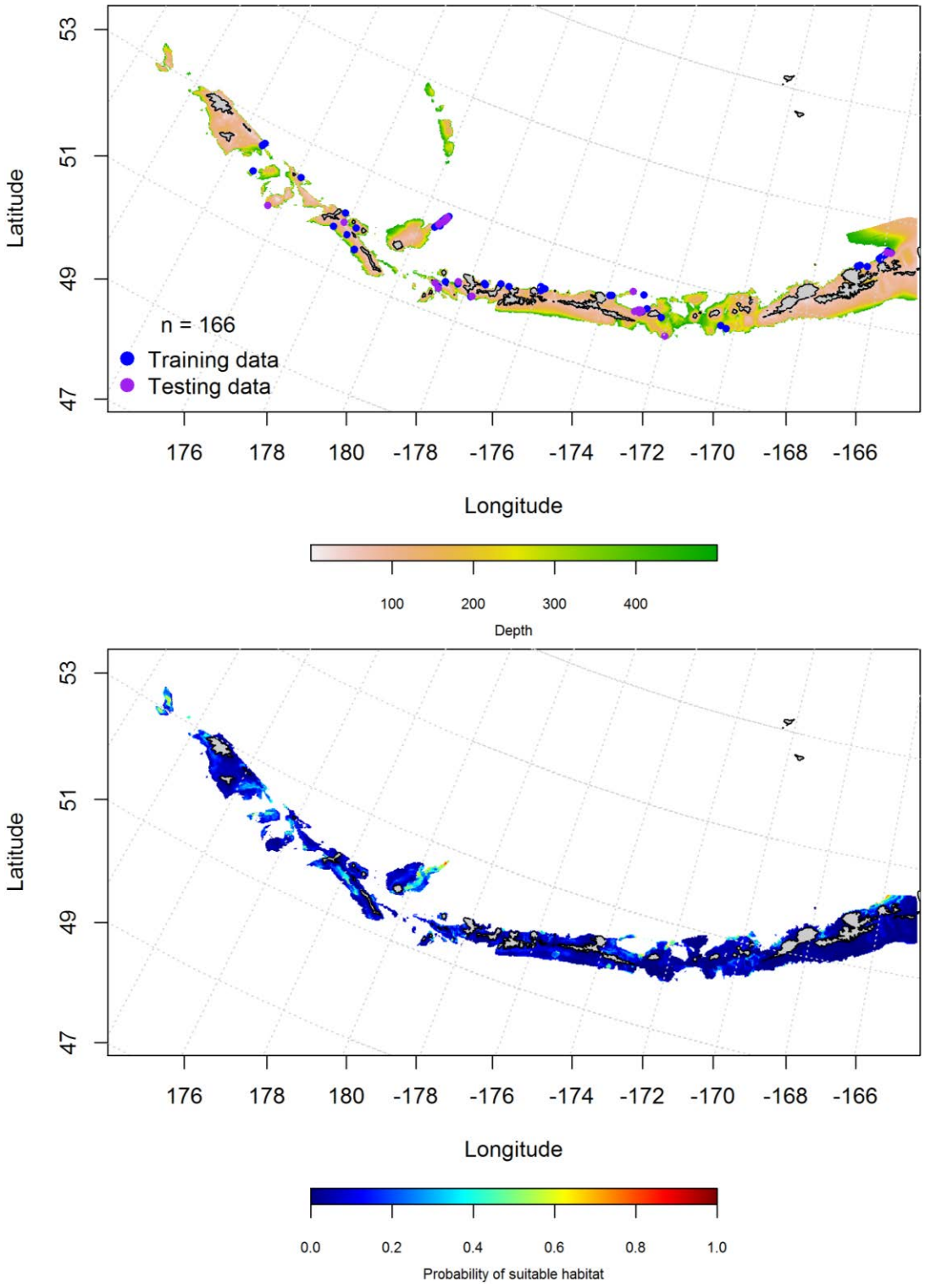

Figure 38. -- Locations of fall (September-November) commercial fisheries catches of Greenland turbot (top panel). Blue points were used to train the maximum entropy model predicting the probability of suitable fall habitat supporting commercial catches of Greenland turbot (bottom panel) and the purple points were used to validate the model.

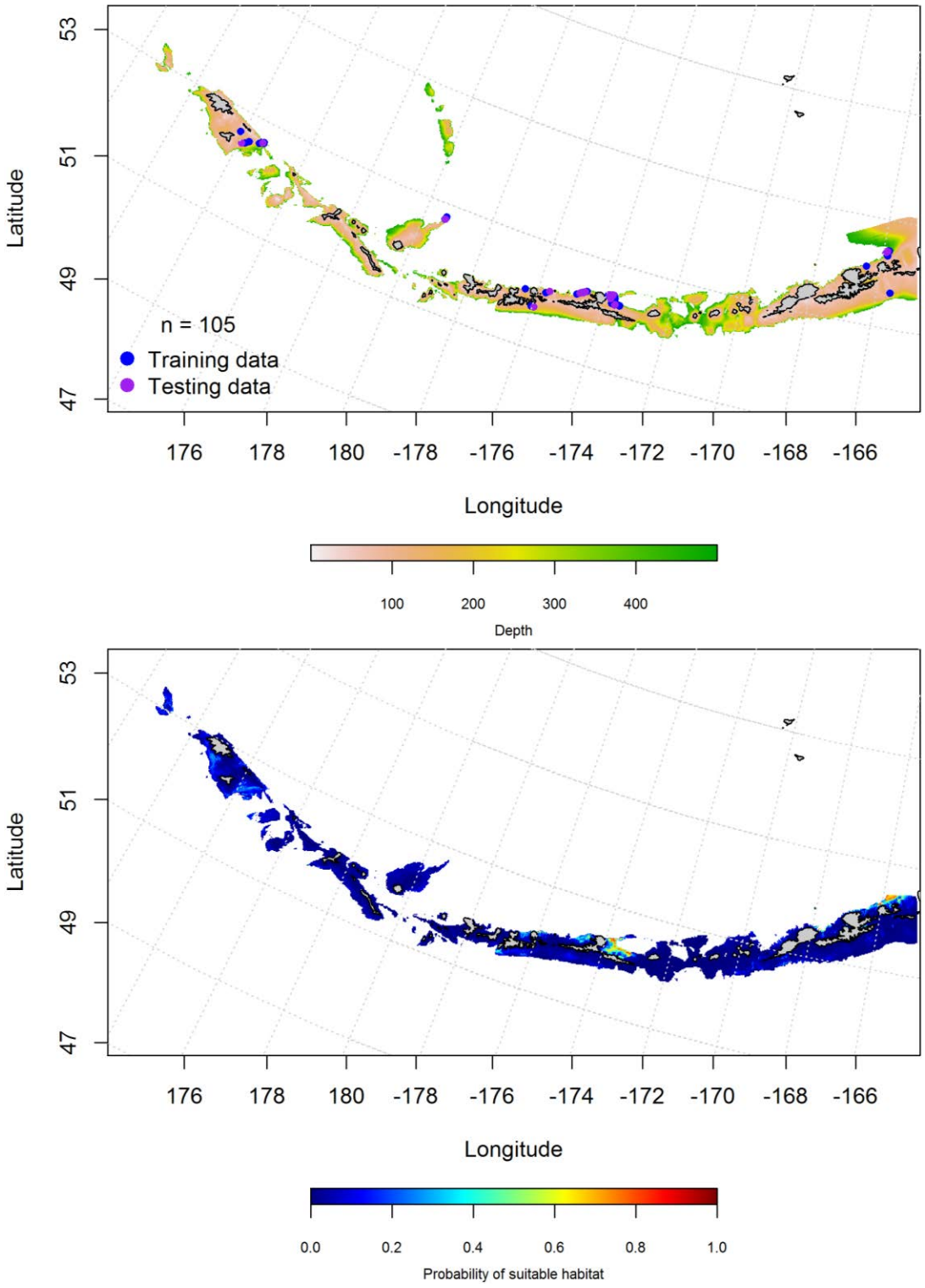

Figure 39. -- Locations of winter (December-February) commercial fisheries catches of Greenland turbot (top panel). Blue points were used to train the maximum entropy model predicting the probability of suitable winter habitat supporting commercial catches of Greenland turbot (bottom panel) and the purple points were used to validate the model.

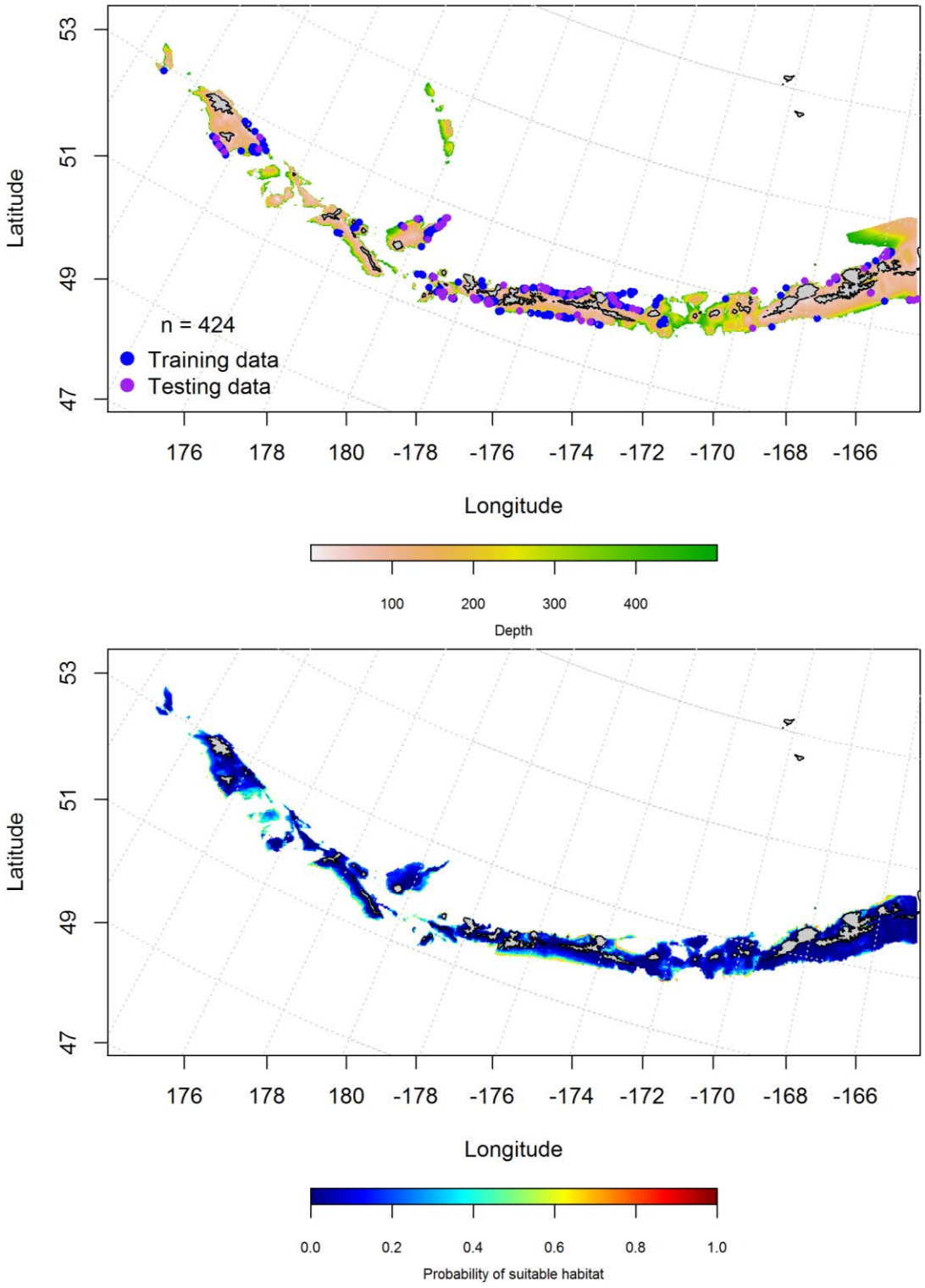

Figure 40. -- Locations of spring (March-May) commercial fisheries catches of Greenland turbot (top panel). Blue points were used to train the maximum entropy model predicting the probability of suitable spring habitat supporting commercial catches of Greenland turbot (bottom panel) and the purple points were used to validate the model.

Aleutian Islands Greenland turbot Essential Fish Habitat Maps and Conclusions --

In general, juvenile and adult Greenland turbot are distributed through the Aleutian Islands chain and co-occur in most places where they are found. Adults were slightly more concentrated in the eastern AI. Those collected in summertime bottom trawl surveys share similar predicted EFH distributions across the Aleutian Islands (Figure 41).

Similar to summertime bottom trawl survey data observations, the EFH predicted from commercial catches of Greenland turbot is distributed throughout the Aleutian Islands chain (Figure 42). There does not appear to be much seasonal variability to the EFH distribution. Commercial Greenland turbot catches coincide with the same EFH distribution pattern observed from summertime bottom trawl surveys.

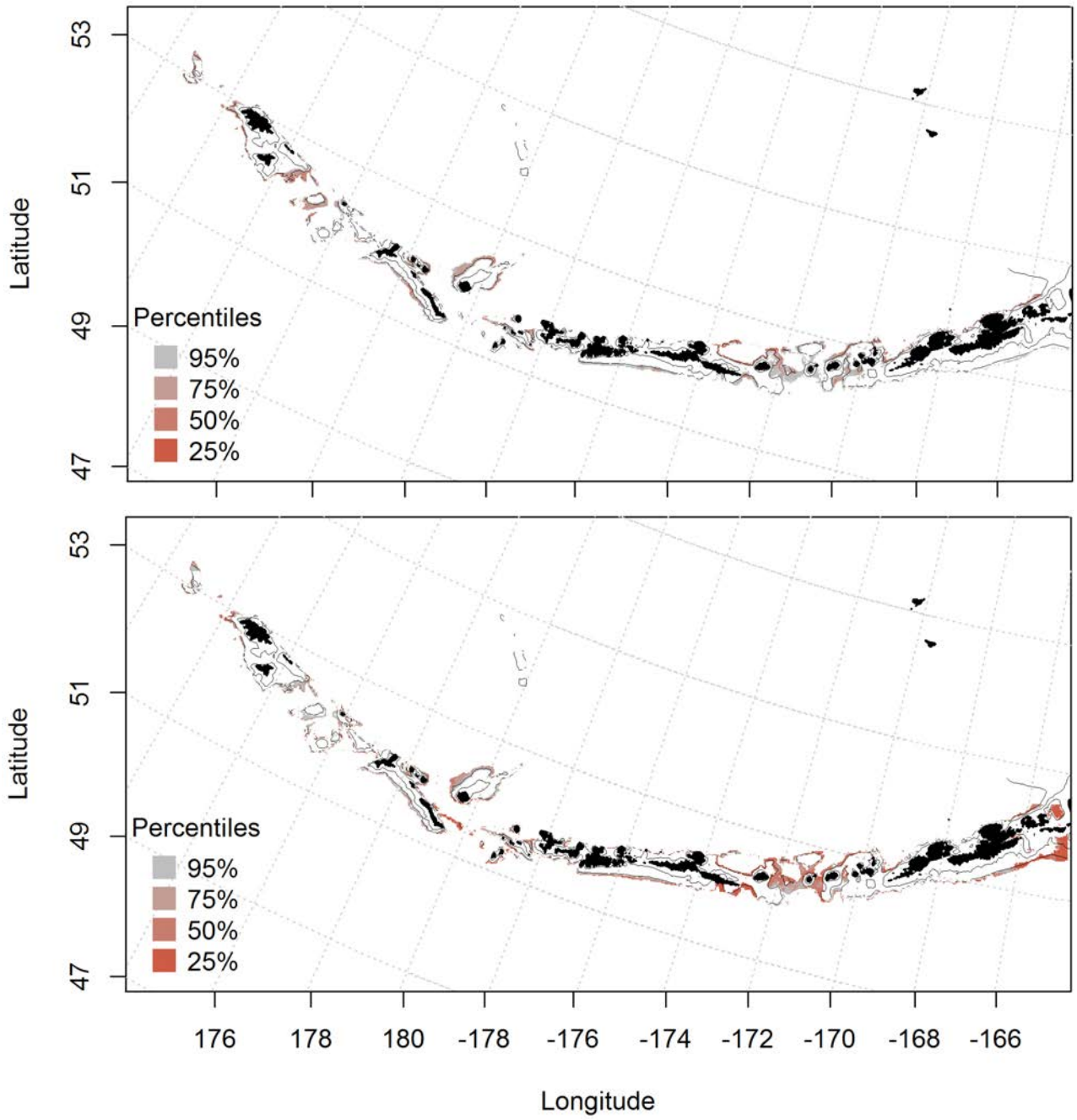

Figure 41. -- Predicted summer essential fish habitat for Greenland turbot juveniles and adults (top and bottom panel) from summertime bottom trawl surveys.

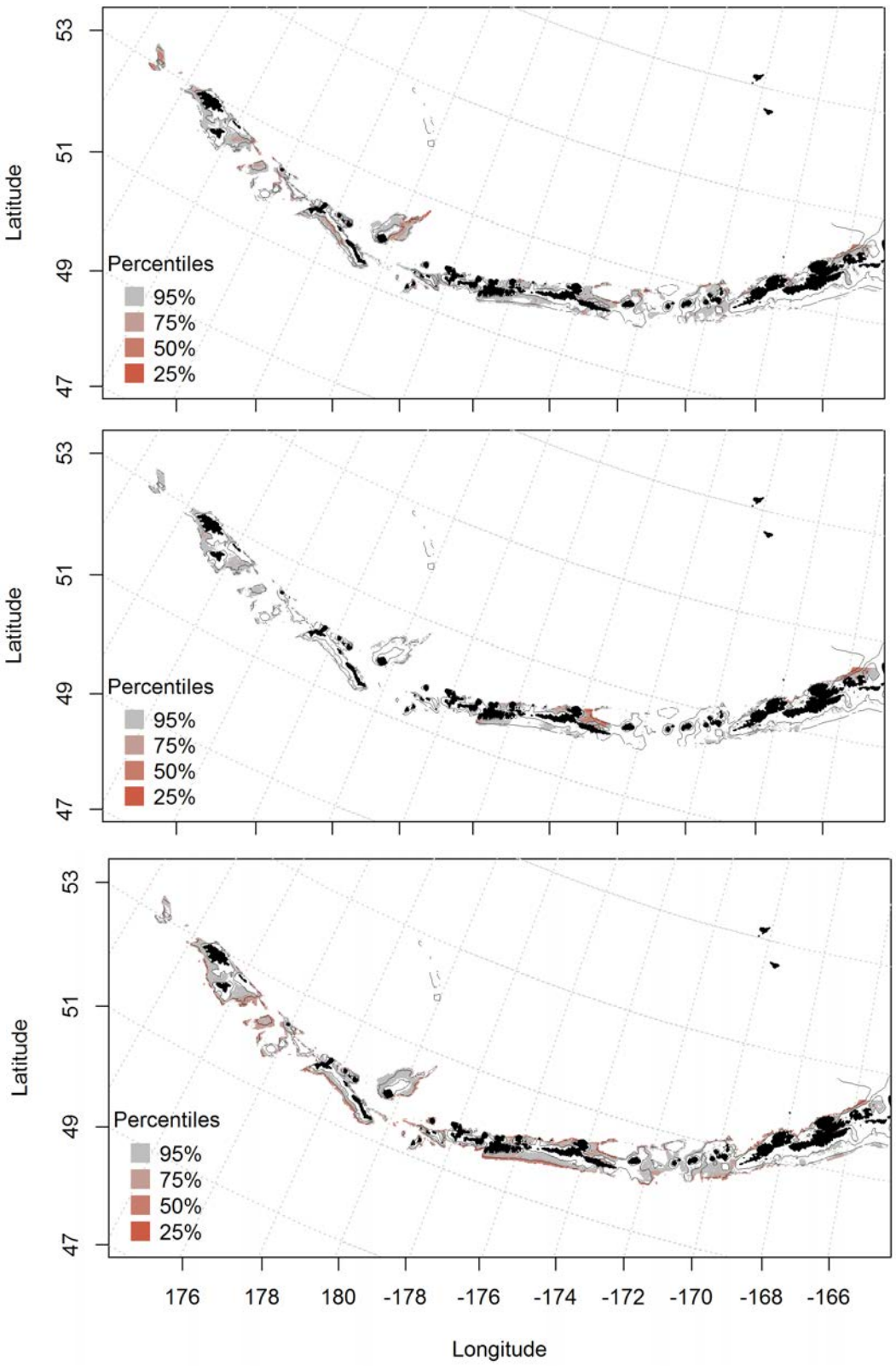

Figure 42. -- Essential fish habitat predicted for Greenland turbot during fall (top panel), winter (middle panel) and spring (bottom panel) from summertime commercial catches.

Flathead sole (*Hippoglossoides elassodon*)

Seasonal distribution of early life history stages of Flathead sole in the Aleutian Islands –

There were only 56 instances of Flathead sole eggs observed in the FOCI database (Figure 43), 55 in the spring and 1 in the summer. All observations, were found in the eastern AI. There were not enough summertime observations to run the summer model. The model predicted abundance of spring Flathead sole eggs throughout the AI, and highest in the eastern AI (Figure 44). The most important variables in modeling spring egg distribution were ocean surface color, current variability and surface temperature (relative importance: 40.2%, 25.4%, and 19.8%, respectively). For the spring model, the AUC was 100% for the training data and 95% for the test data. 98% of the training data and 95% of the test data was correctly classified, indicating a great model fit.

There were 11 observances of Flathead sole larvae in the spring and 5 in the summer months. All observations were found in the eastern AI (and there were not enough cases for modeling spring or summer data) (Figure 45).

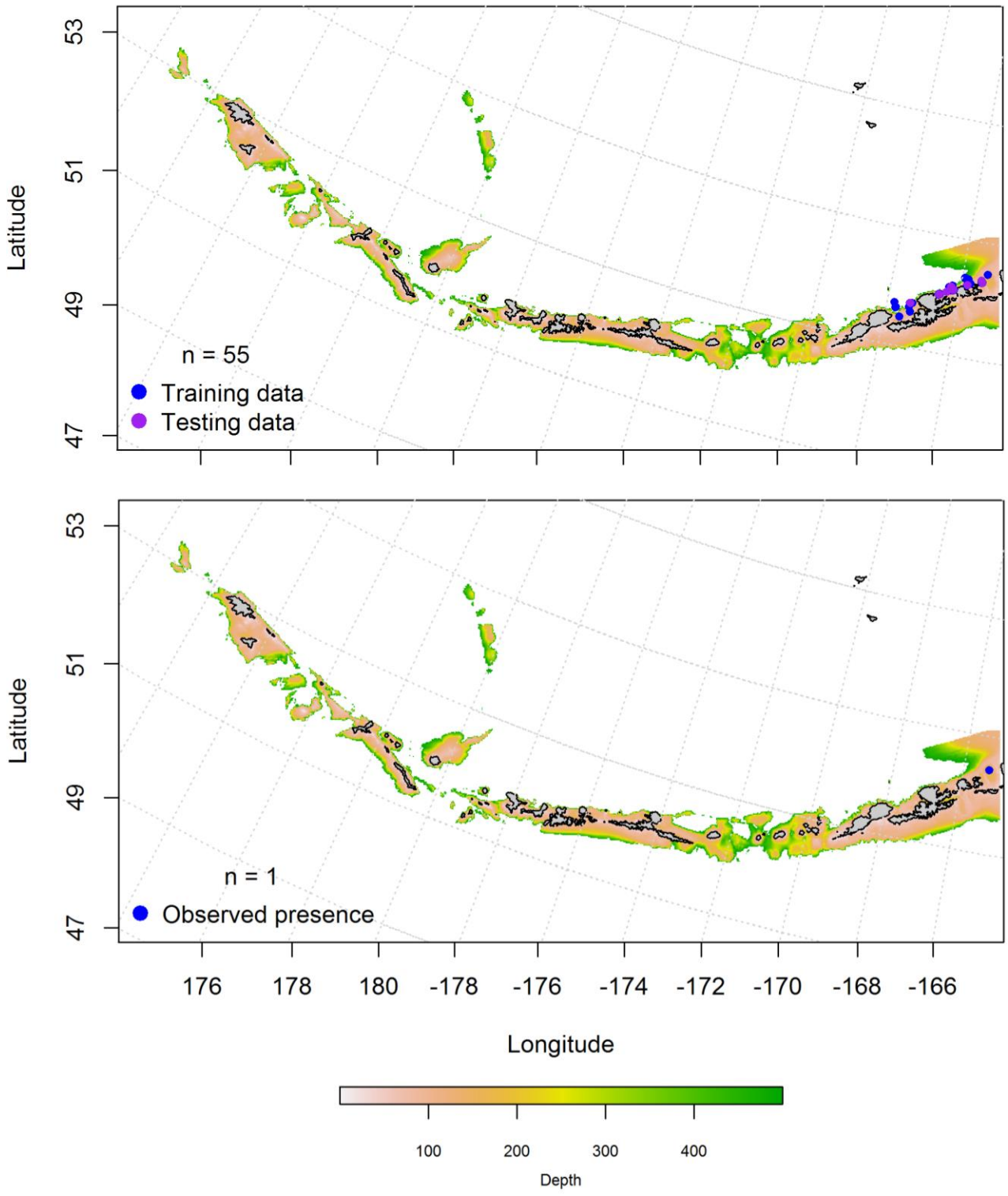

Figure 43. -- Spring and summer observations (top and bottom panel) of Flathead sole eggs from the Aleutian Islands.

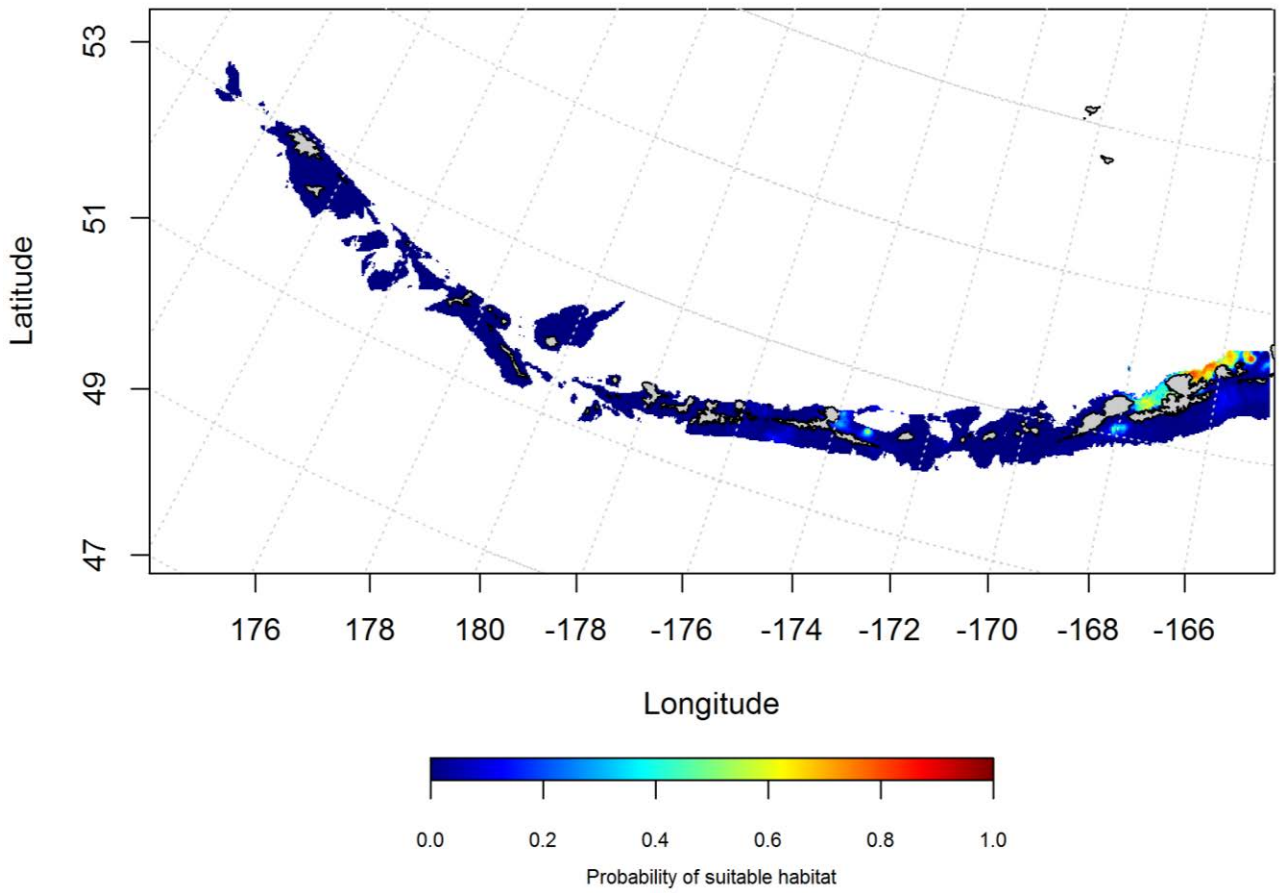

Figure 44. -- Predicted probability of spring distribution of Flathead sole eggs *from maximum entropy modeling of the Aleutian Islands.*

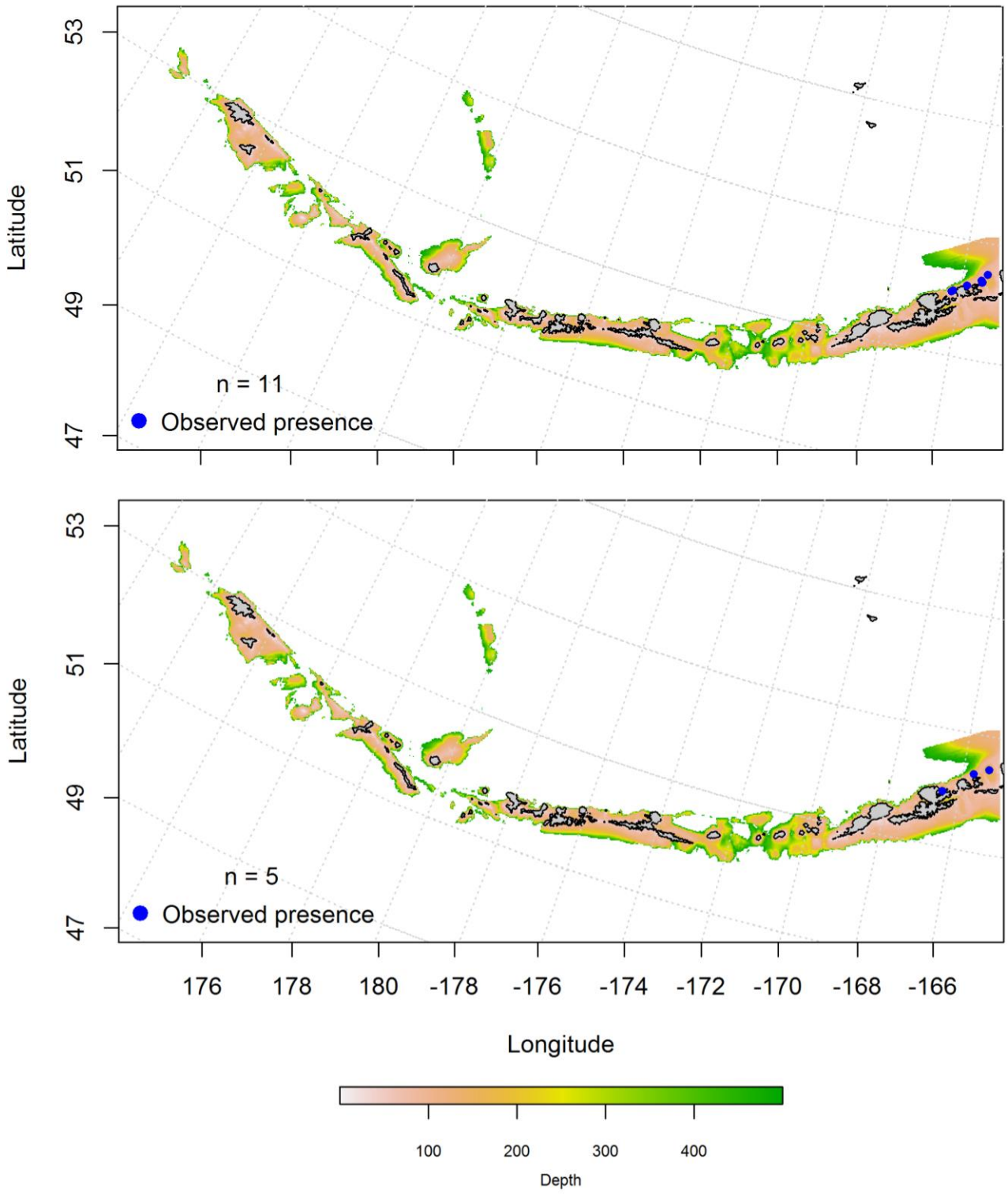

Figure 45. – Spring and summer observations (top and bottom panel) of larval Flathead sole from the Aleutian Islands.

Summertime distribution of juvenile and adult Flathead sole from bottom trawl surveys of the Aleutian Islands. -- The catch of Flathead sole in summer bottom trawl surveys of the Aleutian Islands indicates this species is broadly distributed, and similarly less concentrated around large passes. A two-step hurdle-Generalized additive model predicting the presence absence (PA GAM) of juvenile Flathead sole explained 92% of the variability in CPUE in the bottom trawl survey training data, 91% of the variability in the test data set, and 44.7% of the deviance. Geographic location and bottom depth were the most important variables explaining the distribution of juvenile Flathead sole presence or absence. The model correctly classified 85% of the training data and 83% of the test data. The areas of predicted highest abundance were concentrated around Agattu Island in the western AI, Atka Island in the central AI, and Unalaska in the east (Figure 46).

The second part of the juvenile Flathead sole hurdle-GAM predicted CPUE and explained 43% of the variability of the training data set, 39% of the test data set, and 43.2% of the deviance. Geographic location and ocean color were the most important variables explaining the distribution of juvenile Flathead sole CPUE GAM. The areas of predicted highest abundance were similar to the PA GAM (around Agattu Island in the western AI, Atka Island in the central AI, and Unalaska in the eastern AI) though less abundant (Figure 47).

A two-step hurdle-Generalized additive model predicting the presence absence (PA GAM) of adult Flathead sole explained 90% of the variability in CPUE in the bottom trawl survey training data, and 89% of the variability in the test data set. Surface ocean color, geographic location, and bottom depth were the most important variables explaining the distribution of adult Flathead sole presence or absence. The model correctly classified 82% of the training data, 81% of the test data, and 40.8% of the deviance. The areas of predicted highest abundance were similar to

juvenile Flathead sole, though a higher predicted probability of presence around Agattu Island in the western AI and Unalaska in the east (Figure 48Figure 46).

The second part of the adult Flathead sole hurdle-GAM predicted CPUE and explained 32% of the variability of the training data set, 28% of the test data set, and 32.3% of the deviance. Geographic location and ocean color were the most important variables explaining the distribution of adult Flathead sole CPUE GAM. The areas of predicted highest abundance were similar to the PA GAM though less abundant (Figure 49).

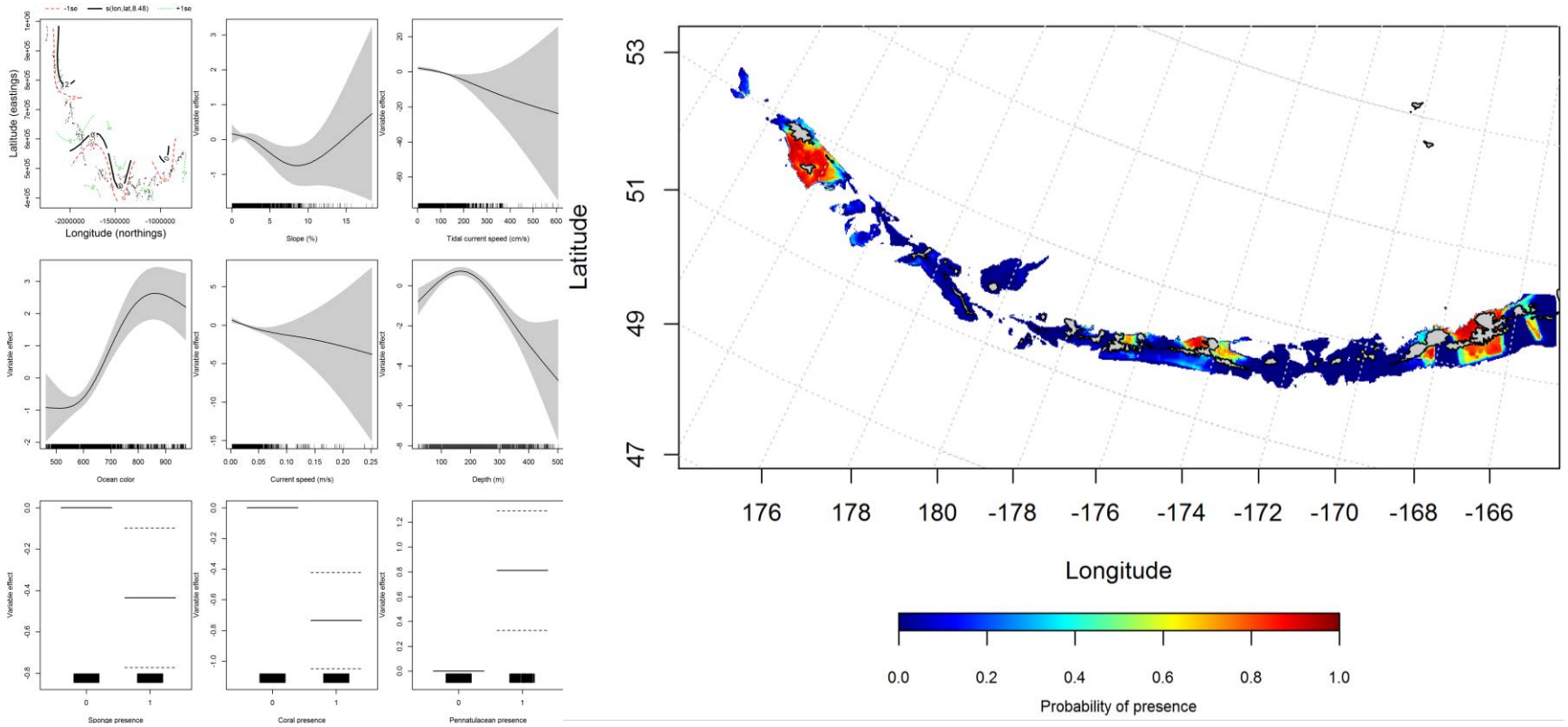

Figure 46. Best-fitting hurdle model effects of retained habitat variables on presence absence (PA) of juvenile Flathead sole from summer bottom trawl surveys of the Aleutian Islands (left panel) alongside hurdle-predicted juvenile Flathead sole PA (right panel).

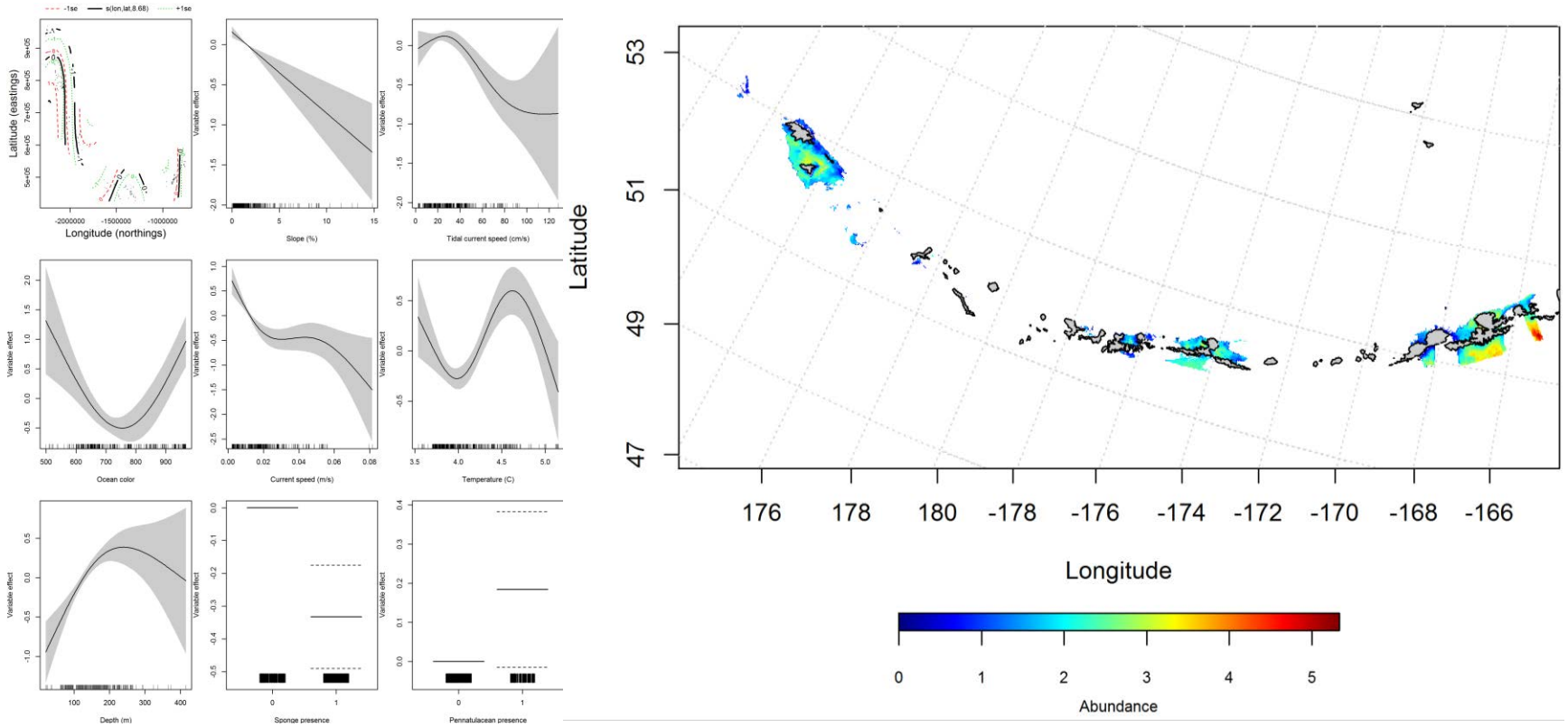

Figure 47. Best-fitting hurdle model effects of retained habitat variables on CPUE of juvenile Flathead sole from summer bottom trawl surveys of the Aleutian Islands (left panel) alongside hurdle-predicted juvenile Flathead sole cpue (right panel).

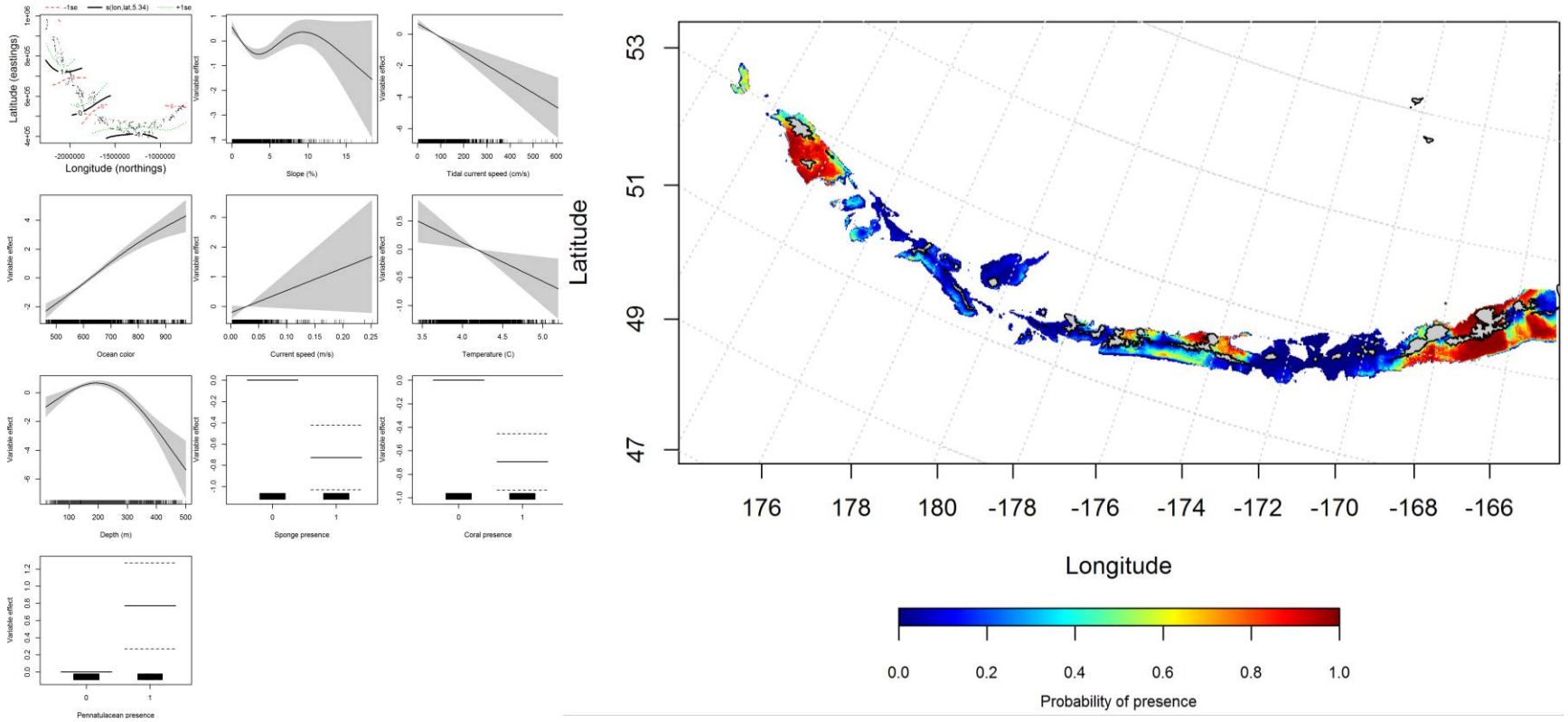

Figure 48. Best-fitting hurdle model effects of retained habitat variables on presence absence (PA) of adult Flathead sole from summer bottom trawl surveys of the Aleutian Islands (left panel) alongside hurdle-predicted adult Flathead sole PA (right panel).

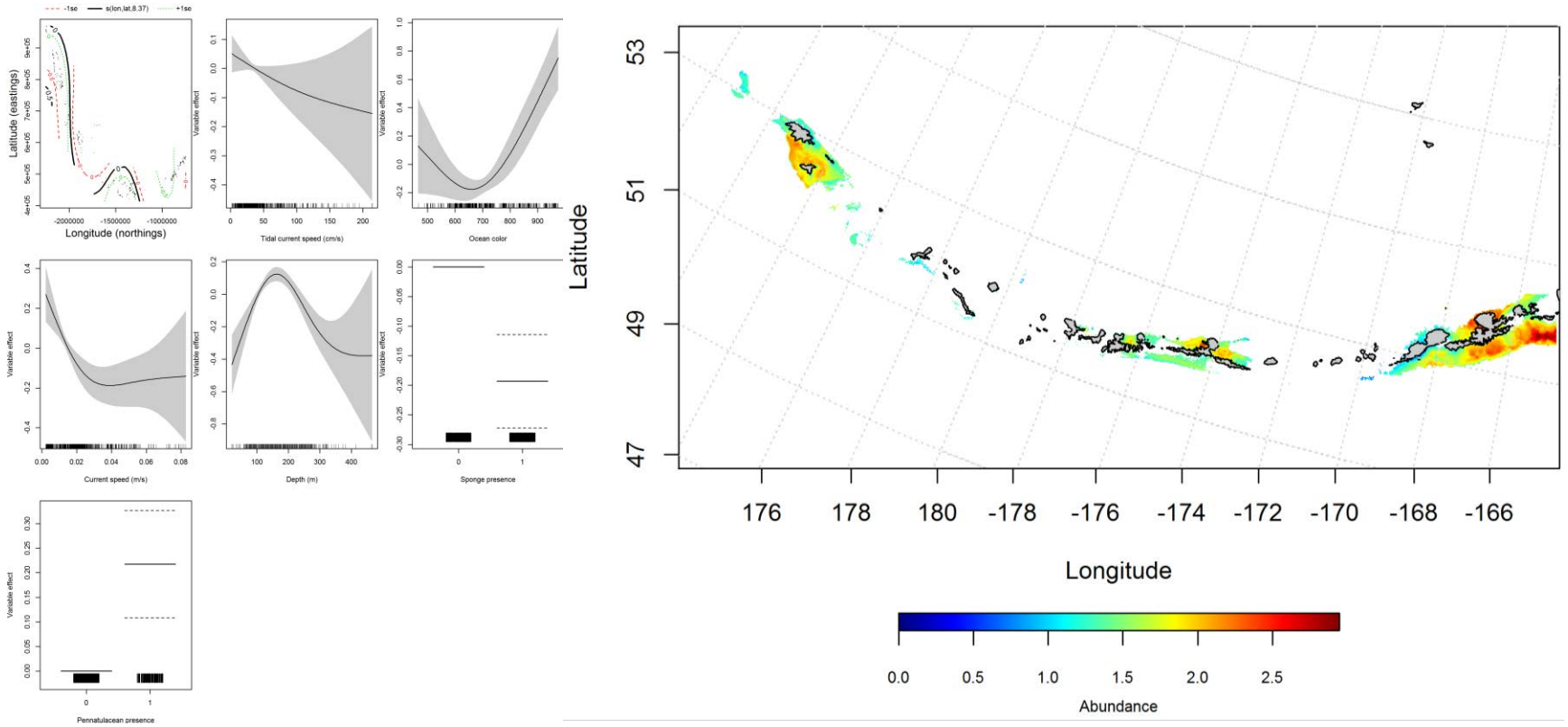

Figure 49. -- Best-fitting hurdle model effects of retained habitat variables on cpue of adult Flathead sole from summer bottom trawl surveys of the Aleutian Islands (left panel) alongside hurdle-predicted adult Flathead sole cpue (right panel).

Seasonal distribution of commercial fisheries catches of adult Flathead sole in the Aleutian Islands -- Adult Flathead sole in the Aleutian Islands in commercial fisheries catches was distributed more broadly in the winter and spring than the fall. In the fall, ocean color, bottom temperature, and bottom depth were the most important variables determining probable suitable habitat of Flathead sole (relative importance: 40.4%, 27%, and 19.9%, respectively). The AUC of the fall maxent model was 96% for the training data and 81%. 90% of the training data and 81% of the test data were predicted correctly. The model predicted probable suitable habitat of Flathead sole throughout the AI, though highest in the eastern AI (Figure 50).

Like the fall, ocean color, bottom depth, and bottom temperature were the most important variables determining probability of suitable habitat of Flathead sole (relative importance: 40.9%, 23.9%, and 18%, respectively) in the winter model. The AUC of the winter maxent model was 97% for the training data and 89% for the test data. 91% of the training data and 89% of the test data sets were correctly classified. As with the fall, the model predicted probable suitable habitat of Flathead sole throughout the AI, but there was a clear clustering in the western, central and eastern AI around islands avoiding large passes (Figure 51).

In the spring, ocean color and bottom depth were the most important variables determining probable suitable habitat of Flathead sole (relative importance: 49.4% and 30.3%). The AUC of the spring maxent model was 94% for the training data and 83% for the test data. 86% of the training data and 83% of the test data were correctly classified. As with the winter, the model predicted probable suitable habitat of adult Flathead sole throughout the AI, but there was a clear clustering in the western, central and eastern AI around islands avoiding large passes (Figure 52).

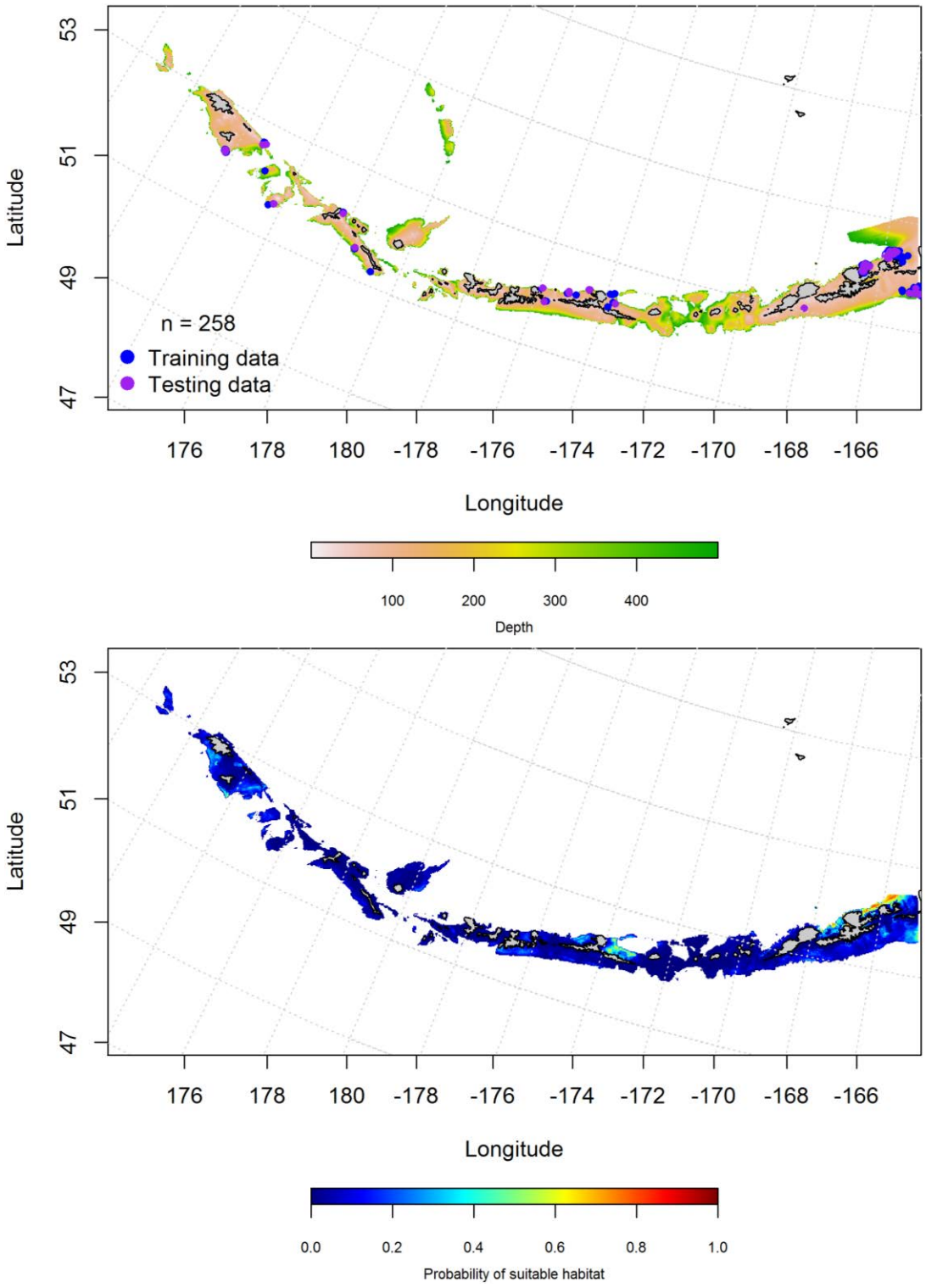

Figure 50. -- Locations of fall (September-November) commercial fisheries catches of Flathead sole (top panel). Blue points were used to train the maximum entropy model predicting the probability of suitable fall habitat supporting commercial fisheries of Flathead sole (bottom panel) and the purple points were used to validate the model.

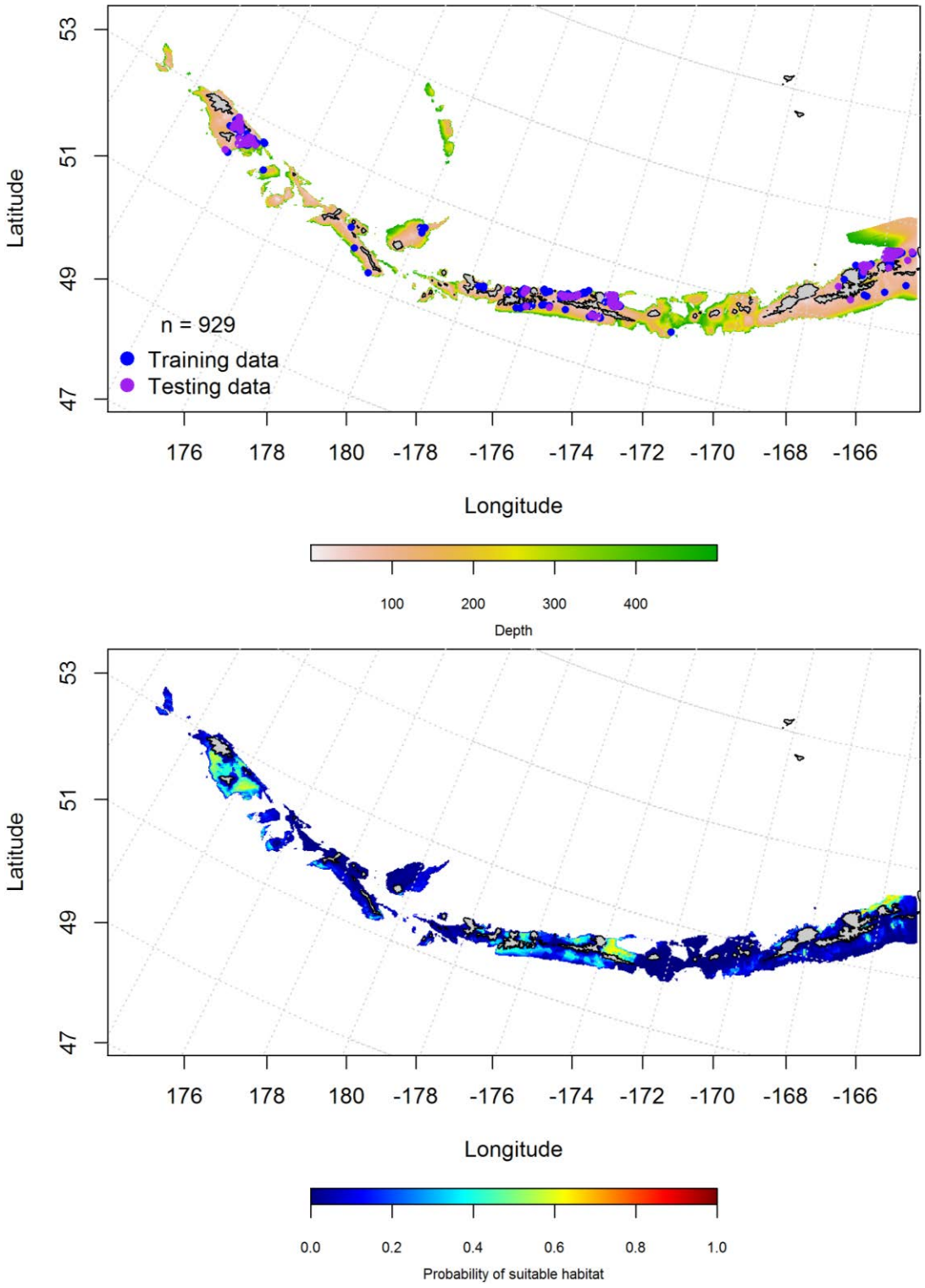

Figure 51. -- Locations of winter (December-February) commercial fisheries catches of Flathead sole (top panel). Blue points were used to train the maximum entropy model predicting the probability of suitable winter habitat supporting commercial catches of Flathead sole (bottom panel) and the purple points were used to validate the model.

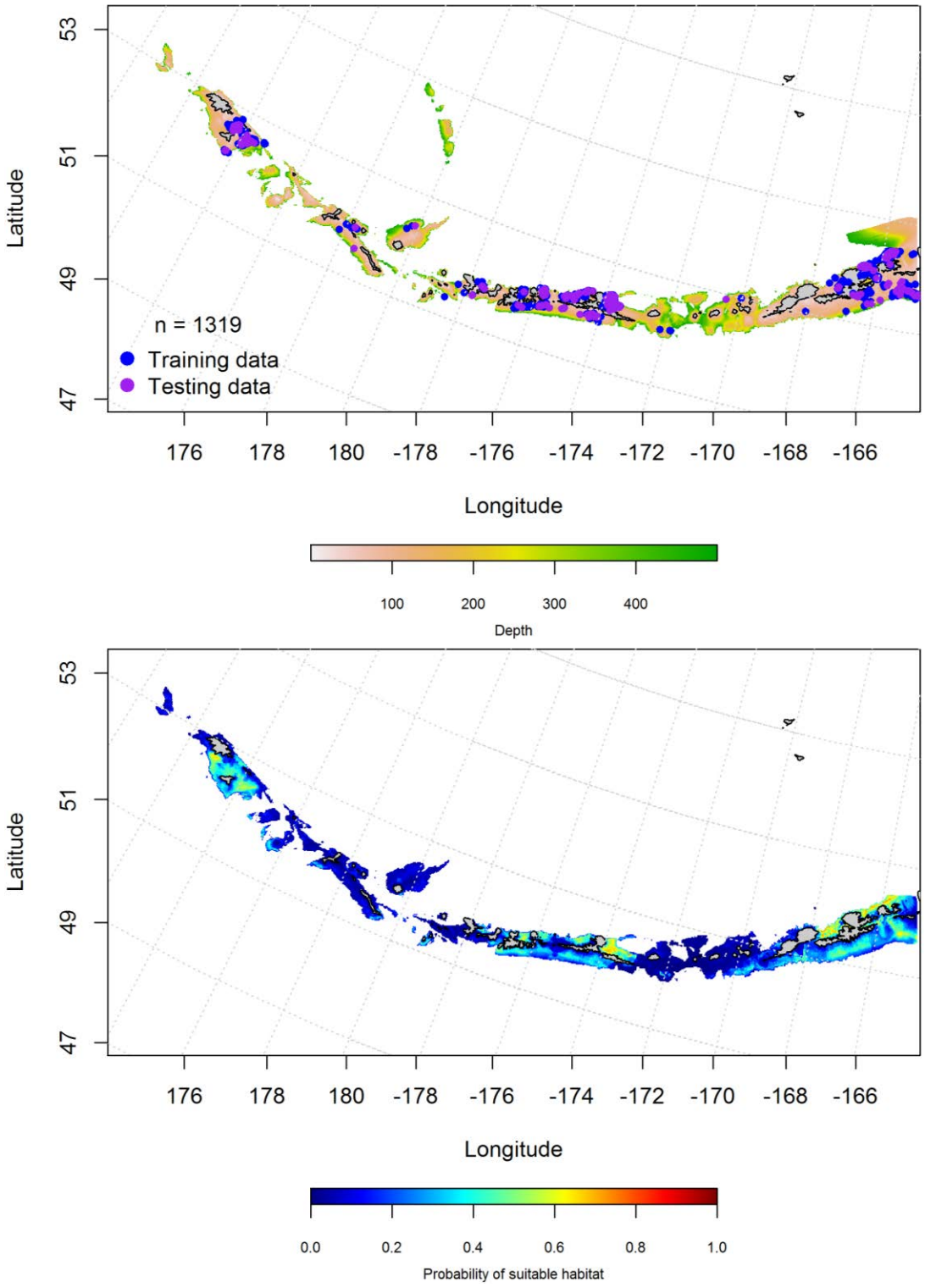

Figure 52. -- Locations of spring (March-May) commercial fisheries catches of Flathead sole (top panel). Blue points were used to train the maximum entropy model predicting the probability suitable spring habitat supporting commercial catches of Flathead sole (bottom panel) and the purple points were used to validate the model.

Aleutian Islands Flathead sole Essential Fish Habitat Maps and Conclusions –

Essential fish habitat for Flathead sole eggs predicted by the modeling is concentrated in the eastern Aleutian Islands, unlike predictions for juveniles and adults from summertime bottom trawl and commercial catches.

In general, juvenile and adult Flathead sole are predicted throughout the AI, but there are clear clusterings in the western AI (Semisopochnoi Island), central (Atka Island) and the eastern AI (Figure 54). These similarities can be observed in both areas of high (areas of higher CPUE exist in the eastern, central, and western Aleutians) and low abundance (e.g., large passes).

The EFH predicted from commercial catches of Flathead sole is distributed throughout the Aleutian Islands chain (Figure 55). There does not appear to be much seasonal variability between the winter and spring months, but the fall has areas of higher concentration around certain islands, consistent with the same EFH pattern distribution observed from summertime bottom trawl surveys.

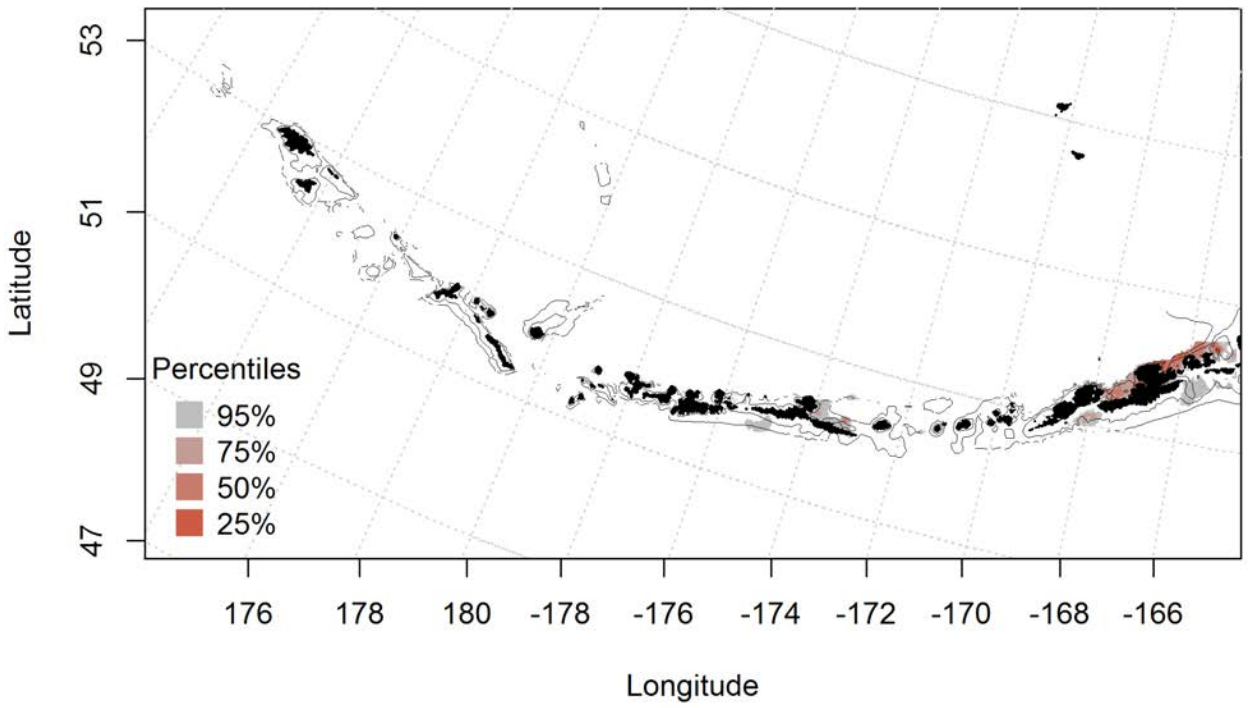

Figure 53. -- Spring essential fish habitat predicted for Flathead sole eggs.

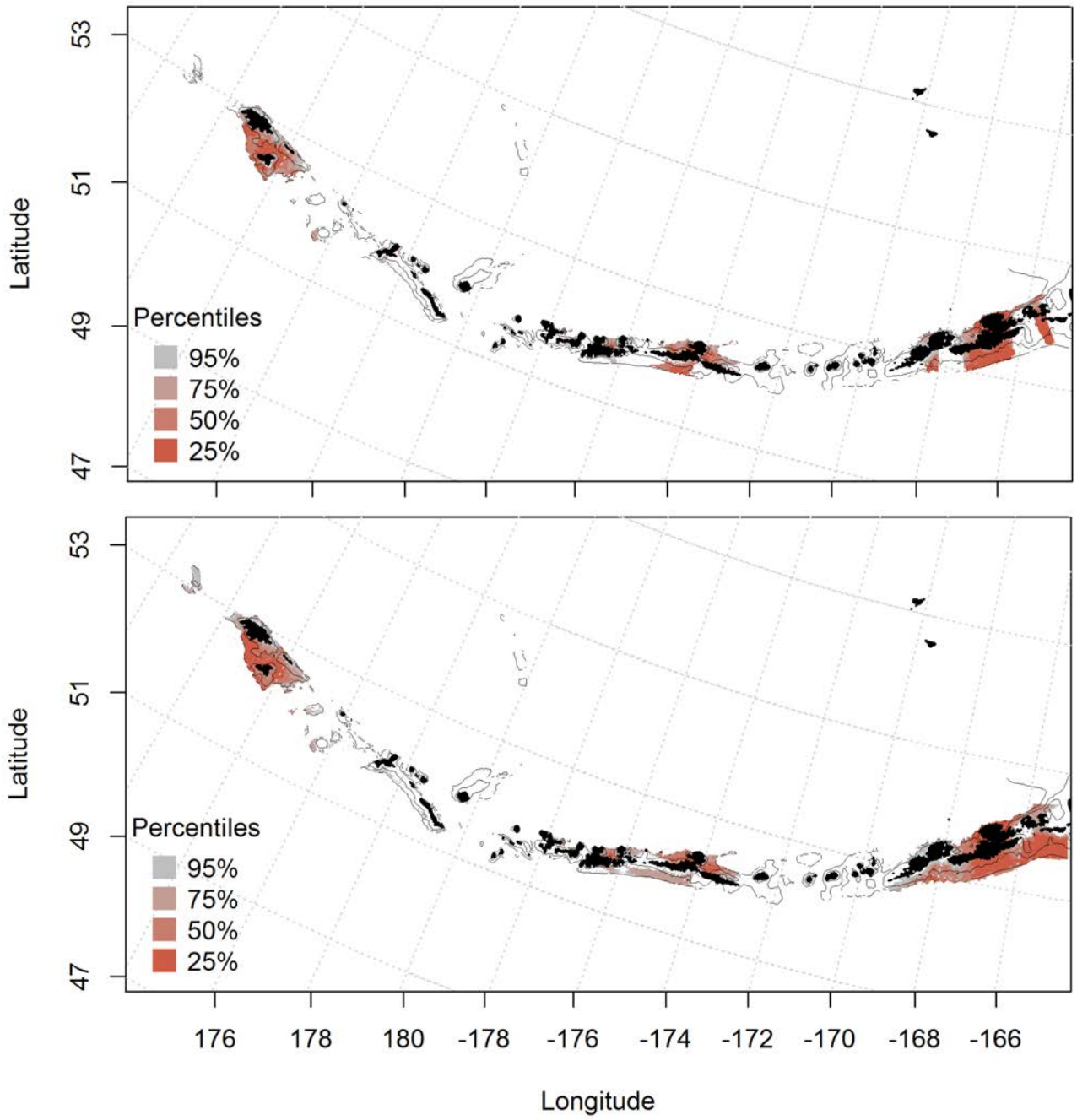

Figure 54. Predicted summer essential fish habitat for Flathead sole juveniles and adults (top and bottom panel) from summertime bottom trawl surveys.

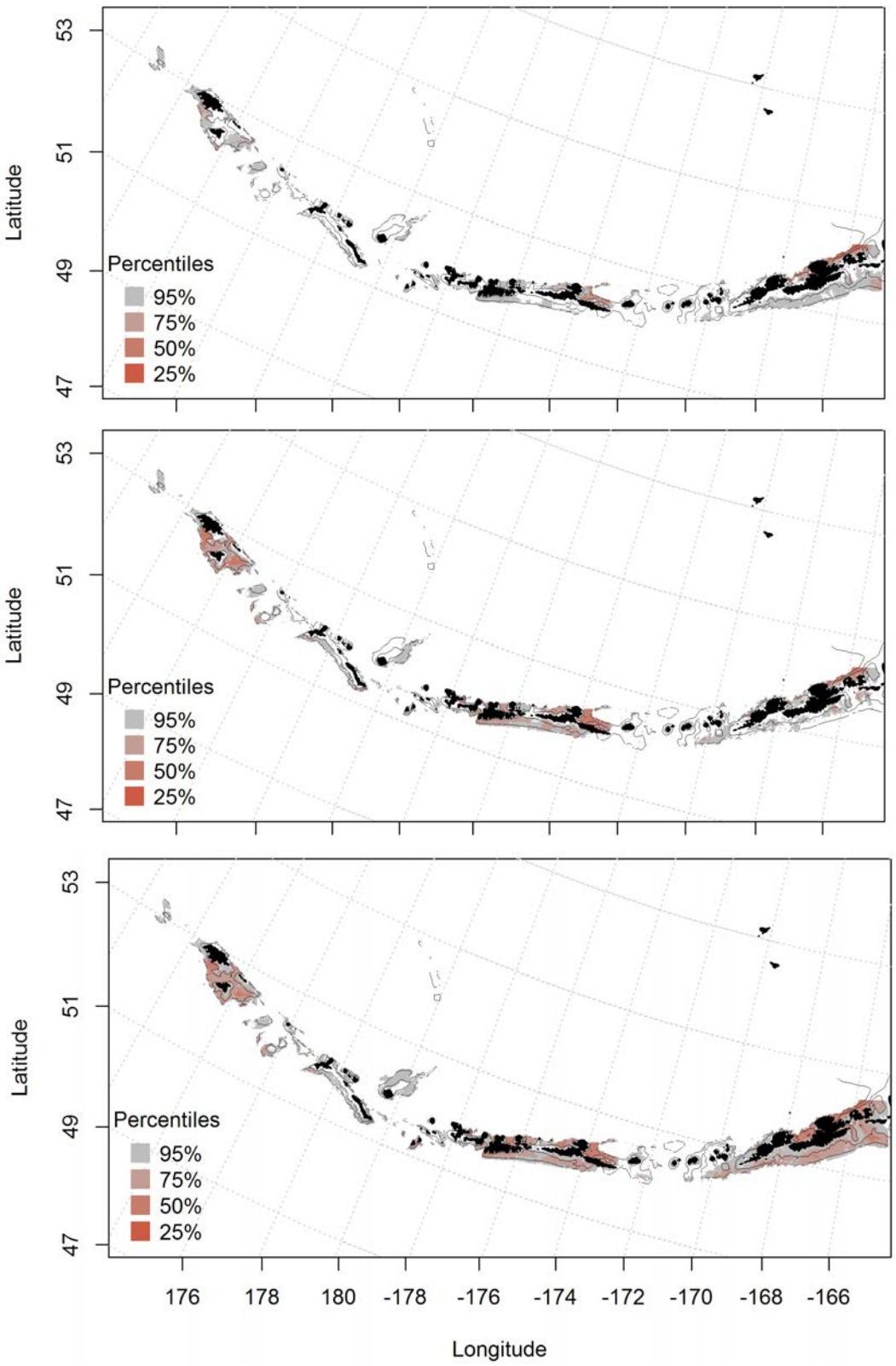

Figure 55. -- Essential fish habitat predicted for Flathead sole during fall (top panel), winter (middle panel) and spring (bottom panel) from summertime commercial catches.

Rex sole *(Glyptocephalus zachirus)*
Species data here

Seasonal distribution of early life history stages of Rex sole in the Aleutian Islands -- There were only 43 instances of Rex sole eggs observed in the FOCI database (Figure 56), 36 in the spring and 7 in the summer. All observations were found in the eastern Aleutian Islands. There were not enough observances to run models for the spring or summer months. There were only 2 observations of larval Rex sole in the eastern AI, not enough to run the model (Figure 57).

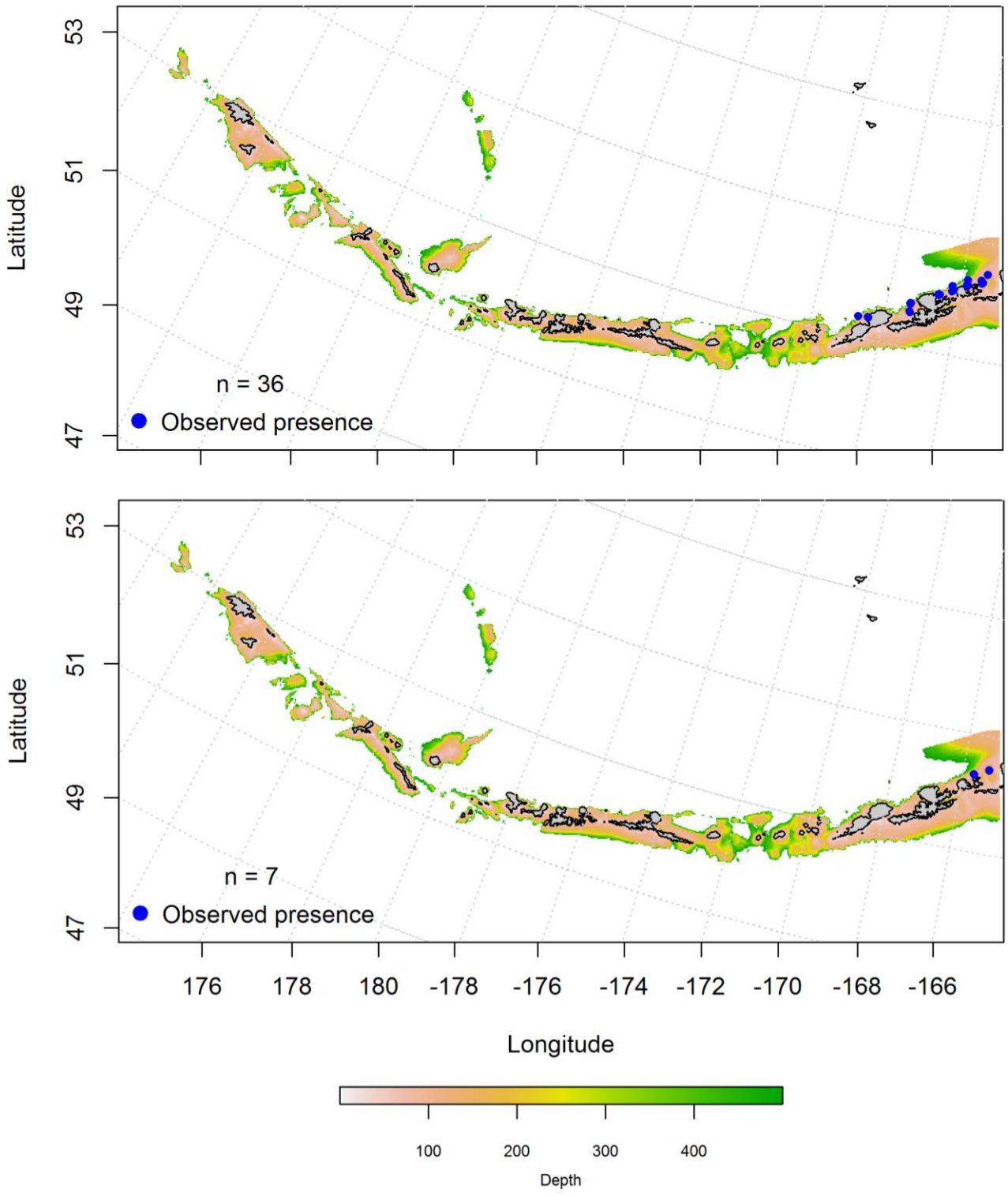

Figure 56. -- Spring and summer observations (top and bottom panel) of Rex sole eggs from the Aleutian Islands.

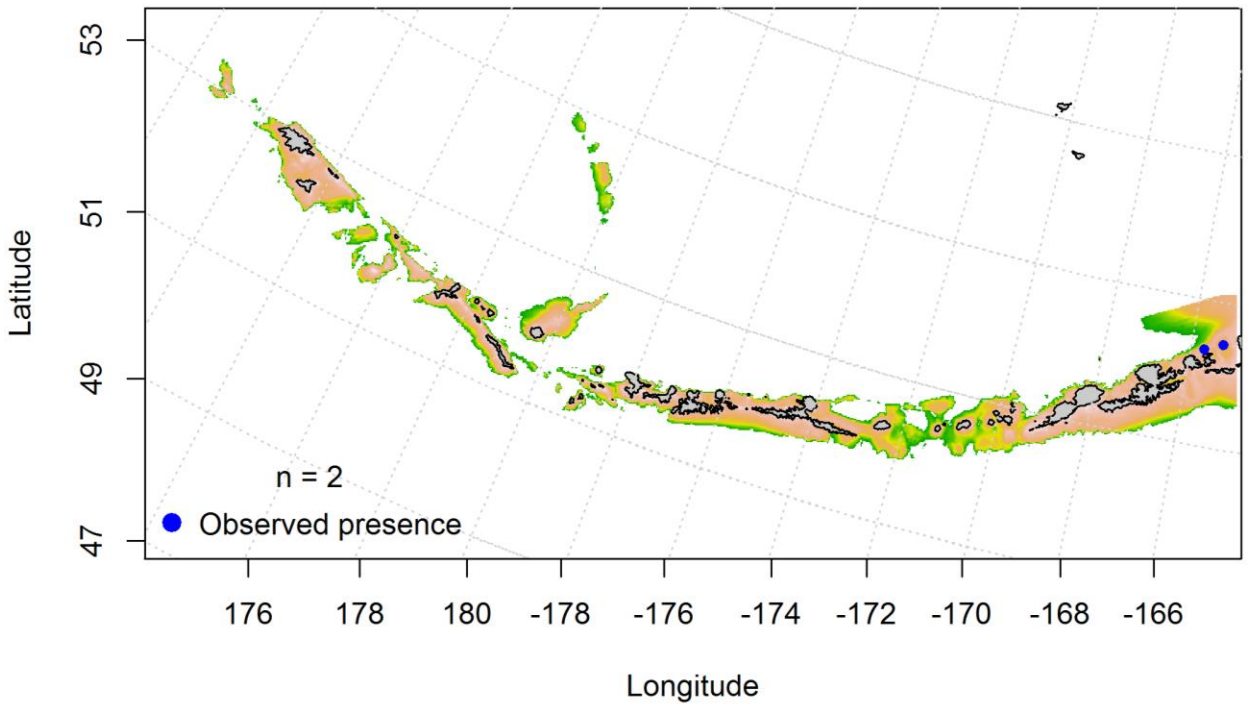

Figure 57. -- Summer observations) of larval Rex sole from the Aleutian Islands.

Summertime distribution of juvenile and adult Rex sole from bottom trawl surveys of the Aleutian Islands -- Juvenile Rex sole were modeled using a hurdle-GAM. The presence absence GAM predicted a higher probability of presence in the eastern Aleutian Islands, though was fairly similar across the Island chain (Figure 58). The best-fitting PA GAM indicated that bottom depth, ocean color, and current speed were the most important factors controlling juvenile Rex sole distribution and the model explained 83% of the variability, and explained 74% of the variability in the test data set. The model correctly predicted 76% of the training data, 71% of the test data set, and 18.7% of the deviance.

The CPUE GAM model found that surface ocean color was the most important variable that explained the distribution of juvenile Rex sole. The model explained 38% of the variability in CPUE in the bottom trawl survey training data, 17% of the test data set, and 38.2% of the

deviance. The predicted abundance was concentrated around larger islands throughout the AI, and absent in large passes (Figure 59).

Adult Rex sole were similarly distributed to juvenile Rex sole in the AI (higher probability of presence in the eastern Aleutian Islands) (Figure 60).The best-fitting GAM model indicated that bottom depth, surface ocean color, and geographic location were the most important factors controlling adult Rex sole. The model explained 33% of the variability in the training data set, 26% of the variability in the test data set, and 33.3% of the deviance.

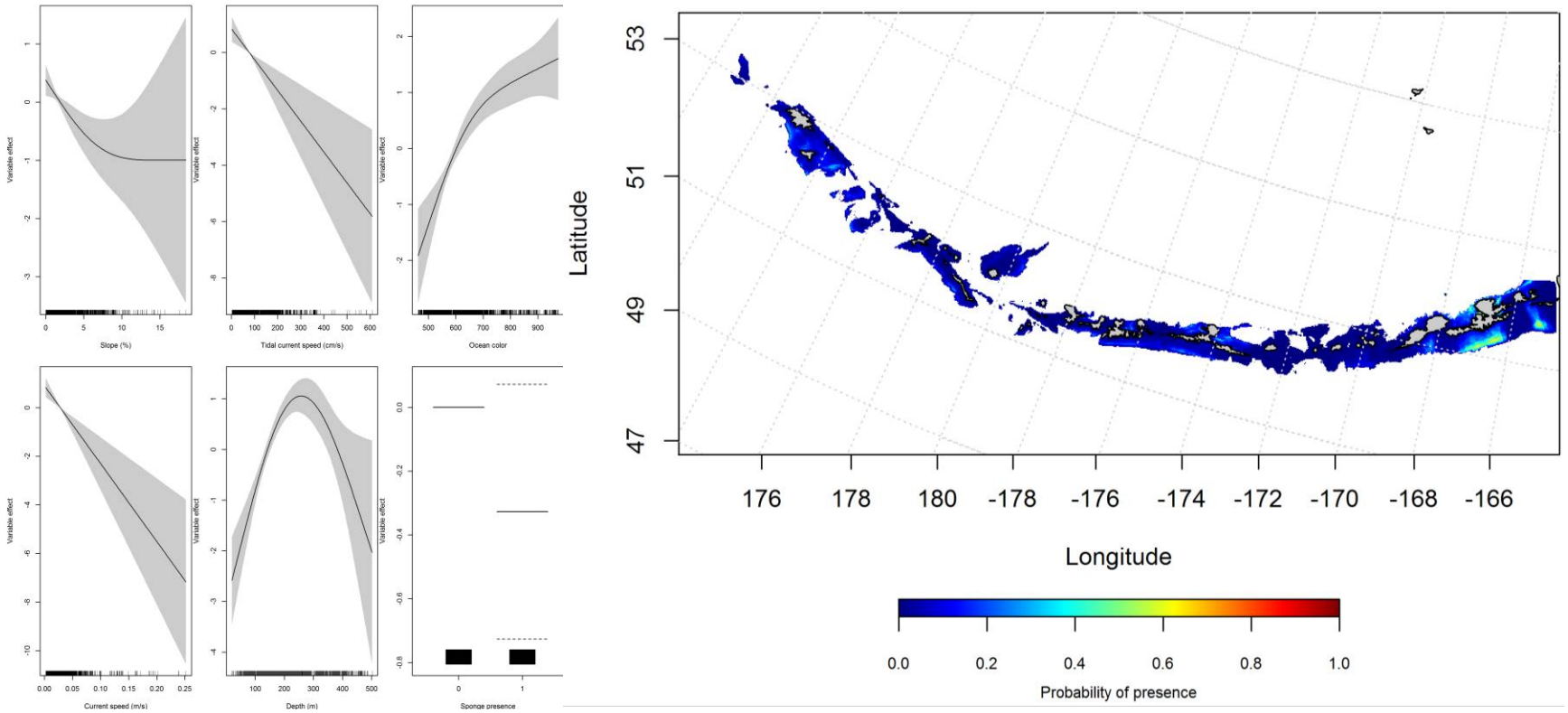

Figure 58. Best-fitting hurdle model effects of retained habitat variables on presence absence (PA) of juvenile Rex sole from summer bottom trawl surveys of the Aleutian Islands (left panel) alongside hurdle-predicted juvenile Rex sole PA (right panel).

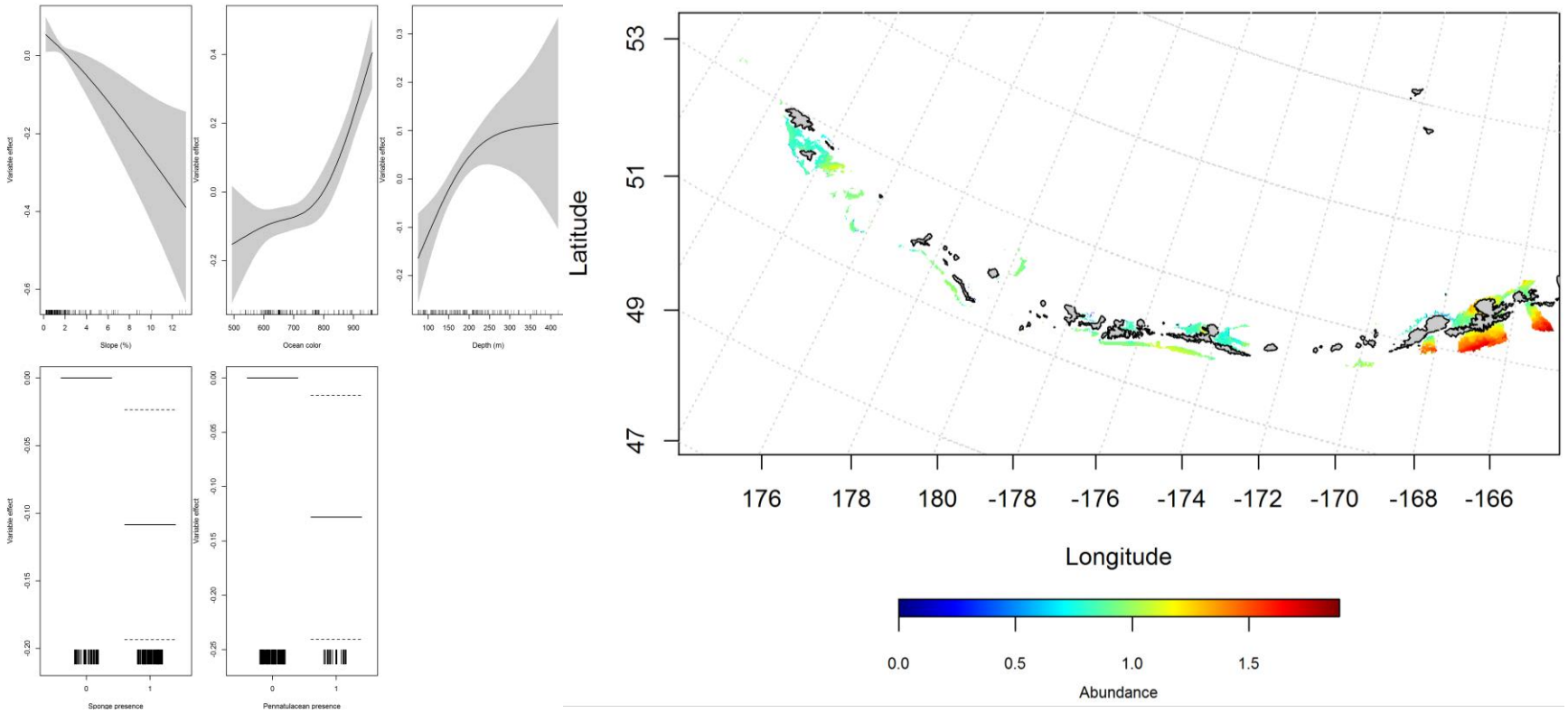

Figure 59. -- Best-fitting hurdle model effects of retained habitat variables on cpue of juvenile Rex sole from summer bottom trawl surveys of the Aleutian Islands (left panel) alongside hurdle-predicted juvenile Rex sole cpue (right panel).

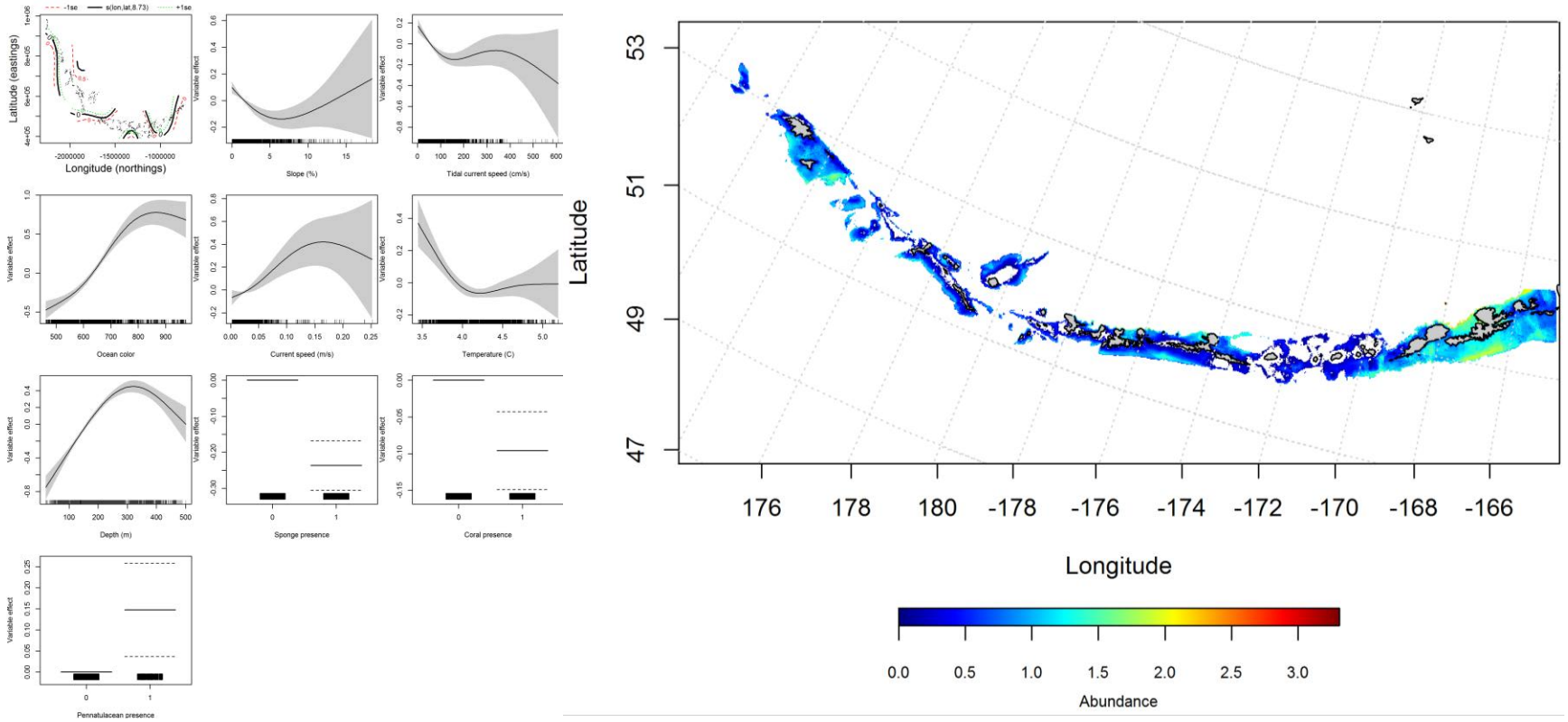

Figure 60. -- Best-fitting generalized additive model (GAM) effects of retained habitat variables on abundance of adult Rex sole from summer bottom trawl surveys of the Aleutian Islands slope and shelf (left panel) alongside GAM-predicted adult Rex sole abundance (right panel).

Seasonal distribution of commercial fisheries catches of adult Rex sole in the Aleutian Islands -- Distribution of adult Rex sole in the Aleutian Islands in commercial fisheries catches was consistent throughout all seasons. In the fall, bottom temperature, bottom depth, and ocean surface color were the most important variables determining probable suitable habitat of rex sole (relative importance: 32.8%, 28.2%, and 23.5%, respectively). The AUC of the fall maxent model was 97% for the training data and 93% for the test data. 91% of the cases in both the training data set and 93% of the cases in the test data set were predicted correctly. The model predicted probable suitable habitat of Rex sole throughout the AI, though absent in large passes (Figure 61).

In the winter, ocean color, bottom depth, and bottom temperature were the most important variables determining probable suitable habitat of adult Rex Sole (relative importance: 33.7%, 27.6%, and 23.3%, respectively). The AUC of the winter maxent model was 98% for the training data and 88% for the test data. 93% of the cases in the training data set, and 88% of the test data were predicted correctly. The model predicted probable suitable habitat of Rex sole throughout the AI (Figure 62).

Ocean color, bottom depth, and current speed were the most important variables determining probable suitable habitat of Rex Sole in the spring (relative importance: 48.2%, 31.2%, and 14.3%, respectively). The AUC of the spring maxent model was 95% for the training data and 86% for the test data. 87% of the training data set and 86% of the test data set were correctly classified. The model predicted probable suitable habitat of Rex Sole in the spring similar to the winter (distributed throughout the AI), though more concentrated in the eastern AI (Figure 63).

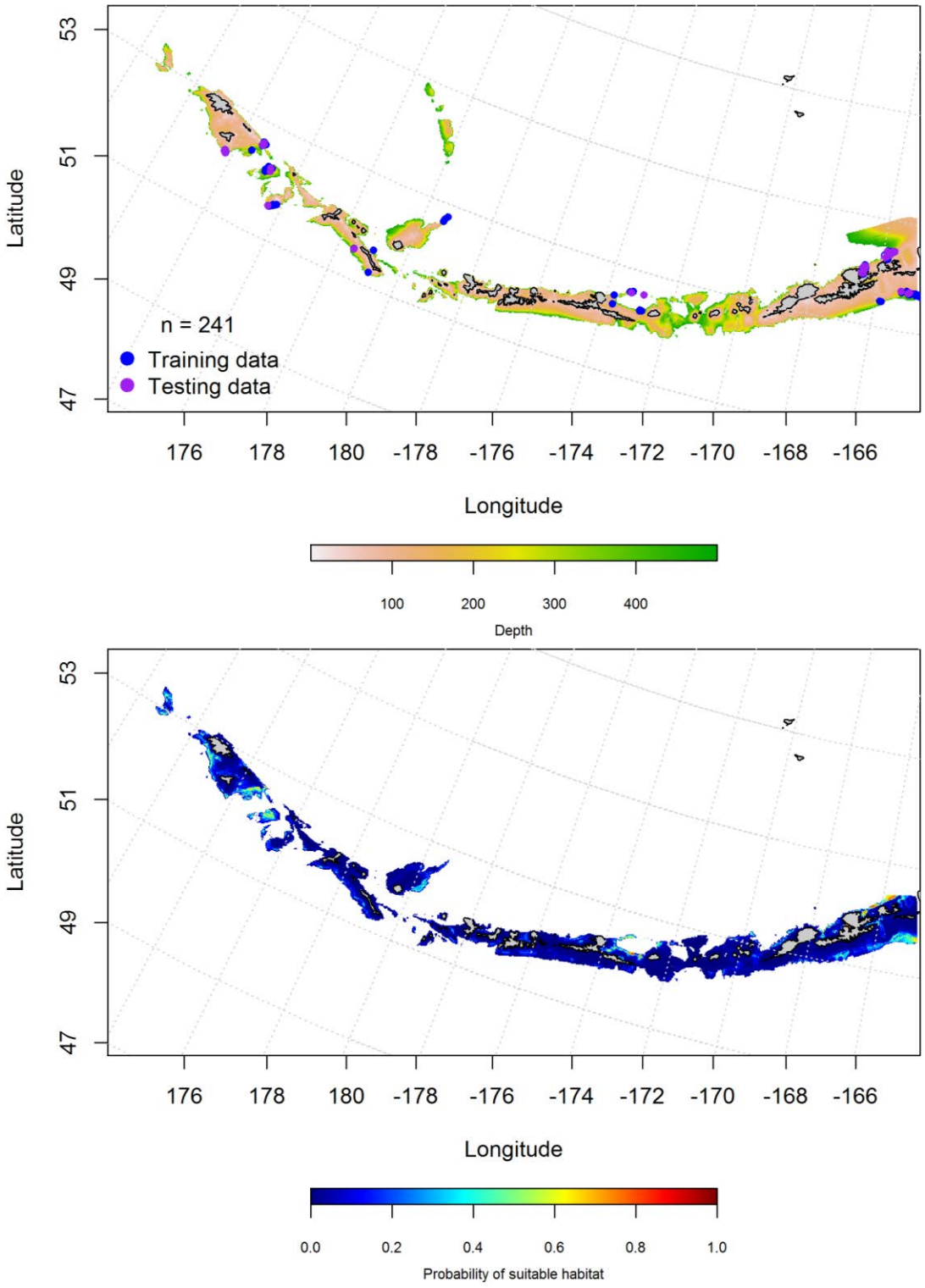

Figure 61. -- Locations of fall (September-November) commercial fisheries catches of Rex sole (top panel). Blue points were used to train the maximum entropy model predicting the probability suitable fall habitat supporting commercial catches of Rex sole (bottom panel) and the purple points were used to validate the model.

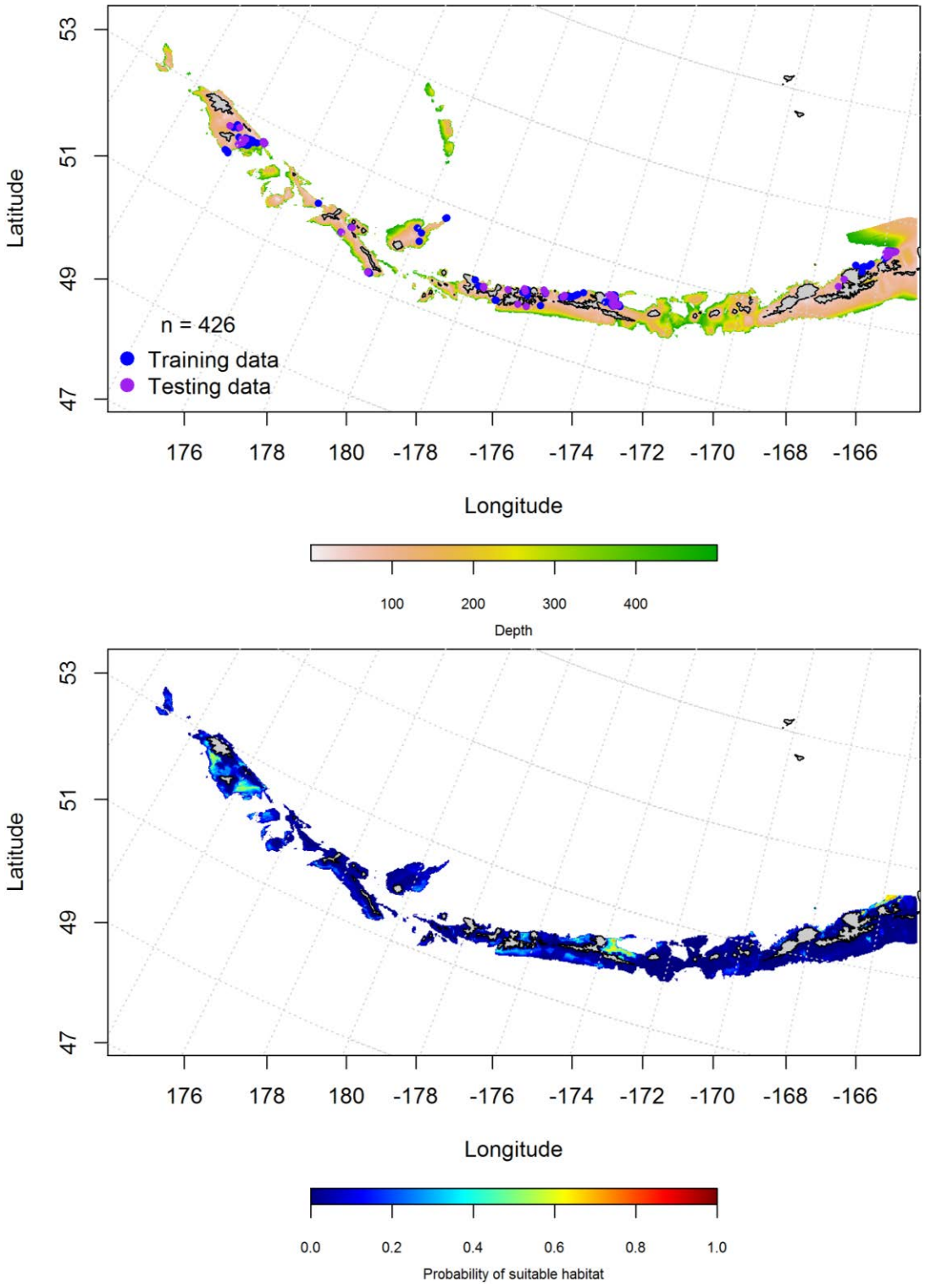

Figure 62. -- Locations of winter (December-February) commercial fisheries catches of Rex sole (top panel). Blue points were used to train the maximum entropy model predicting the probability of suitable winter habitat supporting commercial catches of Rex sole (bottom panel) and the purple points were used to validate the model.

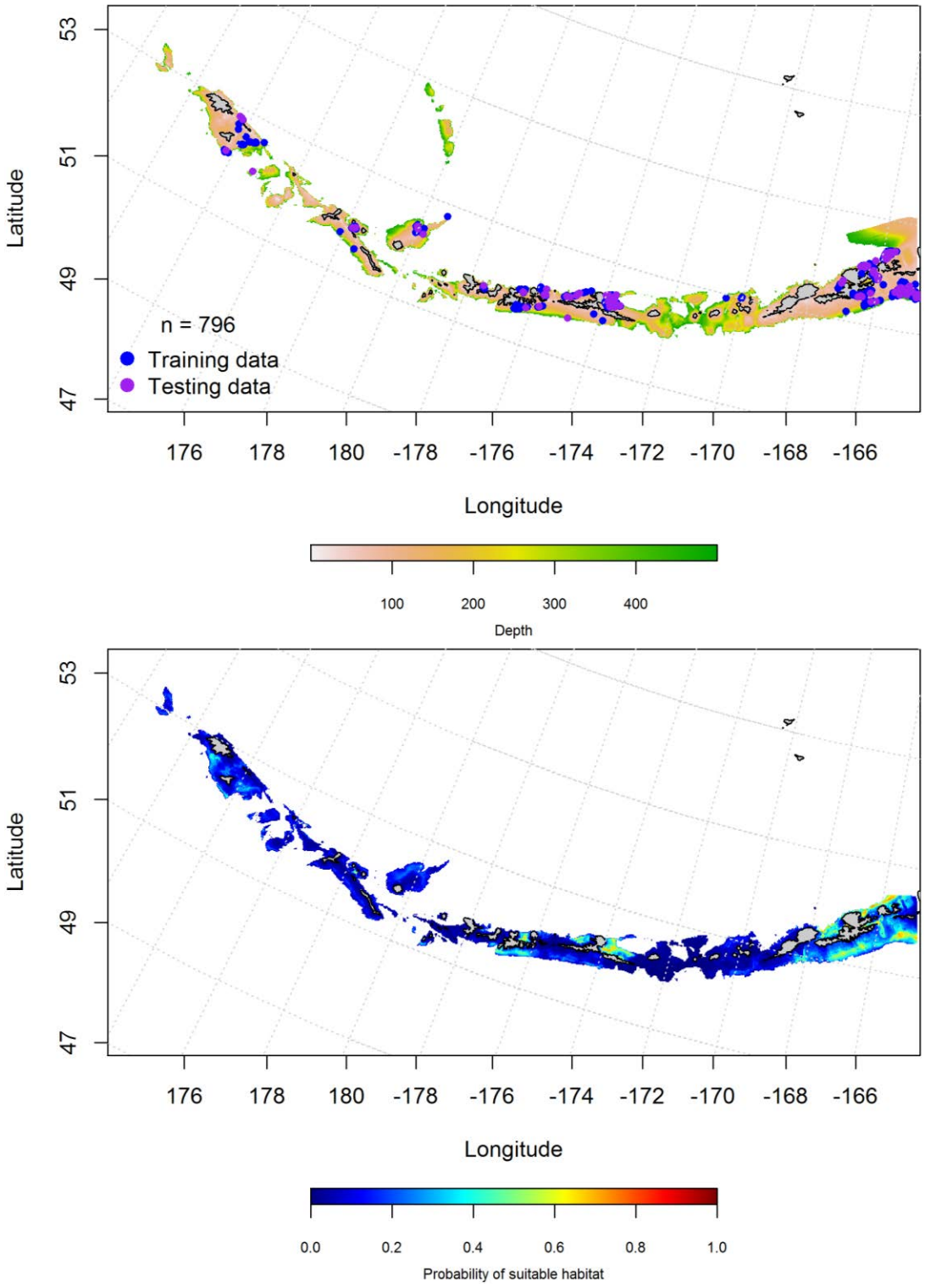

Figure 63. -- Locations of spring (March-May) commercial fisheries catches of Rex sole (top panel). Blue points were used to train the maximum entropy model predicting the probability of suitable spring habitat supporting commercial catches of Rex sole (bottom panel) and the purple points were used to validate the model.

Aleutian Islands Rex sole Essential Fish Habitat Maps and Conclusions – Juvenile and adult Rex sole essential fish habitat predicted by the modeling was distributed differently throughout the Aleutian Islands using summertime bottom trawl surveys (Figure 64). Juveniles are more sparsely distributed, with higher predicted abundance in the eastern AI. Adult rex soles were more widely distributed throughout the AI than the juveniles.

Predicted fall, winter and spring distributions from summertime commercial catches were similarly distributed (Figure 65). EFH was sparse, though slightly more concentrated in the eastern AI in the spring. Areas with large passes were predicted to have low abundance in all seasons.

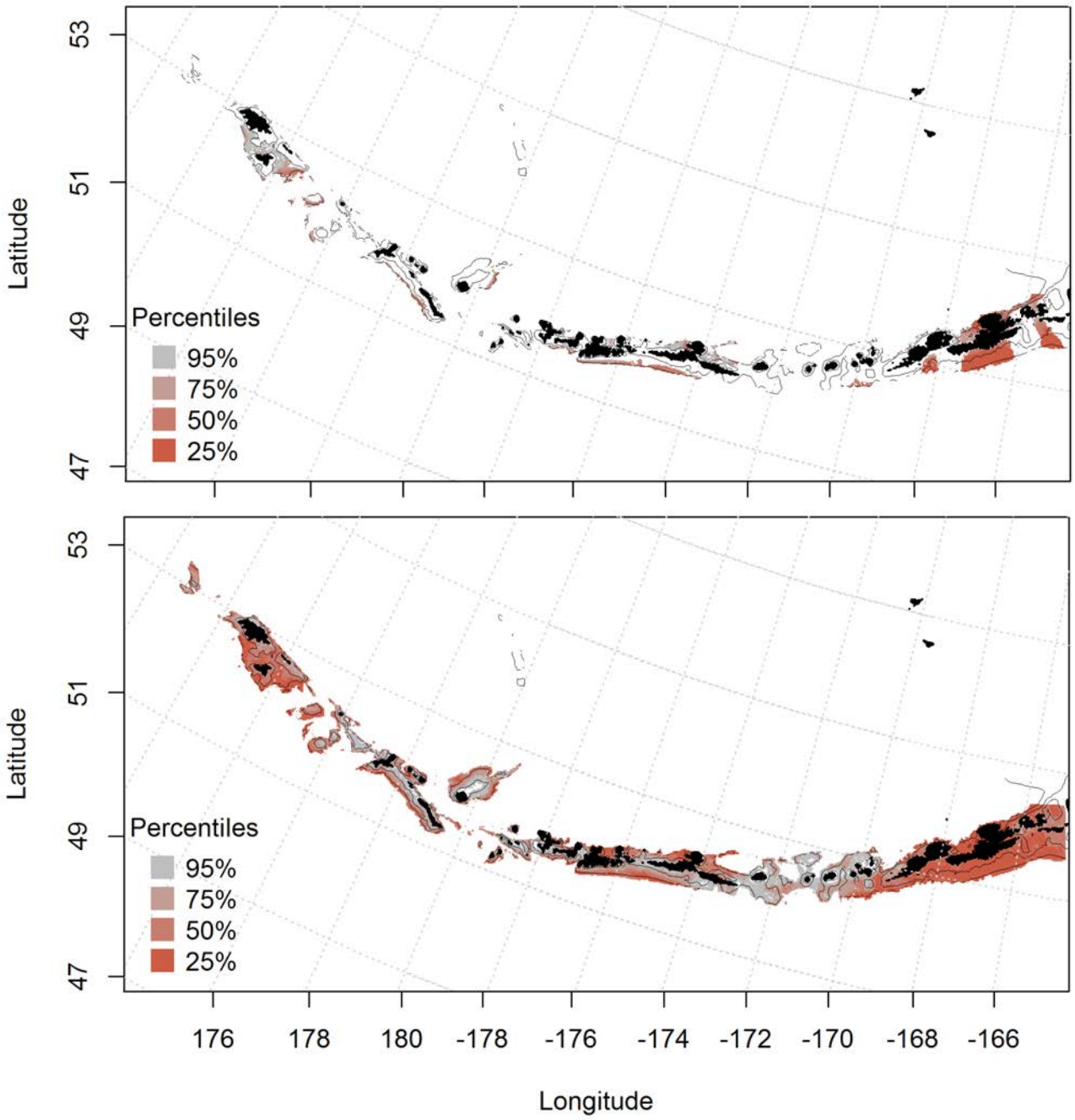

Figure 64. -- Predicted summer essential fish habitat for Rex sole juveniles and adults (top and bottom panel) from summertime bottom trawl surveys.

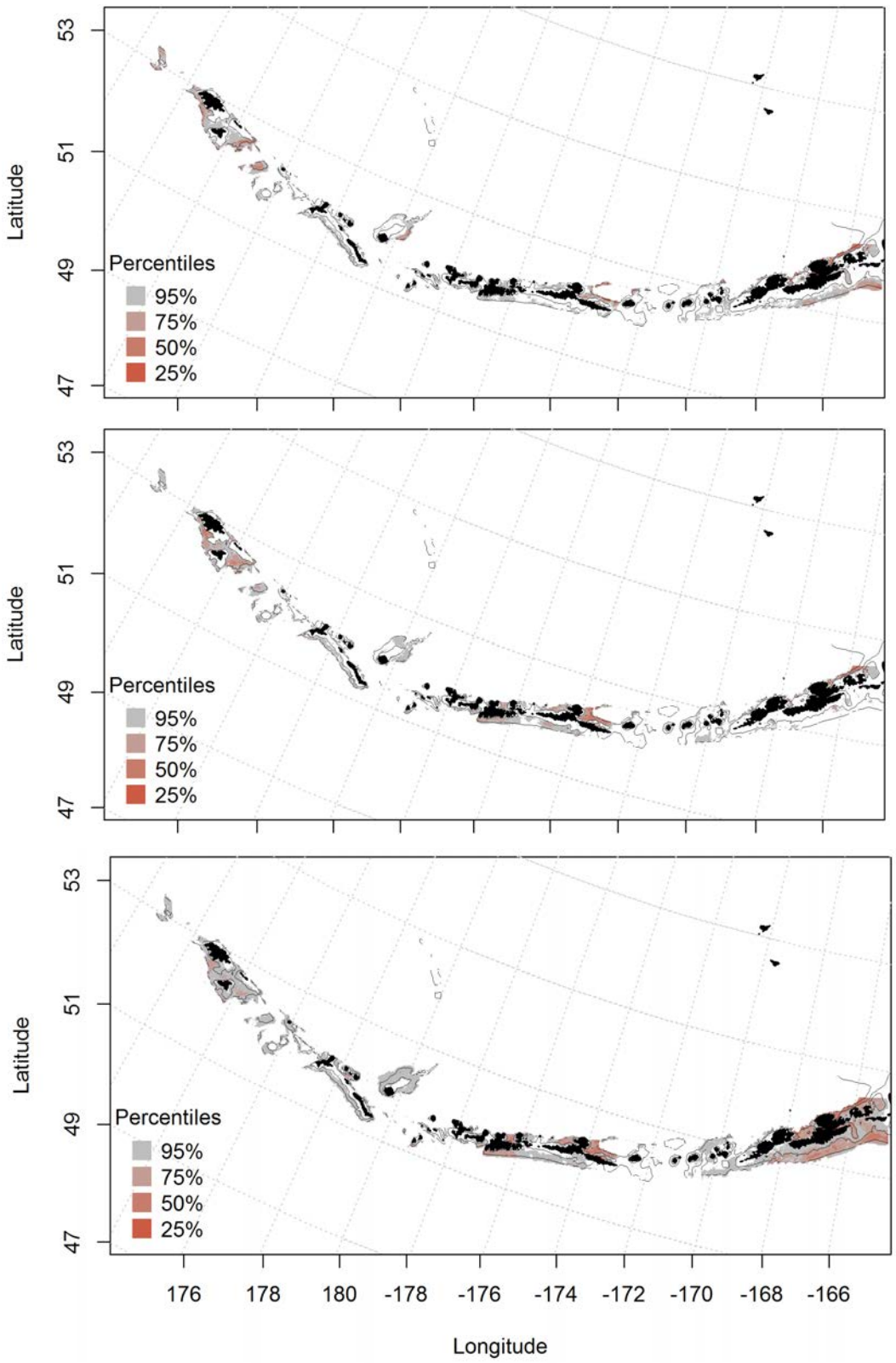

Figure 65. Essential fish habitat predicted for Rex sole during fall (top panel), winter (middle panel) and spring (bottom panel) from summertime commercial catches.

Dover sole *(Microstomus pacificus)*
Species text here.

Seasonal distribution of early life history stages of Dover sole in the Aleutian Islands

-- There were only 8 instances of Dover sole eggs observed in the FOCI database (Figure 66), 3 in the spring and 5 in the summer. All observations, except one were found in the eastern Aleutian Islands, there were not enough cases to run the spring or summer models.

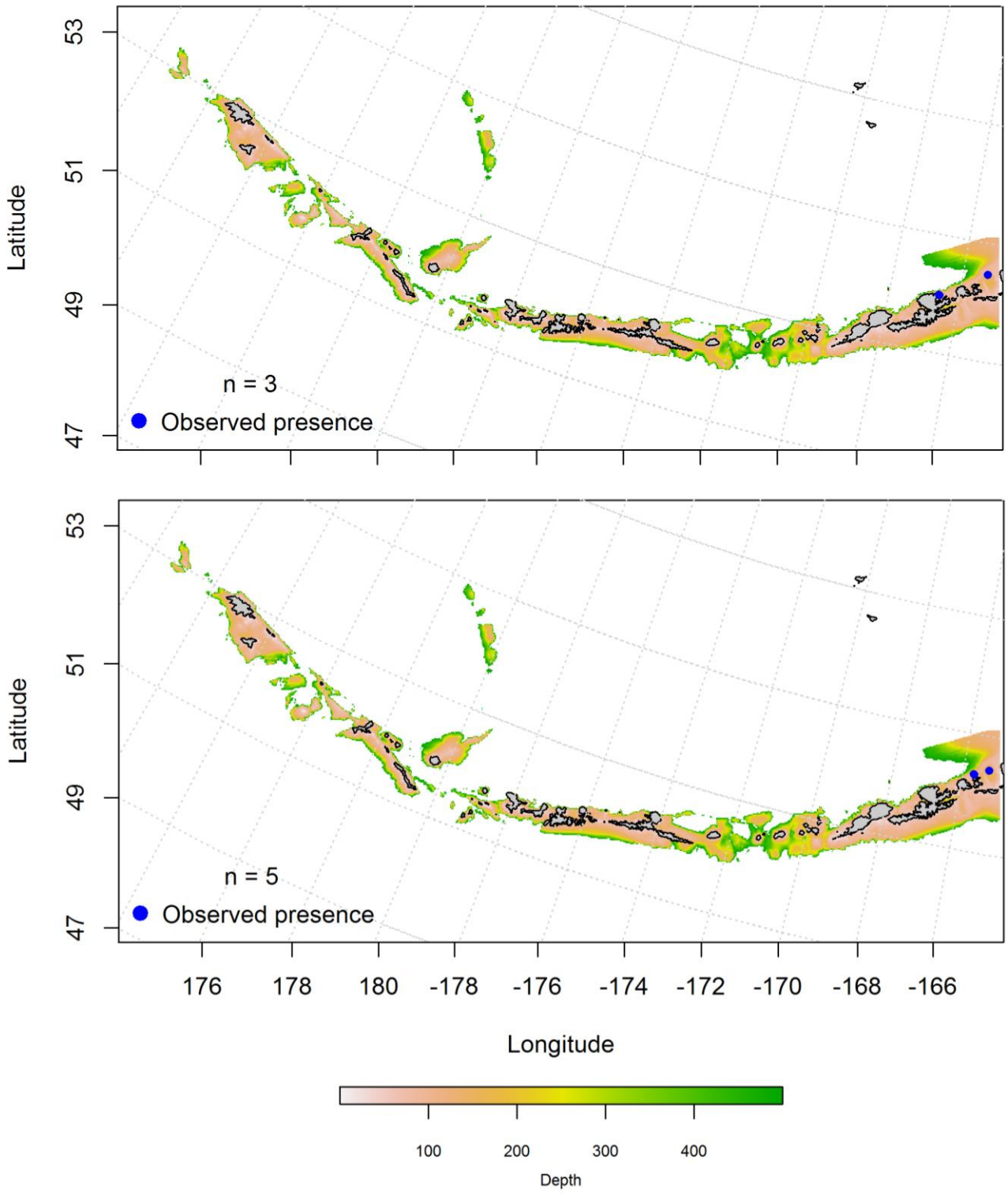

Figure 66. – Spring and summer observations of Dover sole eggs from the Aleutian Islands (top and bottom panel).

Summertime distribution of juvenile and adult Dover sole from bottom trawl surveys of the Aleutian Islands -- Juvenile Dover sole were modeled using a hurdle-GAM. The presence absence GAM predicted probability of presence throughout the AI (Figure 67). The best-fitting PA GAM indicated that geographic location and ocean color were the most important factors controlling juvenile Dover sole distribution. The model explained 84% of the variability in the training data set, 79% of the variability in the test data set, and 21.5% of the deviance. The model correctly predicted 76% of the training and test data sets.

The CPUE GAM model found that slope and surface ocean color were the most important variables that explained the distribution of juvenile Dover sole. The model explained 9% of the variability in CPUE in the bottom trawl survey training data, 6% of the test data set, and 8.5% of the deviance. The predicted abundance was similar to the presence/absence GAM (throughout the AI) (Figure 68).

Adult Dover sole were modeled using a hurdle-GAM. The presence absence GAM predicted probability of presence throughout the AI, similar to the presence prediction for juveniles (Figure 67). The best-fitting PA GAM indicated that geographic location, ocean color, and bottom depth were the most important factors controlling adult Dover sole distribution. The model explained 84% of the variability in the training and test data sets, 23% of the deviance, and correctly predicted 77% of the training and test data sets. The probability of adult Dover sole's presence was distributed across the AI survey area (Figure 69).

The CPUE GAM model found that current speed was the most important variables that explained the distribution of adult Dover sole. The model explained 19% of the variability in training data set, 16% of the test data in CPUE in the bottom trawl survey data, and 18.8% of the deviance.

The predicted abundance was similar to the presence/absence GAM (distributed throughout the AI) (Figure 70).

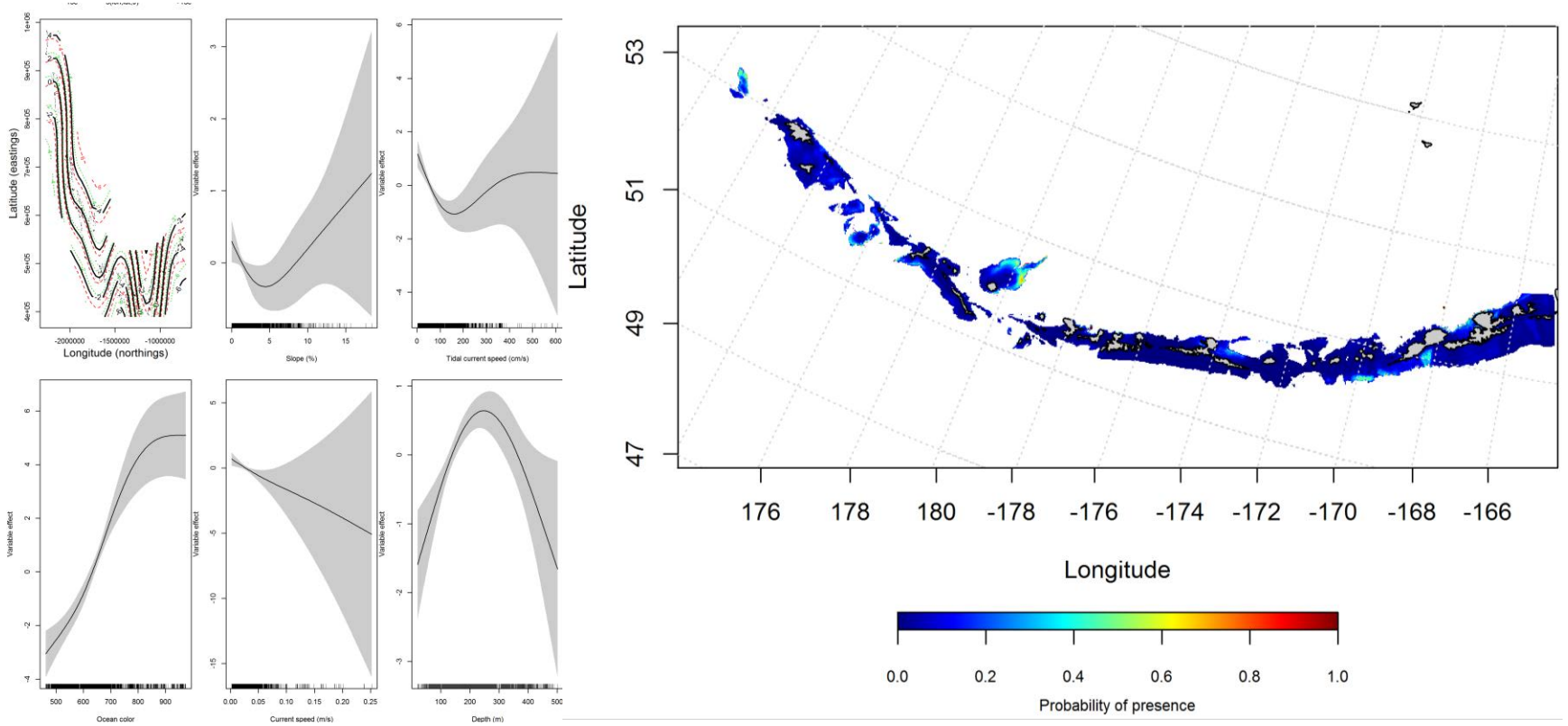

Figure 67. Best-fitting hurdle model effects of retained habitat variables on presence absence (PA) of juvenile Dover sole from summer bottom trawl surveys of Aleutian Islands (left panel) alongside hurdle-predicted juvenile Dover sole PA (right panel).

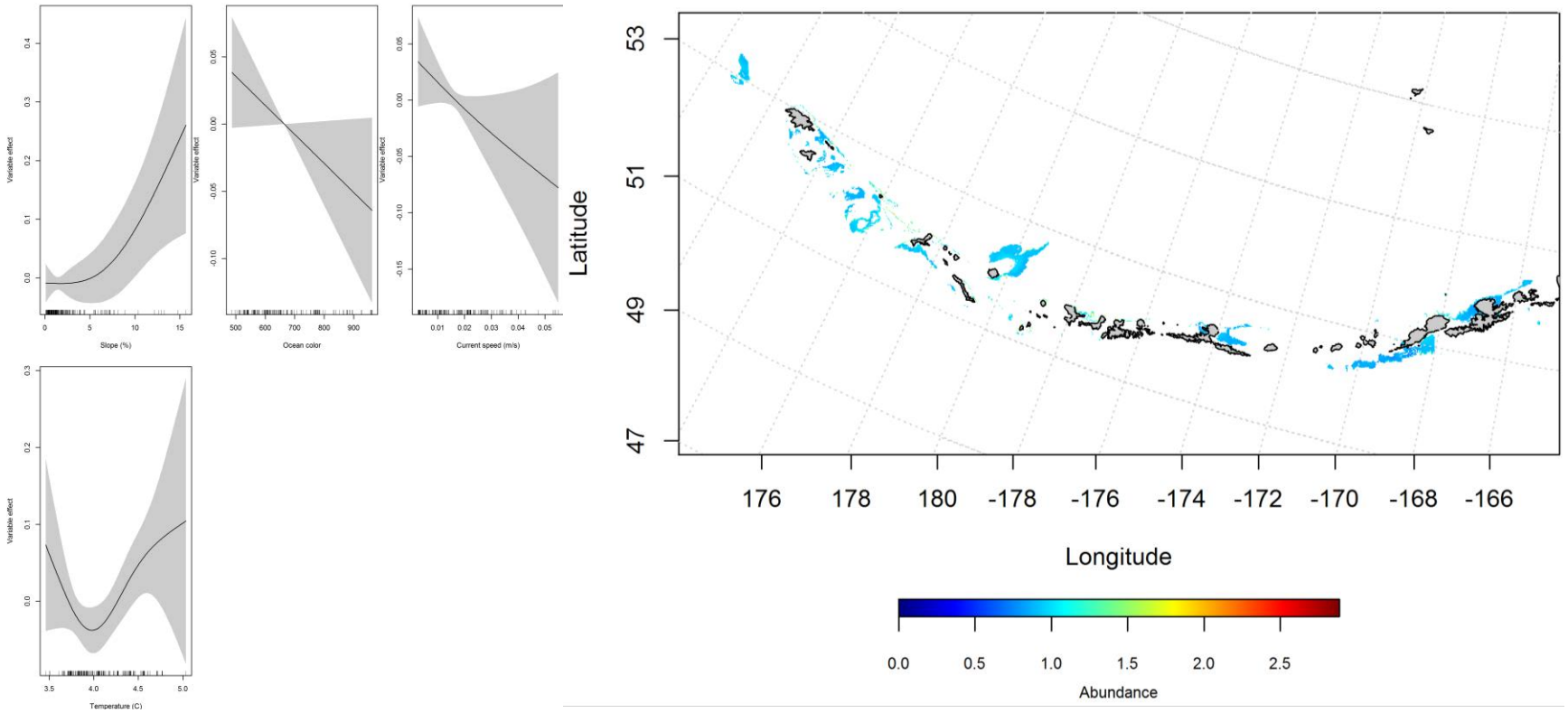

Figure 68. Best-fitting hurdle model effects of retained habitat variables on cpue of juvenile Dover sole from summer bottom trawl surveys of Aleutian Islands (left panel) alongside hurdle-predicted juvenile Dover sole cpue (right panel).

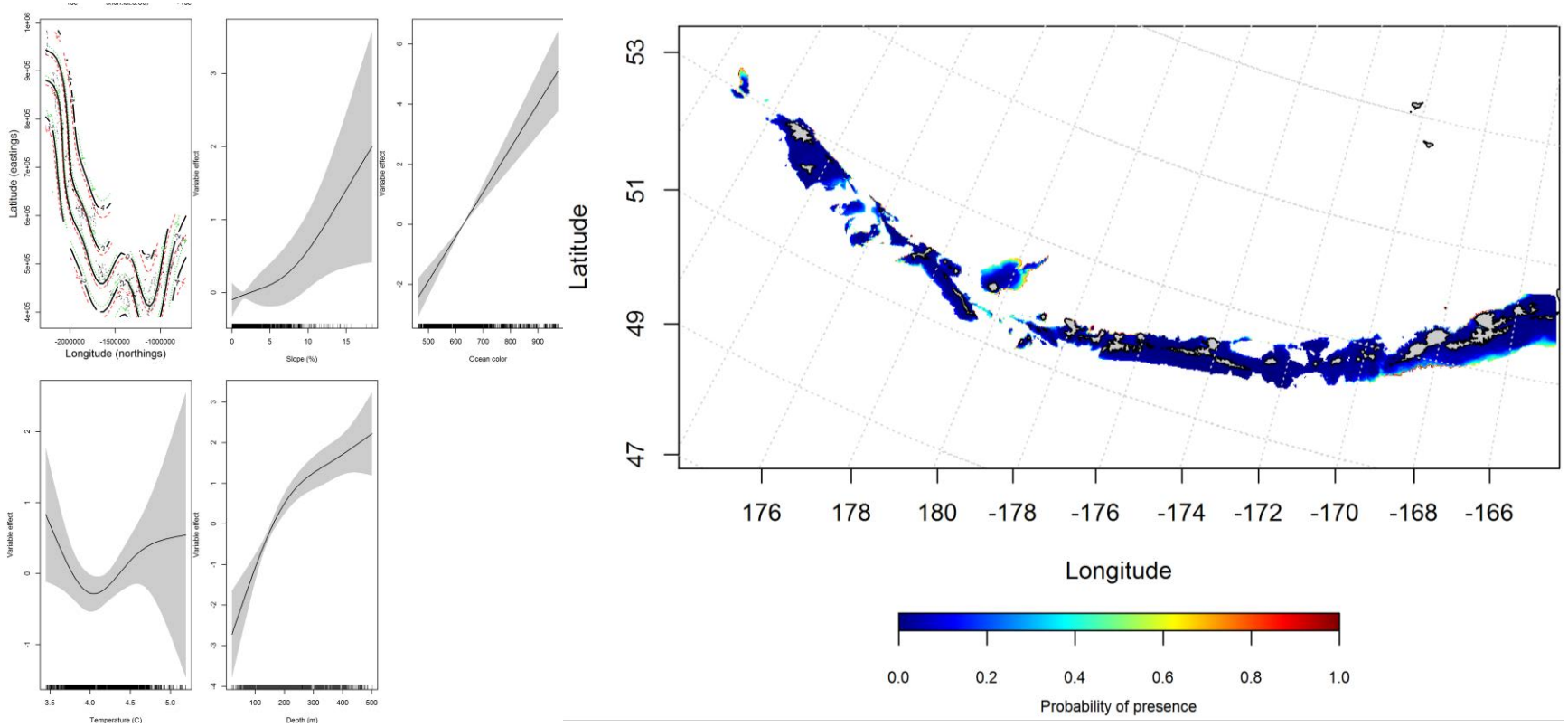

Figure 69. Best-fitting hurdle model effects of retained habitat variables on presence absence (PA) of adult Dover sole from summer bottom trawl surveys of the Aleutian Islands (left panel) alongside hurdle-predicted adult Dover sole PA (right panel).

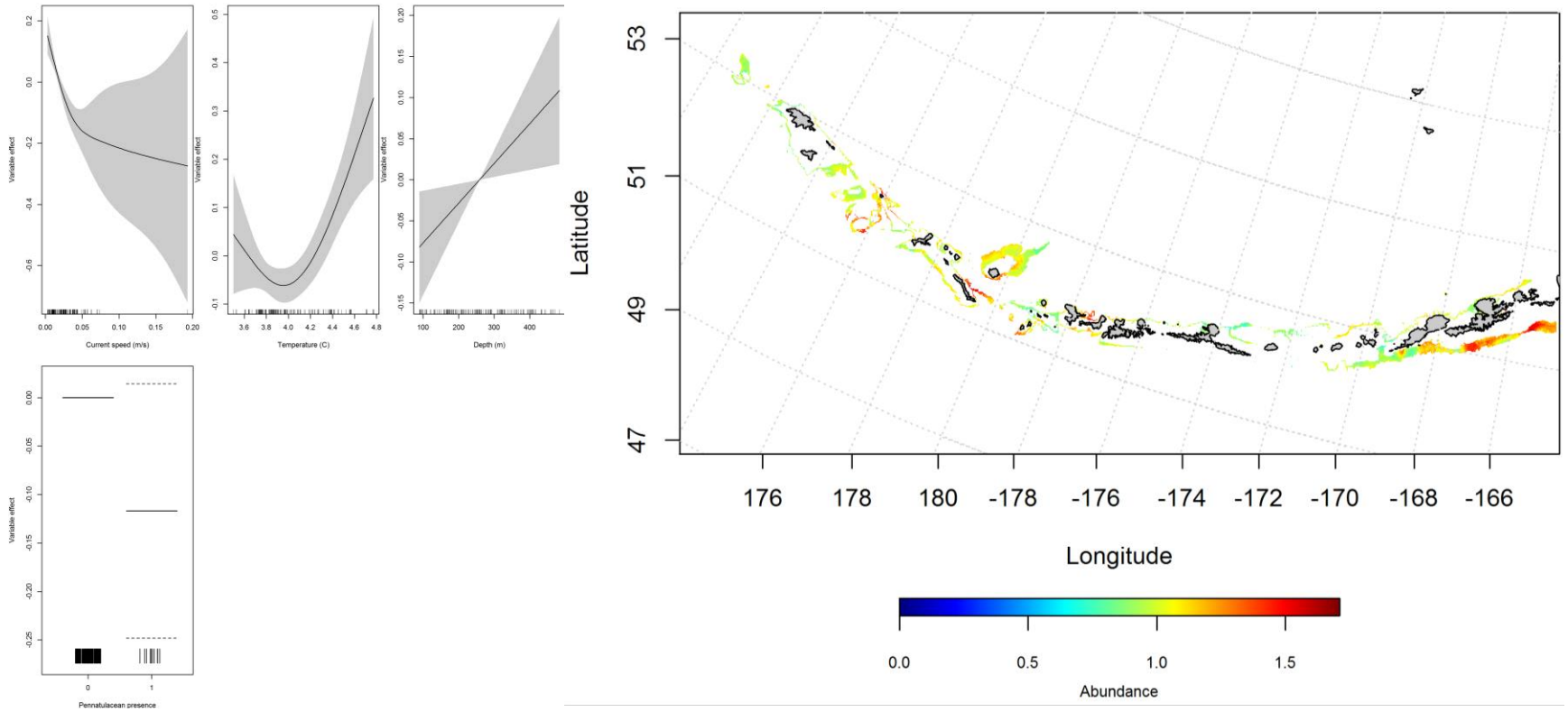

Figure 70. -- Best-fitting hurdle model effects of retained habitat variables on cpue of adult Dover sole from summer bottom trawl surveys of the Aleutian Islands (left panel) alongside hurdle-predicted adult Dover sole cpue (right panel).

Seasonal distribution of commercial fisheries catches of adult Dover sole in the Aleutian Islands -- There were only 41 instances of adult Dover sole observed in the commercial fisheries database, 27 in the fall and 14 in the winter (Figure 71 and Figure 72). All observations were found throughout the Aleutian Islands, and there were not enough cases to run the fall or winter models.

In the spring, bottom depth, ocean color, and current speed were the most important variables determining probable suitable habitat of Dover sole (relative importance: 32.4%, 23.5%, and 22.8%, respectively). The AUC of the spring maxent model was 94% for the training data and 80% for the test data. 83% of the training data and 80% of the test data sets were predicted correctly. The model predicted probable suitable habitat of Dover sole throughout the AI in the spring (Figure 73).

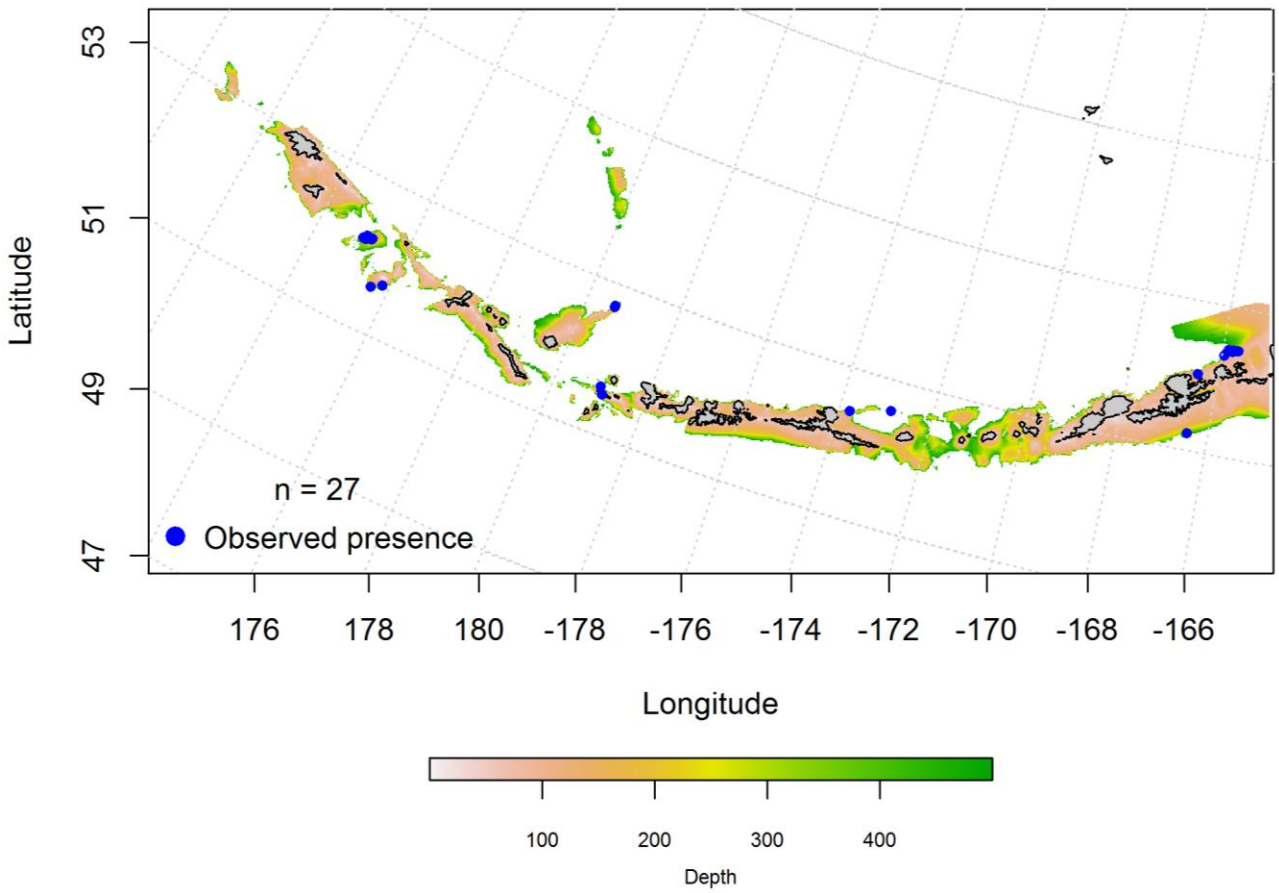

Figure 71. -- Locations of observed instances of Dover sole from commercial fisheries catches in the fall (September-November).

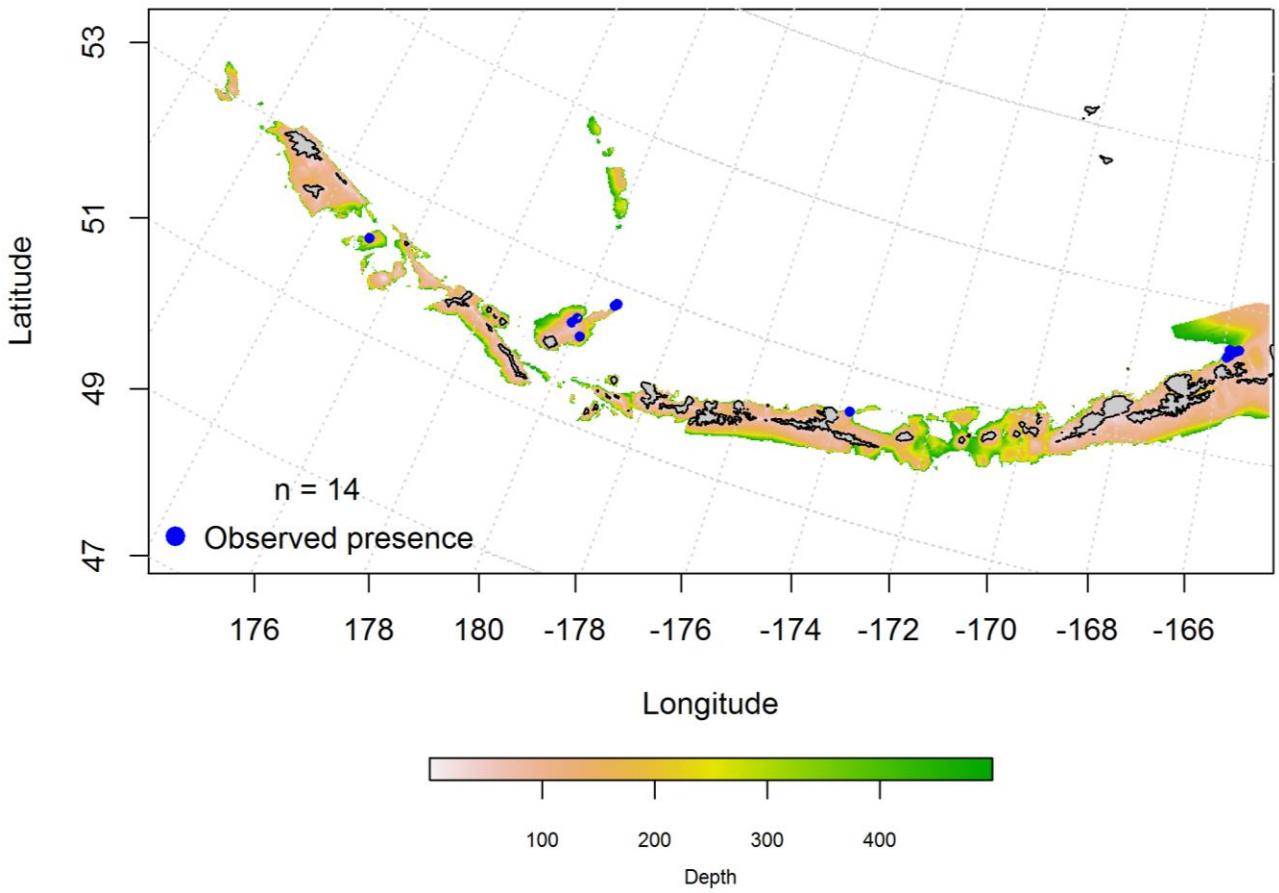

Figure 72. -- Locations of observed instances of Dover sole from commercial fisheries catches in the winter (December-February).

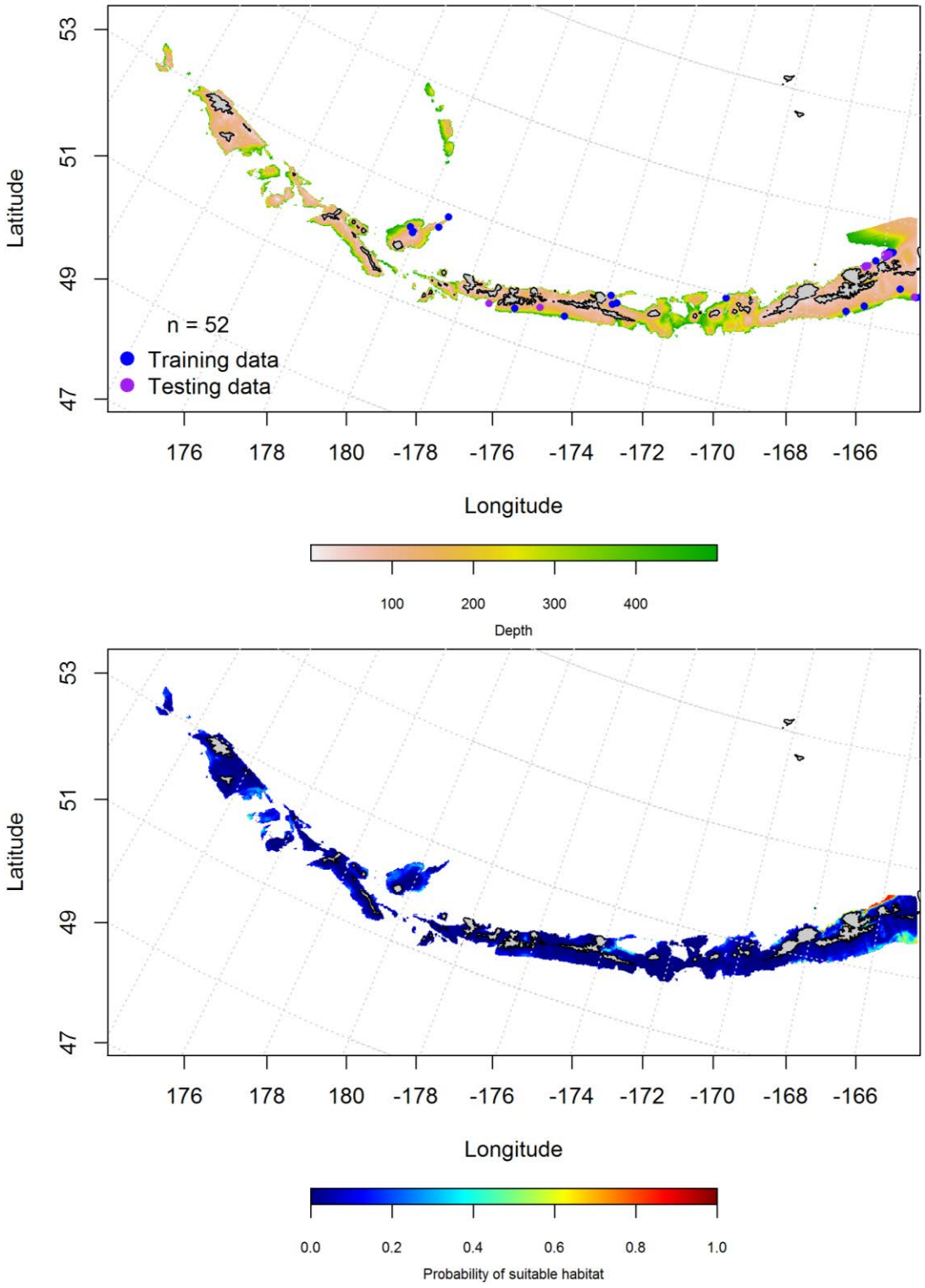

Figure 73. -- Locations of spring (March-May) commercial fisheries catches of Dover sole (top panel). Blue points were used to train the maximum entropy model predicting the probability of suitable spring habitat supporting commercial catches of Dover sole (bottom panel) and the purple points were used to validate the model.

Aleutian Islands Dover sole Essential Fish Habitat Maps and Conclusions -- In general, juvenile and adult Dover sole co-occur in most places where they are found. Those collected in summertime bottom trawl surveys share similar predicted EFH distributions across the Aleutian Islands (Figure 74). These similarities can be observed in both areas of high (western and eastern Aleutian Islands) and low abundance (e.g., central Aleutian Islands and large passes).

There were not enough observations to predict essential fish habitat in the AI during the fall and winter. EFH predicted from spring commercial catches of Dover sole has a limited distribution throughout the Aleutian Islands chain with a slightly higher abundance in the eastern AI north of Unalaska Island (Figure 75).

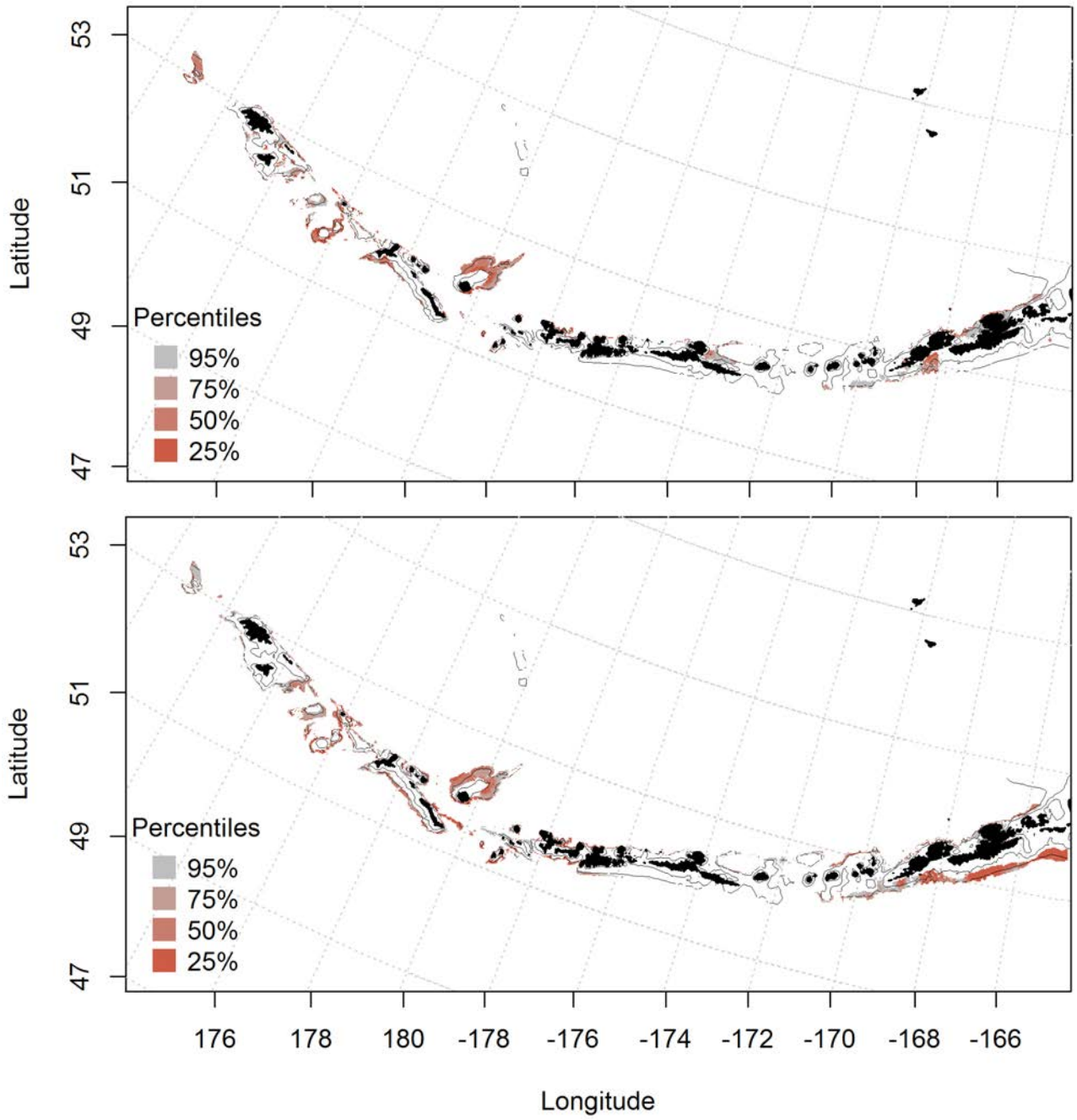

Figure 74. Essential fish habitat predicted for Dover sole juveniles and adults (top and bottom panel) from summertime groundfish trawls.

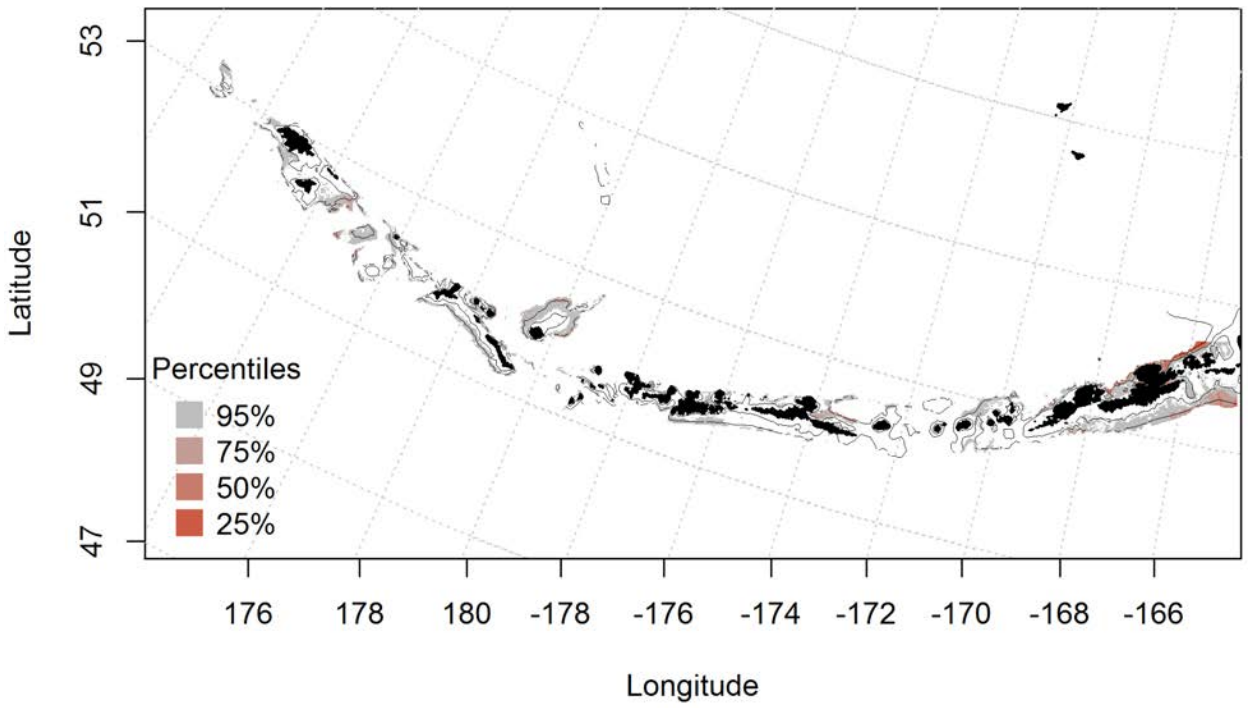

Figure 75. – Spring essential fish habitat predicted for Dover sole from summertime commercial catches.

3.2 Roundfishes

Atka mackerel (*Pleurogrammus monopterygius*)

Seasonal distribution of early life history stages of Atka mackerel in the Aleutian Islands -- Atka mackerel eggs were distributed throughout the AI (

Figure 76) and grouped on an annual basis. All observations are taken from underwater camera work, rather than the FOCI database. Because Atka mackerel are demersal spawners/nesters, the same variables regularly used for the GAM models were used in this maxent model. Bottom depth and coral presence were the most important variables (relative abundance: 34.4% and 14.3%) in modeling egg suitable habitat. The AUC for the training data is 96%, and 76% using the test data. 88% of the training data and 76% of the test data sets were correctly classified. The model predicted Atka mackerel egg probable suitable habitat throughout the AI (Figure 77).

There were only 10 instances of Atka mackerel larvae observed in the FOCI database (Figure 78), 6 in the winter and 4 in the spring. All observations were found in the central and eastern AI. There were not enough cases in the winter or spring to run the maxent models.

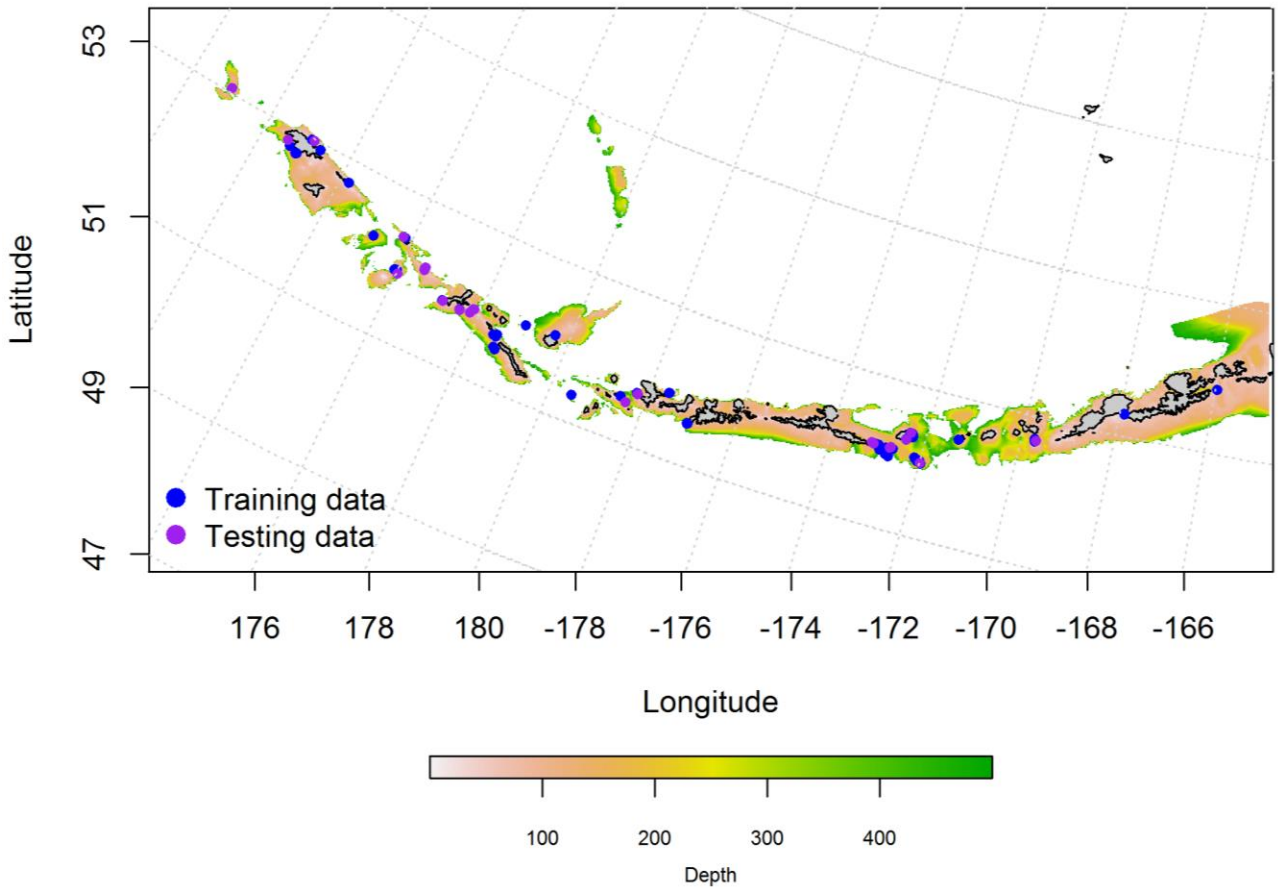

Figure 76.Annual observations of Atka mackerel eggs from the Aleutian Islands.

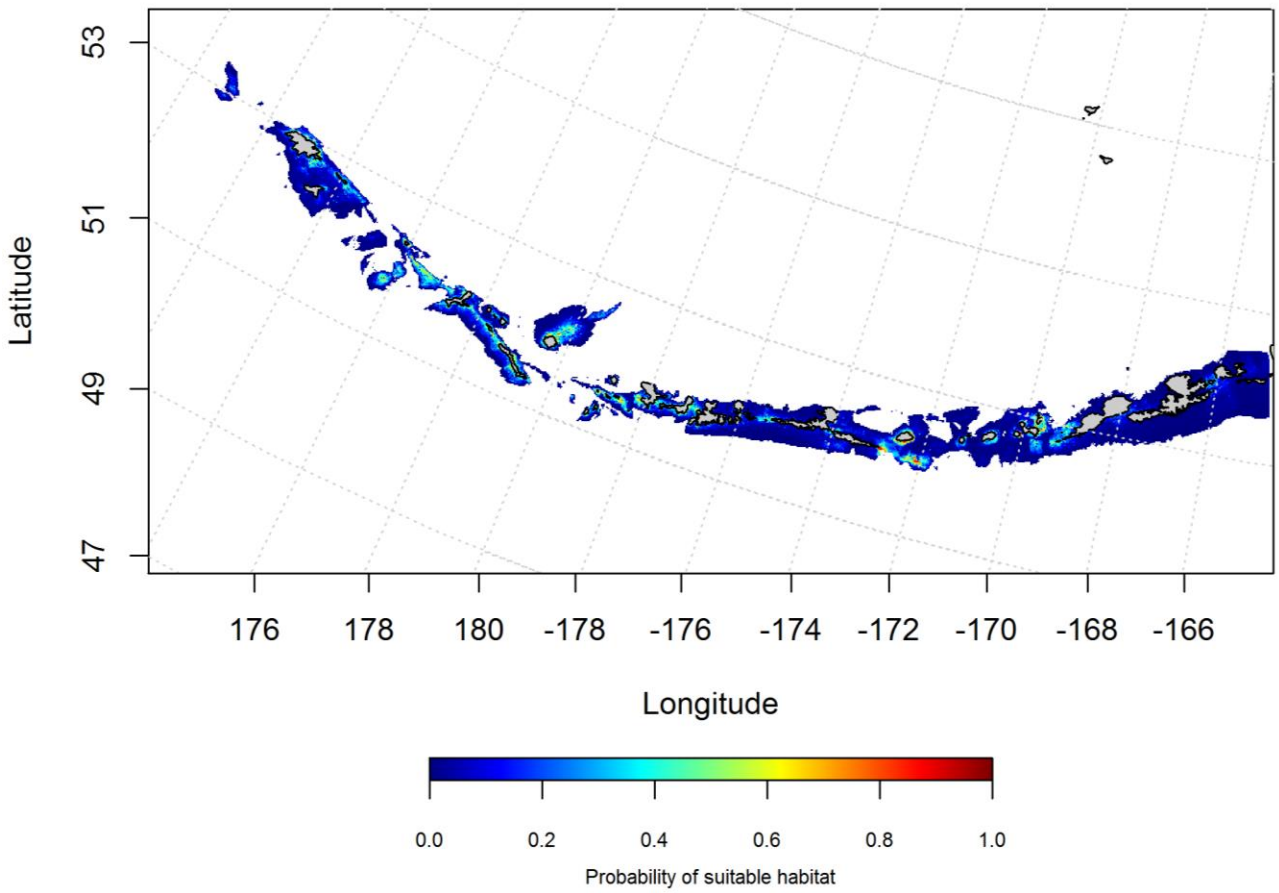

Figure 77. Predicted probability of annual distribution of Atka mackerel eggs from maximum entropy modeling of the Aleutian Islands.

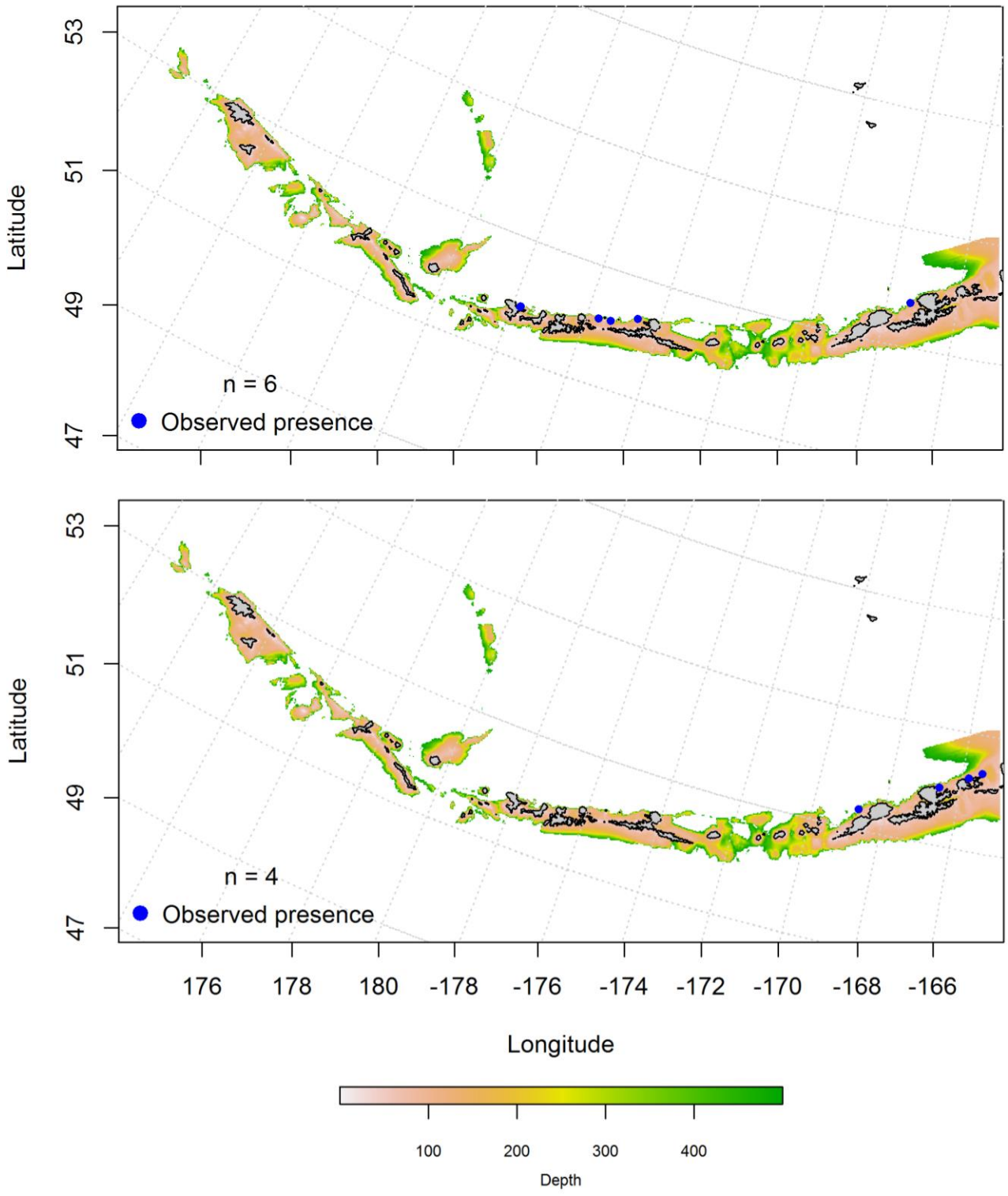

Figure 78. Winter and spring observations (top and bottom panel) of larval Atka mackerel from the Aleutian Islands.

Summertime distribution of juvenile and adult Atka mackerel from bottom trawl surveys of the Aleutian Islands -- A two-step hurdle-Generalized additive model predicting the presence absence (PA GAM) of juvenile Atka mackerel explained 89% of the variability in CPUE in the bottom trawl survey training data, and 87% of the variability in the test data set. Geographic location and bottom depth were the most important variables explaining the distribution of juvenile Atka mackerel presence or absence. The model correctly classified 82% of the training and test data sets, and explained 36.9% of the deviance. Juveniles were distributed throughout the AI, though the highest predicted abundance was in the large pass between Agattu and Kiska Islands (Figure 79).

The second part of the juvenile Atka mackerel hurdle-GAM predicted CPUE and explained 21% of the variability of the training data set, 26% of the test data set, and 20.5% of the deviance. Geographic location and bottom depth were also the most important variables explaining the distribution of juvenile Atka mackerel CPUE GAM. The areas of predicted highest abundance were similar to the PA GAM, in the western AI (Figure 80).

A generalized additive model predicting the abundance of adult Atka mackerel explained 28% of the training data set variability in CPUE in the bottom trawl survey. Bottom depth and geographic location were the most important variables explaining the distribution of adult Atka mackerel. The model explained 26% of the test data set variability, and 27.6% of the deviance. Adult Atka mackerel were distributed throughout the AI (Figure 5).

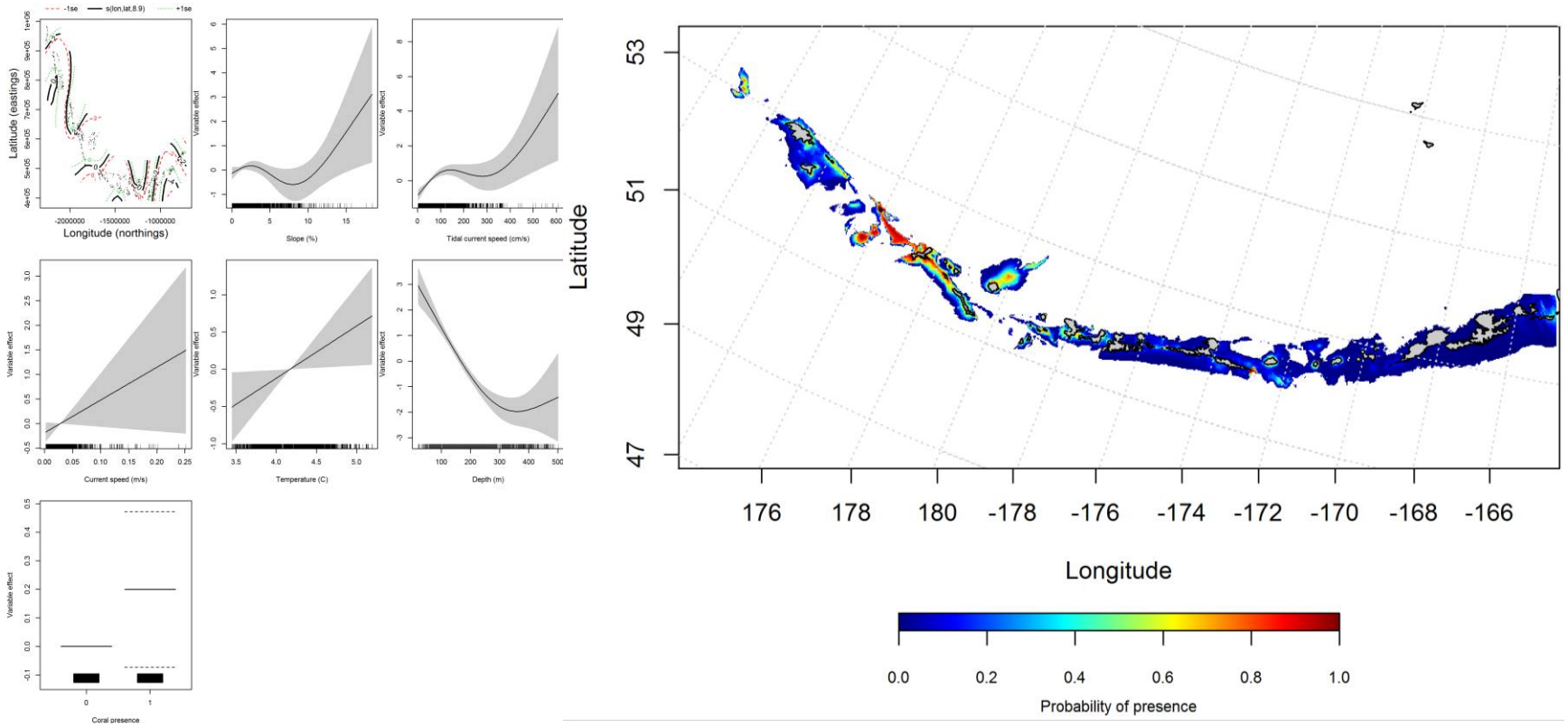

Figure 79. Best-fitting hurdle effects of retained habitat variables on presence absence (PA) of juvenile Atka mackerel from summer bottom trawl surveys of the Aleutian Islands (left panel) alongside hurdle-predicted juvenile Atka mackerel PA (right panel).

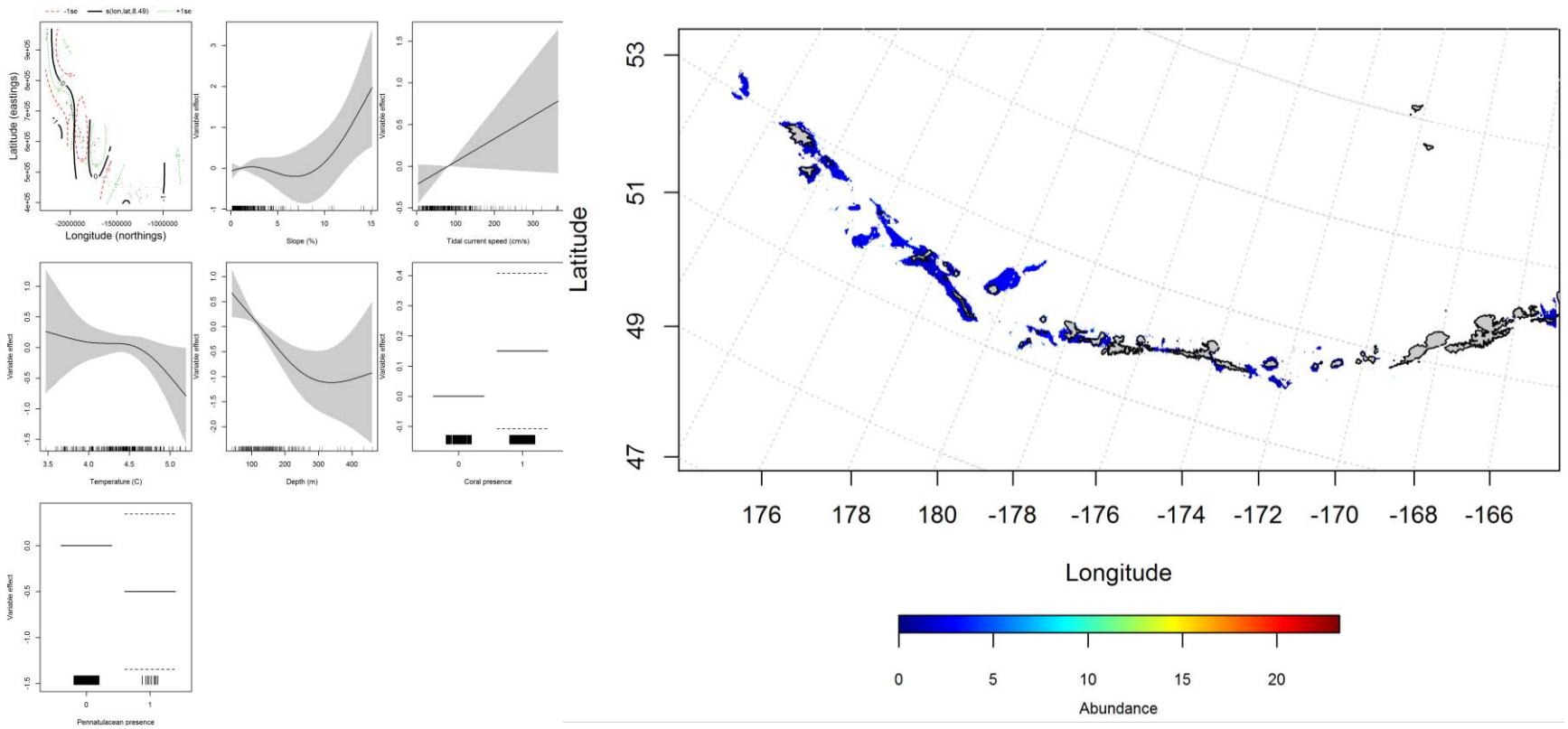

Figure 80.Best-fitting hurdle effects of retained habitat variables on CPUE of juvenile Atka mackerel from summer bottom trawl surveys of the Aleutian Islands (left panel) alongside hurdle-predicted juvenile Atka mackerel CPUE (right panel).

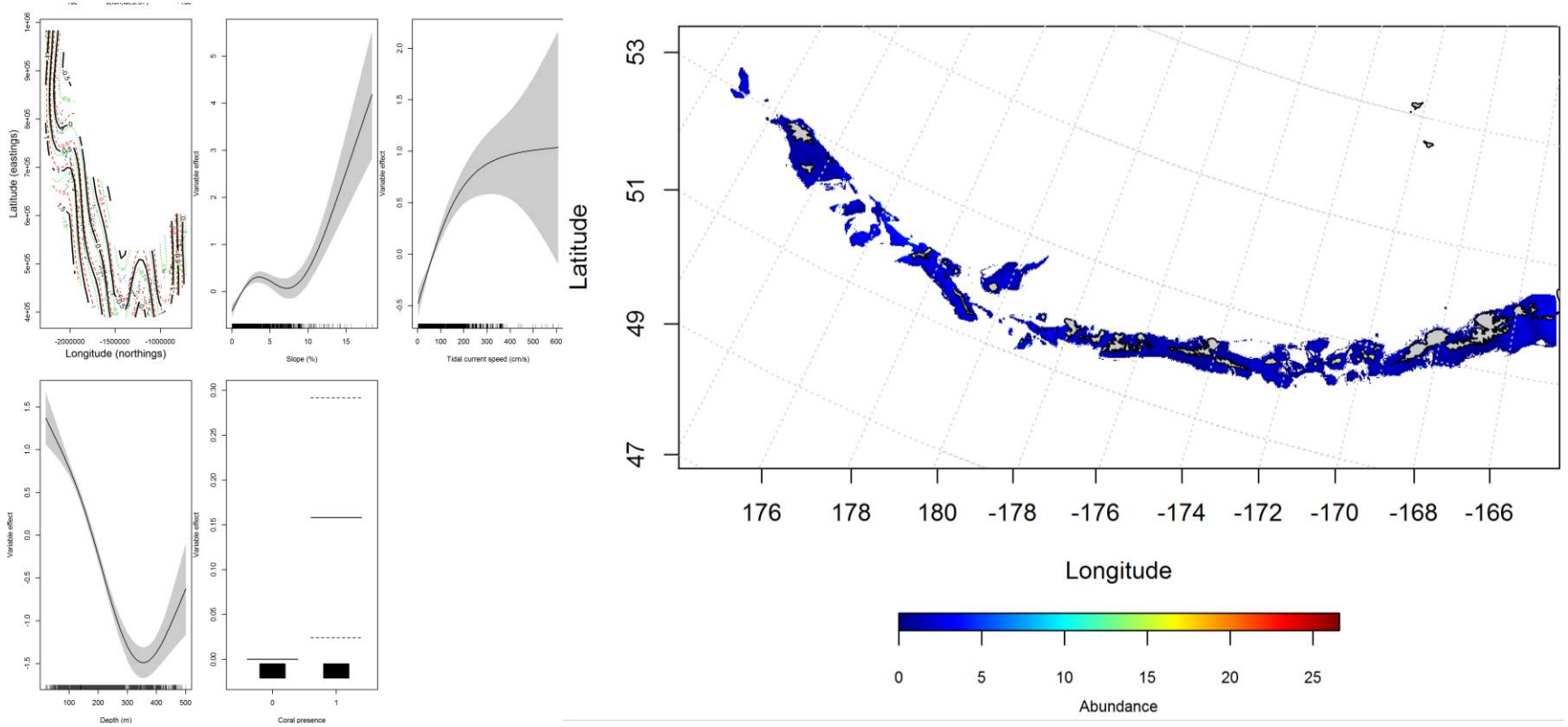

Figure 81. Best-fitting hurdle effects of retained habitat variables on CPUE of adult Atka mackerel from summer bottom trawl surveys of the eastern Aleutian Islands(left panel) alongside hurdle-predicted adult Atka mackerel CPUE (right panel)..

Seasonal distribution of commercial fisheries catches of adult Atka mackerel in the Aleutian Islands -- Distribution of adult Atka mackerel in the Aleutian Islands in commercial fisheries catches was generally consistent throughout all seasons. In the fall, bottom depth, bottom temperature, and tidal current were the most important variables determining probable suitable habitat of Atka mackerel (relative importance: 54.6%, 17.6%, and 11.8%, respectively). The AUC of the fall maxent model was 93% for the training data and 84% for the test data. 85% of the cases in the training data set and 84% of the cases in the test data set were predicted correctly. The model predicted probable suitable habitat of Atka mackerel catches throughout the AI, though less abundant in areas with large passes (Figure 82).

In the winter, bottom depth, bottom temperature, and ocean color were the most important variables determining the probability of suitable habitat of Atka mackerel (relative importance: 46.3%, 25%, and 16.8%, respectively). The AUC of the winter maxent model was 95% for the training data and 86% for the test data. 88% of the cases in both the training data sets and 86% in the test data were predicted correctly. As with the fall, the model predicted probable suitable habitat of Atka mackerel catches throughout the AI, though less abundant in areas with large passes (Figure 83).

In the spring, bottom depth and ocean color were the most important variables determining probable suitable habitat of Atka mackerel (relative importance: 64.3% and 13.9%). The AUC of the spring maxent model was 90% for the training data and 84% for the test data. The model correctly classified 82% of the training data and 84% of the test data sets. As with the fall and winter, the model predicted probable suitable habitat of Atka mackerel catches throughout the AI, though less abundant in areas with large passes (Figure 84).

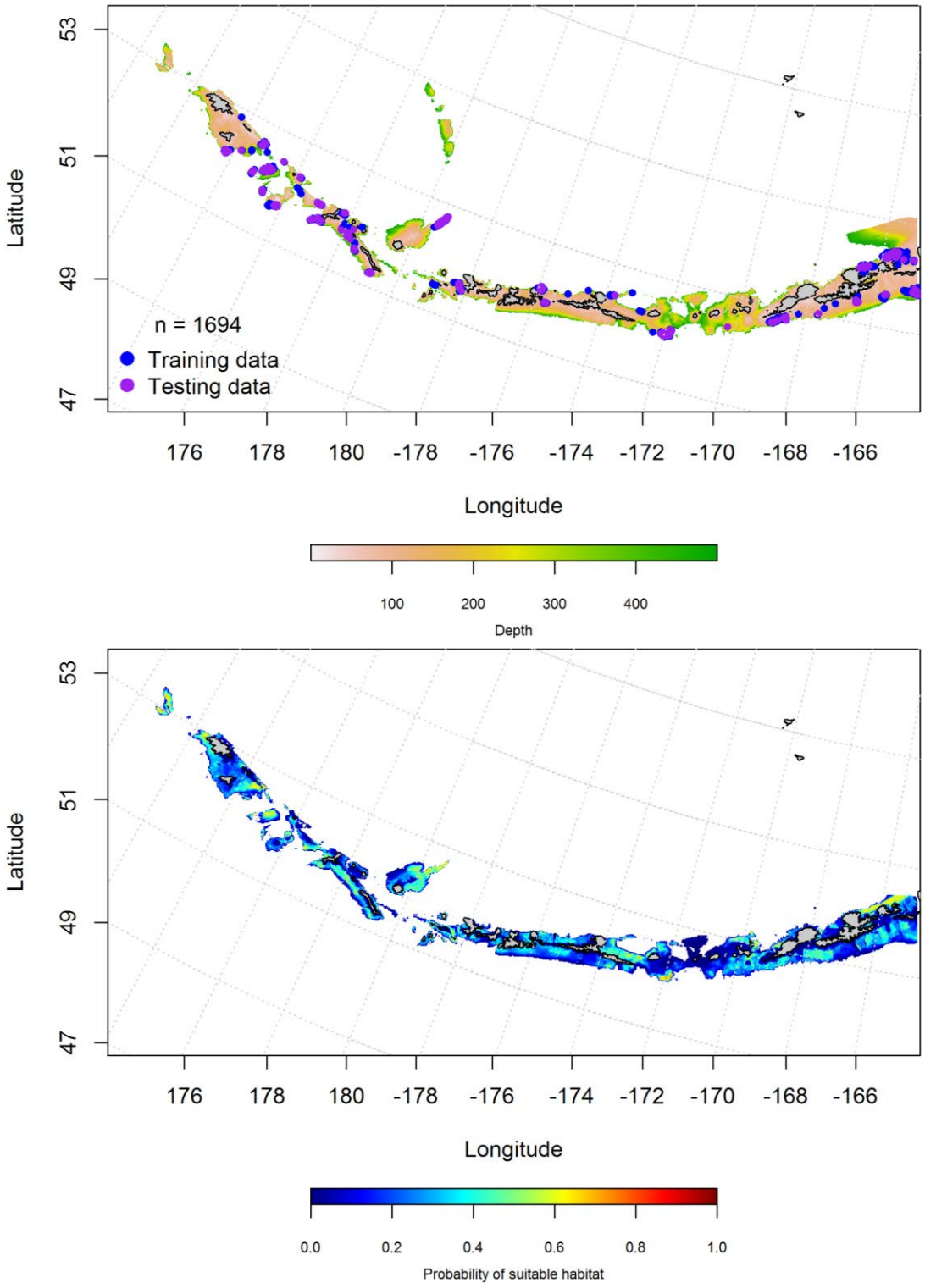

Figure 82. Locations of fall (September-November) commercial fisheries catches of adult Atka mackerel (top panel). Blue points were used to train the maximum entropy model predicting the probability of suitable fall habitat supporting commercial catches of adult Atka mackerel (bottom panel) and the purple points were used to validate the model.

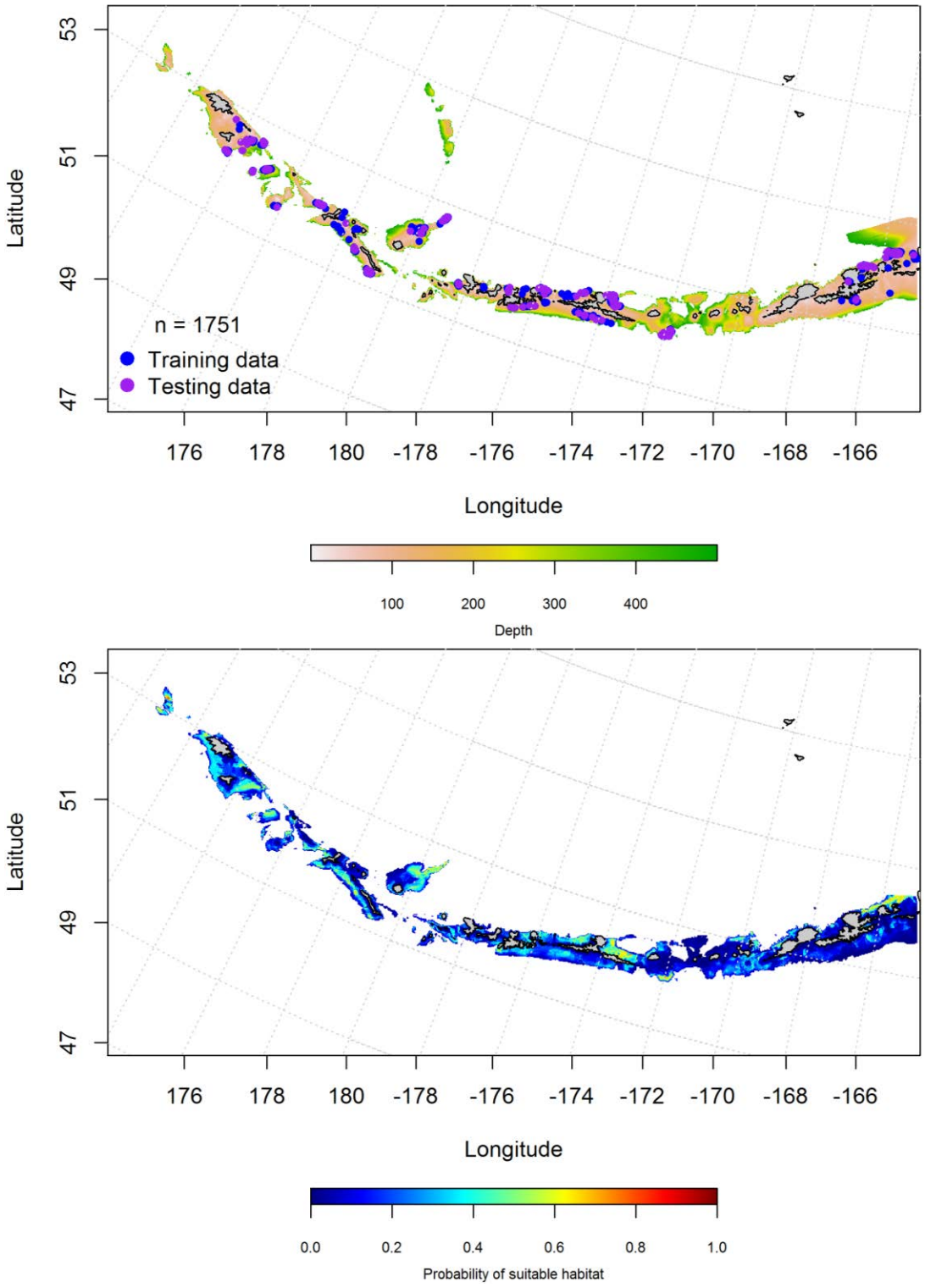

Figure 83. Locations of winter (December-February) commercial fisheries catches of adult Atka mackerel (top panel). Blue points were used to train the maximum entropy model predicting the probability of suitable winter habitat supporting commercial catches of adult Atka mackerel (bottom panel) and the purple points were used to validate the model.

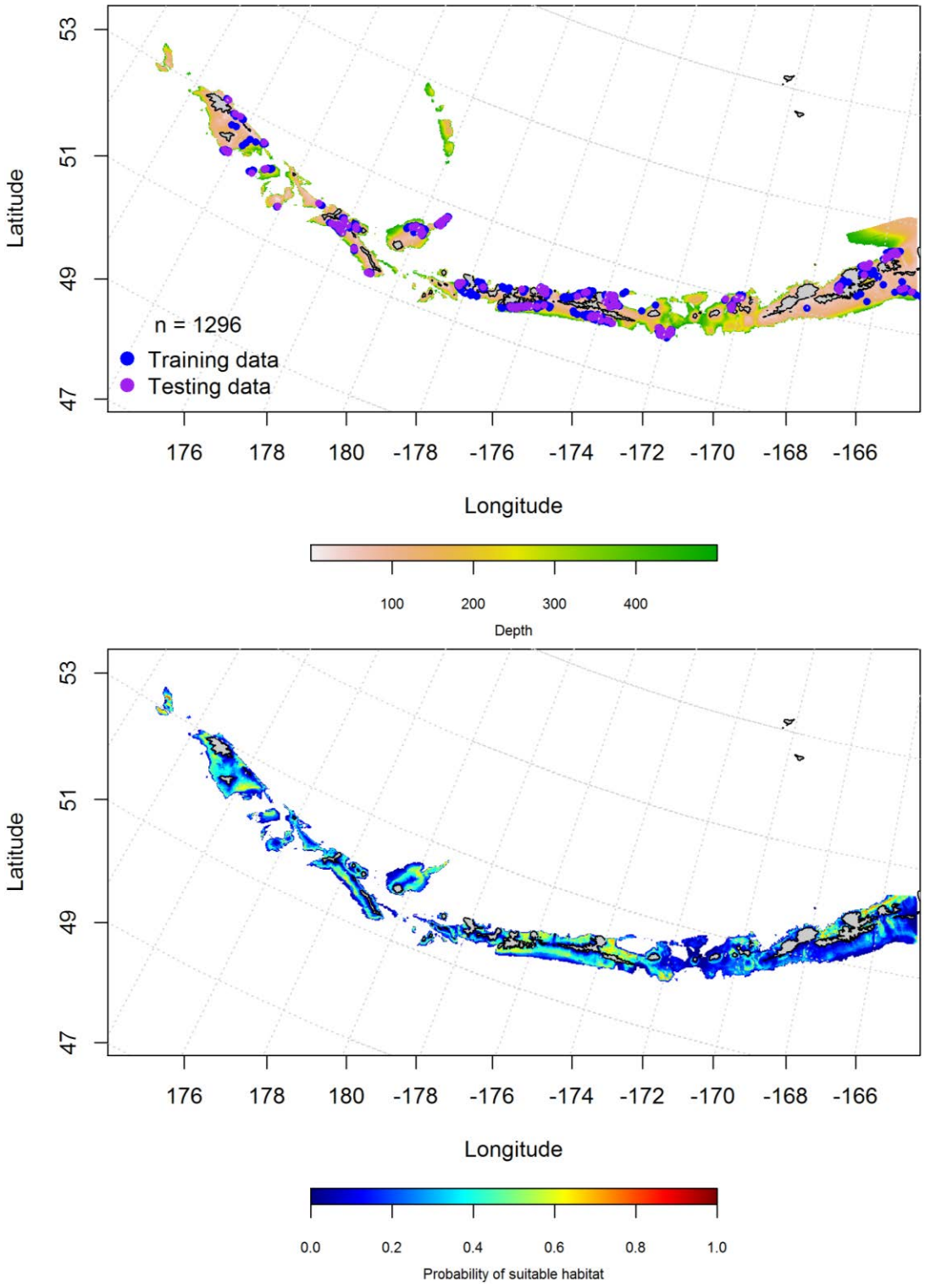

Figure 84. Locations of spring (March-May) commercial fisheries catches of adult Atka mackerel (top panel). Blue points were used to train the maximum entropy model predicting the probability of suitable spring habitat supporting commercial catches of adult Atka mackerel (bottom panel) and the purple points were used to validate the model.

Aleutian Islands Atka mackerel Essential Fish Habitat Maps and Conclusions --

Predicted EFH for Atka mackerel eggs was highest in the western and central AI (Figure 85).

Adult Atka mackerel are distributed throughout the AI whereas juveniles have a more limited predicted EFH in the western AI (Figure 86).

There were no seasonal differences in adult Atka mackerel essential fish habitat. Adults were distributed similarly through the Aleutian Islands (Figure 87).

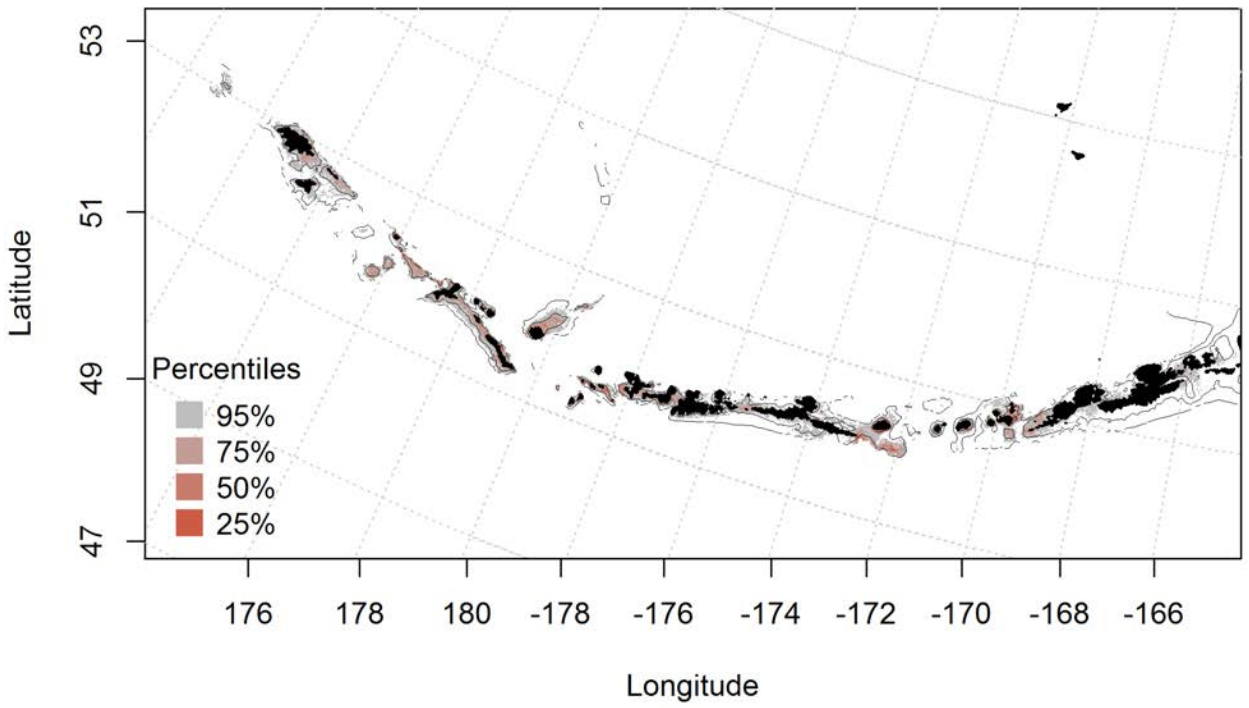

Figure 85. Essential fish habitat predicted for Atka mackerel eggs.

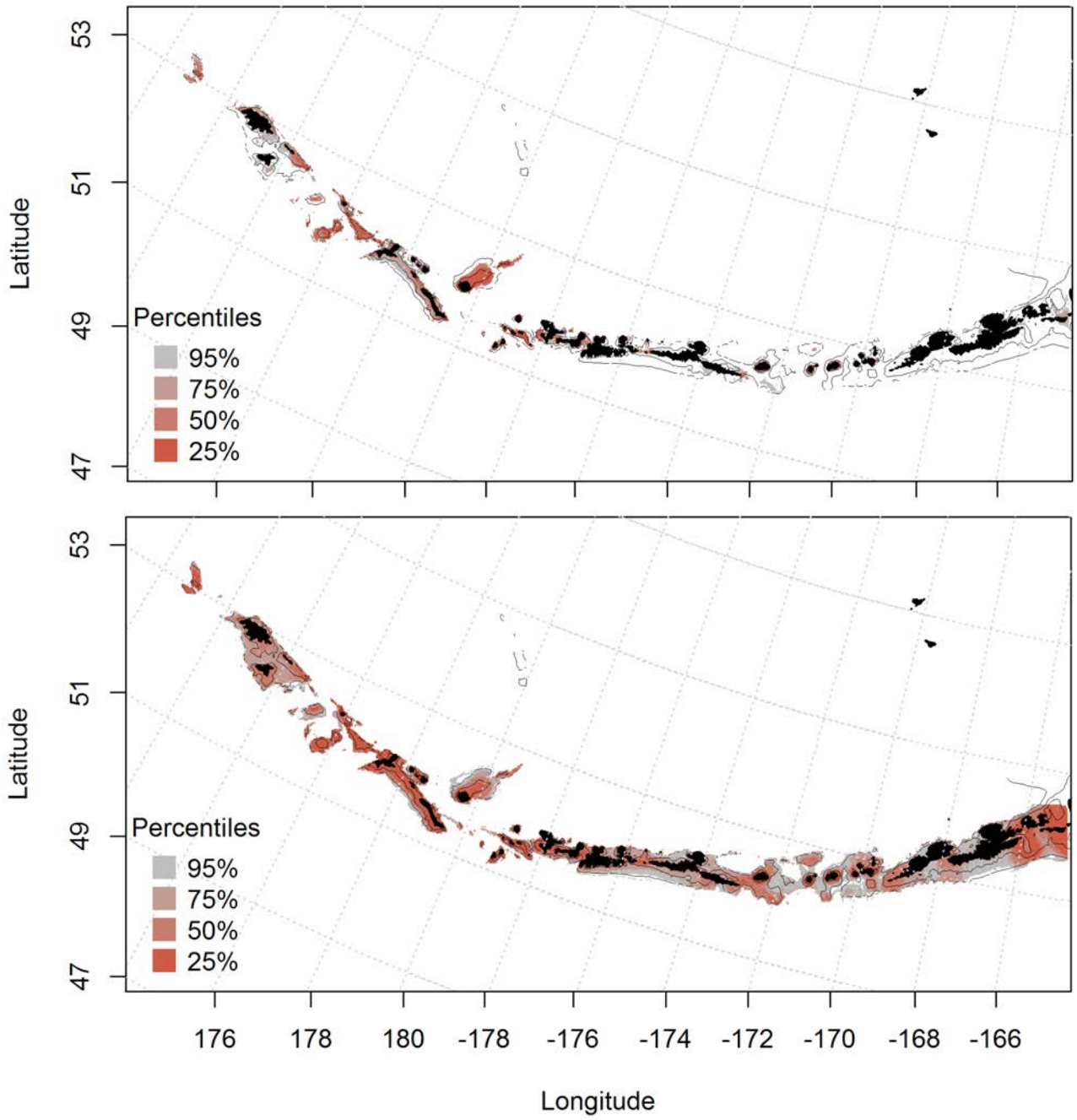

Figure 86. Predicted summer essential fish habitat for Atka mackerel juveniles and adults (top and bottom panel) from summertime bottom trawl surveys.

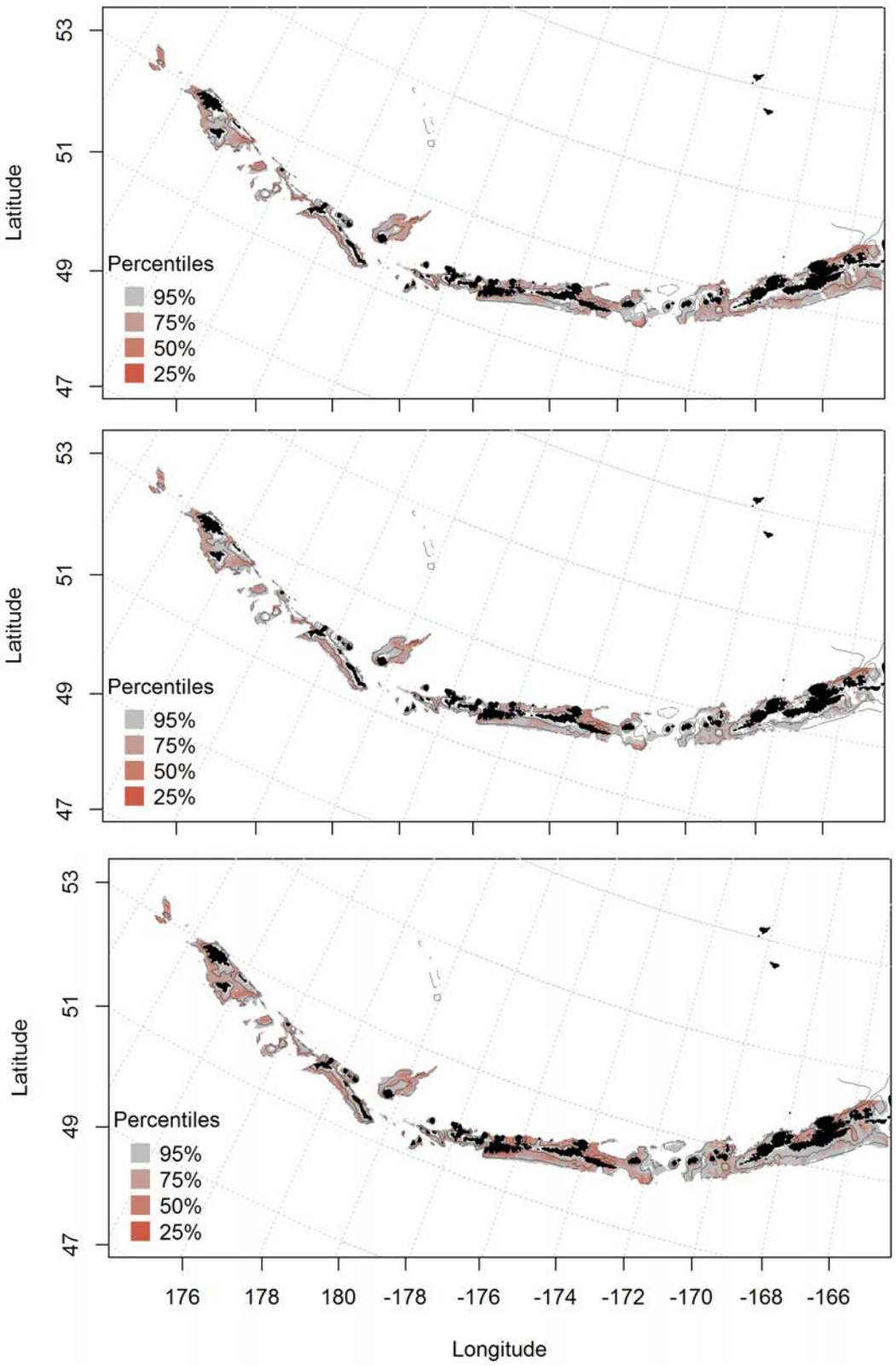

Figure 87. Essential fish habitat predicted for Atka mackerel during fall (top panel), winter (middle panel) and spring (bottom panel) from summertime commercial catches.

Pacific cod (*Gadus macrocephalus*)

Seasonal distribution of early life history stages of Pacific cod in the Aleutian Islands -- There was only 1 instance of Pacific cod eggs observed in the FOCI database (not enough to run the model). All observations were found in the eastern AI (Figure 88).

There were only 45 instances of Pacific cod larvae observed in the FOCI database, 43 in the spring and 2 in the summer. All observations found in the eastern AI (Figure 89). There were not enough cases to run the model in the spring or summer.

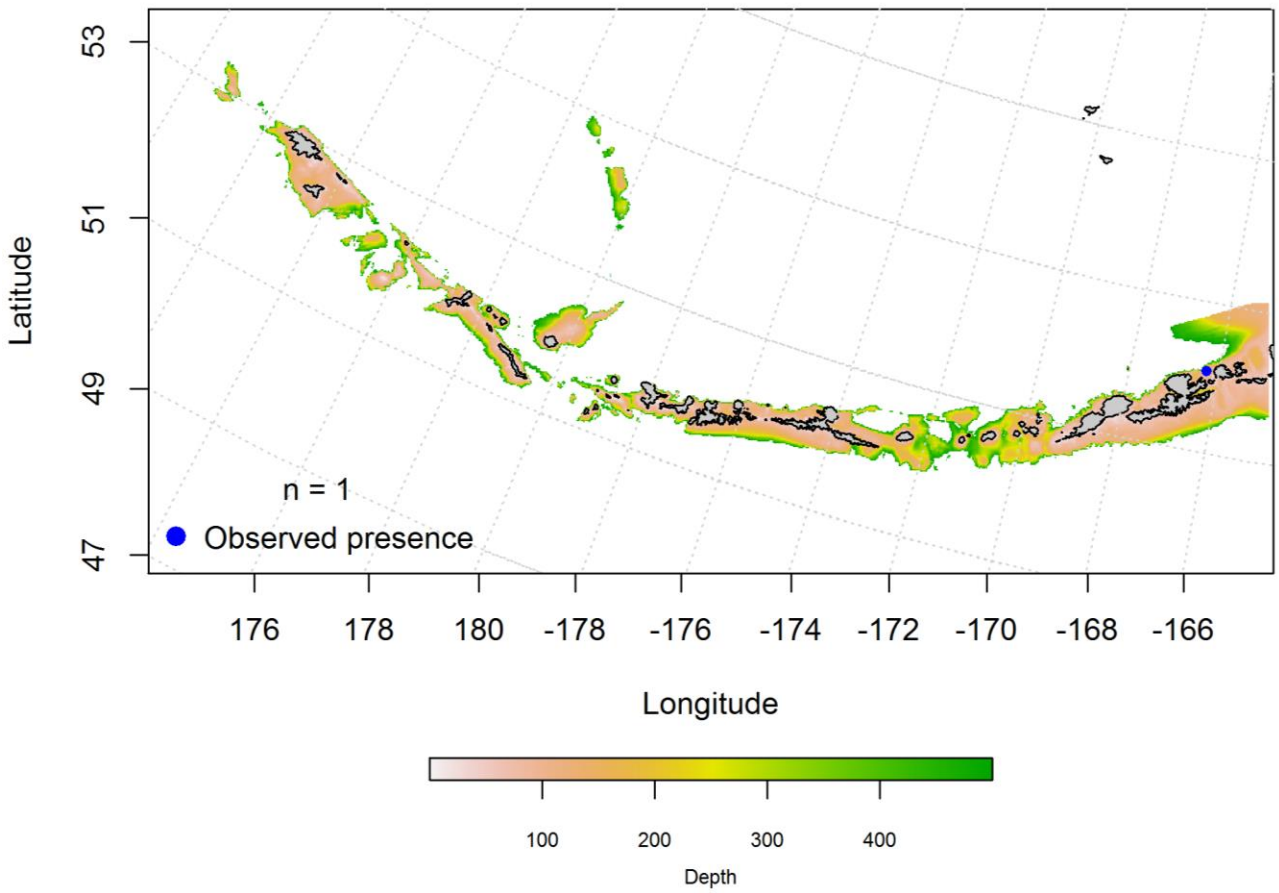

Figure 88. Spring observations of Pacific cod eggs from the Aleutian Islands.

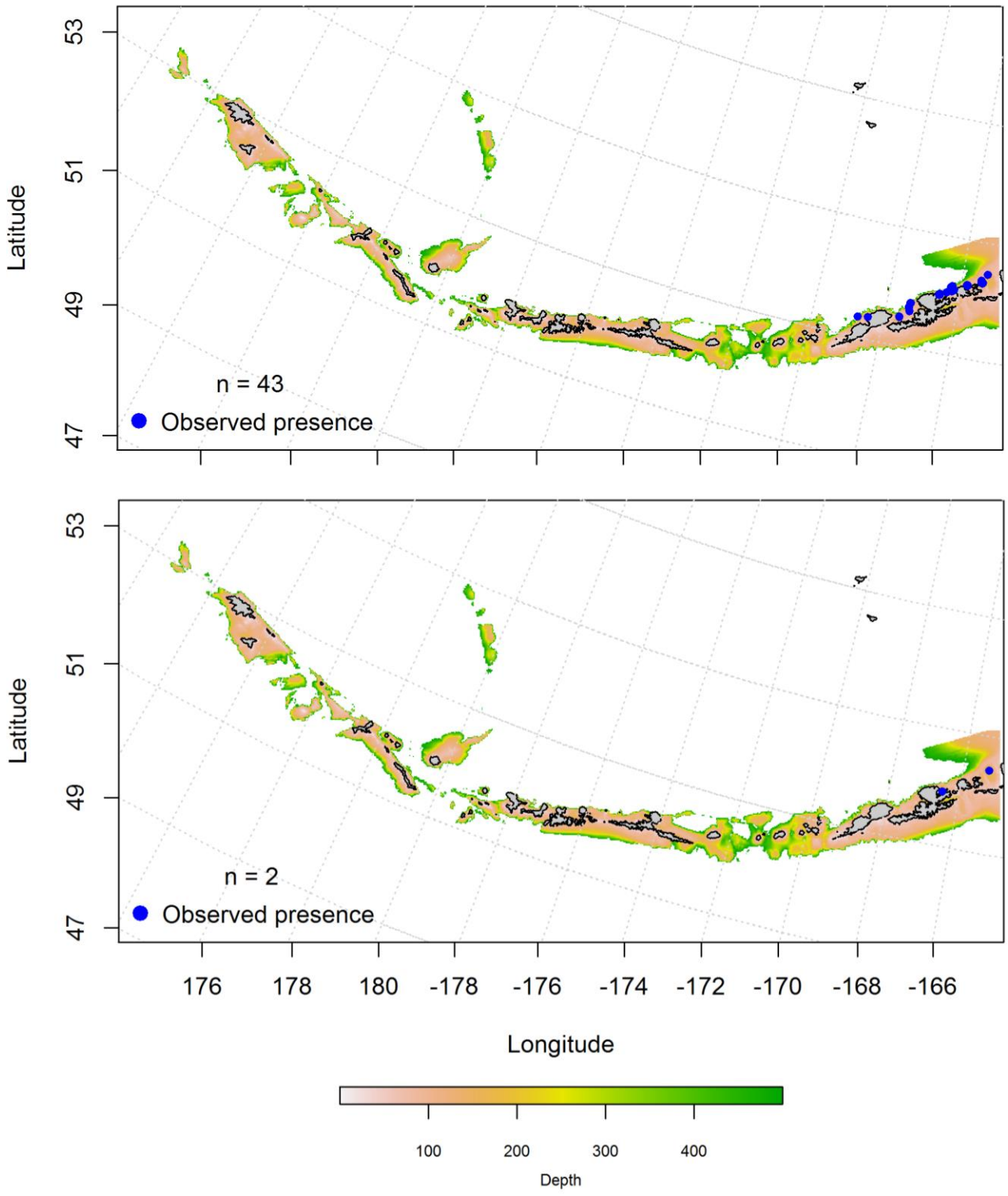

Figure 89. Spring and summer observations (top and bottom panel) of larval Pacific cod from the Aleutian Islands.

Summertime distribution of juvenile and adult Pacific cod from bottom trawl surveys of the Aleutian Islands -- The catch of Pacific cod in summer bottom trawl surveys of the Aleutian Islands indicates this species is broadly distributed. A generalized additive model predicting the abundance of juvenile Pacific cod explained 22% of the training data variability and 24% of the test data variability in CPUE from the bottom trawl survey. The model explained 22.1% of the deviance. Bottom depth and geographic location were the most important variables explaining the distribution of juvenile Pacific cod. Juvenile Pacific cod are distributed throughout the AI, though areas of predicted highest abundance were in the eastern AI (Figure 90).

A generalized additive model predicting the abundance of adult Pacific cod explained 29% of the training data variability and 30% of the test data variability in CPUE from the bottom trawl survey. The model also explained 29.1% of the deviance. Bottom depth and geographic location were the most important variables explaining the distribution of adult Pacific cod. Adults were distributed throughout the AI (Figure 91).

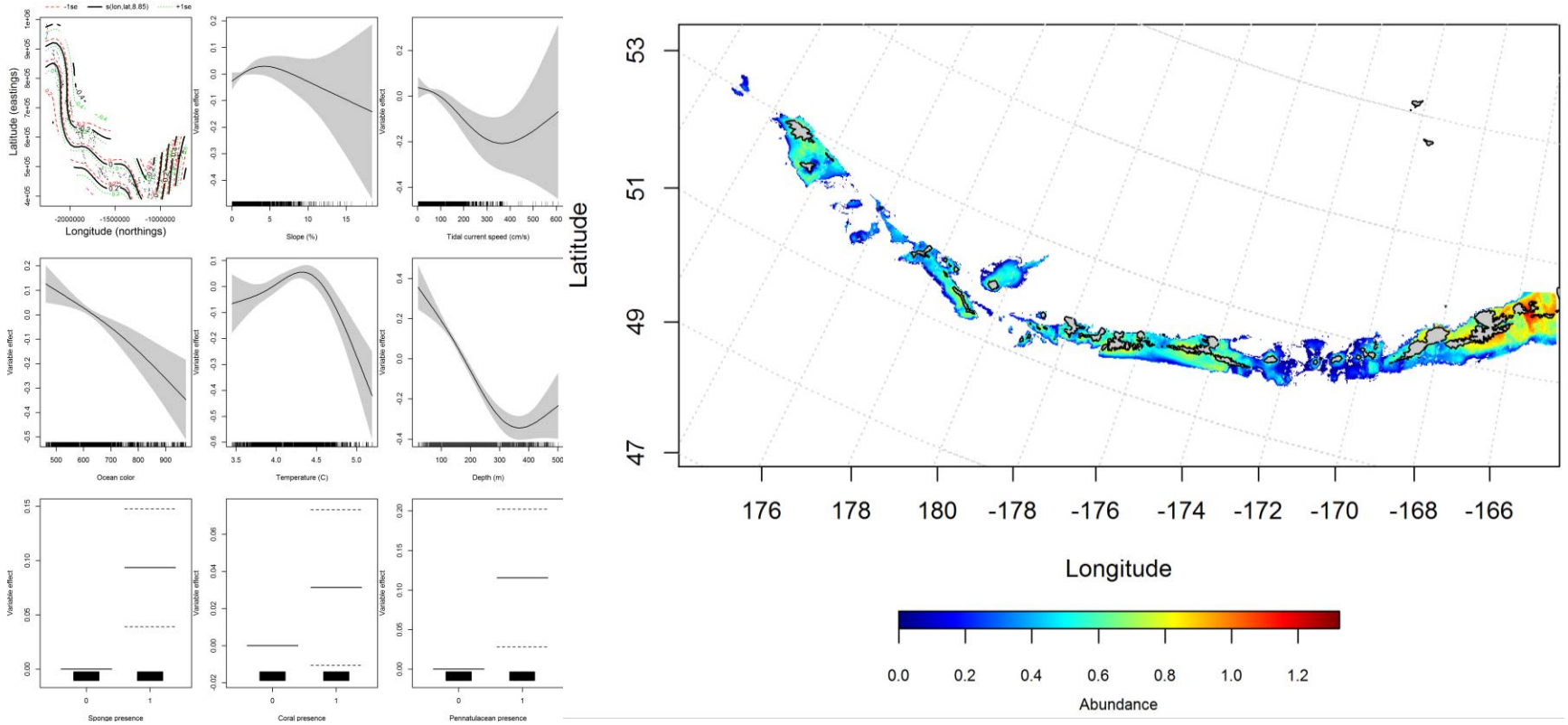

Figure 90. Best-fitting generalized additive model (GAM) effects of retained habitat variables on abundance of juvenile Pacific cod from summer bottom trawl surveys of the Aleutian Islands (left panel) alongside GAM-predicted juvenile Pacific cod abundance (right panel).

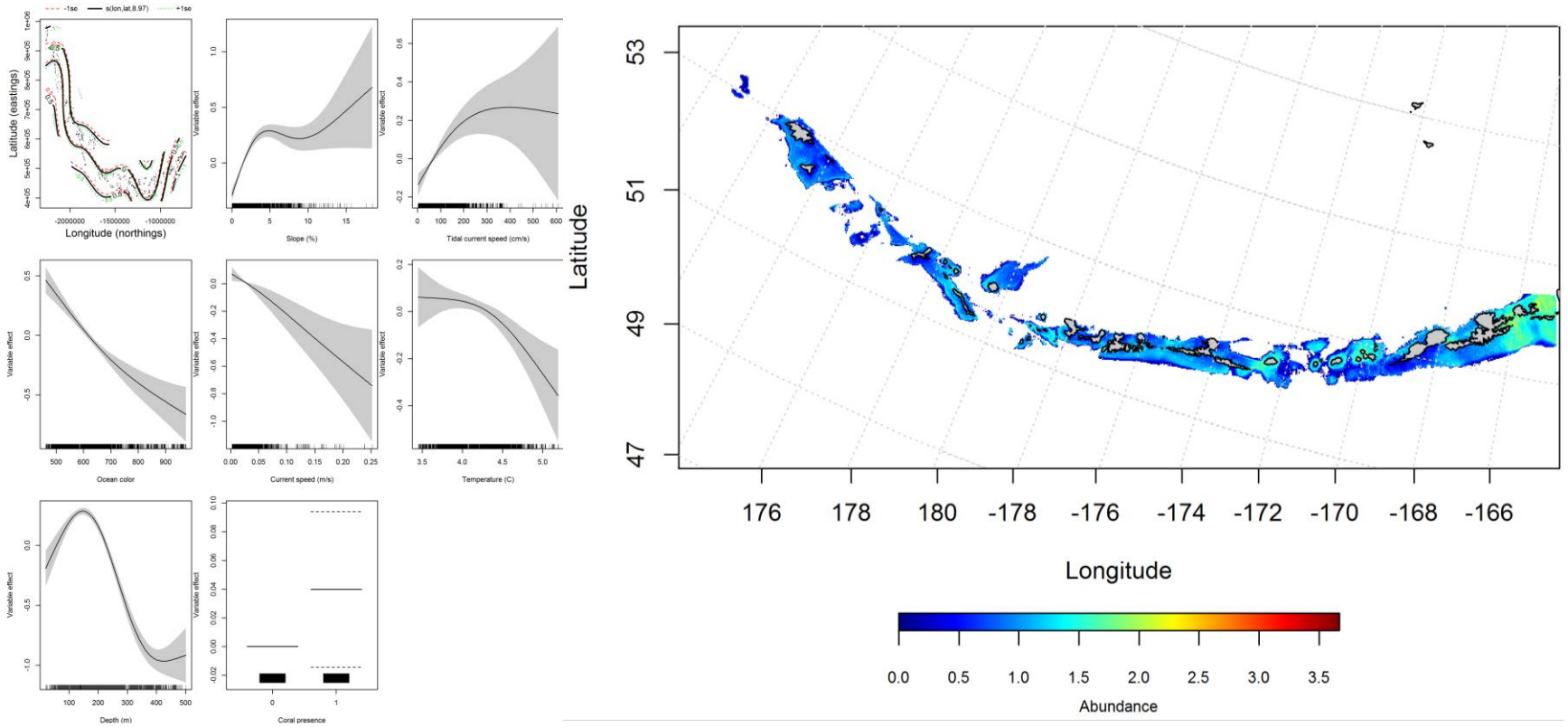

Figure 91. Best-fitting generalized additive model (GAM) effects of retained habitat variables on abundance of adult Pacific cod from summer bottom trawl surveys of the Aleutian Islands (left panel) alongside GAM-predicted adult Pacific cod abundance (right panel).

Seasonal distribution of commercial fisheries catches of adult Pacific cod in the Aleutian Islands-- Distribution of adult Pacific cod in the Aleutian Islands in commercial fisheries catches was generally consistent throughout all seasons. In the fall, bottom depth and ocean color were the most important variables determining probable suitable habitat of adult Pacific cod (relative importance: 69.8% and 11.5%). The AUC of the fall maxent model was 90% for the training data and 85% for the test data. 82% of the cases in the training data and 85% of the test data set were predicted correctly. The model predicted probable suitable habitat of Pacific cod catches throughout the AI with areas of highest abundance in the central and eastern AI (Figure 92).

Bottom depth and ocean color were the most important variables determining probable suitable habitat of Pacific cod in the winter (relative importance: 65.6% and 18.5%). The AUC of the winter maxent model was 92% for the training data and 86% for the test data. The model correctly classified 85% of the training data and 86% of the test data sets. As with the fall, the model predicted probable suitable habitat of Pacific cod catches across the AI with areas of highest abundance in the central and western AI (Figure 93).

In the spring, bottom depth and ocean color were the most important variables determining probable suitable habitat of Pacific cod (relative importance: 78.6% and 12.1%). The AUC of the spring maxent model was 89% for the training data and 79% for the test data. The model correctly classified 81% of the training data and 79% of the test data. As with the fall and winter, the model predicted probable suitable habitat of Pacific cod across the AI with areas of highest abundance in the central and western AI (Figure 94).

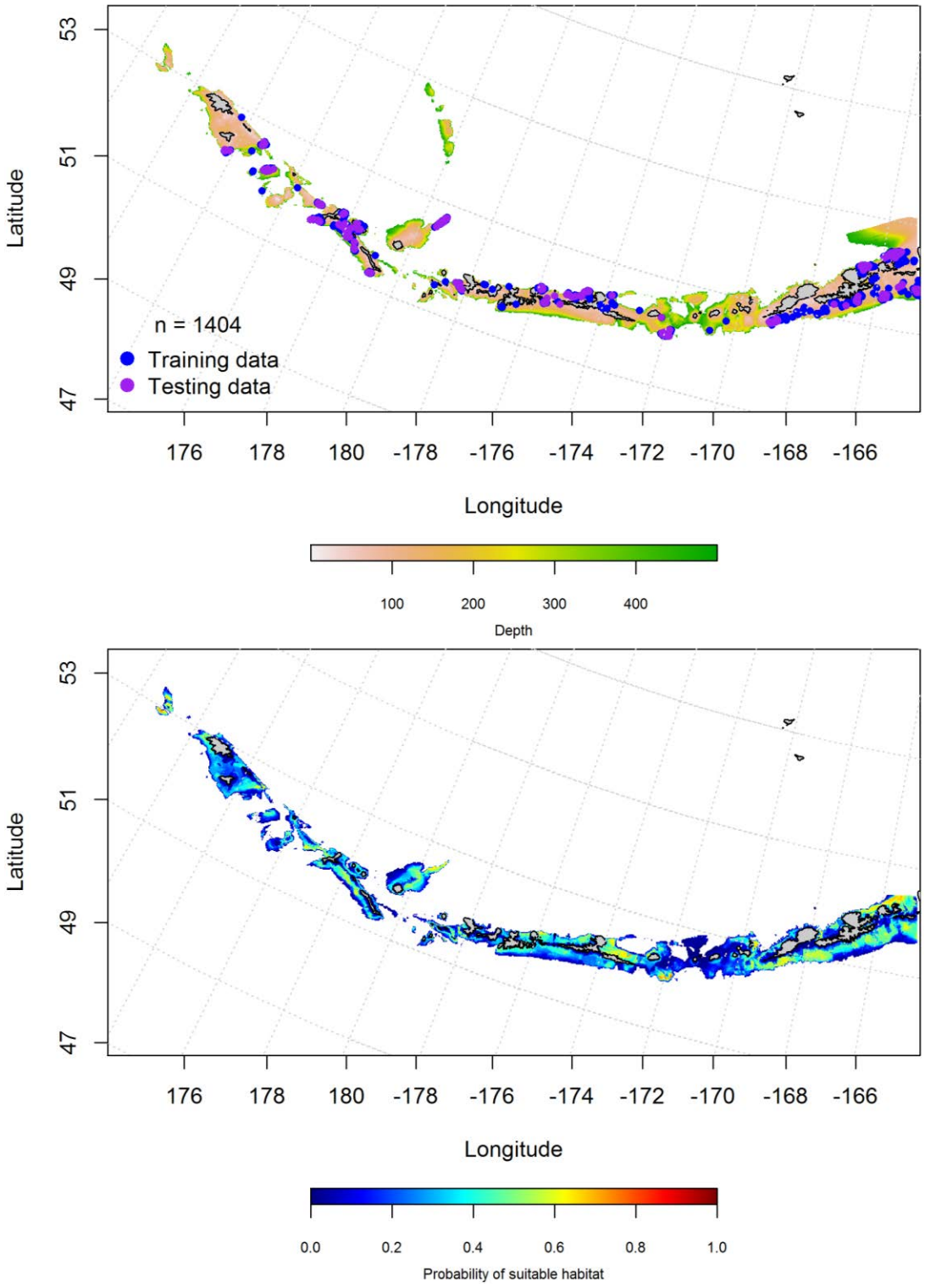

Figure 92. Locations of fall (September-November) commercial fisheries catches of adult Pacific cod (top panel). Blue points were used to train the maximum entropy model predicting the probability of suitable fall habitat supporting commercial catches of adult Pacific cod (bottom panel) and the purple points were used to validate the model.

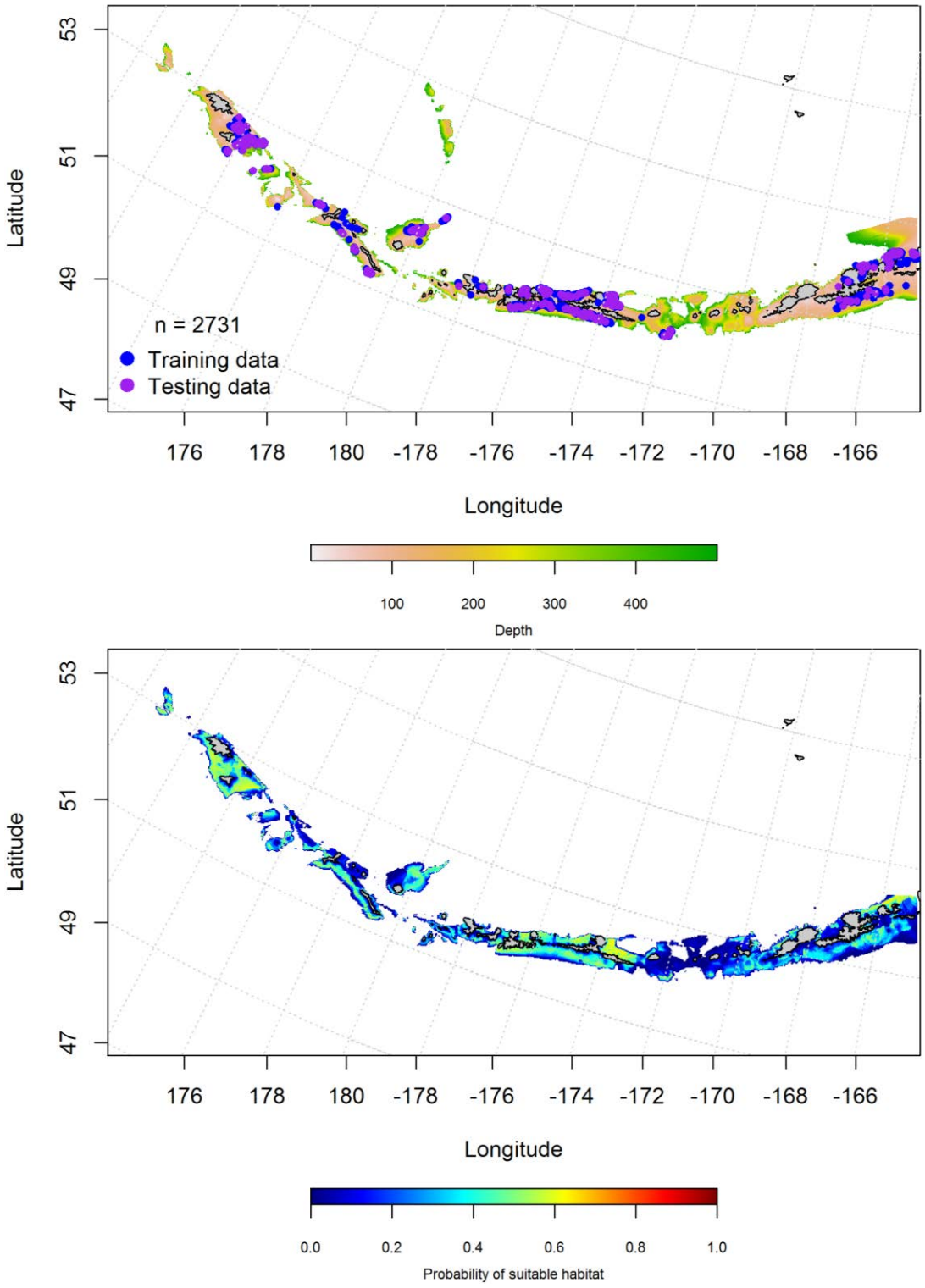

Figure 93. Locations of winter (December-February) commercial fisheries catches of adult Pacific cod (top panel). Blue points were used to train the maximum entropy model predicting the probability of suitable winter habitat supporting commercial catches of adult Pacific cod (bottom panel) and the purple points were used to validate the model.

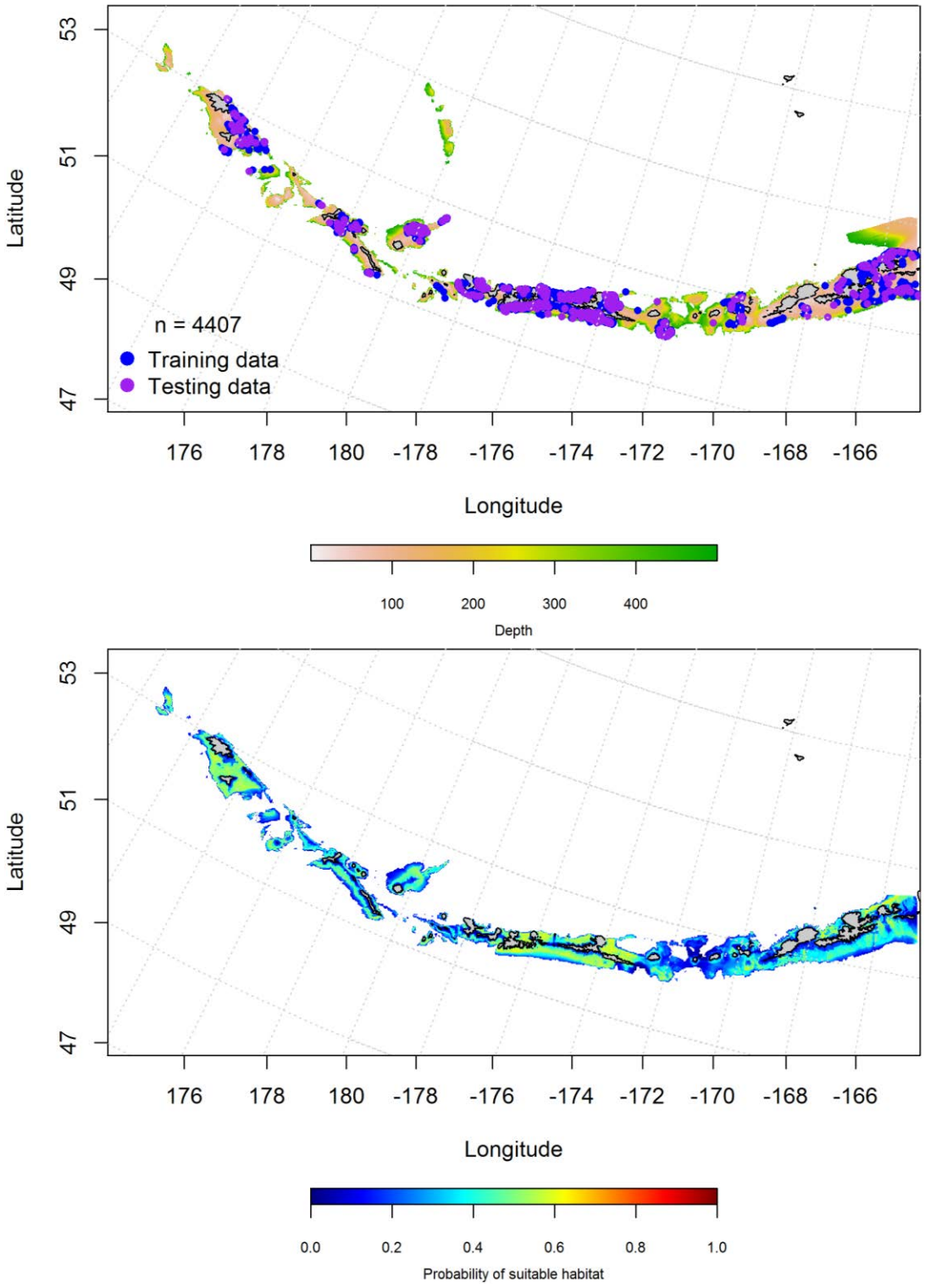

Figure 94. Locations of spring (March-May) commercial fisheries catches of adult Pacific cod (top panel). Blue points were used to train the maximum entropy model predicting the probability of suitable spring habitat supporting commercial catches of adult Pacific cod (bottom panel) and the purple points were used to validate the model.

Aleutian Islands Pacific cod Essential Fish Habitat Maps and Conclusions -- Pacific cod summertime essential fish habitat predicted by the modeling is distributed similarly across the Aleutian Islands for juvenile and adult life history stages (Figure 95).

The fall, winter and spring distribution of Pacific cod EFH was essentially the same throughout the AI (Figure 96). However, spring EFH was more abundant in the central and western AI than in the fall or winter.

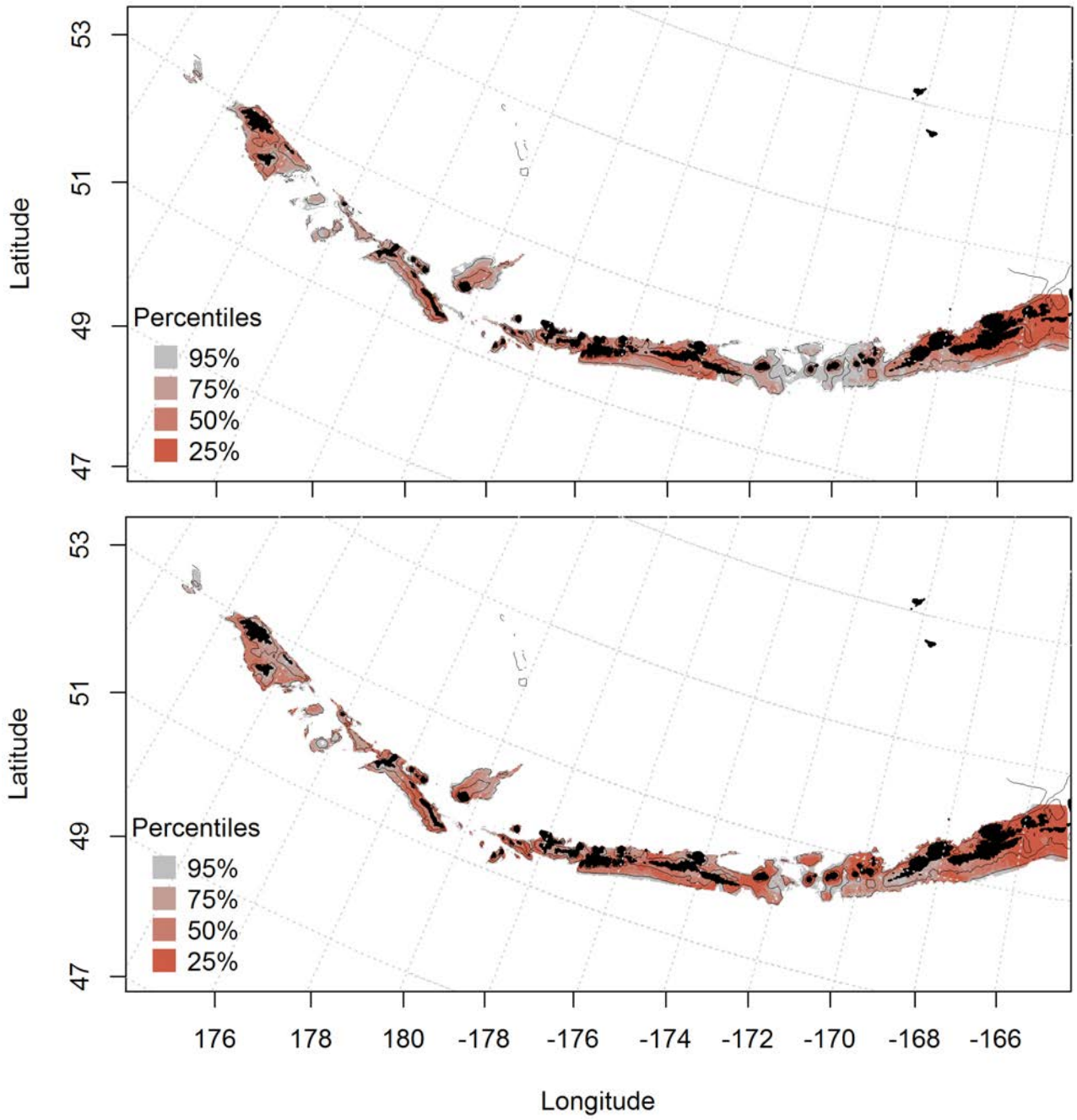

Figure 95. Predicted summer essential fish habitat for Pacific cod juveniles and adults (top and bottom panel) from summertime bottom trawl surveys.

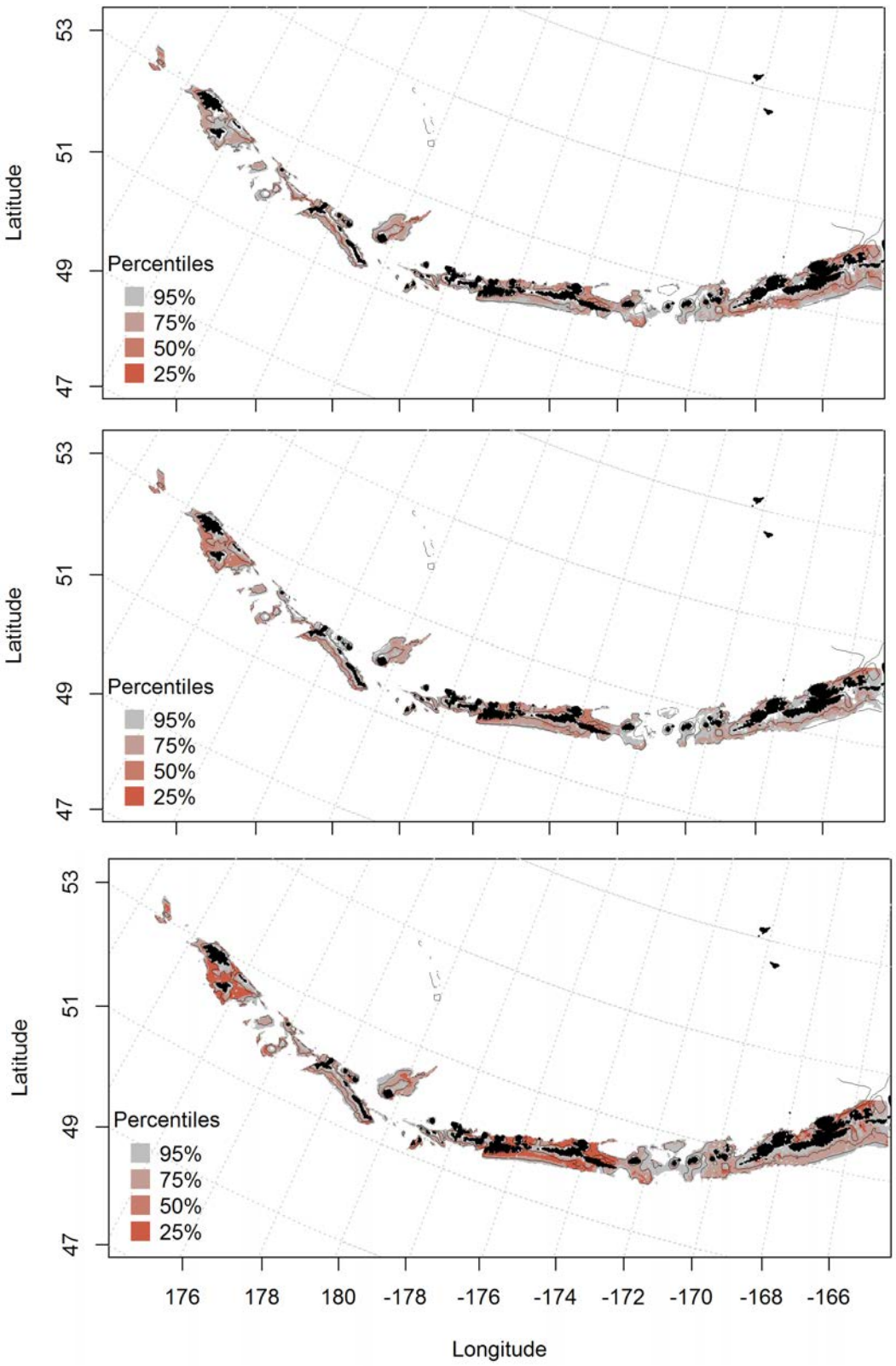

Figure 96.Essential fish habitat predicted for Pacific cod during fall (top panel), winter (middle panel) and spring (bottom panel) from summertime commercial catches.

Walleye pollock (*Theragra chalcogramma*)

Seasonal distribution of early life history stages of Walleye pollock in the Aleutian Islands-- There were 101 instances of Walleye pollock eggs observed in the FOCI database (Figure 97), 1 in the winter, 97 in the spring, and 3 in the summer. All observations were found in eastern AI. There were not enough observations to run the winter or summer models.

Ocean color, surface temperature, and current variability were the most important variables in modeling spring suitable habitat of Walleye pollock eggs (relative importance: 29%, 28.8%, and 19.8%, respectively). The training data AUC was 98%, and 97% for the test data. The model correctly classified 95% of the training data and 97% of the test data sets. The model predicted probable suitable habitat of spring Walleye Pollock egg distribution was predicted throughout the AI, and was most abundant in the eastern AI near Atka Island (Figure 98).

There were 84 instances of larval Walleye pollock observed in the FOCI data base, 79 in the spring, and 5 in the summer (Figure 99). All observations were found in the eastern AI. There were not enough observations to run the larval summer model.

The most important variables in the spring larval model were surface color, surface temperature, current variability, and bottom depth (relative importance: 31.9%, 24.1%, 18.9%, and 11.4%, respectively). The AUC was 99% for the training data and 93% for the testing data, indicating a good model fit. The model correctly classified 95% of the training data and 93% of the test data. In the spring, the model predicted probable suitable habitat of larvae through the AI chain with a higher predicted probability in the eastern AI near Atka Island (Figure 100).

There were only 2 observations of juvenile Walleye pollock in the FOCI database, both in the eastern AI (Figure 101). Both observations were in the summer, and there were not enough cases to run the model.

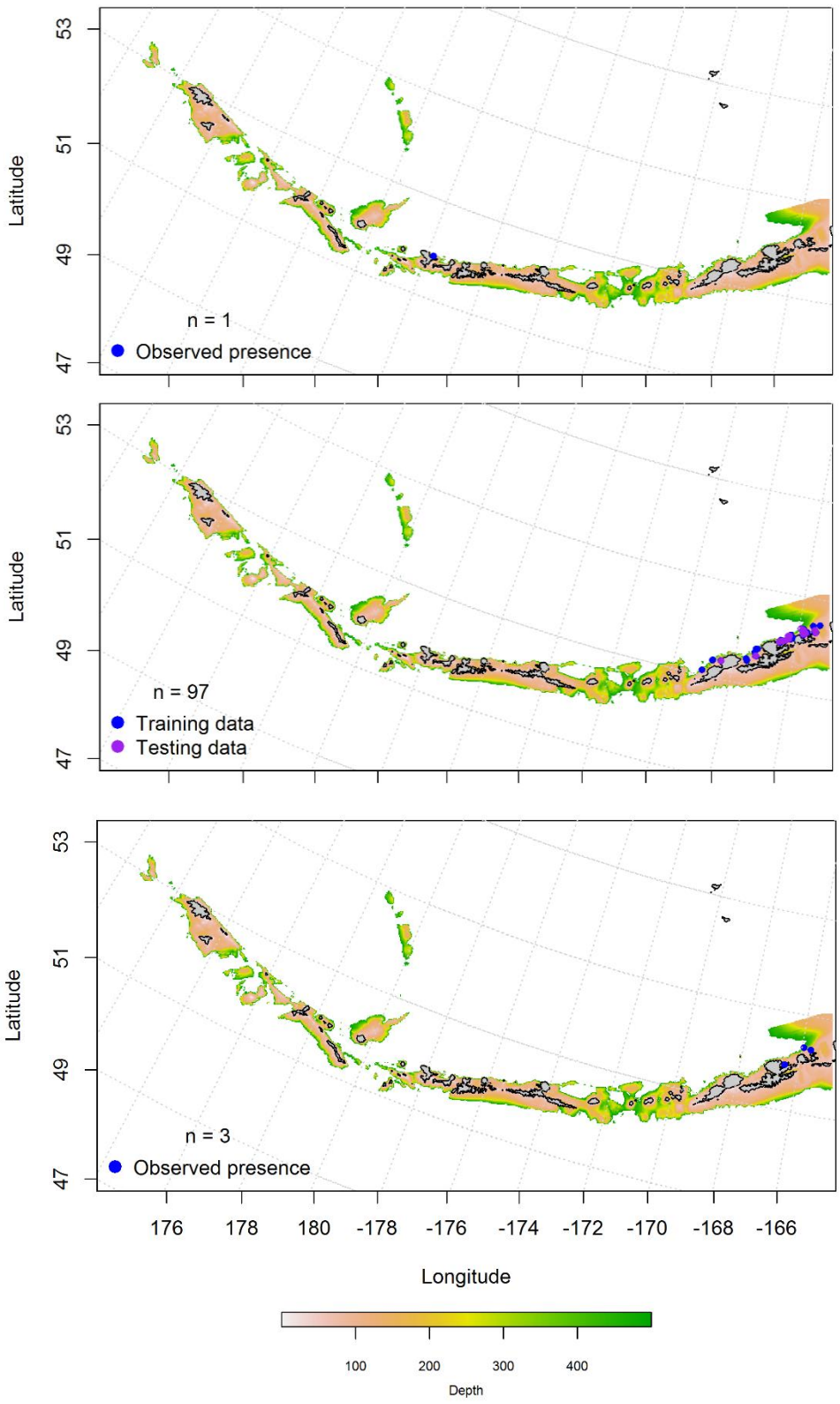

Figure 97.Winter, spring, and summer observations (top, middle, and bottom panel, respectively) of Walleye pollock eggs from the Aleutian Islands.

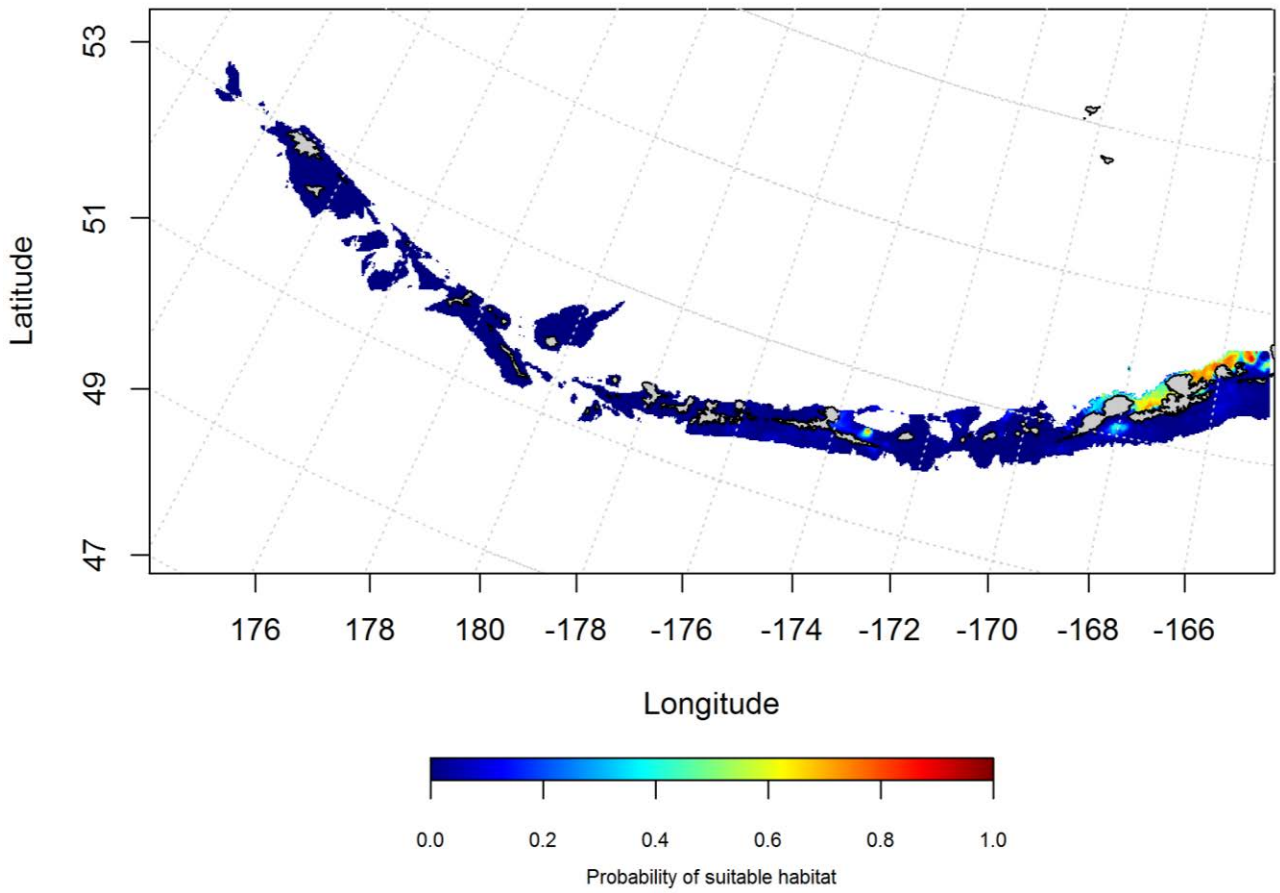

Figure 98. Predicted probability of spring distribution of Walleye pollock eggs from maximum entropy modeling of the Aleutian Islands.

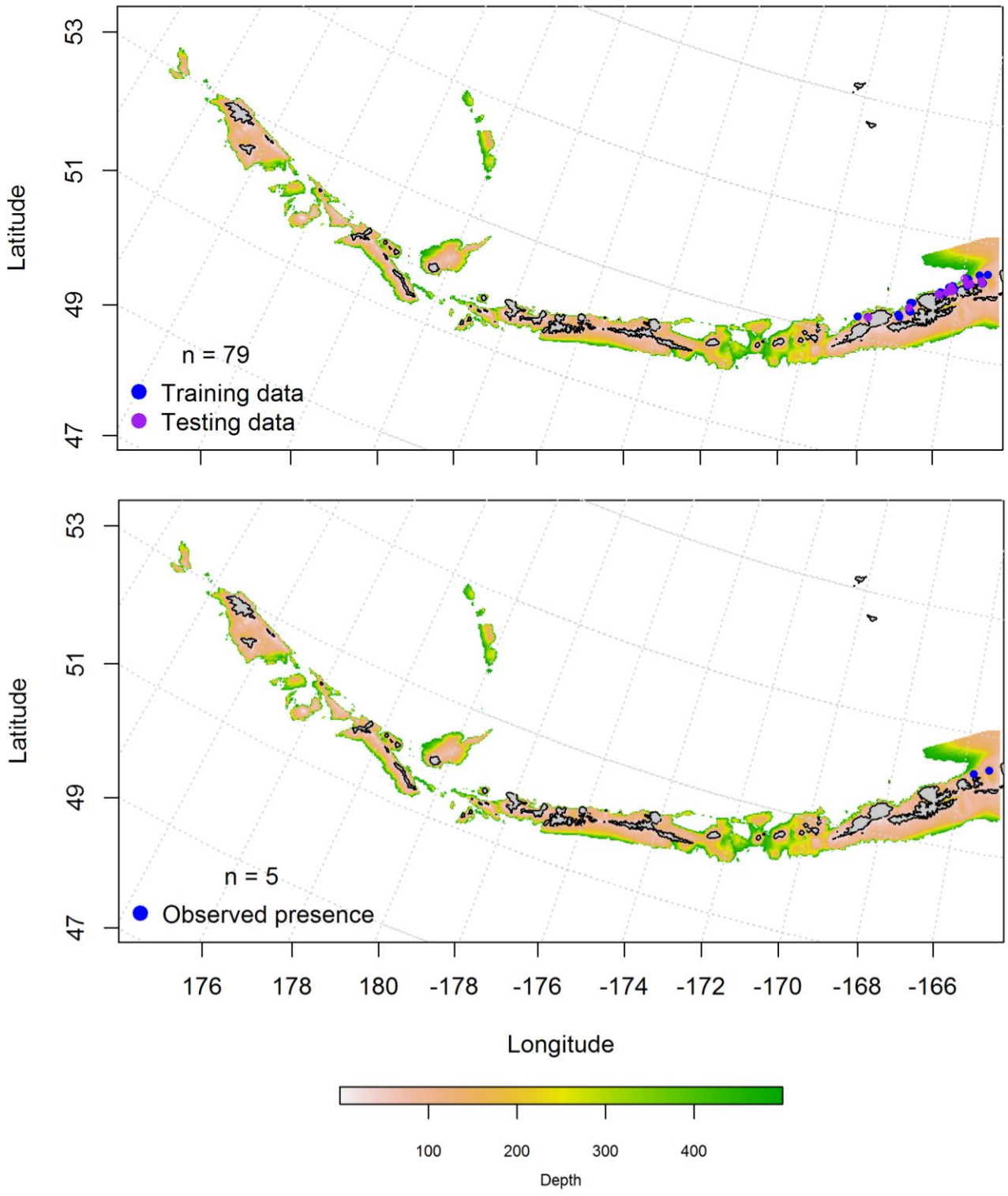

Figure 99. Spring and summer observations (top and bottom panel) of larval Walleye pollock from the Aleutian Islands.

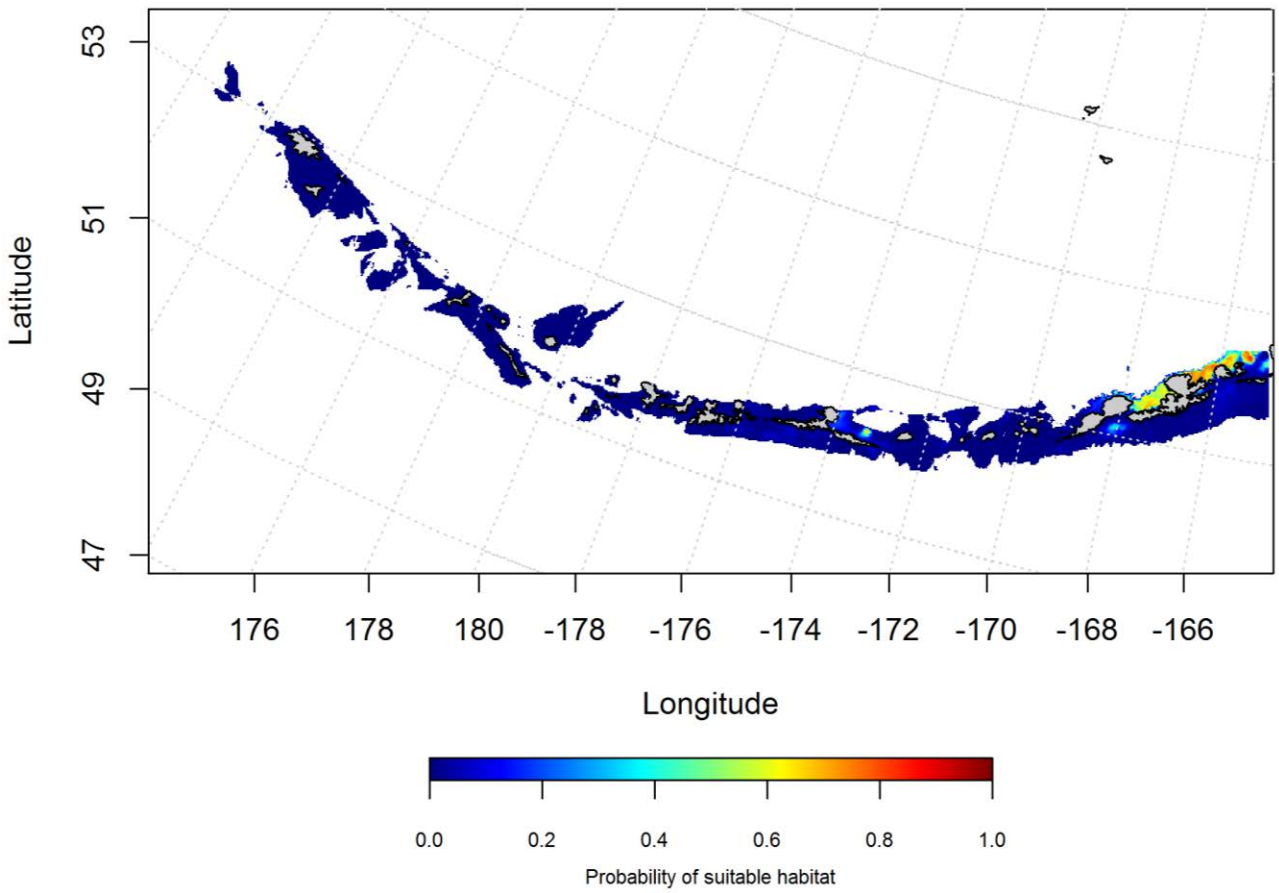

Figure 100. Predicted probability of spring suitable habitat of larval Walleye pollock from maximum entropy modeling of the Aleutian Islands.

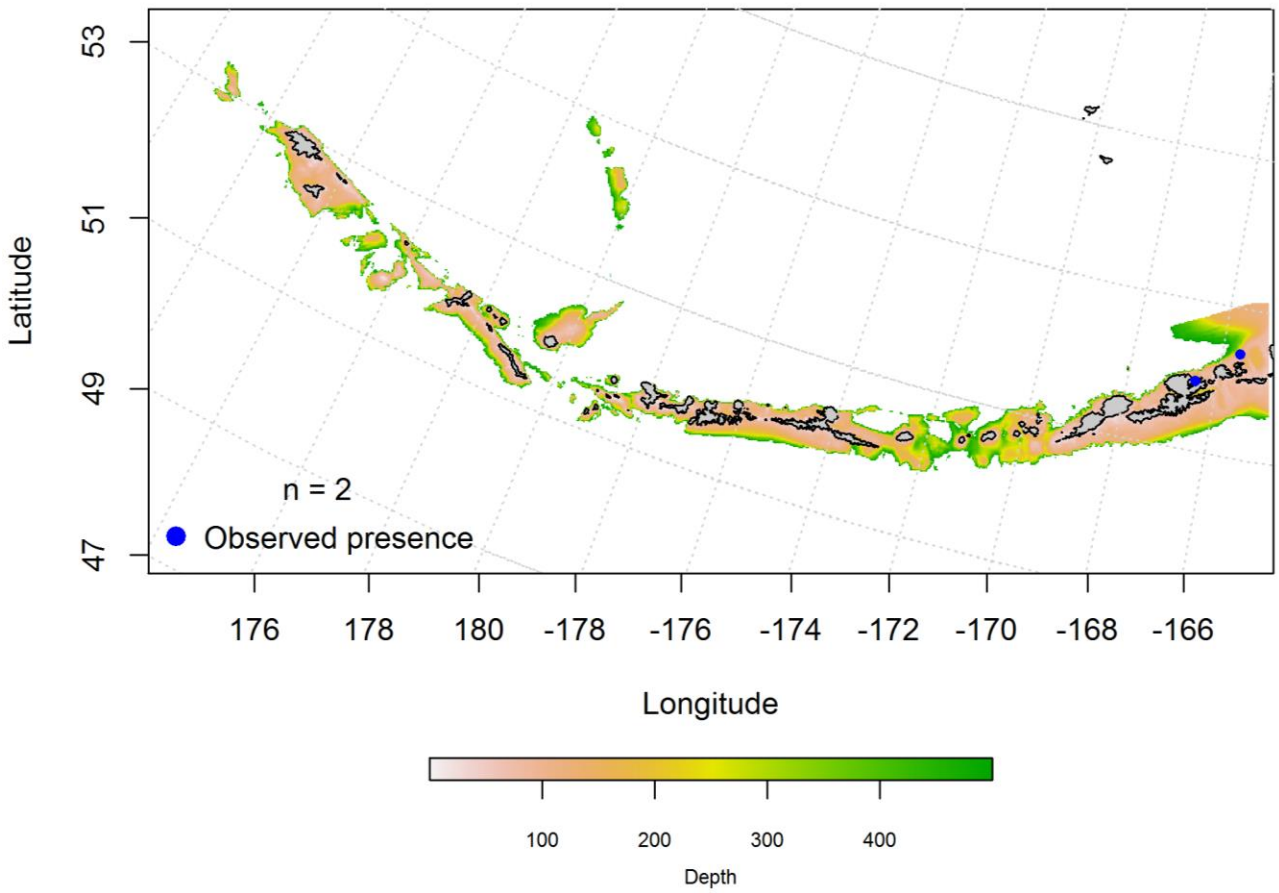

Figure 101. Summer catches of early juvenile Walleye pollock in the Aleutian Islands.

Summertime distribution of juvenile and adult Walleye pollock from bottom trawl surveys of the Aleutian Islands -- Juvenile Walleye pollock were modeled using a hurdle-GAM. The presence absence GAM predicted areas of high and low abundance (e.g. areas with large passes) throughout the AI (Figure 102). The best-fitting PA GAM indicated that bottom depth and geographic location were the most important factors controlling juvenile Walleye pollock distribution and the model explained 79% of the variability in the training and test data sets. The model correctly classified 71% of the training data and 72% of the test data, and explained 17.2% of the deviance.

The CPUE GAM model found that ocean color was the most important variable that explained the distribution of juvenile Walleye pollock. The model explained 12.6% of the deviance, 13% of the variability in CPUE in the bottom trawl survey in the training data and explained 5% of the test data set. The second part of the hurdle-GAM was similarly distributed as the PA GAM (areas of high and low abundance (e.g. areas with large passes) throughout the AI) though more abundant in the eastern AI (Figure 103).

A generalized additive model predicting the abundance of adult Walleye pollock explained 31% of the training data set variability in CPUE in the bottom trawl survey, and 27% of the test data set variability. The model also explained 31.3% of the deviance. Bottom depth and geographic location were the most important variables explaining the distribution of adult Walleye pollock. Adults were distributed throughout the AI, highest predicted abundance was in the eastern AI (Figure 104).

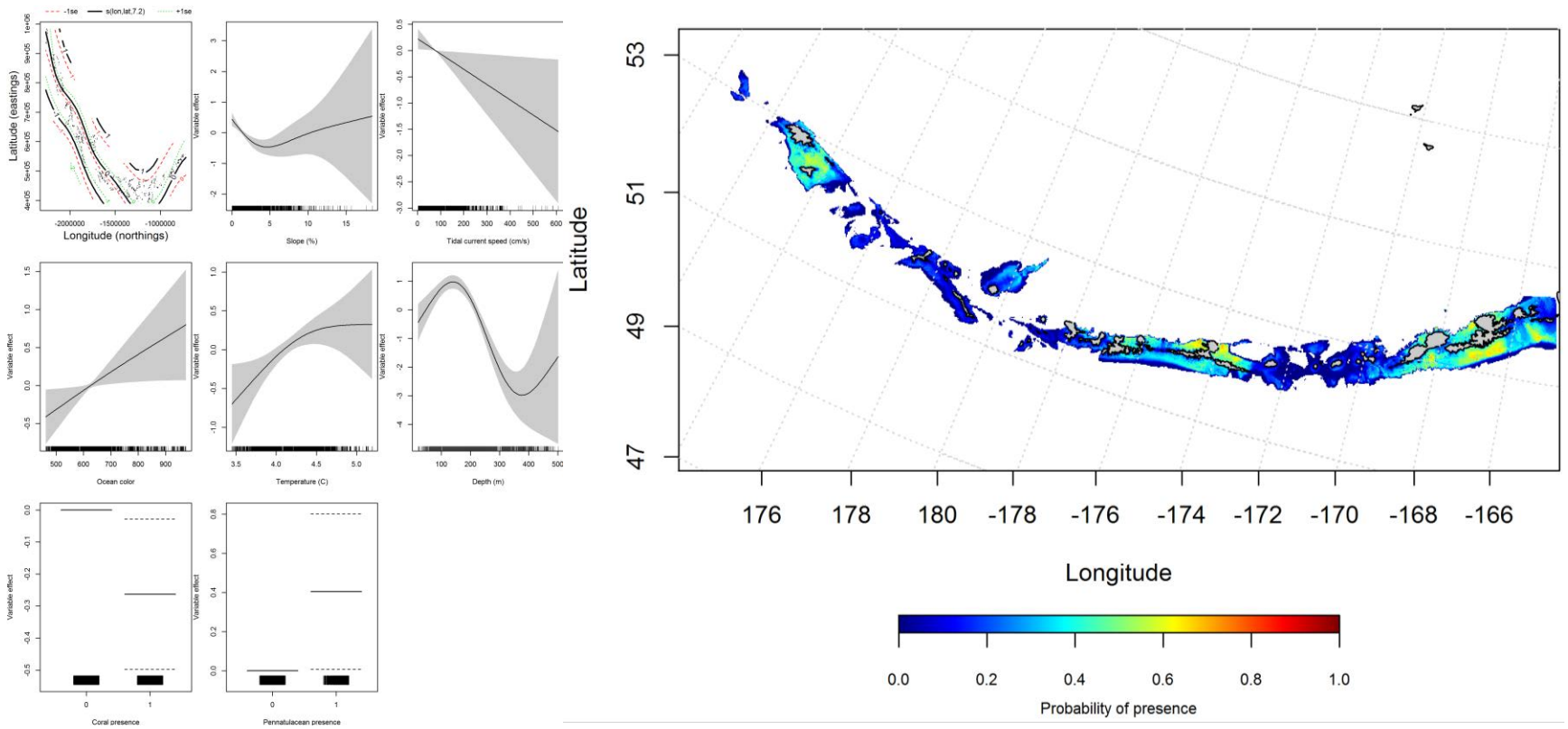

Figure 102. Best-fitting hurdle effects of retained habitat variables on presence absence (PA) of juvenile Walleye pollock from summer bottom trawl surveys of the Aleutian Islands (left panel) alongside hurdle-predicted juvenile Walleye pollock PA (right panel).

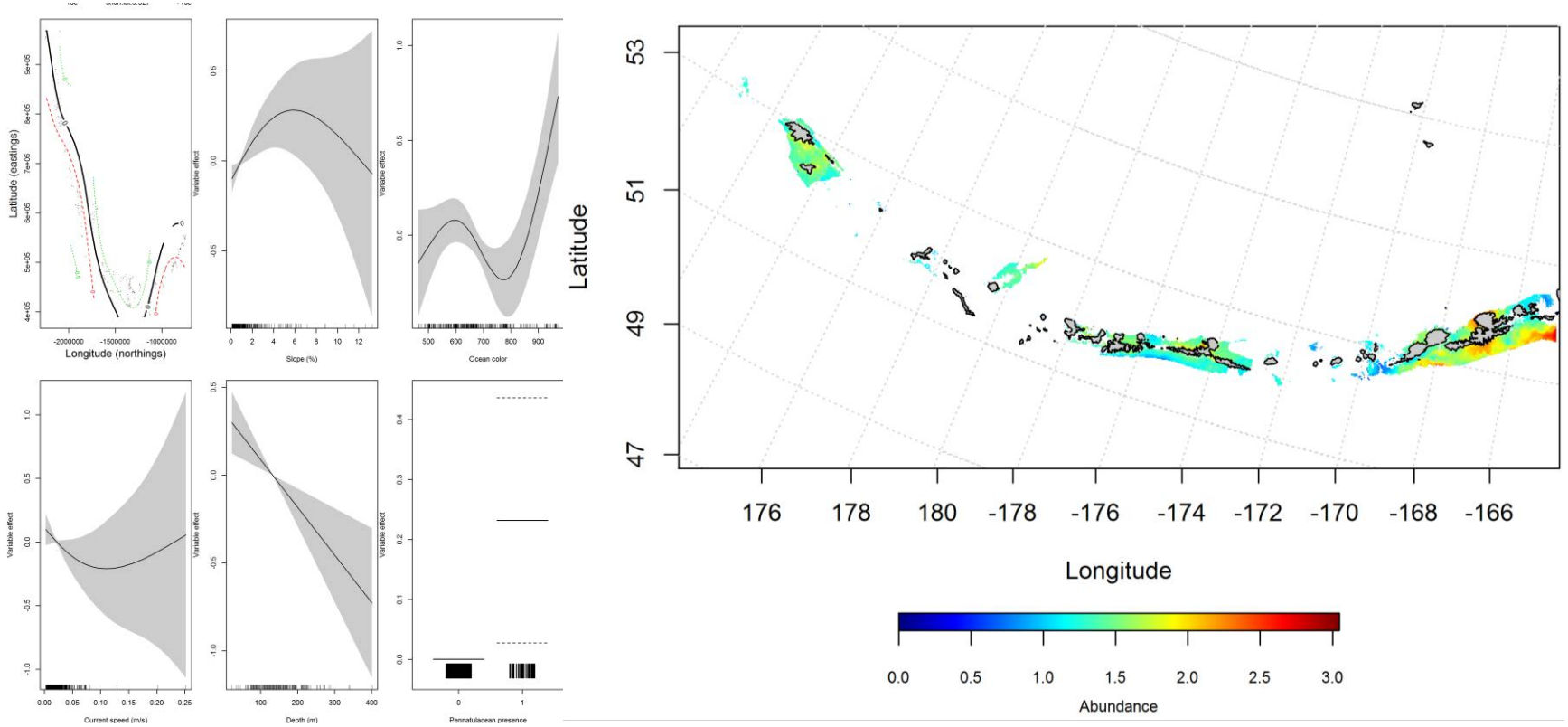

Figure 103. Best-fitting hurdle effects of retained habitat variables on CPUE of juvenile Walleye pollock from summer bottom trawl surveys of the Aleutian Islands (left panel) alongside hurdle-predicted juvenile Walleye pollock CPUE (right panel).

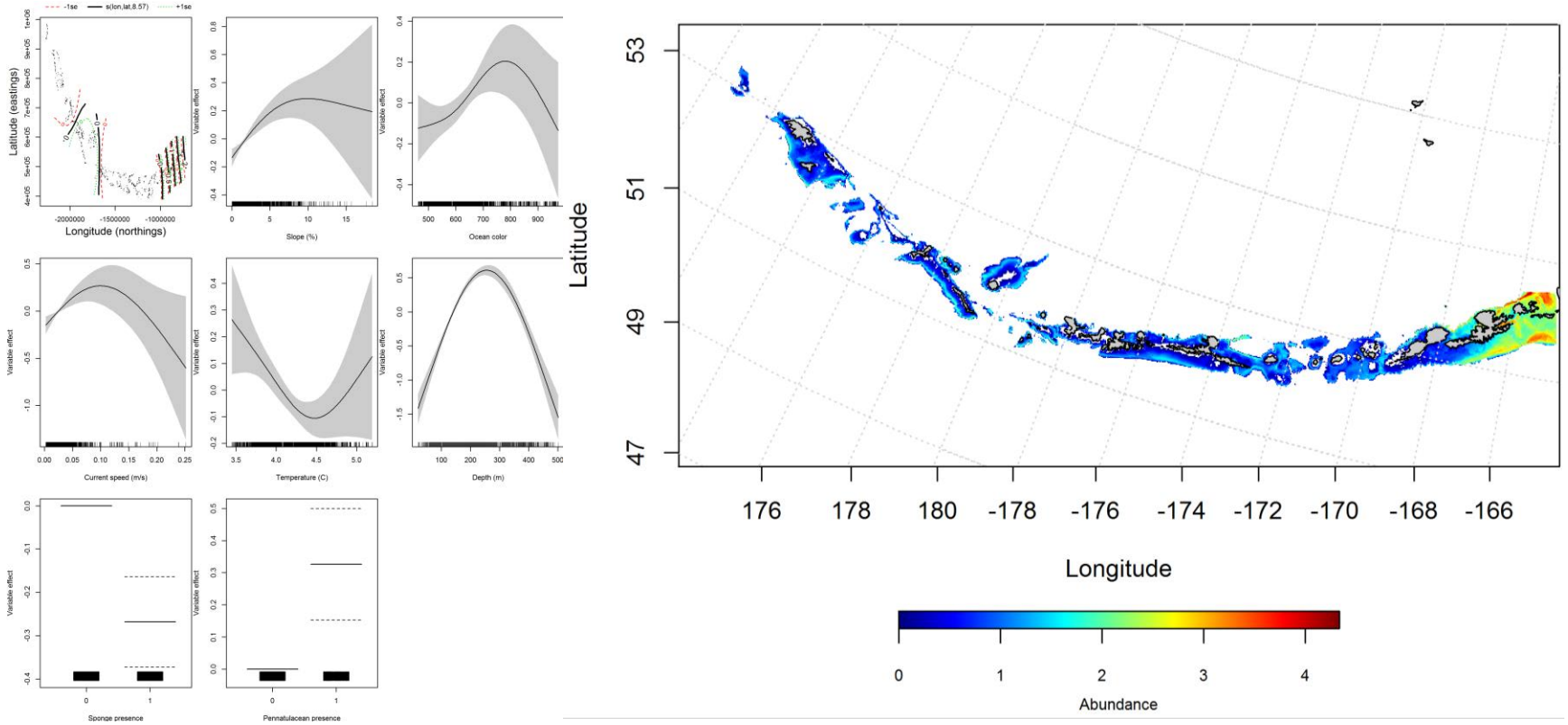

Figure 104. Best-fitting hurdle effects of retained habitat variables on CPUE of adult Walleye pollock from summer bottom trawl surveys of the Aleutian Islands (left panel) alongside hurdle-predicted adult Walleye pollock CPUE (right panel)..

Seasonal distribution of commercial fisheries catches of adult Walleye pollock in the Aleutian Islands-- Distribution of adult Walleye pollock in the Aleutian Islands in commercial fisheries catches was generally consistent throughout all seasons. In the fall, bottom depth, current speed, and bottom temperature were the most important variables determining probable suitable habitat of Walleye pollock (relative importance: 46.6%, 19.1%, and 13.2%, respectively). The AUC of the fall maxent model was 95% for the training data and 88% for the test data. 87% of the training data and 88% of the test data were correctly classified. The model predicted probable suitable habitat of Walleye pollock catches throughout the AI (Figure 105).

In the winter, bottom depth, bottom temperature and surface color were the most important variables determining probable suitable habitat of Walleye pollock (relative importance: 33.7%, 24.6%, and 24.3%, respectively). The AUC of the winter maxent model was 95% for the training data and 84% for the test data. 88% of the training data and 84% of the cases in the test data sets were predicted correctly. The model predicted probable suitable habitat of Walleye pollock across the AI, though more abundant near Agattu, Attu, and Atka Islands (Figure 106).

In the spring, bottom depth and surface ocean color were the most important variables determining probable suitable habitat of Walleye pollock (relative importance: 41.5% and 36.1%). The AUC of the spring maxent model was 92% for the training data and 81% for the test data. 83% of the training data and 81% of the test data sets were correctly classified. As with the fall, the model predicted probable suitable habitat of Walleye pollock throughout the AI (Figure 107).

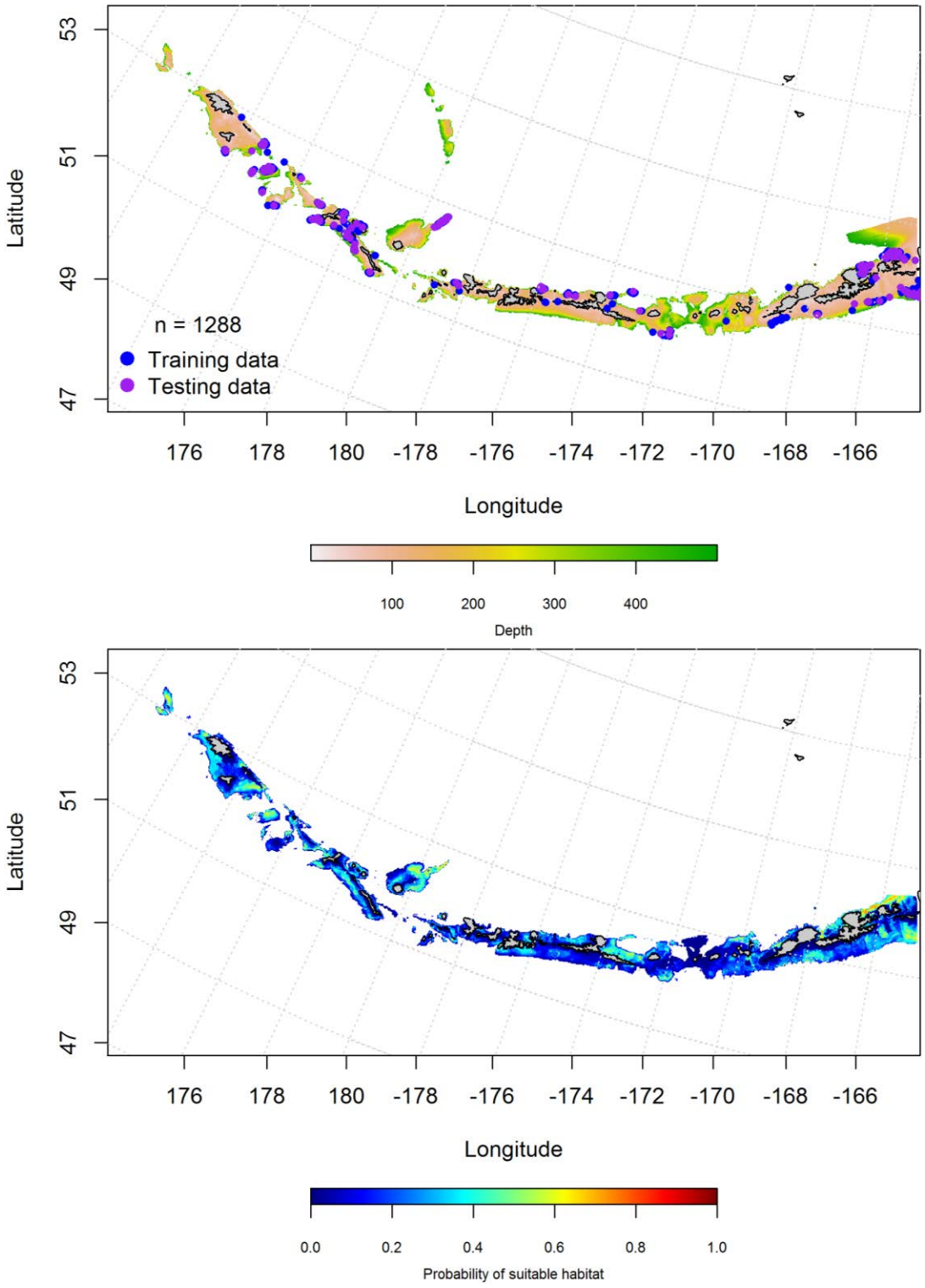

Figure 105. Locations of fall (September-November) commercial fisheries catches of adult Walleye pollock (top panel). Blue points were used to train the maximum entropy model predicting the probability of suitable fall habitat supporting commercial catches of adult Walleye pollock (bottom panel) and the purple points were used to validate the model.

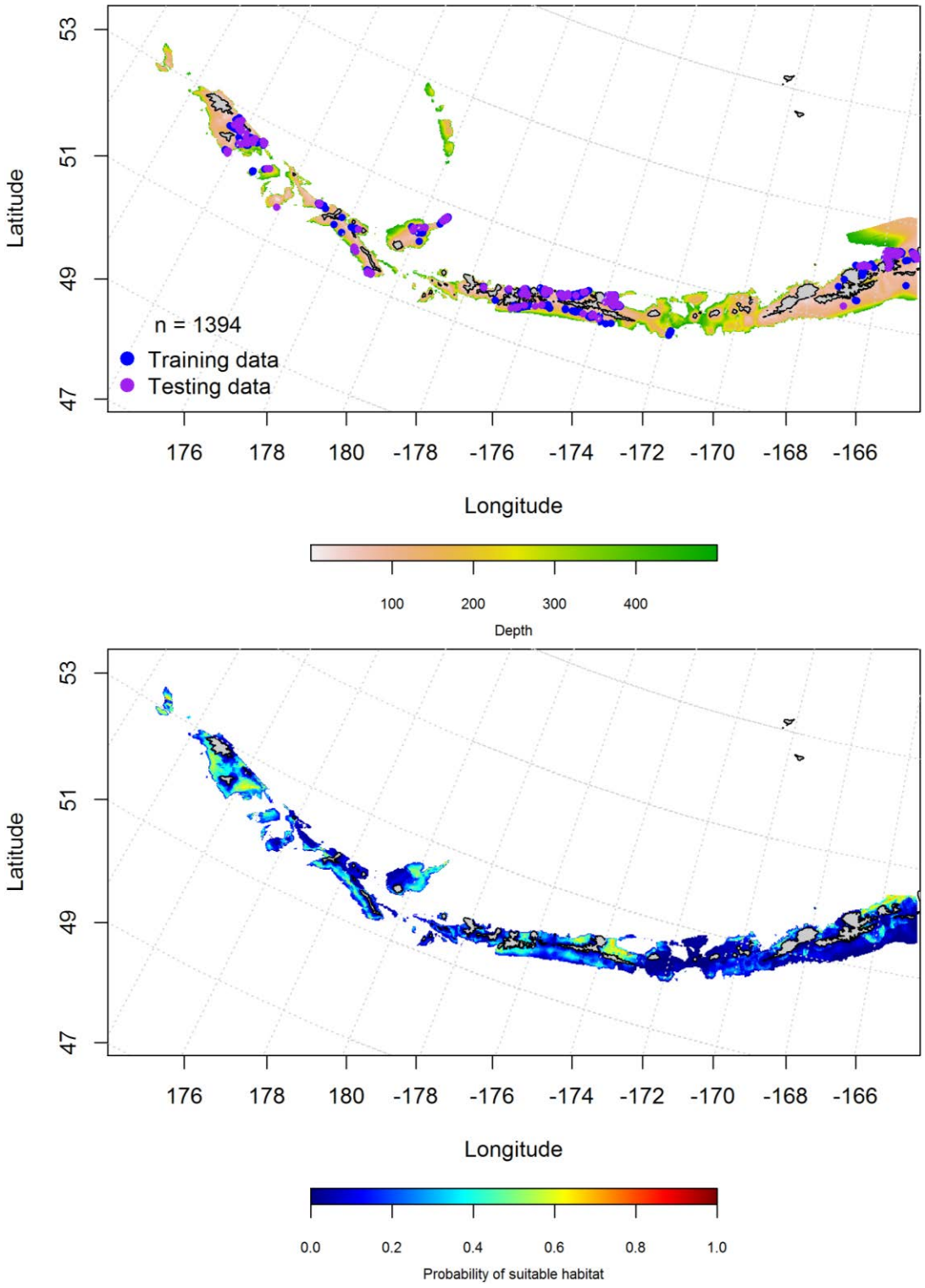

Figure 106. Locations of winter (December-February) commercial fisheries catches of adult Walleye pollock (top panel). Blue points were used to train the maximum entropy model predicting the probability of suitable winter habitat supporting commercial catches of adult Walleye pollock (bottom panel) and the purple points were used to validate the model.

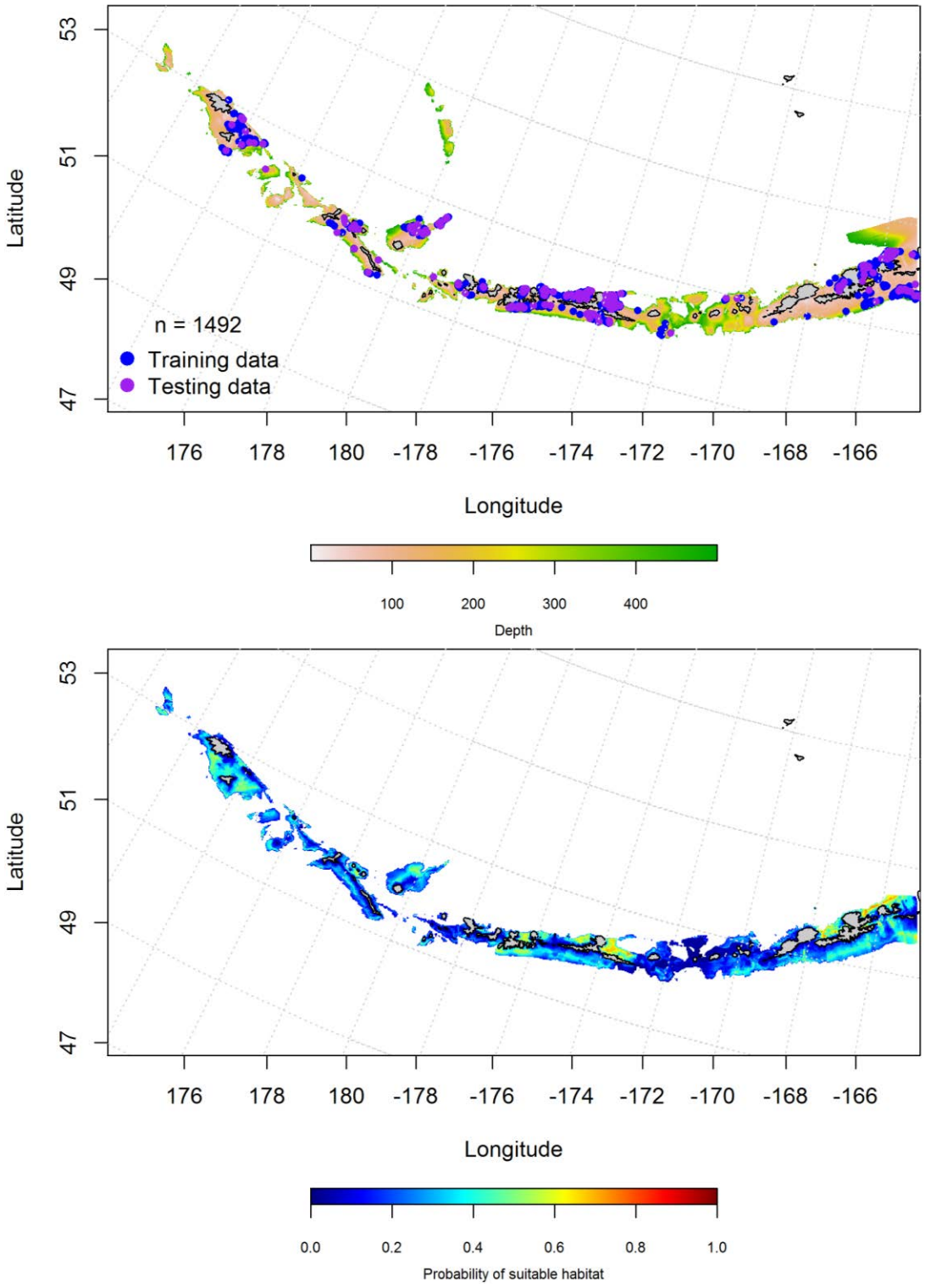

Figure 107. Locations of spring (March-May) commercial fisheries catches of adult Walleye pollock (top panel). Blue points were used to train the maximum entropy model predicting the probability of suitable spring habitat supporting commercial catches of adult Walleye pollock (bottom panel) and the purple points were used to validate the model.

Aleutian Islands Walleye pollock Essential Fish Habitat Maps and Conclusions – EFH for Walleye pollock eggs predicted in the spring were the most abundant in the eastern AI (Figure 108). EFH for Walleye pollock larvae predicted in the spring were also the most abundant in the eastern AI (Figure 109).

Juvenile Walleye pollock had less predicted EFH than the adults, though there were common areas of high abundance (Figure 110). Predicted summertime EFH of juvenile Walleye pollock was distributed throughout the AI, though less abundant in areas of large passes. Adult Walleye pollock were distributed throughout the AI and most abundant in the eastern AI.

The fall, winter and spring distribution of Walleye pollock EFH from commercial catches was essentially the same throughout the seasons and spread throughout the AI (Figure 111).

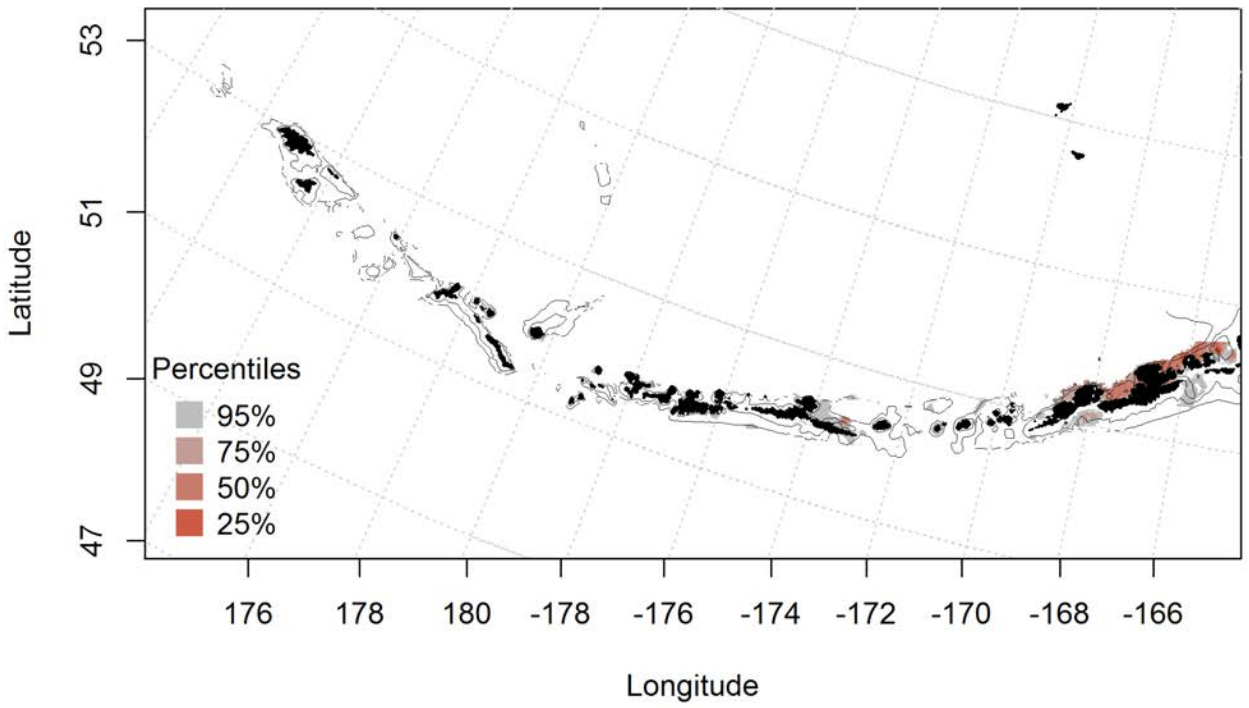

Figure 108. Spring essential fish habitat predicted for Walleye pollock eggs.

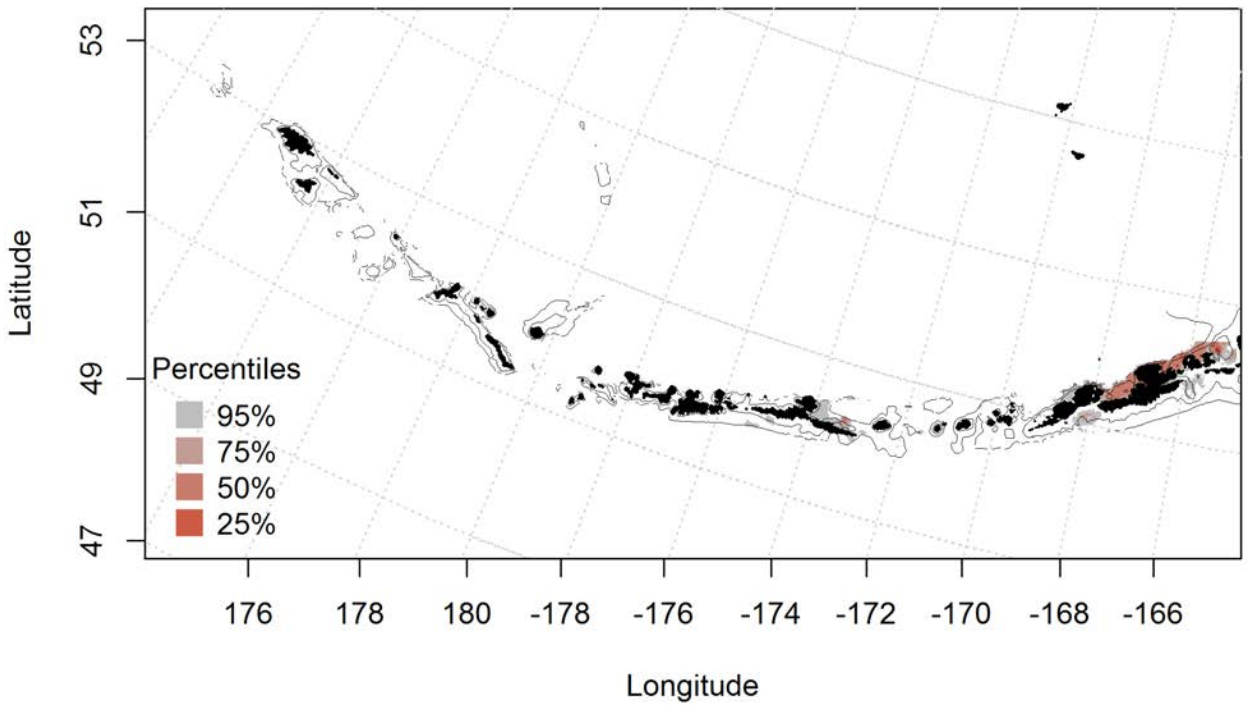

Figure 109. Spring essential fish habitat predicted for larval Walleye pollock.

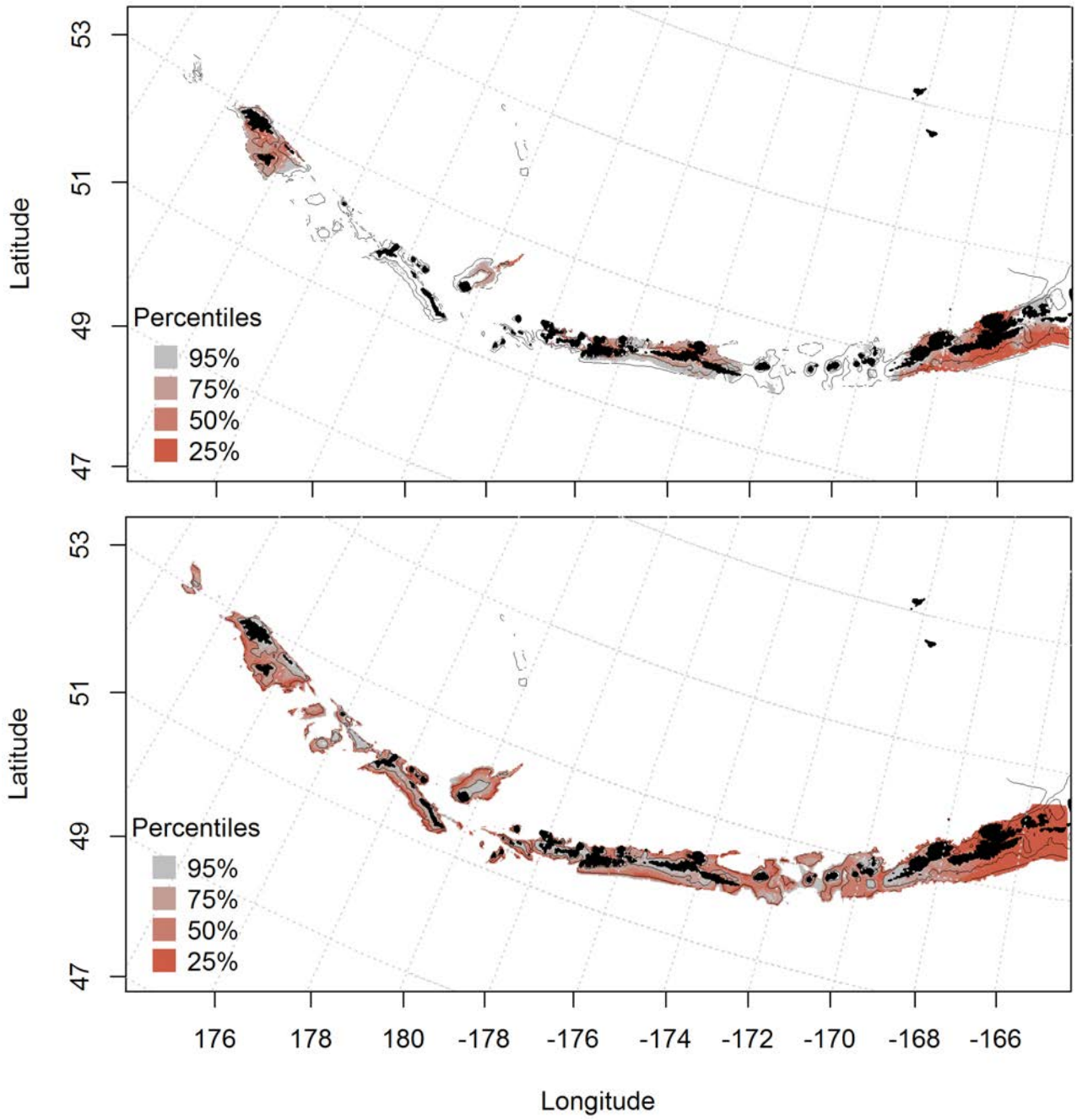

Figure 110. Predicted summer essential fish habitat for Walleye pollock juveniles and adults (top and bottom panel) from summertime bottom trawl surveys.

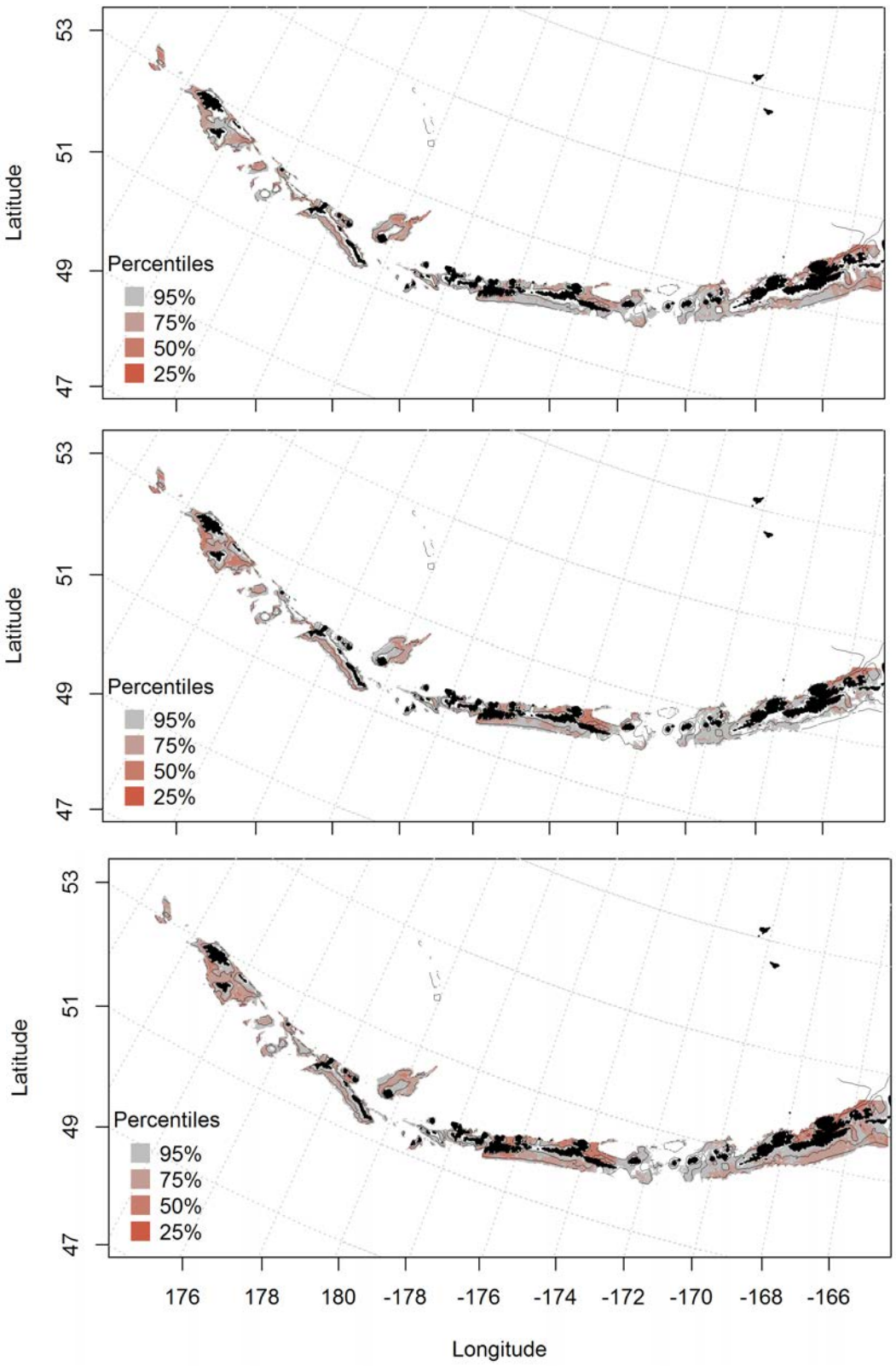

Figure 111. Essential fish habitat predicted for Walleye pollock during fall (top panel), winter (middle panel) and spring (bottom panel) from summertime commercial catches.

Sablefish (*Anoplopoma fimbria*)

Seasonal distribution of early life history stages of Sablefish in the Aleutian Islands-- There were only 9 instances of larval Sablefish observed in the FOCI database, 8 in the spring and 1 in the summer (Figure 112). All observations were found in the eastern AI, and there were not enough cases for modeling spring or summer larvae.

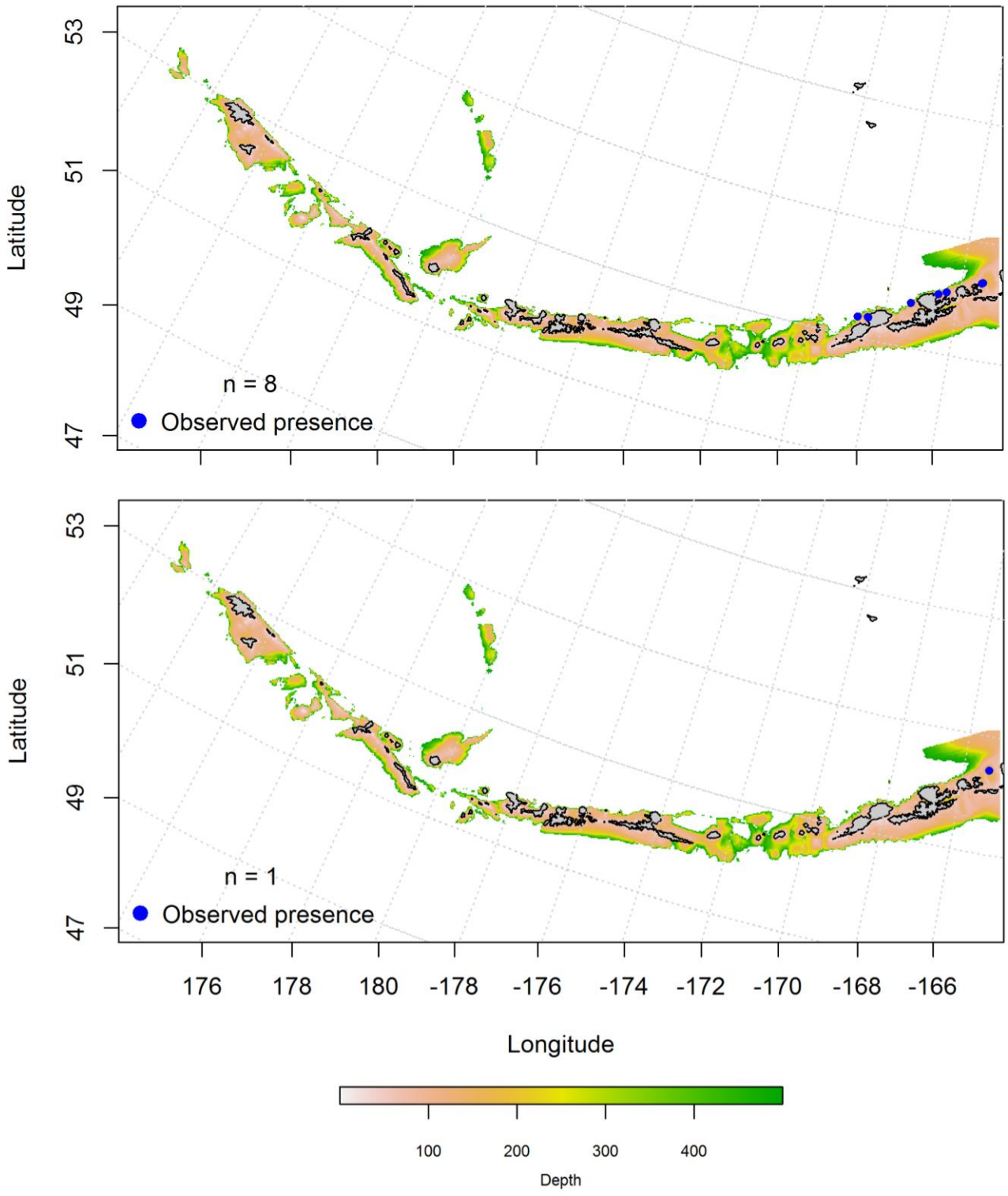

Figure 112. Spring and summer observations (top and bottom panel) of larval Sablefish from the Aleutian Islands.

Summertime distribution of juvenile and adult Sablefish from bottom trawl surveys of the Aleutian Islands – There were not enough instances of juvenile Sablefish from the summertime bottom trawl surveys for modeling. There were only 14 cases, and all were in the eastern AI (Figure 113).

A two-step hurdle-Generalized additive model predicting the presence absence (PA GAM) of adult Sablefish explained 95% of the variability in CPUE in the bottom trawl survey training data, and 96% of the variability in the test data set. Bottom depth and geographic location were the most important variables explaining the distribution of adult Sablefish presence or absence. The model correctly classified 89% of the training and test data sets, and explained 51.1% of the deviance. Adults were distributed throughout the AI, though the highest predicted abundance was in eastern AI (Figure 114).

The second part of the adult Sablefish hurdle-GAM predicted CPUE and explained 35.4% of the deviance, 36% of the variability of the training data set and 22% of the test data set. Geographic location and tidal current were the most important variables explaining the distribution of adult Sablefish CPUE GAM. Adults were distributed across the AI, though the central AI had the highest predicted abundance (Figure 115).

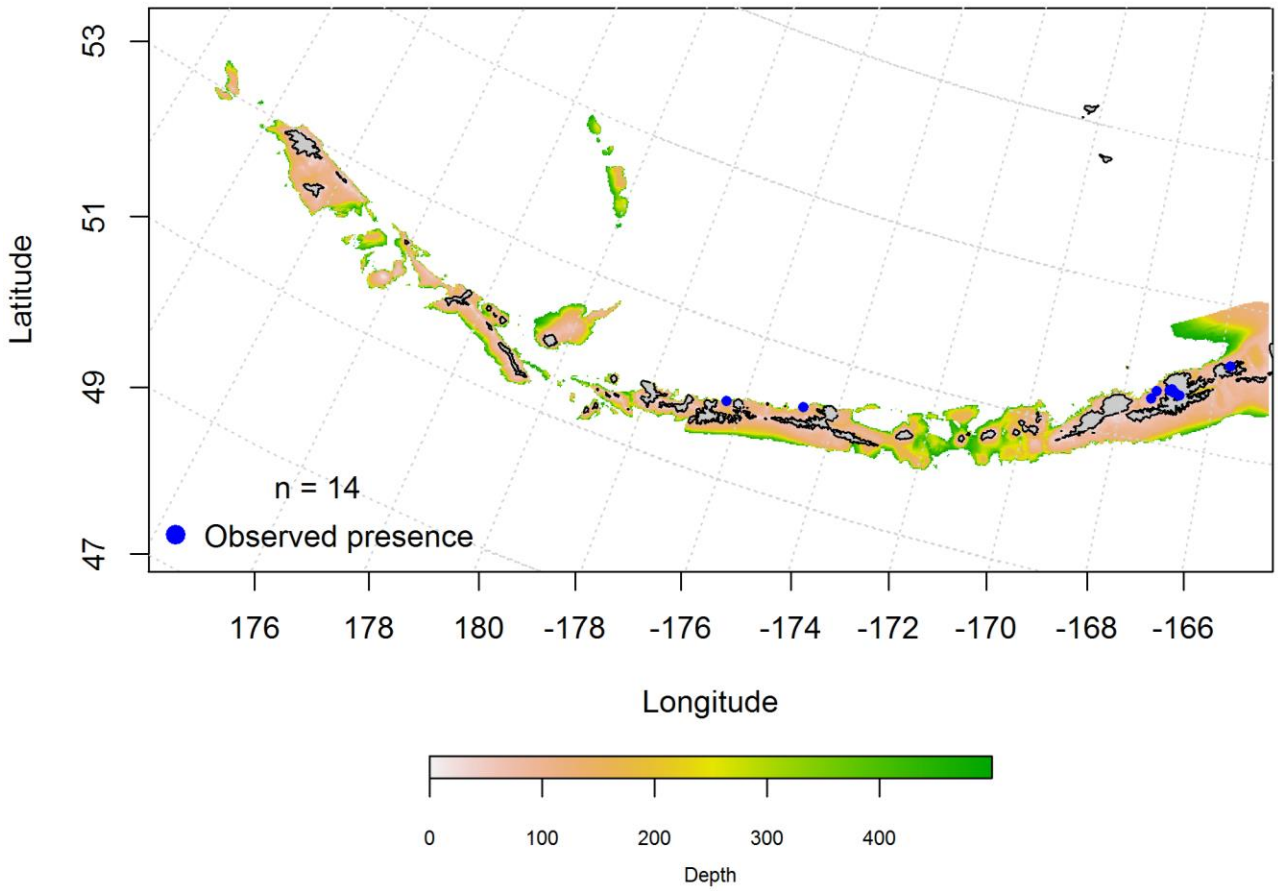

Figure 113. Blue points indicate instances where juvenile Sablefish were observed during summertime bottom trawl survey catches.

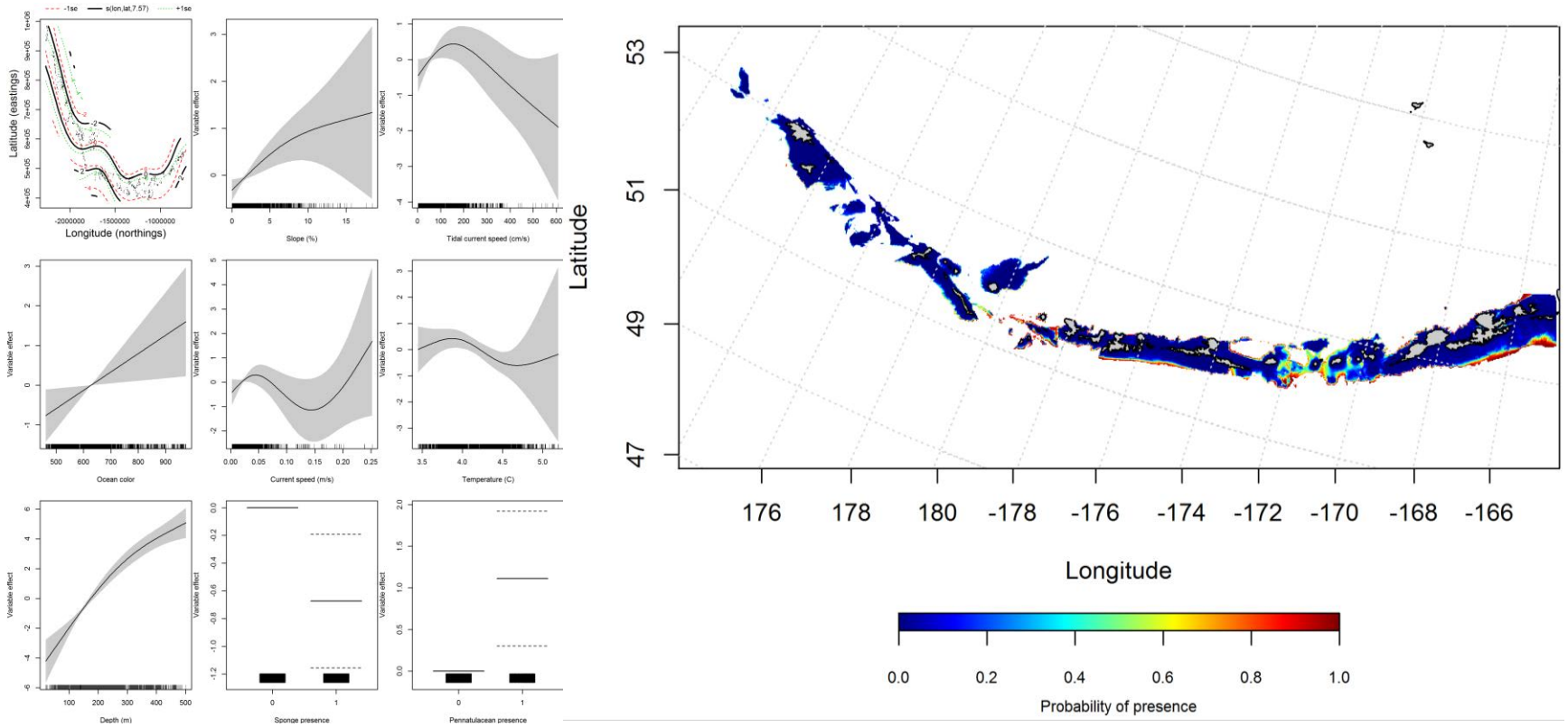

Figure 114. Best-fitting hurdle effects of retained habitat variables on presence absence (PA) of adult Sablefish from summer bottom trawl surveys of the Aleutian Islands (left panel) alongside hurdle-predicted adult Sablefish PA (right panel).

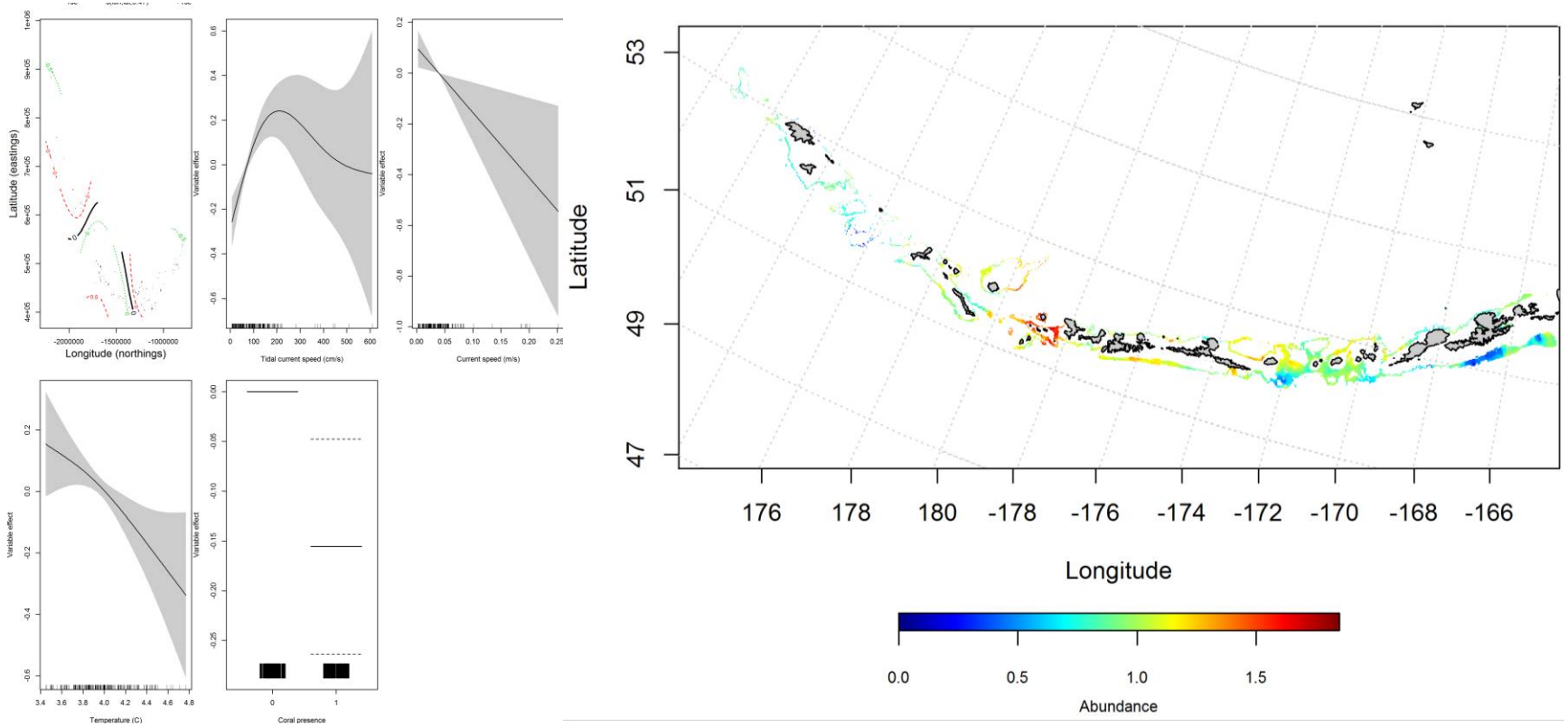

Figure 115. Best-fitting hurdle effects of retained habitat variables on CPUE of adult Sablefish from summer bottom trawl surveys of the Aleutian Islands (left panel) alongside hurdle-predicted adult Sablefish CPUE (right panel).

Seasonal distribution of commercial fisheries catches of adult Sablefish in the Aleutian Islands—Commercial fisheries catches of adult Sablefish in the Aleutian Islands were generally consistent throughout the fall and winter, though were more abundant in the western AI in the spring than in other seasons. In the fall, surface ocean color, bottom depth, and bottom temperature were the most important variables determining probable suitable habitat of adult Sablefish (relative importance: 34.8%, 26%, and 24.4%, respectively). The AUC of the fall maxent model was 91% for the training data and 81% for the test data, and 81% of the cases in both the test and training data sets were predicted correctly. The model predicted probable suitable habitat of adult Sablefish across the AI though most probable in the eastern AI near Nikolski and Unalaska Islands(Figure 116).

In the winter, surface ocean color, bottom temperature, and tidal current were the most important variables determining probable suitable habitat of Sablefish (relative importance: 36.6%, 31.9%, and 19.7%, respectively). The AUC of the winter maxent model was 97% for the training data and 92% for the test data. 94% of the training data and 92% of the test data cases were predicted correctly. As with the fall, the winter model predicted probable suitable habitat of Sablefish across the AI with a higher probability near Atka Island (Figure 117).

In the spring, bottom depth and surface ocean color were the most important variables determining probability of suitable habitat for Sablefish (relative importance: 65% and 25.3%). The AUC of the spring maxent model was 94% for the training data and 83% for the test data. The model correctly classified 86% of the training data and 83% of the test data. The model predicted probable suitable habitat of Sablefish across the AI (Figure 118).

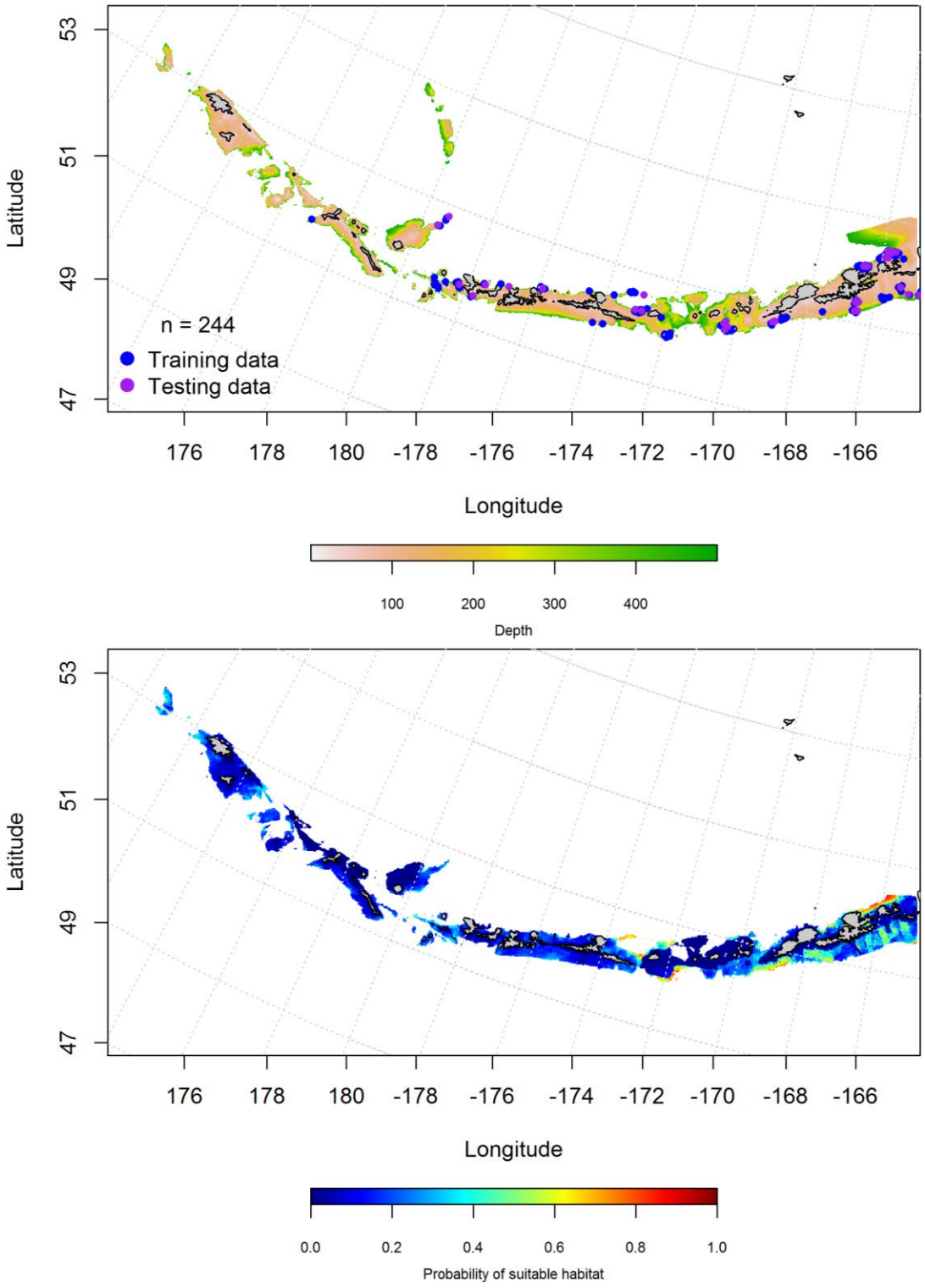

Figure 116. Locations of fall (September-November) commercial fisheries catches of adult Sablefish (top panel). Blue points were used to train the maximum entropy model predicting the probability of suitable fall habitat supporting commercial catches of adult Sablefish (bottom panel) and the purple points were used to validate the model.

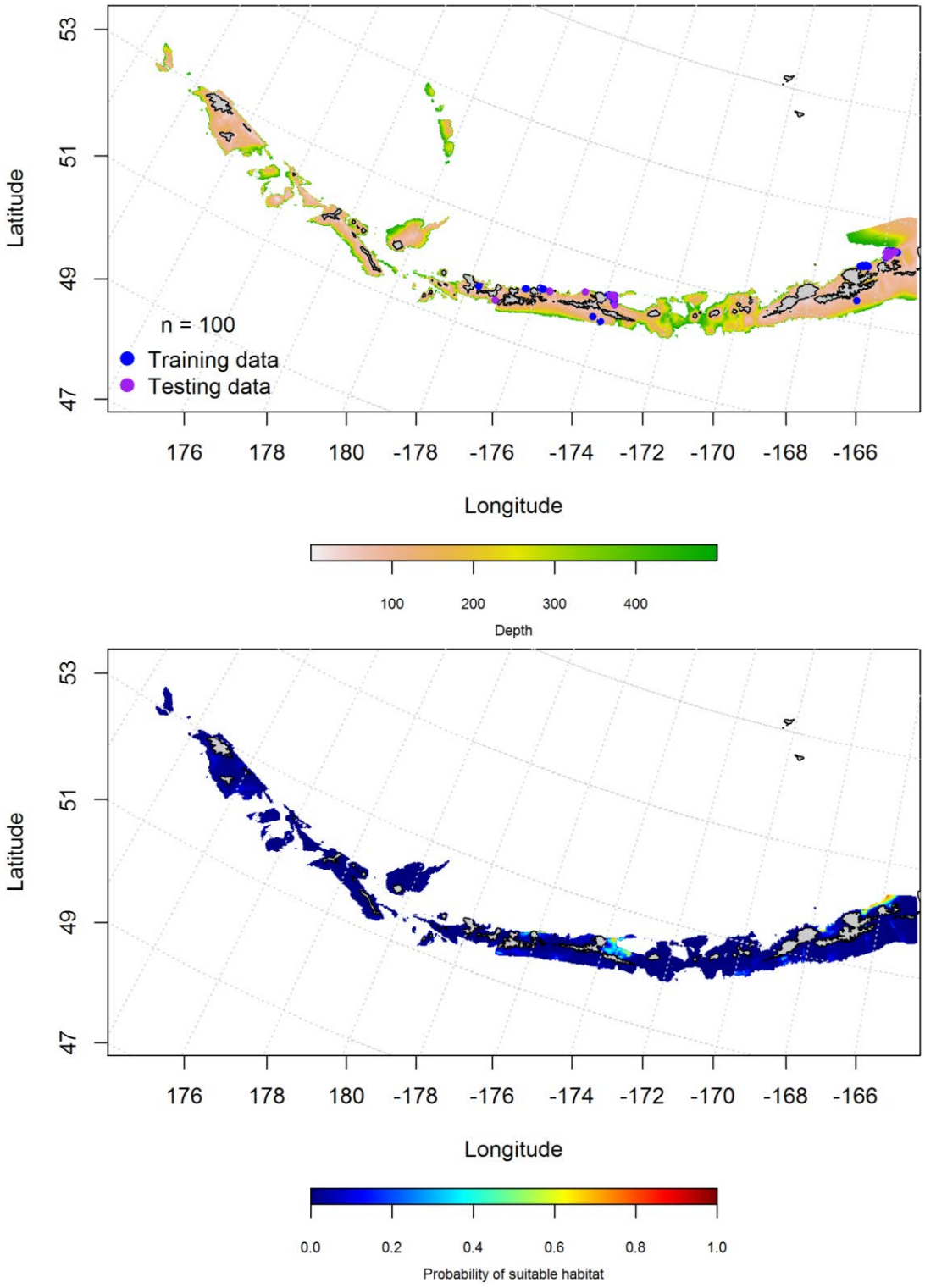

Figure 117. Locations of winter (December-February) commercial fisheries catches of adult Sablefish (top panel). Blue points were used to train the maximum entropy model predicting the probability of suitable winter habitat supporting commercial catches of adult Sablefish commercial catches (bottom panel) and the purple points were used to validate the model.

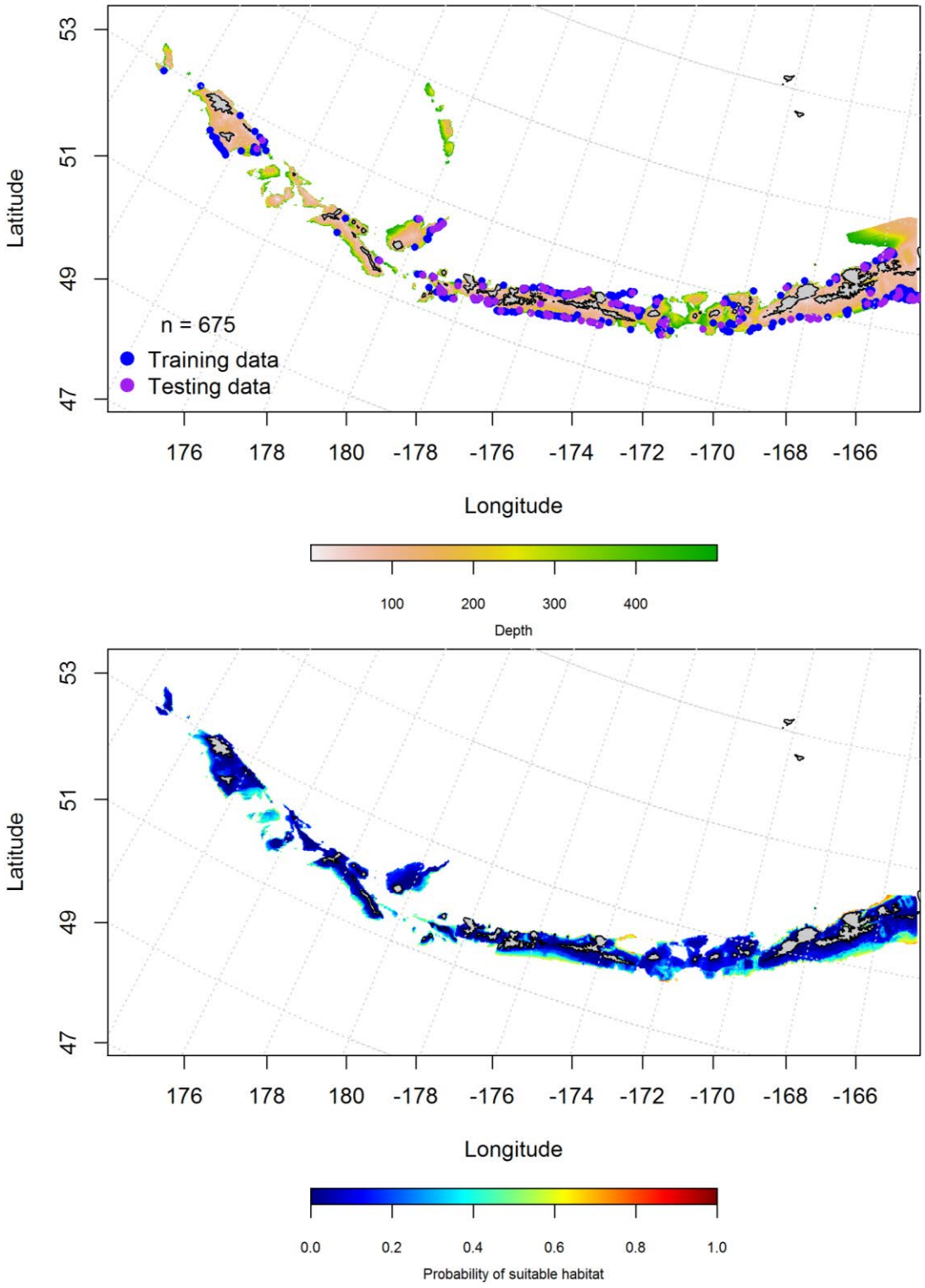

Figure 118. Locations of spring (March-May) commercial fisheries catches of adult Sablefish (top panel). Blue points were used to train the maximum entropy model predicting the probability of suitable spring habitat supporting commercial catches of adult Sablefish (bottom panel) and the purple points were used to validate the model.

Aleutian Islands Sablefish Essential Fish Habitat Maps and Conclusions --

Summertime EFH of Sablefish juveniles and adults had different distributions (Figure 119). Predicted EFH supports presence of juvenile Sablefish in the eastern AI, whereas adults had higher suitable probable habitat in the central and eastern AI.

The fall and spring predicted EFH of Sablefish were similar whereas there was lower probability in the winter (Figure 120).

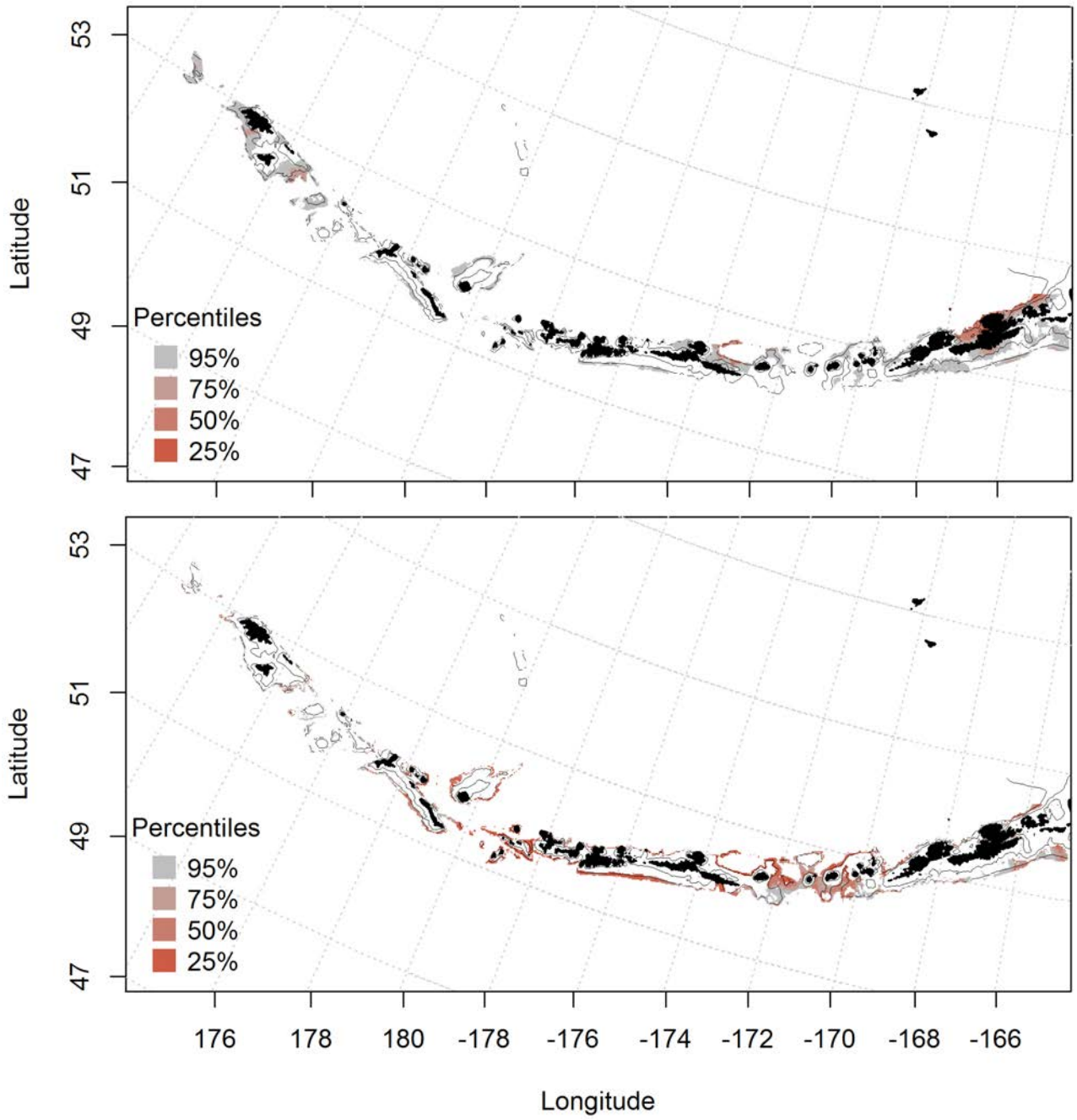

Figure 119. Predicted summer essential fish habitat for Sablefish juveniles and adults (top and bottom panel) from summertime bottom trawl surveys.

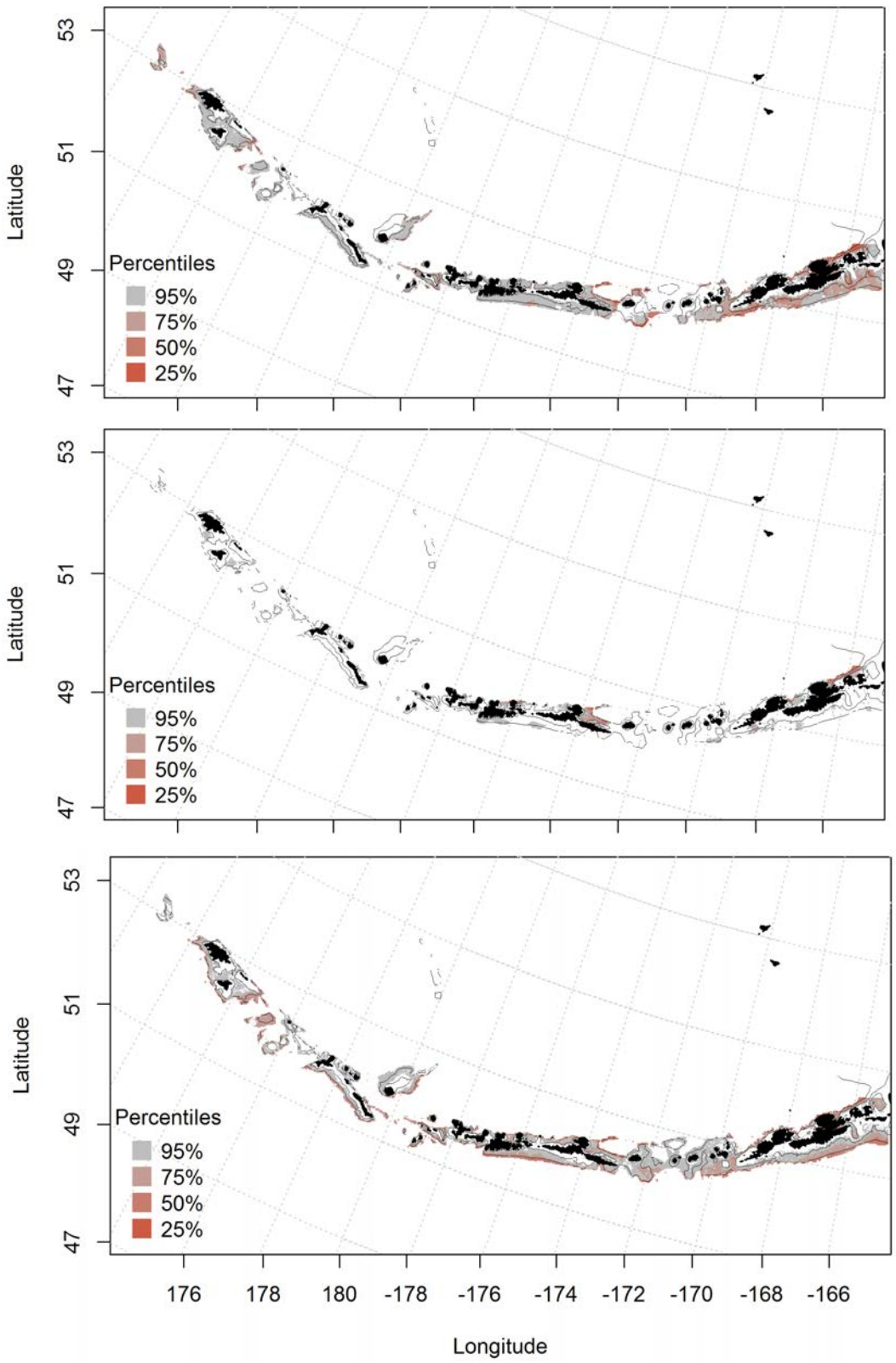

Figure 120. Essential fish habitat predicted for Sablefish during fall (top panel), winter (middle panel) and spring (bottom panel) from summertime commercial catches.

Great sculpin (*Myoxocephalus polyacanthocephalus*)

Summertime distribution of juvenile and adult Great sculpin from bottom trawl surveys of the Aleutian Islands -- The catch of Great sculpin in summer bottom trawl surveys of the Aleutian Islands indicates this species is broadly distributed. A maximum entropy model predicting probable suitable habitat of juvenile Great sculpin explained 95% of the training data variability in CPUE in the bottom trawl survey, and 97% of the test data variability. 88% of the training data and 97% of the test data were correctly classified. Bottom depth and tidal current were the most important variables explaining the distribution of juvenile Great sculpin (relative importance: 57.8% and 28.8%). The model predicted probable suitable habitat of juvenile Great sculpin throughout the AI, though highest near Attu and Agattu Island in the west, and Unalaska Island in the east (Figure 121).

A Maxent model predicting the suitable winter habitat of adult Great sculpin explained 89% of the training data variability in CPUE in the bottom trawl survey, and 84% of the test data variability. 80% of the training data and 84% of the test data were correctly classified. Bottom depth and tidal current were also the most important variables explaining probable suitable habitat of adult Great sculpin (relative importance: 64% and 13.8%). The predicted probability of suitable habitat was similar to juveniles (throughout the AI, though highest near Attu and Agattu Island, and Unalaska Island in the east) (Figure 122).

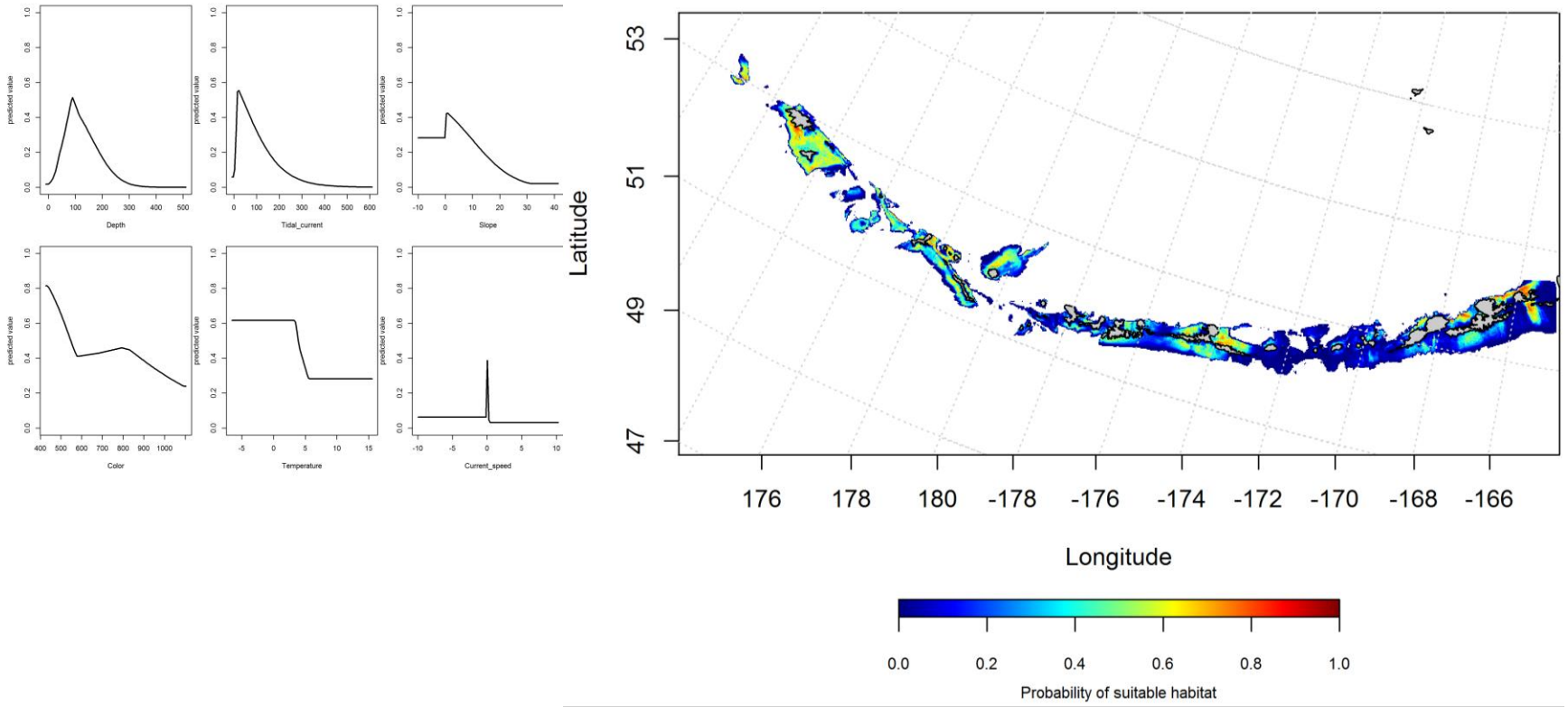

Figure 121. Best-fitting maximum entropy model effects of retained habitat variables on predicted suitable habitat of juvenile Great sculpin from summer bottom trawl surveys of the Aleutian Islands (left panel) alongside maxent-predicted probable juvenile Great sculpin suitable habitat (right panel).

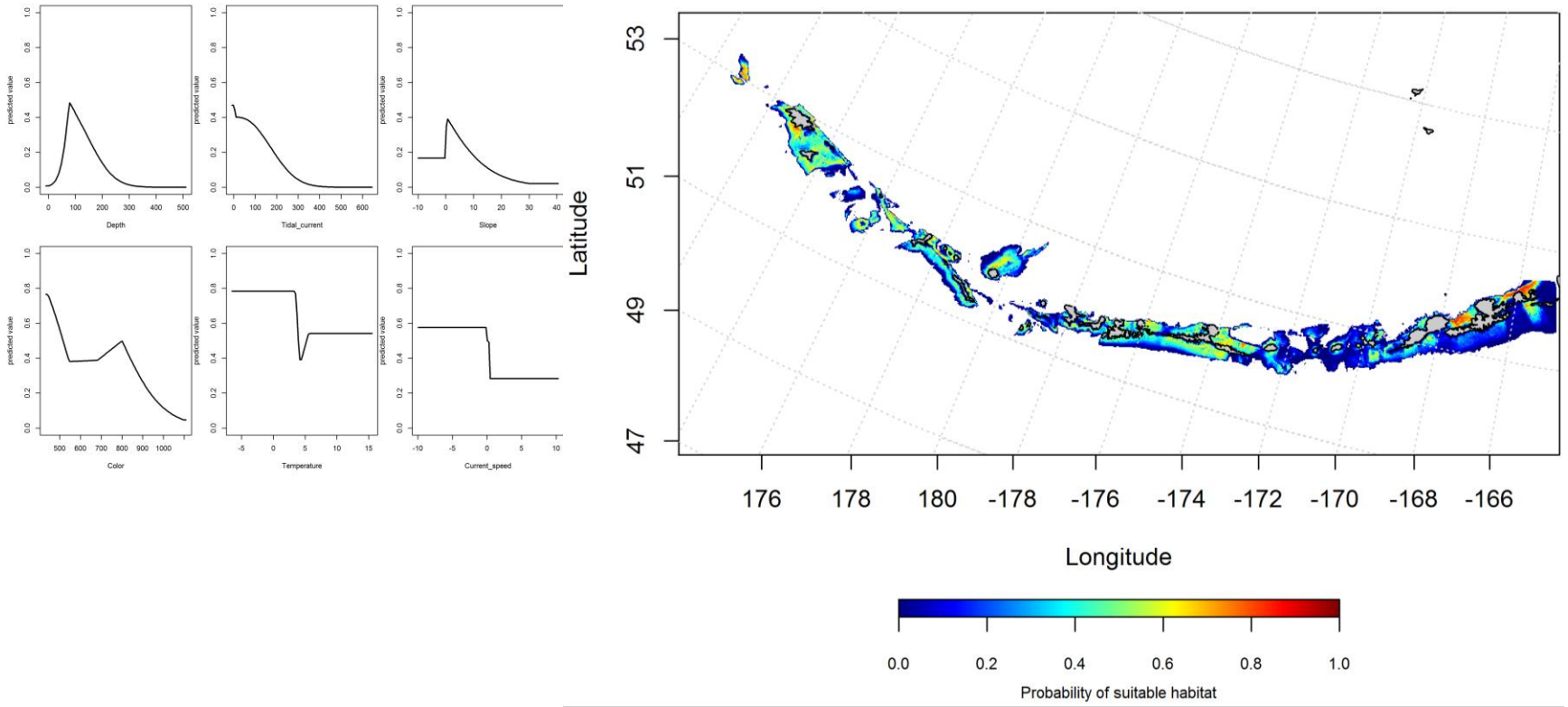

Figure 122. Best-fitting maximum entropy model effects of retained habitat variables on predicted probability of suitable habitat of adult Great sculpin from summer bottom trawl surveys of the Aleutian Islands (left panel) alongside adult Great sculpin probable suitable habitat as predicted by the maxent model (right panel).

Seasonal distribution of commercial fisheries catches of adult Great sculpin in the Aleutian Islands -- There were only 9 observances of Great sculpin in the fall across the AI (Figure 123). There were not enough cases to run the model.

In the winter, bottom depth, ocean color, tidal current, and bottom temperature were the most important variables determining probable suitable habitat of Great sculpin (relative importance: 26.5%, 22.6%, 21.7%, and 13.5%, respectively). The AUC of the winter maxent model was 97% for the training data and 88% for the test data. 93% of the cases in the training data, and 88% of the test data set were predicted correctly. The model predicted probable suitable winter habitat of Great sculpin near Agattu Island in the west, and Atka and Unalaska Islands in the east (Figure 124).

In the spring, ocean color, and bottom depth were the most important variables determining probable suitable habitat of Great sculpin (relative importance: 42.9% and 42.7%). The AUC of the spring maxent model was 95% for the training data and 81% for the test data, and the model correctly predicted 88% of the training data and 81% of the test data. As with the winter, the model predicted probable suitable habitat of Great sculpin near Agattu Island in the west, and Atka Island in the east (Figure 125).

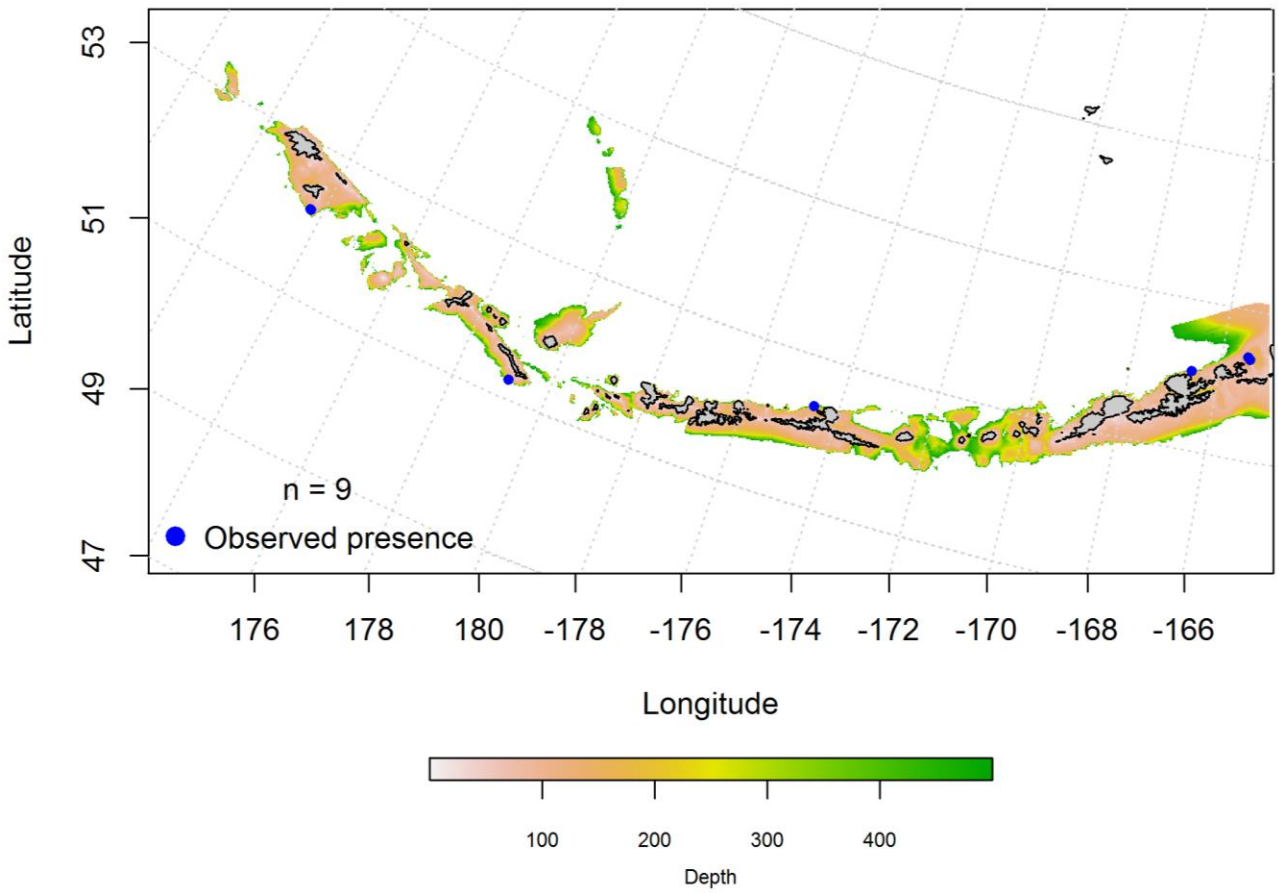

Figure 123. Blue points indicate locations where Great sculpin were observed during fall (September-November) commercial fisheries catches.

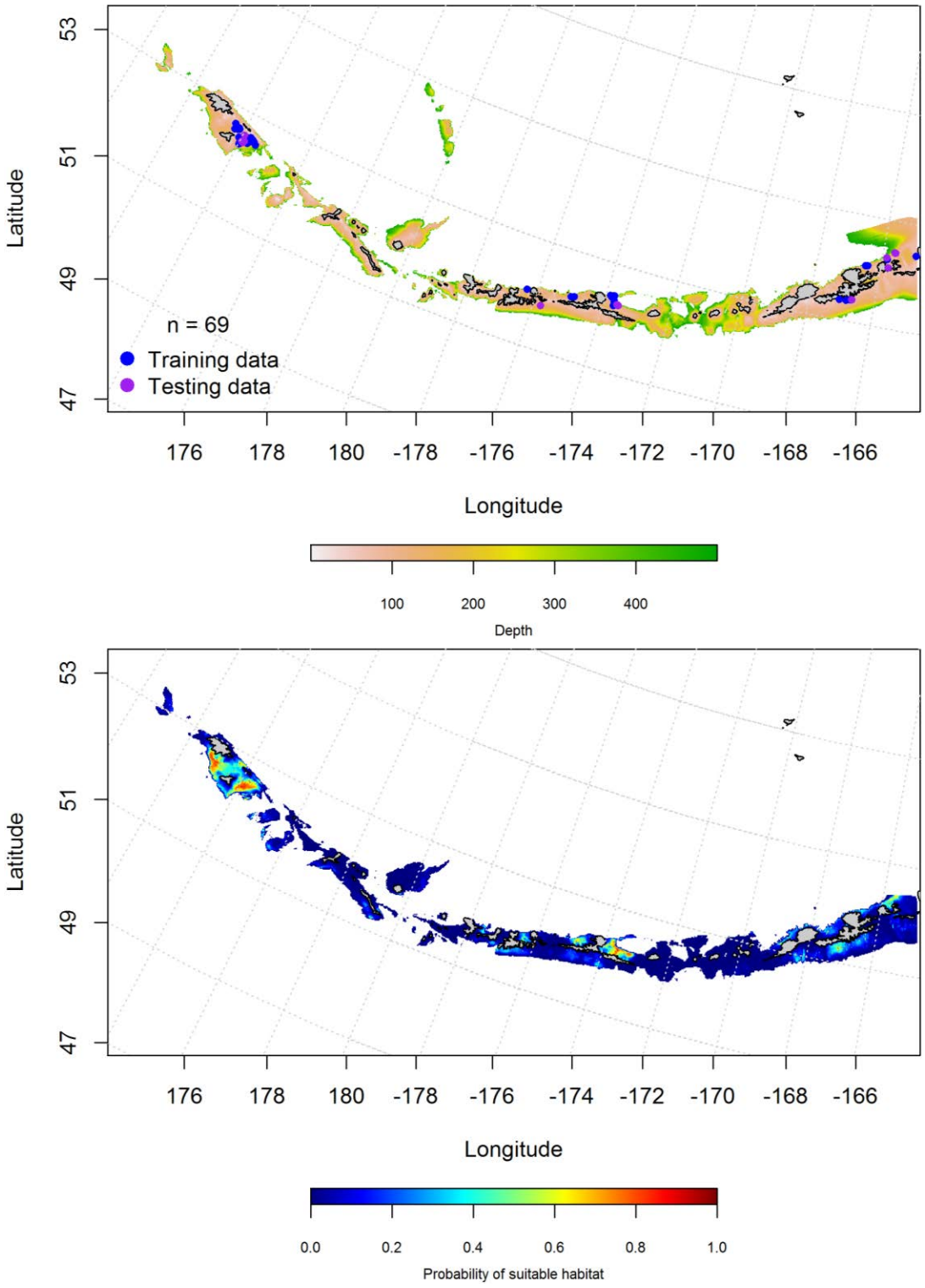

Figure 124. Locations of winter (December-February) commercial fisheries catches of Great sculpin (top panel). Blue points were used to train the maximum entropy model predicting the probability of suitable winter habitat supporting commercial catches of Great sculpin (bottom panel) and the purple points were used to validate the model.

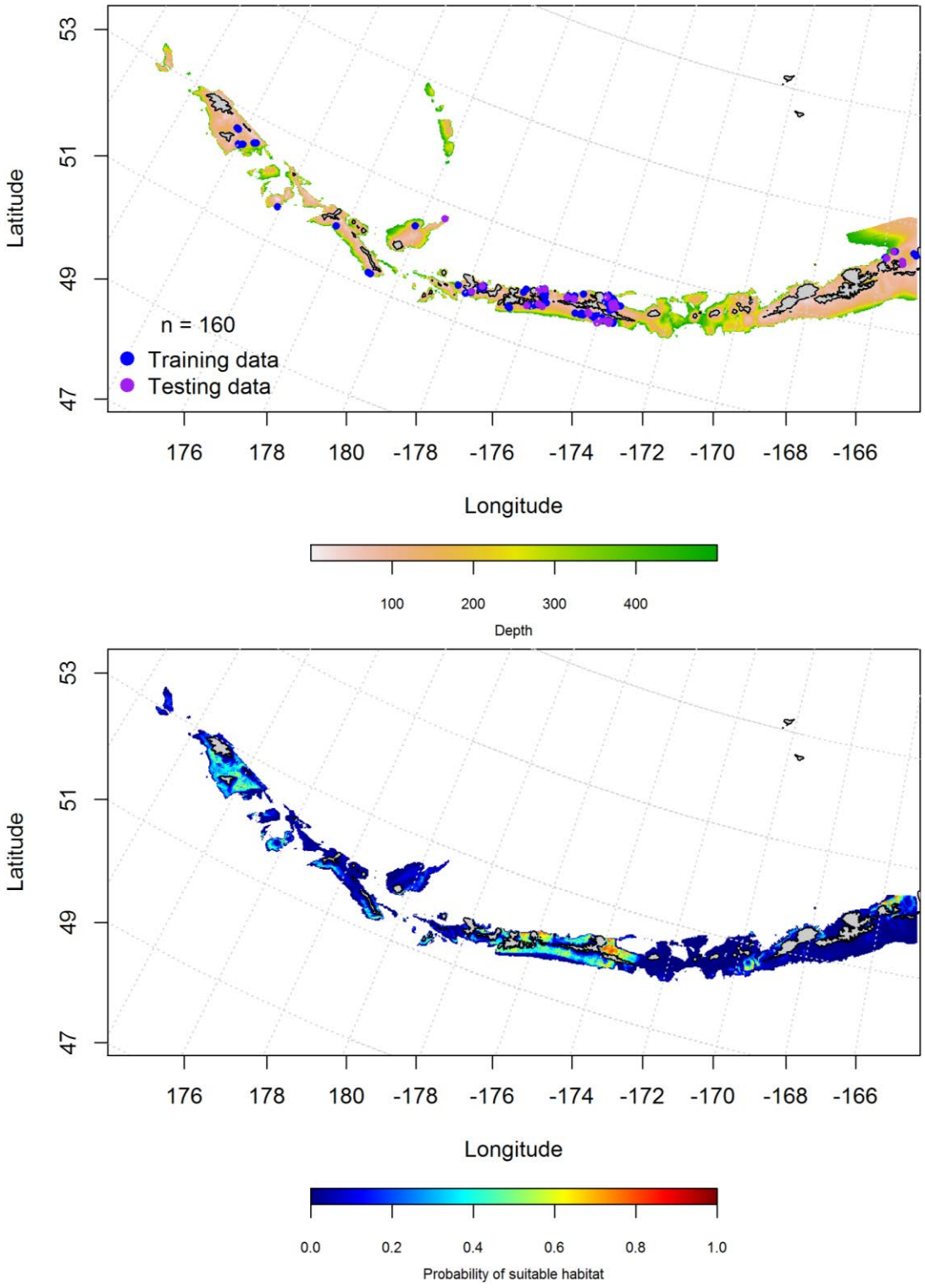

Figure 125. Locations of spring (March-May) commercial fisheries catches of Great sculpin (top panel). Blue points were used to train the maximum entropy model predicting the probability of spring habitat supporting commercial catches of Great sculpin commercial catches (bottom panel) and the purple points were used to validate the model.

Aleutian Islands Great sculpin Essential Fish Habitat Maps and Conclusions – Great sculpin essential fish habitat predicted by the modeling is similarly distributed across the Aleutian Islands for juvenile and adult life stages from summer bottom trawl surveys (Figure 126). For both life stages, there is less suitable habitat for Great sculpin in areas with large passes.

The winter and spring distribution of Great sculpin EFH was generally the same in each season (Figure 127), though more probable near Attu and Agattu Island in the winter.

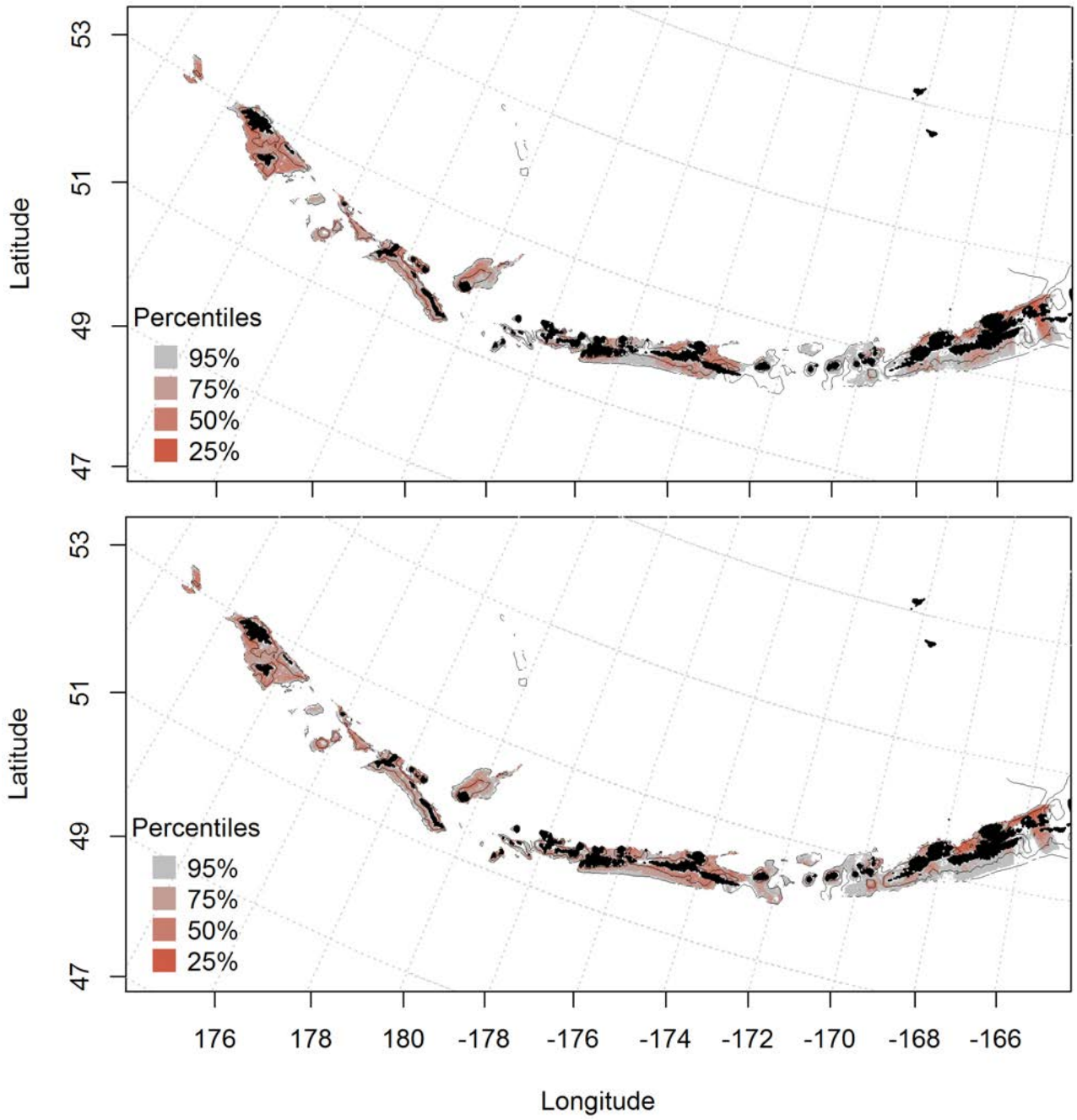

Figure 126. Predicted summer essential fish habitat for Great sculpin juveniles and adults (top and bottom panel) from summertime bottom trawl surveys.

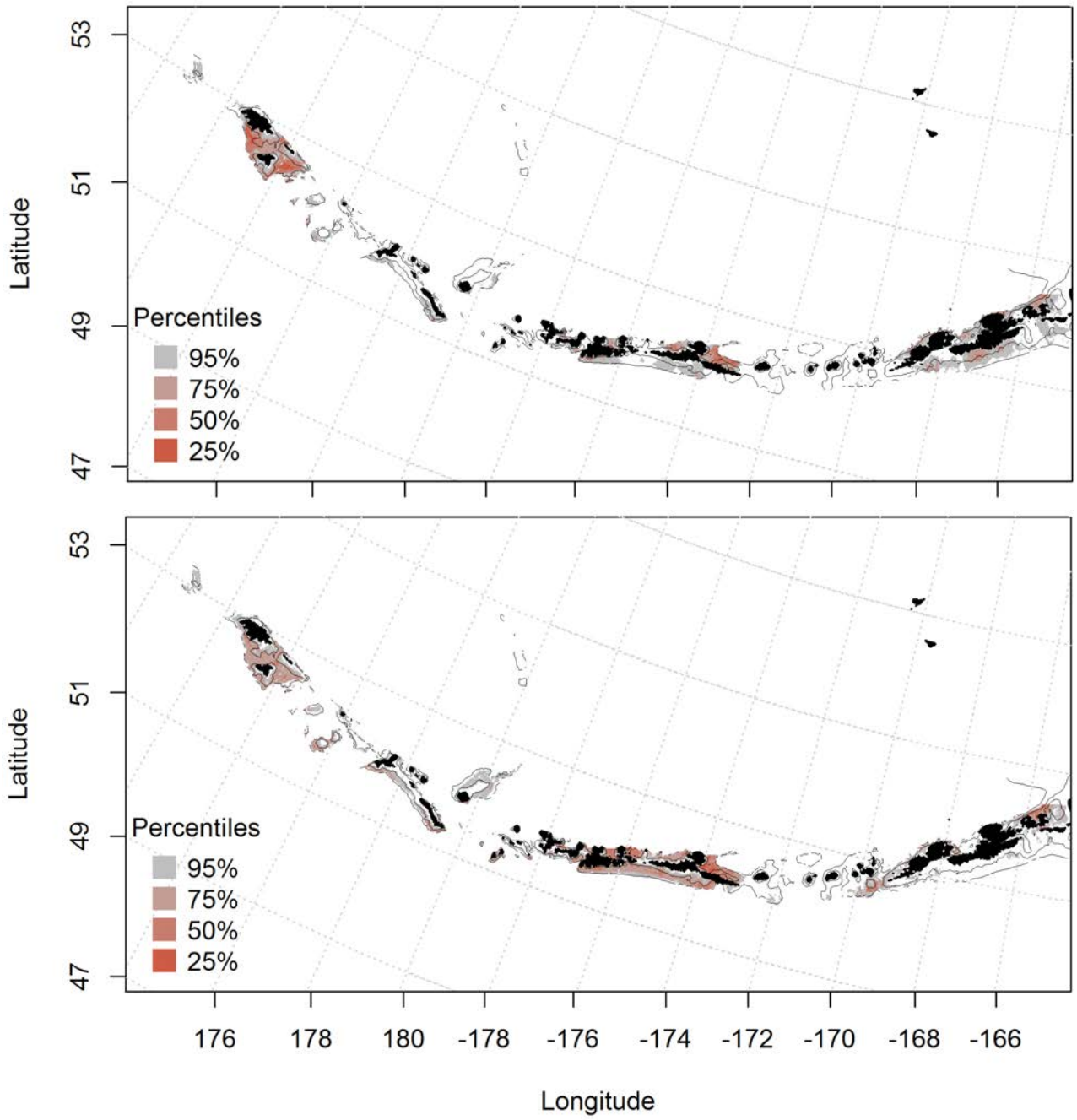

Figure 127. Essential fish habitat predicted for Great sculpin during winter (top panel) and spring (bottom panel) from summertime commercial catches.

Yellow Irish Lord (*Hemilepidotus jordani*)

Summertime distribution of juvenile and adult Yellow Irish Lord from bottom trawl surveys of the Aleutian Islands -- The catch of Yellow Irish Lord in summer bottom trawl surveys of the Aleutian Islands indicates this species is broadly distributed. A maximum entropy model predicting the suitable habitat of juvenile Yellow Irish Lord explained 93% of the variability in the training data, 80% of the variability in the test data set, and correctly classified 86% of the training data and 80% of the test data. Bottom depth and ocean color were the most important variables explaining the probability of suitable habitat of juvenile Yellow Irish Lord across the AI (Figure 128).

A two-step hurdle-Generalized additive model predicting the presence absence (PA GAM) of adult Yellow Irish Lord explained 81% of the variability in CPUE in the bottom trawl survey training data, and 80% of the variability in the test data set. Bottom depth and geographic location were the most important variables explaining the distribution of adult Yellow Irish Lord presence or absence. The model correctly classified 74% of the training and test data sets, and explained 21.8% of the deviance. Predicted juvenile suitable habitat were distributed throughout the AI, though the highest predicted abundance was in the eastern AI (Figure 129).

The second part of the adult Yellow Irish Lord hurdle-GAM predicted CPUE and explained 30% of the variability of the training data set, 18% of the test data set, and 30.5% of the deviance. Tidal current and geographic location were also the most important variables explaining the distribution of adult Yellow Irish Lord CPUE GAM. The areas of predicted highest abundance were similar to the PA GAM, the highest predicted abundance was in the eastern AI (Figure 130).

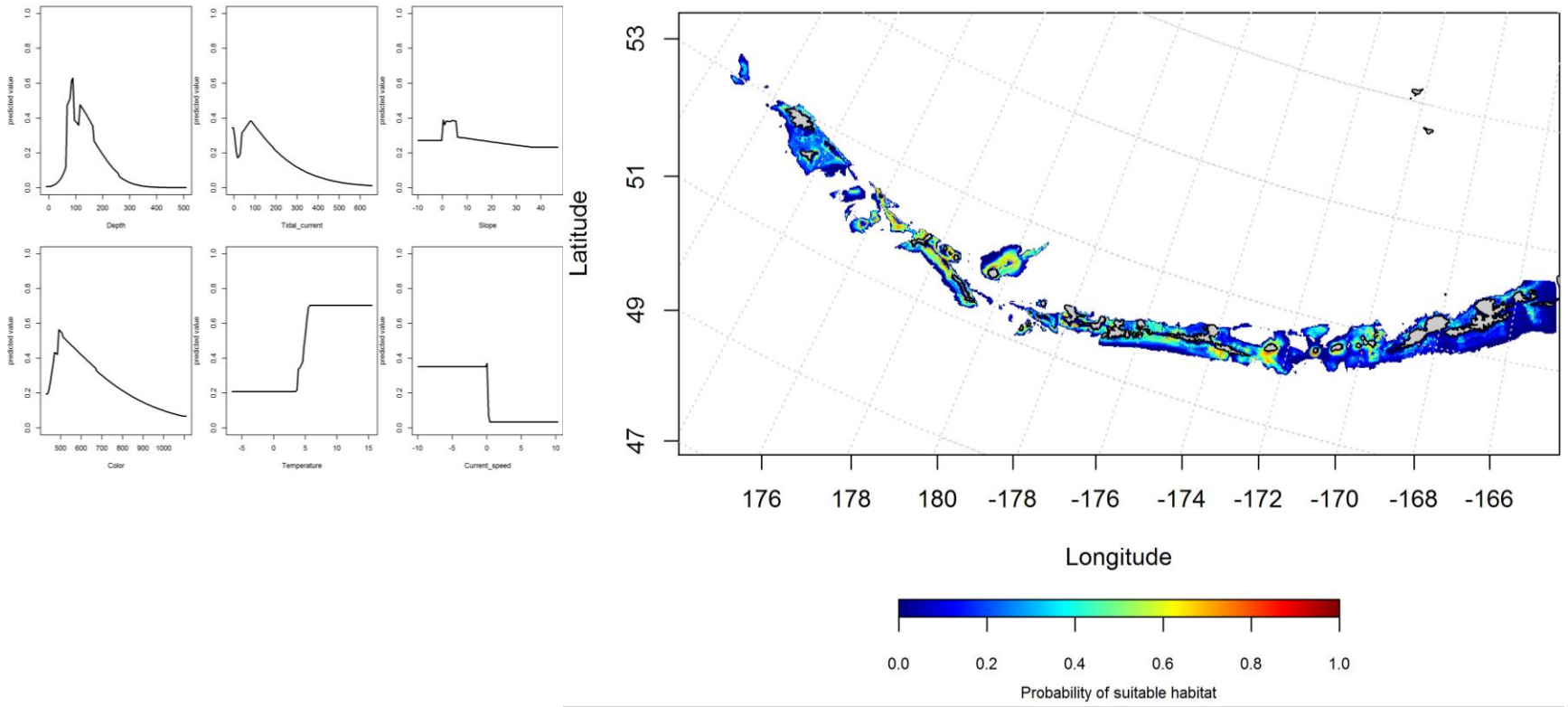

Figure 128. Best-fitting maximum entropy model effects of retained habitat variables on suitable habitat of juvenile Yellow Irish Lord from summer bottom trawl surveys of the Aleutian Islands (left panel) alongside maxent-predicted juvenile Yellow Irish Lord suitable habitat (right panel).

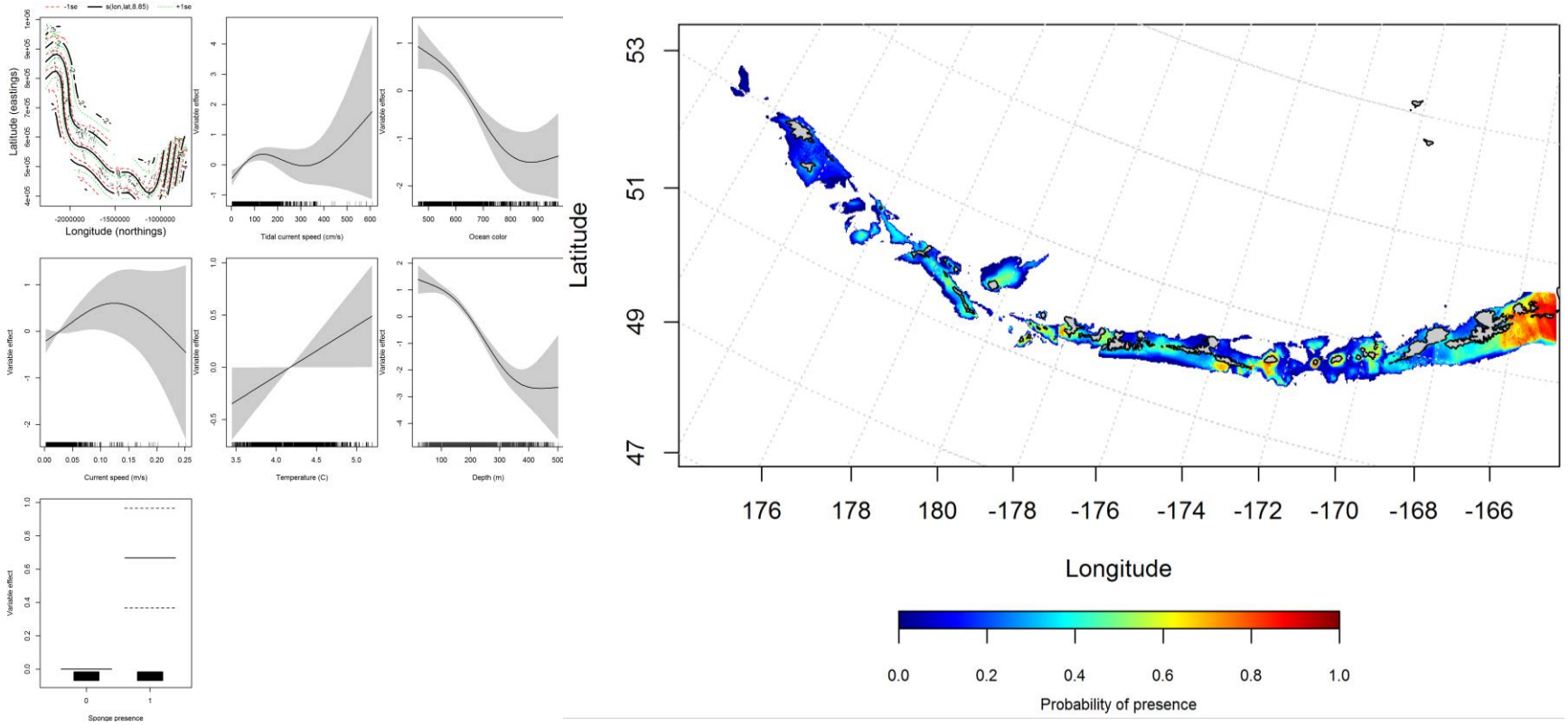

Figure 129. Best-fitting hurdle model effects of retained habitat variables on presence absence (PA) of adult Yellow Irish Lord from summer bottom trawl surveys of the Aleutian Islands (left panel) alongside hurdle-predicted adult Yellow Irish Lord PA (right panel).

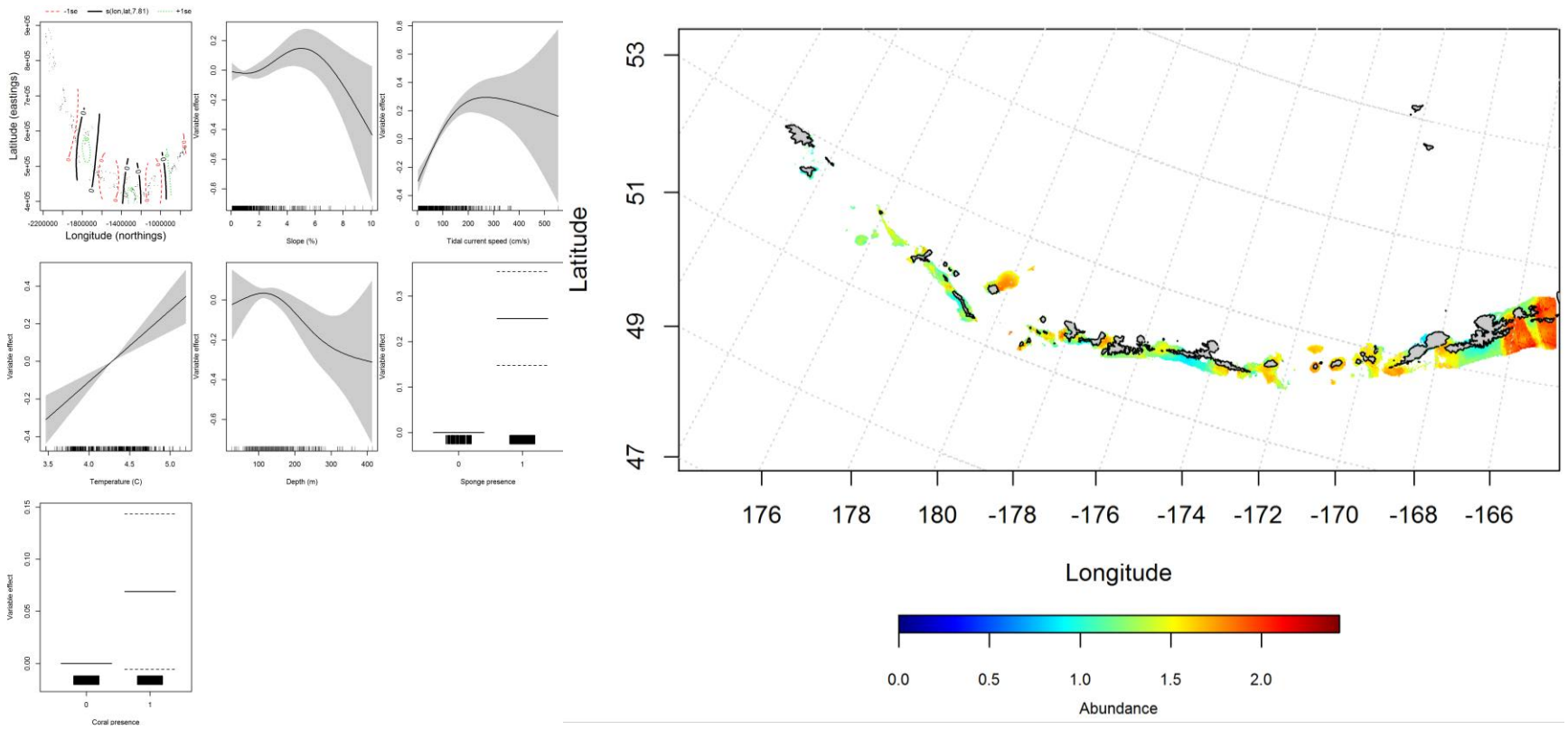

Figure 130. Best-fitting hurdle model effects of retained habitat variables on CPUE of adult Yellow Irish Lord from summer bottom trawl surveys of the Aleutian Islands (left panel) alongside hurdle-predicted adult Yellow Irish Lord CPUE (right panel)..

Seasonal distribution of commercial fisheries catches of adult Yellow Irish Lord in the Aleutian Islands-- Distribution of adult Yellow Irish Lord in the Aleutian Islands in commercial fisheries catches was generally consistent throughout all seasons. In the fall, current speed, bottom depth, and bottom temperature were the most important variables determining probable suitable habitat of Yellow Irish Lord (relative importance: 30.2%, 28%, and 17.7%, respectively). The AUC of the fall maxent model was 97% for the training data and 90% for the test data and 89% of the cases in both the training data and 90% of the test data sets were predicted correctly. The model predicted suitable habitat of Yellow Irish Lord across the AI (Figure 131).

In the winter, bottom depth, current speed, and tidal current were the most important variables determining probable suitable habitat of Yellow Irish Lord (relative importance: 50.5%, 26.3%, and 9.9%, respectively). The AUC of the winter maxent model was 94% for the training data and 86% for the test data. 84% of the cases in the training data and 86% of the test data sets were predicted correctly. As with the fall, the model predicted probable suitable habitat of Yellow Irish Lord across the AI, though more probable in the winter than in the fall (Figure 132).

In the spring, bottom depth, and ocean color were the most important variables determining probable suitable habitat of Yellow Irish Lord (relative importance: 57.6% and 18.8%). The AUC of the spring maxent model was 95% for the training data and 89% for the test data. The model correctly classified 88% of the training data and 89% of the test data. The model predicted suitable habitat of Yellow Irish Lord across the AI, though were more suitable in the western AI near Attu and Agatuu Island, and in the central AI (Figure 133).

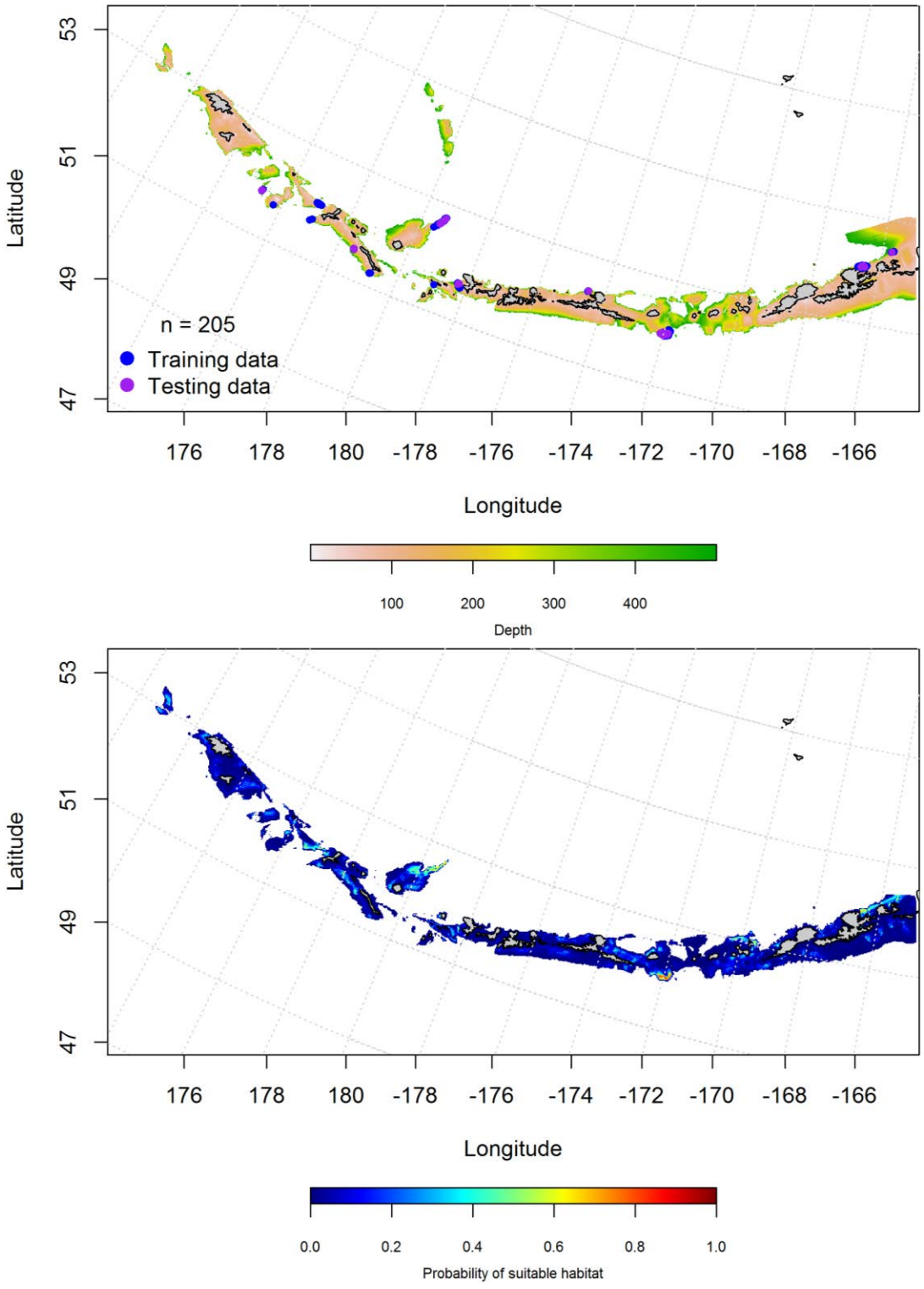

Figure 131. Locations of fall (September-November) commercial fisheries catches of Yellow Irish Lord (top panel). Blue points were used to train the maximum entropy model predicting the probability of suitable fall habitat supporting commercial catches of Yellow Irish Lord (bottom panel) and the purple points were used to validate the model.

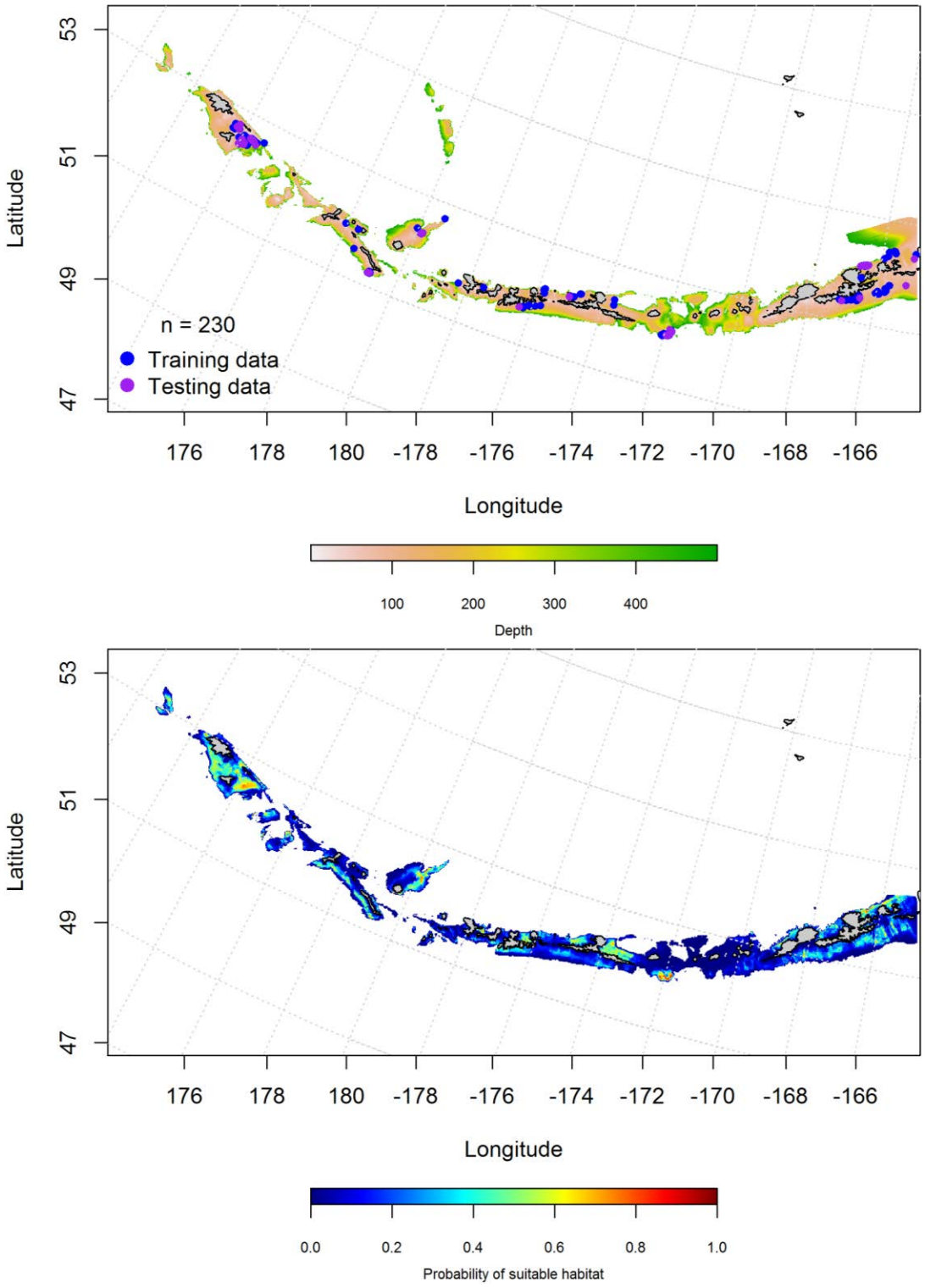

Figure 132. Locations of winter (December-February) commercial fisheries catches of Yellow Irish Lord (top panel). Blue points were used to train the maximum entropy model predicting the probability of suitable winter habitat supporting commercial catches of Yellow Irish Lord (bottom panel) and the purple points were used to validate the model.

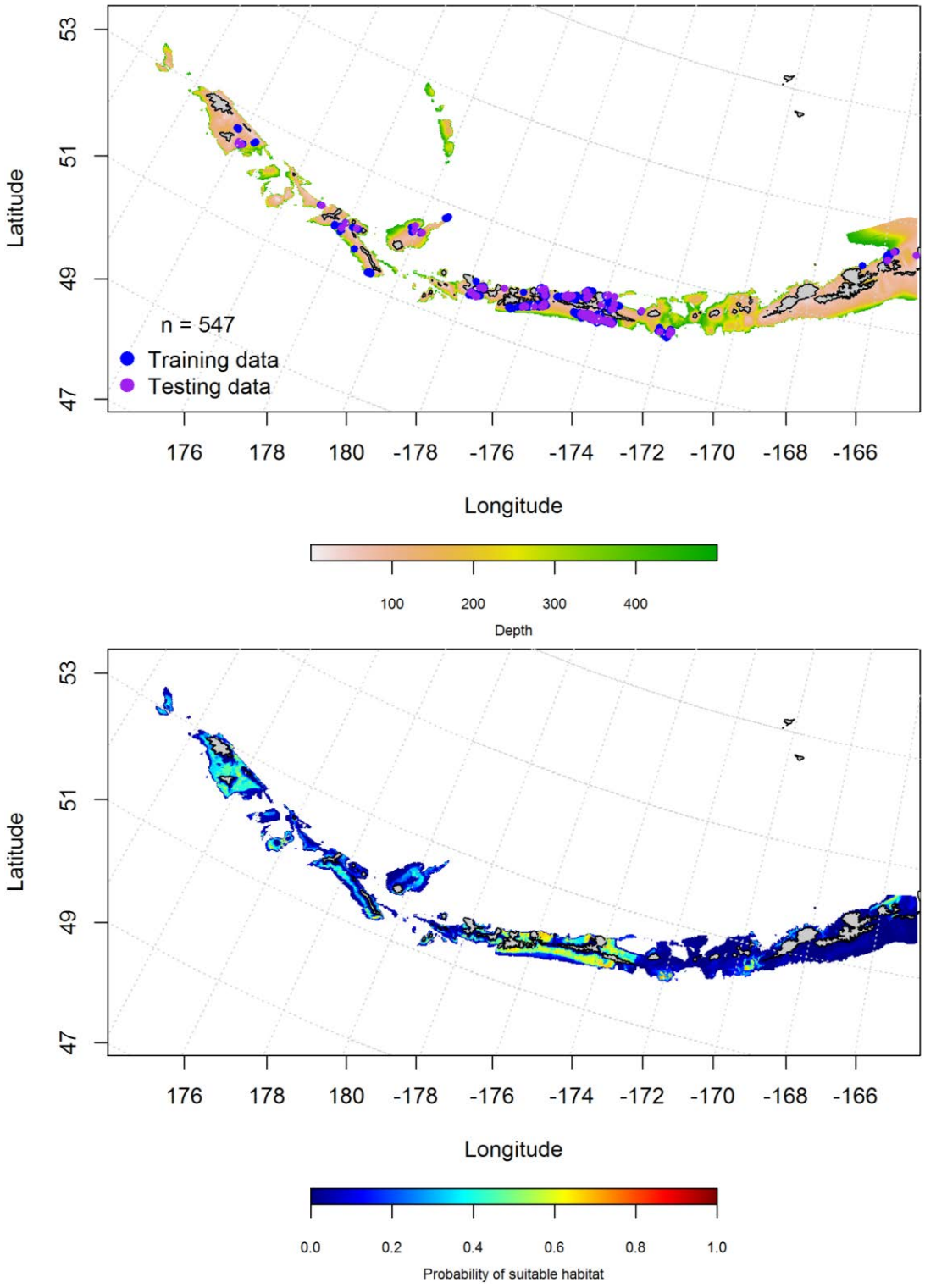

Figure 133. Locations of spring (March-May) commercial fisheries catches of Yellow Irish Lord (top panel). Blue points were used to train the maximum entropy model predicting the probability of suitable spring habitat supporting commercial catches of Yellow Irish Lord (bottom panel) and the purple points were used to validate the model.

Aleutian Islands Yellow Irish Lord Essential Fish Habitat Maps and Conclusions --

Summertime EFH of Yellow Irish Lord juveniles and adults varied in the western AI (Figure 134). Juveniles EFH was more probable in the central AI according to the model. Adult Yellow Irish Lords were distributed across the AI and less abundant in the western AI, though more abundant in the eastern AI than the juveniles.

The fall, winter and spring distribution of Yellow Irish Lord was essentially the same throughout the seasons (Figure 135). EFH was distributed across the AI, though was more abundant in the central AI in the spring.

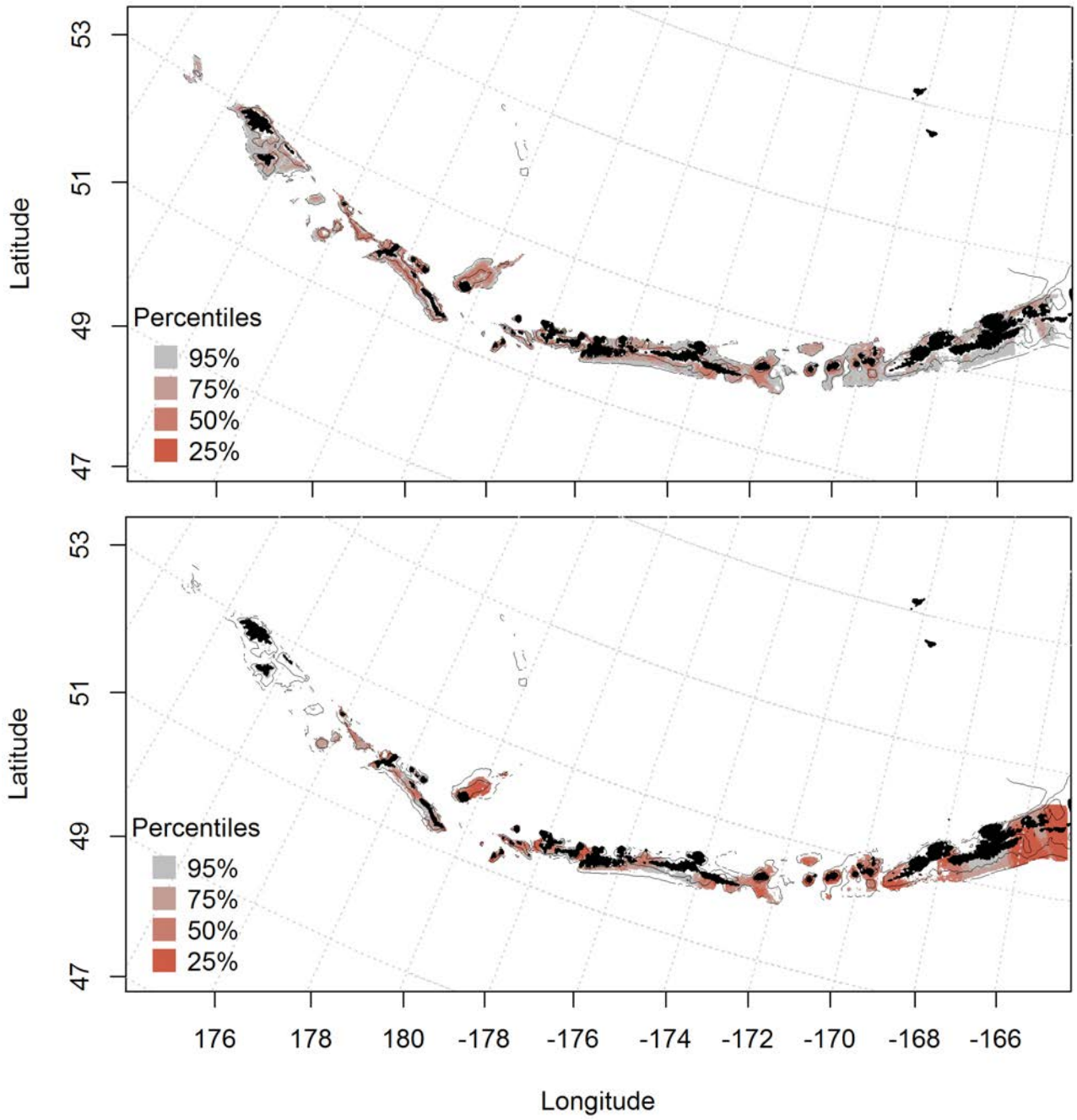

Figure 134. Predicted summer essential fish habitat for Yellow Irish Lord juveniles and adults (top and bottom panel) from summertime bottom trawl surveys.

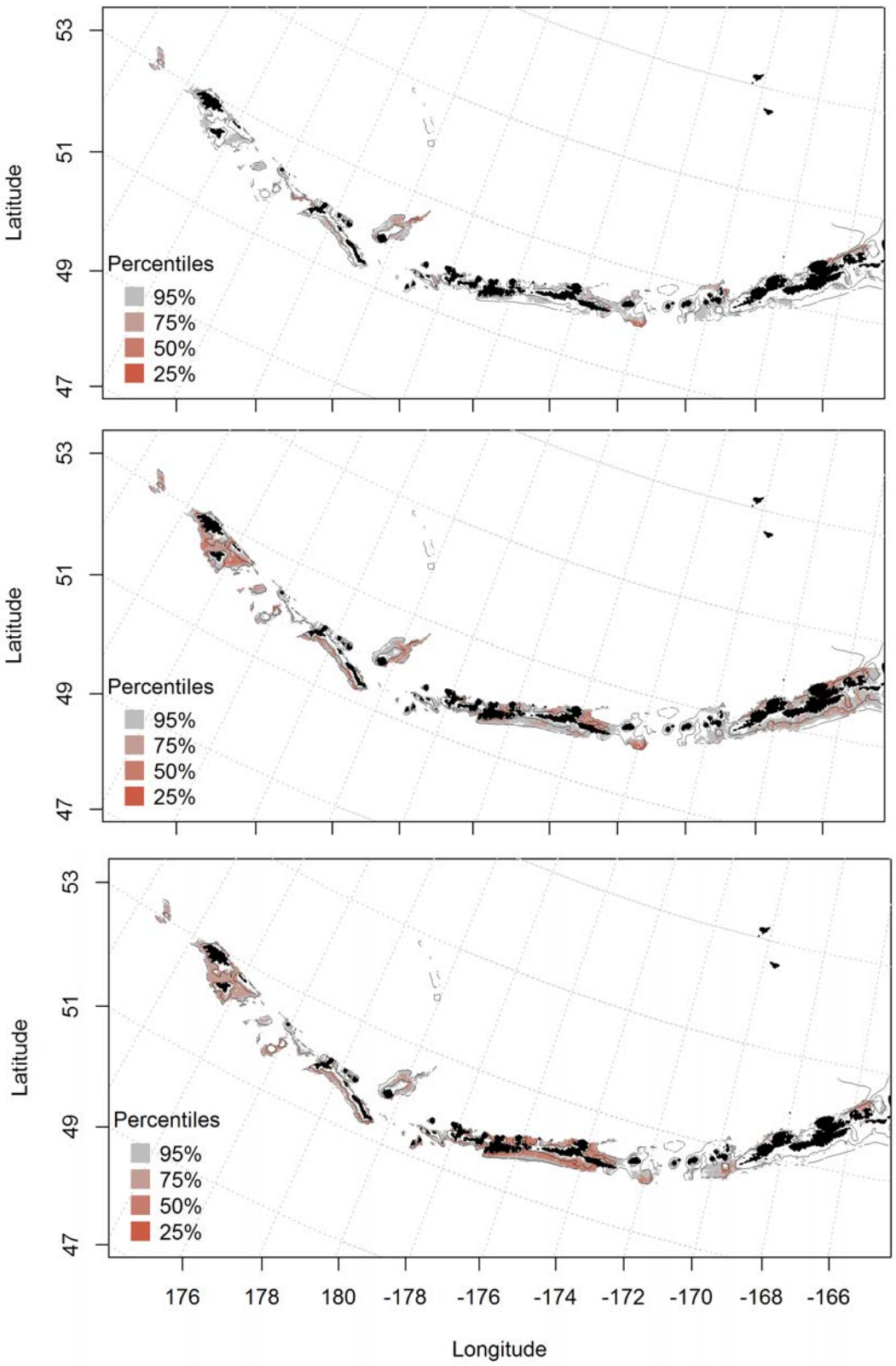

Figure 135. Essential fish habitat predicted for Yellow Irish Lord during fall (top panel), winter (middle panel) and spring (bottom panel) from summertime commercial catches.

Bigmouth sculpin (*Hemitripterus bolini*)

Seasonal distribution of early life history stages of Bigmouth sculpin in the Aleutian Islands-- There were only 14 instances of spring Bigmouth sculpin larvae observed in the FOCI database in the eastern AI (Figure 136). There were not enough cases to run the model.

There was only 1 instance of spring Bigmouth sculpin juvenile observed in the FOCI database in the eastern AI (Figure 137). There were not enough cases to run the model.

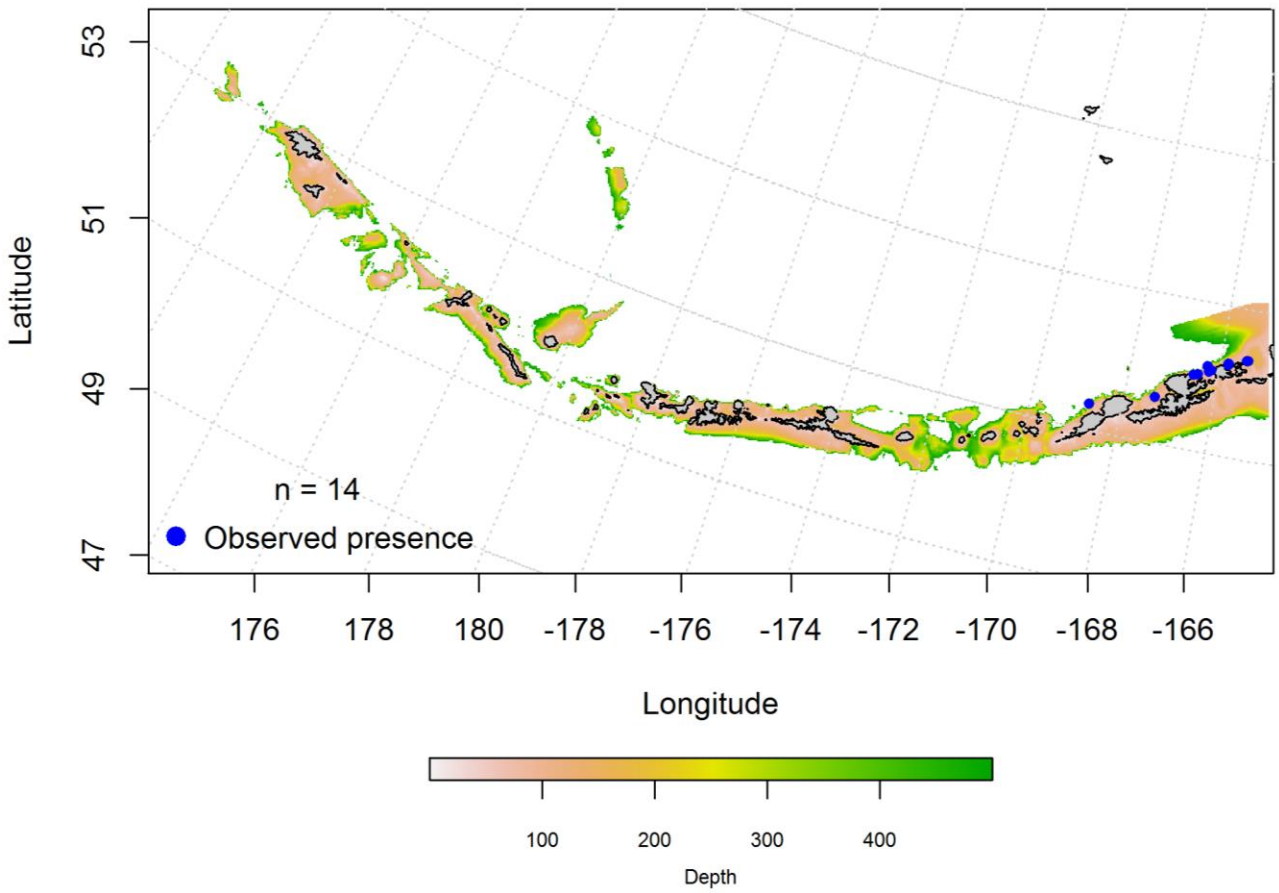

Figure 136. Spring observations of larval Bigmouth sculpin from the Aleutian Islands.

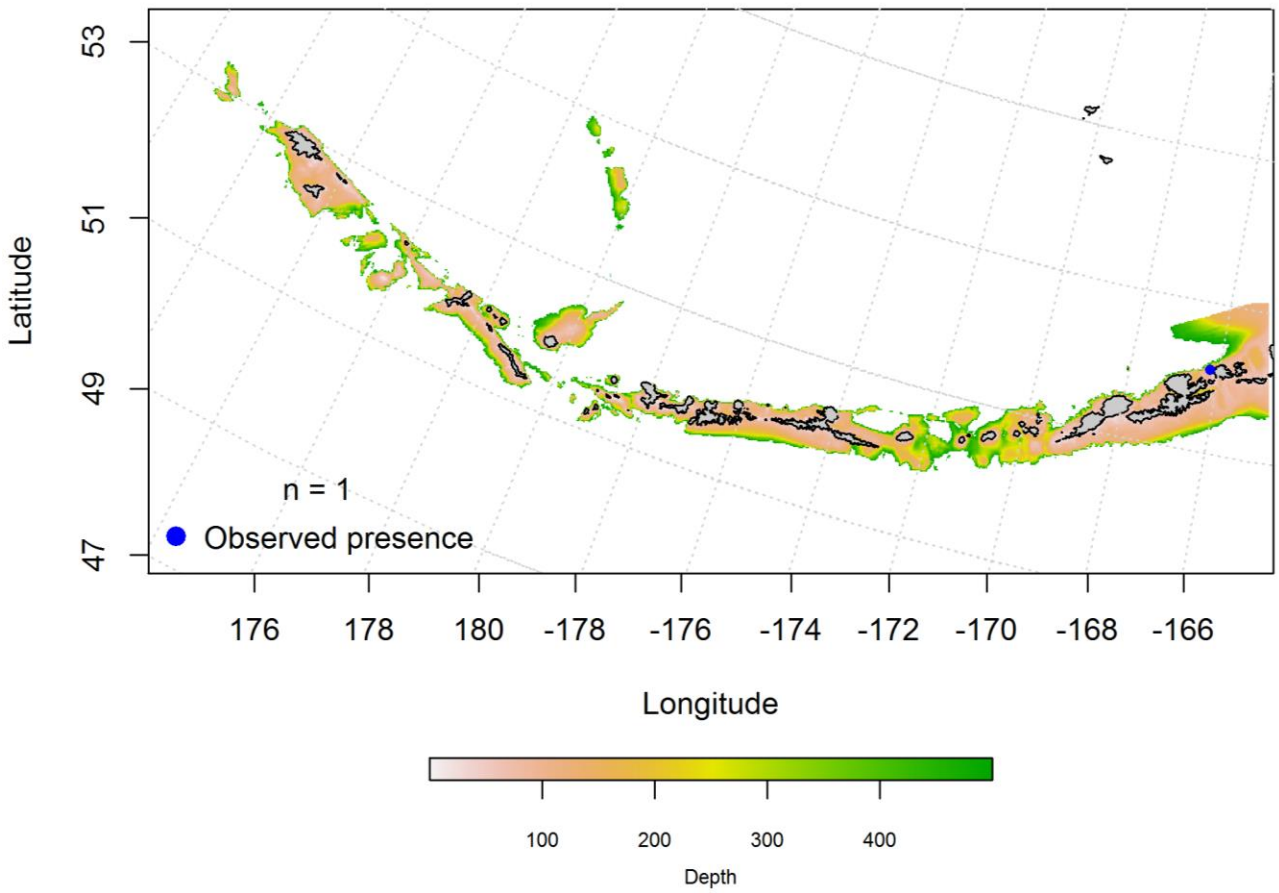

Figure 137. Spring observations of early juvenile Bigmouth sculpin in the Aleutian Islands.

Summertime distribution of juvenile and adult Bigmouth sculpin from bottom trawl surveys of the Aleutian Islands -- The catch of Bigmouth sculpin in summer bottom trawl surveys of the Aleutian Islands indicates this species is broadly distributed. A maximum entropy model predicting suitable habitat of juvenile Bigmouth sculpin explained 89% of the variability in CPUE in the bottom trawl survey in the training data and 92% of the variability in the test data. The model correctly classified 79% of the training data and 92% of the test data. Ocean color, bottom depth, and bottom temperature were the most important variables explaining probable suitable habitat of juvenile Bigmouth sculpin (relative abundance: 43.2%, 31.2%, and 16.6%, respectively). The model predicted probable suitable habitat of juvenile Bigmouth

sculpin across the AI, though highest near Attu and Agattu Island in the west, Adak Island in the central AI, and Akutan Island in the eastern AI (Figure 138).

A maxent model predicting probable suitable habitat of adult Bigmouth sculpin explained 76% of the variability in CPUE in the bottom trawl survey in the training data and 71% of the variability in the test data. The model correctly classified 69% of the training data and 71% of the test data. Bottom depth, current speed, and bottom temperature were the most important variables explaining probable suitable habitat of adult Bigmouth sculpin suitable habitat (relative abundance: 57.3%, 15.7%, and 14.3%, respectively). The model predicted probable suitable habitat of adult Bigmouth sculpin across the AI, though highest near Attu and Agattu Island in the west, Seguam Island in the central AI, and Akutan Island in the eastern AI (Figure 139).

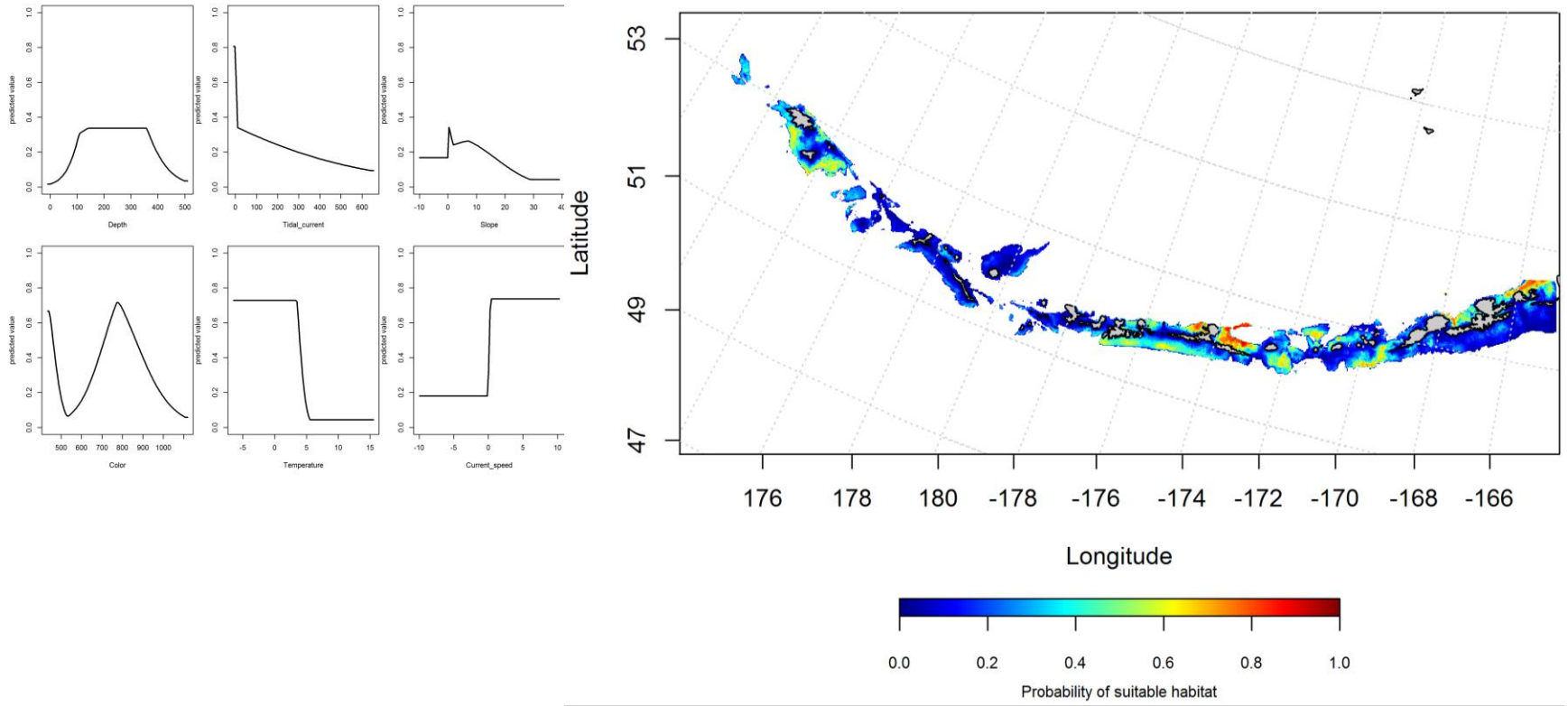

Figure 138. Best-fitting maximum entropy model effects of retained habitat variables on probable suitable habitat of juvenile Bigmouth sculpin from summer bottom trawl surveys of the Aleutian Islands (left panel) alongside maxent-predicted juvenile Bigmouth sculpin probable suitable habitat (right panel).

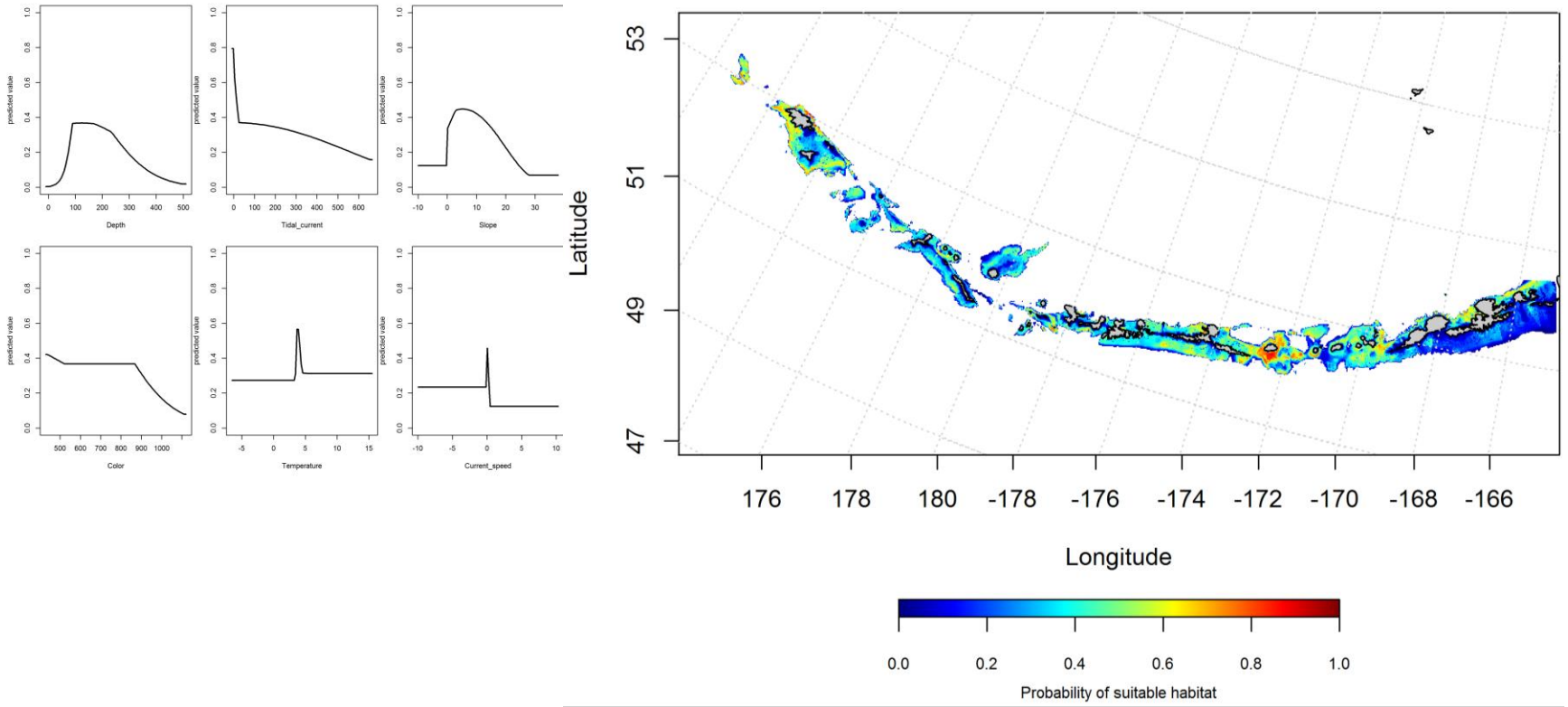

Figure 139. Best-fitting maximum entropy model effects of retained habitat variables on probable suitable habitat of adult Bigmouth sculpin from summer bottom trawl surveys of the Aleutian Islands (left panel) alongside probable suitable habitat of adult Bigmouth sculpin from the maxent model (right panel).

Seasonal distribution of commercial fisheries catches of adult Bigmouth sculpin in the Aleutian Islands-- Distribution of adult Bigmouth sculpin in the Aleutian Islands in commercial fisheries catches was generally consistent throughout all seasons. In the fall, bottom depth, bottom temperature, and tidal current were the most important variables determining probable suitable habitat of Bigmouth sculpin (relative importance: 34%, 32%, and 12.2%, respectively). The AUC of the fall maxent model was 97% for the training data and 88% for the test data. 91% of the training data and 88% of the test data were correctly classified. The model predicted probable suitable habitat of adult Bigmouth sculpin across the AI (Figure 140).

In the winter, bottom depth, tidal current and ocean color were the most important variables determining probable suitable habitat of Bigmouth sculpin (relative importance: 38.5%, 25.8%, and 17.8%, respectively). The AUC of the winter maxent model was 97% for the training data and 87% for the test data. 90% of the training data and 87% of the test data sets were predicted correctly. The model predicted probable suitable winter habitat of adult Bigmouth sculpin across the AI, though highest suitable habitat was predicted in the western AI near Agattu and Attu Islands, and in the central AI near Atka Island (Figure 141).

In the spring, bottom depth and ocean color were the most important variables determining probable suitable habitat of Bigmouth sculpin (relative importance: 42.2% and 37.6%). The AUC of the spring maxent model was 94% for the training data and 87% for the test data, and 87% of the training and test data sets were correctly classified. The model predicted probable spring suitable habitat of Bigmouth sculpin similar to the winter (across the AI, though highest suitable habitat was predicted in the western AI near Agattu and Attu Islands, and in the central AI near Atka Island) (Figure 142).

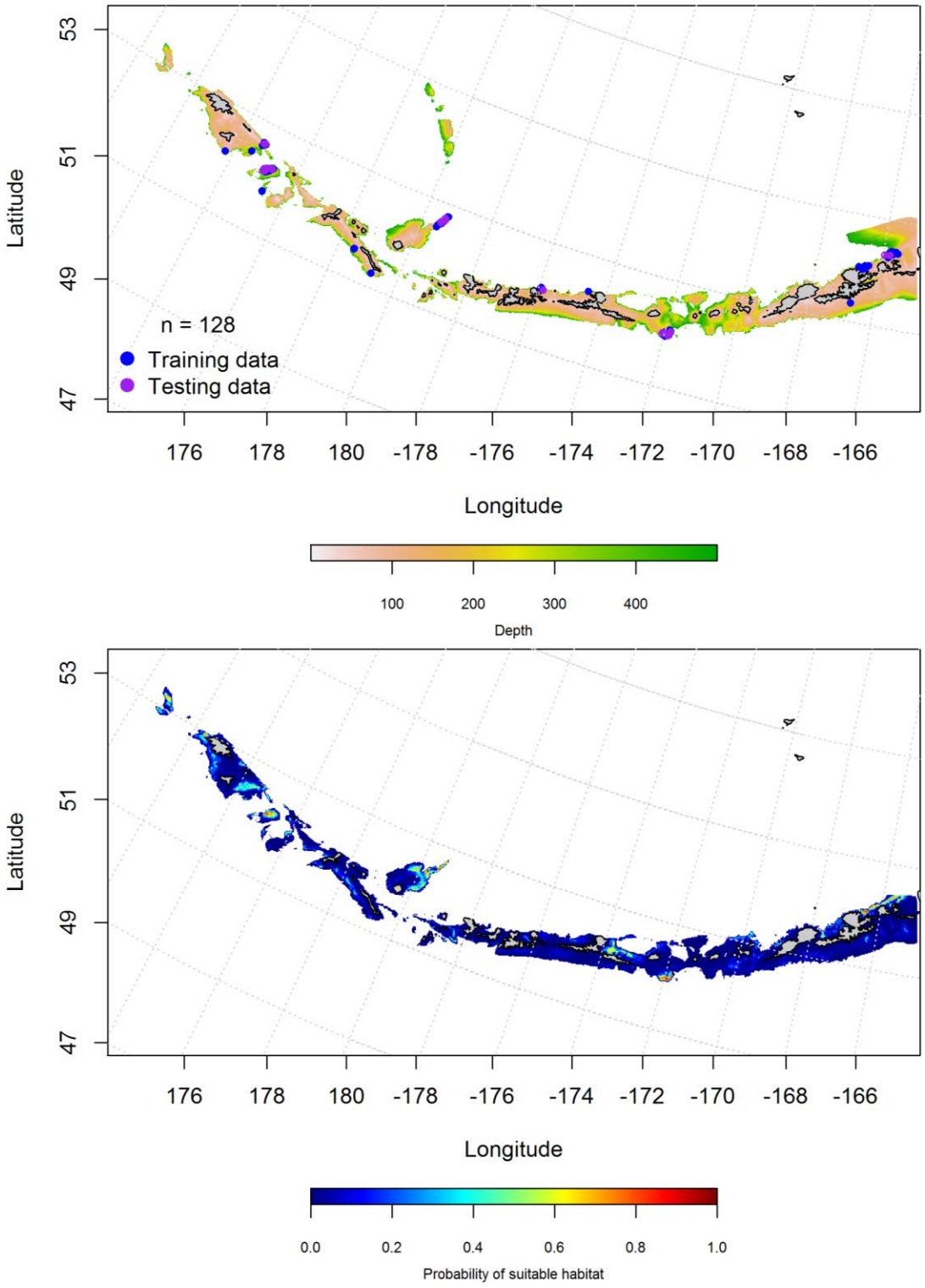

Figure 140. Locations of fall (September-November) commercial fisheries catches of adult Bigmouth sculpin (top panel). Blue points were used to train the maximum entropy model predicting the probability of suitable fall habitat supporting commercial catches of adult Bigmouth sculpin (bottom panel) and the purple points were used to validate the model.

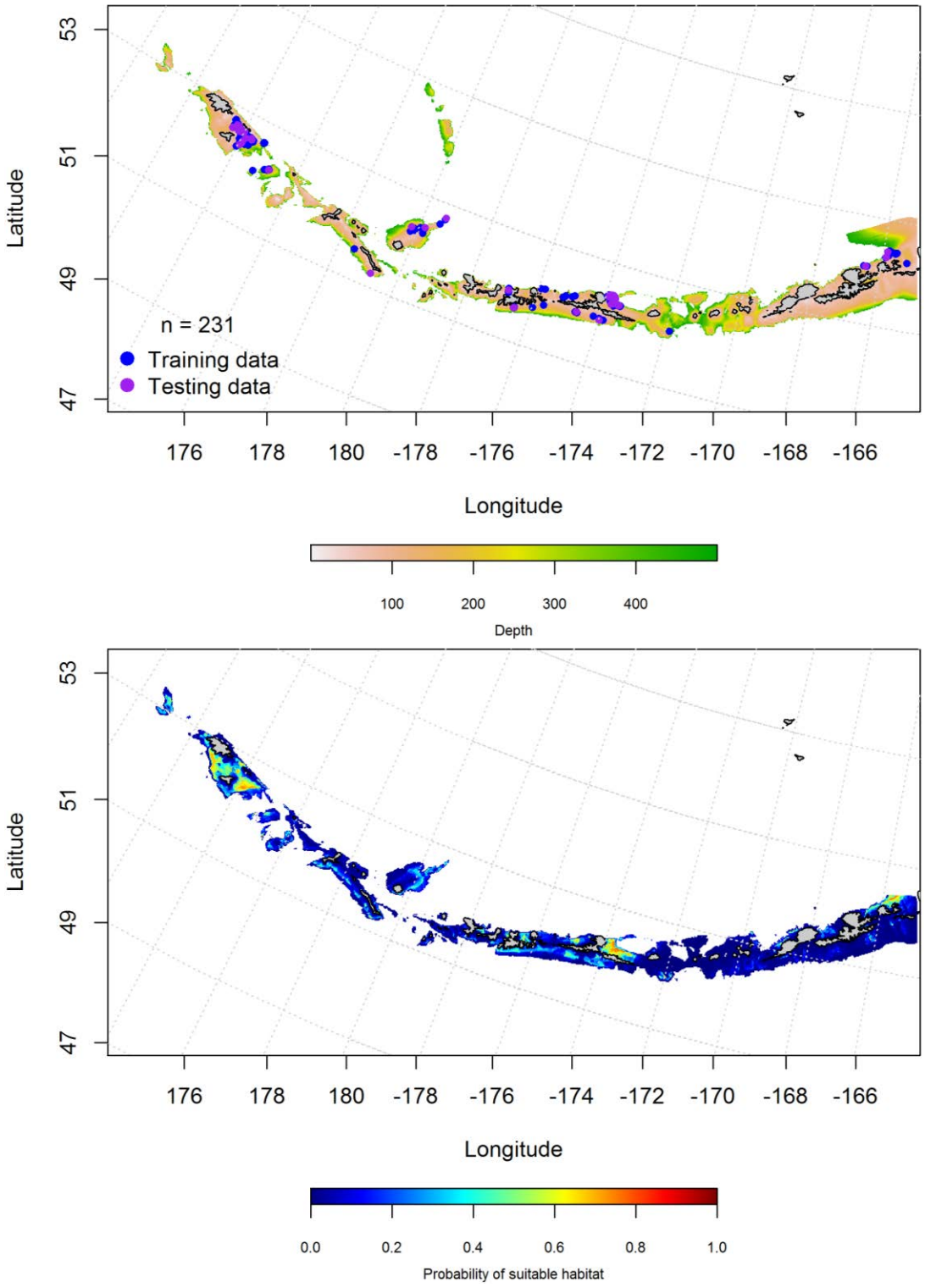

Figure 141. Locations of winter (December-February) commercial fisheries catches of adult Bigmouth sculpin (top panel). Blue points were used to train the maximum entropy model predicting the probability of suitable winter habitat supporting commercial catches of adult Bigmouth sculpin (bottom panel) and the purple points were used to validate the model.

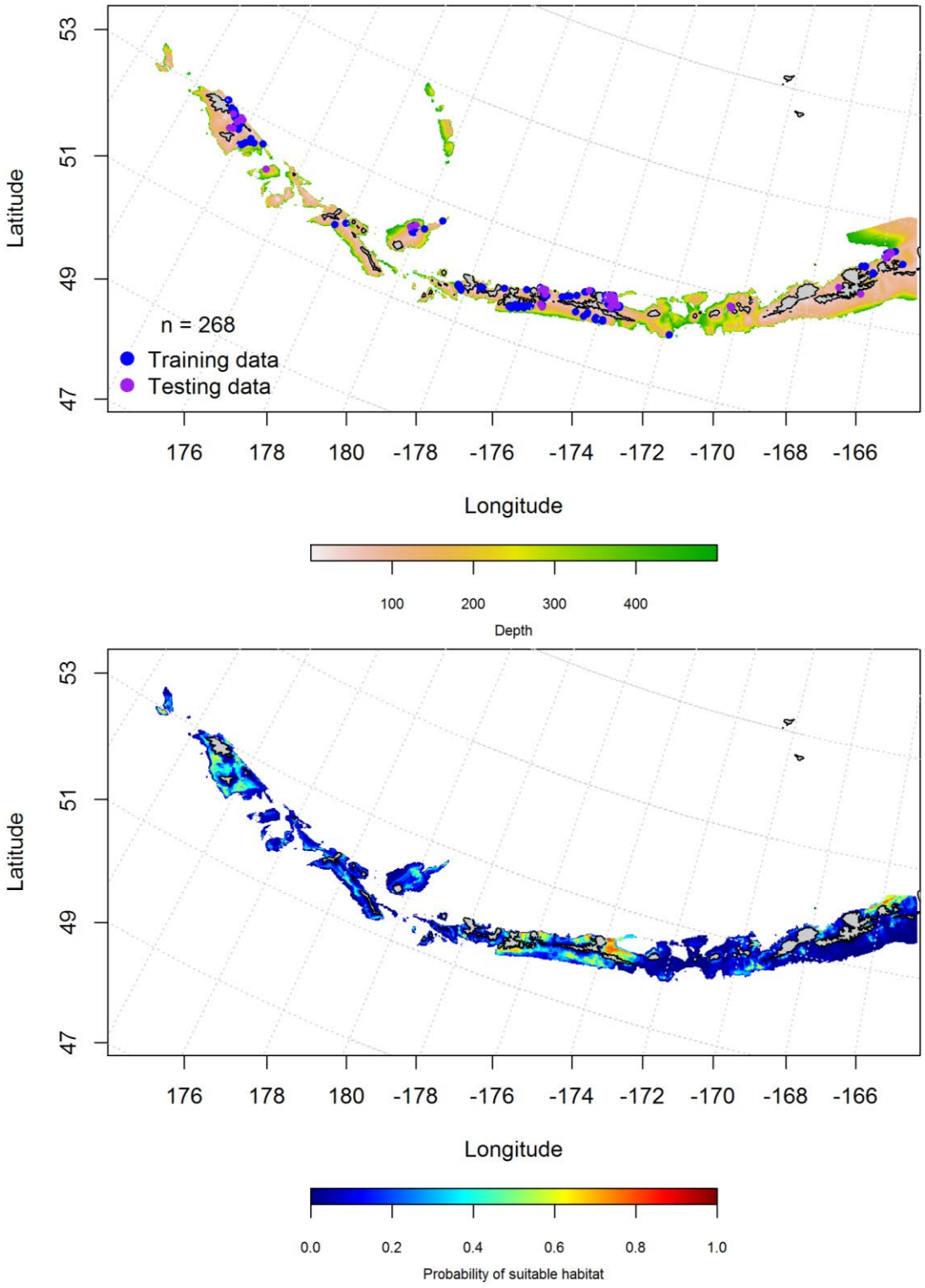

Figure 142. Locations of spring (March-May) commercial fisheries catches of adult Bigmouth sculpin (top panel). Blue points were used to train the maximum entropy model predicting the probability of suitable spring habitat supporting commercial catches of adult Bigmouth sculpin (bottom panel) and the purple points were used to validate the model.

Aleutian Islands Bigmouth sculpin Essential Fish Habitat Maps and Conclusions -- Bigmouth sculpin essential fish habitat predicted by the modeling is extensively distributed across the Aleutian Islands for juvenile and adult life history stages (Figure 143). Juvenile EFH was similarly distributed as the adults, and less abundant in areas of large passes.

The fall, winter and spring distribution of Bigmouth sculpin EFH was generally the same throughout the seasons in the Aleutian Islands (Figure 144). Bigmouth sculpin were predicted to be more abundant in the western AI near Agattu and Attu Islands in the winter, and in the central AI near Atka Island in the spring than in other seasons.

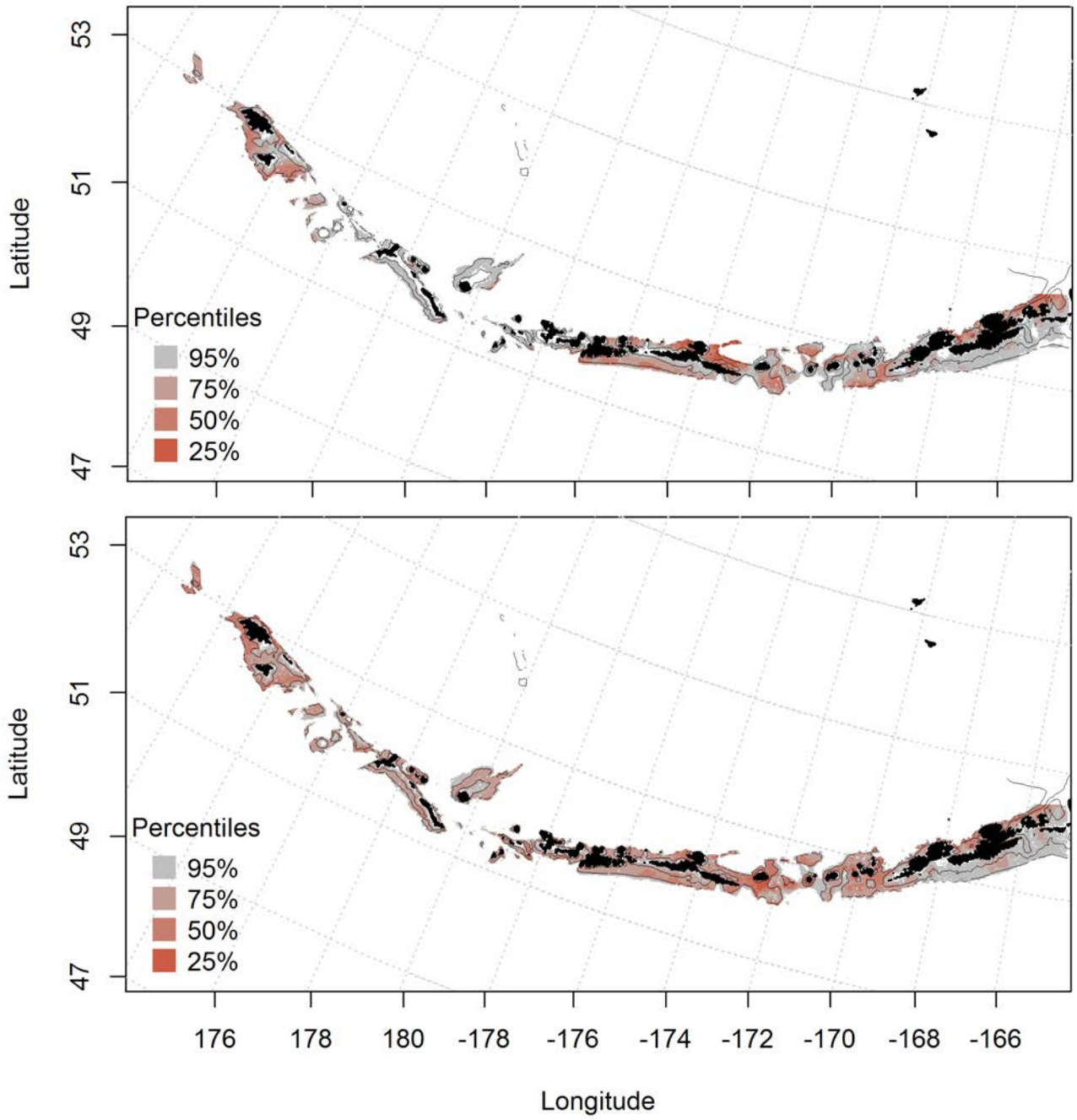

Figure 143. Predicted summer essential fish habitat for Bigmouth sculpin juveniles and adults (top and bottom panel) from summertime bottom trawl surveys.

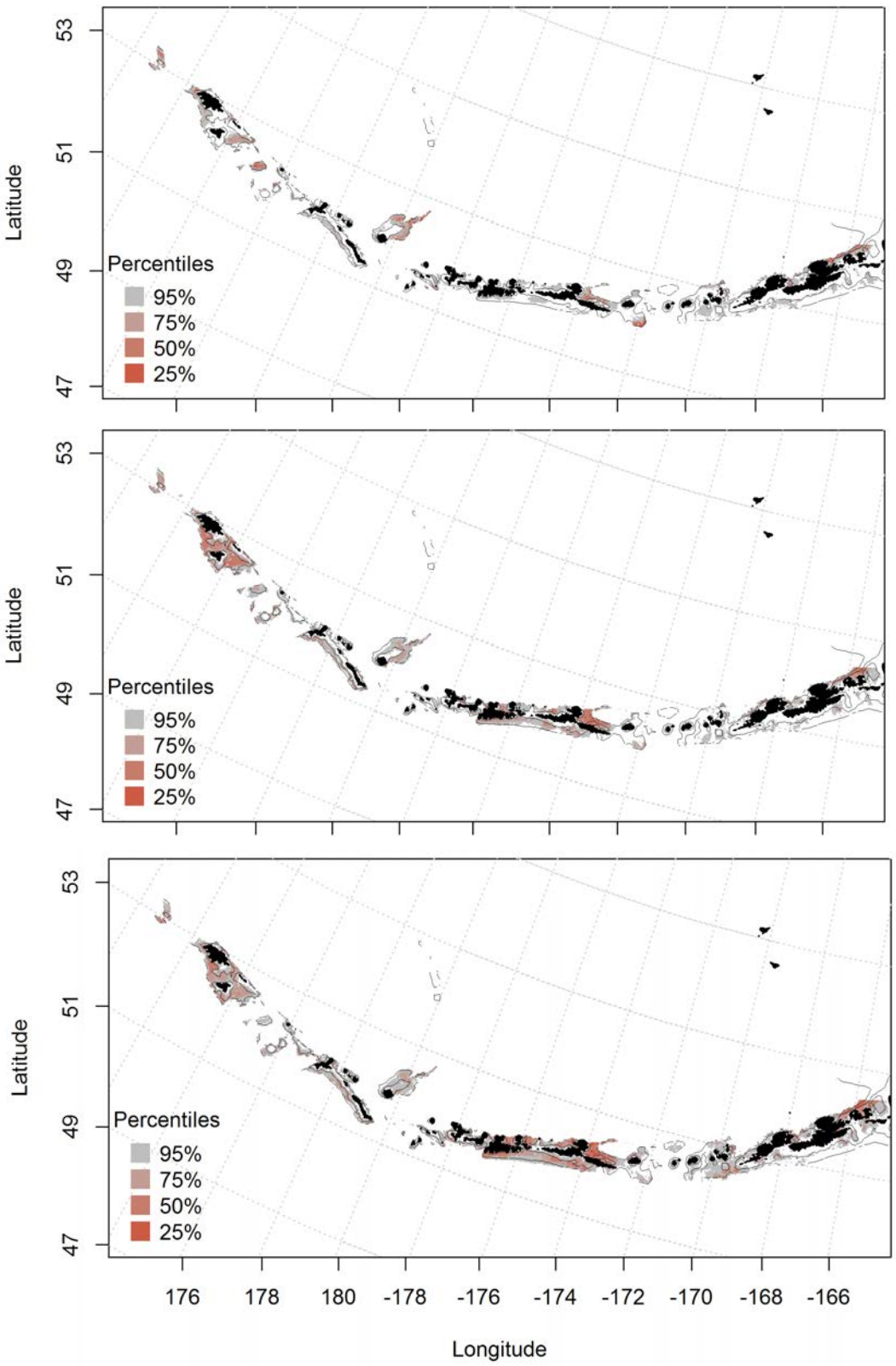

Figure 144. Essential fish habitat predicted for Bigmouth sculpin during fall (top panel), winter (middle panel) and spring (bottom panel) from summertime commercial catches.

3.3 Rockfishes

***Sebastes* spp.**

Collected FOCI data grouped all early life stage *Sebastes* species together in the Aleutian Islands.

Seasonal distribution of early life history stages of *Sebastes* spp. in the Aleutian Islands-- There were 85 instances of larval *Sebastes* observed in the FOCI database (Figure 145), 75 in the spring and 10 in the summer. All observations were found in the eastern AI. Surface temperature, surface color and current variability were the most significant variables in modeling probability of larval *Sebastes* species suitable habitat (relative importance: 30.6%, 27.7%, and 19.1%, respectively).The maximum entropy model explained 100% of the variability in the training and test data sets, and correctly classified 97% of the training data and 100% of the test data set. The model predicted probable suitable habitat of spring *Sebastes* larvae in the eastern AI (Figure 146). There were not enough observations to run the summer *Sebastes* larval model. Spring essential fish habitat predicted larval *Sebastes* species in the eastern AI (Figure 147).

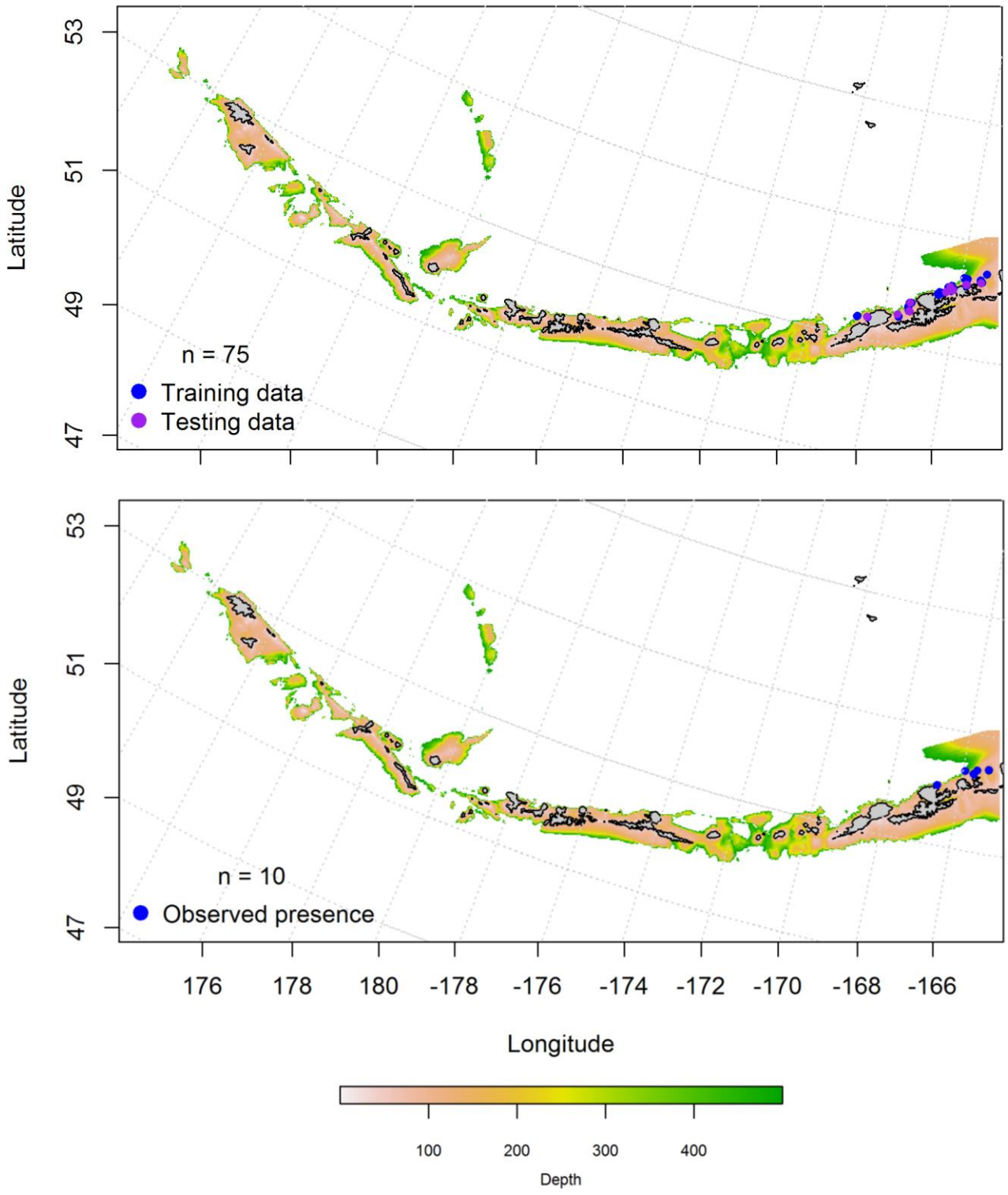

Figure 145. Spring and summer observations (top and bottom panel) of larval Sebastes spp. from the Aleutian Islands.

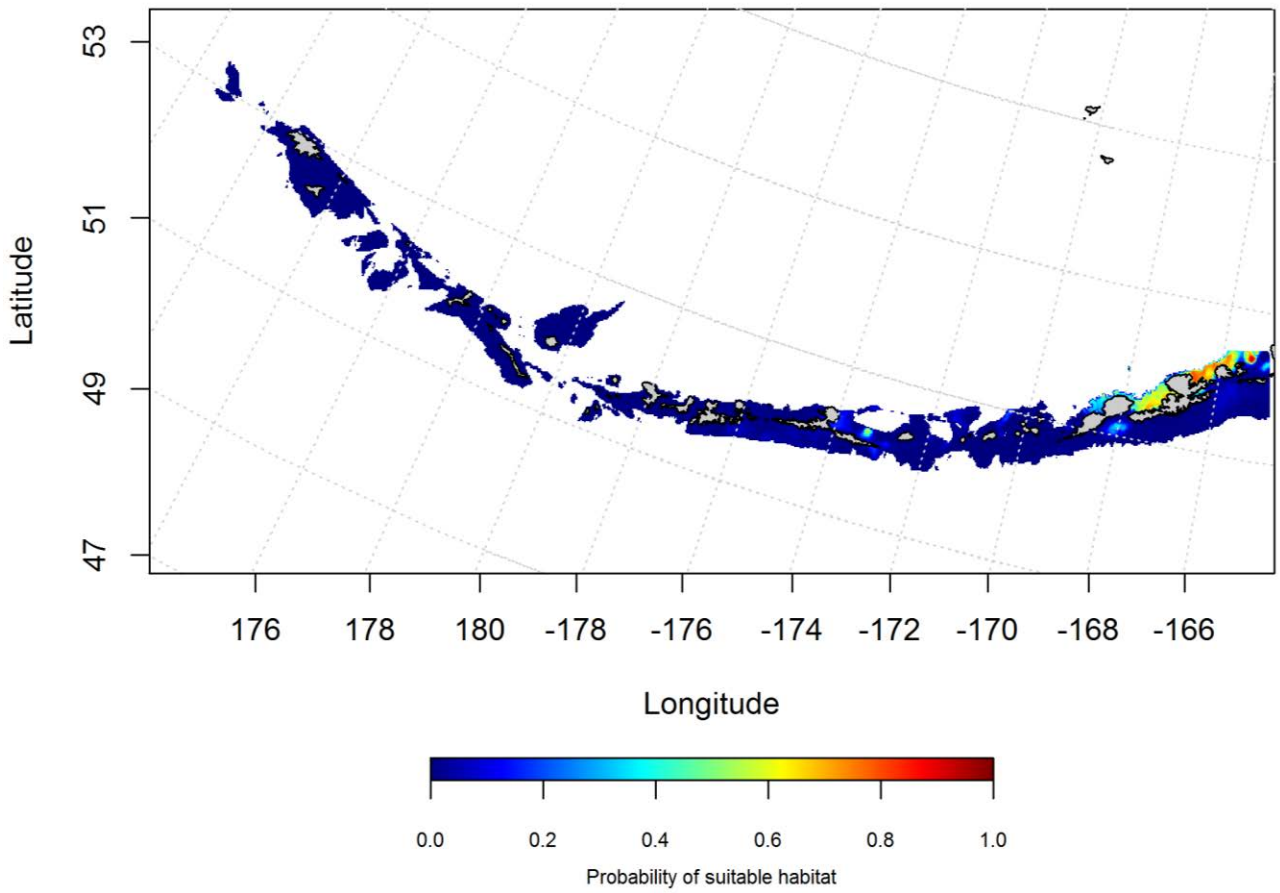

Figure 146. Predicted probability of spring distribution of larval Sebastes spp. from maximum entropy modeling of the Aleutian Islands.

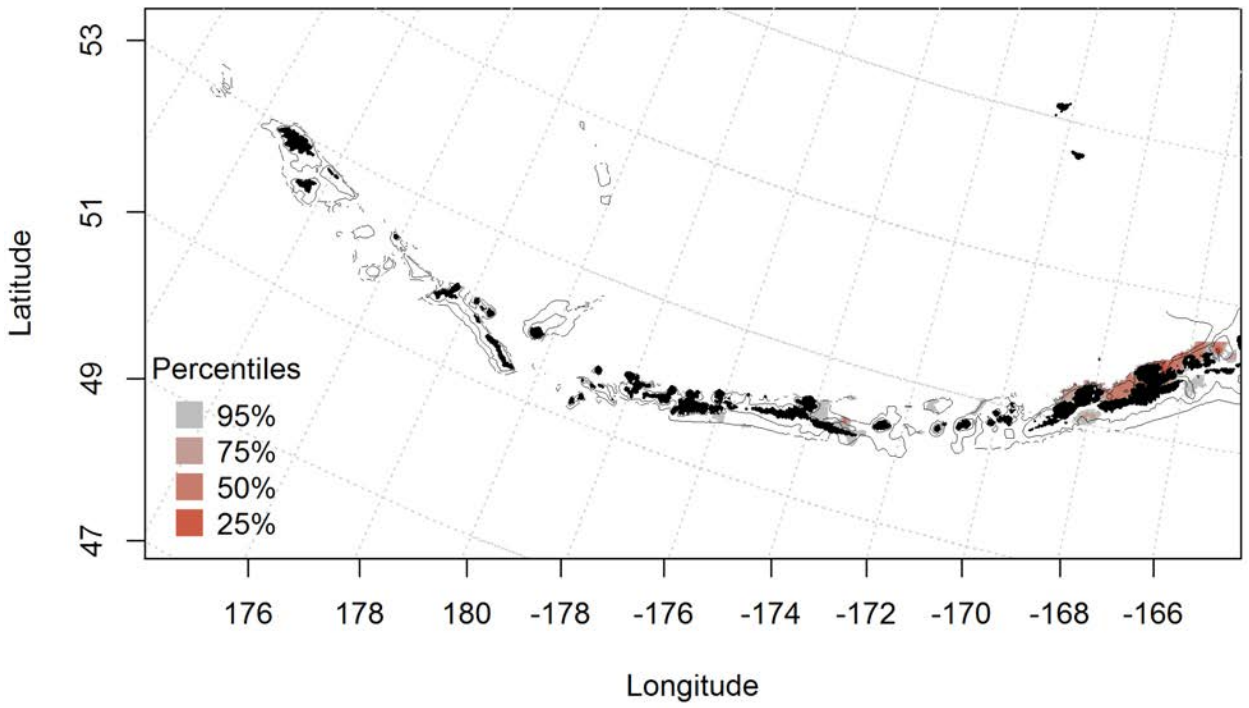

Figure 147. Spring essential fish habitat predicted for larval Sebastes spp.

Pacific ocean perch (*Sebastes alutus*)
Species text here

Summertime distribution of juvenile and adult Pacific ocean perch from bottom trawl surveys of the Aleutian Islands -- The catch of Pacific ocean perch (POP) in summer bottom trawl surveys in the Aleutian Islands indicates this species is broadly distributed. A hurdle-GAM model was used to predict the presence of absence of juvenile Pacific ocean perch and explained 80% of the variability in the training and test data sets. Bottom depth, geographic location, and coral presence were the most important variables explaining the distribution of juvenile POP. The model explained 19.8% of the deviance, and correctly classified 72% of the training data set and 73% of the test data set. The areas of predicted highest presence were concentrated in the eastern and western AI (Figure 148).

The second part of the hurdle model found bottom temperature and bottom depth influence the CPUE of juvenile POP the most, and explained 20.8% of the deviance, 21% of the

training data and 14% of the test data. The model predicted highest CPUE in a similar pattern as the PA GAM (concentrated in the eastern and western AI), but also indicated a small concentration in the central AI (Figure 149).

Generalized additive models predicting the abundance of adult POP explained 46% of the variability in CPUE in the bottom trawl survey training data, and 44% of the variability in the test data set. Bottom depth, geographic location, and slope were the most important variables explaining the distribution of adult POP. Predicted abundance was distributed throughout the AI chain (Figure 150).

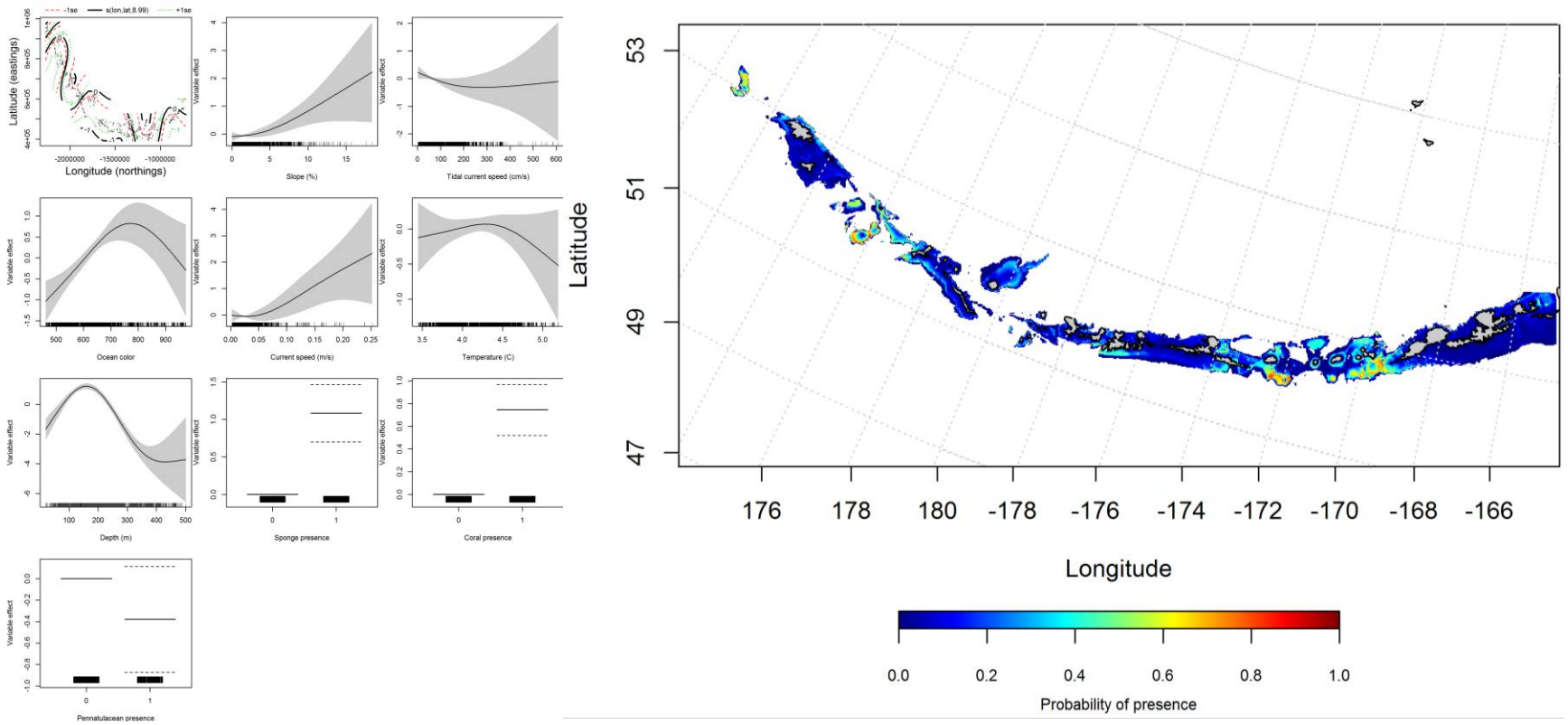

Figure 148. Best-fitting hurdle model effects of retained habitat variables on presence absence (PA) of juvenile Pacific ocean perch from summer bottom trawl surveys of the Aleutian Islands (left panel) alongside hurdle-predicted juvenile Pacific ocean perch PA (right panel).

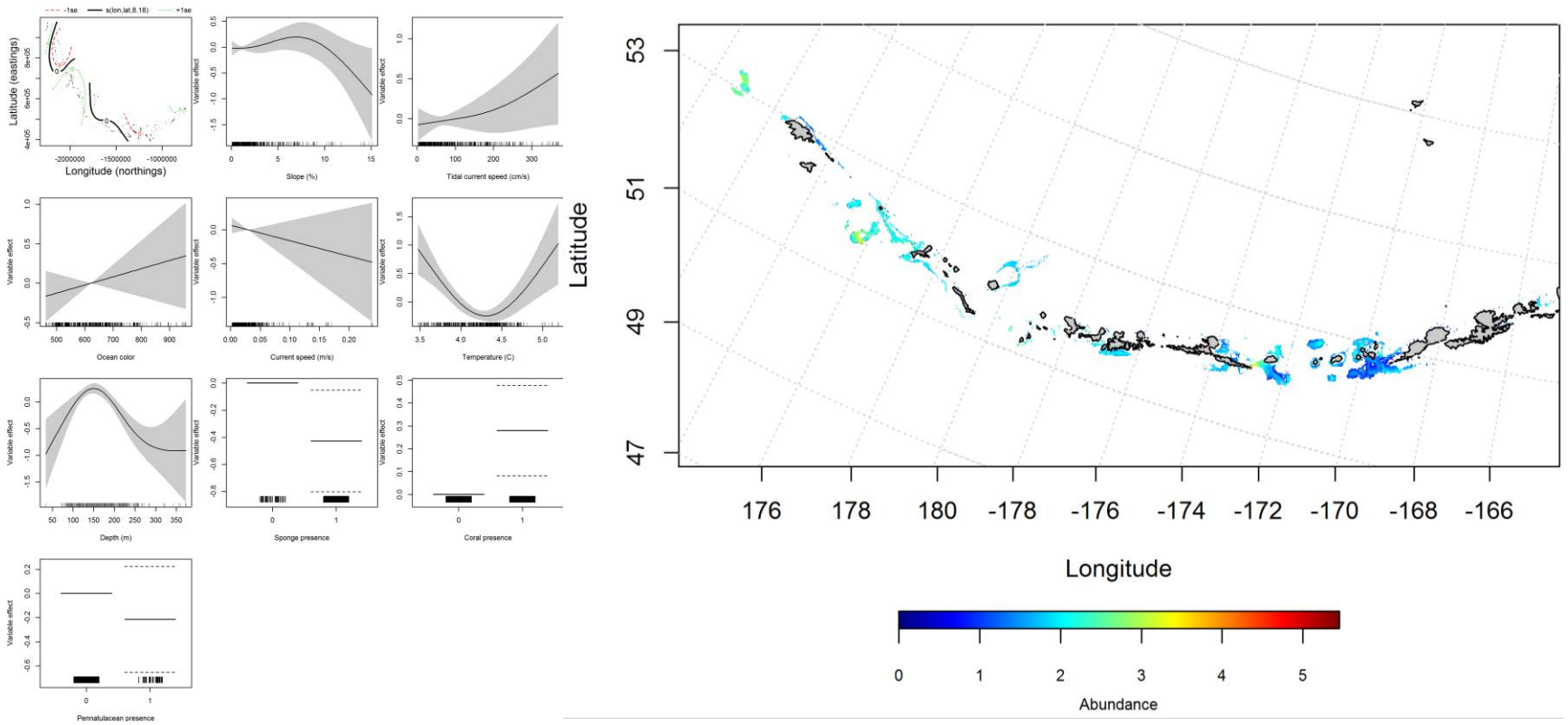

Figure 149. Best-fitting hurdle model effects of retained habitat variables on CPUE of juvenile Pacific ocean perch from summer bottom trawl surveys of the Aleutian Islands (left panel) alongside hurdle-predicted juvenile Pacific ocean perch CPUE (right panel).

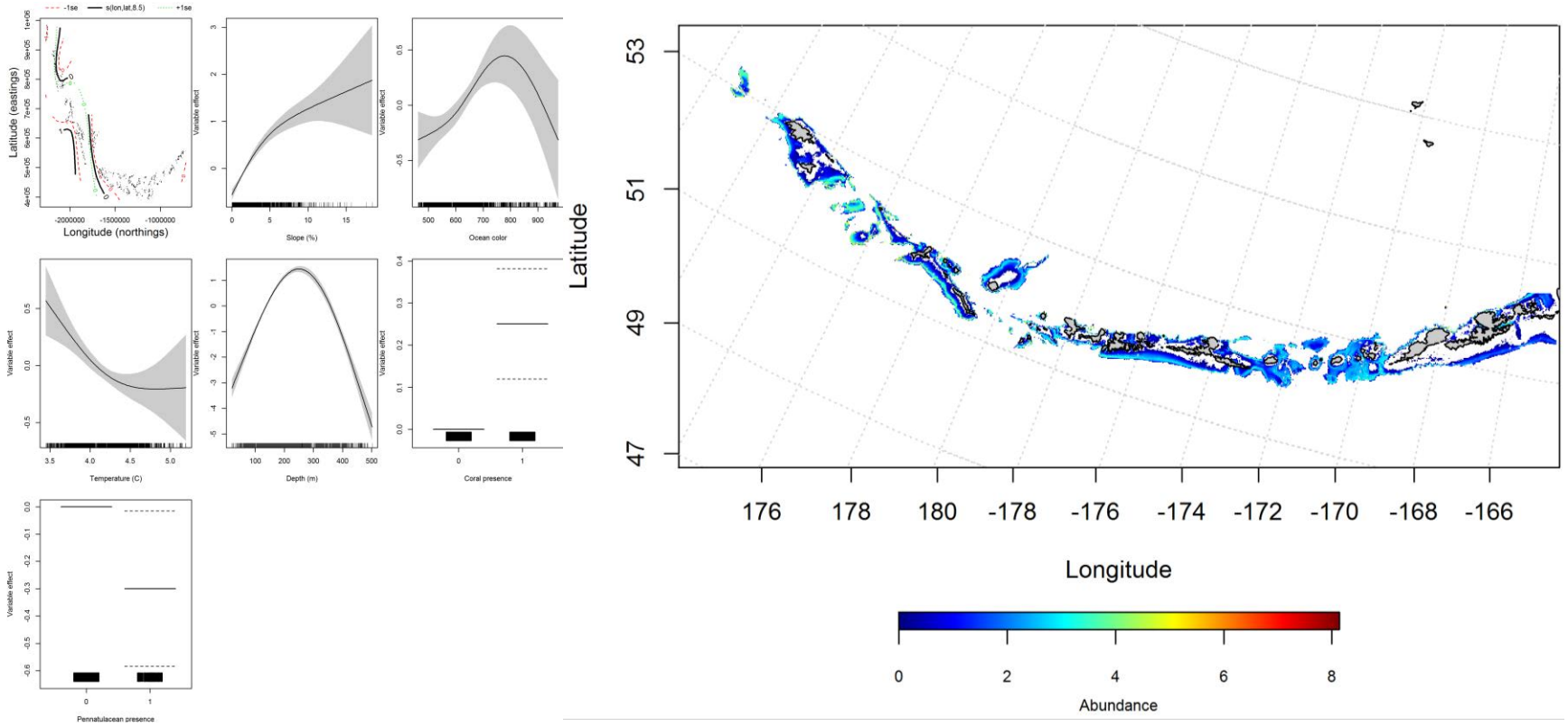

Figure 150. Best-fitting generalized additive model (GAM) effects of retained habitat variables on abundance of adult Pacific ocean perch from summer bottom trawl surveys of the Aleutian Islands (left panel) alongside GAM-predicted adult Pacific ocean perch abundance (right panel).

Seasonal distribution of commercial fisheries catches of adult Pacific ocean perch in the Aleutian Islands-- Distribution of adult Pacific ocean perch in the Aleutian Islands in commercial fisheries catches was generally consistent throughout all seasons. In the fall, bottom depth, and bottom temperature were the most important variables determining the distribution of POP (relative importance: 49.1% and 25.3%). The AUC of the fall maxent model was 94% for the training data and 83% for the test data. The model correctly predicted 86% of the training data set and 83% of the test data set. The model predicted probable suitable habitat of POP across the AI (Figure 151).

In the winter, bottom depth, bottom temperature, and ocean color were the most important variables determining the distribution of POP (relative importance:45.4%, 19.5%, and 18.1%, respectively). The AUC of the winter maxent model was 96% for the training data and 89% for the test data sets. 90% of the cases in the training data and 89% of the test data were predicted correctly. As with the fall, the model predicted probable suitable habitat of POP throughout the AI (Figure 152).

In the spring, bottom depth and ocean color were the most important variables determining the distribution of adult POP (relative importance: 61.1% and 21.6%). The AUC of the fall model was 93% for the training data and 83% for the test data. 85% of the training data and 83% of the test data sets were predicted correctly. As with the fall and winter, the model predicted probable suitable habitat of POP throughout the AI (Figure 152).

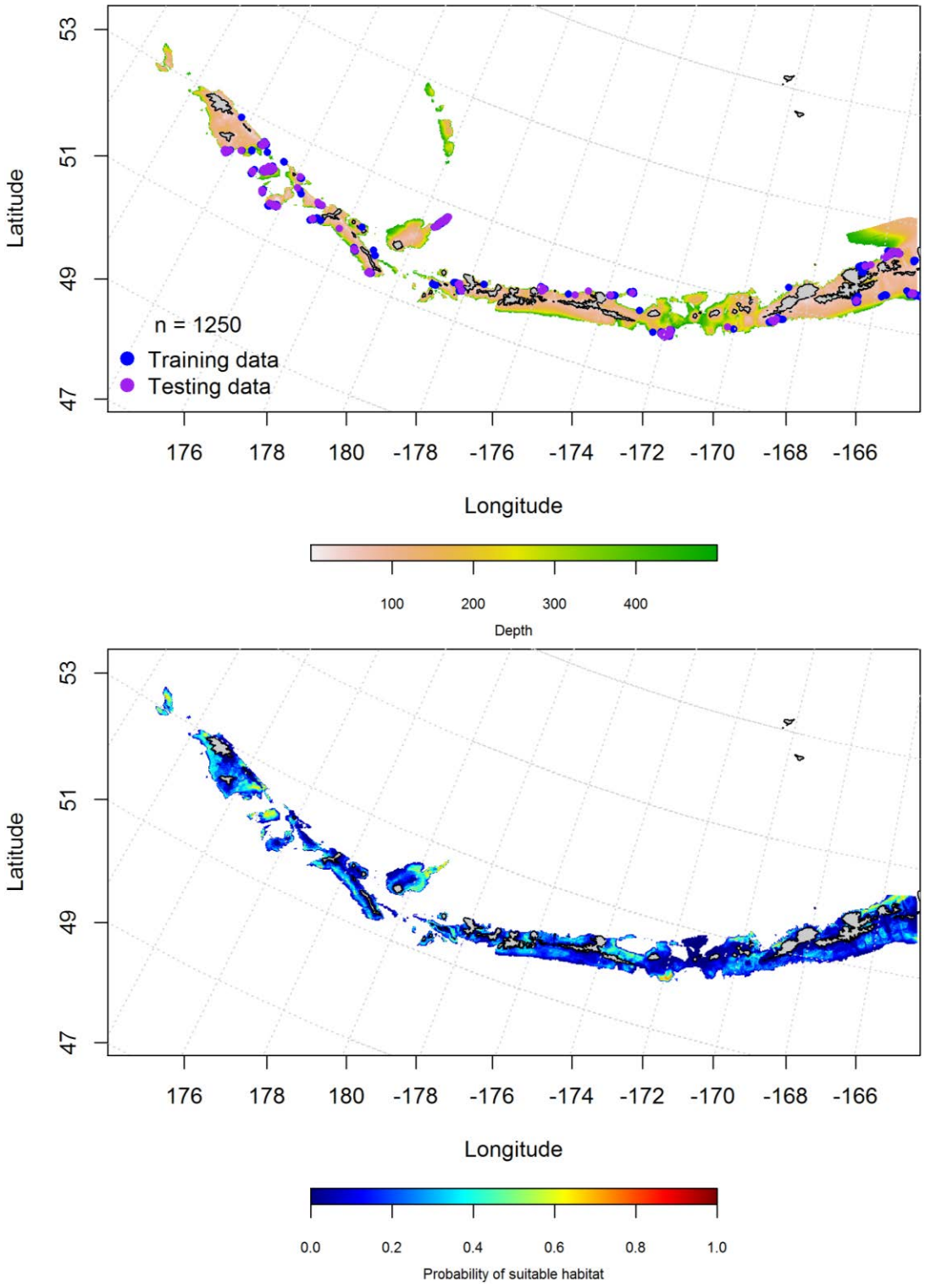

Figure 151. Locations of fall (September-November) commercial fisheries catches of Pacific ocean perch (top panel). Blue points were used to train the maximum entropy model predicting the probability of the suitable fall habitat supporting commercial catches of Pacific ocean perch (bottom panel) and the purple points were used to validate the model.

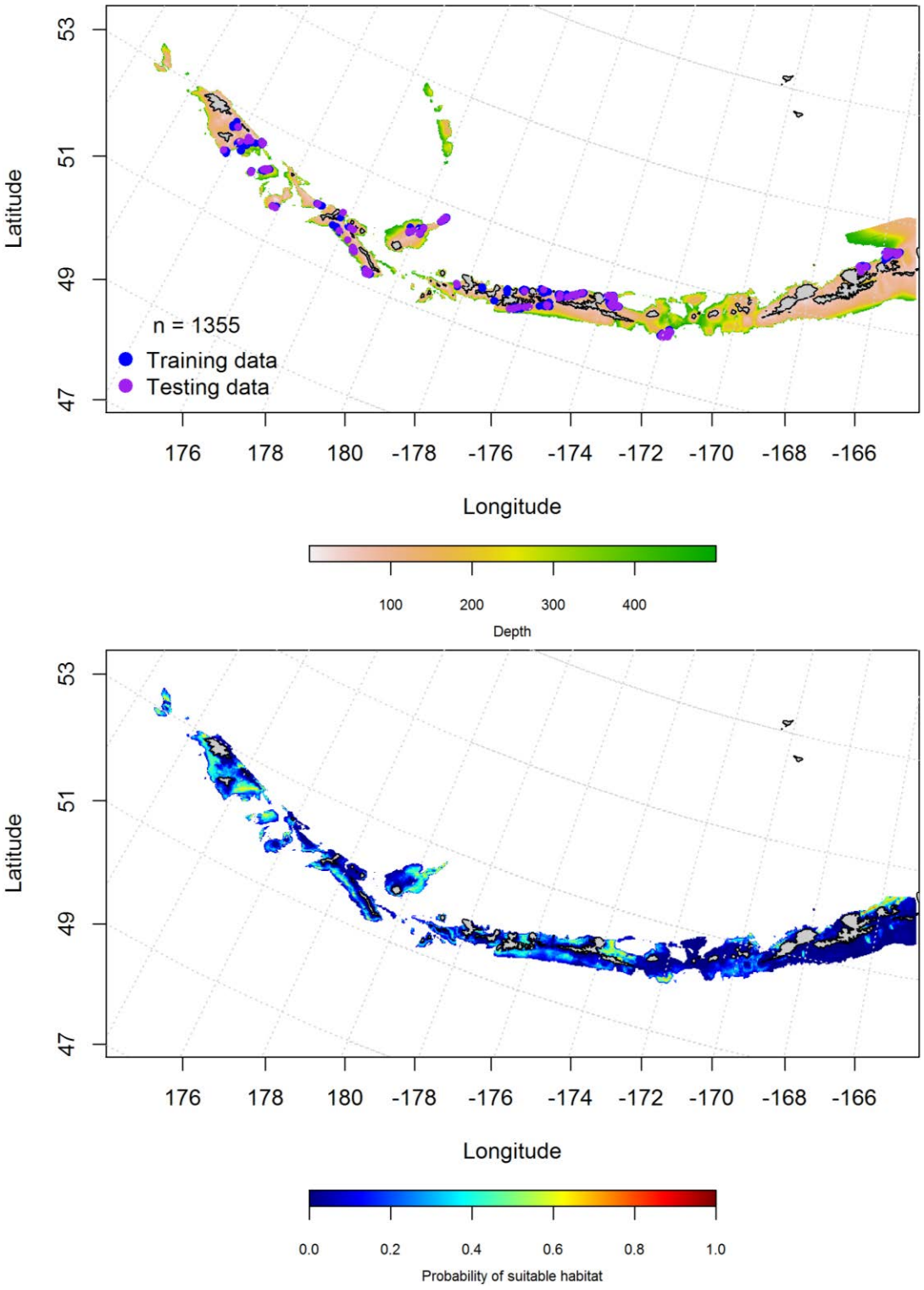

Figure 152. Locations of winter (December-February) commercial fisheries catches of Pacific ocean perch (top panel). Blue points were used to train the maximum entropy model predicting the probability of suitable winter habitat supporting commercial catches of Pacific ocean perch (bottom panel) and the purple points were used to validate the model.

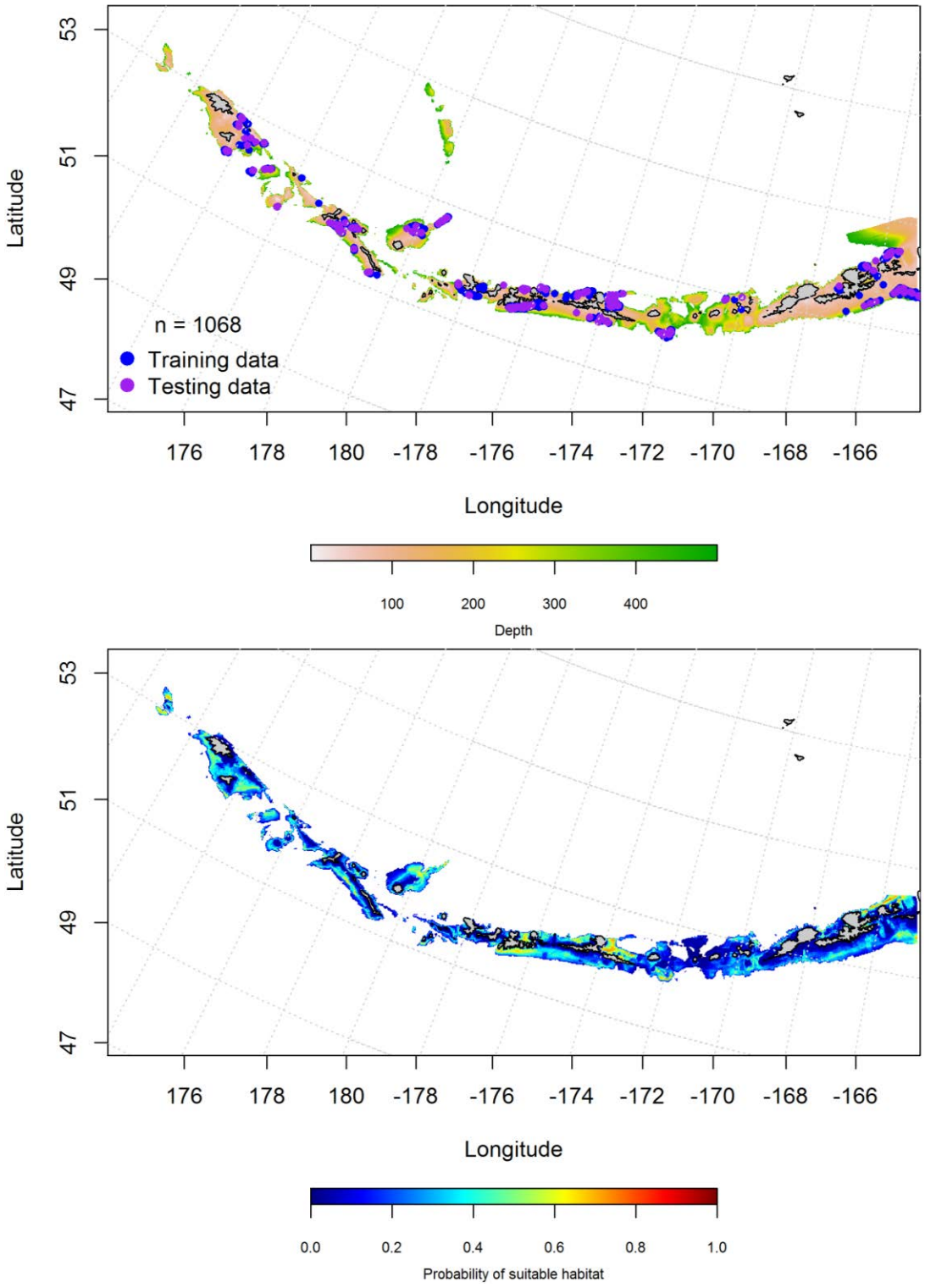

Figure 153. Locations of spring (March-May) commercial fisheries catches of Pacific ocean perch (top panel). Blue points were used to train the maximum entropy model predicting the probability of suitable spring habitat supporting commercial catches of Pacific ocean perch (bottom panel) and the purple points were used to validate the model.

Aleutian Islands Pacific ocean perch Essential Fish Habitat Maps and Conclusions -

- Summertime EFH of juvenile POP was less broadly distributed throughout the AI as the adult POP (Figure 154).

Similar to adult summertime bottom trawl survey data observations, the EFH predicted from commercial catches of POP in the fall, winter and spring is distributed throughout the Aleutian Islands chain (Figure 155). There does not appear to be much seasonal variability to the EFH distribution and areas of high concentration are interspersed with areas of low concentration.

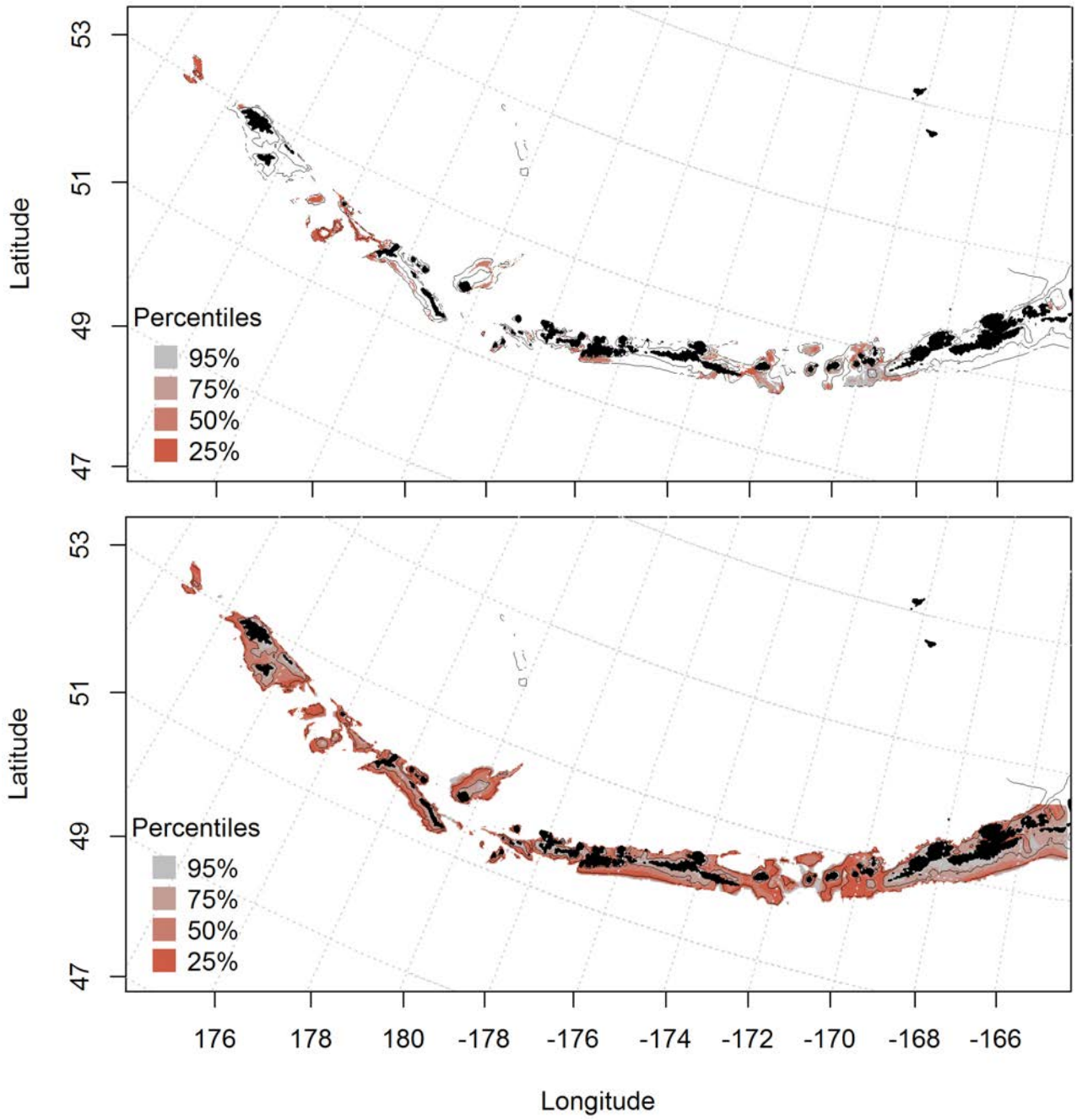

Figure 154. Predicted summer essential fish habitat for Pacific ocean perch juveniles and adults (top and bottom panel) from summertime bottom trawl surveys.

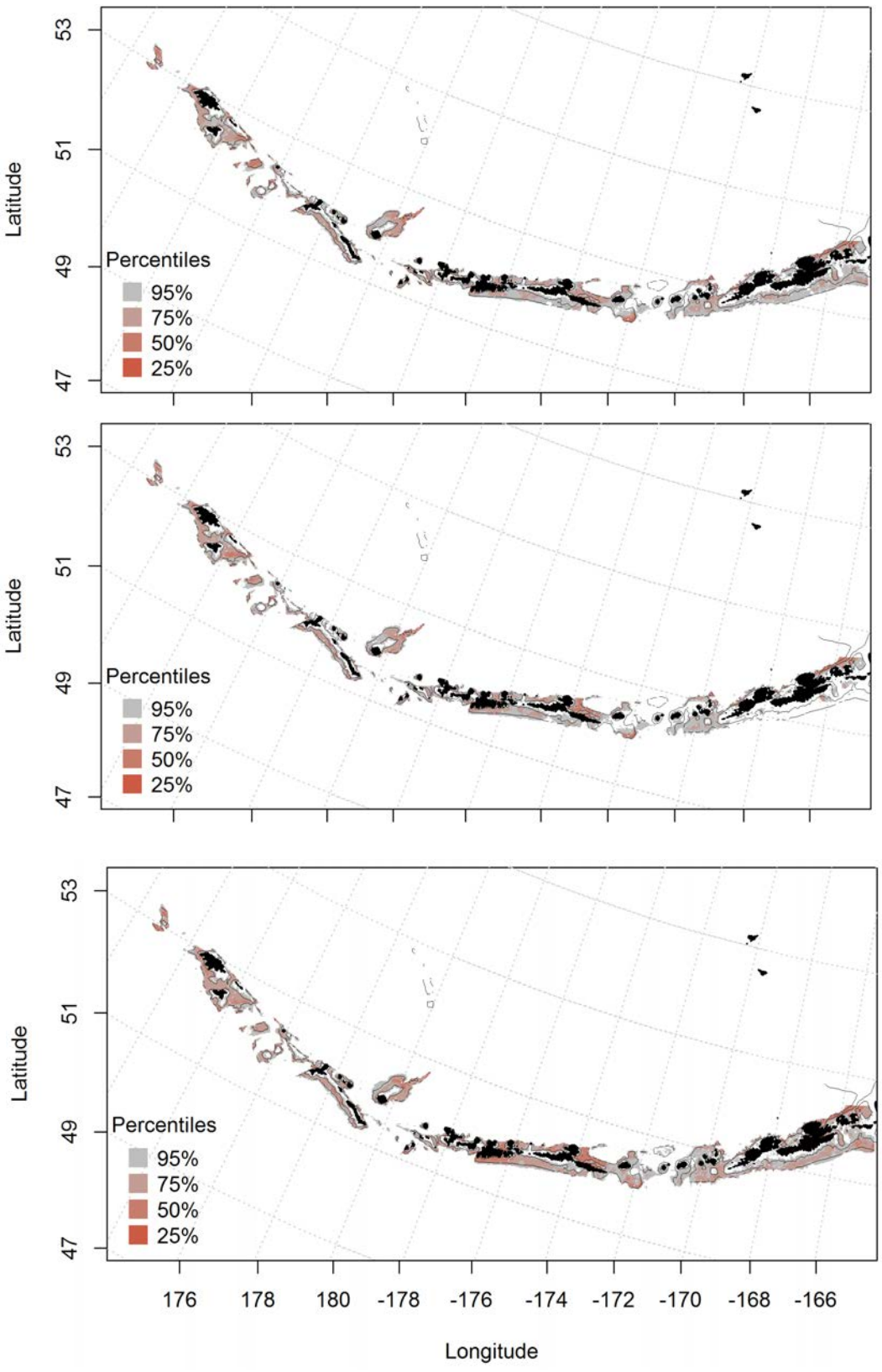

Figure 155. Essential fish habitat predicted for Pacific ocean perch during fall (top panel), winter (middle panel) and spring (bottom panel) from summertime commercial catches.

Northern rockfish (*Sebastes polyspinus*)

Summertime distribution of juvenile and adult Northern rockfish from bottom trawl surveys of the Aleutian Islands –

The catch of Northern rockfish (NRF) in summer bottom trawl surveys in the Aleutian Islands indicates this specie's presence varied across the Aleutian Islands survey area and was highest in the western AI (Figure 156). A hurdle-GAM model was used to predict the presence and absence of juvenile Northern rockfish. The PA GAM explained 30.9% of the deviance, 87% of the variability in the bottom trawl survey training data and 88% of the variability in the test data set. Geographic location and bottom depth were the most important variables explaining the distribution of juvenile NRF. The model correctly classified 78% of the training and test data sets.

The second part of the hurdle model found geographic location and bottom depth were also the most influential variables influencing the CPUE of juvenile NRF. The model explained 45.1% of the deviance, 45% of the training data and 47% of the test data. The model predicted highest abundance in a similar pattern as the PA GAM (with the highest abundance in the western AI) (Figure 157).

The catch of adult NRF in summer bottom trawl surveys of the Aleutian Islands is similar to juvenile NRF (Figure 158). A generalized additive model predicting the abundance of juvenile NRF explained 31.3% of the deviance, and 31% of the variability in the bottom trawl survey using the training and test data sets. Geographic location and bottom depth were the most important variables explaining the distribution of juvenile NRF.

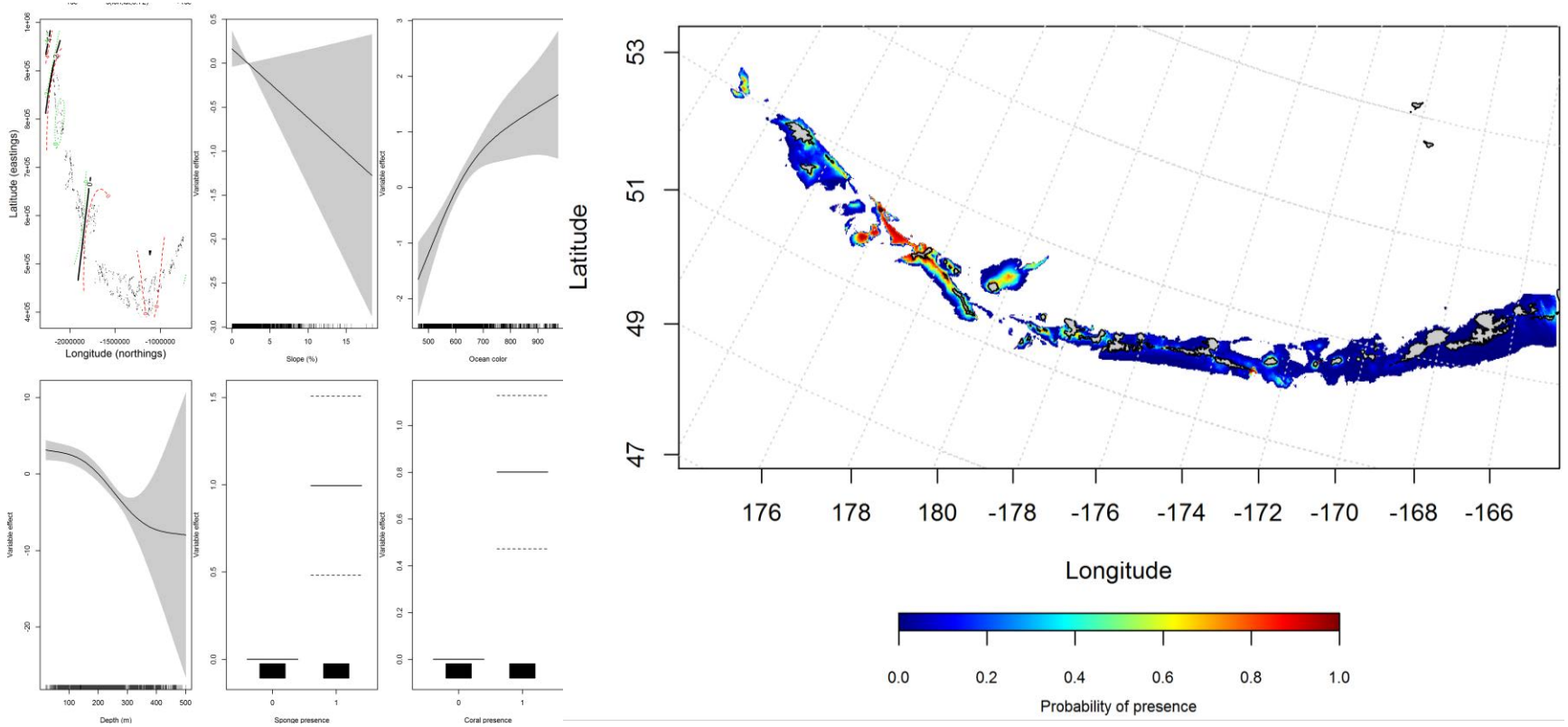

Figure 156. Best-fitting hurdle model effects of retained habitat variables on presence absence (PA) of juvenile Northern rockfish from summer bottom trawl surveys of the Aleutian Islands (left panel) alongside hurdle-predicted juvenile Northern rockfish PA (right panel).

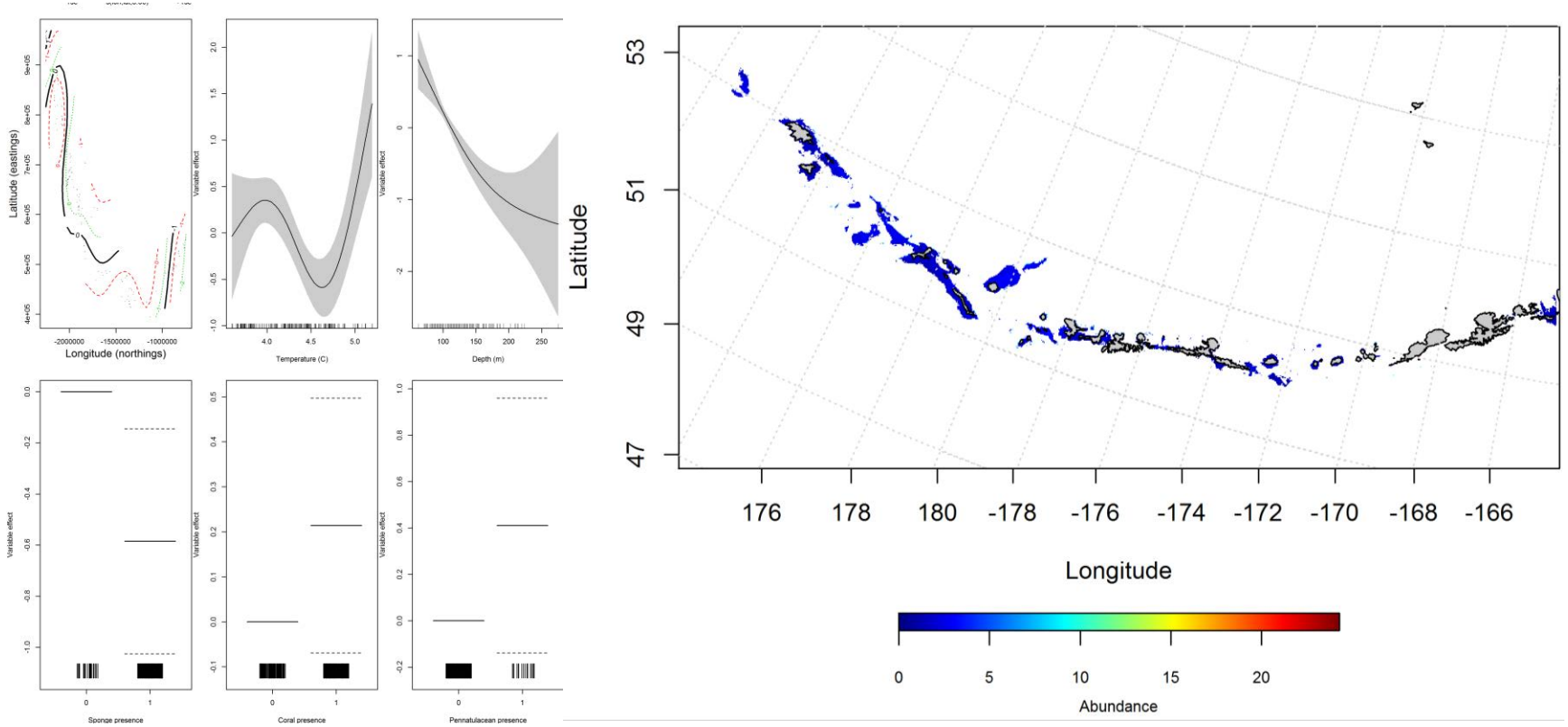

Figure 157. Best-fitting hurdle model effects of retained habitat variables on CPUE of juvenile Northern rockfish from summer bottom trawl surveys of the Aleutian Islands (left panel) alongside hurdle-predicted juvenile Northern rockfish CPUE (right panel).

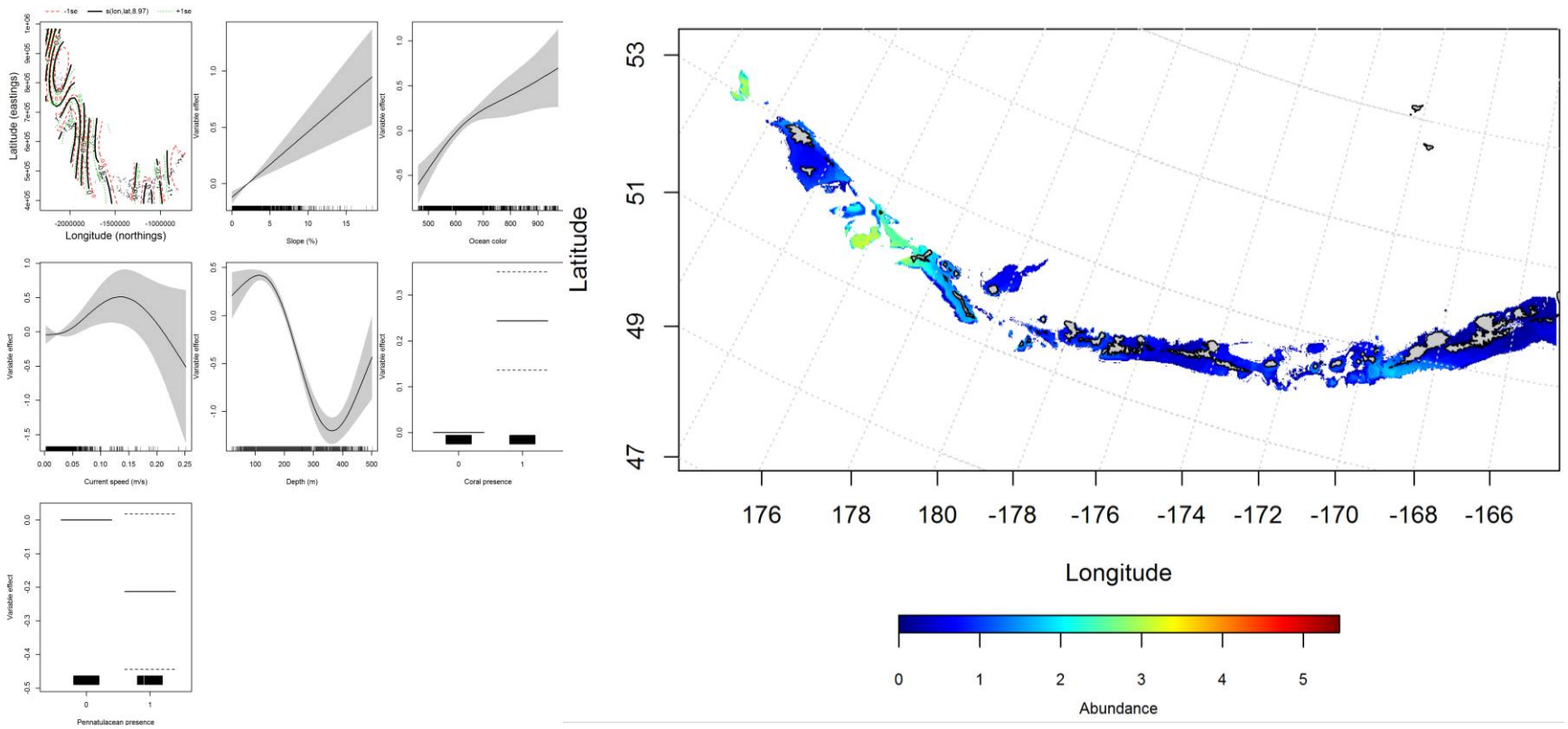

Figure 158. Best-fitting generalized additive model (GAM) effects of retained habitat variables on abundance of adult Northern rockfish from summer bottom trawl surveys of the Aleutian Islands (left panel) alongside GAM-predicted adult Northern rockfish abundance (right panel).

Seasonal distribution of commercial fisheries catches of adult Northern rockfish in the Aleutian Islands-- Distribution of adult Northern rockfish (NRF) in the Aleutian Islands in commercial fisheries catches was generally consistent throughout all seasons. In the fall, bottom depth and ocean color were the most important variables determining the distribution of NRF (relative importance: 65.6% and 14.5%). The AUC of the maxent fall model was 93% for the training data and 86% for the test data, 85% of the cases in the training data set, and 86% of the test data set were predicted correctly. The model predicted probable suitable habitat of NRF throughout the AI chain (Figure 159).

In the winter, bottom depth and ocean color were also the most important variables determining the distribution of NRF (relative importance: 61.5% and 16.1%). The AUC of the winter maxent model was 95% for the training data and 88% for the test data. 87% of the training data set and 88$ of the test data set were predicted correctly. As with the fall, the model predicted probable suitable habitat of NRF throughout the AI chain, though less abundant in the eastern AI (Figure 160).

Like the fall and winter, bottom depth and ocean color in the spring were the most important variables determining the distribution of NRF (relative importance: 79.5% and 10.1%). The AUC of the spring maxent model was 91% for the training data and 83% for the test data. The model correctly classified 84% of the training data and 83% of the test data. The model predicted probable suitable habitat of NRF catches were distributed throughout the AI (Figure 161).

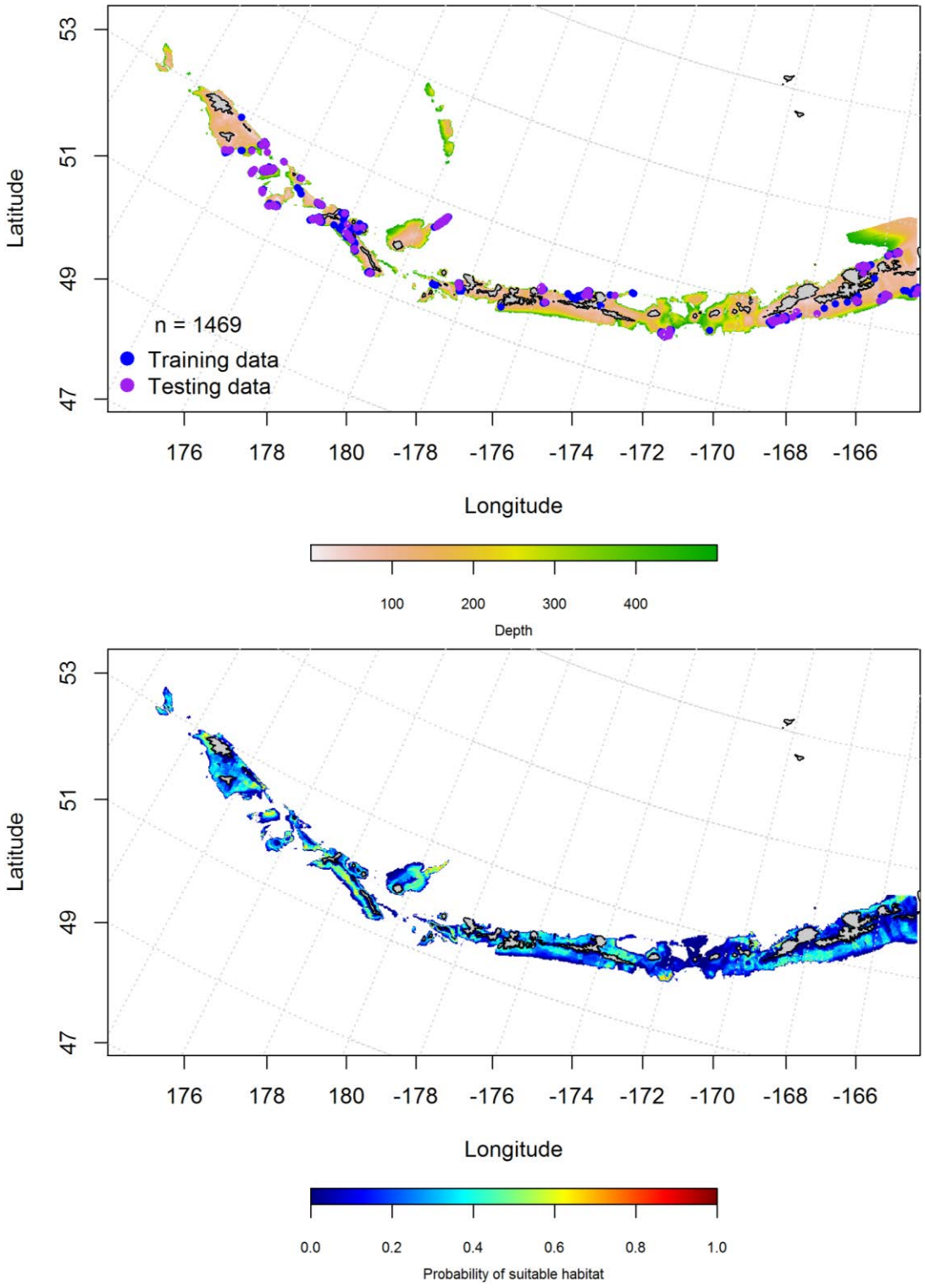

Figure 159. Locations of fall (September-November) commercial fisheries catches of Northern rockfish (top panel). Blue points were used to train the maximum entropy model predicting the probability of suitable fall habitat supporting commercial catches of Northern rockfish (bottom panel) and the purple points were used to validate the model.

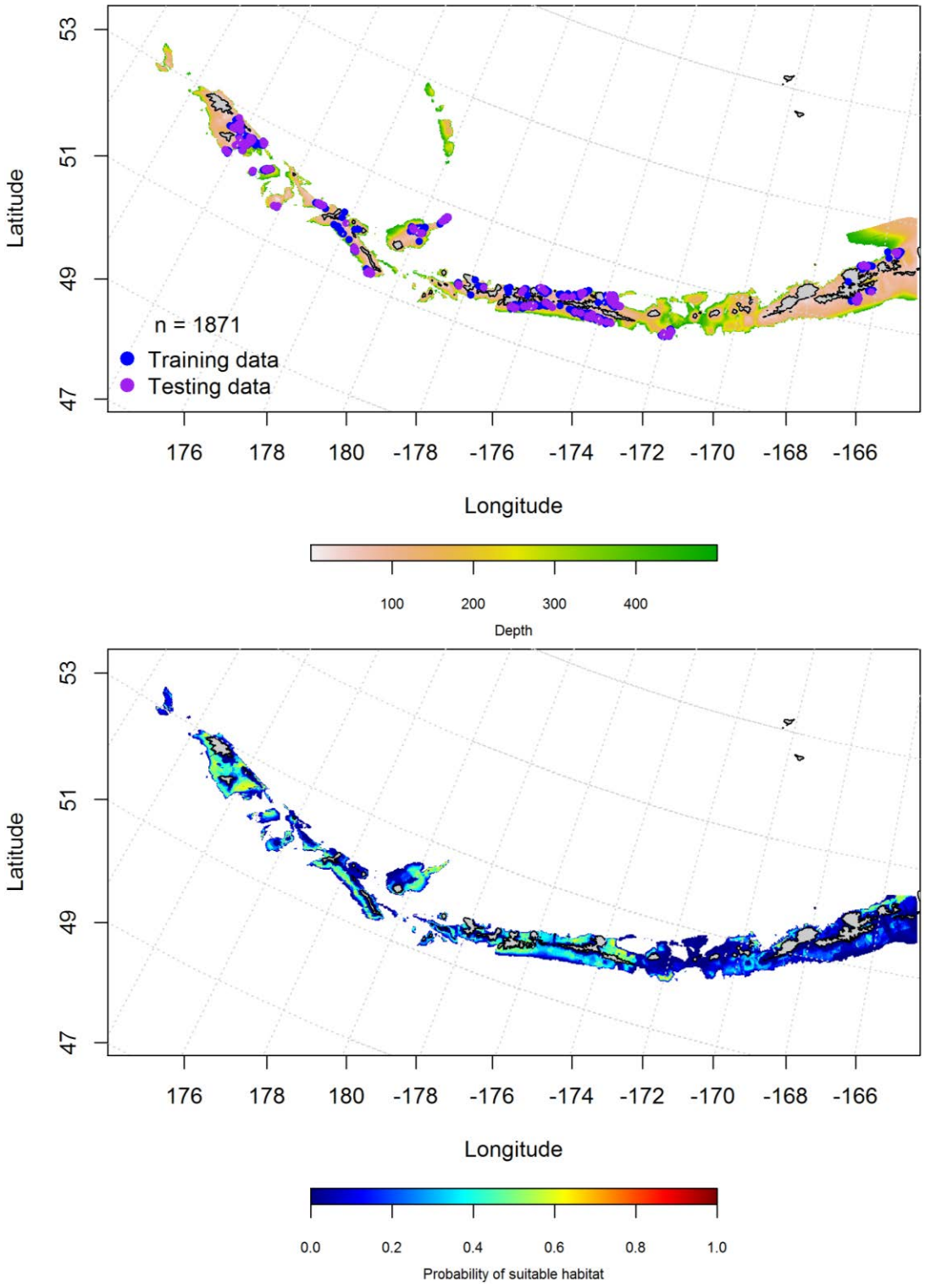

Figure 160. Locations of winter (December-February) commercial fisheries catches of Northern rockfish (top panel). Blue points were used to train the maximum entropy model predicting the probability of suitable winter habitat supporting commercial catches of Northern rockfish (bottom panel) and the purple points were used to validate the model.

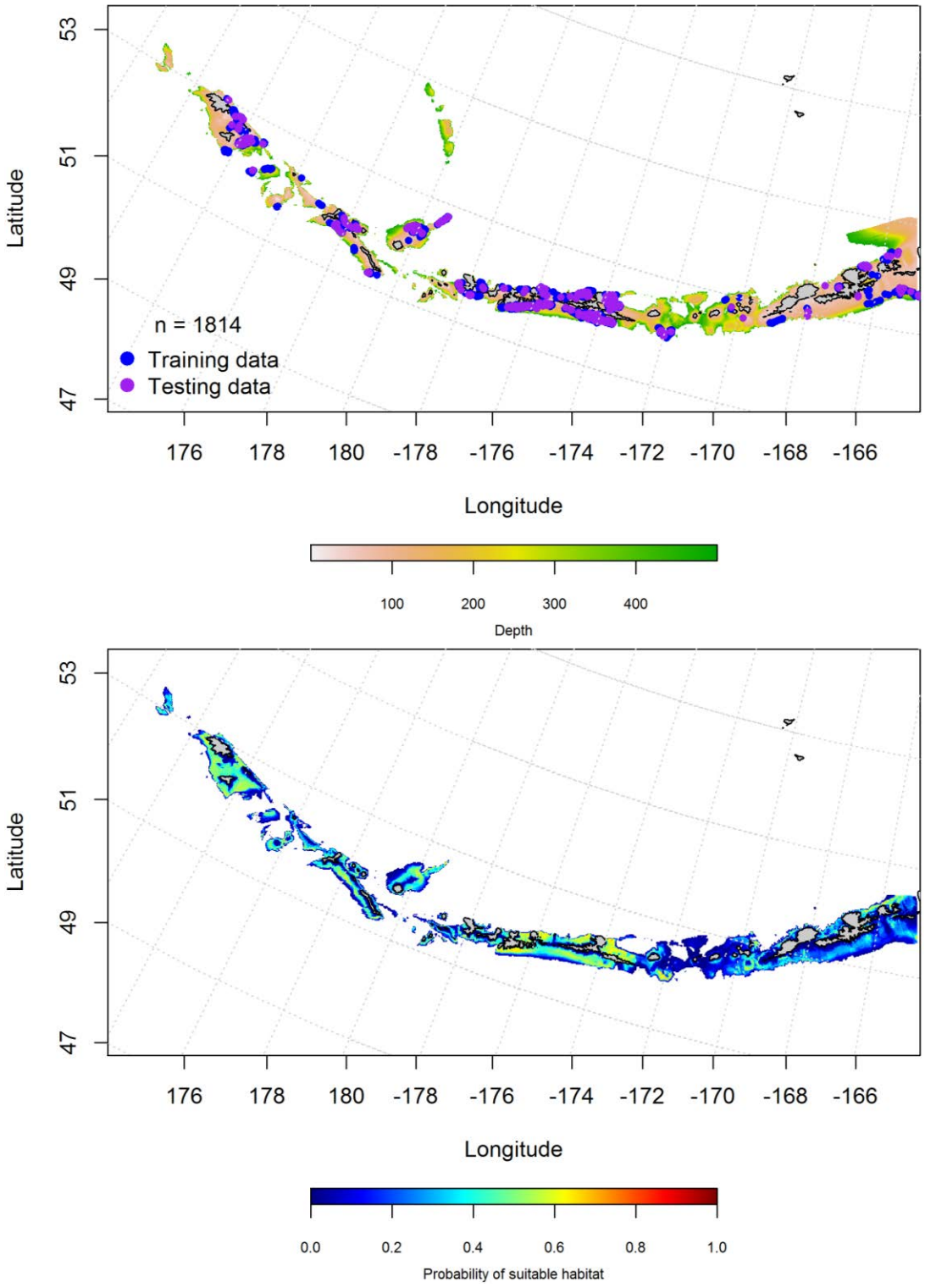

Figure 161. Locations of spring (March-May) commercial fisheries catches of Northern rockfish (top panel). Blue points were used to train the maximum entropy model predicting the probability of suitable spring habitat supporting commercial catches of Northern rockfish (bottom panel) and the purple points were used to validate the model.

Aleutian Islands Northern rockfish Essential Fish Habitat Maps and Conclusions --

In general, adult NRF were widely distributed through the Aleutian Islands chain whereas the juveniles were more abundant in the central and western AI (Figure 162).

In general, EFH predicted from commercial catches of adult NRF are widely distributed through the Aleutian Islands chain and co-occur in most places where they are found (Figure 163). These similarities can be observed in areas of low abundance (e.g., large passes). There does not appear to be much seasonal variability to the EFH distribution from fall, winter and spring summertime commercial catches.

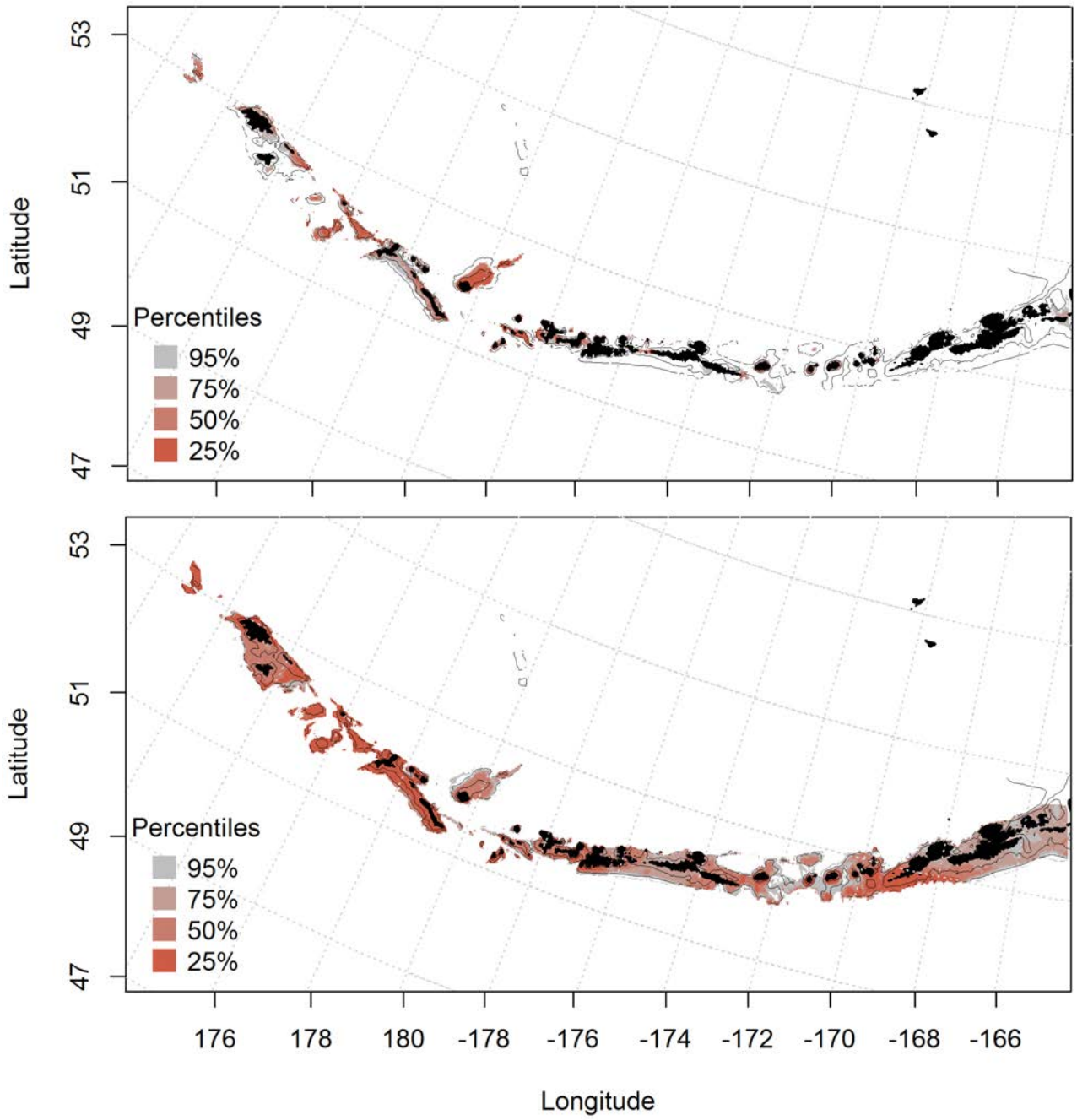

Figure 162. Predicted summer essential fish habitat for Northern rockfish juveniles and adults (top and bottom panel) from summertime bottom trawl surveys.

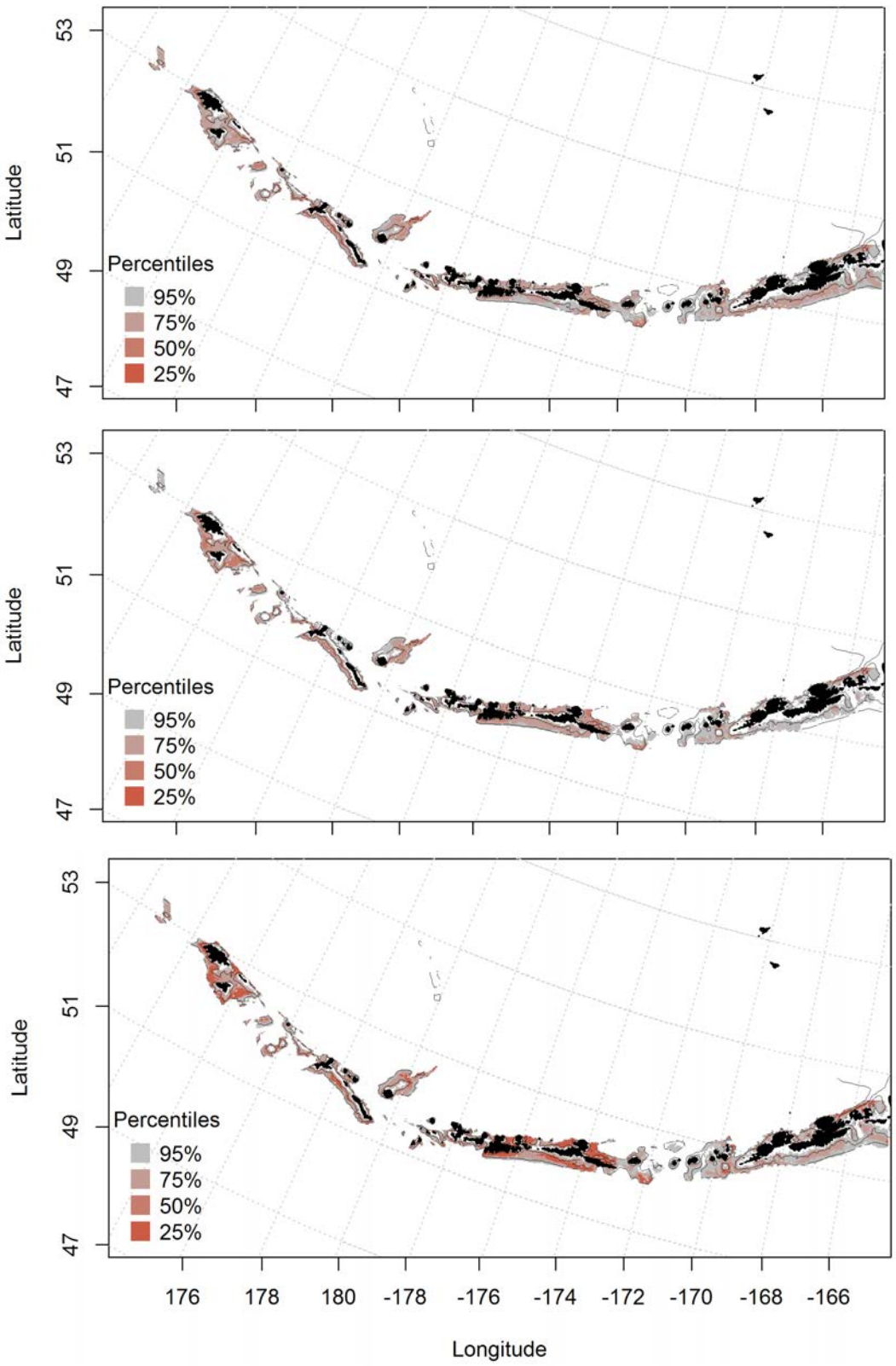

Figure 163. Essential fish habitat predicted for Northern rockfish during fall (top panel), winter (middle panel) and spring (bottom panel) from summertime commercial catches.

Shortraker rockfish (*Sebastes borealis*)

Summertime distribution of juvenile and adult Shortraker rockfish from bottom trawl surveys of the Aleutian Islands -- The catch of Shortraker rockfish in summer bottom trawl surveys was similarly distributed in the Aleutian Islands. A hurdle-GAM model was used to predict the presence and absence of juvenile Shortraker rockfish. The PA GAM explained 99% of the variability in the bottom trawl survey training and test data sets, and 71.5% of the deviance. Bottom depth, geographic location, and ocean color were the most important variables explaining the distribution of juvenile Shortraker rockfish. The model correctly classified 95% of the training data and 96% of the test data. Juvenile Shortraker rockfish were distributed throughout the AI (Figure 164).

The second part of the hurdle model found geographic location and slope were the most influential variables influencing the CPUE of juvenile Shortraker rockfish. The model explained 42.8% of the deviance, 43% of the training data and 36% of the test data. The model predicted abundance in a similar pattern as the PA GAM (throughout the AI) (Figure 165).

A hurdle-GAM model was used to predict the presence and absence of adult Shortraker rockfish. The PA GAM explained 98% of the variability in the bottom trawl survey training data, 96% of the variability in the test data set, and 67.1% of the deviance. Bottom depth and geographic location were the most important variables explaining the distribution of adult Shortraker rockfish. The model correctly classified 92% of the training and test data sets. Juvenile Shortraker rockfish were distributed throughout the AI (Figure 166).

The second part of the hurdle model found geographic location and bottom depth were the most influential variables influencing the CPUE of adult Shortraker rockfish. The model

explained 34.8% of the deviance, 35% of the training data and 25% of the test data. The model predicted abundance in a similar pattern as the PA GAM (throughout the AI) (Figure 167).

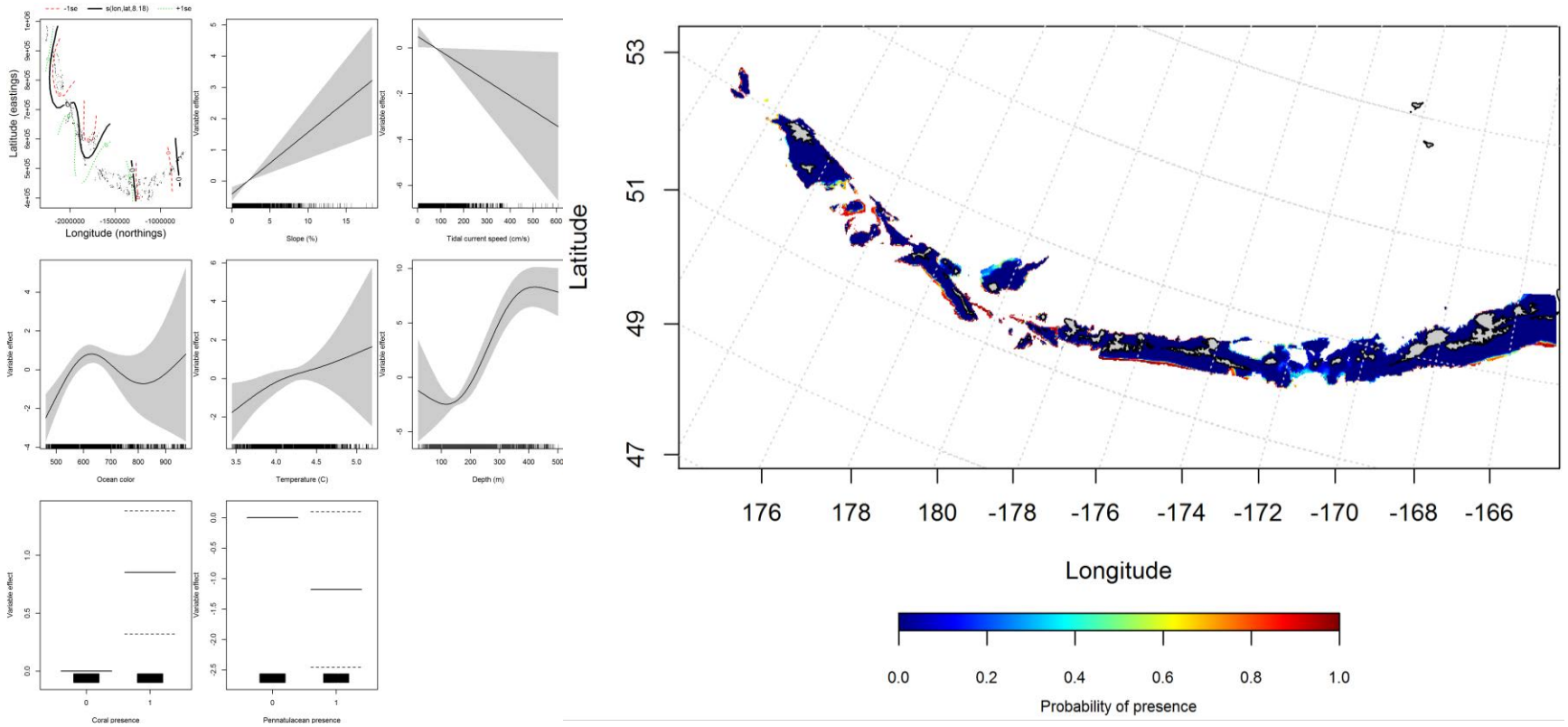

Figure 164. Best-fitting hurdle model effects of retained habitat variables on presence absence (PA) of juvenile Shortraker rockfish from summer bottom trawl surveys of the Aleutian Islands (left panel) alongside hurdle-predicted juvenile Shortraker rockfish PA (right panel).

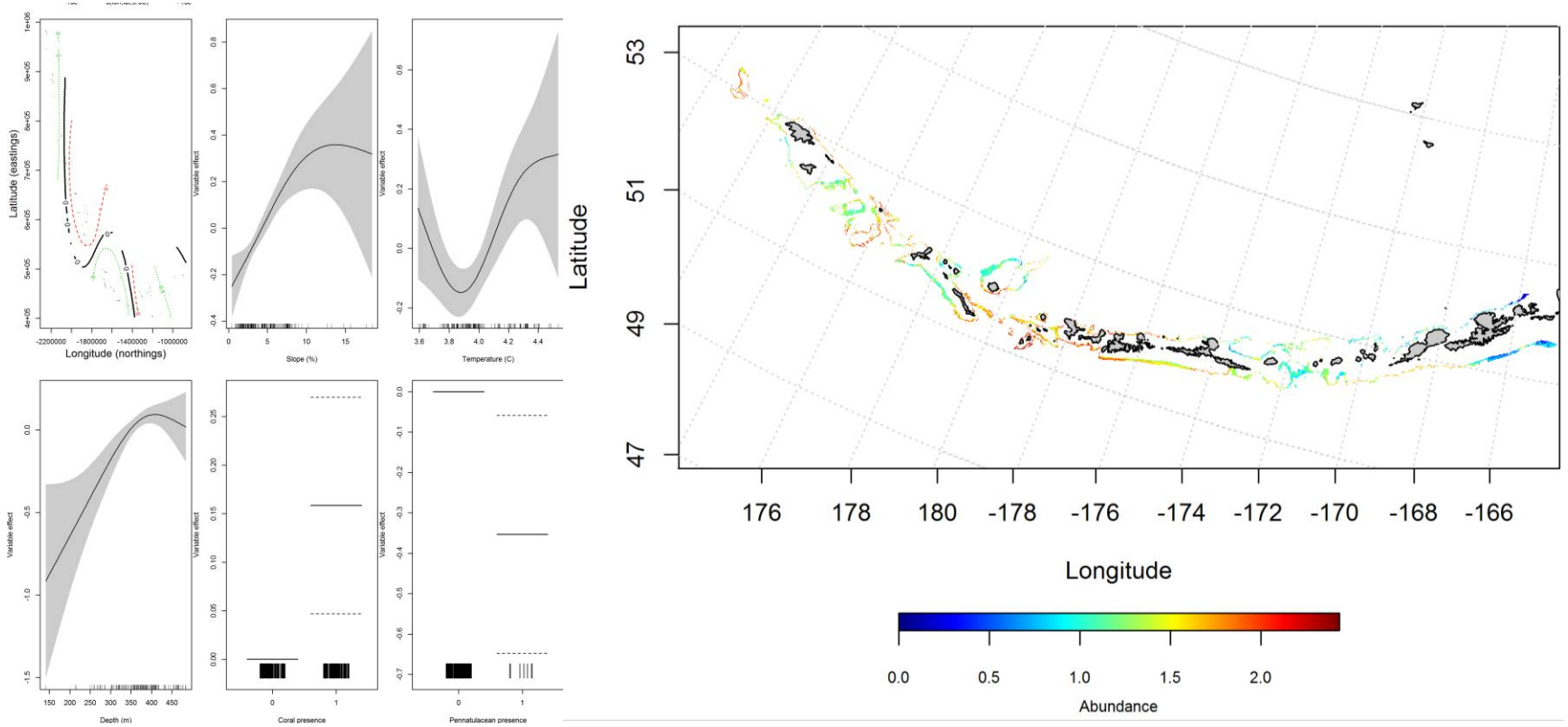

Figure 165. Best-fitting hurdle model effects of retained habitat variables on CPUE of juvenile Shortraker rockfish from summer bottom trawl surveys of the Aleutian Islands (left panel) alongside hurdle-predicted juvenile Shortraker rockfish CPUE (right panel).

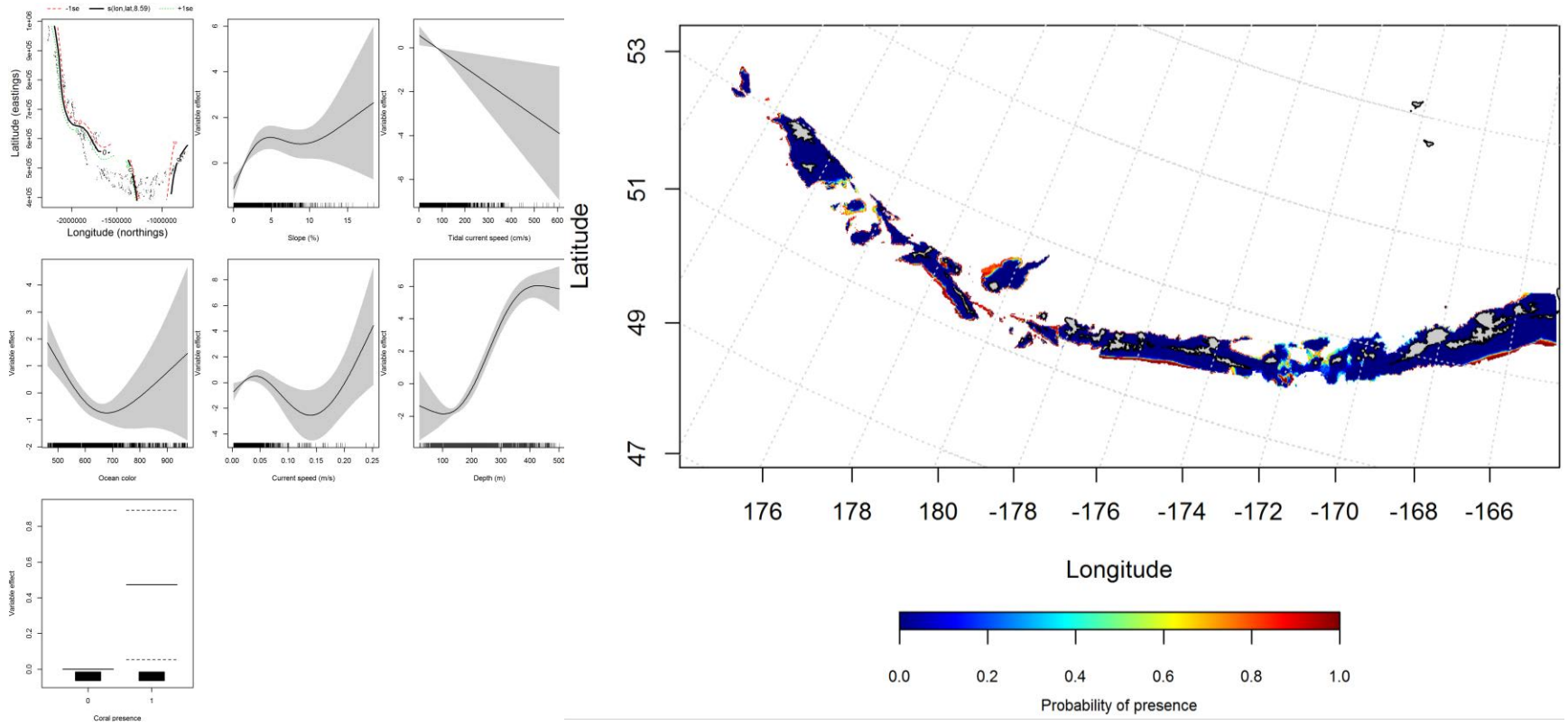

Figure 166. Best-fitting hurdle model effects of retained habitat variables on presence absence (PA) of adult Shortraker rockfish from summer bottom trawl surveys of the Aleutian Islands (left panel) alongside hurdle-predicted adult Shortraker rockfish PA (right panel).

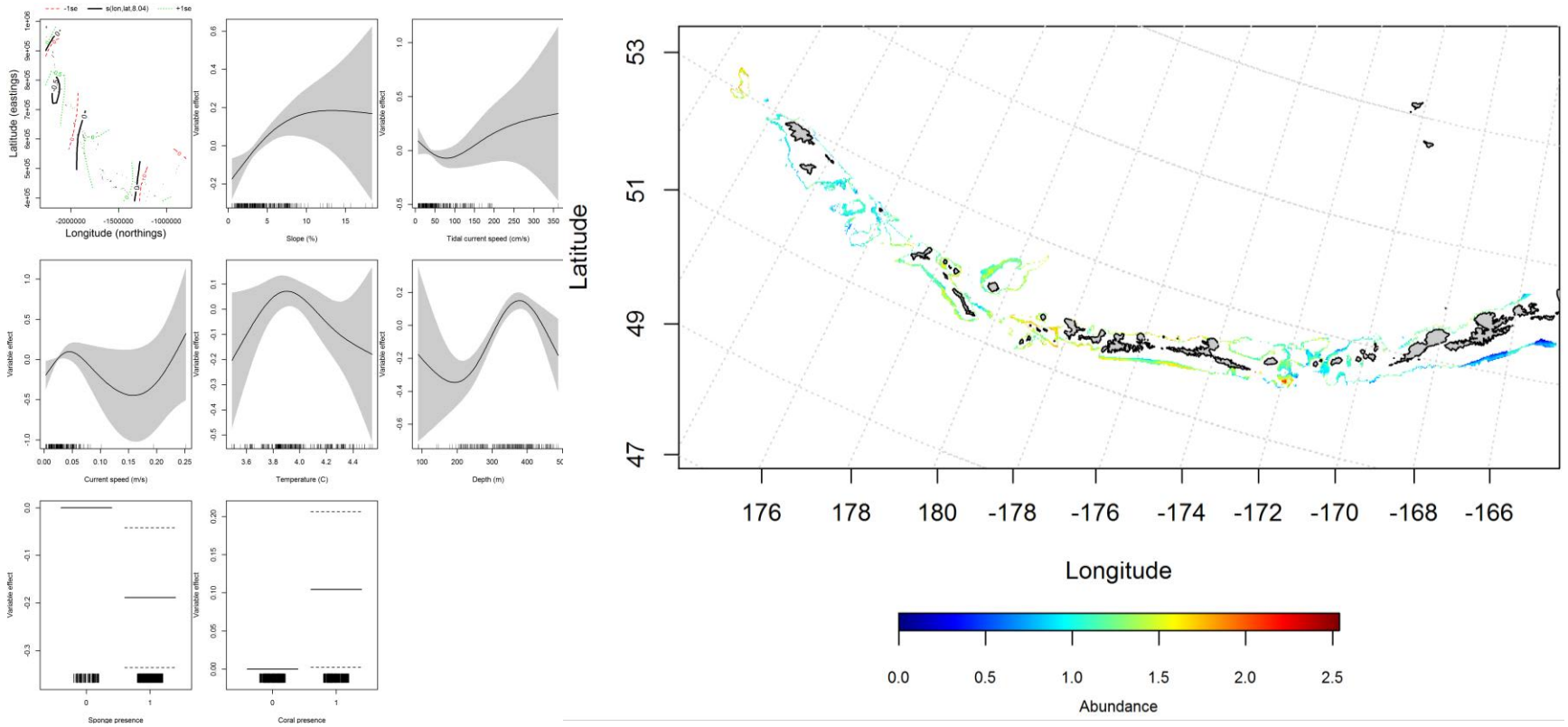

Figure 167. Best-fitting hurdle model effects of retained habitat variables on CPUE of adult Shortraker rockfish from summer bottom trawl surveys of the Aleutian Islands (left panel) alongside hurdle-predicted adult Shortraker rockfish CPUE (right panel).

Seasonal distribution of commercial fisheries catches of adult Shortraker rockfish in the Aleutian Islands-- Distribution of adult Shortraker rockfish in the Aleutian Islands in commercial fisheries catches was generally consistent throughout all seasons. In the fall, bottom depth, ocean color and tidal current were the most important variables determining the distribution of Shortraker rockfish (relative importance: 47.1%, 21.9%, and 12.7%, respectively). The AUC of the fall maxent model was 86% for the training data and 81% for the test data. 80% of the training data and 81% of the test data sets were predicted correctly. The model predicted probable suitable habitat of Shortraker rockfish throughout the AI chain (Figure 168).

In the winter, bottom depth, ocean color and tidal current were also the most important variables determining the distribution of Shortraker rockfish (relative importance:36.2%, 28.3%, and 23.2%, respectively). The AUC of the winter maxent model was 89% for the training data and 78% for the test data. The model correctly classified 76% of the training data and 78% of the test data sets. As with the fall, the model predicted probable suitable habitat of Shortraker rockfish throughout the AI, although there was higher predicted probability in the eastern AI (Figure 169).

In the spring, bottom depth and ocean color were the most important variables determining the distribution of Shortraker rockfish (relative importance: 62% and 20.3%). The AUC of the spring maxent model was 93% for the training data and 84% for the test data. Similar to the fall, the model predicted probable suitable habitat of Shortraker rockfish throughout the AI (Figure 170).

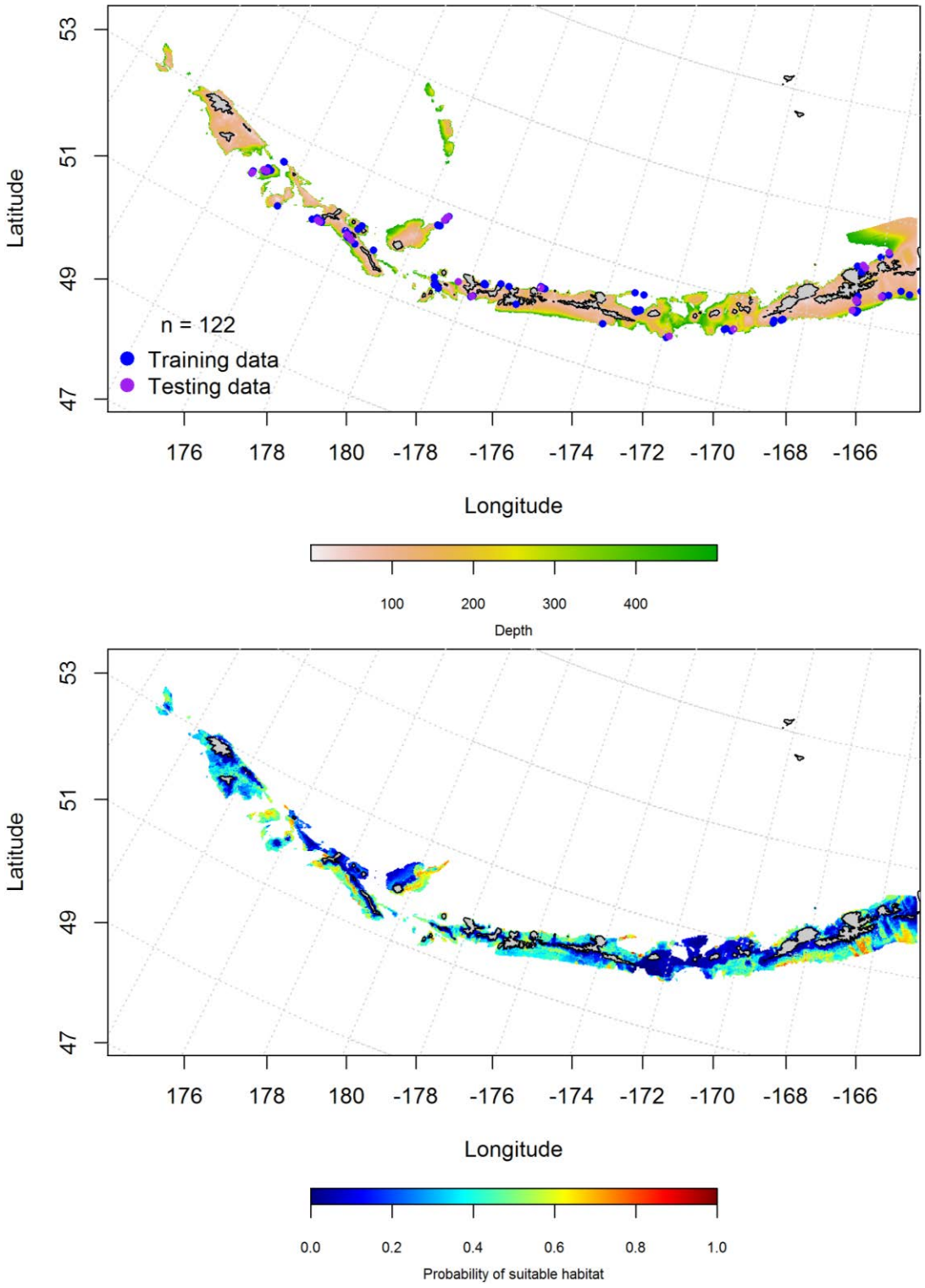

Figure 168. Locations of fall (September-November) commercial fisheries catches of Shortraker rockfish (top panel). Blue points were used to train the maximum entropy model predicting the probability of suitable fall habitat supporting commercial catches of Shortraker rockfish (bottom panel) and the purple points were used to validate the model.

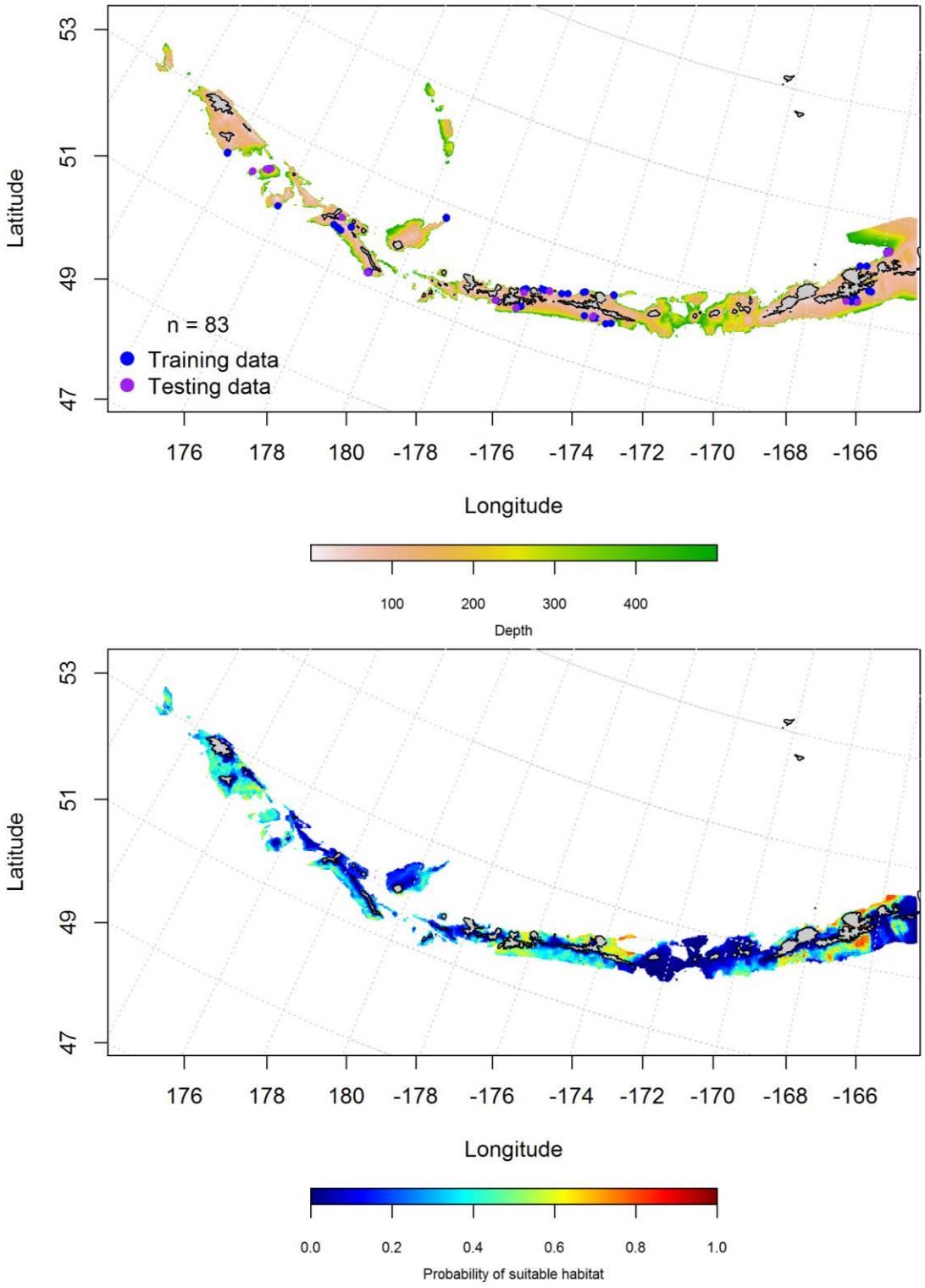

Figure 169. Locations of winter (December-February) commercial fisheries catches of Shortraker rockfish (top panel). Blue points were used to train the maximum entropy model predicting the probability suitable winter habitat supporting commercial catches of Shortraker rockfish (bottom panel) and the purple points were used to validate the model.

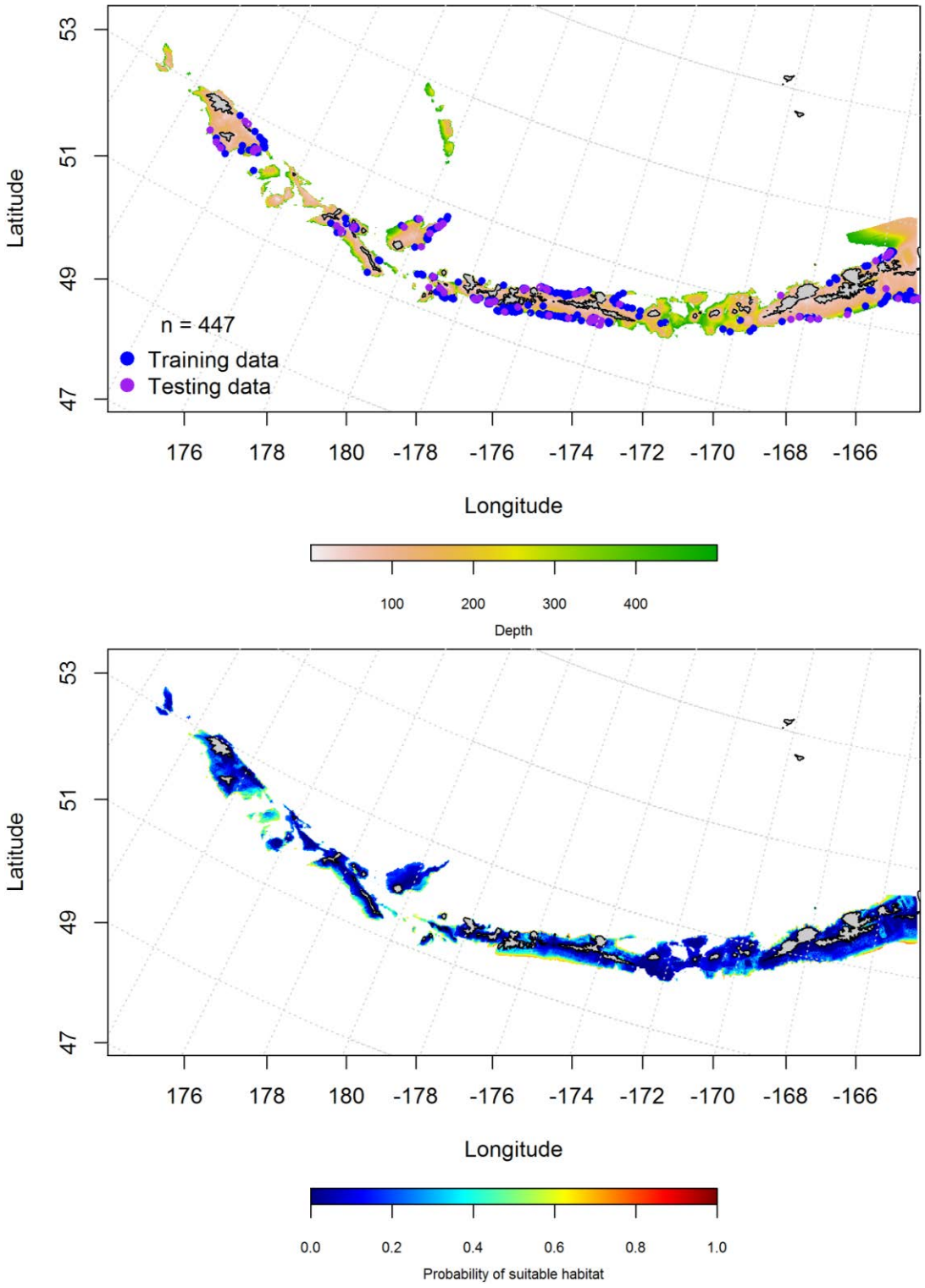

Figure 170. Locations of spring (March-May) commercial fisheries catches of Shortraker rockfish (top panel). Blue points were used to train the maximum entropy model predicting the probability of suitable spring habitat supporting commercial catches of Shortraker rockfish (bottom panel) and the purple points were used to validate the model.

Aleutian Islands Shortraker rockfish Essential Fish Habitat Maps and Conclusions -- In general, juvenile and adult Shortraker rockfish are similarly distributed through the Aleutian Islands chain and co-occur in most places where they are found. Those collected in summertime bottom trawl surveys share similar predicted EFH distributions across the Aleutian Islands (Figure 171). These similarities can be observed in both areas of higher and low abundance (e.g., large passes and the eastern AI).

Similar to summertime bottom trawl survey data observations, the EFH predicted from commercial catches of Shortraker rockfish is distributed throughout the Aleutian Islands chain (Figure 172). There does not appear to be much seasonal variability to the EFH location throughout the AI, though the fall model predicts a larger percent of suitable habitat, followed by winter than spring. Large passes result in of low concentration in all seasons.

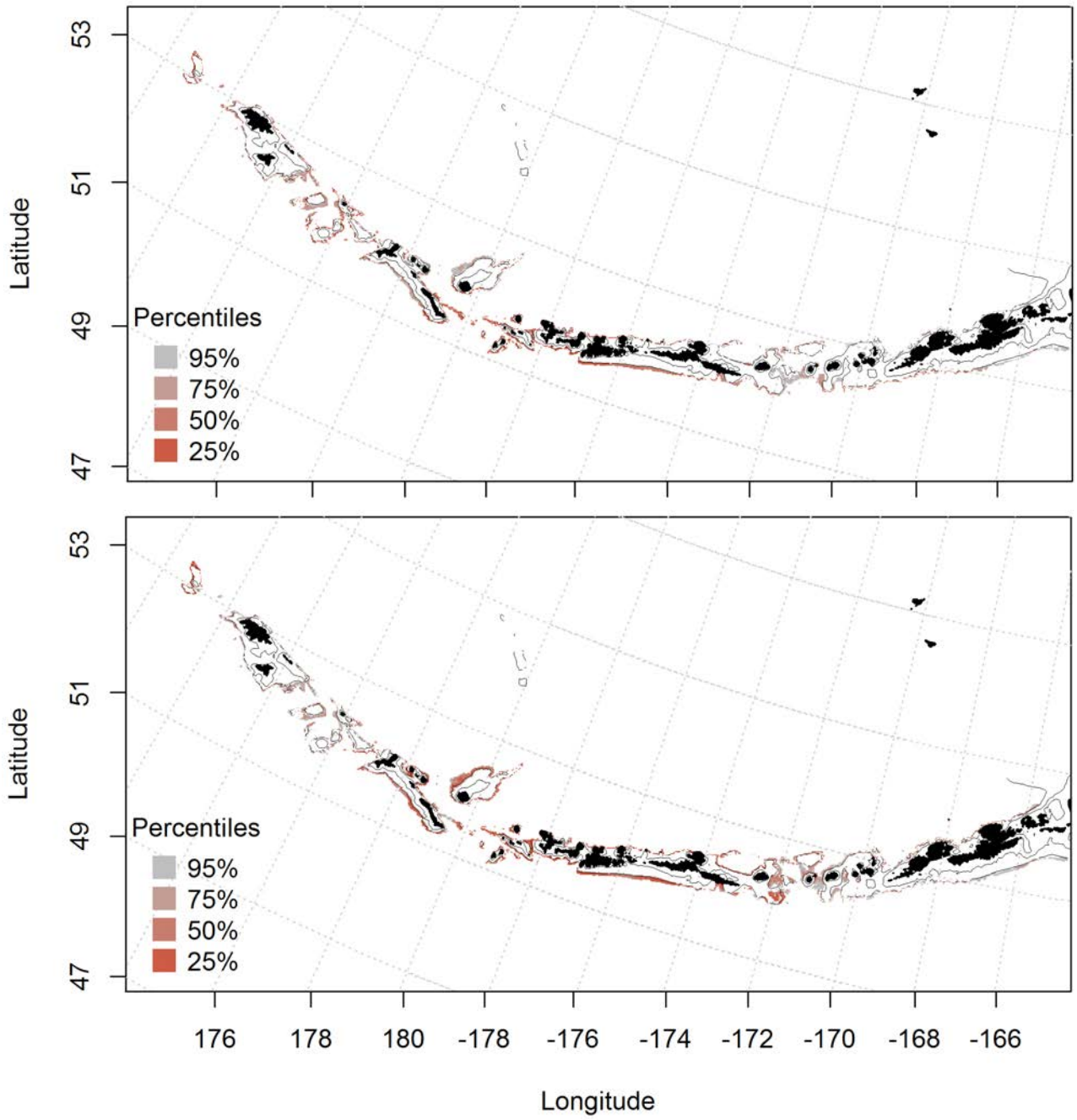

Figure 171. Predicted summer essential fish habitat for Shortraker rockfish juveniles and adults (top and bottom panel) from summertime bottom trawl surveys.

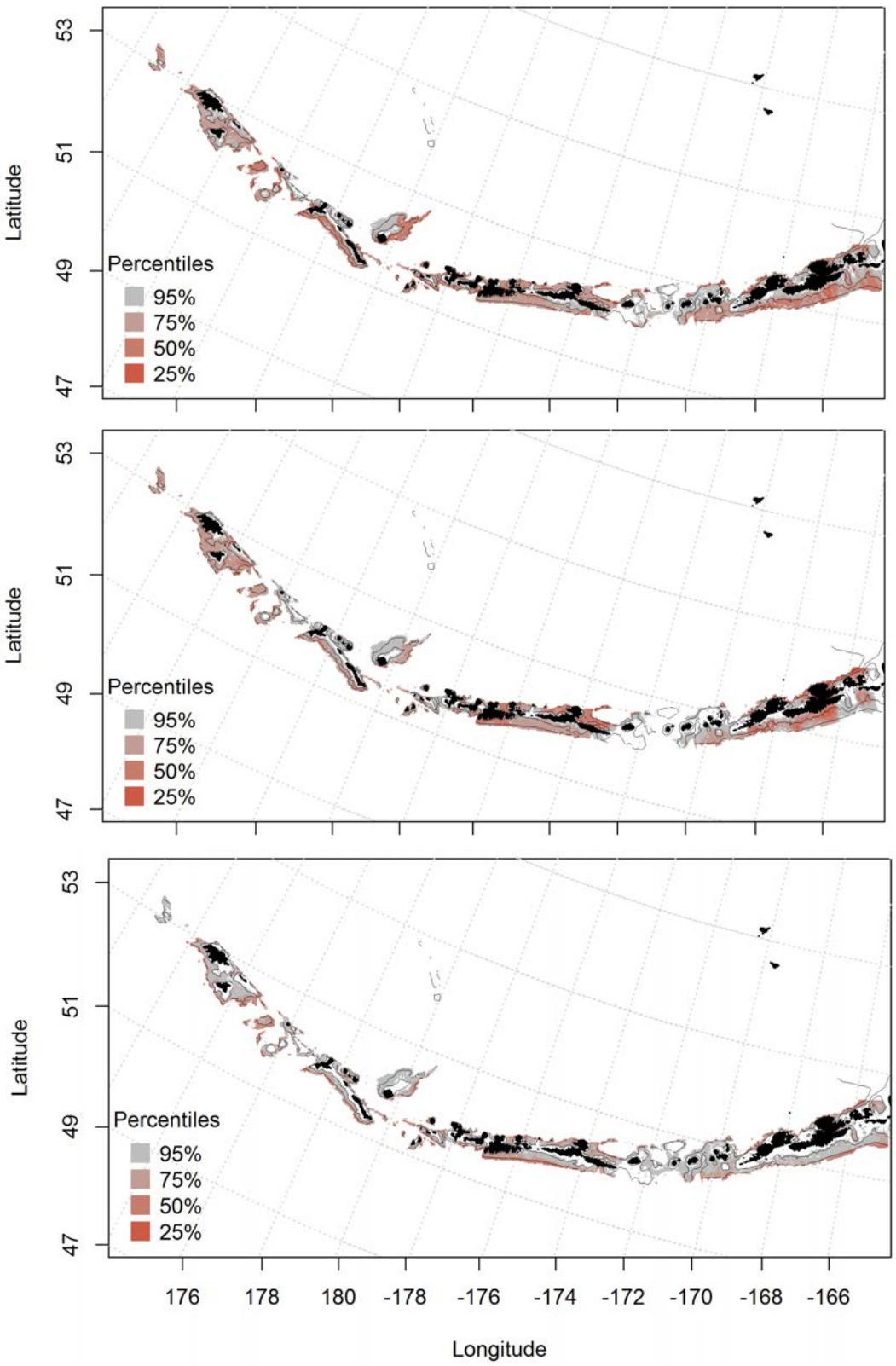

Figure 172. Essential fish habitat predicted for Shortraker rockfish during fall (top panel), winter (middle panel) and spring (bottom panel) from summertime commercial catches.

Rougheye rockfish (*Sebastes aleutianus*)

Summertime distribution of juvenile and adult Rougheye rockfish from bottom trawl surveys of the Aleutian Islands -- The catch of Rougheye rockfish in summer bottom trawl surveys of the Aleutian Islands indicates this species is similarly distributed throughout the AI. Bottom depth, current speed and bottom temperature were the most important variables explaining the distribution of juvenile Rougheye rockfish (relative importance: 61%, 14.3%, and 13.6%, respectively). A maximum entropy model predicting probable suitable habitat of juvenile Rougheye rockfish explained 95% of the training data set variability and 75% of the test data set. The model correctly classified 88% of the training data and 75% of the test data. The model predicted probable suitable habitat of juvenile Rougheye rockfish across the AI and was highest near Kiska and Adak Islands (Figure 173).

Bottom depth, slope, and bottom temperature were the most important variables explaining the distribution of adult Rougheye rockfish (relative importance: 56.7%, 23.9%, and 10.9%, respectively). A maximum entropy model predicting probable suitable habitat of adult Rougheye rockfish explained 92% of the training and test data sets. The model correctly classified 88% of the training data and 92% of the test data. The model predicted probable suitable habitat of adult Rougheye rockfish similar to the juveniles (varied across the AI and was highest near Kiska and Adak Islands) (Figure 174).

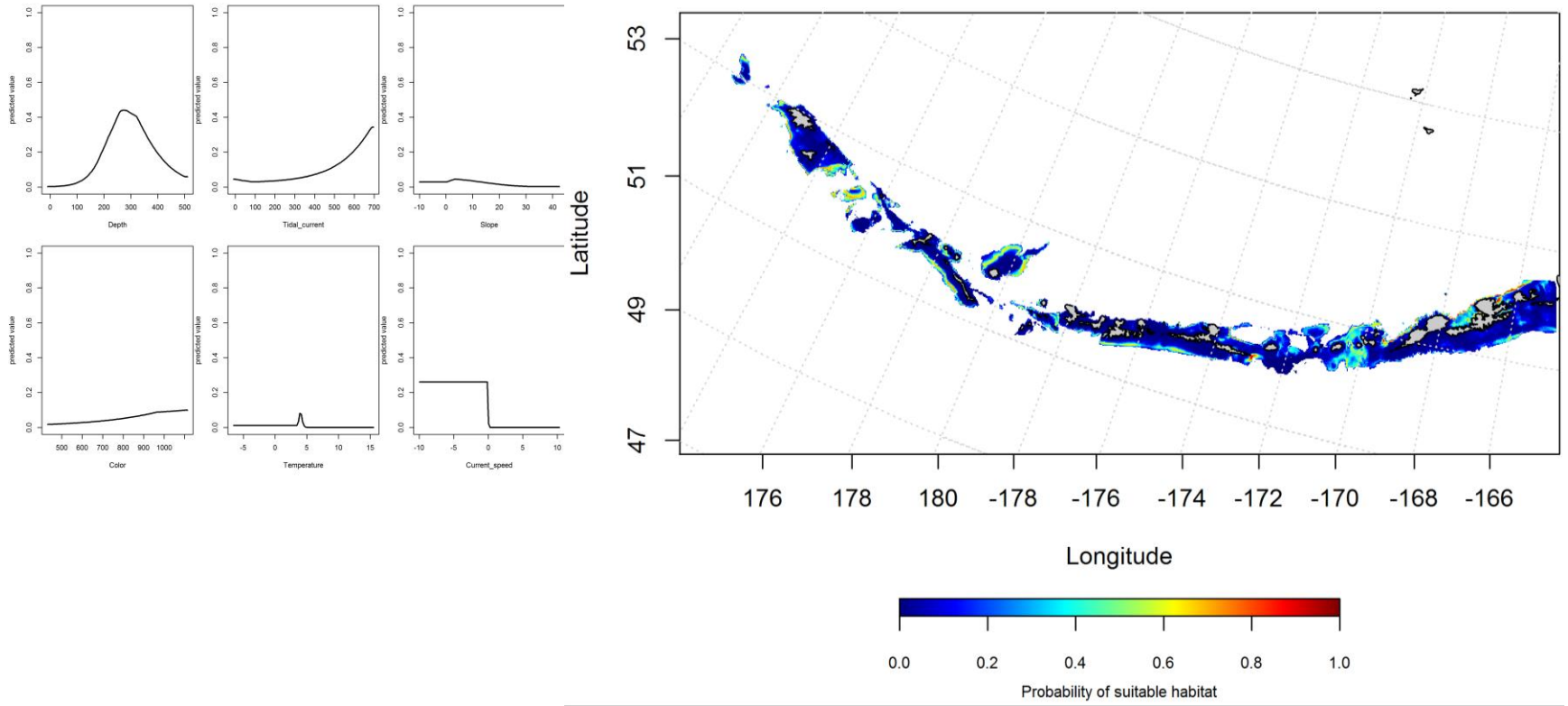

Figure 173. Best-fitting maxent model effects of retained habitat variables on suitable habitat of juvenile Rougheye rockfish from summer bottom trawl surveys of the Aleutian Islands (left panel) alongside maxent-predicted juvenile Rougheye rockfish probable suitable habitat (right panel).

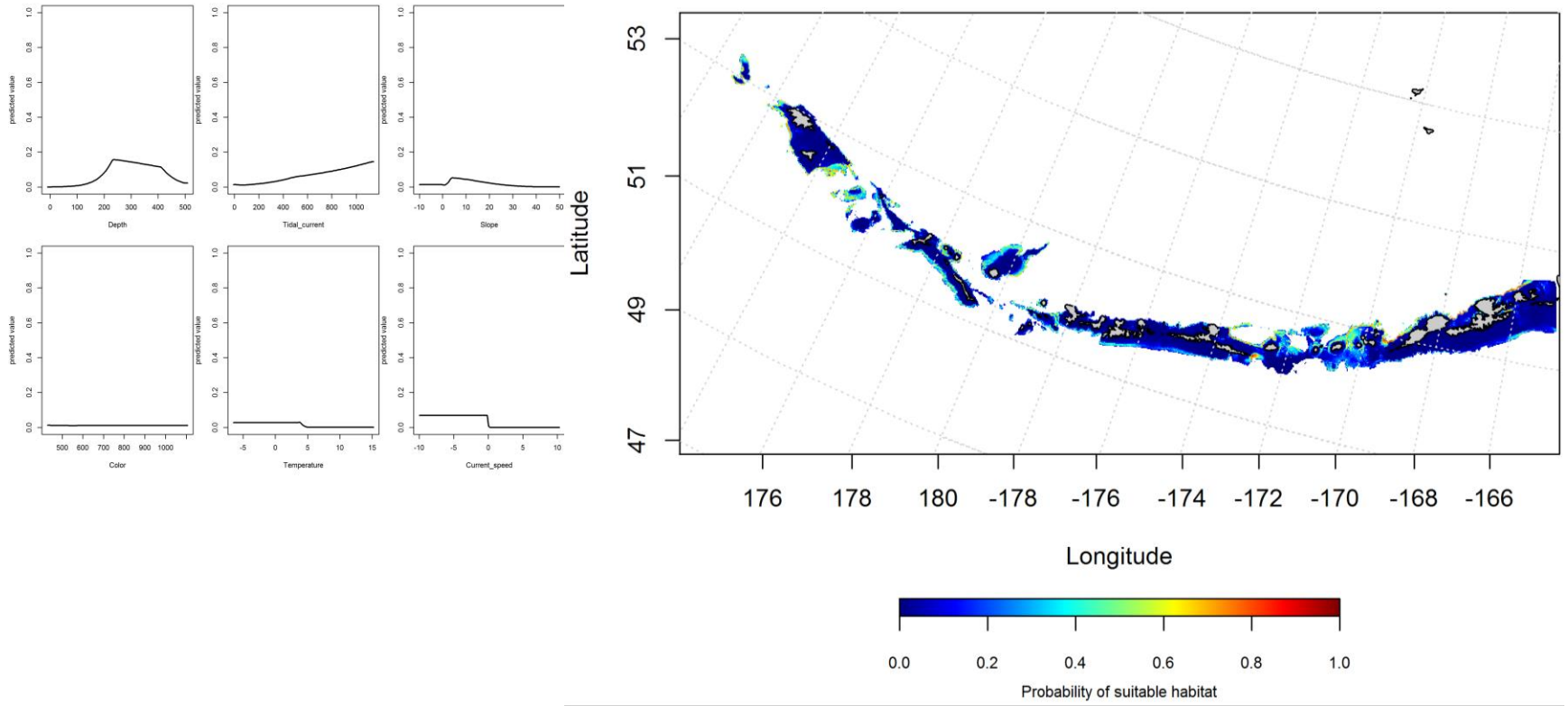

Figure 174. Best-fitting maxent model effects of retained habitat variables on probable suitable habitat of adult Rougheye rockfish from summer bottom trawl surveys of the Aleutian Islands (left panel) alongside maxent-predicted adult Rougheye rockfish suitable habitat (right panel).

Blackspotted rockfish (*Sebastes melanostictus*)

Summertime distribution of juvenile and adult Blackspotted rockfish from bottom trawl surveys of the Aleutian Islands -- The catch of Blackspotted rockfish in summer bottom trawl surveys was similarly distributed in the Aleutian Islands. A hurdle-GAM model was used to predict the presence and absence of juvenile Blackspotted rockfish. Bottom depth and geographic location were most important variables explaining the distribution of juvenile Blackspotted rockfish. The PA GAM explained 89% of the training data variability, 86% of the test data variability, and 34.2% of the deviance. The model correctly classified 80% of the training data and 79% of the test data. Juvenile Blackspotted rockfish were suitable habitat was predicted across the AI though higher near Kiska and Adak Islands, and the ?? pass (Figure 175).

The second part of the hurdle model found geographic location and coral presence were the most influential variables influencing the CPUE of juvenile Blackspotted rockfish. The model explained 24.9% of the deviance, 25% of the training data and 30% of the test data. The model predicted suitable habitat across the AI (Figure 176).

The catch of Blackspotted rockfish in summer bottom trawl surveys was similarly distributed in the Aleutian Islands. A hurdle-GAM model was used to predict the presence and absence of adult Blackspotted rockfish. Bottom depth and slope were the most important variables explaining the distribution of adult Blackspotted rockfish. The PA GAM explained 95% of the training data variability, 94% of the test data variability, and 50.7% of the deviance. The model correctly classified 86% of the training and test data sets. Adult Blackspotted rockfish suitable habitat was predicted across the AI though higher near ?? and ?? passes (Figure 177).

The second part of the hurdle model found ocean color and slope were the most influential variables influencing the CPUE of adult Blackspotted rockfish. The model explained 38.6% of the deviance, 39% of the training data and 35% of the test data. The model predicted suitable habitat across the AI (Figure 178).

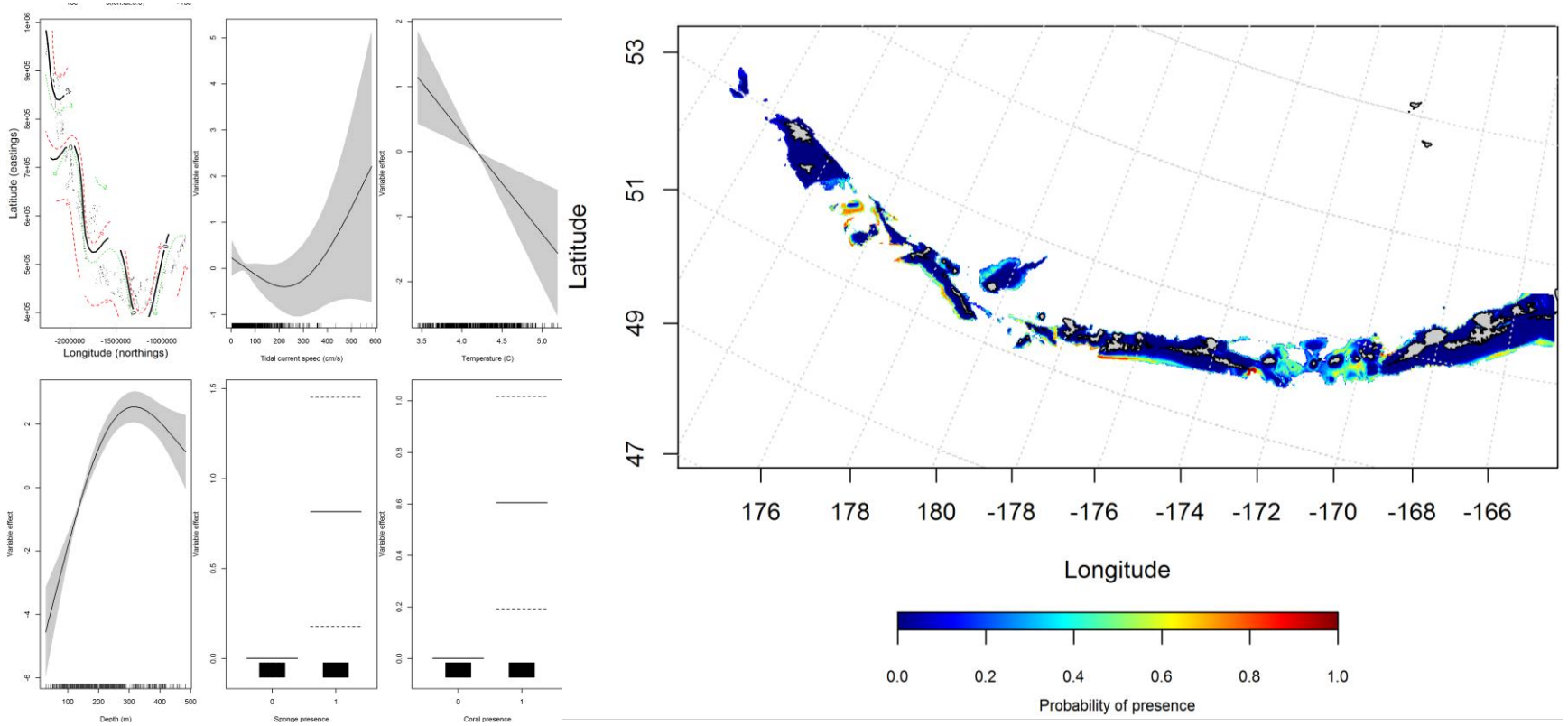

Figure 175. Best-fitting hurdle model effects of retained habitat variables on presence absence (PA) of juvenile Blackspotted rockfish from summer bottom trawl surveys of the Aleutian Islands (left panel) alongside hurdle-predicted juvenile Blackspotted rockfish PA (right panel).

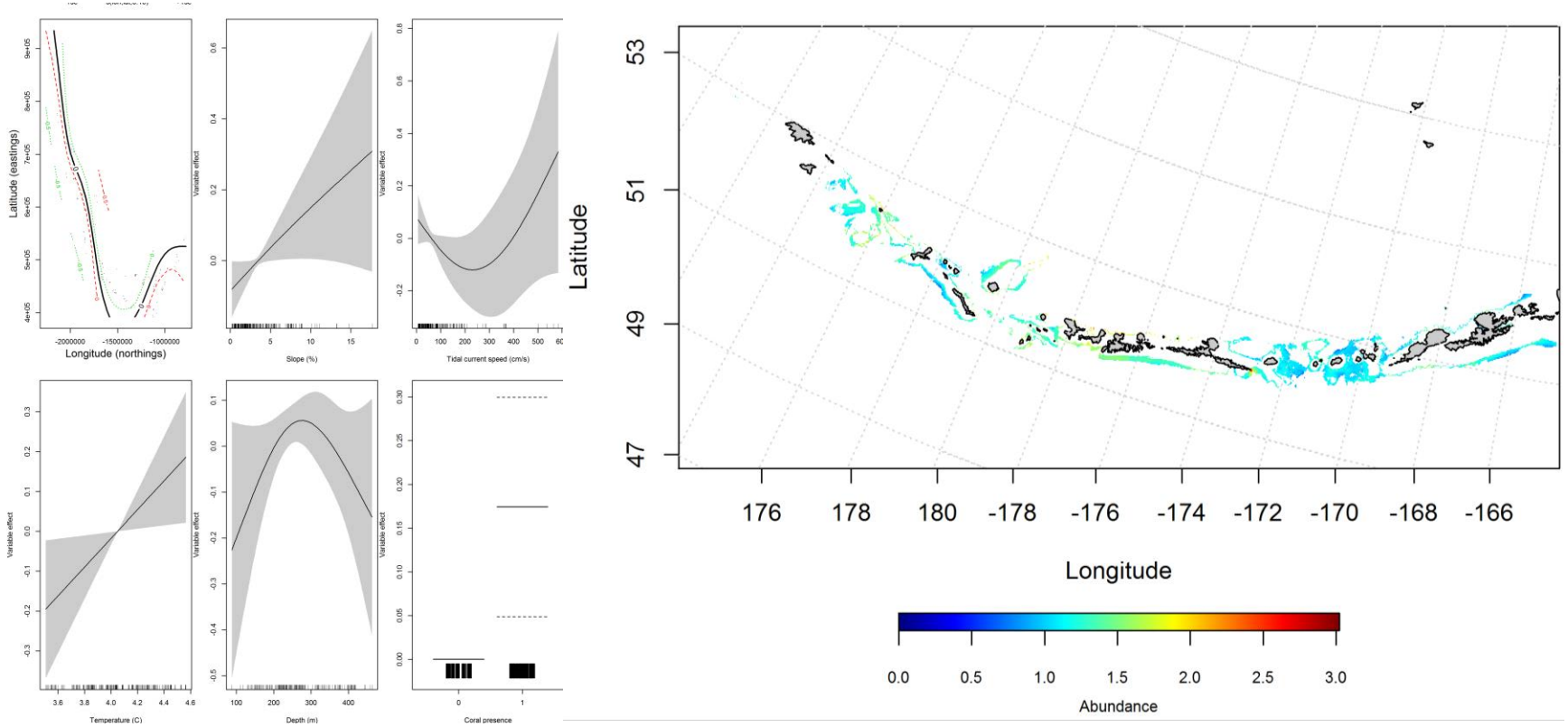

Figure 176. Best-fitting hurdle model effects of retained habitat variables on CPUE of juvenile Blackspotted rockfish from summer bottom trawl surveys of the Aleutian Islands (left panel) alongside hurdle-predicted juvenile Blackspotted rockfish CPUE (right panel).

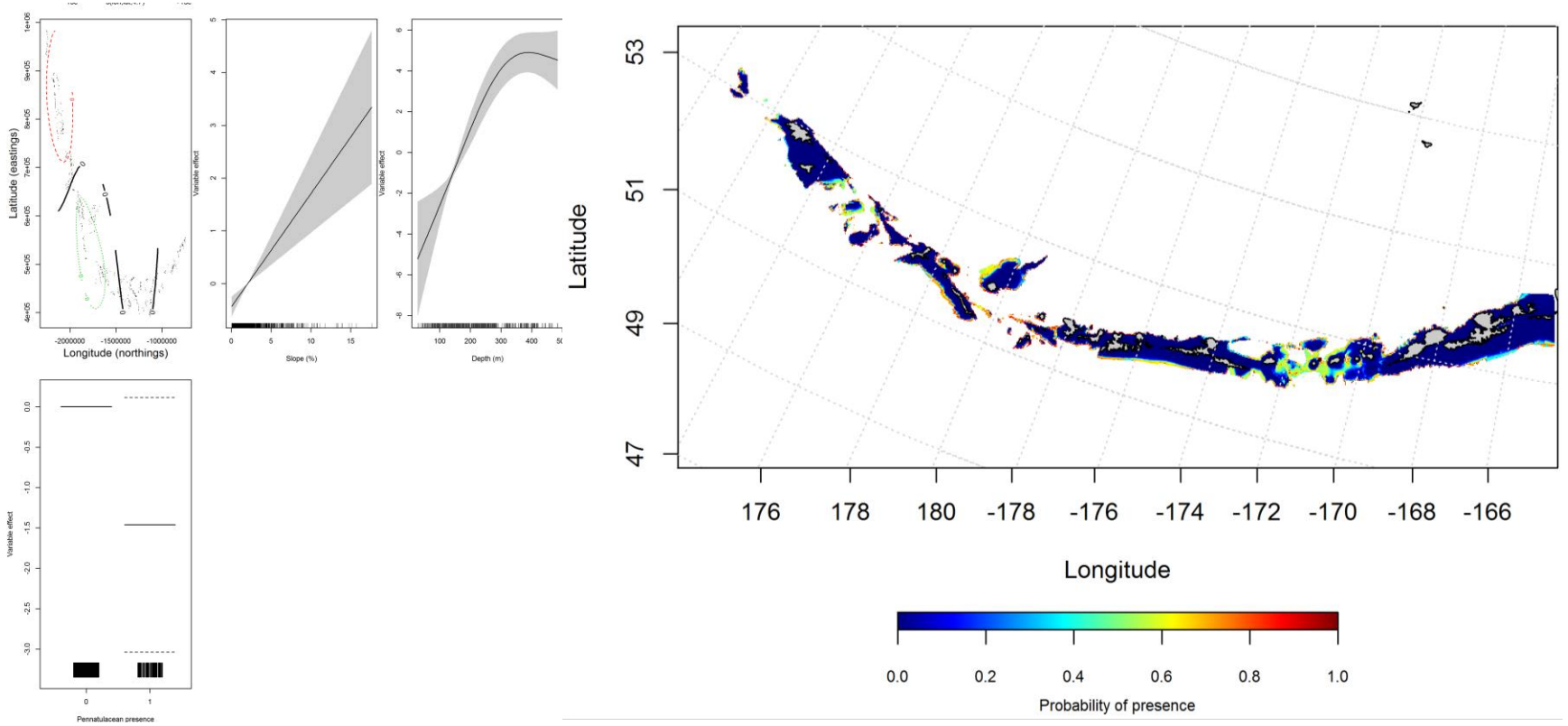

Figure 177. Best-fitting hurdle model effects of retained habitat variables on presence absence (PA) of adult Blackspotted rockfish from summer bottom trawl surveys of the Aleutian Islands (left panel) alongside hurdle-predicted adult Blackspotted rockfish PA (right panel).

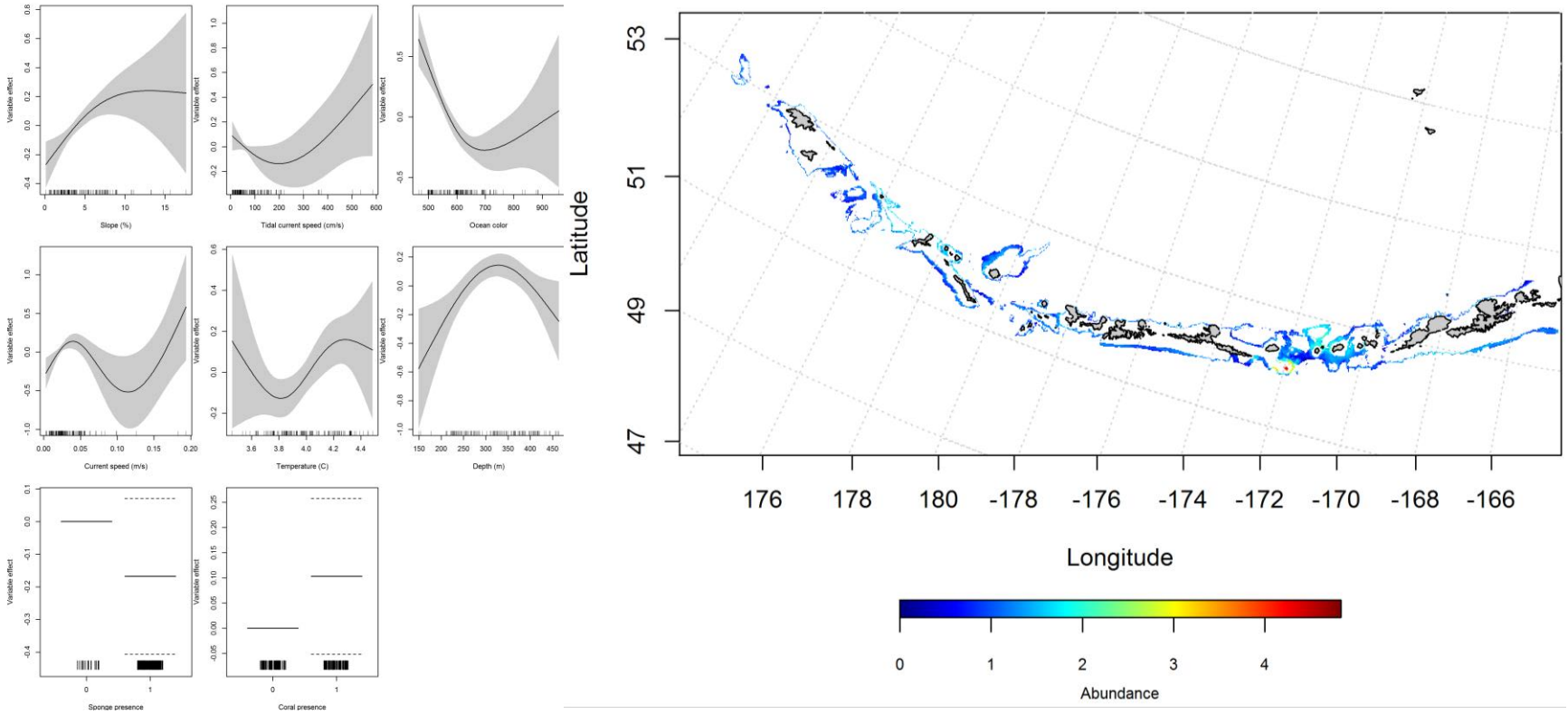

Figure 178. Best-fitting hurdle model effects of retained habitat variables on CPUE of adult Blackspotted rockfish from summer bottom trawl surveys of the Aleutian Islands (left panel) alongside hurdle-predicted adult Blackspotted rockfish CPUE (right panel).

Rougheye rockfish (*Sebastes aleutianus*) and Blackspotted rockfish (*Sebastes melanostictus*) were combined in Sean's observer data, but separate in my groundfish data

Seasonal distribution of commercial fisheries catches of adult Rougheye rockfish and Blackspotted rockfish in the Aleutian Islands-- Distribution of adult Rougheye rockfish and Blackspotted rockfish in the Aleutian Islands in commercial fisheries catches was generally consistent throughout all seasons. In the fall, bottom depth, surface color and tidal current were the most important variables determining probable suitable habitat of Rougheye rockfish and Blackspotted rockfish (relative importance: 48.4%, 22.8%, and 10.1%, respectively). The AUC of the fall maxent model was 92% for the training data and 75% for the test data. The model correctly classified 84% of the training data and 75% of the test data. The model predicted probable suitable habitat of Rougheye rockfish and Blackspotted rockfish across the AI, and higher north of Semisopochnoi Island (Figure 179).

In the winter, bottom depth, tidal current, surface color, and current speed were the most important variables determining probable suitable habitat of Rougheye rockfish and Blackspotted rockfish (relative importance: 38.8%, 18.3%, 17.1%, and 15.6%, respectively). The AUC of the winter maxent model was 96% for the training data and 85% for the test data. 91% of the cases in the training data and 85% of the test data sets were predicted correctly. As with the fall, the model predicted probable suitable habitat of Rougheye rockfish and Blackspotted rockfish through the AI (Figure 180).

In the spring, bottom depth, surface color, and bottom temperature were the most important variables determining probable suitable habitat of Rougheye rockfish and Blackspotted rockfish (relative importance: 50.8%, 23.6%, and 10%, respectively). The AUC of the spring model was 87% for the training data and 75% for the test data. The model correctly classified 79% of the

training data and 75% of the test data. As with the fall and winter, the model predicted probable suitable habitat of Rougheye rockfish and Blackspotted rockfish across the AI and highest near Adak and Atka Islands (Figure 181).

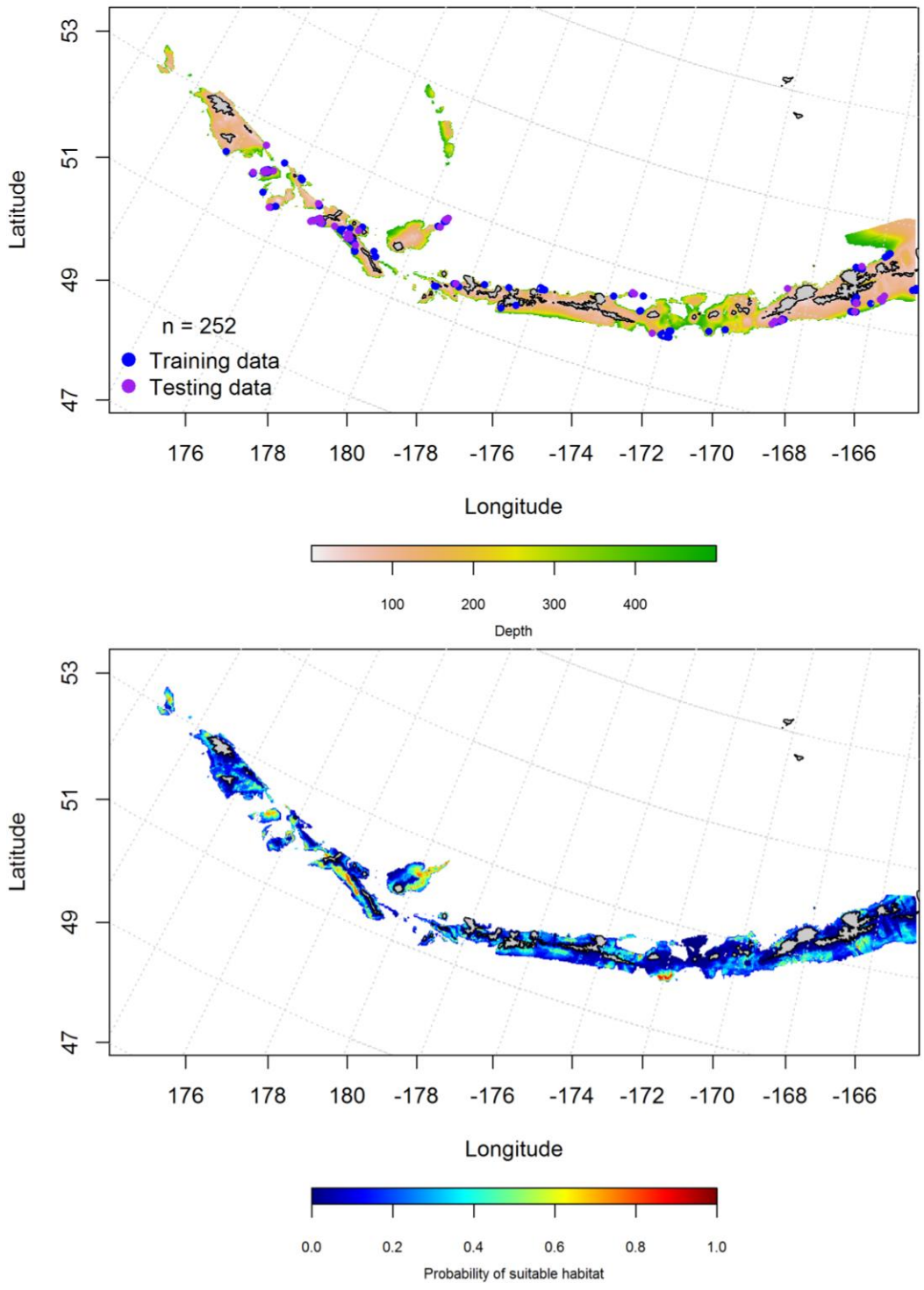

Figure 179. Locations of fall (September-November) commercial fisheries catches of Rougheye rockfish and Blackspotted rockfish combined (top panel). Blue points were used to train the maximum entropy model predicting the probability of suitable fall habitat supporting commercial catches of Rougheye rockfish and Blackspotted rockfish (bottom panel) and the purple points were used to validate the model.

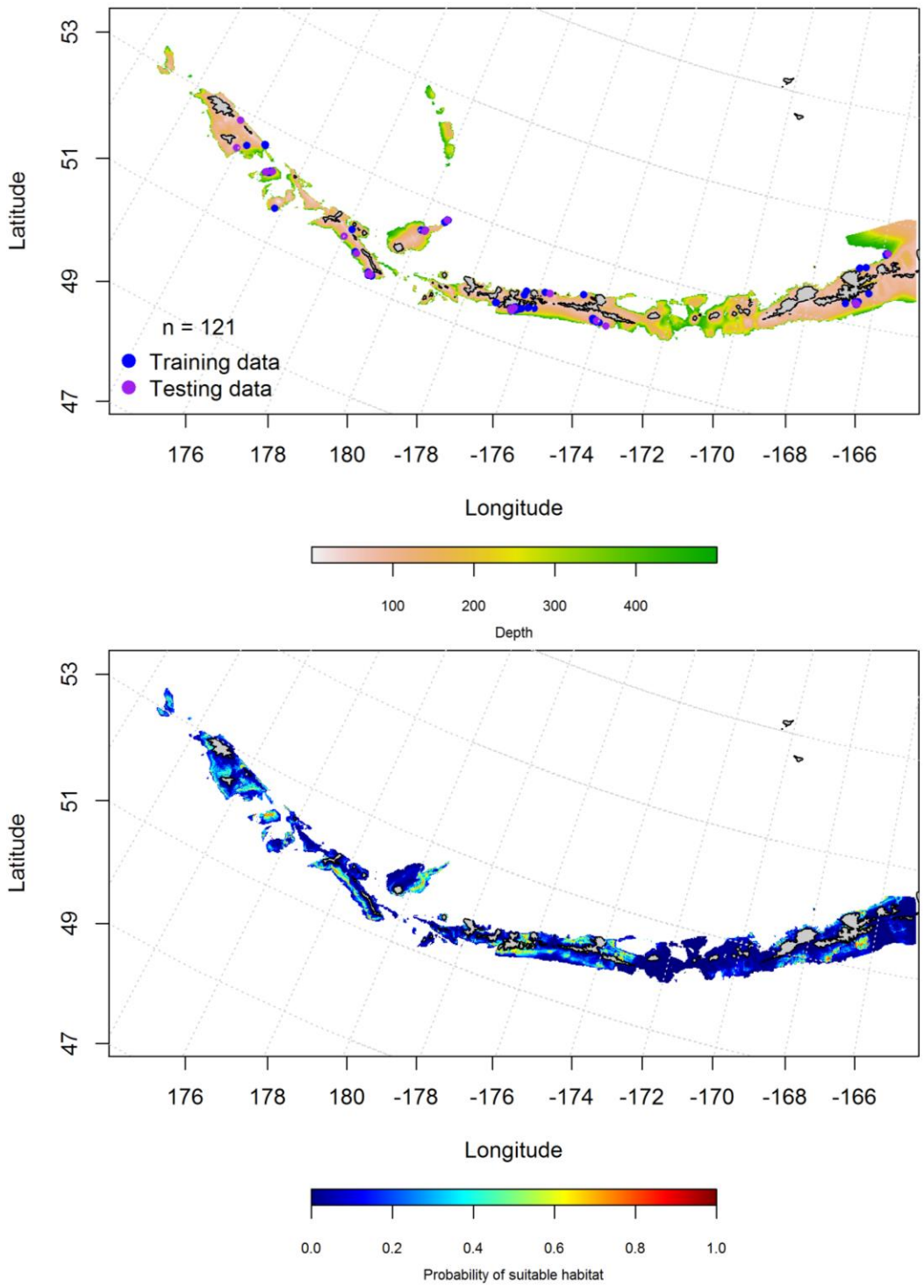

Figure 180. Locations of winter (December-February) commercial fisheries catches of Rougheye rockfish and Blackspotted rockfish combined (top panel). Blue points were used to train the maximum entropy model predicting the probability of suitable winter habitat supporting commercial catches of Rougheye rockfish and Blackspotted rockfish (bottom panel) and the purple points were used to validate the model.

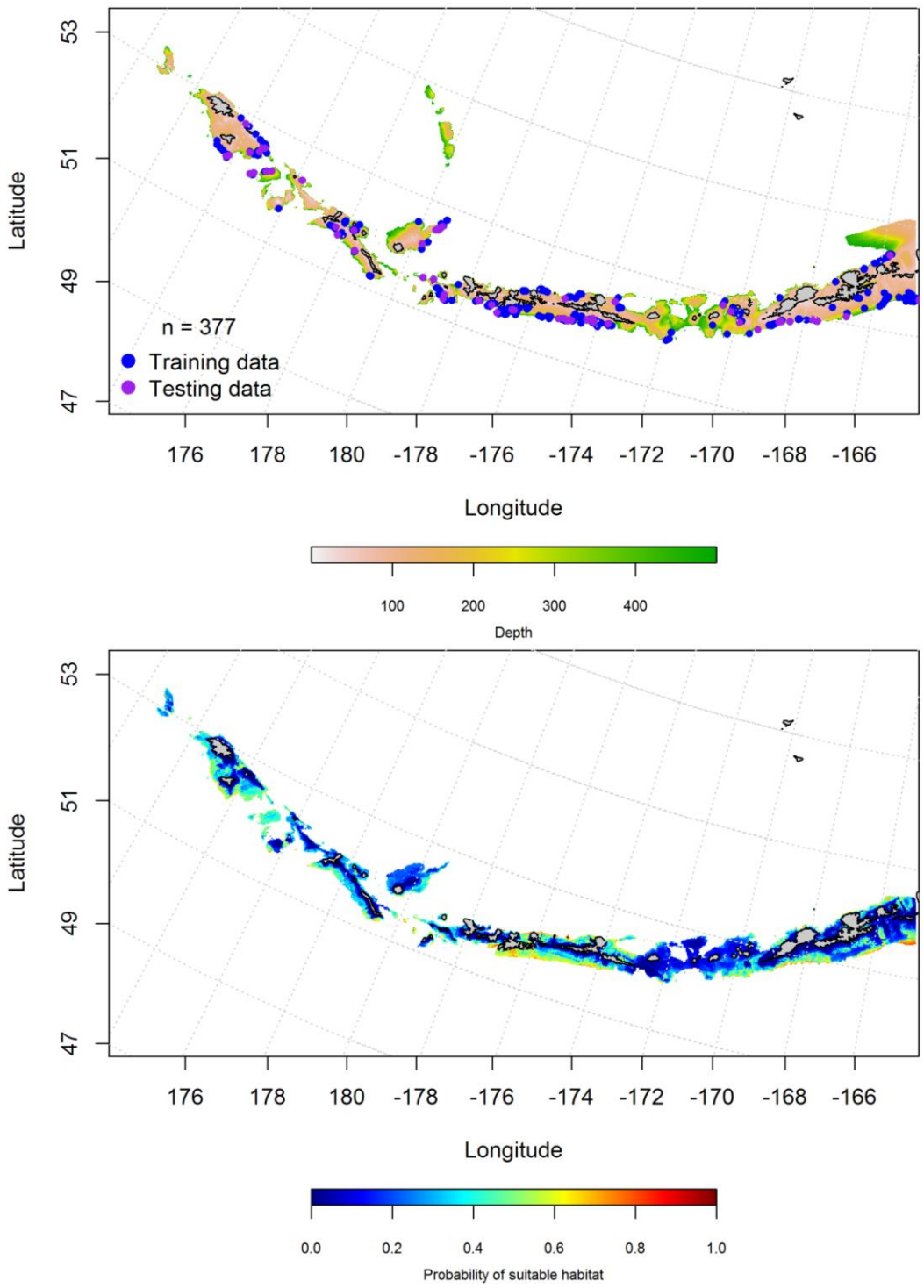

Figure 181. Locations of spring (March-May) commercial fisheries catches of Rougheye rockfish and Blackspotted rockfish combined (top panel). Blue points were used to train the maximum entropy model predicting the probability of suitable spring habitat supporting commercial catches of Rougheye rockfish and Blackspotted rockfish (bottom panel) and the purple points were used to validate the model.

Aleutian Islands Rougheye rockfish and Blackspotted rockfish Essential Fish Habitat Maps and Conclusions -- Rougheye rockfish summertime EFH of juveniles and adults was low, but similarly distributed across the AI (Figure 182). Blackspotted rockfish summertime EFH of juveniles and adults was also similarly distributed across the AI (Figure 183).

The fall, winter and spring distribution of Rougheye rockfish and Blackspotted rockfish data was combined. EFH was essentially the same in all seasons (Figure 184). The highest EFH was predicted in the eastern AI near Adak and Atka Islands.

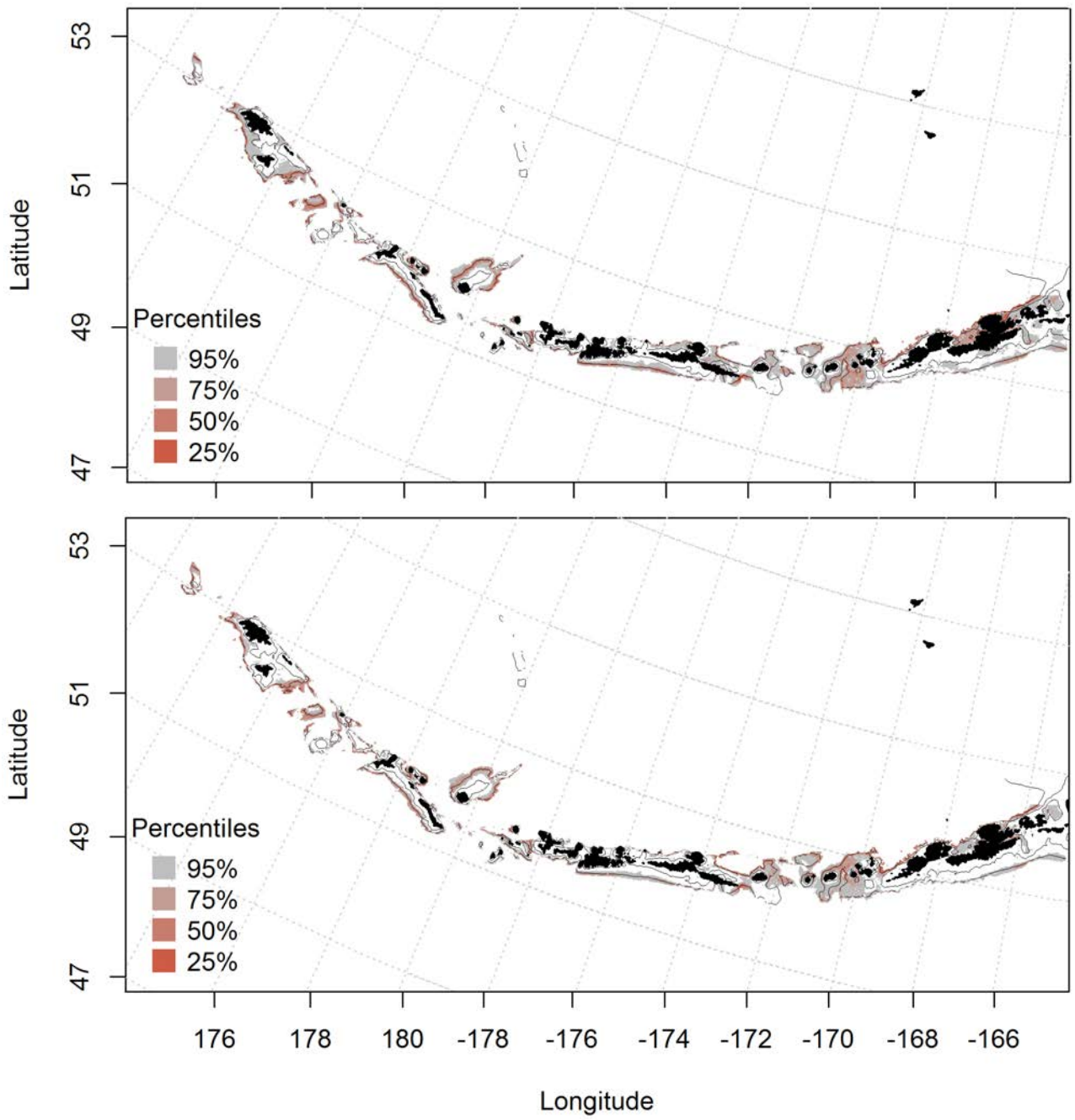

Figure 182. Predicted summer essential fish habitat for Rougheye rockfish juveniles and adults (top and bottom panel) from summertime bottom trawl surveys.

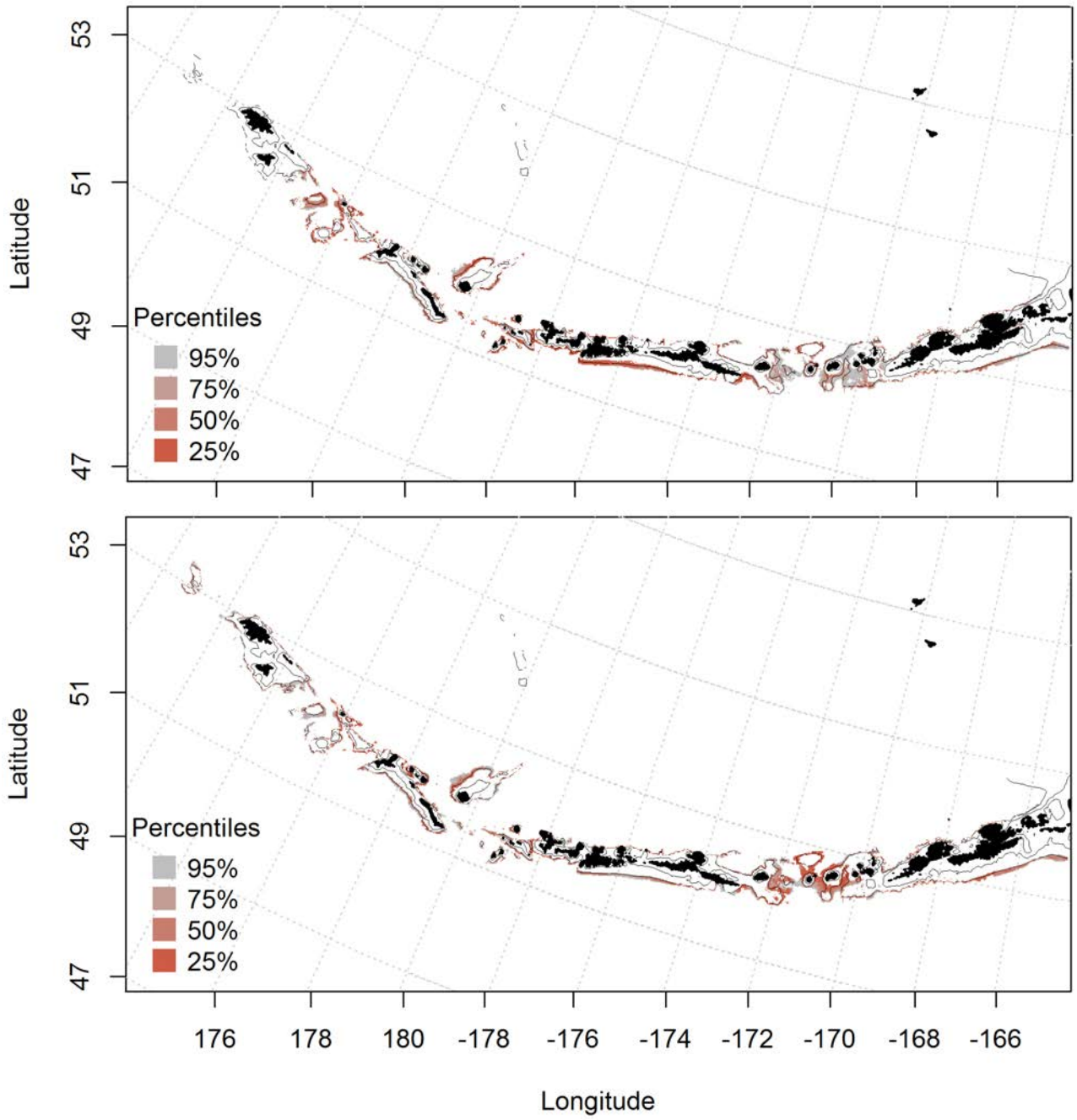

Figure 183. Predicted summer essential fish habitat for Blackspotted rockfish juveniles and adults (top and bottom panel) from summertime bottom trawl surveys.

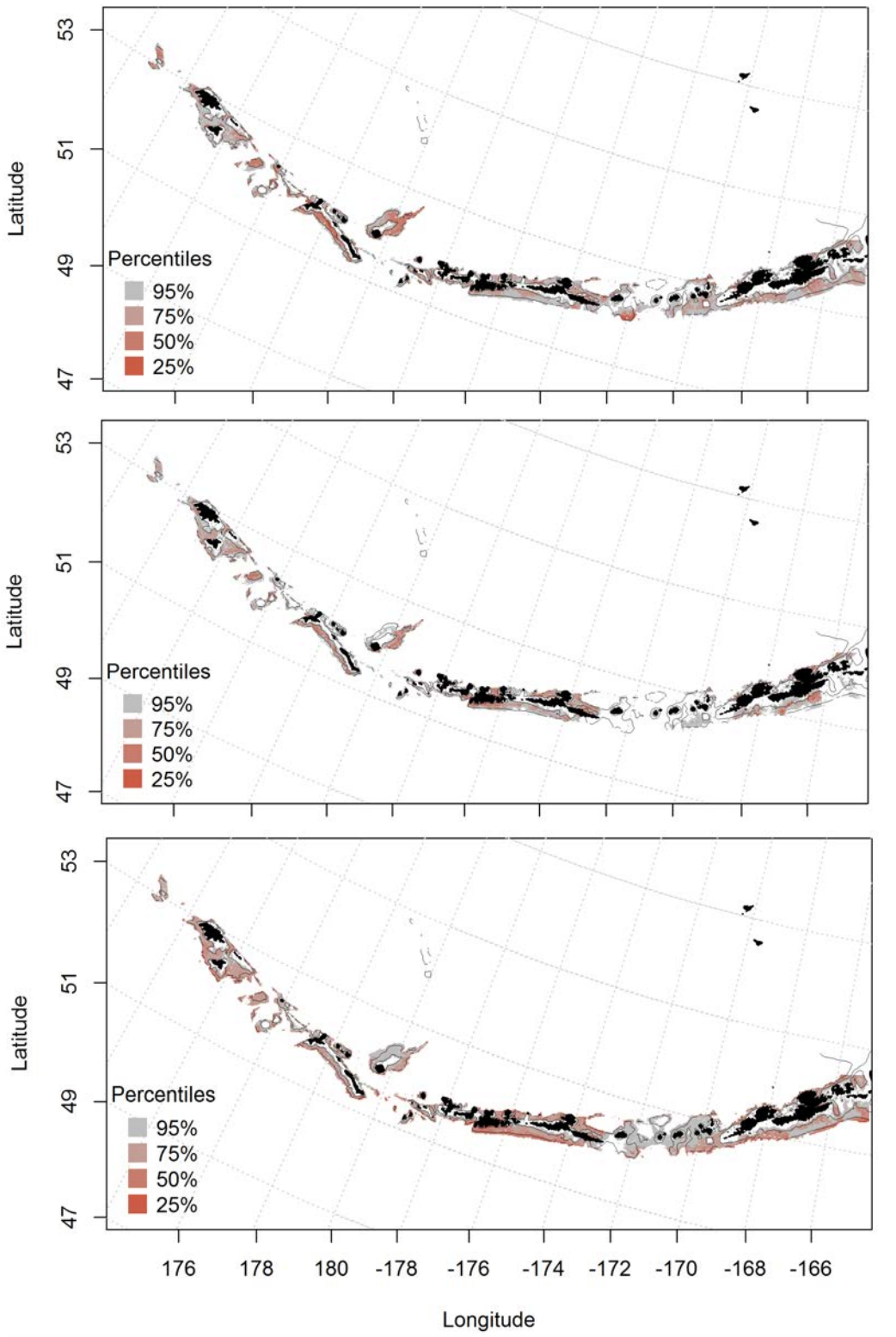

Figure 184. Essential fish habitat predicted for Rougheye rockfish and Blackspotted rockfish during fall (top panel), winter (middle panel) and spring (bottom panel) from summertime commercial catches.

Dusky rockfish (*Sebastes variabilis)*
Text about species here

Summertime distribution of juvenile and adult Dusky rockfish from bottom trawl surveys of the Aleutian Islands – There were only 22 instances of juvenile Dusky rockfish from summertime bottom trawl survey catches (Figure 185). Cases were across the AI, though there were not enough cases to run the maxent model.

A hurdle-GAM model was used to predict the presence and absence of adult Dusky rockfish and explained 79% of the variability in CPUE in the bottom trawl survey training data, and 76% of the variability in the test data set. Geographic location, slope, and bottom depth were the most important variables explaining the distribution of adult Dusky rockfish. The model explained 16.7% of the deviance, and correctly classified 70% of the training data and 67% of the test data set. The areas of predicted highest presence were similar to the juveniles, across the AI and highest in the eastern AI near Unalaska Island (Figure 186).

The second part of the hurdle model found bottom depth and geographic location influence the CPUE of adult Dusky rockfish the most, and explained 12.2% of the deviance, 12% of the training data and 17% of the test data. The model predicted highest CPUE in a similar pattern as the PA GAM (across the AI and highest in the eastern AI near Unalaska Island), but also indicated a high CPUE around Kiska Island (Figure 187).

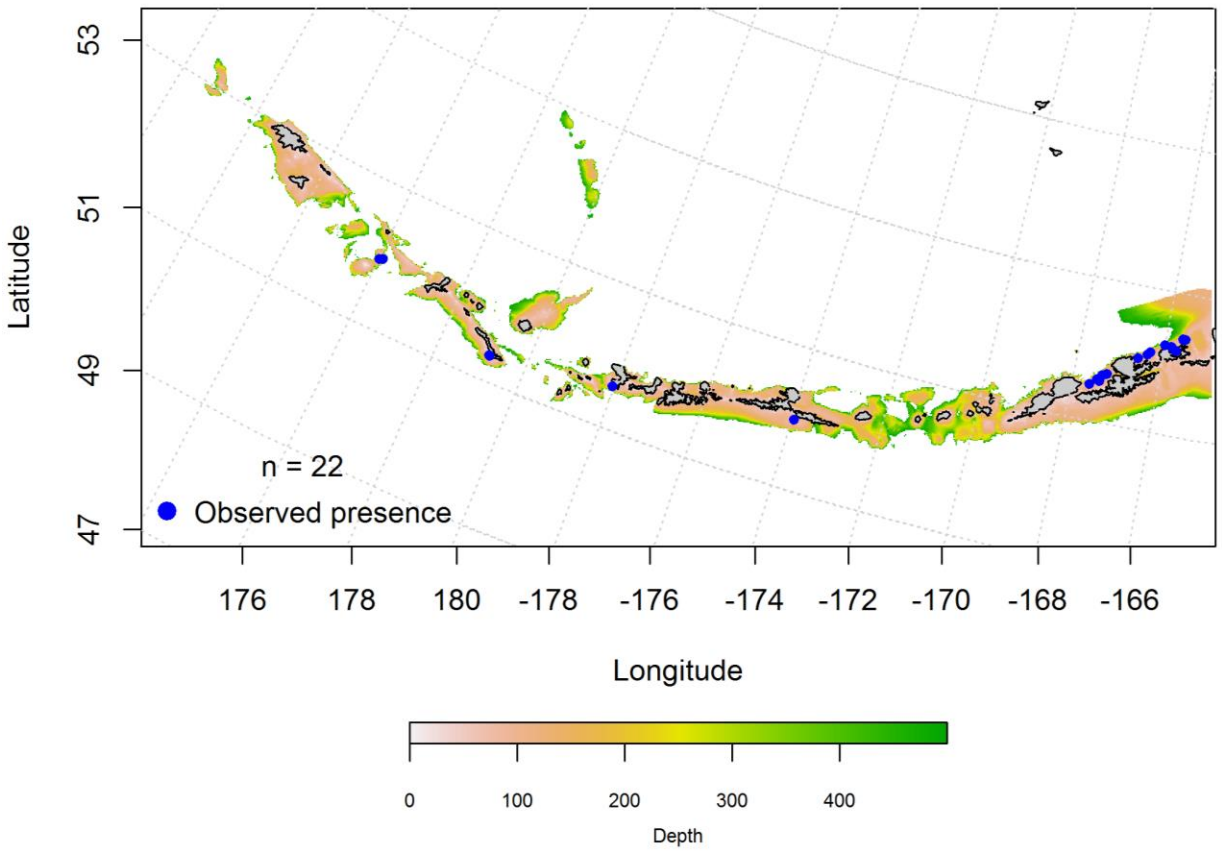

Figure 185. Blue points indicate instances where juvenile Dusky rockfish were observed during summertime trawl survey catches.

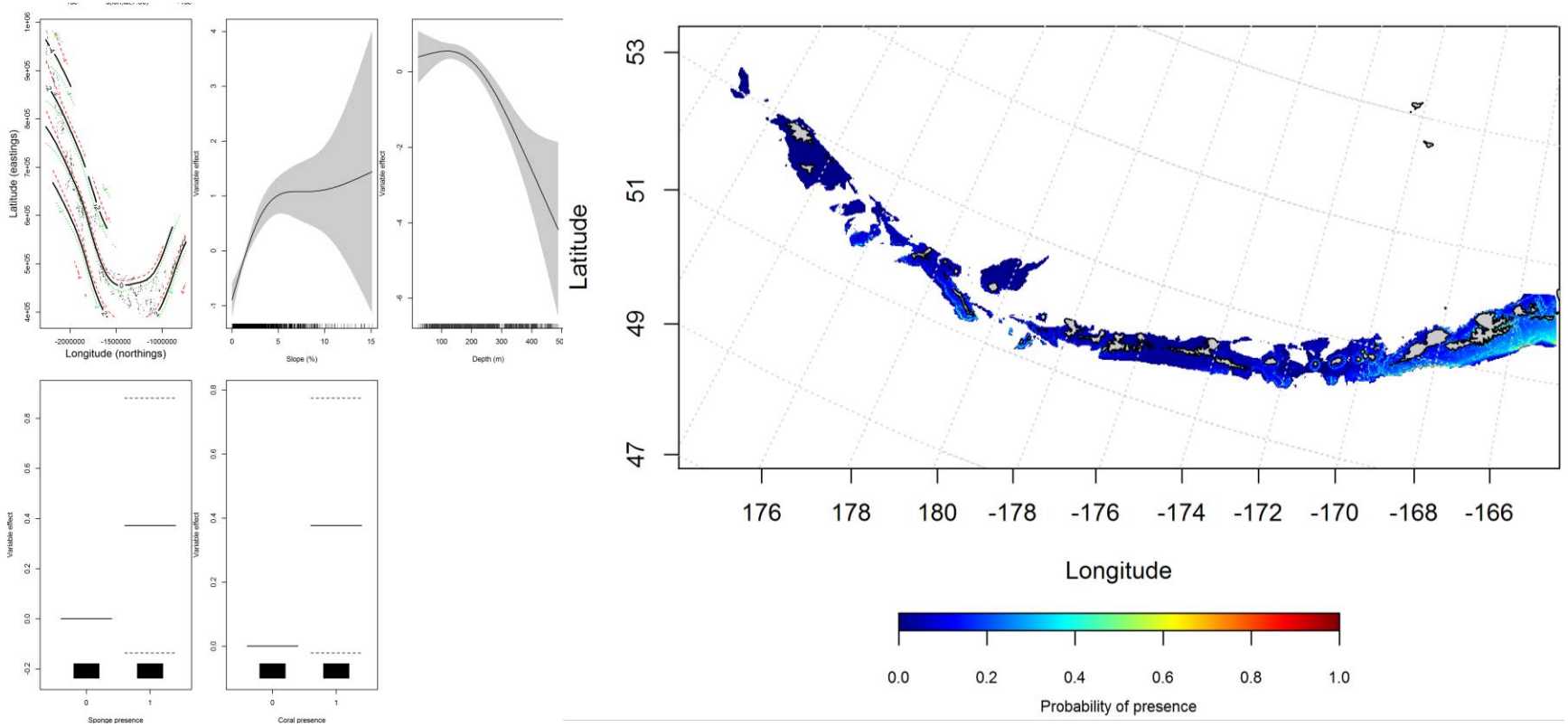

Figure 186. Best-fitting hurdle model effects of retained habitat variables on presence absence (PA) of adult Dusky rockfish from summer bottom trawl surveys of the Aleutian Islands (left panel) alongside hurdle-predicted adult Dusky rockfish PA (right panel).

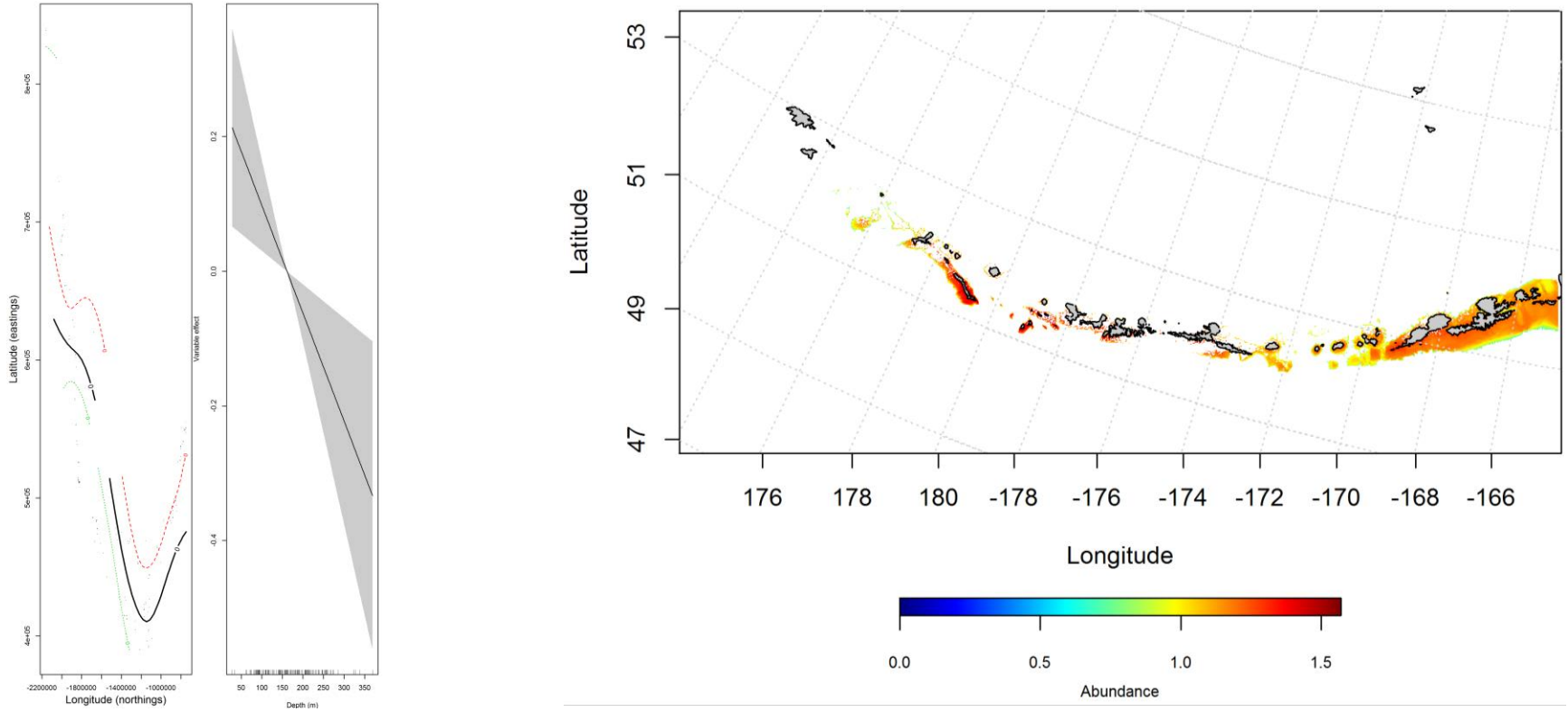

Figure 187. Best-fitting hurdle model effects of retained habitat variables on CPUE of adult Dusky rockfish from summer bottom trawl surveys of the Aleutian Islands (left panel) alongside hurdle-predicted adult Dusky rockfish CPUE (right panel).

Seasonal distribution of commercial fisheries catches of adult Dusky rockfish in the Aleutian Islands-- Distribution of adult Dusky rockfish in the Aleutian Islands in commercial fisheries catches was generally consistent throughout all seasons. In the fall, bottom depth, current speed, and tidal current were the most important variables determining probable suitable habitat of Dusky rockfish (relative importance: 51.9%, 13.3%, and 12.6%, respectively). The AUC of the fall maxent model was 94% for the training data and 84% for the test data. The model correctly classified 86% of the training data and 84% of the test data. The model predicted probable suitable habitat of Dusky rockfish across the AI, and highest north of Semisopochnoi Island, and in the eastern AI near Unalaska Island (Figure 188).

In the winter, bottom depth, bottom temperature, and surface color were the most important variables determining probable suitable habitat of Dusky rockfish (relative importance: 51.1%, 16.3%, and 11.6%, respectively). The AUC of the winter maxent model was 94% for the training data and 87% for the test data. 86% of the training data set and 87% of the test data set was correctly classified. The winter model predicted probable suitable habitat of Dusky rockfish across the AI (Figure 189).

In the spring, bottom depth, and surface ocean color were the most important variables determining probable suitable habitat of Dusky rockfish (relative importance: 66.8% and 11.6%). The AUC of the spring model was 93% for the training data and 83% for the test data. The spring model predicted probable suitable habitat of Dusky rockfish across the AI, and was highest near Agattu, Attu, Adak, and Atka Islands (Figure 190).

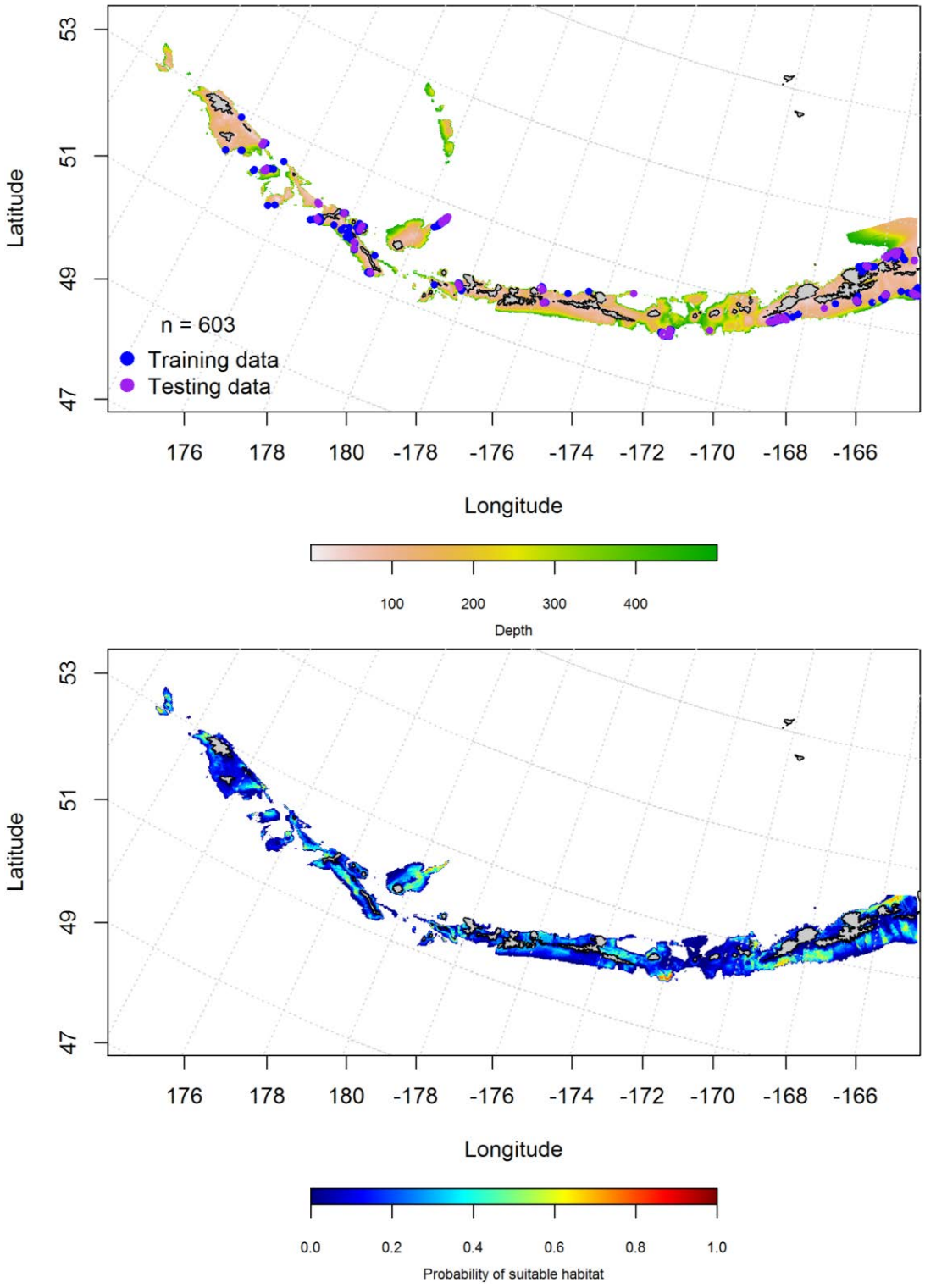

Figure 188. Locations of fall (September-November) commercial fisheries catches of Dusky rockfish (top panel). Blue points were used to train the maximum entropy model predicting the probability of suitable fall habitat supporting commercial catches of Dusky rockfish (bottom panel) and the purple points were used to validate the model.

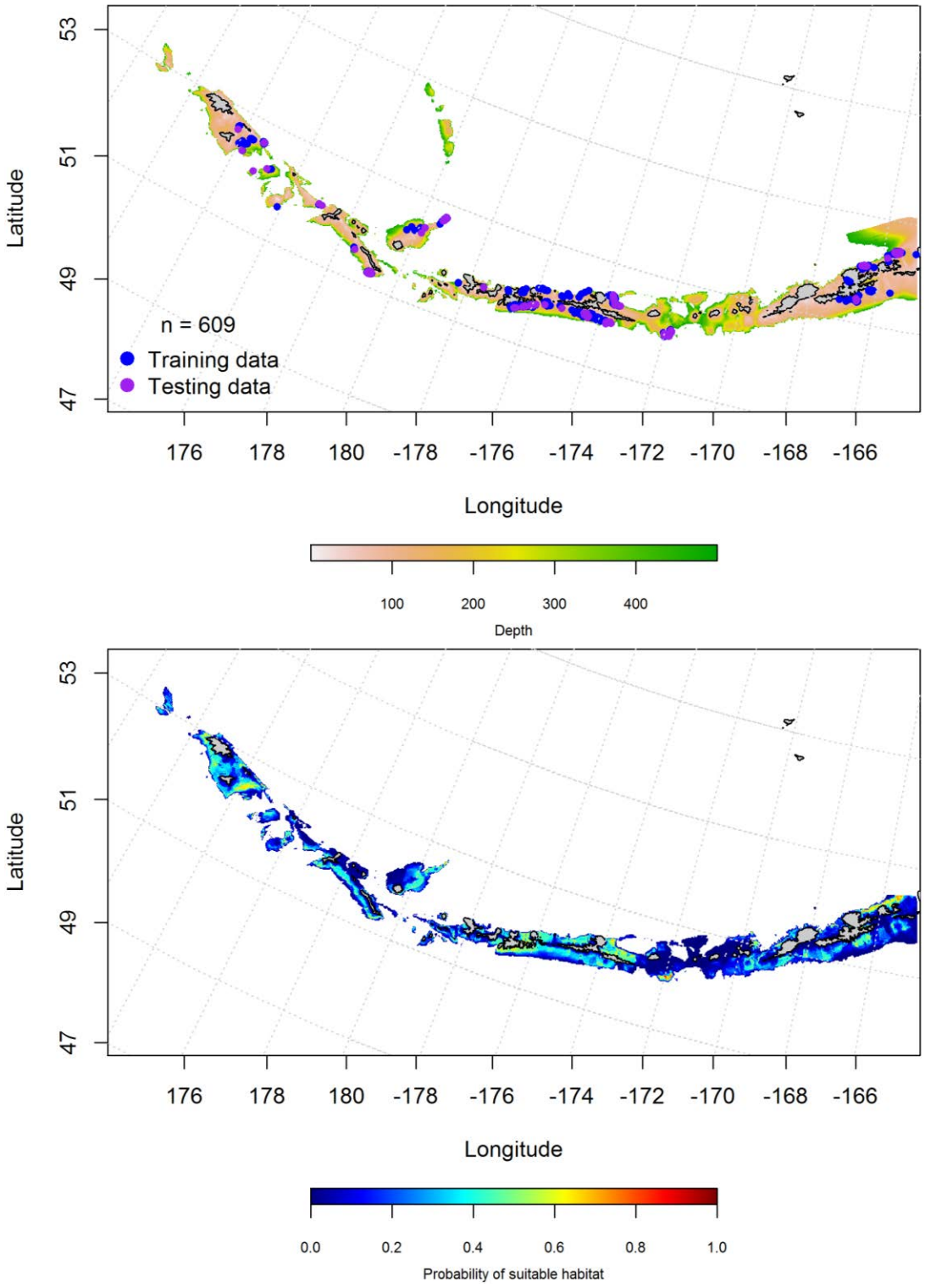

Figure 189. Locations of winter (December-February) commercial fisheries catches of Dusky rockfish (top panel). Blue points were used to train the maximum entropy model predicting the probability of suitable winter habitat supporting commercial catches of Dusky rockfish (bottom panel) and the purple points were used to validate the model.

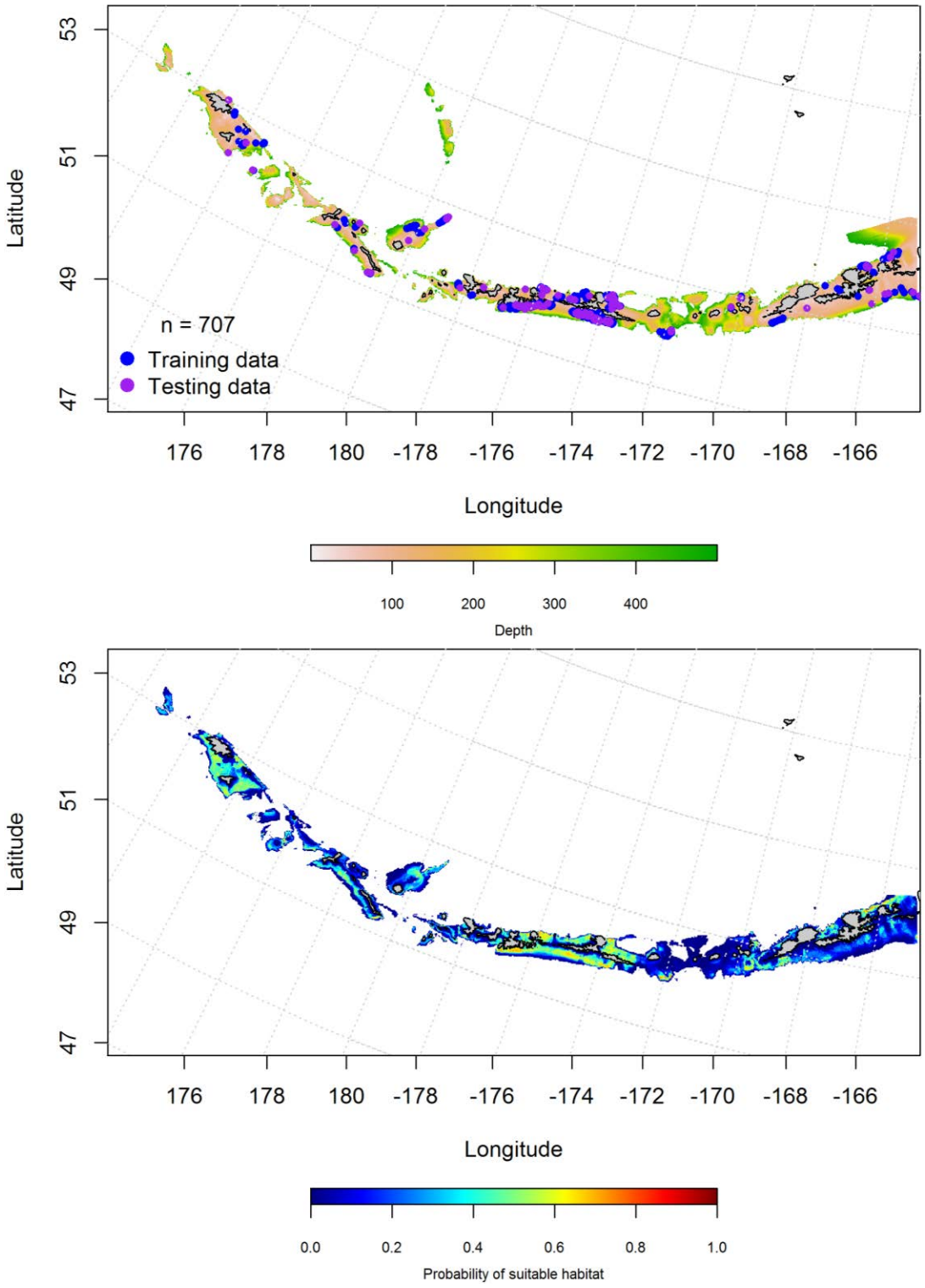

Figure 190. Locations of spring (March-May) commercial fisheries catches of Dusky rockfish (top panel). Blue points were used to train the maximum entropy model predicting the probability of suitable spring habitat supporting commercial catches of Dusky rockfish (bottom panel) and the purple points were used to validate the model.

Aleutian Islands Dusky rockfish Essential Fish Habitat Maps and Conclusions --.

Summertime EFH of Dusky rockfish juveniles and adults was distributed across AI, but had different patterns (Figure 191). Predicted juvenile EFH was less abundant than adults overall, but most abundant on the north side of Unalaska Island. Adult dusky rockfish predicted essential fish habitat was highest near Kiska Island and in the eastern AI around Nikolsi and Unalaska Islands.

The fall, winter and spring distribution of Dusky rockfish predicted EFH was essentially the same across the seasons (Figure 192). The highest percentage of suitable habitat in all seasons surrounded Adak and Atka Islands.

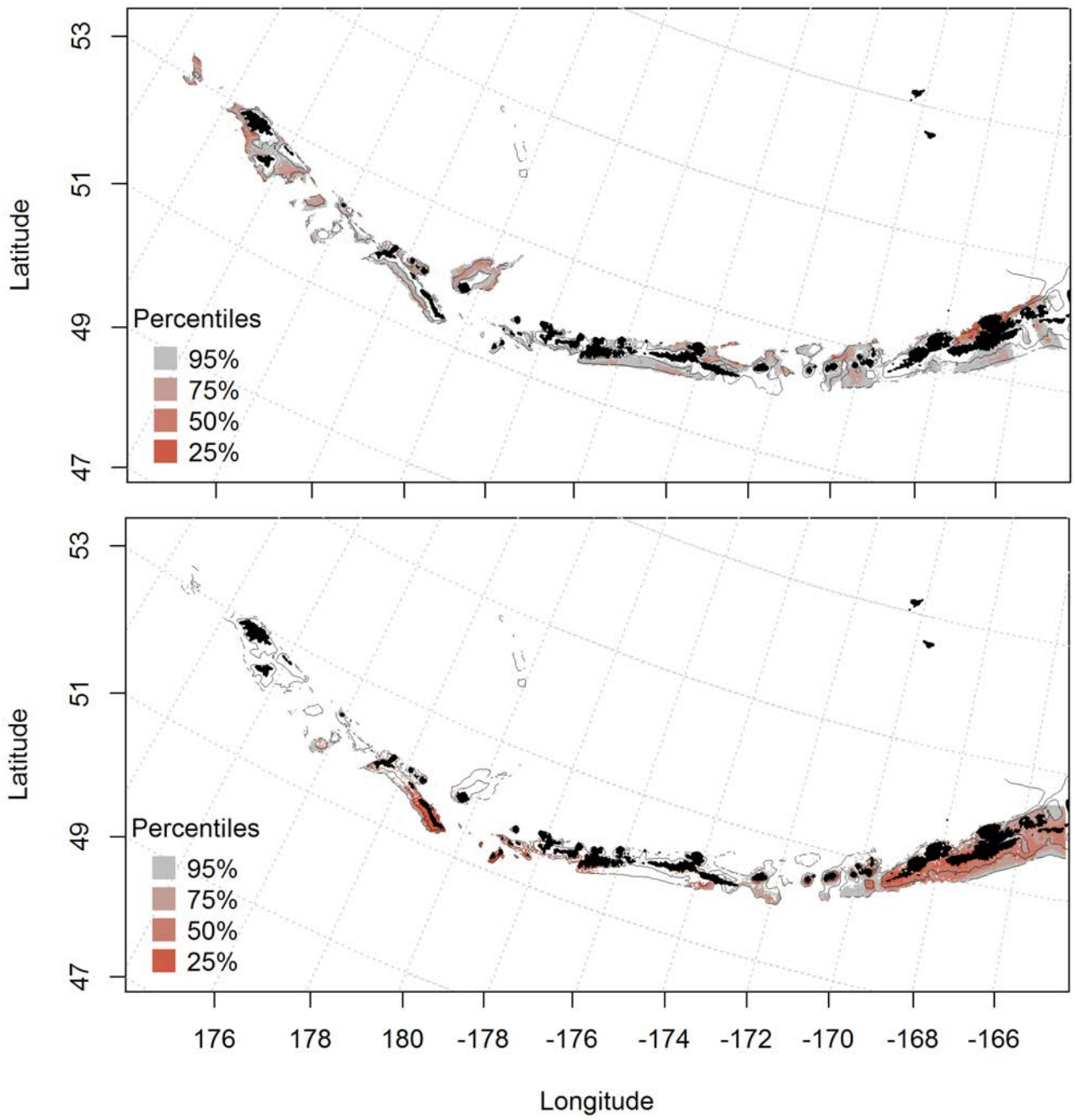

Figure 191. Predicted summer essential fish habitat for Dusky rockfish juveniles and adults (top and bottom panel) from summertime bottom trawl surveys.

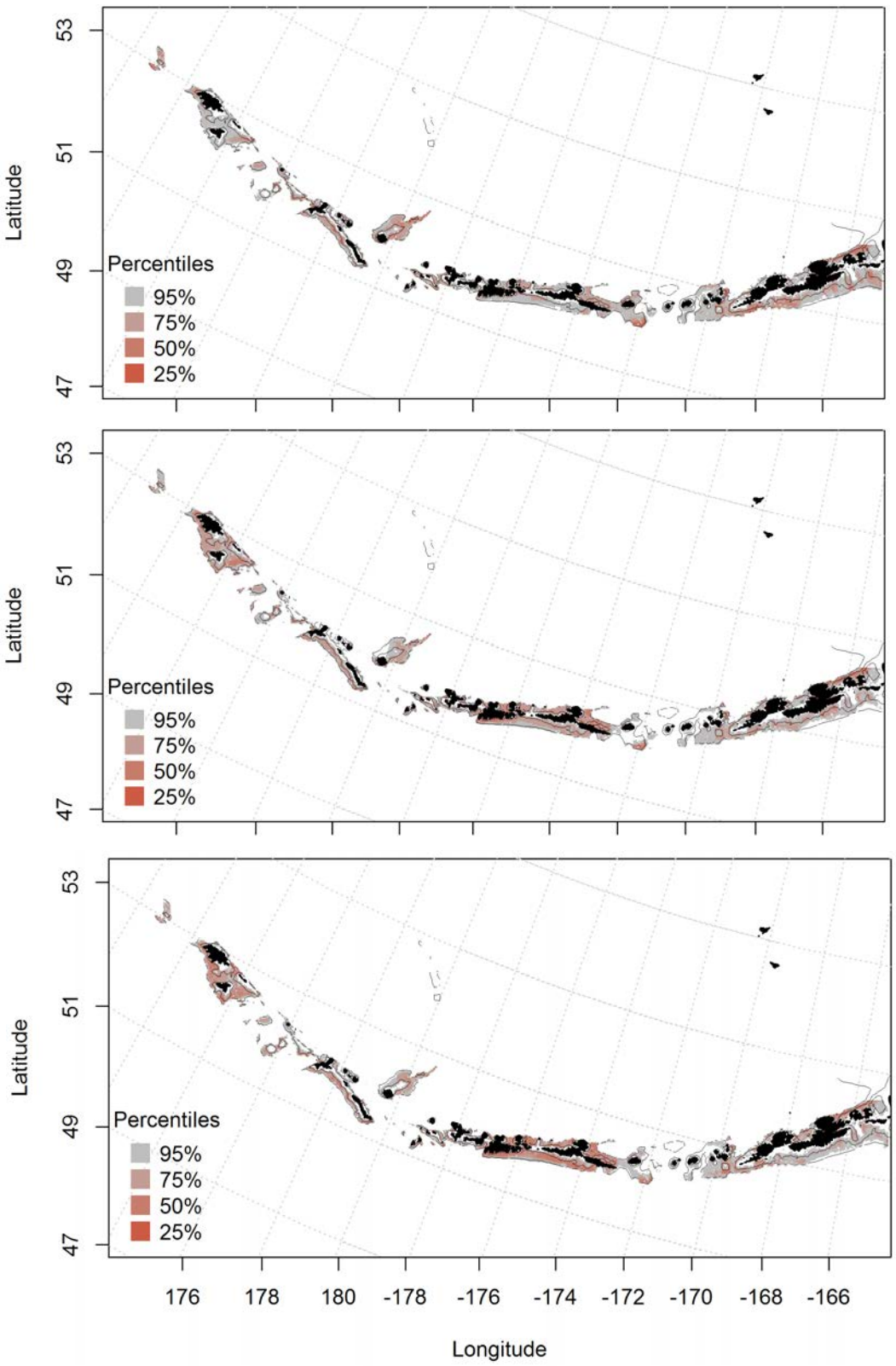

Figure 192. Essential fish habitat predicted for Dusky rockfish during fall (top panel), winter (middle panel) and spring (bottom panel) from summertime commercial catches.

Dark rockfish (*Sebastes ciliatus*)

Summertime distribution of juvenile and adult Dark rockfish from bottom trawl surveys of the Aleutian Islands – A maximum entropy model predicting the abundance of juvenile Dark rockfish explained 94% of the training data variability in CPUE in the bottom trawl survey, and 81% of the test data set variability. Bottom depth, bottom temperature, and tidal current were the most important variables explaining probable suitable habitat of juvenile Dark rockfish (48.1%, 25.9%, and 10.9%, respectively). The model correctly classified 84% of the training data and 81% of the test data. The model predicted probable suitable habitat of juvenile Dark rockfish across the AI (Figure 193).

There were only 10 instances of adult Dark rockfish in the central and eastern AI from summertime bottom trawl surveys (Figure 194). There were not enough cases to model the data.

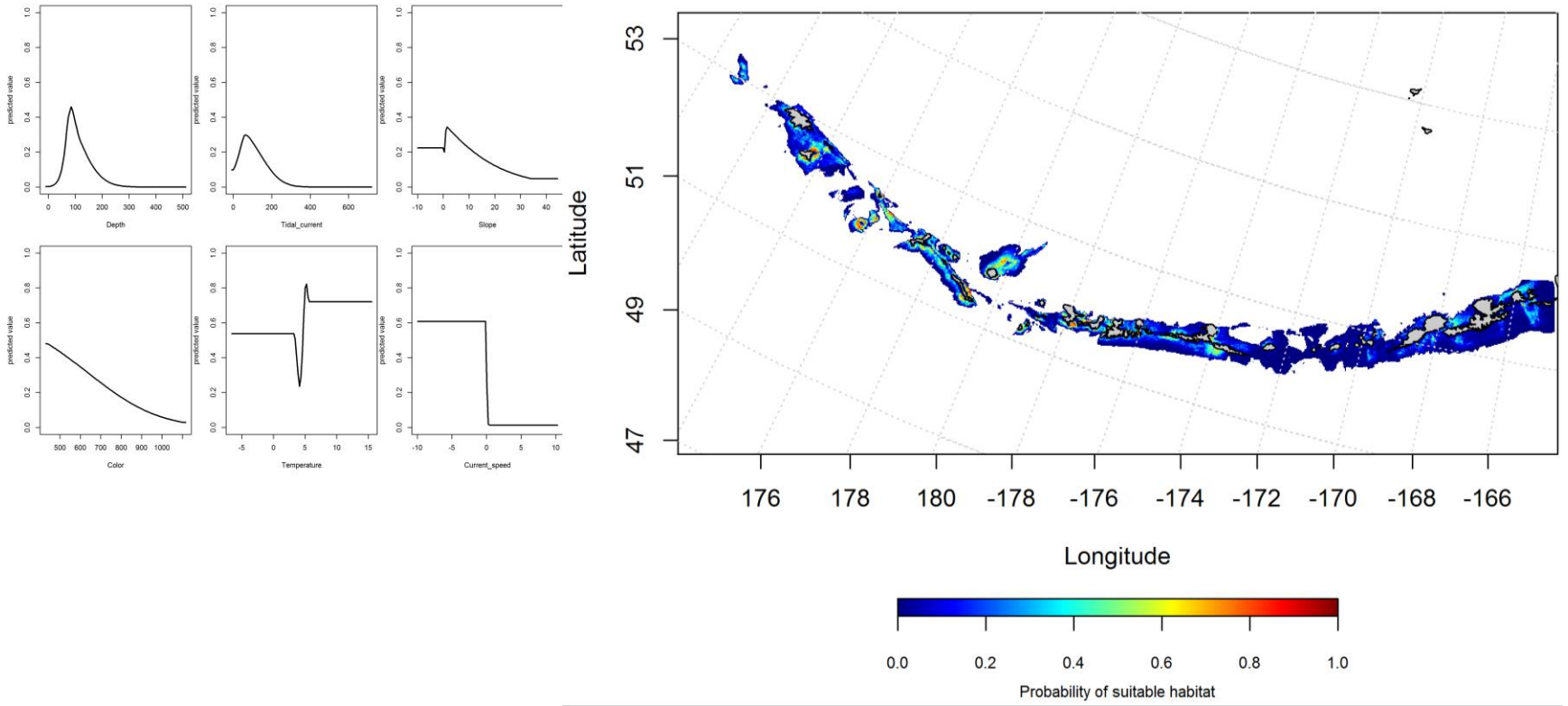

Figure 193. Best-fitting maximum entropy model effects of retained habitat variables on probable suitable habitat of juvenile Dark rockfish from summer bottom trawl surveys of the Aleutian Islands (left panel) alongside maxent-predicted juvenile Dark rockfish suitable habitat (right panel).

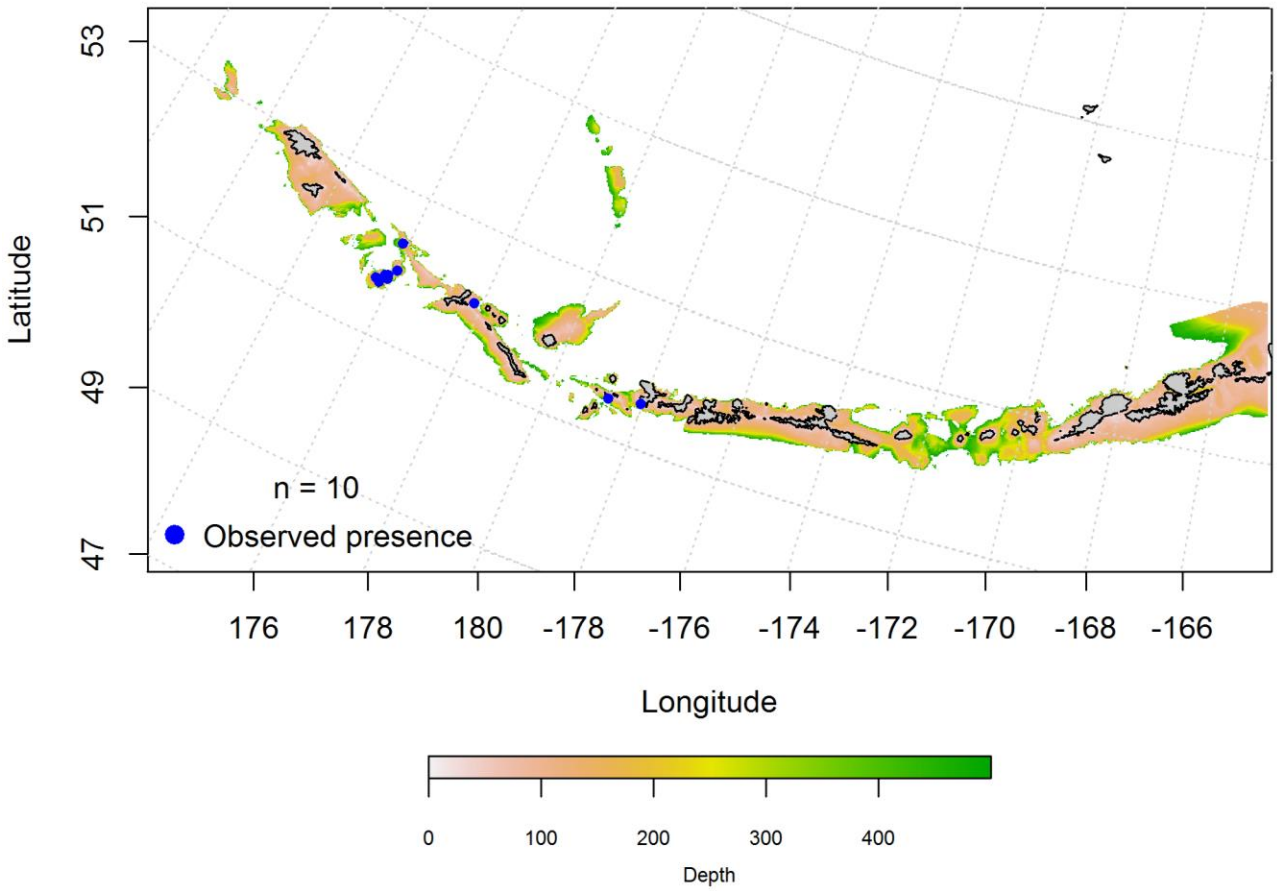

Figure 194. Blue points indicate instances where juvenile Dark rockfish were observed during summertime trawl survey catches.

Seasonal distribution of commercial fisheries catches of adult Dark rockfish in the Aleutian Islands – There were only 133 instances of adult Dark rockfish, 44 in the fall, 48 in the winter, and 41 in the spring (Figure 195). There was not enough data to run the models for any season.

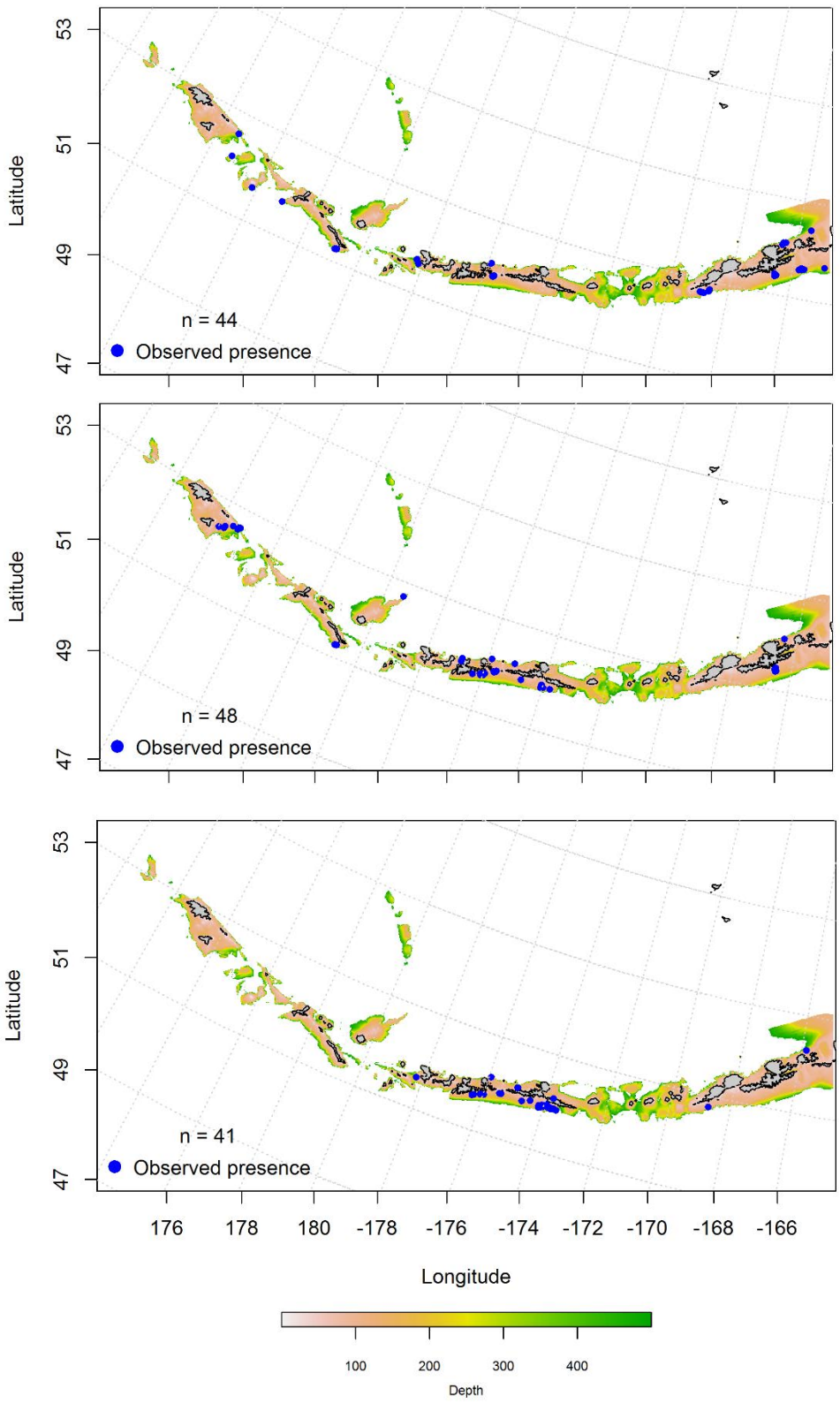

Figure 195. Blue points indicate locations where adult Dark rockfish were observed during fall (September-November), winter (December-February), and spring (March-May) commercial fisheries catches (top, middle, and bottom panel, respectively).

Aleutian Islands Dark rockfish Essential Fish Habitat Maps and Conclusions --

Summertime EFH of juvenile Dark rockfish was predicted across the AI, avoiding areas of large passes (Figure 196).

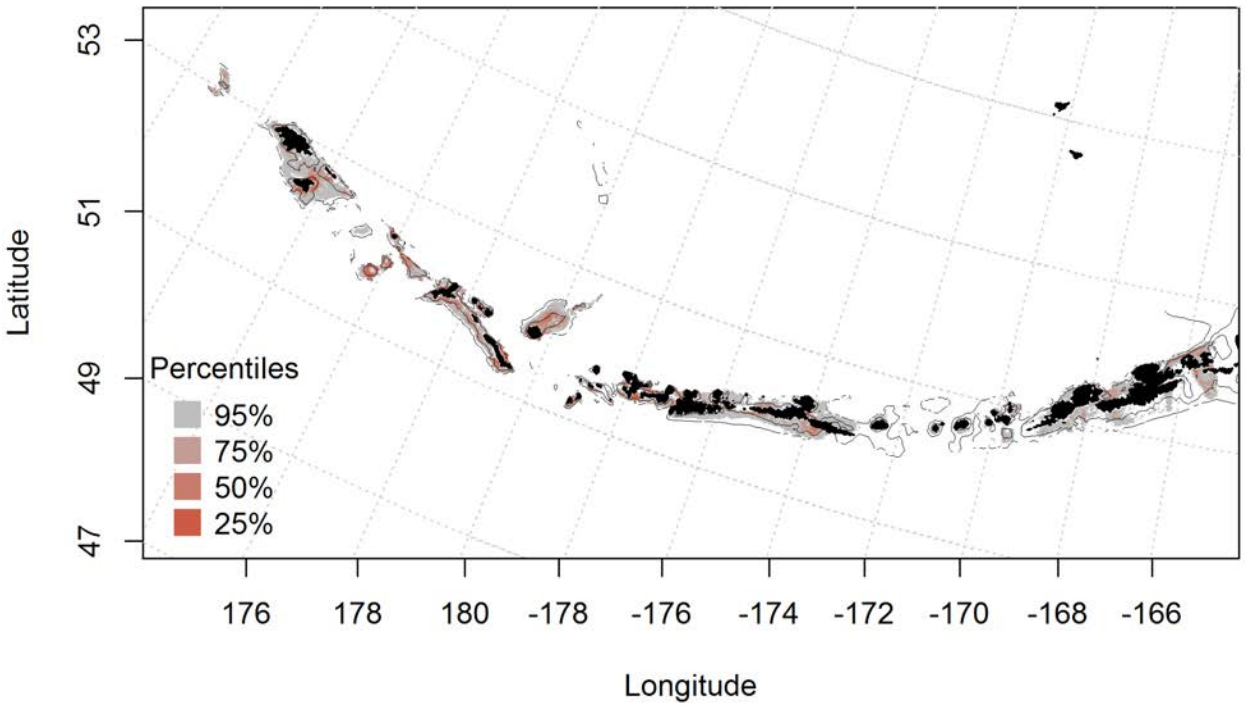

Figure 196. Predicted summer essential fish habitat for Dark rockfish juveniles from summertime bottom trawl surveys.

Harlequin rockfish (*Sebastes variegatus*)

Species text here

Summertime distribution of juvenile and adult Harlequin rockfish from bottom trawl surveys of the Aleutian Islands -- There were only 5 instances of juvenile Harlequin rockfish in the central and western AI (Figure 197), not enough data to run a model.

A maximum entropy model predicting the probability of suitable habitat of adult Harlequin rockfish explained 92% of the variability in CPUE in the bottom trawl survey training data and 82% of the variability in the test data set. Bottom depth and slope were the most

important variables explaining probable suitable habitat of adult Harlequin rockfish (relative importance: 56.7% and 26.4%). The model explained 85% of the training data and 82% of the test data. The model predicted probable suitable habitat of adult Harlequin rockfish across the AI (Figure 197).

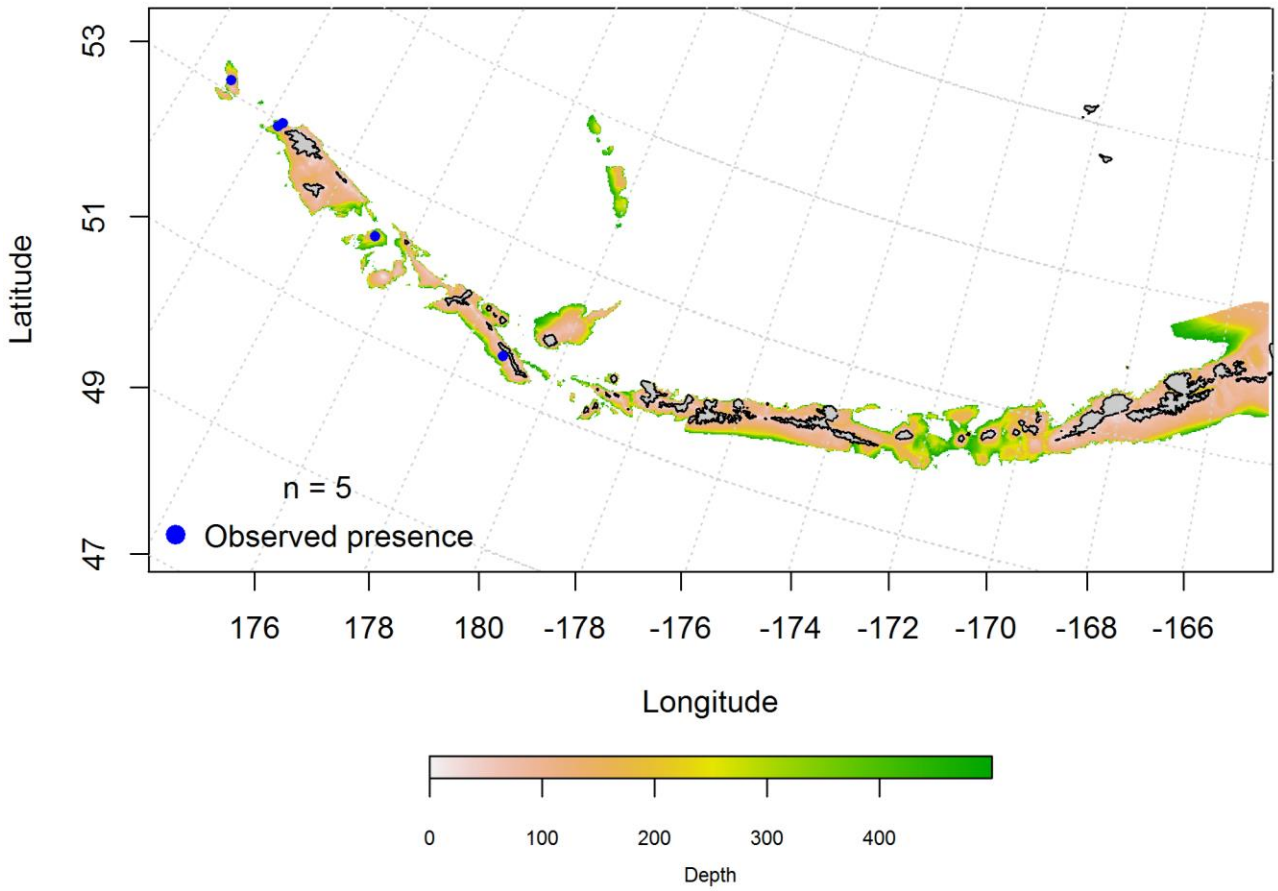

Figure 197. Blue points indicate instances where juvenile Harlequin rockfish were observed during summertime trawl survey catches.

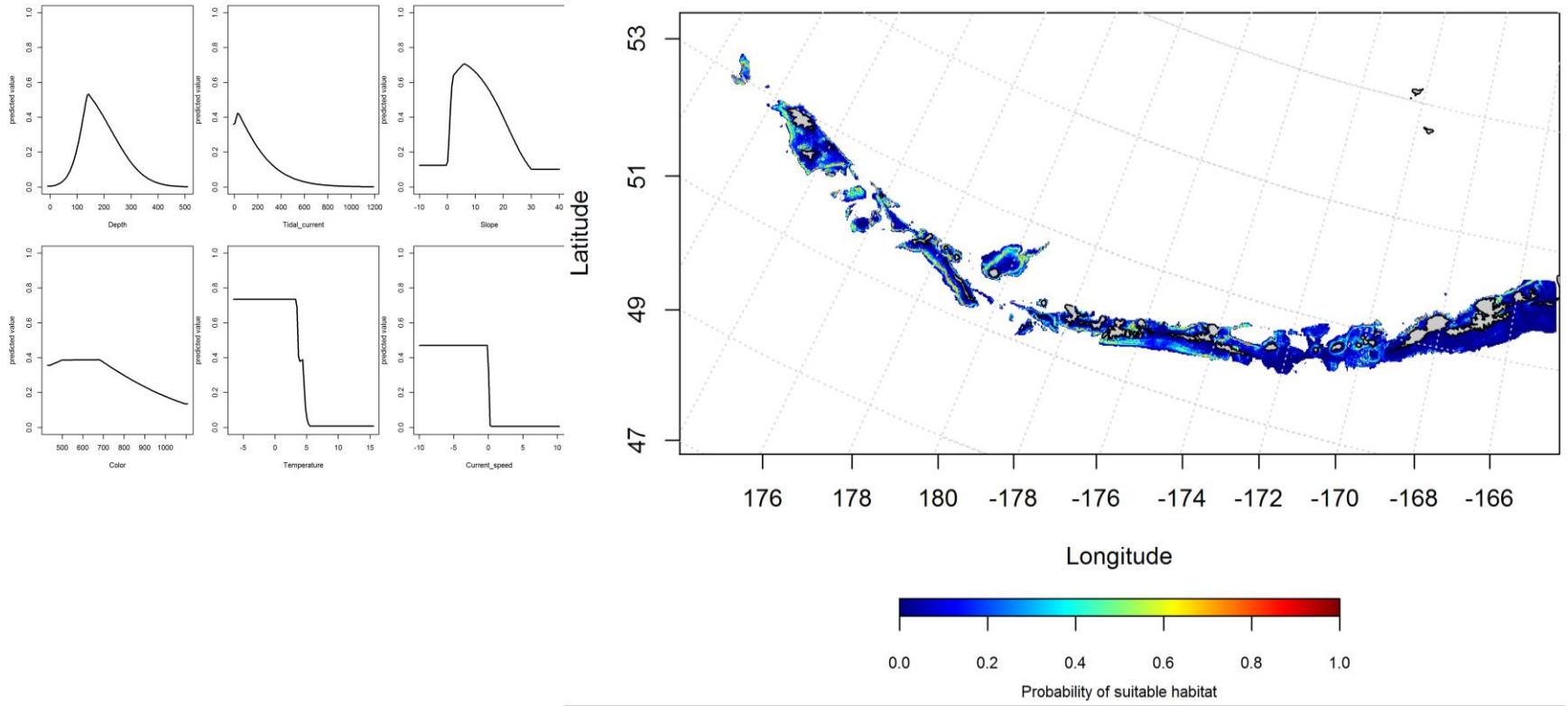

Figure 198. Best-fitting maximum entropy model effects of retained habitat variables on suitable habitat of adult Harlequin rockfish from summer bottom trawl surveys of the Aleutian Islands (left panel) alongside maxent-predicted adult Harlequin rockfish probable suitable habitat (right panel).

Seasonal distribution of commercial fisheries catches of adult Harlequin rockfish in the Aleutian Islands-- Distribution of adult Harlequin rockfish in the Aleutian Islands in commercial fisheries catches was generally consistent throughout all seasons. In the fall, bottom depth, ocean color and current speed were the most important variables determining proability of suitable habitat of Harlequin rockfish (relative importance: 32.1%, 24.2%, and 23.4%, respectively). The AUC of the fall maxent model was 97% for the training data and 92% for the test data. The model correctly classified 90% of the training data and 92% of the test data, a good fit. The model predicted probable suitable habitat of adult Harlequin rockfish across the AI and slightly higher north of Semisopochnoi Island (Figure 199).

In the winter, bottom depth, current speed, and bottom temperature were the most important variables determining probability of suitable habitat of Harlequin rockfish (relative importance: 28.7%, 20.5%, and 19.7%, respectively). The AUC of the winter maxent model was 97% for the training data and 94% for the test data. The model correctly classified 94% of the training and test data sets. As with the fall, the model predicted probable suitable habitat of adult Harlequin rockfish across the AI and slightly higher north of Semisopochnoi Island (Figure 200).

In the spring, bottom depth, current speed, and surface color were also the most important variables determining the probability of suitable habitat of Harlequin rockfish (relative importance: 49.4%, 17.8%, and 14.5%, respectively). The AUC of the spring maxent model was 94% for the training data and 93% for the test data. The model correctly classified 88% of the training data and 93% of the test data. The model predicted probable suitable habitat of Harlequin rockfish in the spring across the AI and higher north of Semisopochnoi Island, Adak, Atka, and Agattu Islands (Figure 201).

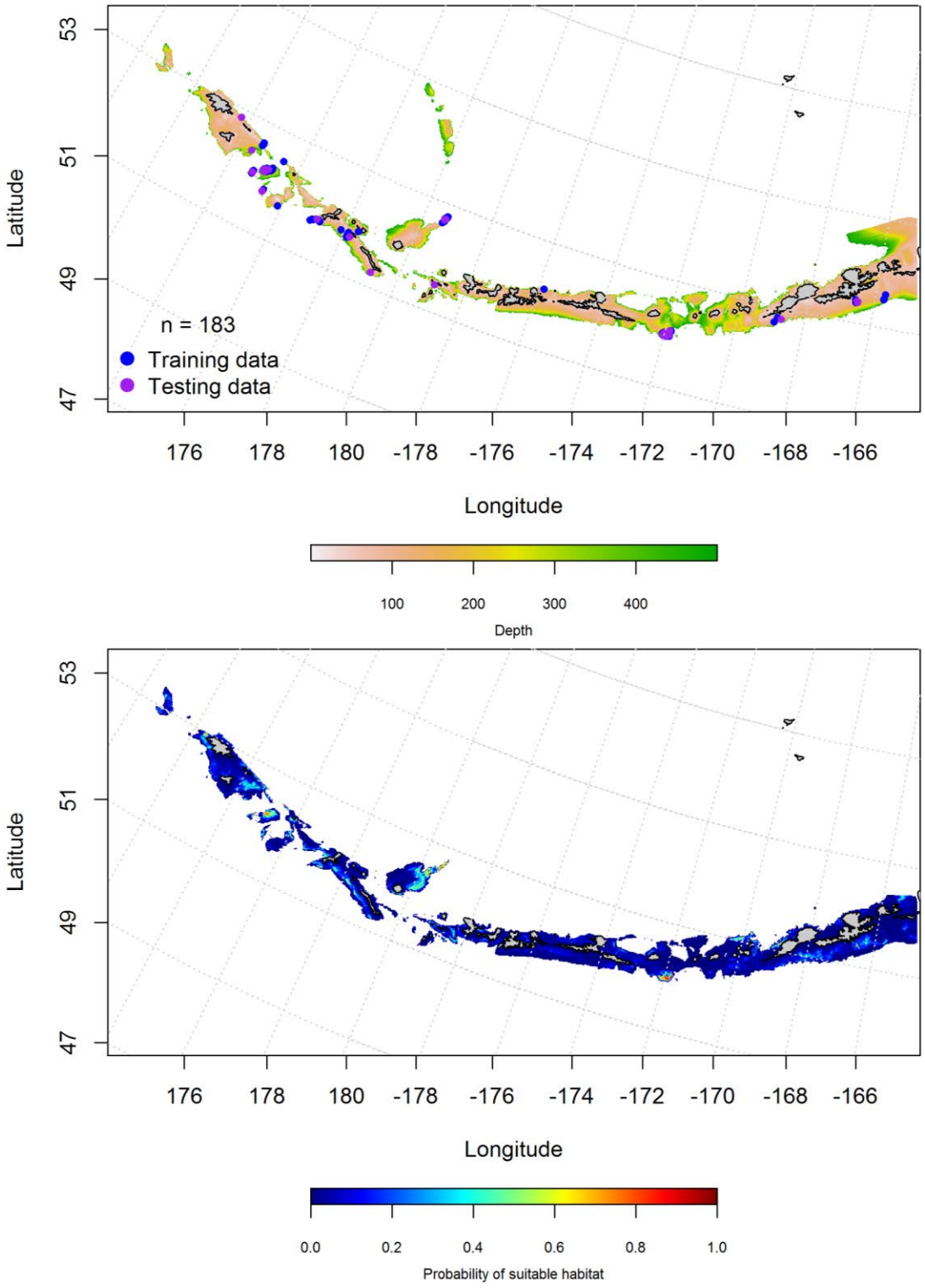

Figure 199. Locations of fall (September-November) commercial fisheries catches of adult Harlequin rockfish (top panel). Blue points were used to train the maximum entropy model predicting the probability of suitable fall habitat supporting commercial catches of adult Harlequin rockfish (bottom panel) and the purple points were used to validate the model.

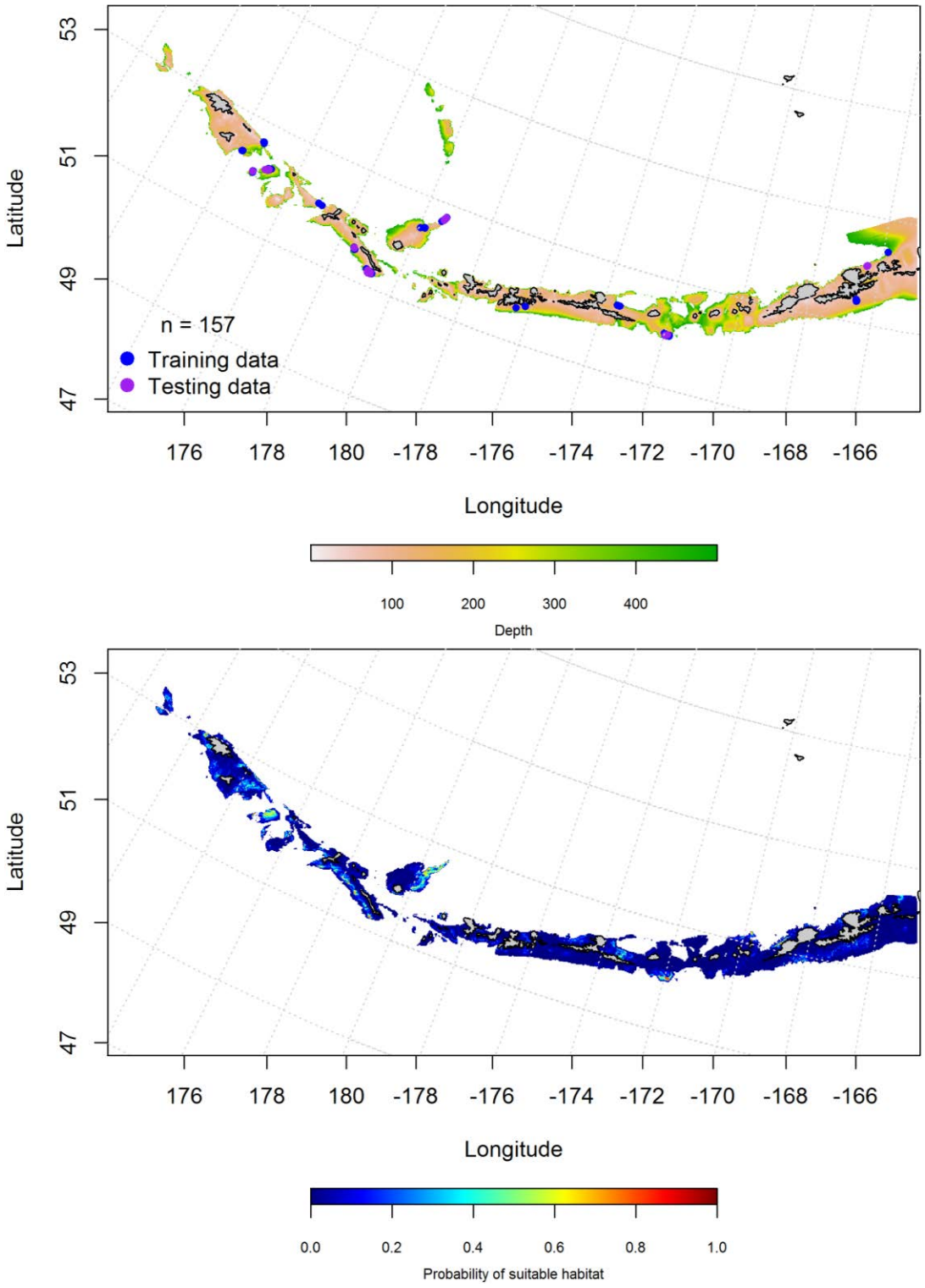

Figure 200. Locations of winter (December-February) commercial fisheries catches of adult Harlequin rockfish (top panel). Blue points were used to train the maximum entropy model predicting the probability of suitable winter habitat supporting commercial catches of adult Harlequin rockfish (bottom panel) and the purple points were used to validate the model.

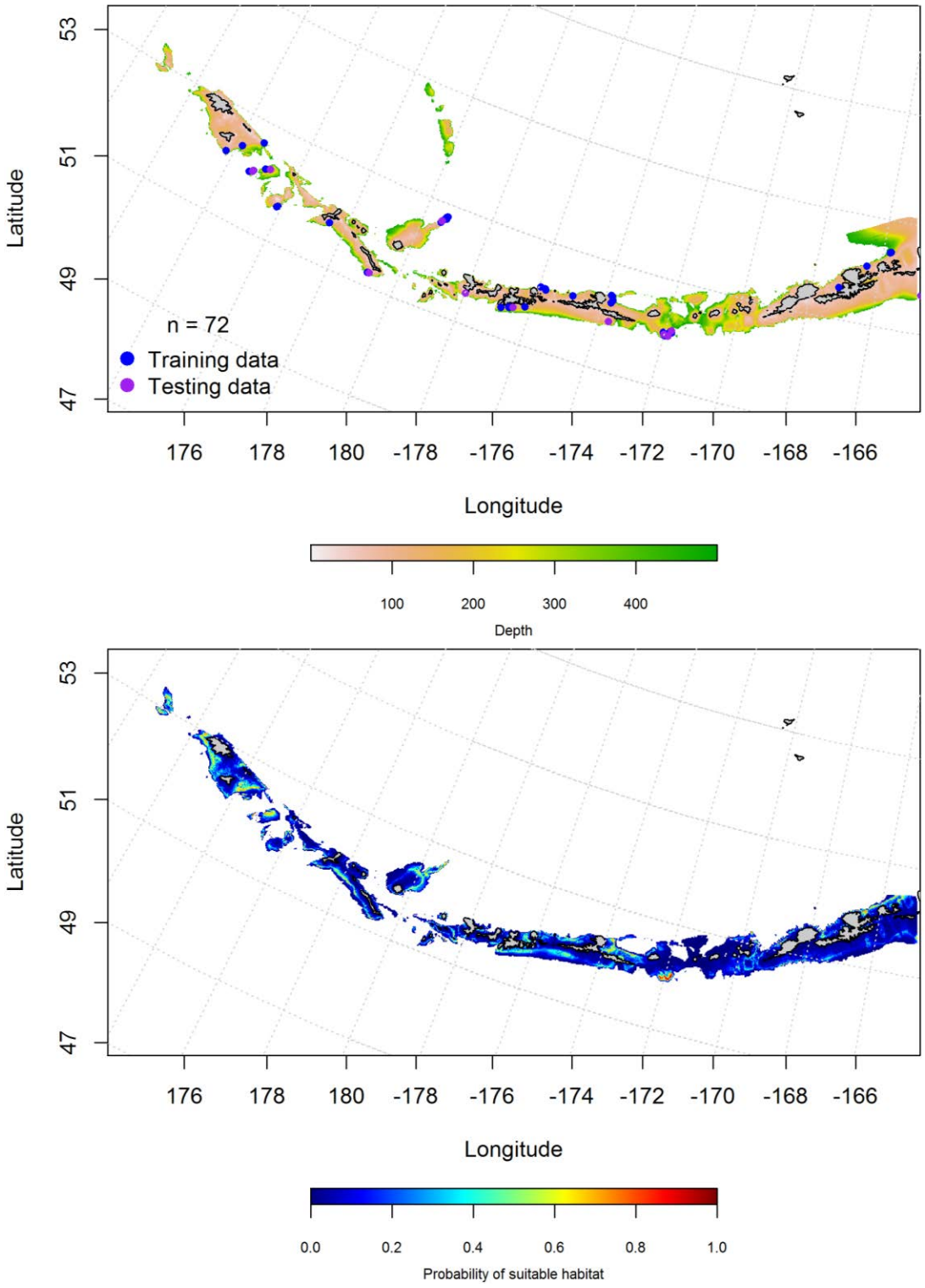

Figure 201. Locations of spring (March-May) commercial fisheries catches of adult Harlequin rockfish (top panel). Blue points were used to train the maximum entropy model predicting the probability of suitable spring habitat supporting commercial catches of adult Harlequin rockfish (bottom panel) and the purple points were used to validate the model.

Aleutian Islands Harlequin rockfish Essential Fish Habitat Maps and Conclusions --

Summertime EFH of adult Harlequin rockfish was predicted across the AI (Figure 202).

The fall, winter and spring predicted EFH of Harlequin rockfish was low, but lowest in area with large passes (Figure 203).

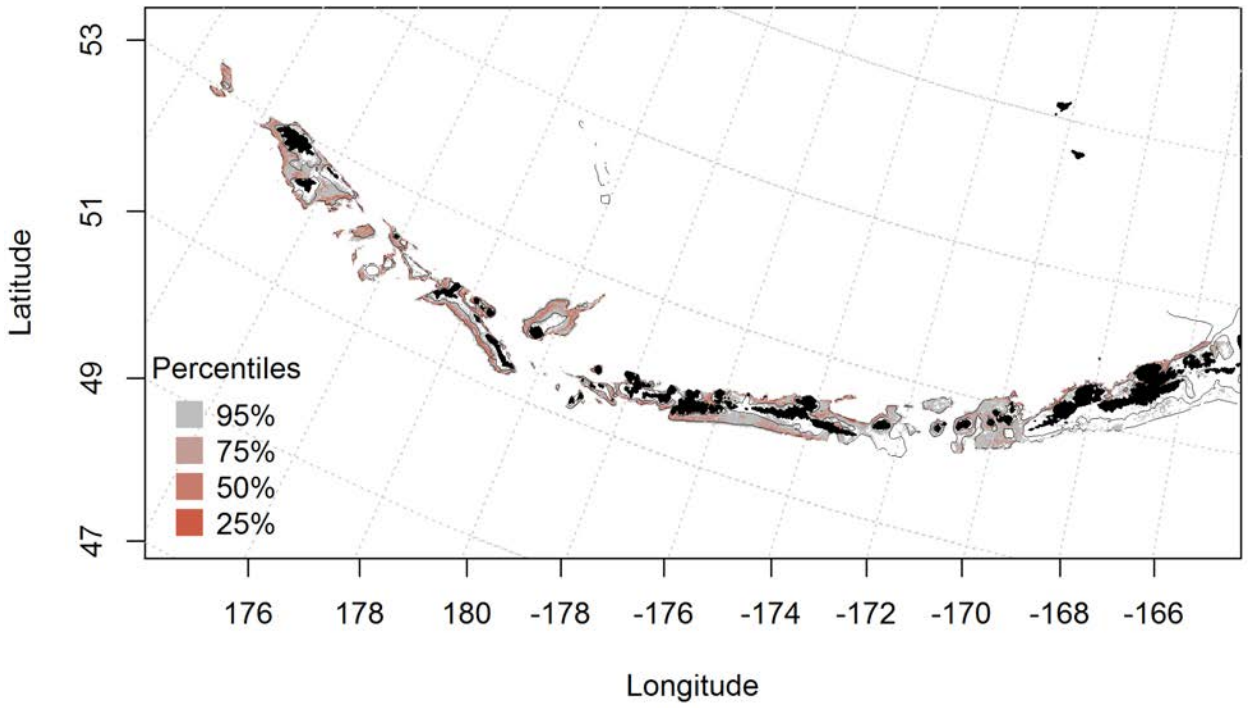

Figure 202. Predicted summer essential fish habitat for adult Harlequin rockfish from summertime bottom trawl surveys.

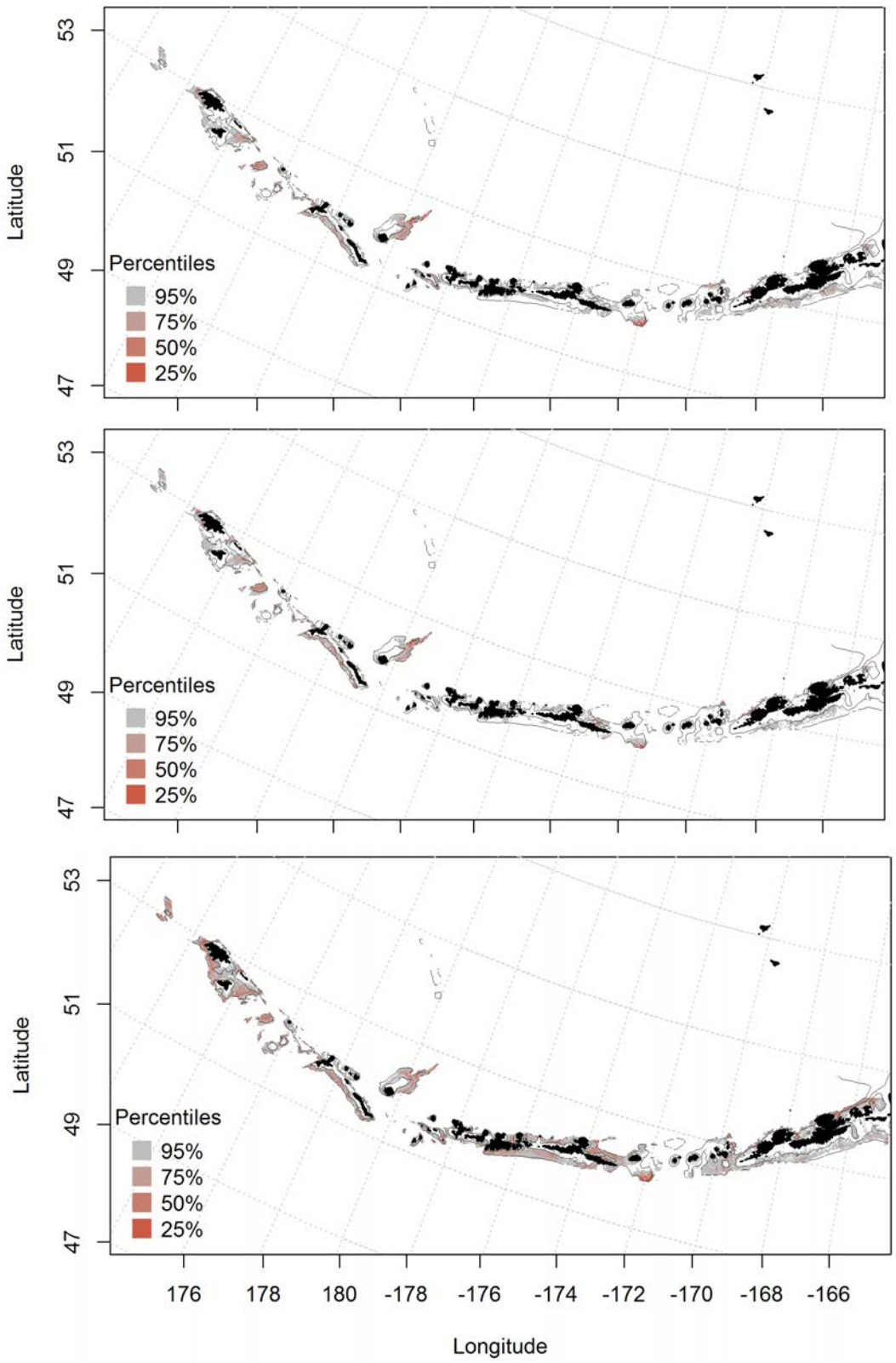

Figure 203. Essential fish habitat predicted for adult Harlequin rockfish during fall (top panel), winter (middle panel) and spring (bottom panel) from summertime commercial catches.

Shortspine thornyhead (*Sebastolobus alascanus*)

Species text here

Summertime distribution of juvenile and adult Shortspine thornyhead from bottom trawl surveys of the Aleutian Islands -- A hurdle-GAM model was used to predict the presence of absence of juvenile Shortspine thornyhead and explained 99% of the variability in CPUE in the bottom trawl survey training data and 98% of the test data set. Bottom depth, geographic location, and ocean color were the most important variables explaining the distribution of juvenile Shortspine thornyhead. The model correctly explained 71.4% of the deviance, classified 95% of the training and data sets. The areas of predicted suitable habitat were across the AI and highest in the central and western AI (Figure 204).

The second part of the hurdle model found bottom depth and bottom temperature influence the CPUE of juvenile Shortspine thornyhead the most, and explained 27.1% of the deviance, 27% of the training data and 18% of the test data. The model predicted probable suitable habitat across the AI (Figure 205).

A hurdle-GAM model was used to predict the presence of absence of adult Shortspine thornyhead and explained 96% of the variability in CPUE in the bottom trawl survey training data and 95% of the test data set. Bottom depth, geographic location, and ocean color were the most important variables explaining the distribution of adult Shortspine thornyhead. The model explained 61.2%% of the deviance, and correctly classified 90% of the training data and 86% of the test data sets. The model predicted probable suitable habitat across the AI (Figure 206).

The second part of the hurdle model found geographic location and bottom depth influence the CPUE of adult Shortspine thornyhead the most, and explained 47% of the

deviance, 47% of the training data and 43% of the test data. The model predicted probable suitable habitat across the AI (Figure 207).

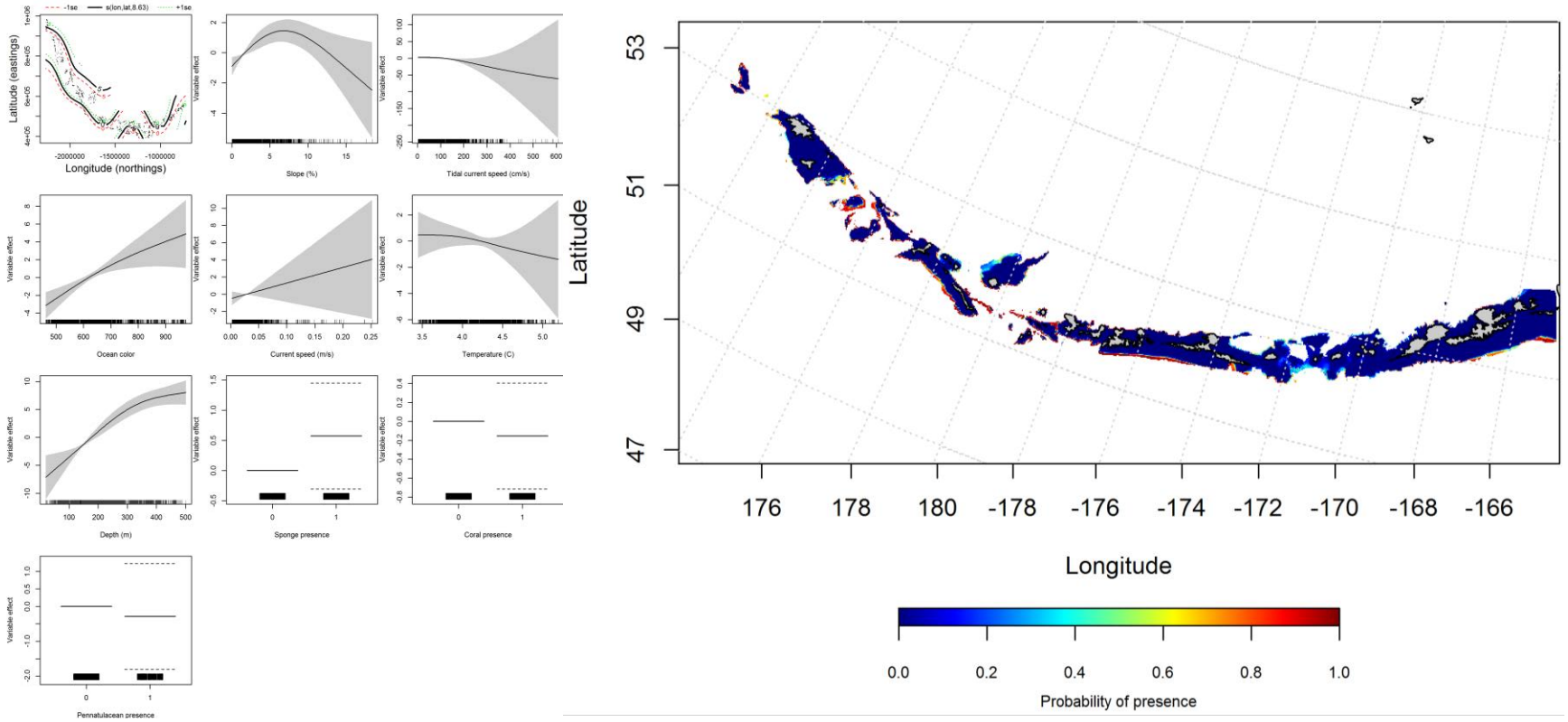

Figure 204. Best-fitting hurdle model effects of retained habitat variables on presence absence (PA) of juvenile Shortspine thornyhead from summer bottom trawl surveys of the Aleutian Islands (left panel) alongside hurdle-predicted juvenile Shortspine thornyhead PA (right panel).

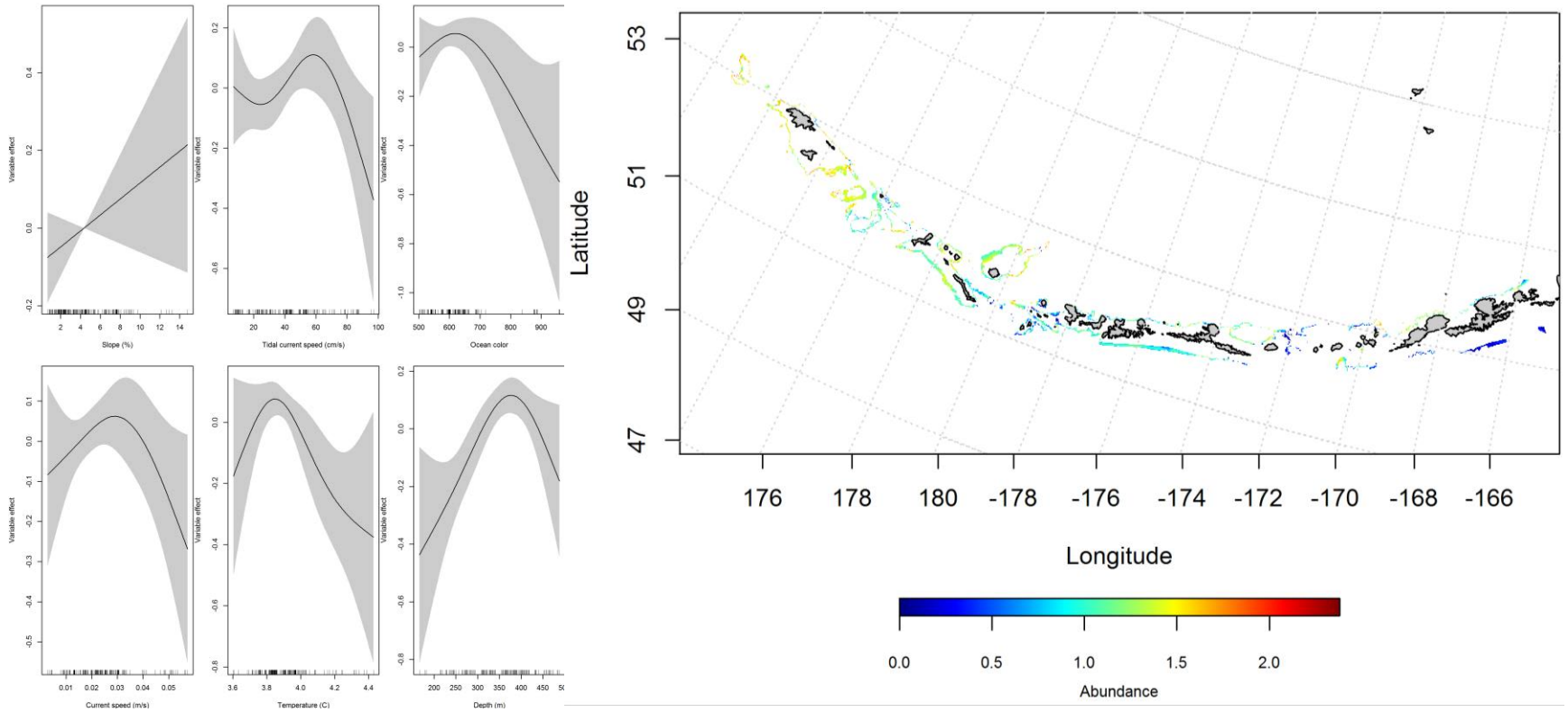

Figure 205. Best-fitting hurdle model effects of retained habitat variables on CPUE of juvenile Shortspine thornyhead from summer bottom trawl surveys of the Aleutian Islands (left panel) alongside hurdle-predicted juvenile Shortspine thornyhead CPUE (right panel).

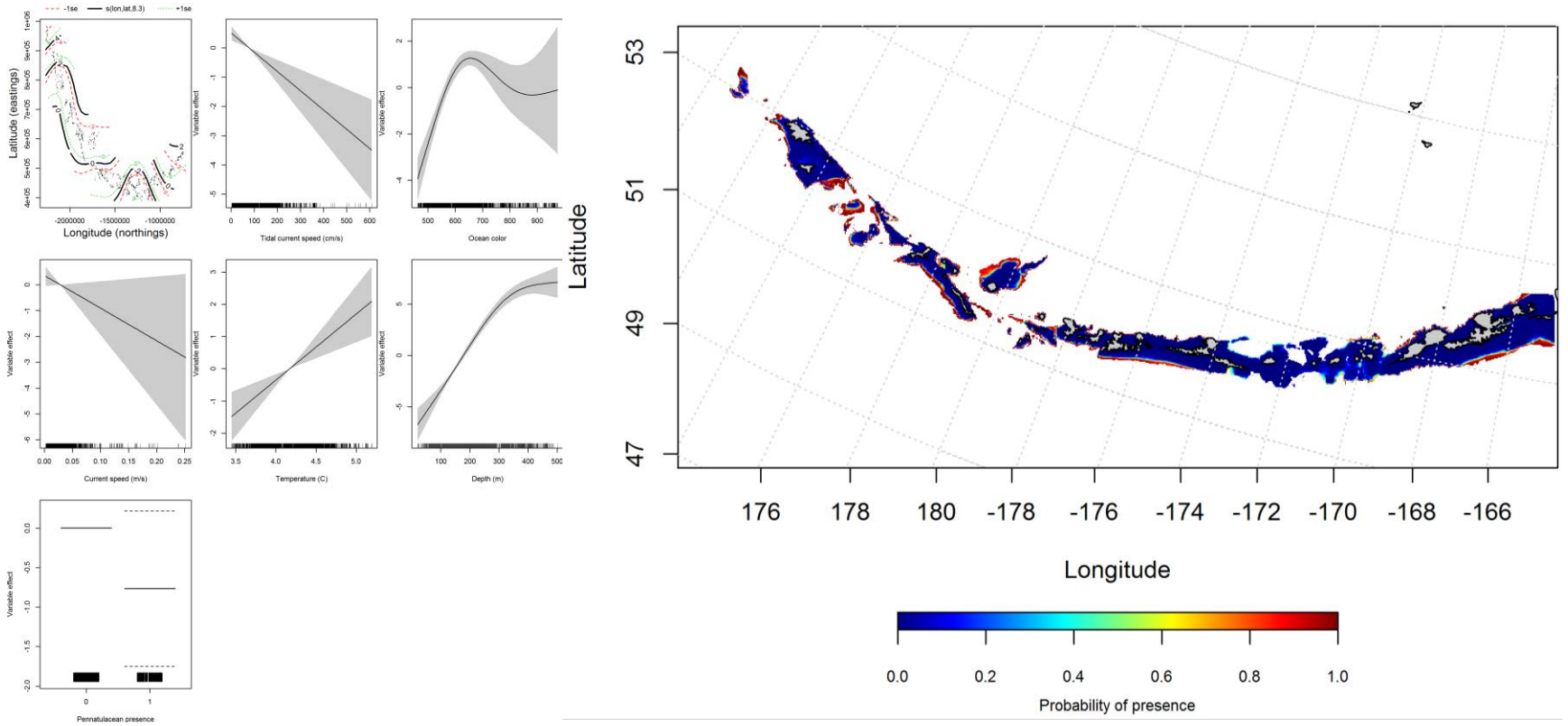

Figure 206. Best-fitting hurdle model effects of retained habitat variables on presence absence (PA) of adult Shortspine thornyhead from summer bottom trawl surveys of the Aleutian Islands (left panel) alongside hurdle-predicted adult Shortspine thornyhead PA (right panel).

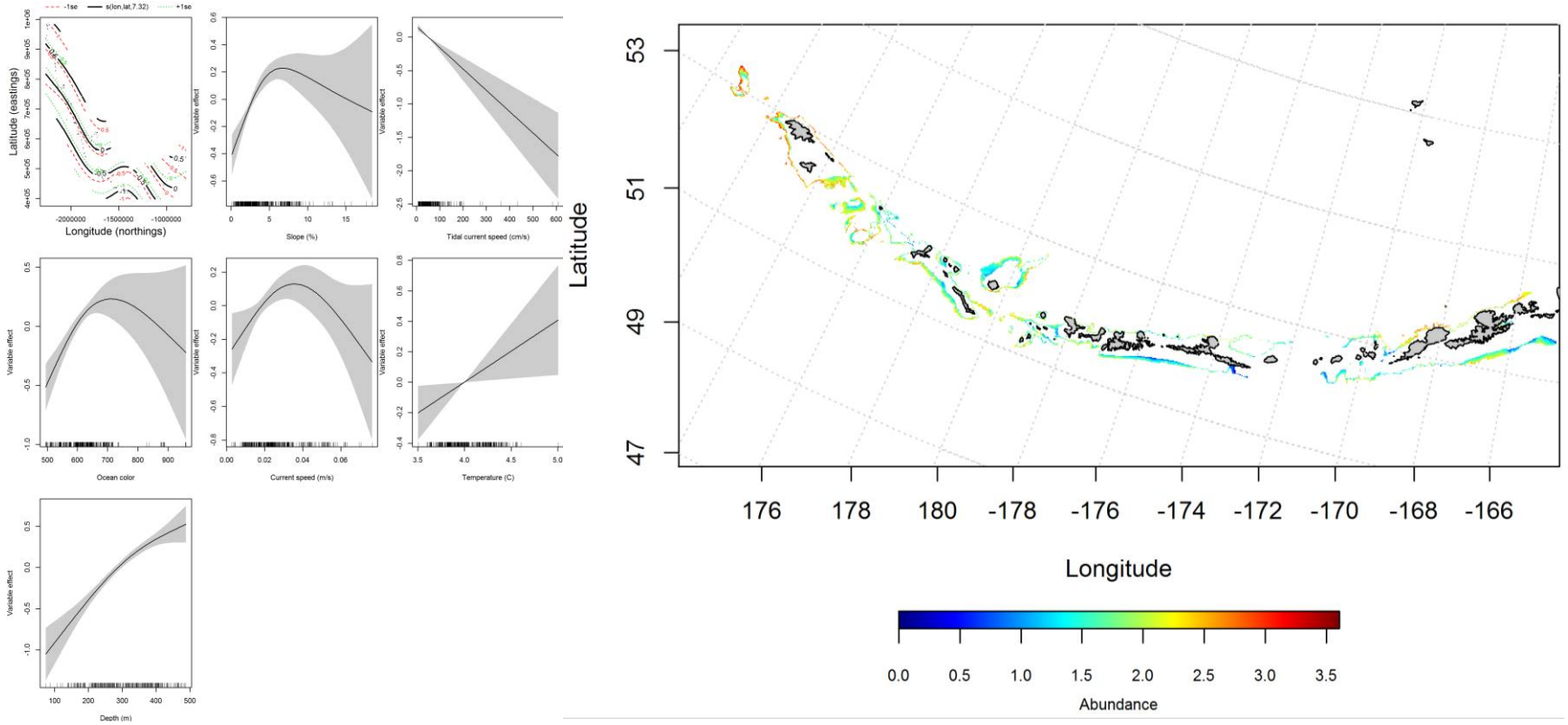

Figure 207. Best-fitting hurdle model effects of retained habitat variables on CPUE of adult Shortspine thornyhead from summer bottom trawl surveys of the Aleutian Islands (left panel) alongside hurdle-predicted adult Shortspine thornyhead CPUE (right panel).

Seasonal distribution of commercial fisheries catches of adult Shortspine thornyhead in the Aleutian Islands-- Distribution of adult Shortspine thornyhead in the Aleutian Islands in commercial fisheries catches was generally consistent throughout all seasons. In the fall, bottom depth, ocean surface color, and slope were the most important variables determining probable suitable habitat of Shortspine thornyhead (relative importance: 46.8%, 20.4%, and 17.2%, respectively). The AUC of the fall maxent model was 92% for the training data and 74% for the test data. 84% of the training data and 74% of the test data sets were predicted correctly. The model predicted probable suitable habitat of Shortspine thornyhead in the fall across the AI and highest in the ??pass and in the eastern AI near Unalaska Island (Figure 208).

There were only 38 instances of adult Shortspine thornyhead in the central and eastern AI in winter commercial catches (Figure 209), this was not enough data to run the model.

In the spring, bottom depth and surface ocean color were the most important variables determining probable suitable habitat of Shortspine thornyhead (relative importance: 56.4% and 26.6%). The AUC of the spring maxent model was 95% for the training data and 86% for the test data. The model correctly classified 88% of the training data and 86% of the test data. The model predicted probable suitable habitat of Shortspine thornyhead in the spring across the AI and highest in the ??pass and in the eastern AI near Unalaska Island (Figure 210).

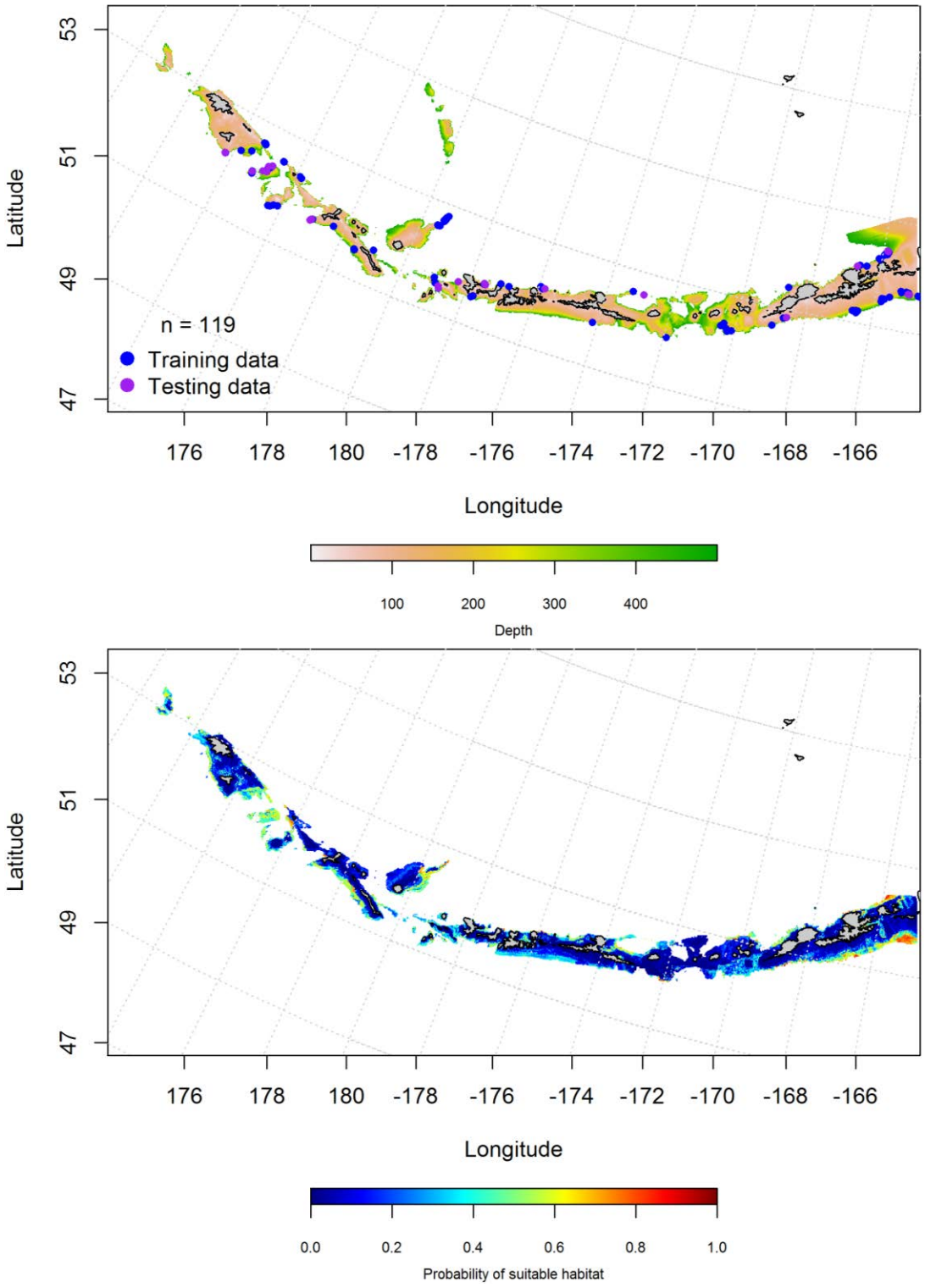

Figure 208. Locations of fall (September-November) commercial fisheries catches of adult Shortspine thornyhead (top panel). Blue points were used to train the maximum entropy model predicting the probability of suitable fall habitat supporting commercial catches of adult Shortspine thornyhead (bottom panel) and the purple points were used to validate the model.

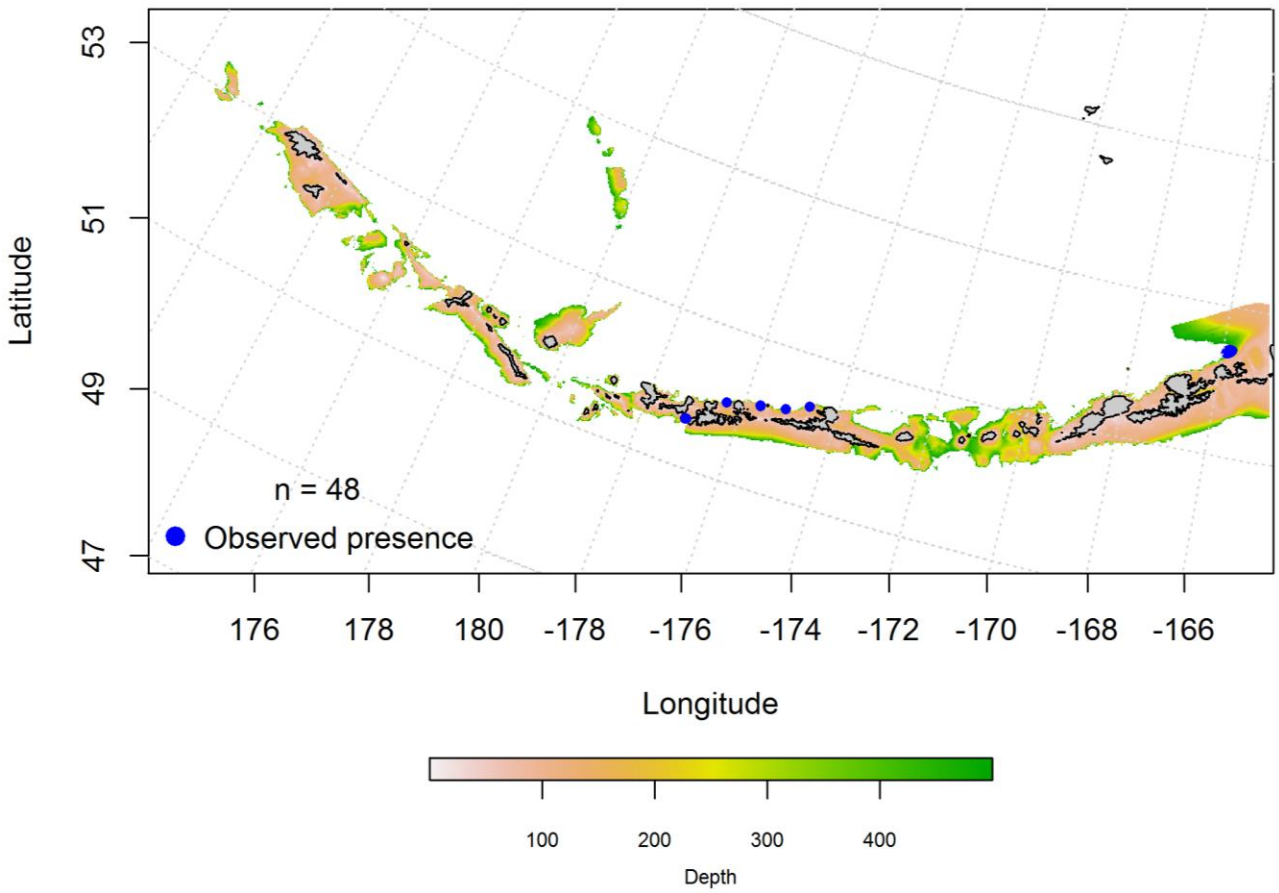

Figure 209. Blue points indicate locations where adult Shortspine thornyhead were observed during winter (December-February) commercial fisheries catches.

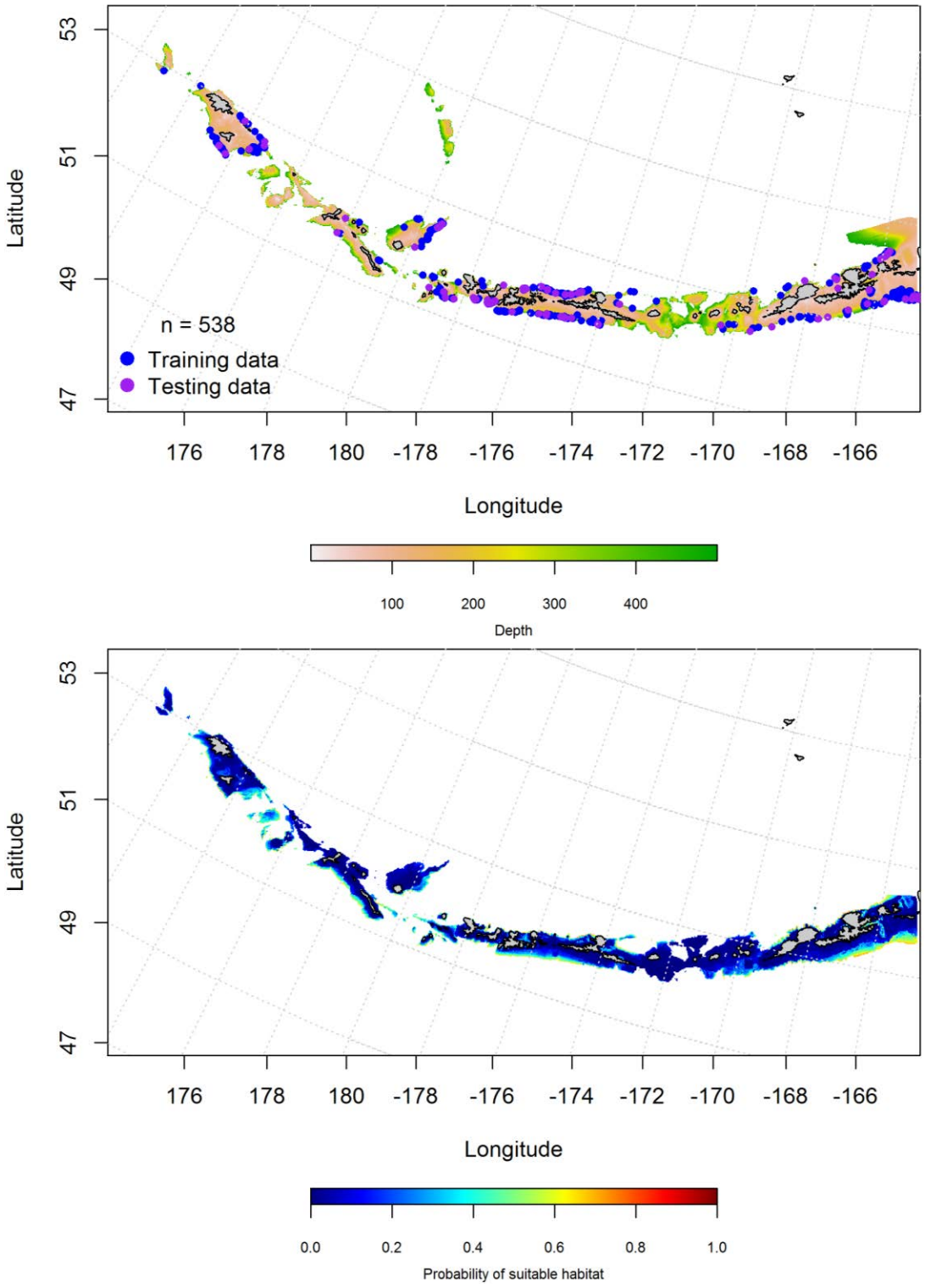

Figure 210. Locations of spring (March-May) commercial fisheries catches of Shortspine thornyhead (top panel). Blue points were used to train the maximum entropy model predicting the probability of suitable spring habitat supporting commercial catches of Shortspine thornyhead (bottom panel) and the purple points were used to validate the model.

Aleutian Islands Shortspine thornyhead Essential Fish Habitat Maps and Conclusions -- Predicted summertime EFH of Shortspine thornyhead juveniles and adults was similar across the AI (Figure 211).

The fall and winter distribution of arrowtooth flounder EFH was essentially the same across seasons (Figure 212). Suitable habitat was predicted, though a low percentile, across the AI, and lowest in areas of large passes. There was not enough data to model spring EFH.

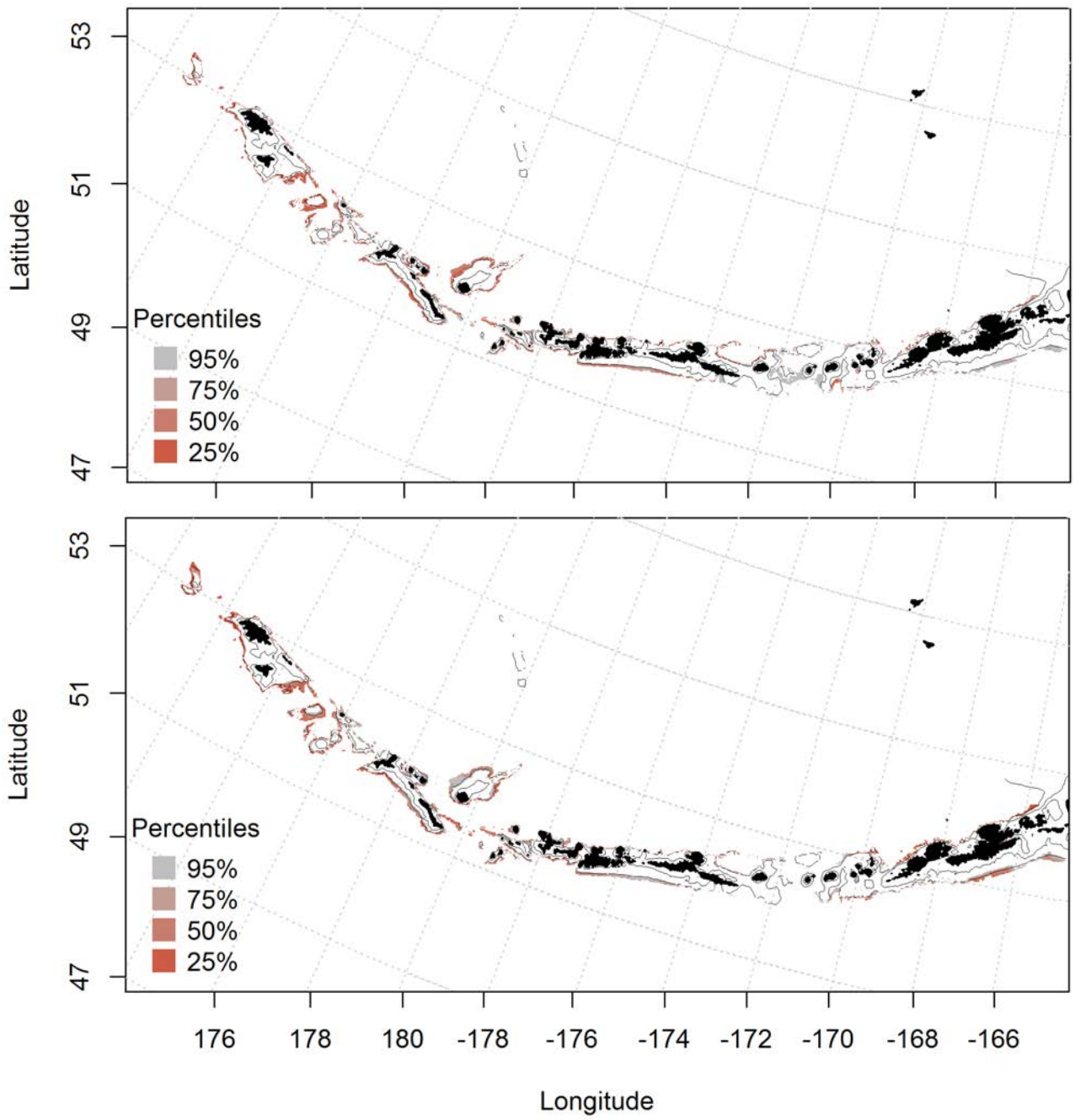

Figure 211. Predicted summer essential fish habitat for Shortspine thornyhead juveniles and adults (top and bottom panel) from summertime bottom trawl surveys.

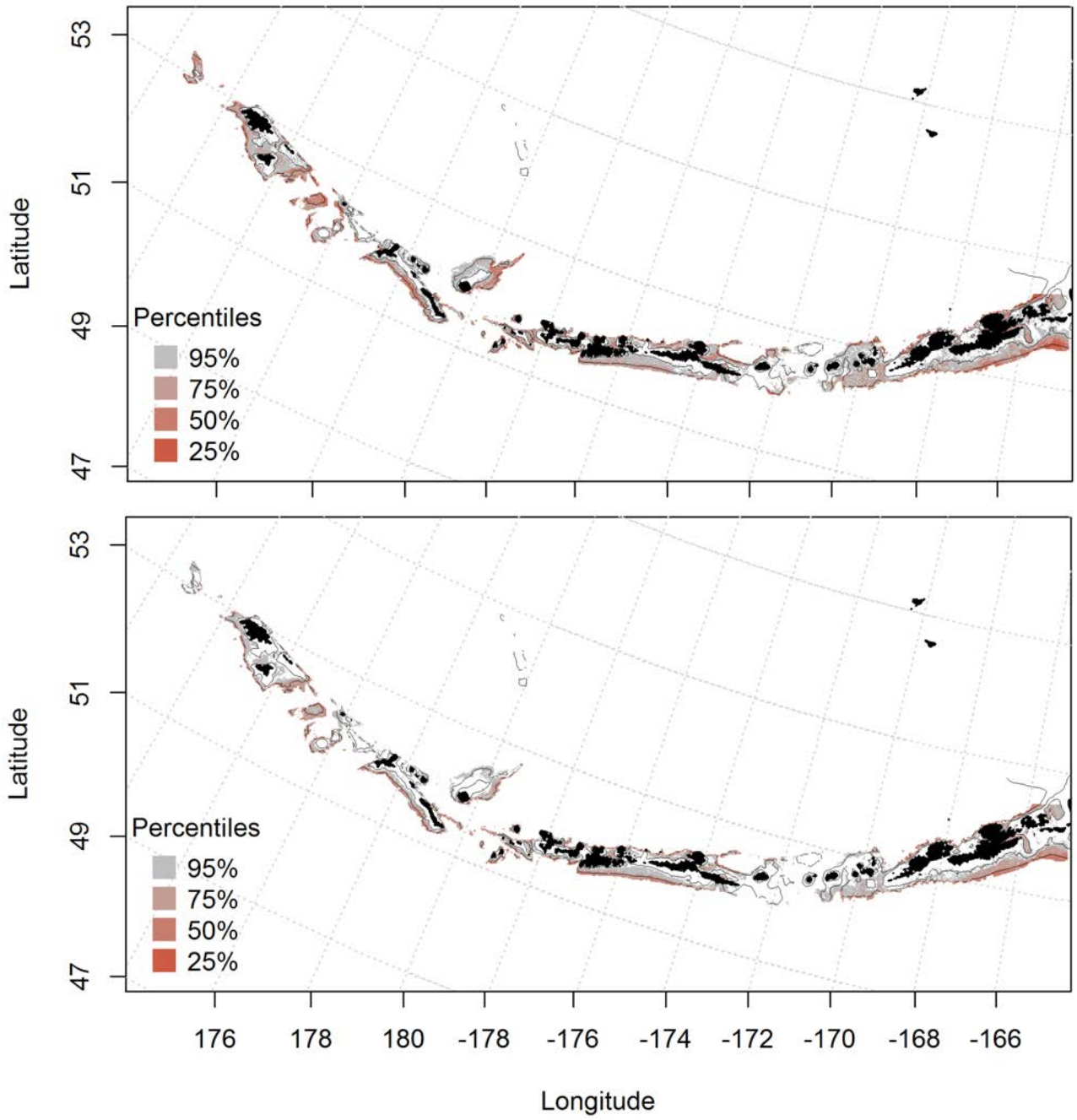

Figure 212. Essential fish habitat predicted for Shortspine thornyhead during fall (top panel) and spring (bottom panel) from summertime commercial catches.

3.4 Skates

Bering skate (*Bathyraja interrupta*)
Species text here

Summertime distribution of juvenile and adult Bering skate from bottom trawl surveys of the Aleutian Islands -- A maximum entropy model predicting the probability of suitable habitat of juvenile Bering skate explained 96% of the training set variability in CPUE in the bottom trawl survey, and 75% of the test data set variability. Bottom depth, bottom temperature, and current speed were the most important variables explaining probable suitable habitat of juvenile Bering skate (relative importance: 30.4%, 24.6%, and 23.5%, respectively). The model correctly classified 88% of the training data and 75% of the test data set. The most probable suitable habitat for juvenile Bering skate is in the eastern AI near Unalaska Island, though juvenile habitat suitability is predicted across the AI (Figure 213).

There were only 18 instances of adult Bering skate from summer bottom trawl survey catches, located in the central and eastern AI (Figure 214). There were not enough cases to the run a model.

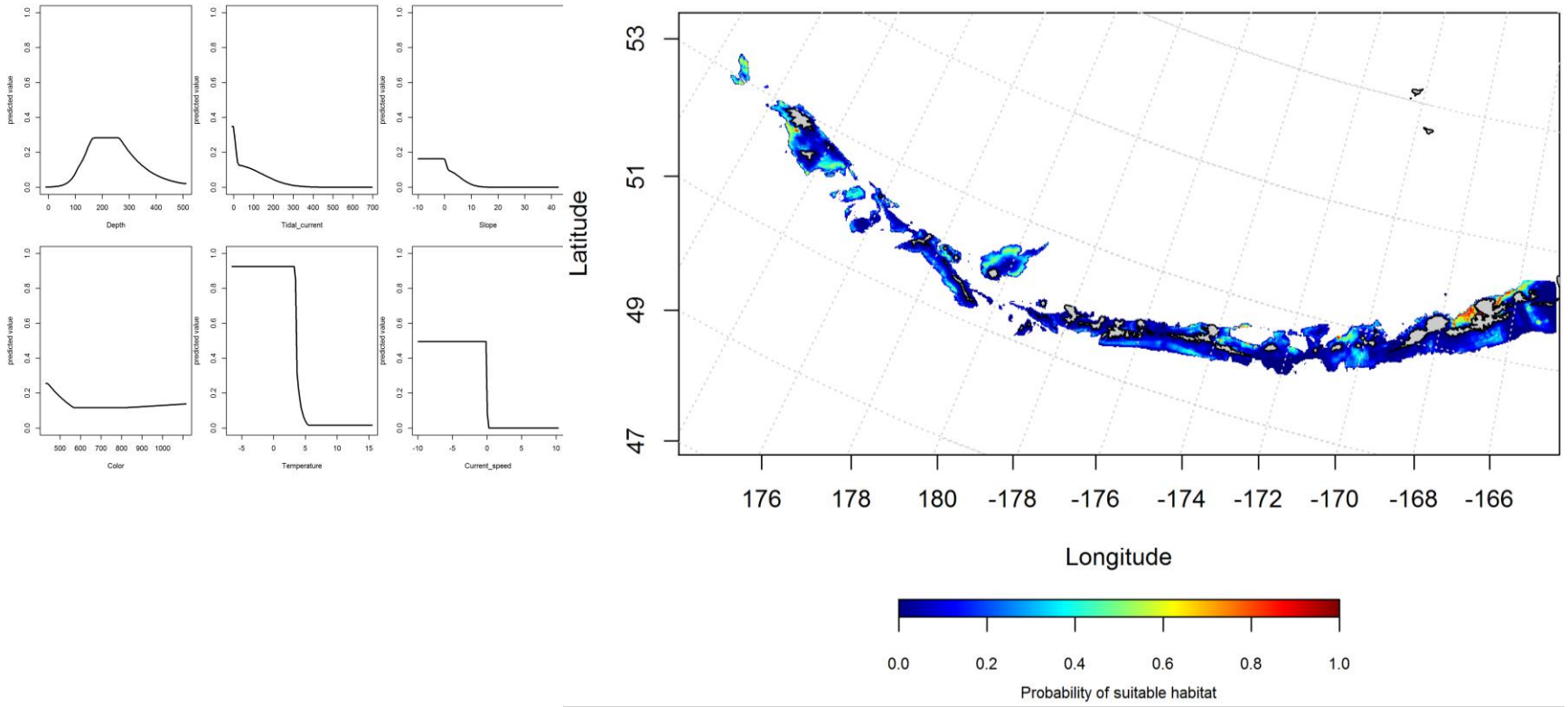

Figure 213. Best-fitting maximum entropy model effects of retained habitat variables on suitable habitat of juvenile Bering skate from summer bottom trawl surveys of the Aleutian Islands (left panel) alongside maxent-predicted juvenile Bering skate probable suitable habitat (right panel).

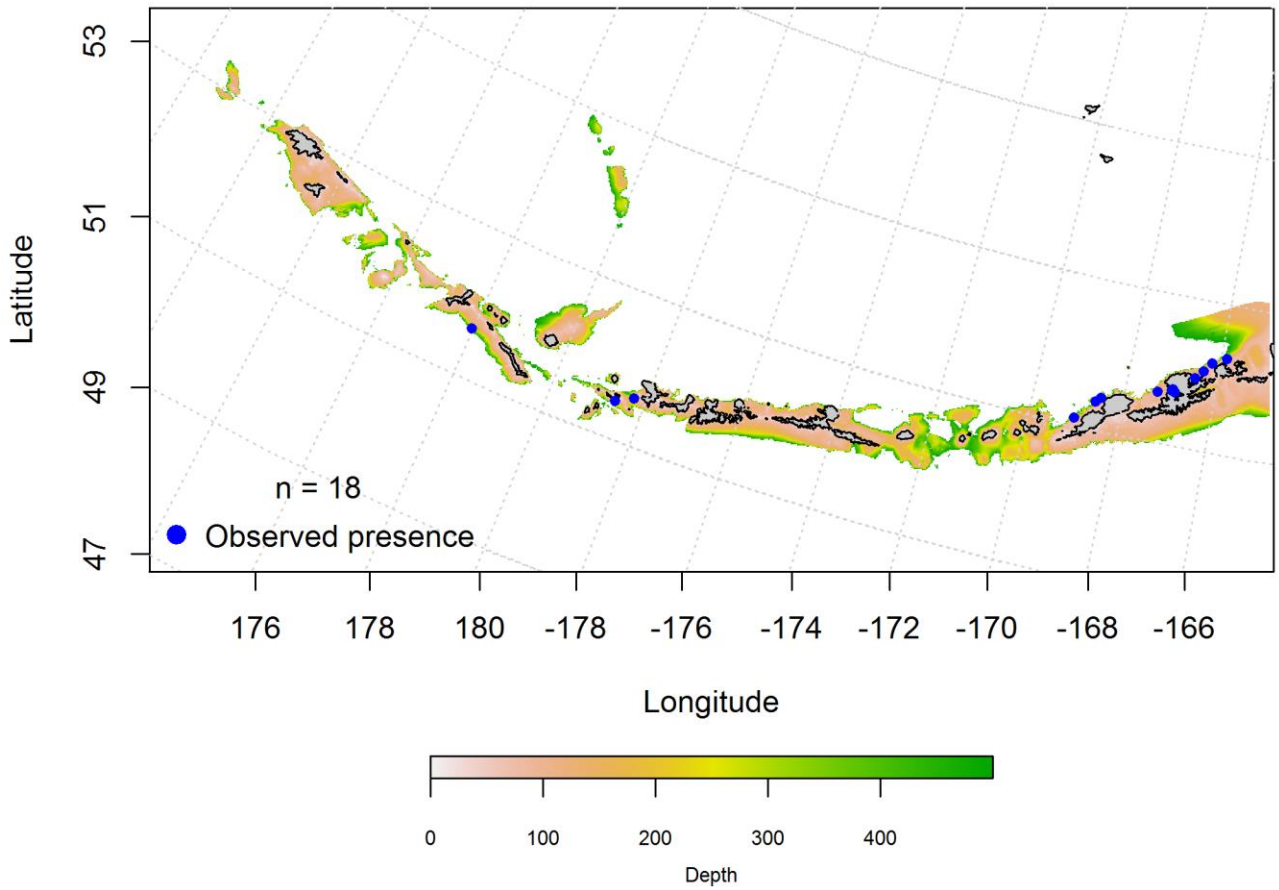

Figure 214. Blue points indicate instances where adult Bering skate were observed during summertime bottom trawl survey catches.

Aleutian Islands Bering skate Essential Fish Habitat Maps and Conclusions --

Summertime EFH of juvenile Bering skate was distributed across the AI (Figure 215). Predicted EFH was generally low, though slightly higher in the eastern AI near Unalaska Island. There was not enough data to map EFH for adult Bering skate.

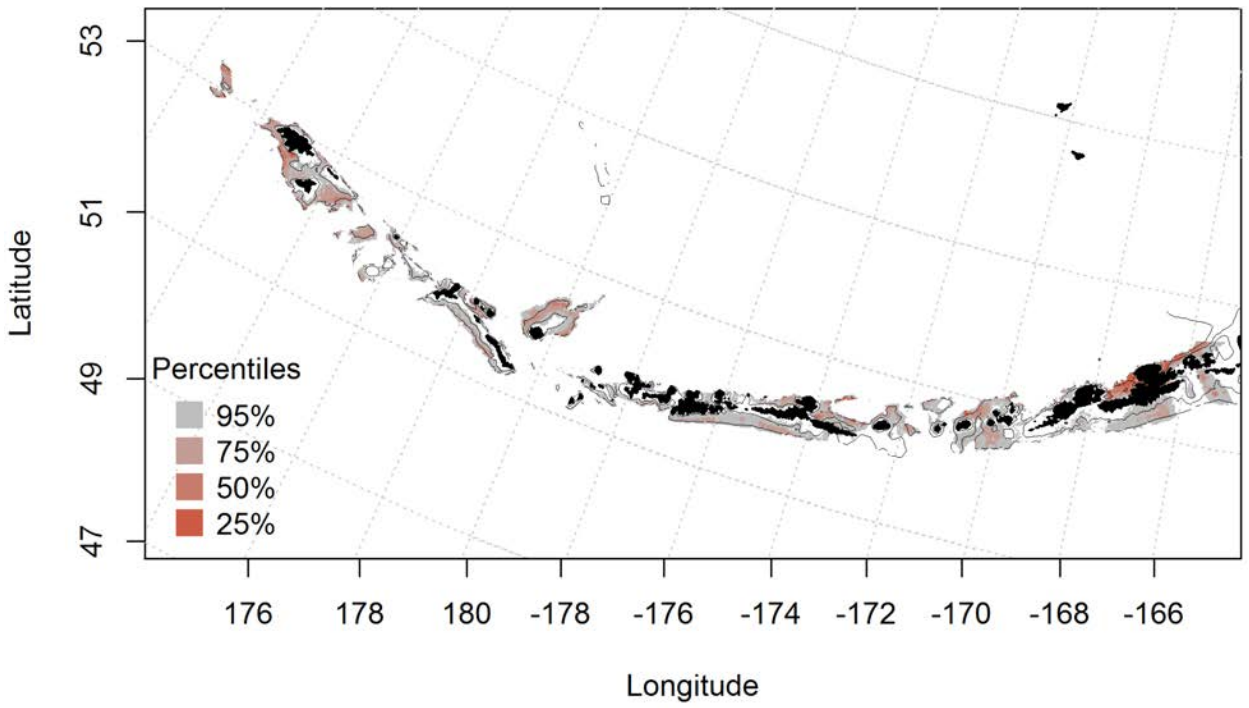

Figure 215. Predicted summer essential fish habitat for Bering skate juveniles from summertime bottom trawl surveys.

Alaska skate (*Bathyraja parmifera*)

Summertime distribution of juvenile and adult Alaska skate from bottom trawl surveys of the Aleutian Islands -- The catch of Alaska skate in summer bottom trawl surveys of the Aleutian Islands indicates this species is broadly distributed. A maximum entropy model predicting suitable habitat of juvenile Alaska skate explained 88% of the training data variability in CPUE in the bottom trawl survey, and 69% of the test data variability. Bottom depth and tidal current were the most important variables explaining the distribution of juvenile Alaska skate (62.4% and 20.2%). The model correctly classified 79% of the training data and 69% of the test data. The juvenile Alaska skate model predicted highest suitable habitat in the central and western AI (Figure 216).

A hurdle-GAM model was used to predict the presence and absence of adult Alaska skate and explained 77% of the variability in CPUE in the bottom trawl survey training data, 72% of the variability in the test data set, and 14% of the deviance. Geographic location and bottom depth were the most important variables explaining the distribution of adult Alaska skate. The model correctly classified 70% of the training and test data sets. Predicted suitable habitat of adult Alaska skate was across the AI (Figure 217).

The second part of the hurdle model found geographic location influenced the cpue of adult Alaska skate the most, and explained 18% of the training data, 13% of the test data, and 17.6% of the deviance. The model predicted highest CPUE across the AI, and highest in the central and western AI (Figure 218).

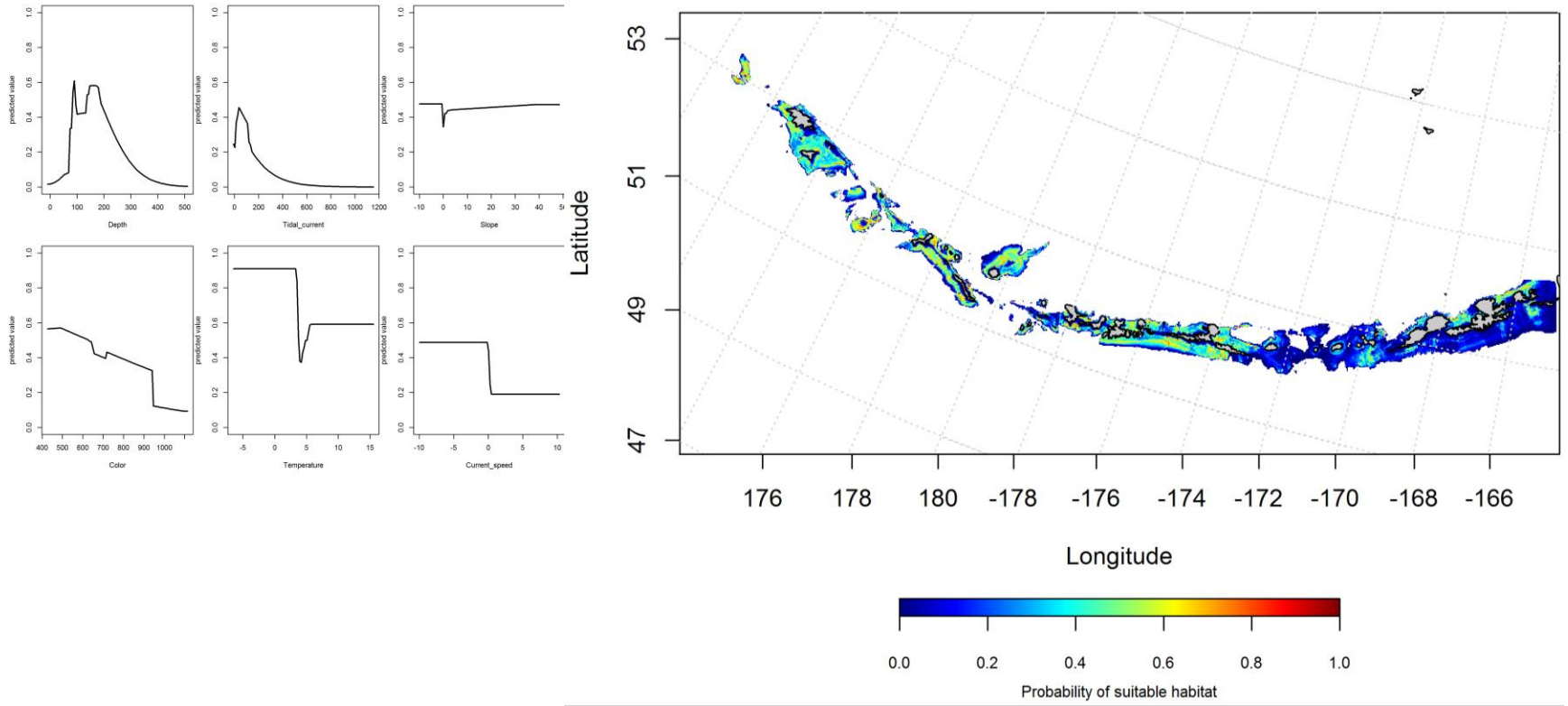

Figure 216. Best-fitting maximum entropy model effects of retained habitat variables on probability of suitable habitat of juvenile Alaska skate from summer bottom trawl surveys of the Aleutian Islands (left panel), alongside maxent-predicted juvenile Alaska skate suitable habitat (right panel).

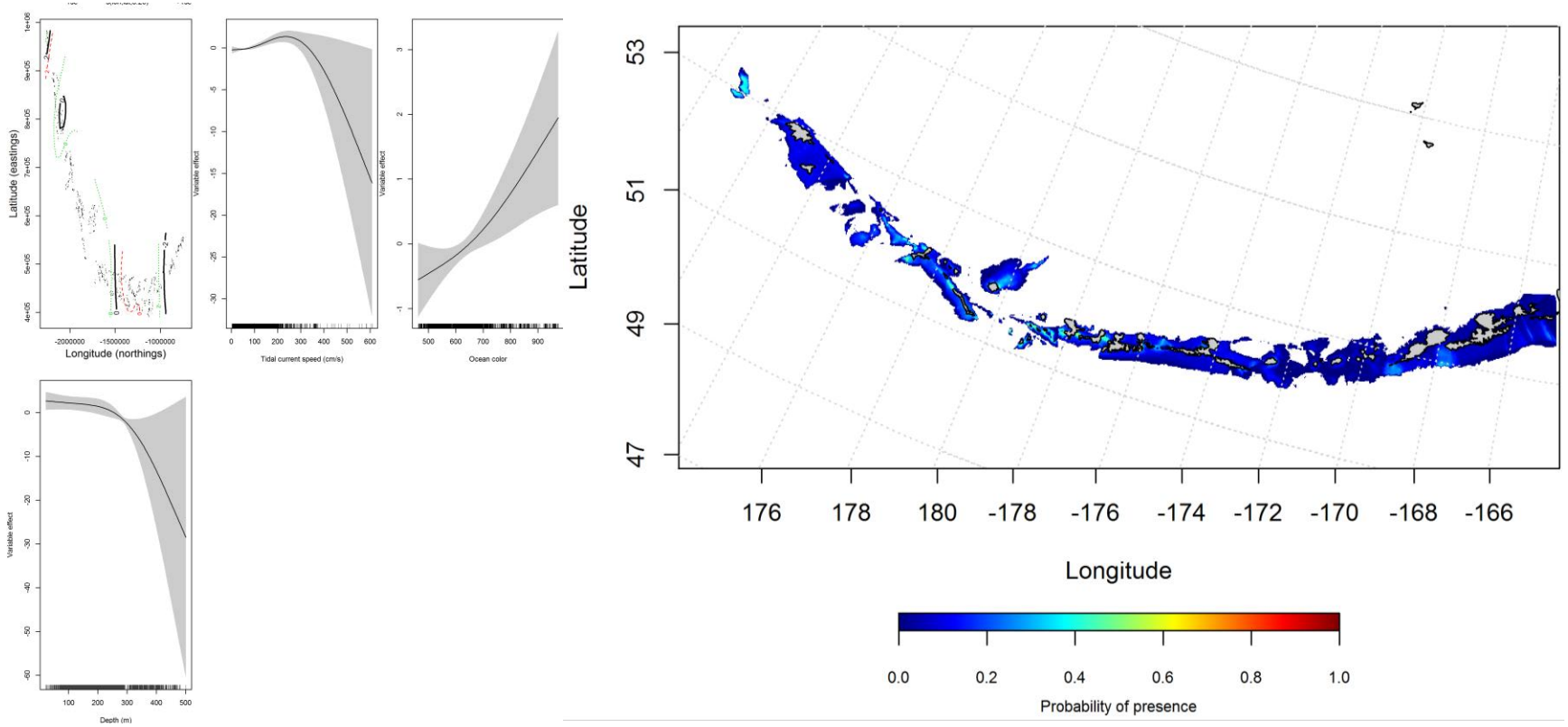

Figure 217.Best-fitting hurdle model effects of retained habitat variables on presence absence (PA) of adult Alaska skate from summer bottom trawl surveys of the Aleutian Islands (left panel) alongside hurdle-predicted adult Alaska skate PA (right panel).

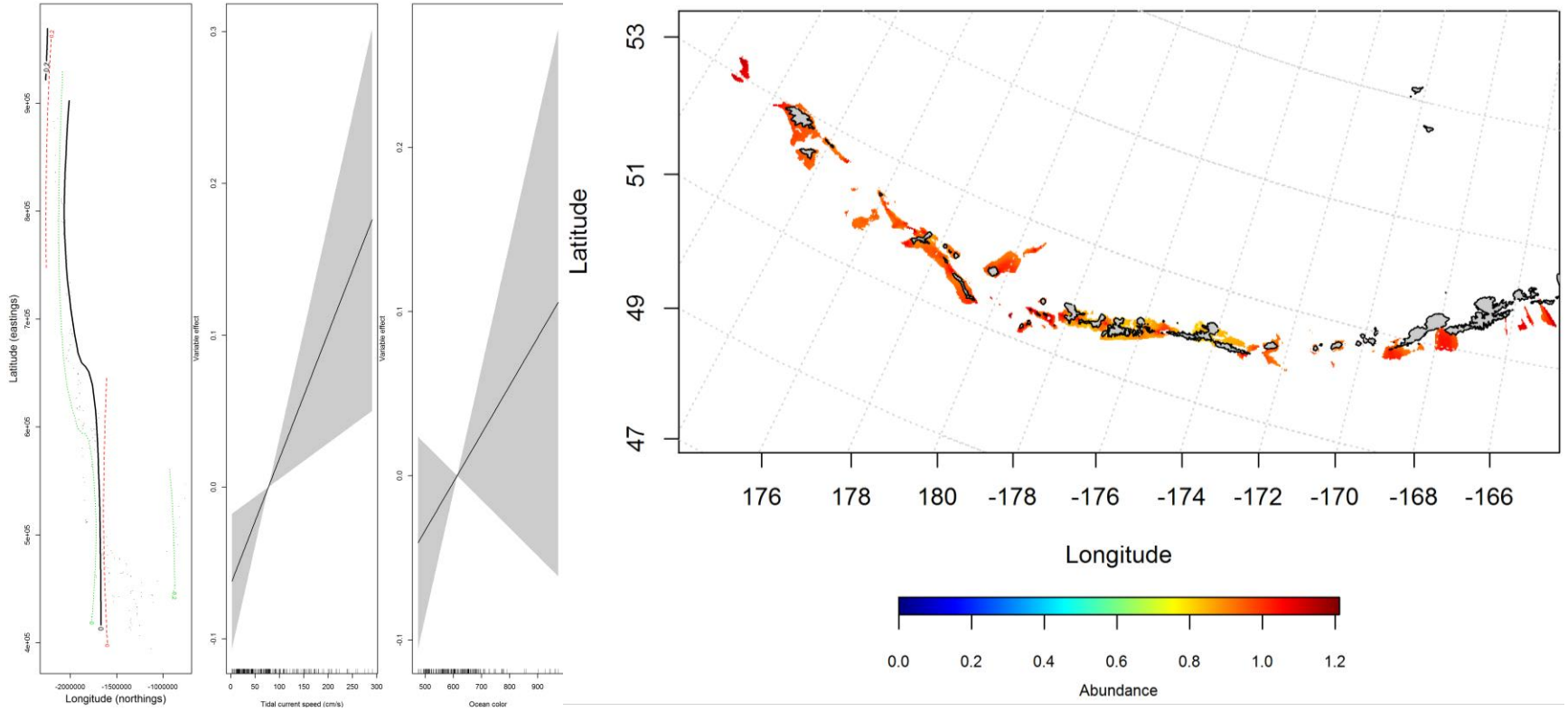

Figure 218. Best-fitting hurdle model effects of retained habitat variables on cpue of adult Alaska skate from summer bottom trawl surveys of the Aleutian Islands (left panel) alongside hurdle-predicted adult Alaska skate cpue (right panel).

Seasonal distribution of commercial fisheries catches of adult Alaska skate in the Aleutian Islands-- Distribution of adult Alaska skate in the Aleutian Islands in commercial fisheries catches was consistent in winter and spring and more abundant in the fall. In the fall, bottom depth and tidal current were the most important variables determining the distribution of Alaska skate (relative importance: 72.7% and 11.6%). The AUC of the fall maxent model was 90% for the training data and 81% for the test data. 83% of the cases in the training data and 81% of the test data were predicted correctly. Areas of high predicted suitable habitat of Alaska skate in the fall were distributed throughout the AI, avoiding large passes (Figure 219).

In the winter, bottom depth and ocean color were the most important variables determining the distribution of Alaska skate (relative importance: 553.9% and 23.5%). The AUC of the winter maxent model was 92% for the training data, 85% for the test data, and 85% of the cases in the training and test data sets were predicted correctly. The model predicted probable suitable habitat of Alaska skate near Agattu and Attu Islands in the western AI, and Atka Island in the central AI (Figure 220).

In the spring, bottom depth and ocean surface color were also the most important variables determining the distribution of Alaska skate (relative importance: 57.7% and 22.9%). The AUC of the spring maxent model was 92% for the training data and 85% for the test data. The model correctly classified 84% of the training data and 85% of the test data. The model predicted probable suitable habitat of spring Alaska skate throughout the AI, though higher near Agattu and Attu Islands in the western AI, and Atka Island in the central AI (Figure 221).

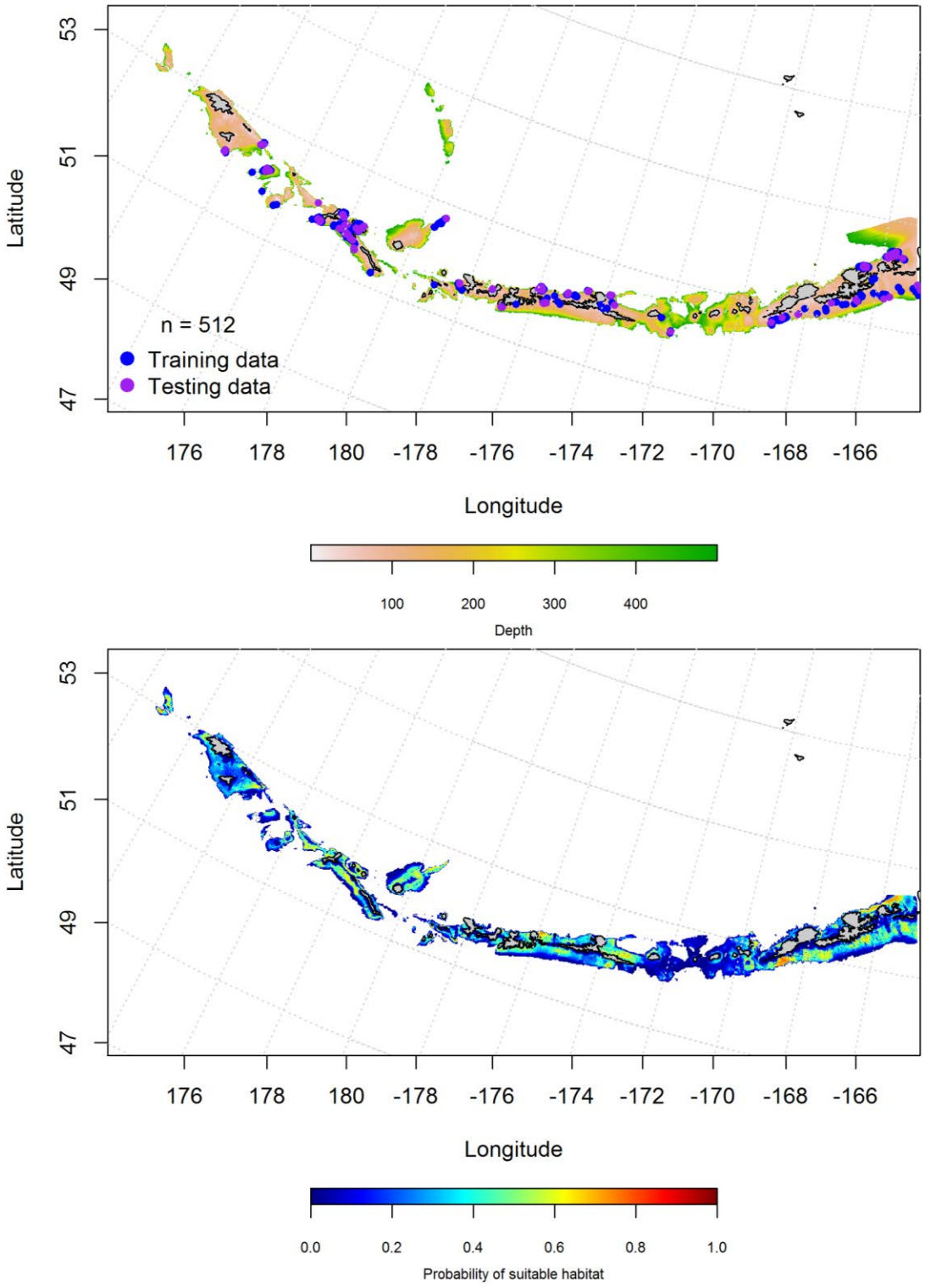

Figure 219. Locations of fall (September-November) commercial fisheries catches of adult Alaska skate (top panel). Blue points were used to train the maximum entropy model predicting the probability of suitable fall habitat supporting commercial catches of adult Alaska skate commercial catches (bottom panel) and the purple points were used to validate the model.

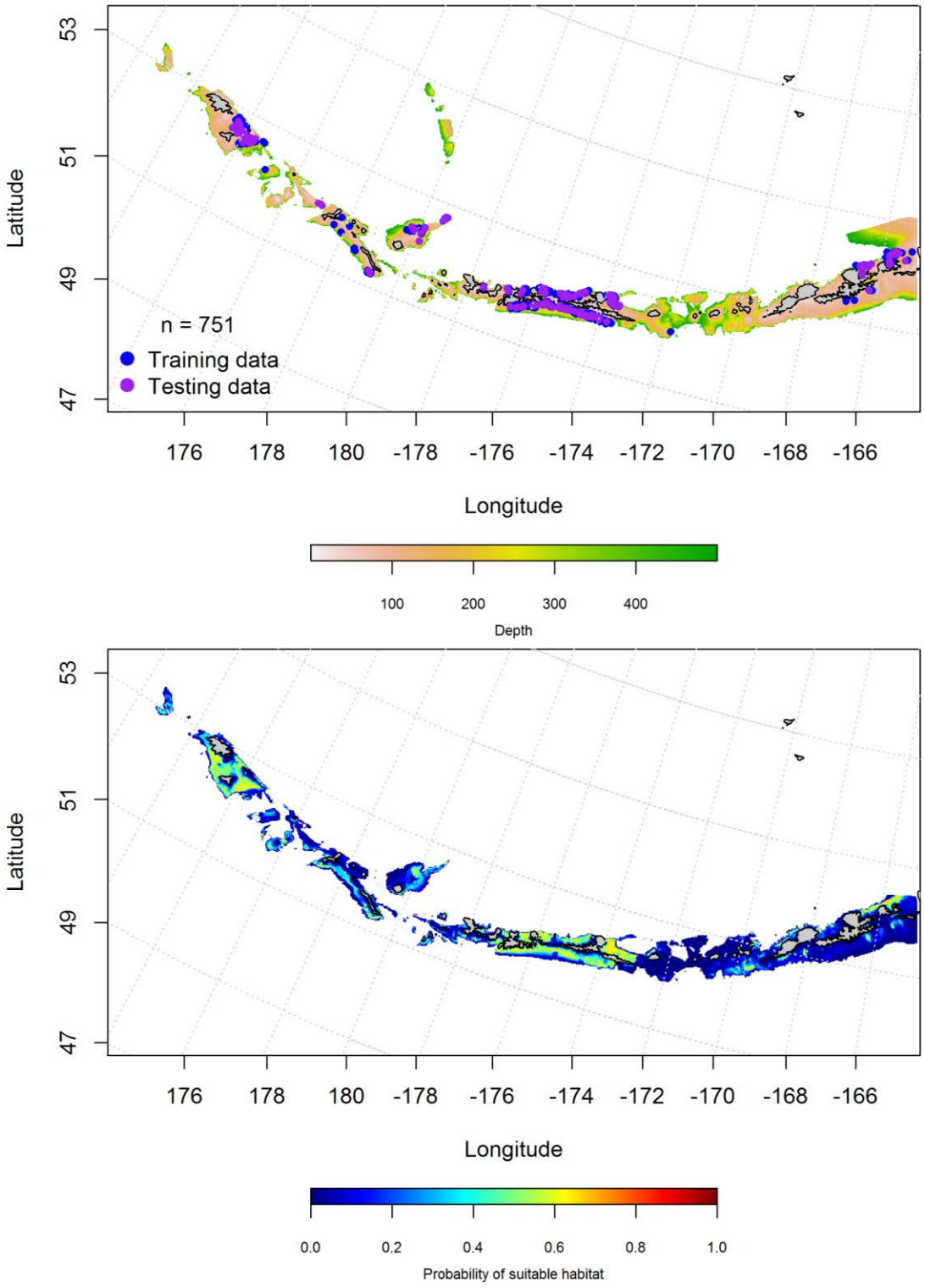

Figure 220. Locations of winter (December-February) commercial fisheries catches of adult Alaska skate (top panel). Blue points were used to train the maximum entropy model predicting the probability of suitable winter habitat supporting commercial catches of adult Alaska skate (bottom panel) and the purple points were used to validate the model.

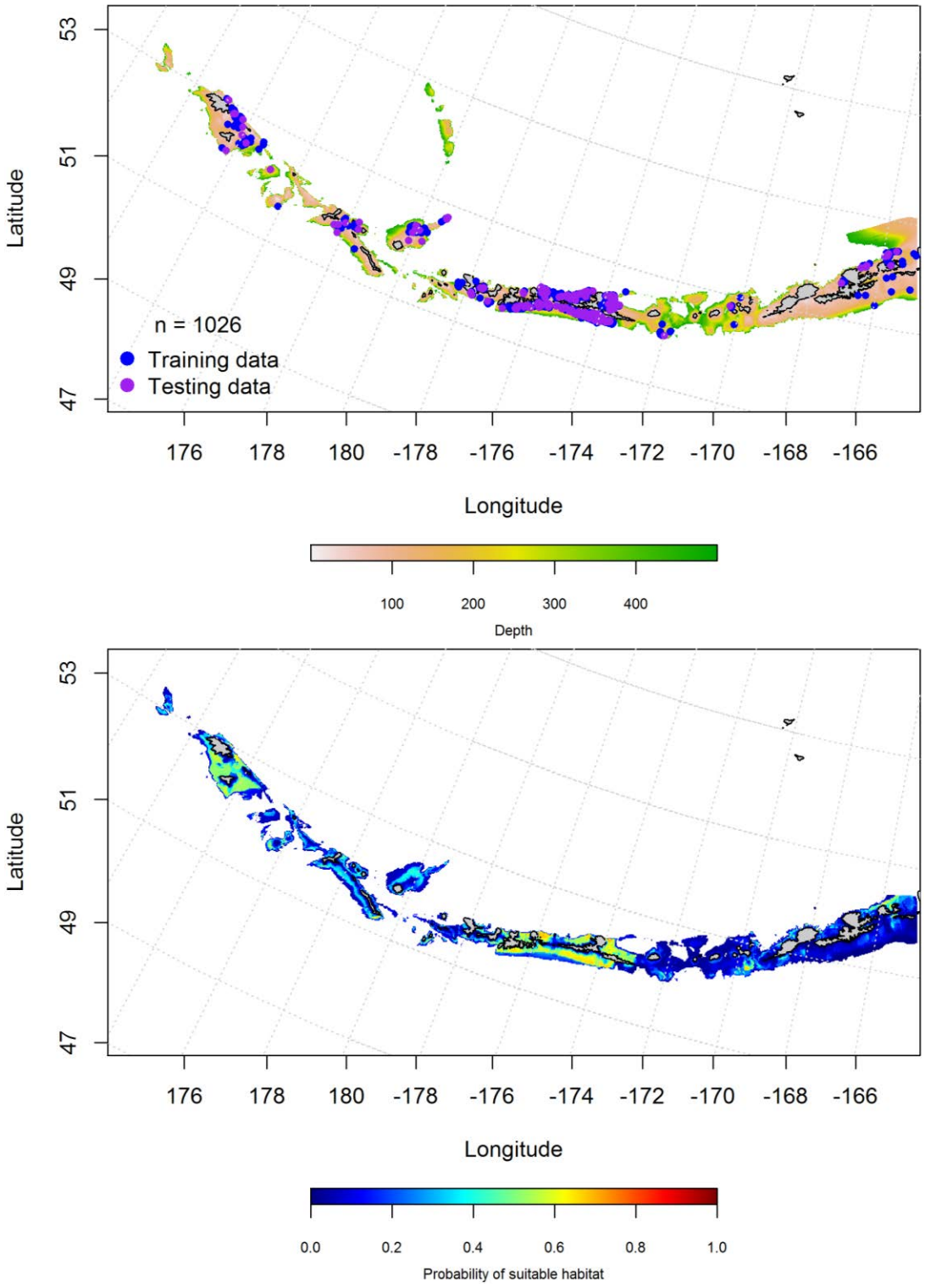

Figure 221.Locations of spring (March-May) commercial fisheries catches of adult Alaska skate (top panel). Blue points were used to train the maximum entropy model predicting the probability of suitable spring habitat supporting commercial catches of adult Alaska skate (bottom panel) and the purple points were used to validate the model.

Aleutian Islands Alaska skate Essential Fish Habitat Maps and Conclusions –Alaska skate were distributed across AI, and less abundant in the passes. Predicted summertime EFH of Alaska skate juveniles was similar to the adults (Figure 222).

The fall, winter and spring distribution of Alaska skate EFH was essentially the same in all seasons (Figure 223). Areas of higher predicted EFH was in the western AI near Agattu and Attu Islands, and in the central AI near Adak and Atka Islands. Fall Alaska skate EFH was higher in the eastern AI near Unalaska Island than in the winter or spring.

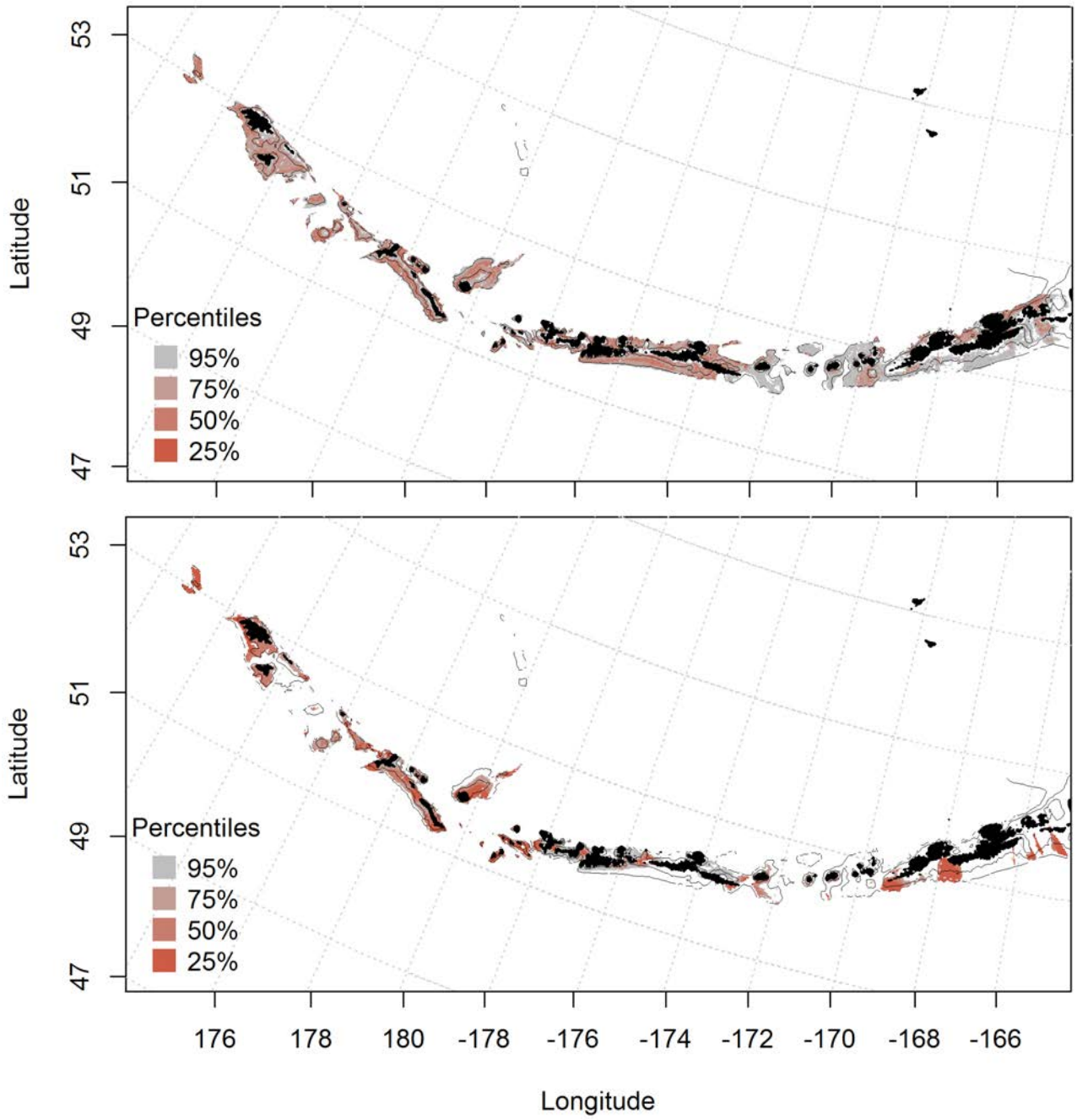

Figure 222. Predicted summer essential fish habitat for Alaska skate juveniles and adults (top and bottom panel) from summertime bottom trawl surveys.

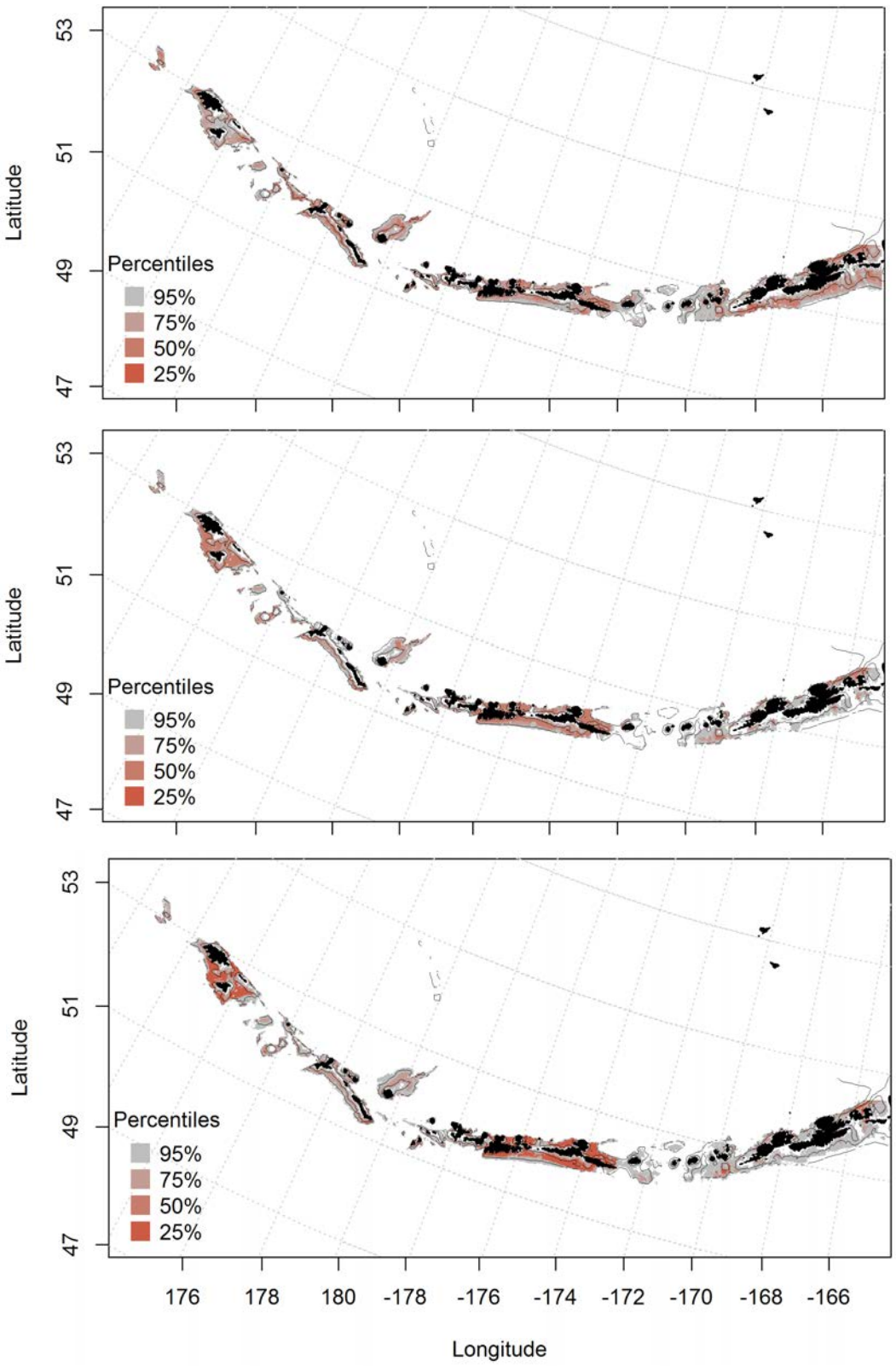

Figure 223. Essential fish habitat predicted for Alaska skate during fall (top panel), winter (middle panel) and spring (bottom panel) from summertime commercial catches.

Aleutian skate (*Bathyraja aleutica*)

Summertime distribution of juvenile and adult Aleutian skate from bottom trawl surveys of the Aleutian Islands – A hurdle-GAM model was used to predict the presence and absence of juvenile Aleutian skate and explained 10.5% of the deviance, 74% of the variability in CPUE in the bottom trawl survey training data and 71% of the variability in the test data set. Geographic location and bottom depth were the most important variables explaining the distribution of juvenile Aleutian skate. The model correctly classified 66% of the training data set and 68% of the test data set. Predicted suitable habitat of juvenile Aleutian skate was distributed across the AI (Figure 224).

The second part of the hurdle model found slope influenced the cpue of juvenile Aleutian skate the best, and explained 11% of the training data, 2% of the test data, and 11.3% of the deviance. The model predicted highest CPUE in a similar pattern as the PA GAM (across the AI), though more abundant in the central AI near Adak and Atka Islands (Figure 225).

A maximum entropy model predicting the probability of suitable habitat of adult Aleutian skate explained 91% of the training data variability, and 77% of the variability in the test data set. Bottom depth, ocean color and bottom temperature were the most important variables explaining the probability of suitable habitat of adult Aleutian skate (relative abundance: 64.3%, 11.1%, and 9.7%, respectively). 84% of the training data and 77% of the test data sets were predicted correctly. Predicted probable suitable habitat was predicted throughout the AI (Figure 226).

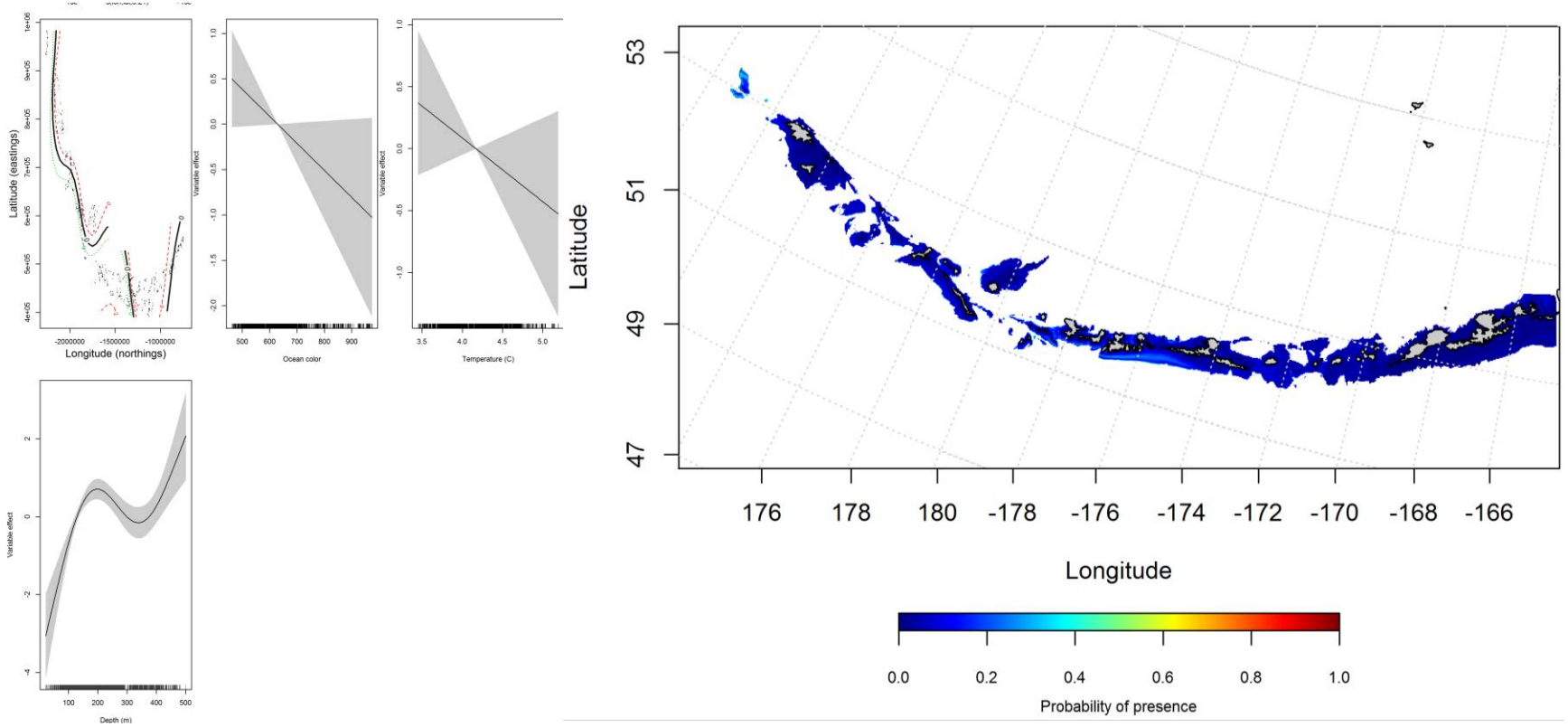

Figure 224. -- Best-fitting hurdle model effects of retained habitat variables on presence absence (PA) of juvenile Aleutian skate from summer bottom trawl surveys of the Aleutian Islands (left panel) alongside hurdle-predicted juvenile Aleutian skate PA (right panel).

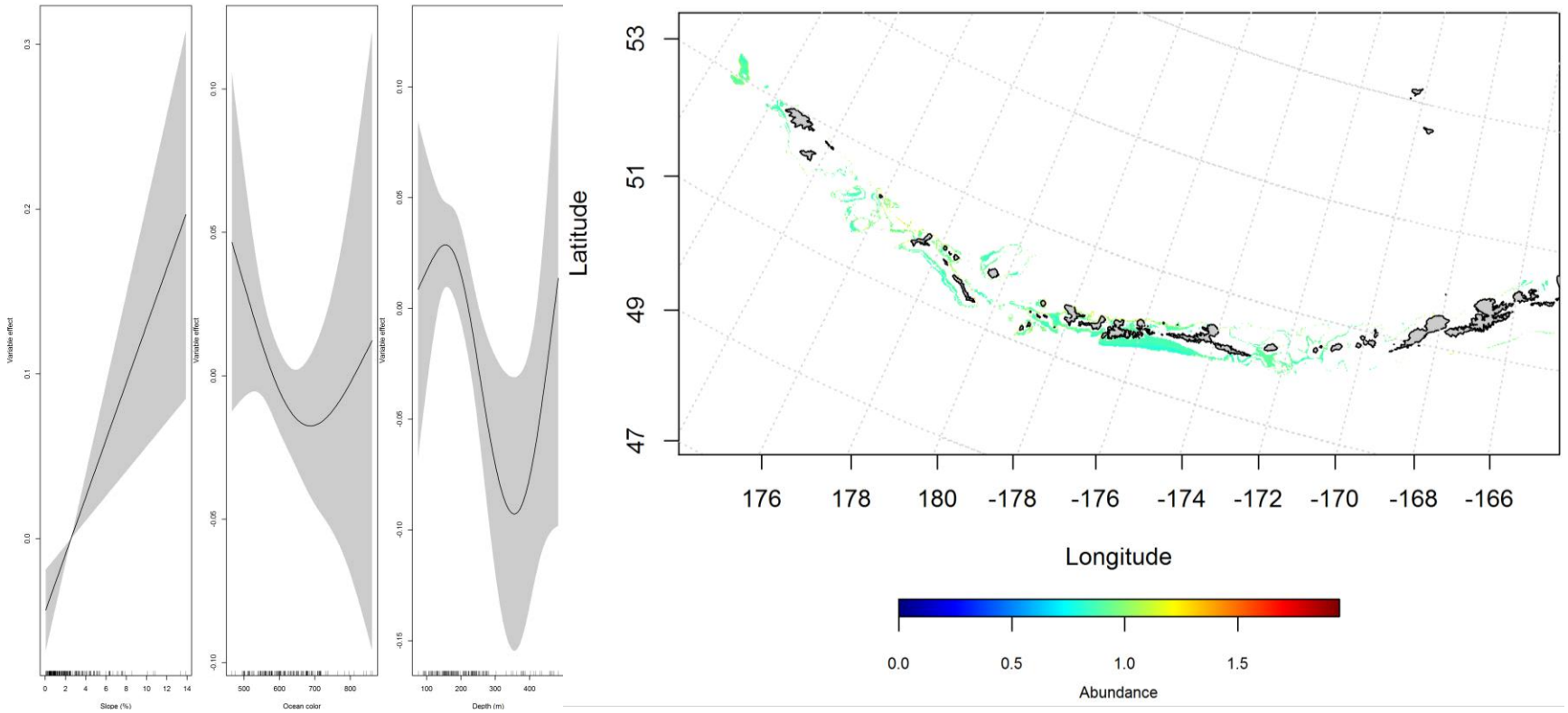

Figure 225. Best-fitting hurdle model effects of retained habitat variables on cpue of juvenile Aleutian skate from summer bottom trawl surveys of the Aleutian Islands (left panel) alongside hurdle-predicted juvenile Aleutian skate cpue (right panel)..

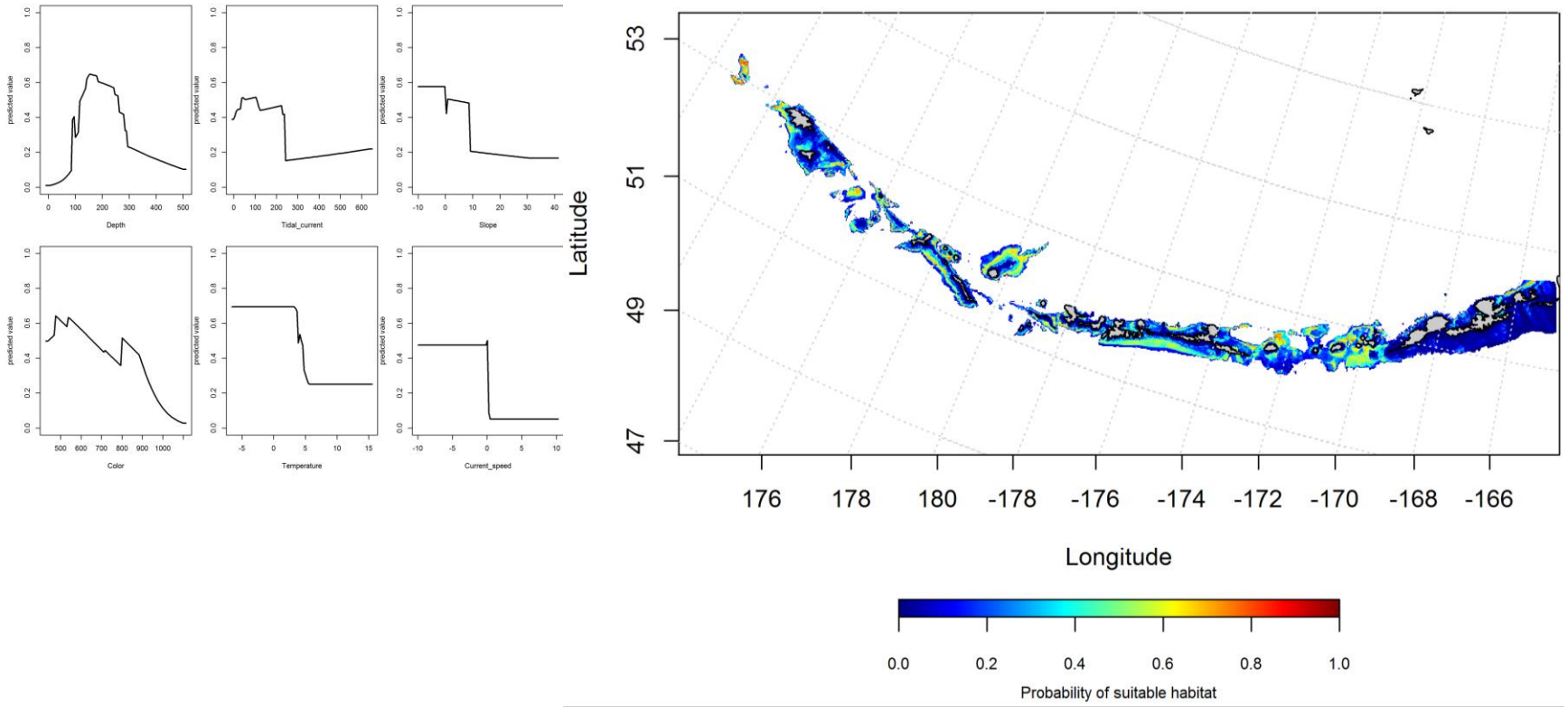

Figure 226. Best-fitting maximum entropy model effects of retained habitat variables on probability of suitable habitat of adult Aleutian skate from summer bottom trawl surveys of the Aleutian Islands (left panel), alongside maxent-predicted adult Aleutian skate suitable habitat (right panel).

Seasonal distribution of commercial fisheries catches of adult Aleutian skate in the Aleutian Islands-- In the fall, ocean color and bottom depth were the most important variables determining the distribution of Aleutian skate (relative importance: 52.4% and 36%). The AUC of the fall maxent model was 94% for the training data and 86% for the test data. 85% of the training data and 86% of the test data sets were predicted correctly. The model predicted probable suitable habitat of Aleutian skate across the AI, though higher in the eastern AI near Adak and Atka Islands (Figure 227).

In the winter, bottom depth and ocean color were the most important variables determining the distribution of Aleutian skate (relative importance: 50.4% and 27.6%). The AUC of the winter maxent model was 91% for the training data and 79% for the test data. 82% of the cases in the training data set, and 79% of the test data set were predicted correctly. The model predicted probable suitable habitat Aleutian skate catches was across the AI with areas of higher abundance near Agattu, Attu, Atka, and Unalaska Islands (Figure 228).

In the spring, bottom depth and ocean color were also the most important variables determining the distribution of Aleutian skate (relative importance: 45.9% and 40.3%). The AUC of the maxent spring model was 87% for the training data and 76% for the test data. Like the winter model, predicted probable suitable habitat of Aleutian skate catches in the spring were across the AI with areas of higher abundance near Agattu, Attu, Atka, and Unalaska Islands (Figure 229).

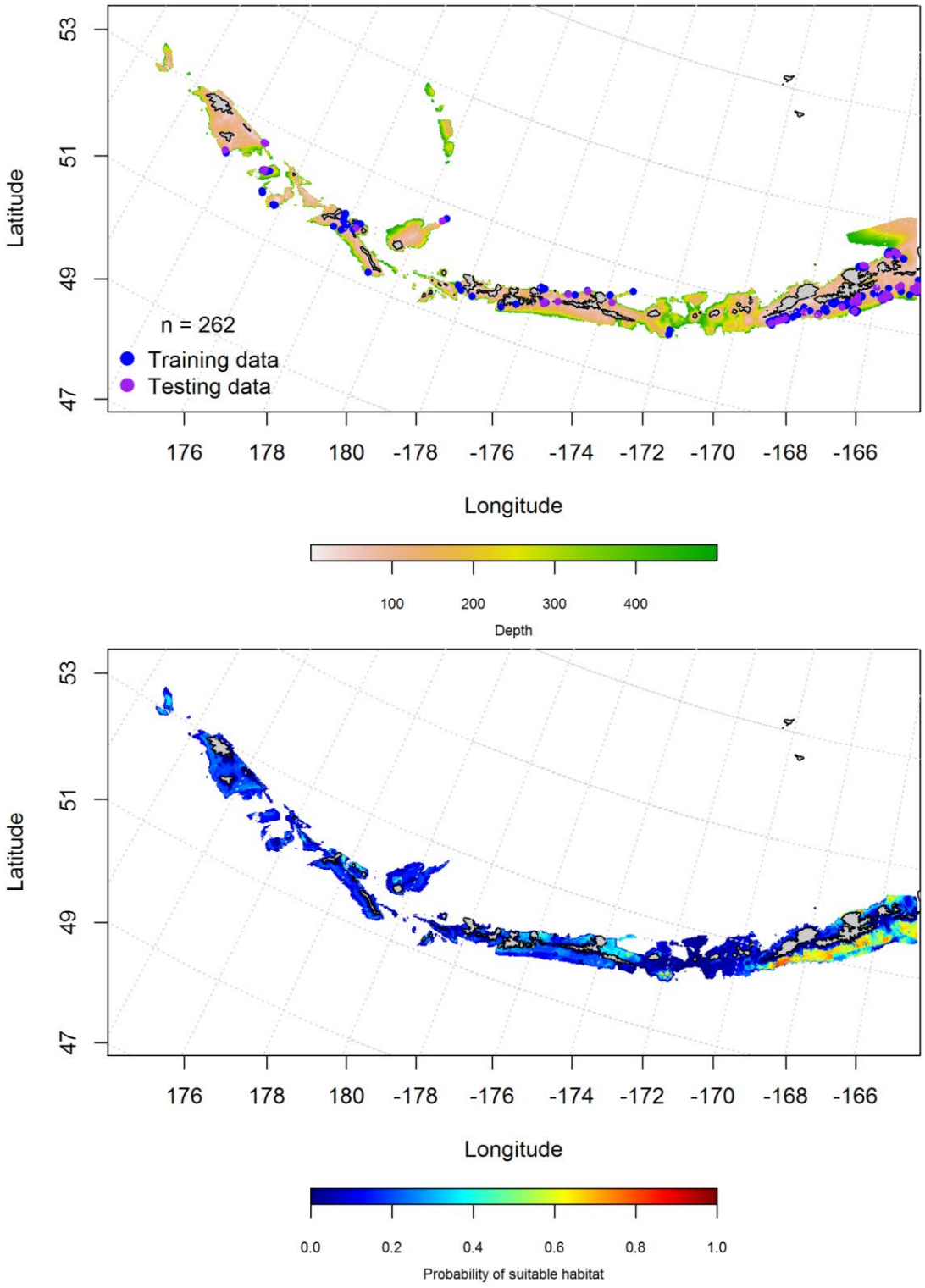

Figure 227. Locations of fall (September-November) commercial fisheries catches of adult Aleutian skate (top panel). Blue points were used to train the maximum entropy model predicting the probability of suitable fall habitat supporting commercial catches of adult Aleutian skate (bottom panel) and the purple points were used to validate the model.

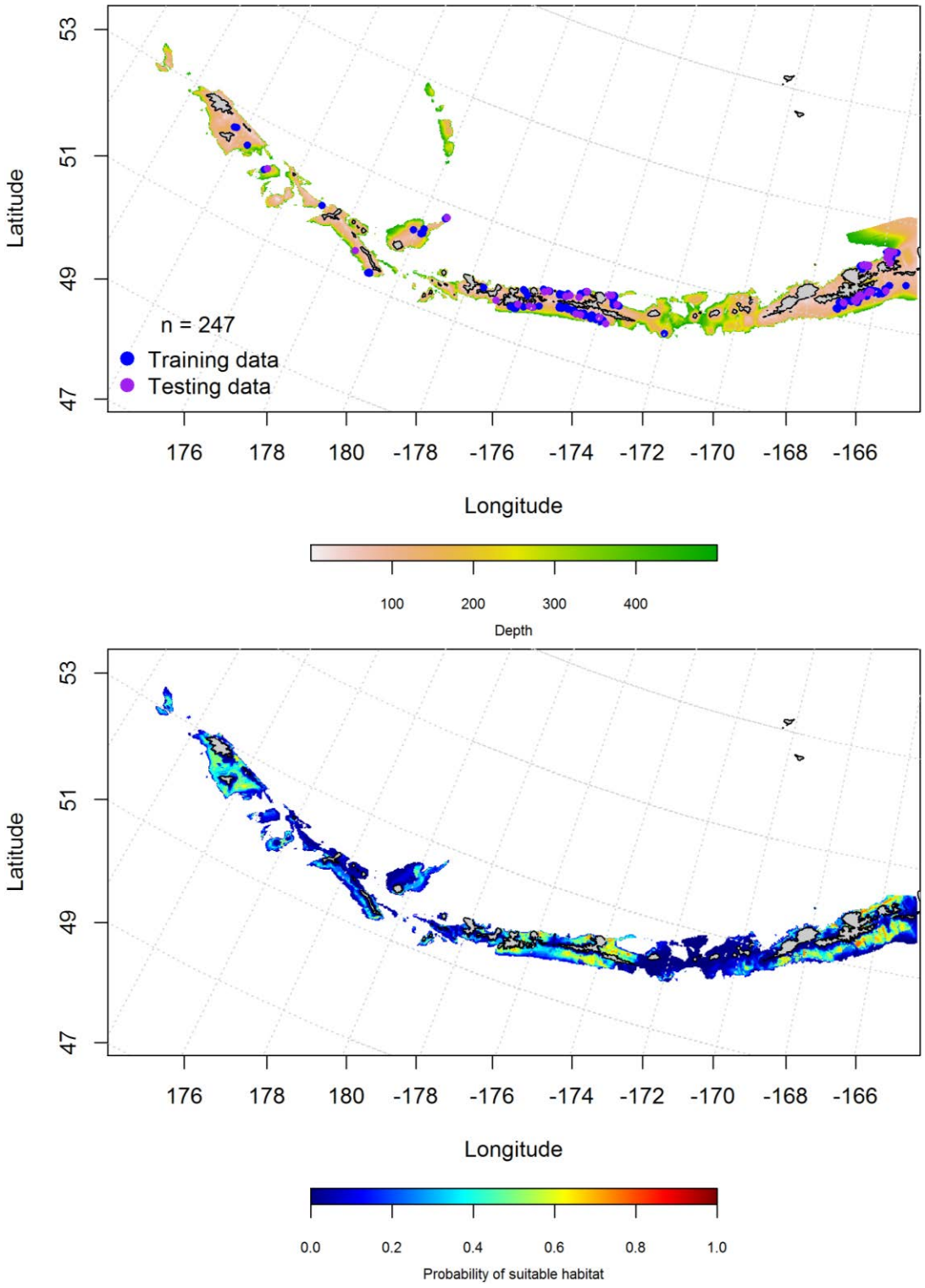

Figure 228. Locations of winter (December-February) commercial fisheries catches of adult Aleutian skate (top panel). Blue points were used to train the maximum entropy model predicting the probability of suitable winter habitat supporting commercial catches of adult Aleutian skate (bottom panel) and the purple points were used to validate the model.

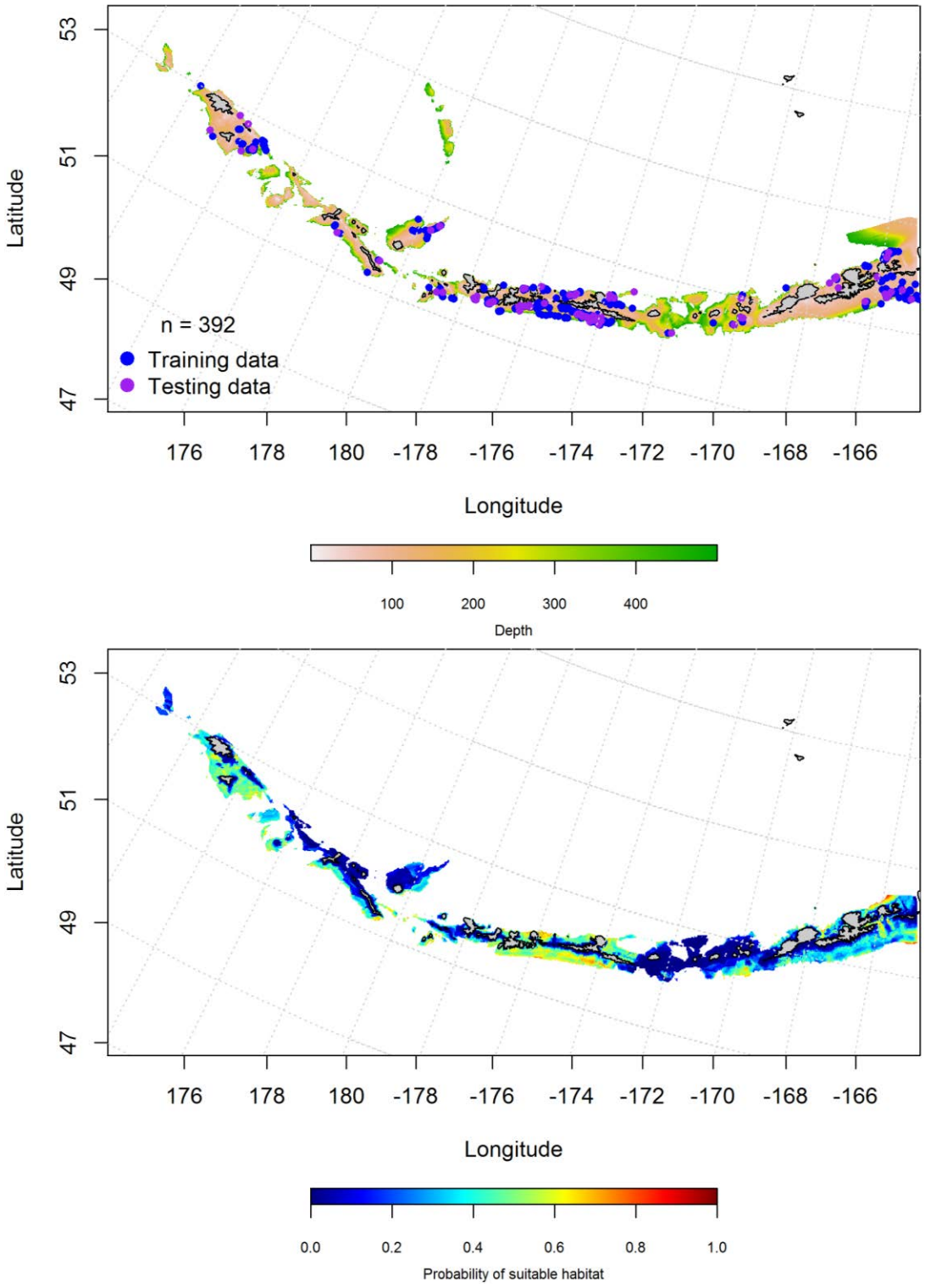

Figure 229. Locations of spring (March-May) commercial fisheries catches of adult Aleutian skate (top panel). Blue points were used to train the maximum entropy model predicting the probability of suitable spring habitat supporting commercial catches of adult Aleutian skate (bottom panel) and the purple points were used to validate the model.

Aleutian Islands Aleutian skate Essential Fish Habitat Maps and Conclusions --

Summertime EFH of Aleutian skate juveniles and adults were similarly distributed in the western AI, though varied in the rest of the AI chain (Figure 230). Predictions of juvenile Aleutian skate EFH is distributed in the central and western AI. Juvenile EFH was predicted throughout the AI though was less abundant than the adults.

The fall, winter and spring distribution of arrowtooth flounder EFH was similarly distributed (Figure 231). The eastern AI near Unalaska Island was the most essential habitat in all seasons, followed by Atka and Adak Islands in the central AI.

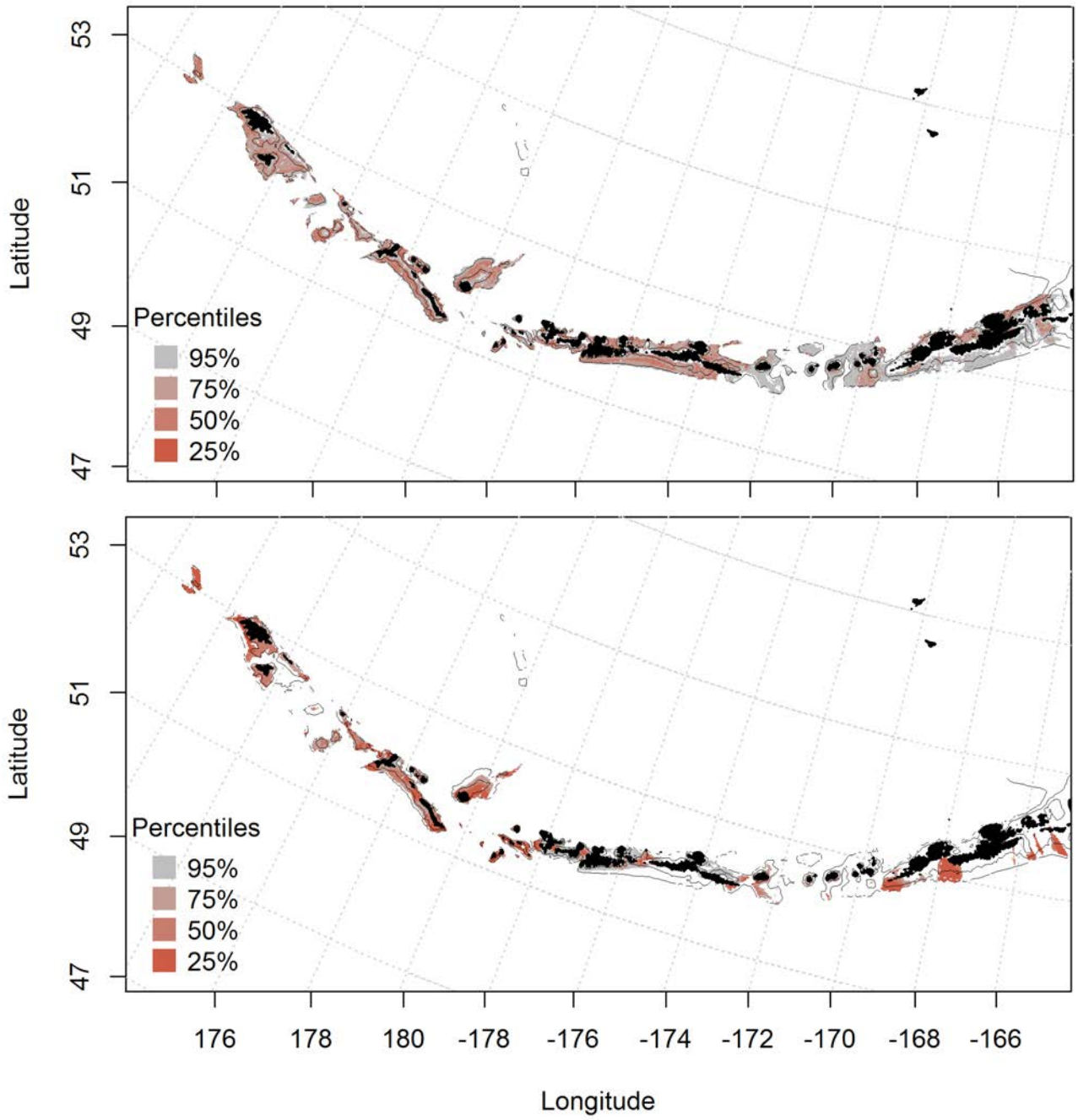

Figure 230. Predicted summer essential fish habitat for Aleutian skate juveniles and adults (top and bottom panel) from summertime bottom trawl surveys.

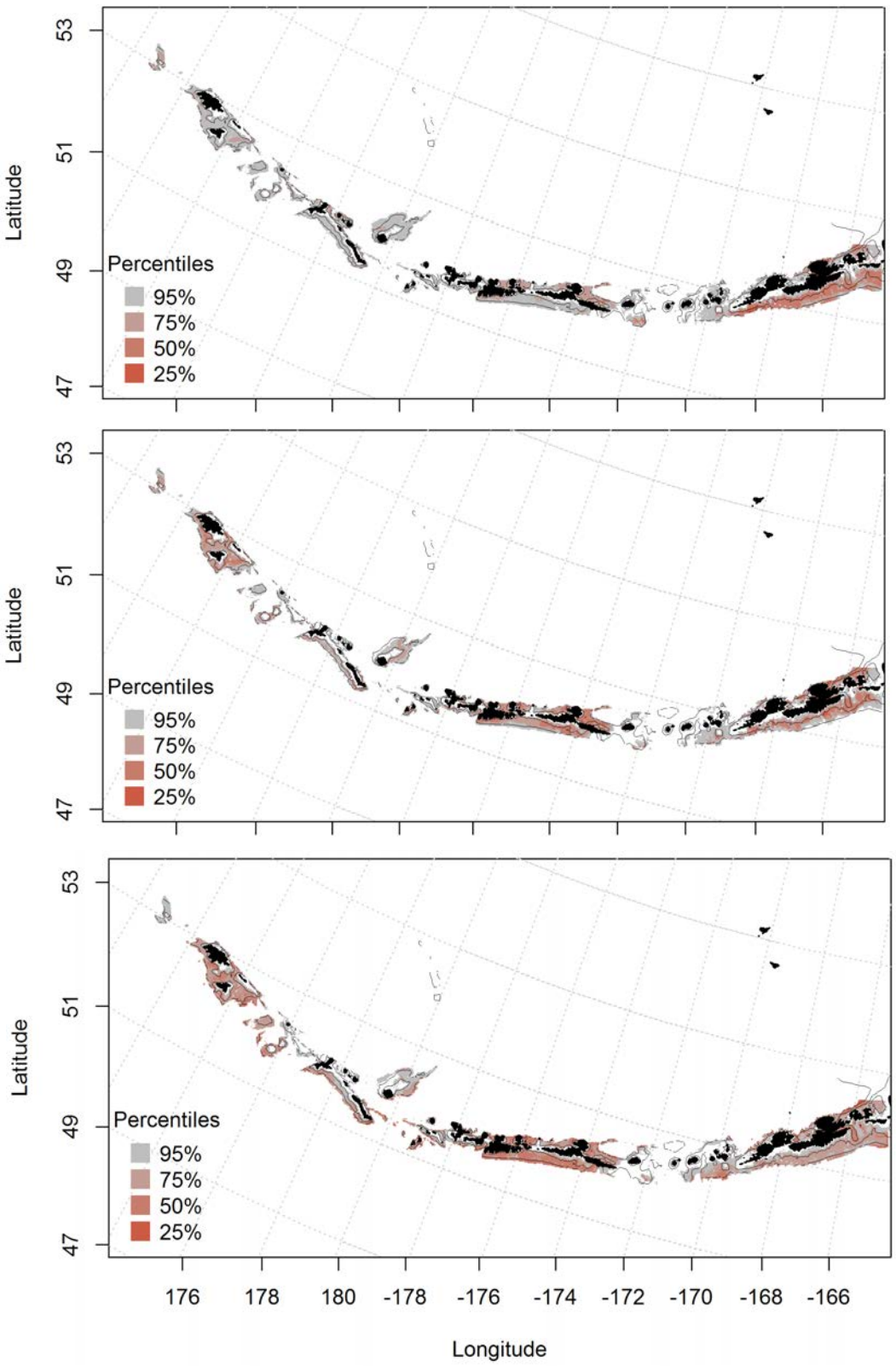

Figure 231. Essential fish habitat predicted for Aleutian skate during fall (top panel), winter (middle panel) and spring (bottom panel) from summertime commercial catches.

Mud skate (*Bathyraja taranetzi*)

Summertime distribution of juvenile and adult Mud skate from bottom trawl surveys of the Aleutian Islands -- A hurdle-GAM model was used to predict the presence and absence of juvenile Mud skate and explained 85% of the variability in CPUE in the bottom trawl survey training data and 86% of the variability in the test data set. Bottom depth and geographic location were the most important variables explaining the distribution of juvenile Mud skate. The model explained 26% of the deviance, and correctly classified 78% of the training and test data sets. Predicted suitable habitat was strongest near Agattu, Attu, Atka, and Unalaska Island (Figure 232).

The second part of the hurdle model found geographic location and ocean color influence the cpue of juvenile Mud skate the most. The model explained 28% of the training data, 10% of the test data, and 28% of the deviance. The model predicted higher CPUE throughout the AI than in the PA GAM (though was similarly distributed), and was absent in large passes (Figure 233).

A maximum entropy model predicting the probability of suitable habitat of adult Mud skate explained 90% of the training data variability in CPUE in the bottom trawl survey, and 79% of the variability in the test data set. Bottom depth, slope, and current speed were the most important variables explaining probable suitable habitat of adult Mud skate (relative importance: 47.5%, 17.2%, and 11.8%, respectively). 80% of the training data and 79% of the test data sets were predicted correctly. The model predicted probable suitable habitat of Mud skates throughout the AI and highest near Nikolsi and Attu Islands (Figure 234).

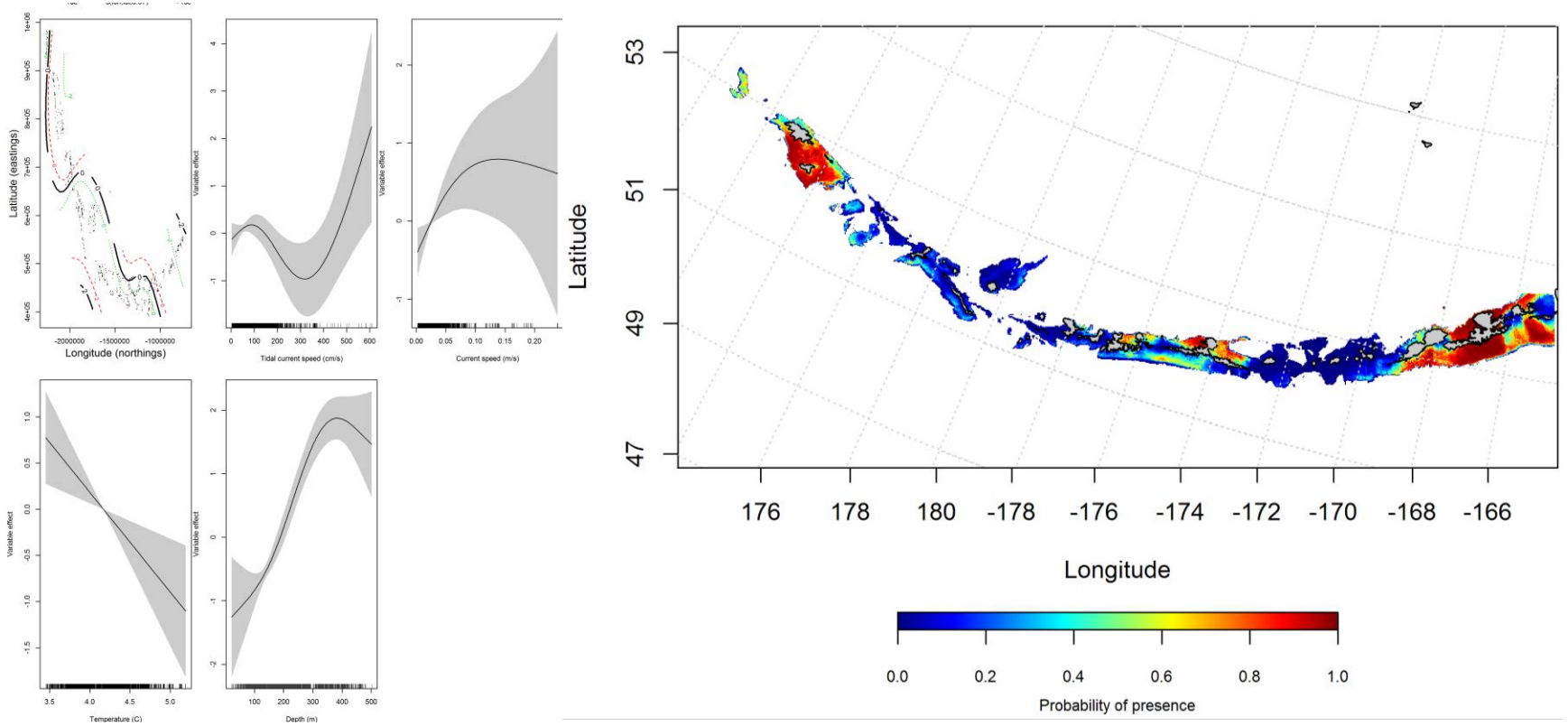

Figure 232. Best-fitting hurdle model effects of retained habitat variables on presence absence (PA) of juvenile Mud skate from summer bottom trawl surveys of the Aleutian Islands (left panel) alongside hurdle-predicted juvenile Mud skate PA (right panel).

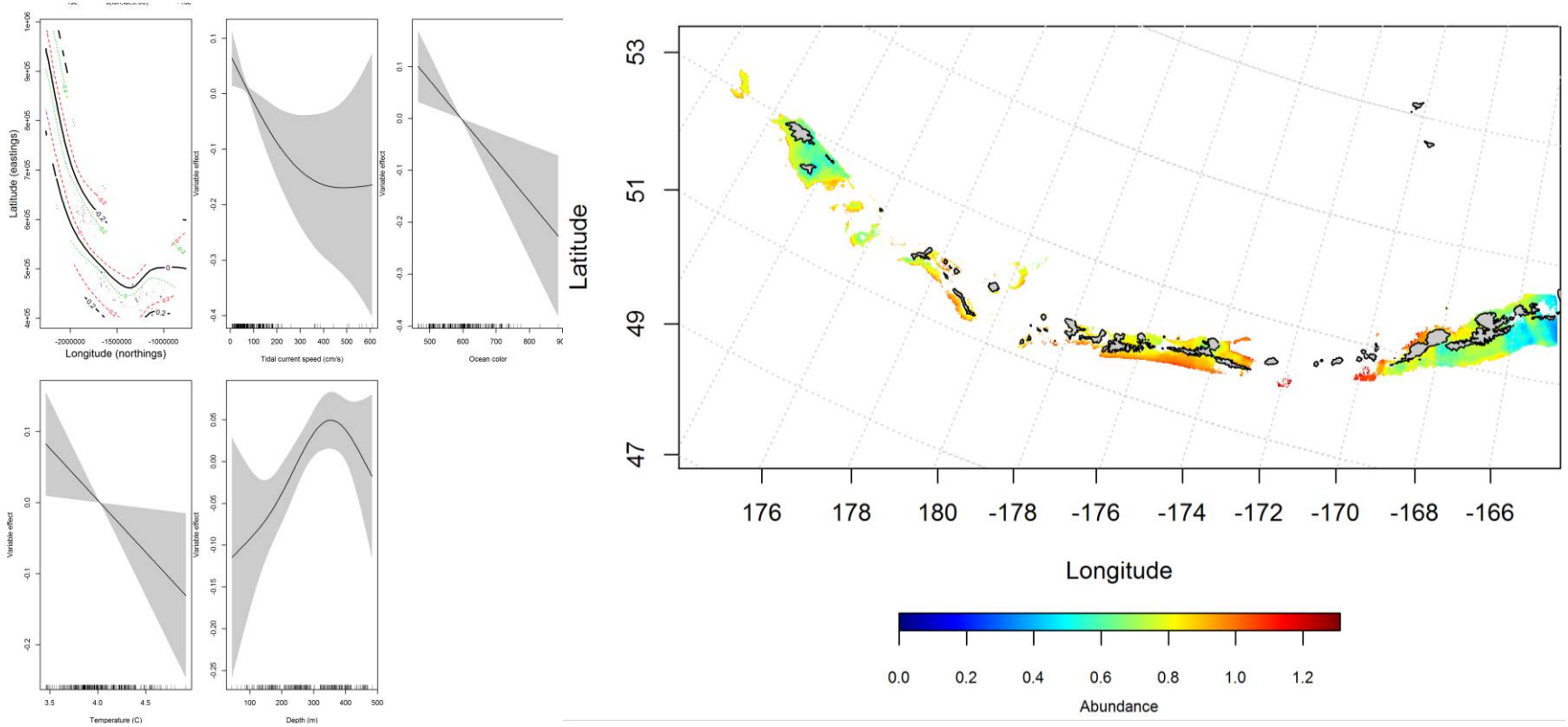

Figure 233. Best-fitting hurdle model effects of retained habitat variables on cpue of juvenile Mud skate from summer bottom trawl surveys of the Aleutian Islands (left panel) alongside hurdle-predicted juvenile Mud skate cpue (right panel).

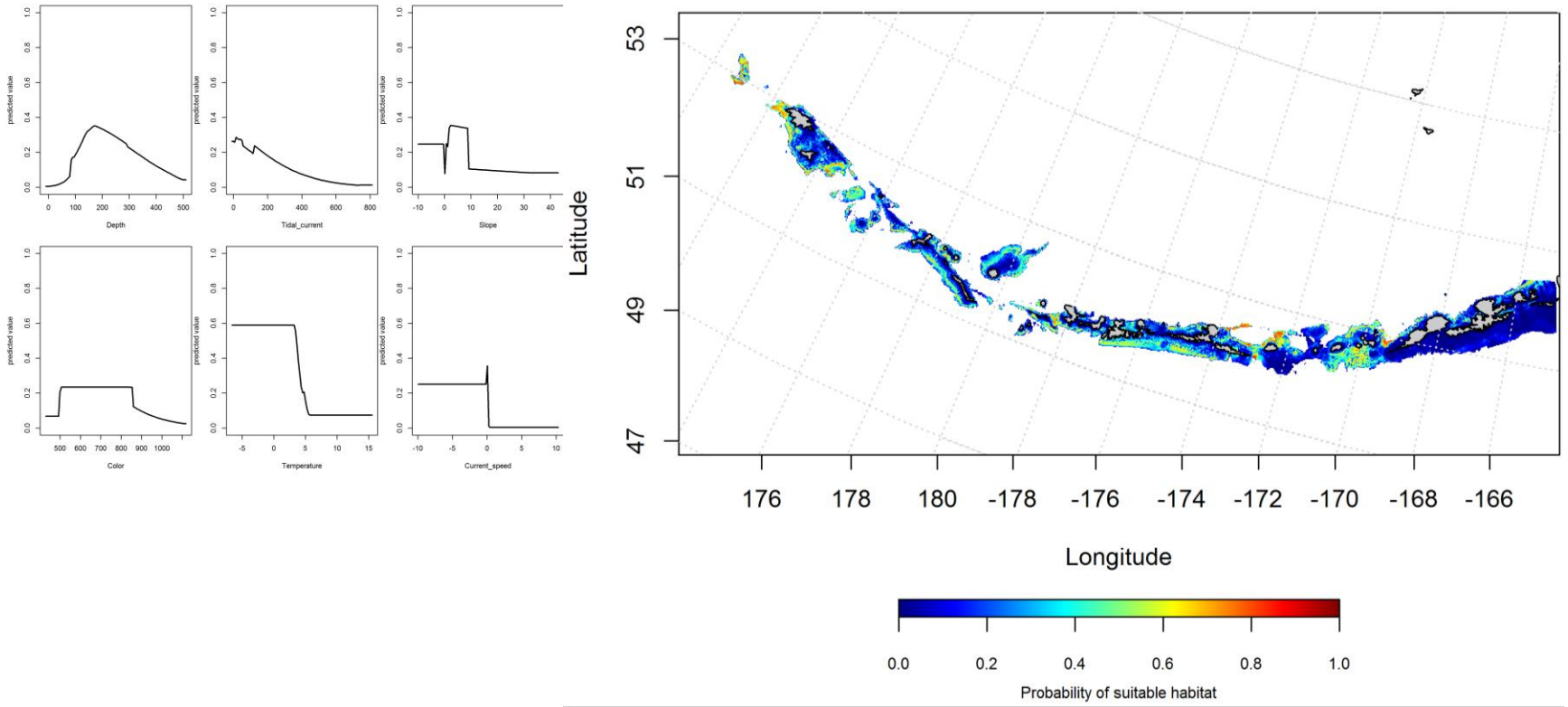

Figure 234. Best-fitting maximum entropy model effects of retained habitat variables on probability of suitable habitat of adult Mud skate from summer bottom trawl surveys of the Aleutian Islands (left panel), alongside maxent-predicted adult Mud skate probable suitable habitat (right panel).

Seasonal distribution of commercial fisheries catches of adult Mud skate in the Aleutian Islands-- Distribution of adult Mud skate in the Aleutian Islands in commercial fisheries catches was generally consistent throughout all seasons. In the fall, bottom depth and ocean color were the most important variables determining the distribution of Mud skate (relative importance: 45.4% and 28.7%). The AUC of the fall maxent model was 93% for the training data and 91% for the test data. 85% of the training data and 91% of the test data sets were predicted correctly. The model predicted probable suitable habitat of Mud skate catches across the AI and highest near Kiska and Amchitka Islands (Figure 235).

In the winter, bottom depth, ocean color, and tidal current were the most important variables determining the distribution of Mud skate (relative importance: 51.3%, 26.8%, and 16.1%, respectively). The AUC of the winter maxent model was 98% for the training data and 91% for the test data. 93% of the training data cases and 91% of the test data sets were predicted correctly. The model predicted probable winter suitable habitat Mud skate across the AI and highest near Atka Island (Figure 236).

In the spring, bottom depth and ocean color were also the most important variables determining the distribution of Mud skate (relative importance: 46.7% and 31.9%). The AUC of the spring model was 92% for the training data and 89% for the test data. 82% of the training data and 89% of the test data was correctly classified. The spring model predicted probable suitable habitat of Mud skate across the AI, but highest near Adak and Atka Islands (Figure 237).

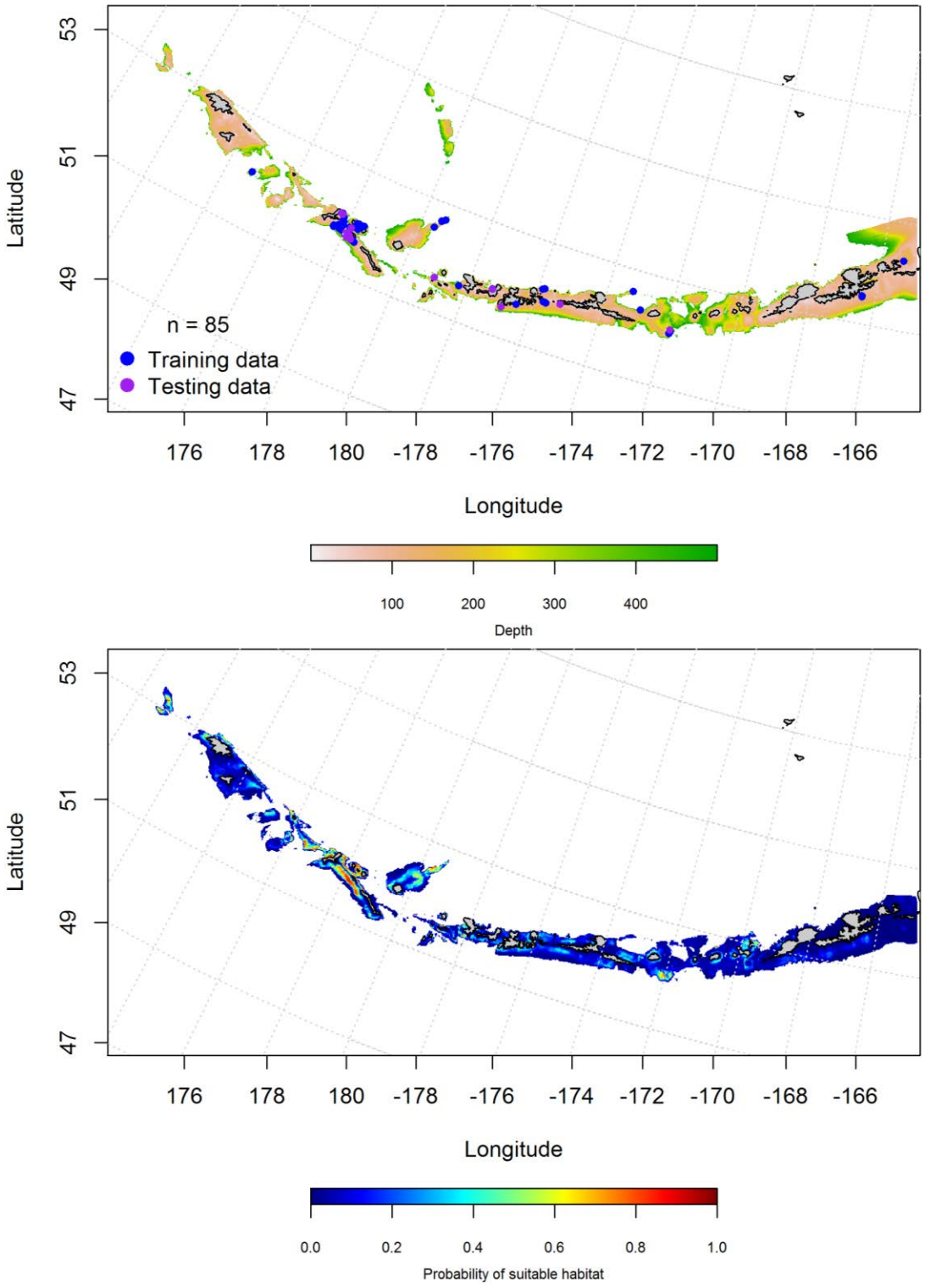

Figure 235. Locations of fall (September-November) commercial fisheries catches of adult Mud skate (top panel). Blue points were used to train the maximum entropy model predicting the probability of suitable fall habitat supporting commercial catches of adult Mud skate (bottom panel) and the purple points were used to validate the model.

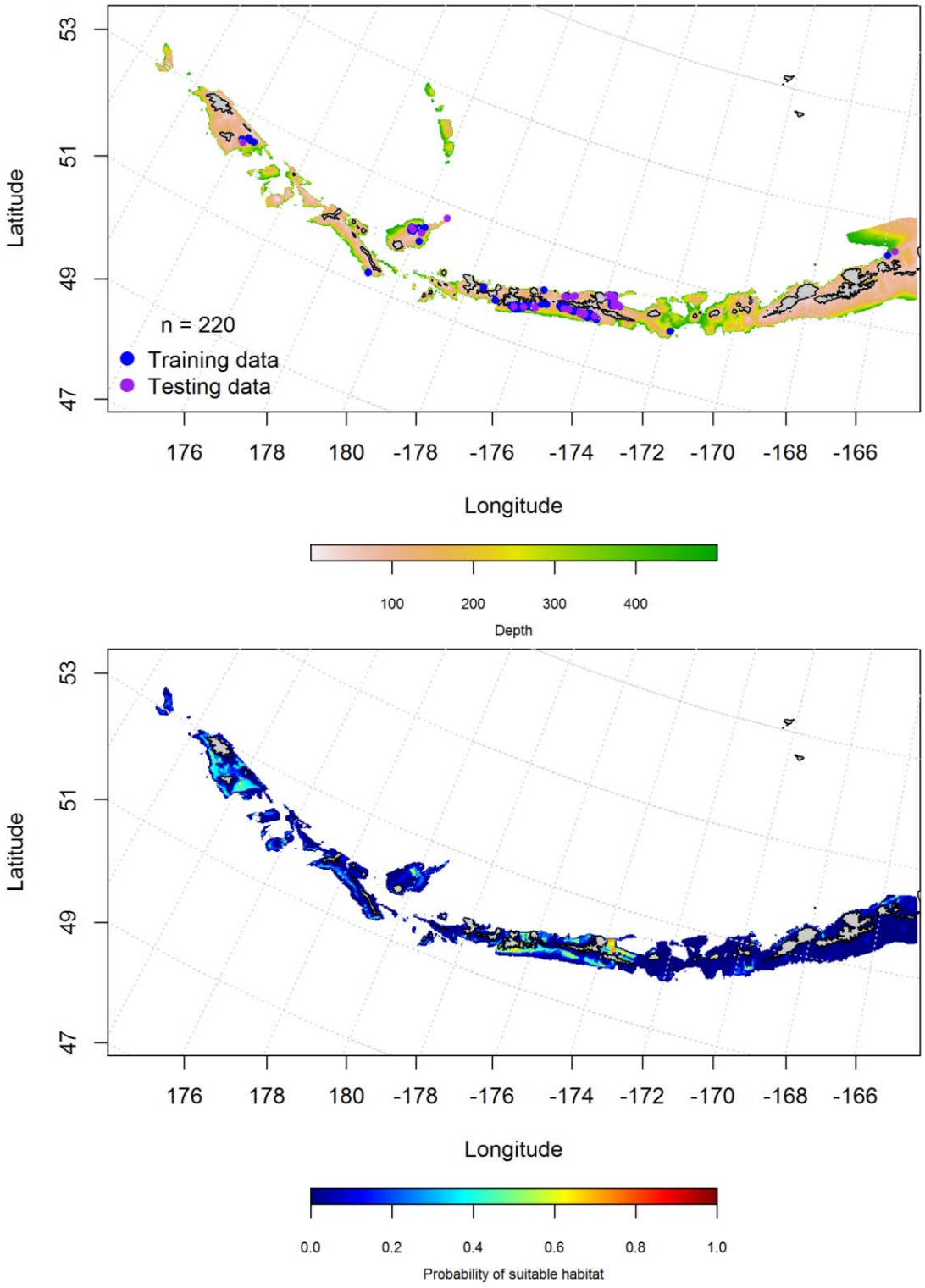

Figure 236. Locations of winter (December-February) commercial fisheries catches of adult Mud skate (top panel). Blue points were used to train the maximum entropy model predicting the probability of suitable winter habitat supporting commercial catches of adult Mud skate (bottom panel) and the purple points were used to validate the model.

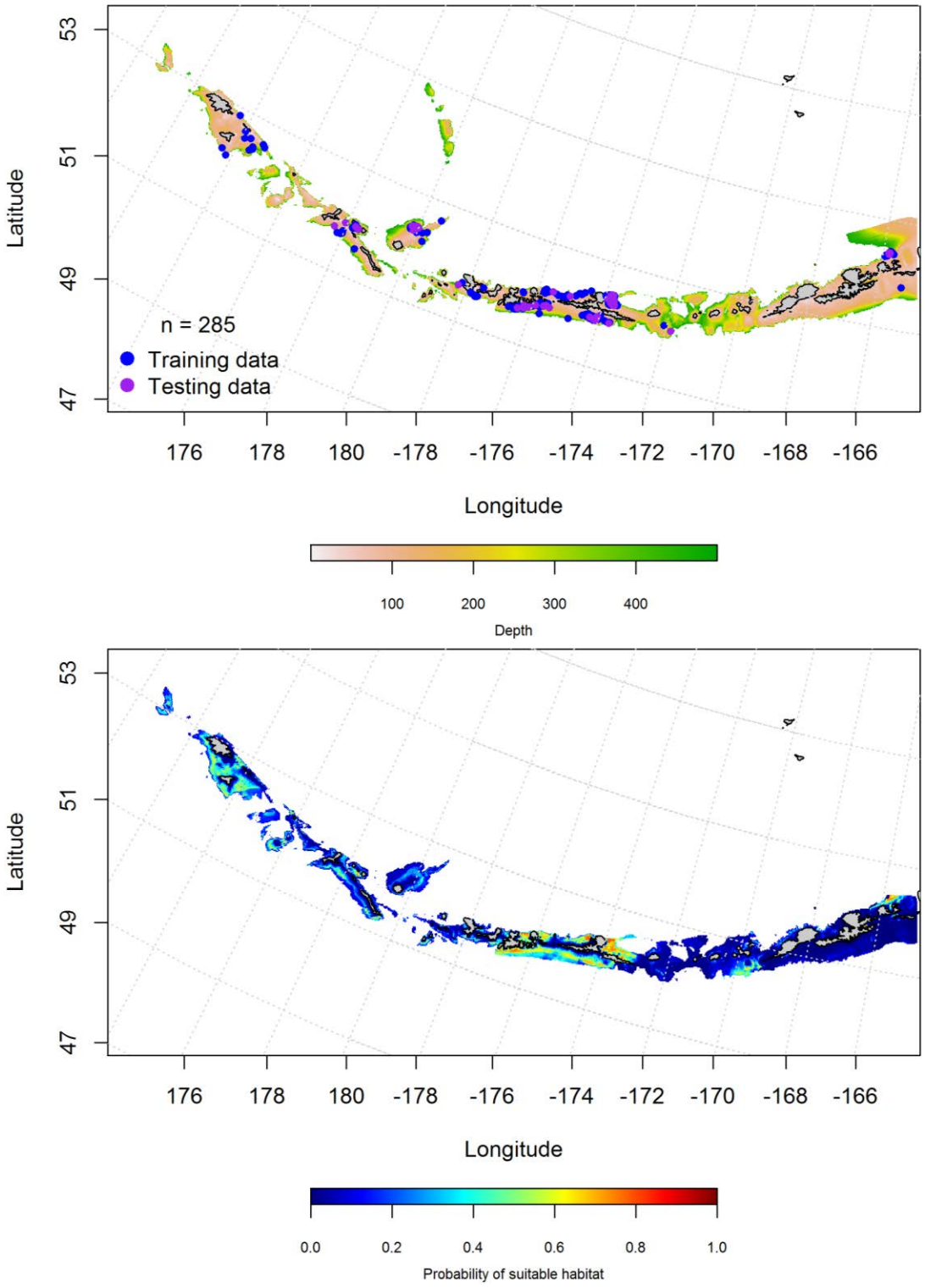

Figure 237. Locations of spring (March-May) commercial fisheries catches of adult Mud skate (top panel). Blue points were used to train the maximum entropy model predicting the probability of suitable spring habitat supporting commercial catches of adult Mud skate (bottom panel) and the purple points were used to validate the model.

Aleutian Islands Mud skate Essential Fish Habitat Maps and Conclusions --

Summertime EFH of Mud skate juveniles and adults was distributed across the AI, though less abundant with adults (Figure 238). Juveniles were more abundant near Adak and Atka Islands, unlike adult Mud skates.

The fall, winter and spring distribution of Mud skate EFH was essentially the same through the seasons (Figure 239). Predicted EFH was not abundant for this species.

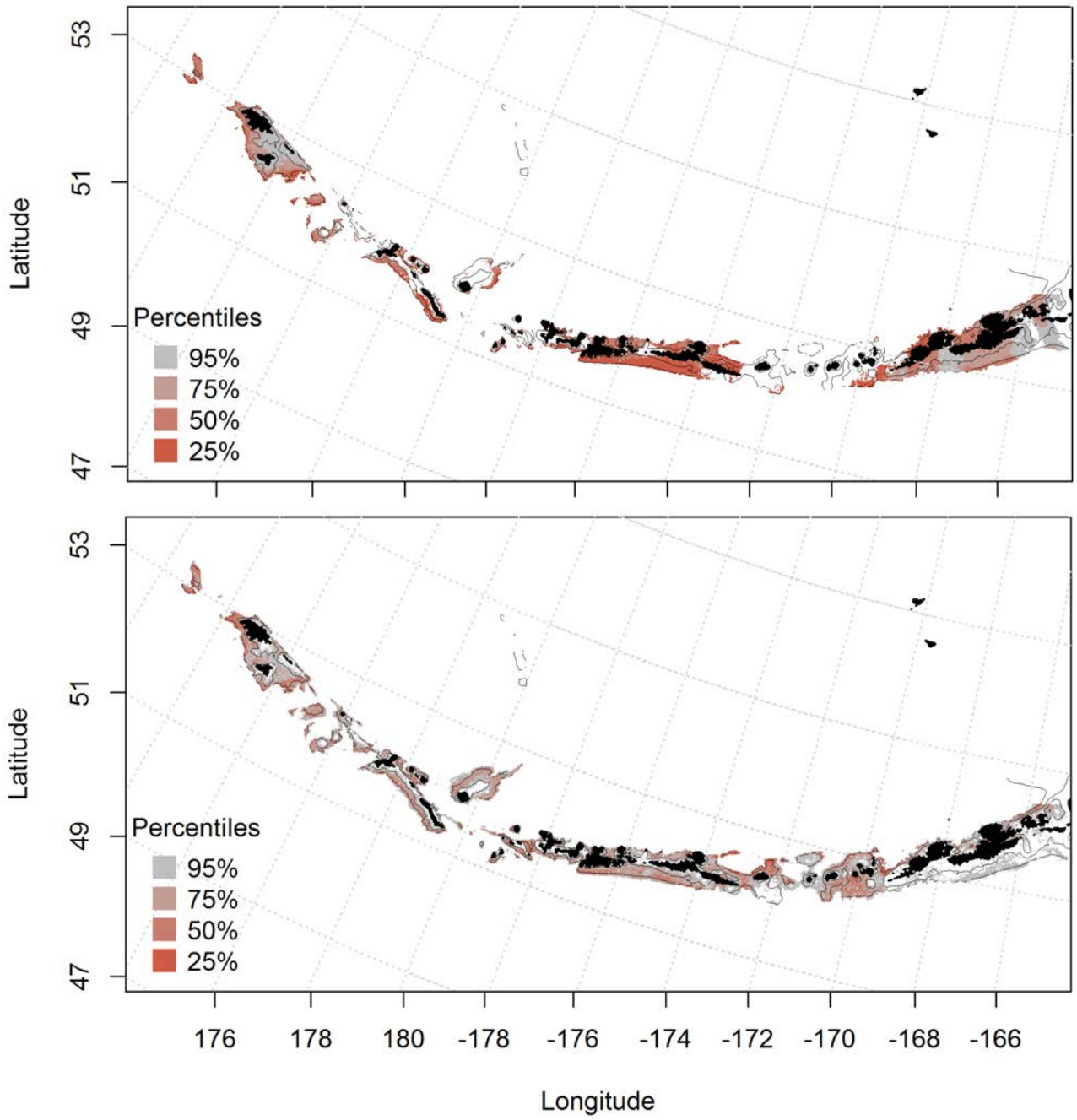

Figure 238. Predicted summer essential fish habitat for Mud skate juveniles and adults (top and bottom panel) from summertime bottom trawl surveys.

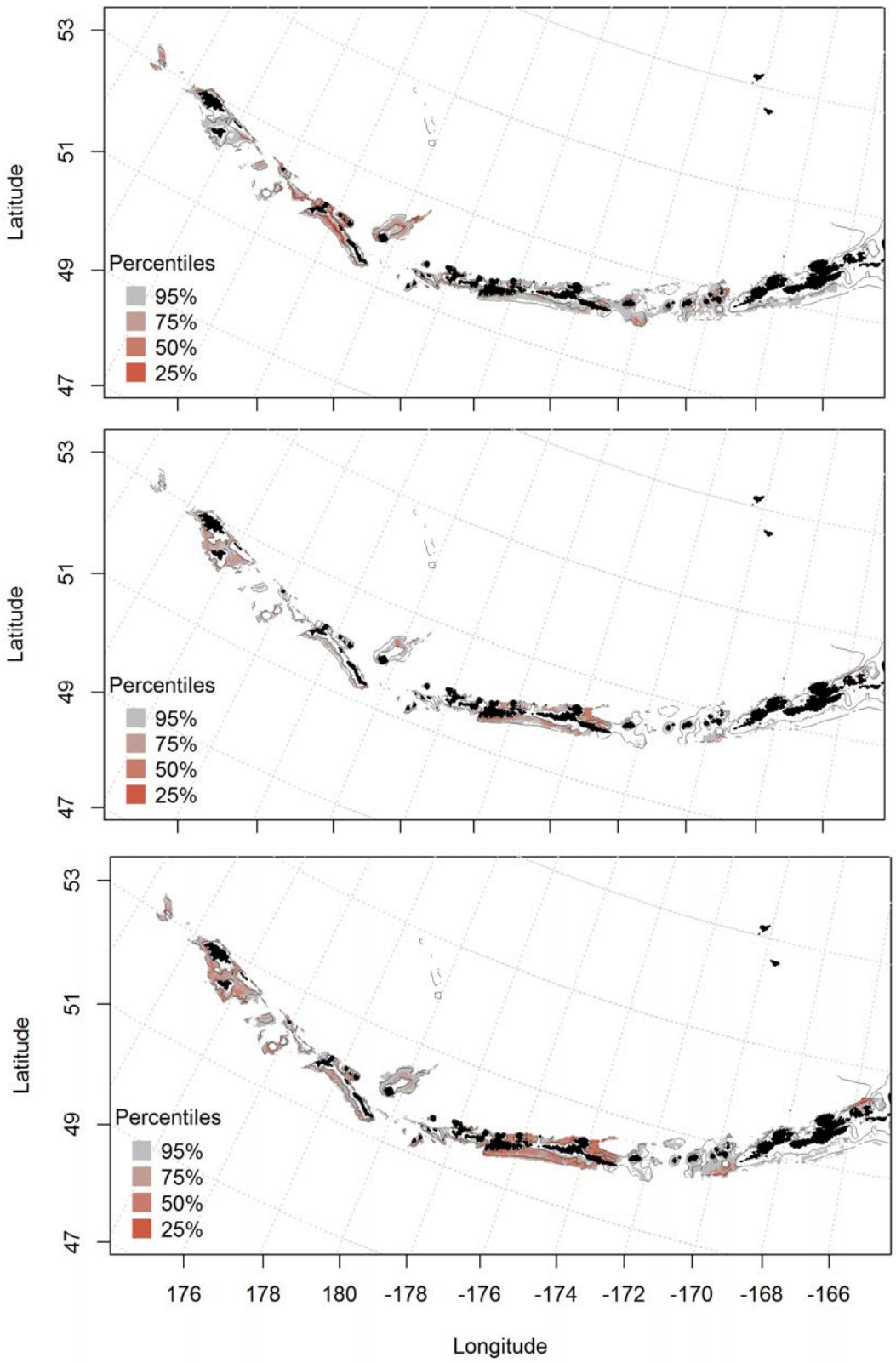

Figure 239. Essential fish habitat predicted for Mud skate during fall (top panel), winter (middle panel) and spring (bottom panel) from summertime commercial catches.

3.5 Invertebrates

Golden king crab (*Lithodes aequispinus*)

Summertime distribution of Golden king crab from bottom trawl surveys of the Aleutian Islands -- A hurdle-GAM model was used to predict the presence and absence of Golden king crab and explained 36.4% of the deviance, 88% of the variability in the training data, and 89% of the variability in the test data set. Bottom depth, geographic location, and coral presence were the most important variables explaining the distribution of Golden king crab. The model correctly classified 82% of the training data set and 84% of the test data set. The model predicted suitable habitat highest in Seguam pass and Near pass in the western AI (Figure 240).

The second part of the hurdle model found current speed influenced the CPUE of Golden king crab the most, and explained 9.5% of the deviance, 10% of the training data, and 4% of the test data. The model predicted highest suitable habitat in a similar pattern as the PA GAM, but also predicted suitable habitat north of Semisopochnoi Island (Figure 241).

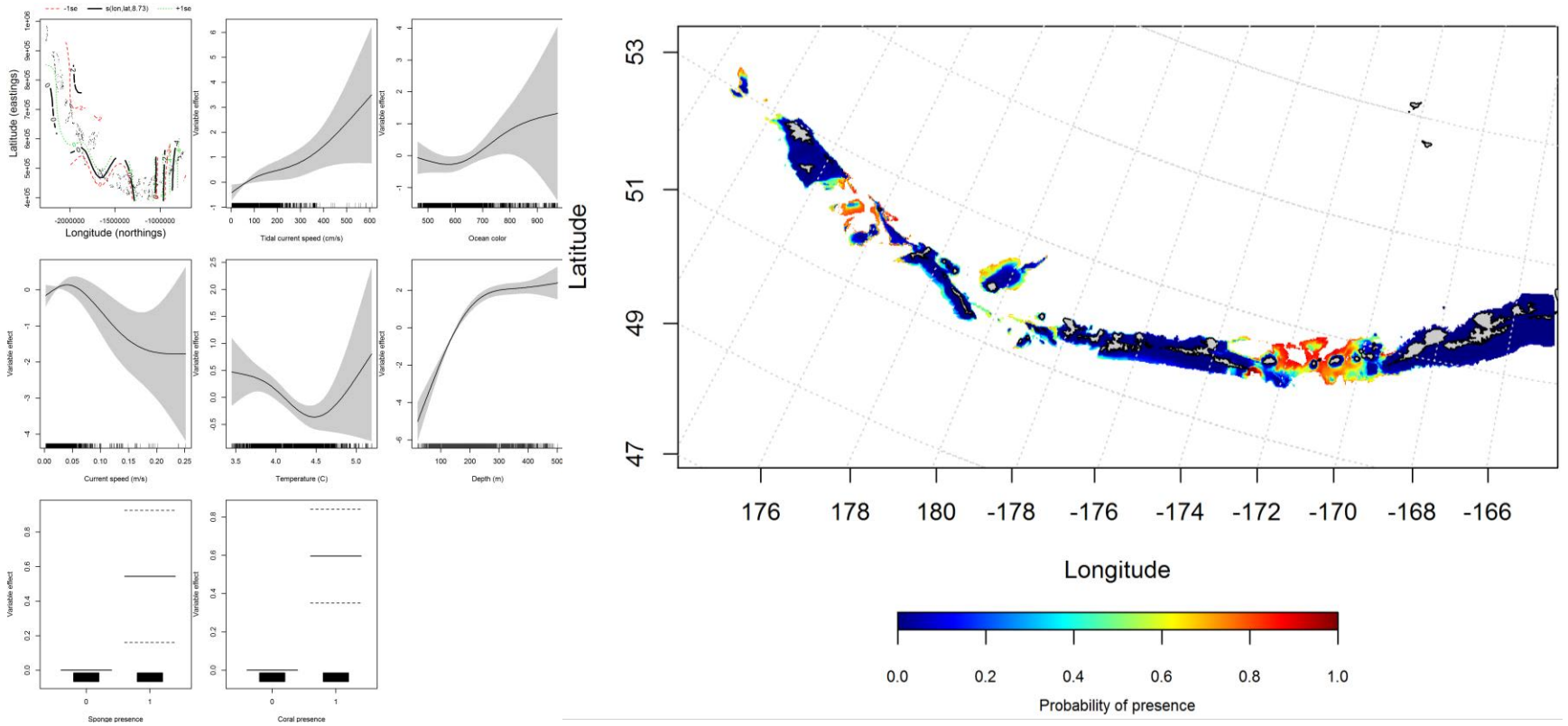

Figure 240. Best-fitting hurdle model effects of retained habitat variables on presence absence (PA) of Golden king crab from summer bottom trawl surveys of the Aleutian Islands (left panel) alongside hurdle-predicted Golden king crab PA (right panel).

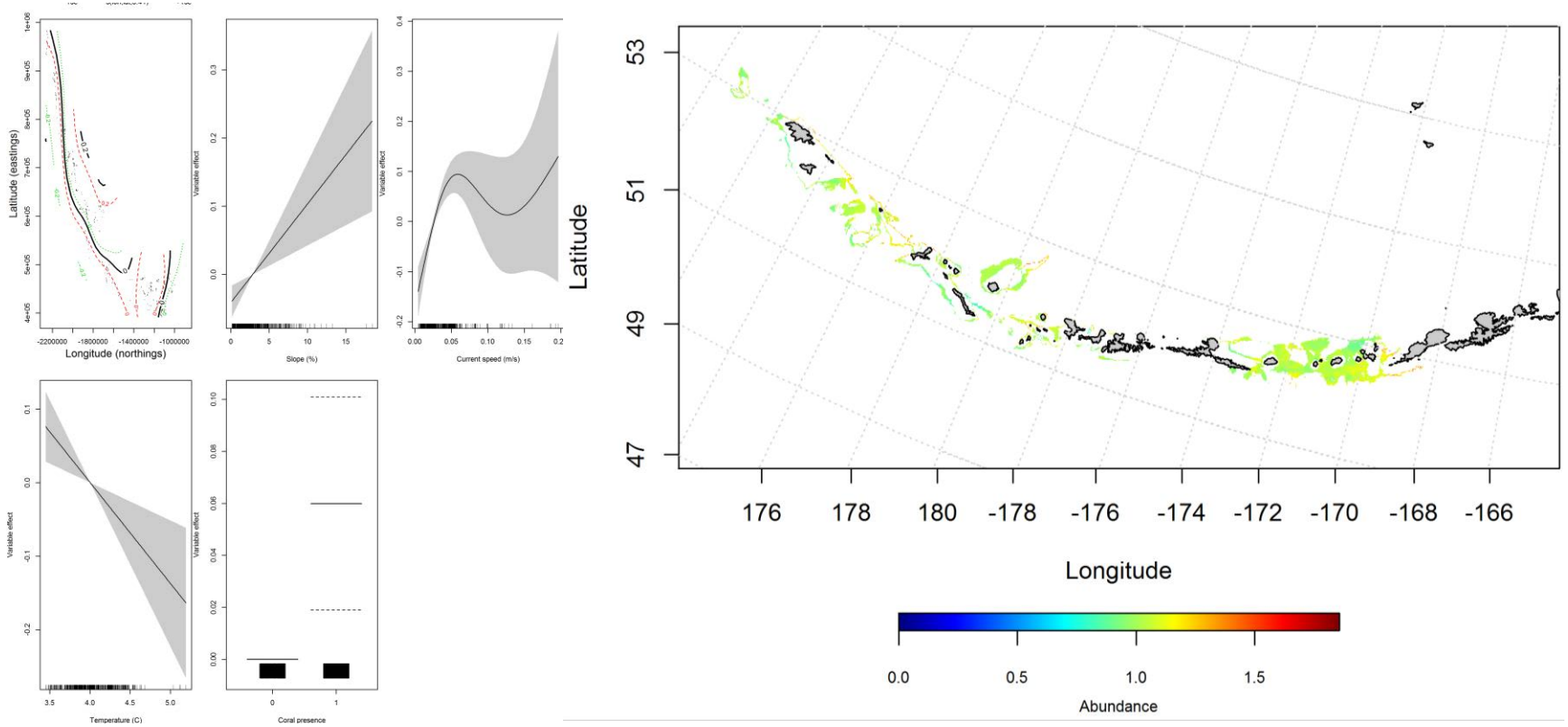

Figure 241. Best-fitting hurdle model effects of retained habitat variables on cpue of Golden king crab from summer bottom trawl surveys of the Aleutian Islands (left panel) alongside hurdle-predicted Golden king crab cpue (right panel).

Seasonal distribution of commercial fisheries catches of Golden king crab in the Aleutian Islands-- Distribution of Golden king crab in the Aleutian Islands in commercial fisheries catches was generally consistent throughout all seasons. In the fall, bottom temperature, surface color, tidal current, and bottom depth were the most important variables determining the distribution of Golden king crab (relative importance: 31.6%, 26.9%, 18.1%, and 11.4%, respectively). The AUC of the fall maxent model was 93% for the training data and 85% for the test data. The model correctly correctly classified 86% of the training data and 85% of the test data. The model predicted probable suitable habitat of Golden king crab across the AI and highest in areas with large passes (Figure 242).

There were only 6 instances of Golden King crab across the AI in the winter months (Figure 243). There were not enough cases to run the winter model.

In the spring, bottom depth and bottom temperature were the most important variables determining the distribution of Golden king crab (relative importance: 65.3% and 13.9%). The AUC of the spring maxent model was 92% for the training data and 85% for the test data. The model correctly classified 83% of the training data and 85% of the test data. As with the fall, the model predicted probable suitable habitat of Golden king crab across the AI and highest in areas with large passes (Figure 244).

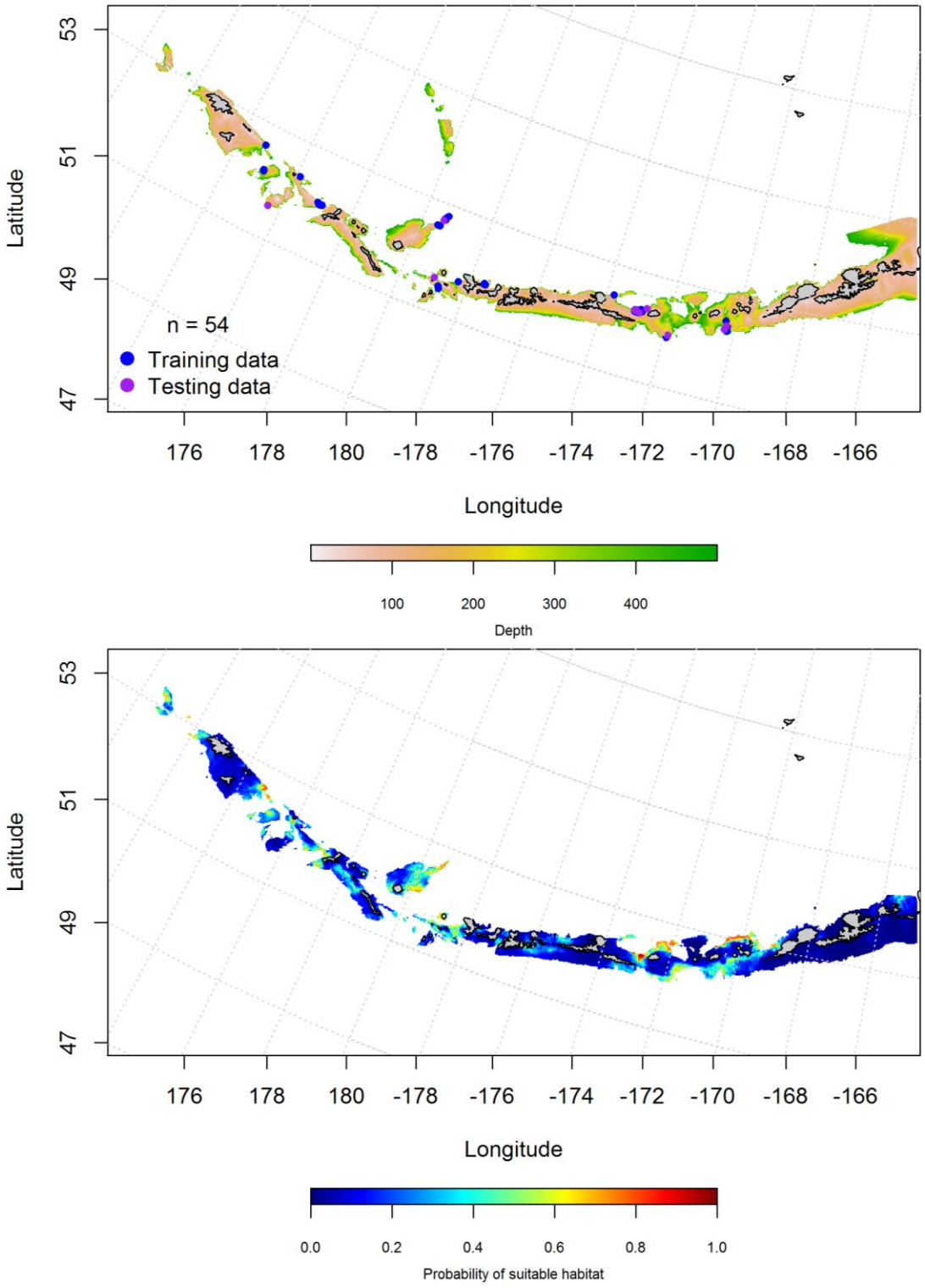

Figure 242. Locations of fall (September-November) commercial fisheries catches of Golden king crab (top panel). Blue points were used to train the maximum entropy model predicting the probability of suitable fall habitat supporting commercial catches of Golden king crab (bottom panel) and the purple points were used to validate the model.

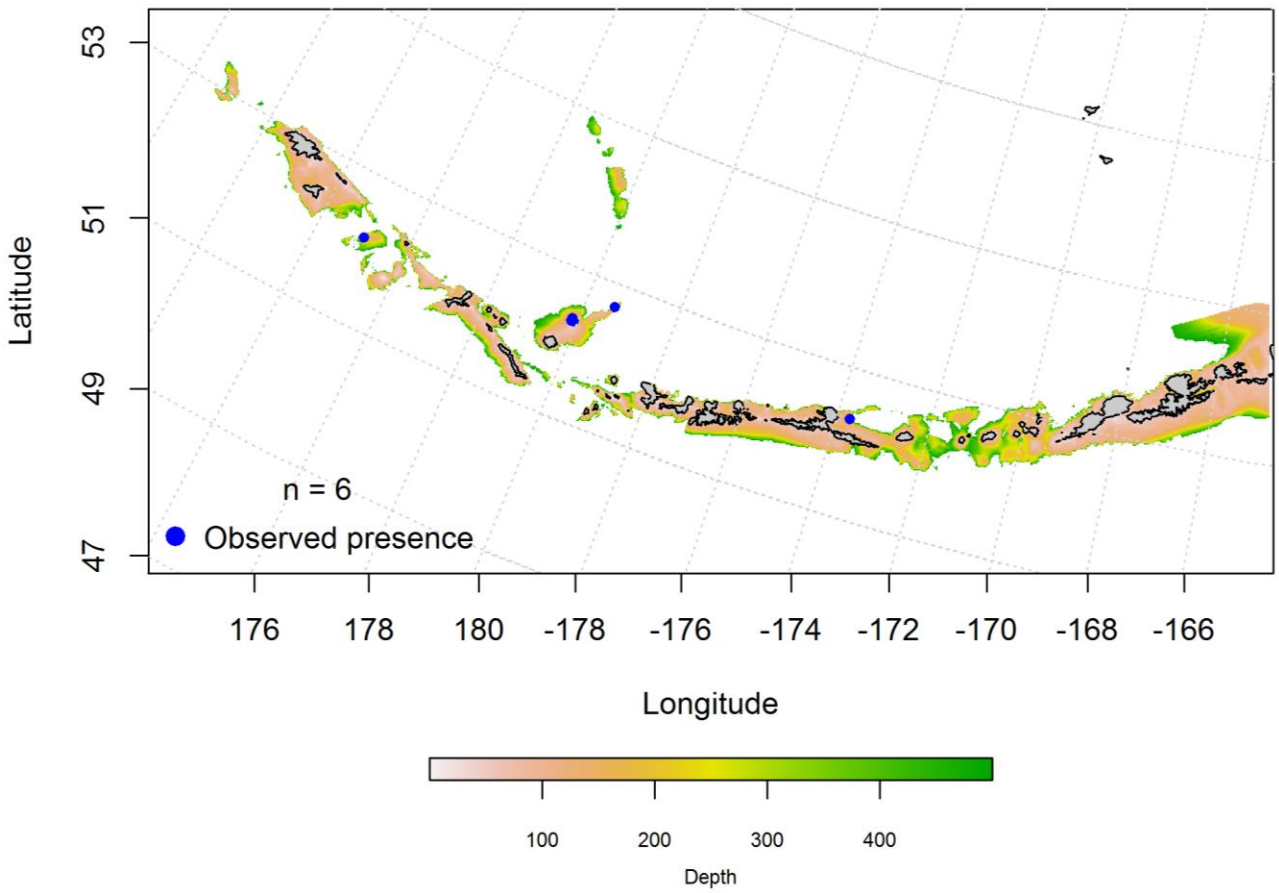

Figure 243. Blue points indicate observed instances of Golden king crab from winter (December-February) commercial fisheries catches.

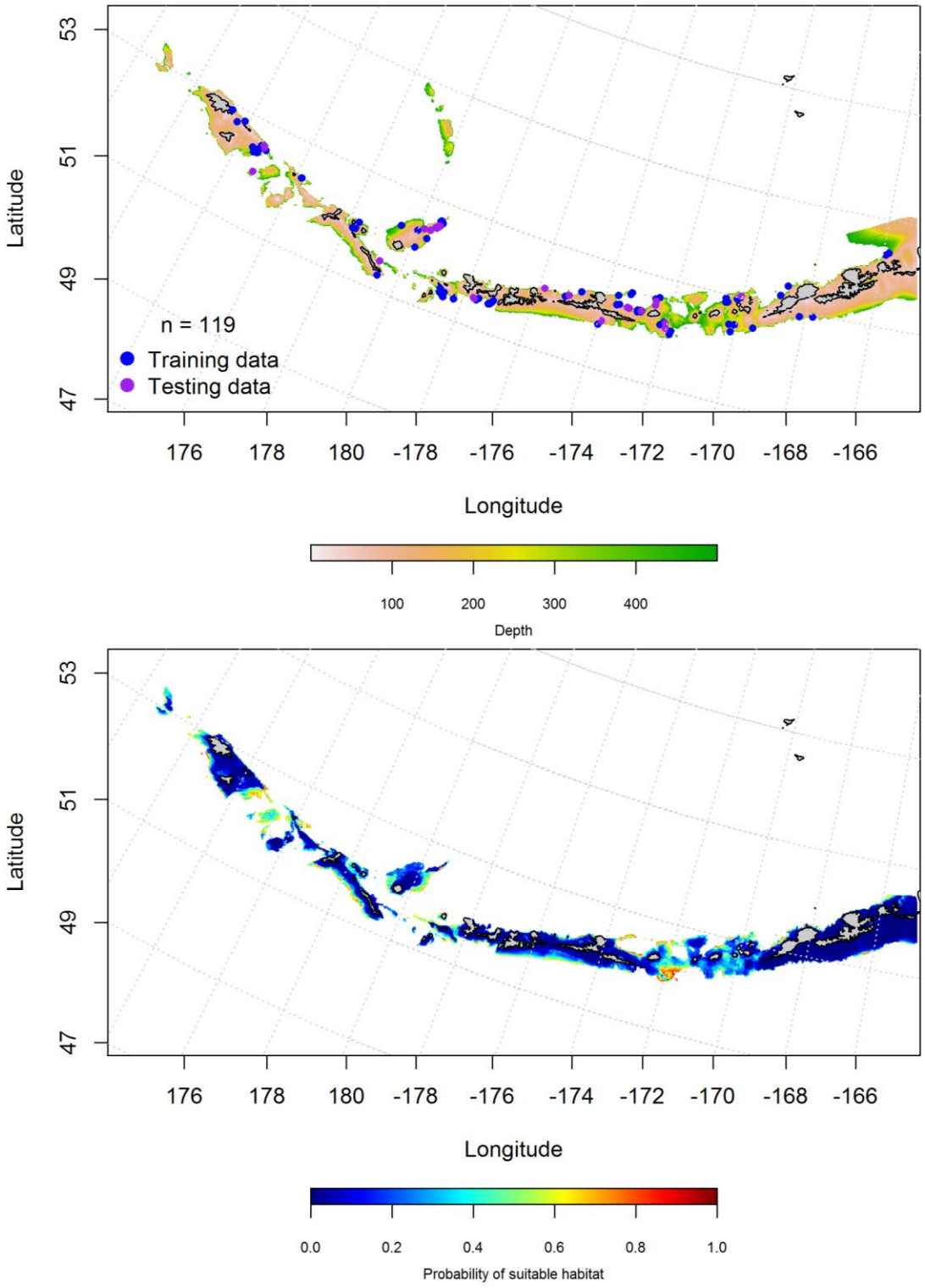

Figure 244. Locations of spring (March-May) commercial fisheries catches of Golden king crab (top panel). Blue points were used to train the maximum entropy model predicting the probability of suitable habitat supporting commercial catches of Golden king crab (bottom panel) and the purple points were used to validate the model.

Aleutian Islands Golden king crab Essential Fish Habitat Maps and Conclusions -- Golden king crab essential fish habitat predicted by the model using summertime bottom trawls is distributed across the AI, though highest in areas with large passes (Figure 245).

The fall and spring distribution of Golden king crab EFH was essentially the same as the summer, with EFH distributed across the AI and highest in areas with large passes (Figure 246).

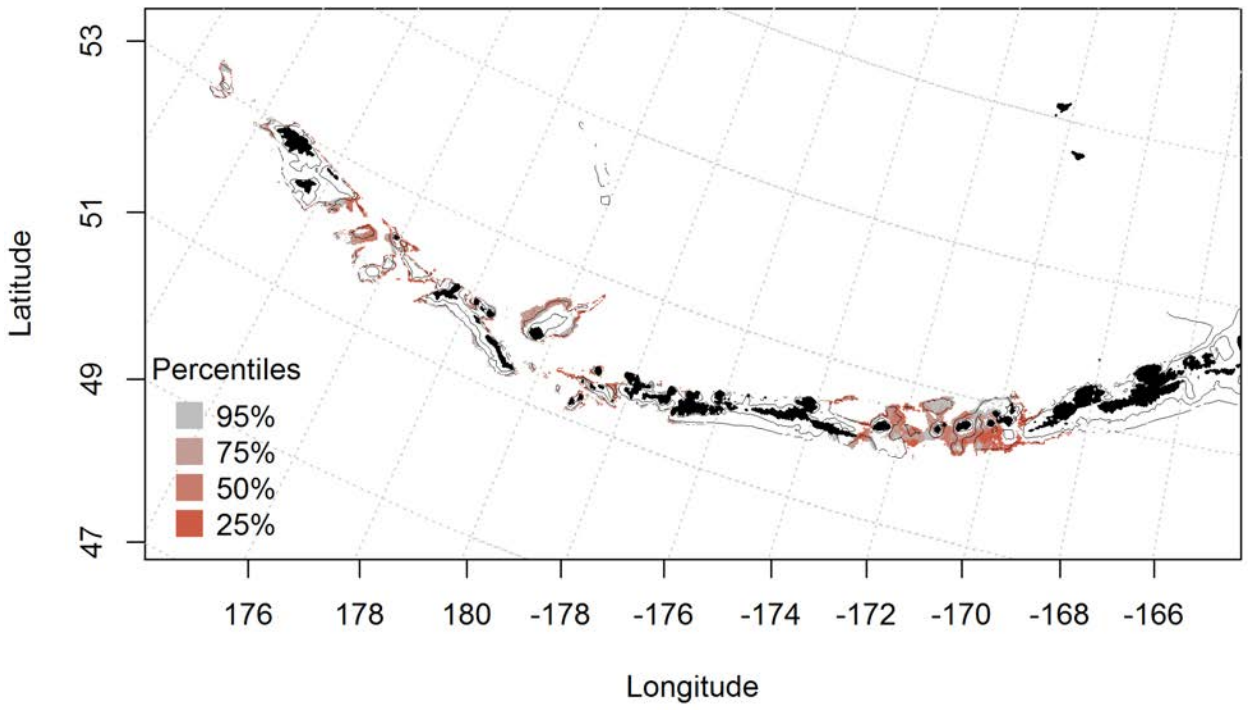

Figure 245. Predicted summer essential fish habitat for Golden king crab from summertime bottom trawl surveys.

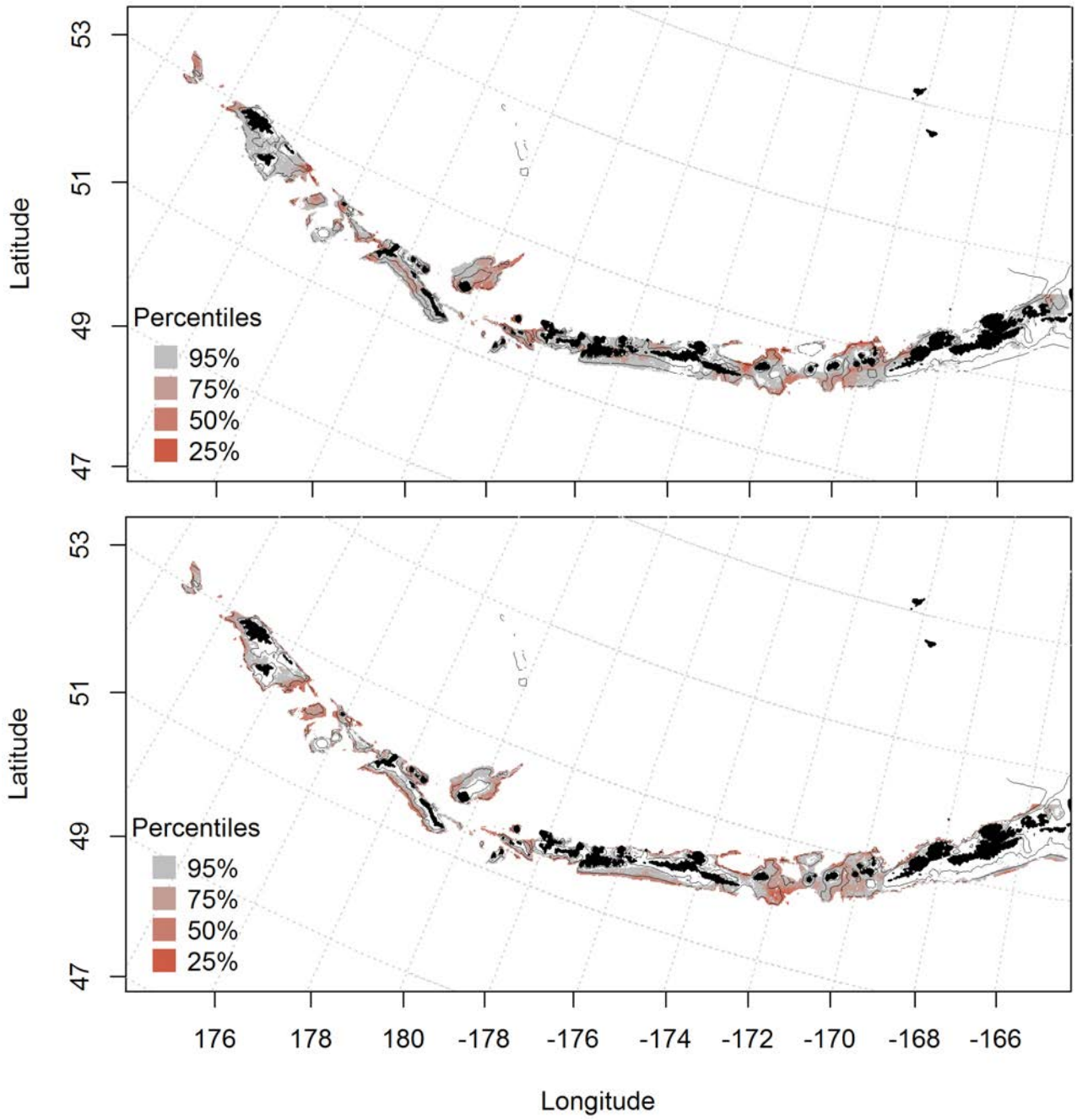

Figure 246. Essential fish habitat predicted for Golden king crab during fall (top panel) and spring (bottom panel) from summertime commercial catches.

Pacific giant octopus (*Enteroctopus dofleini*)

Summertime distribution of Pacific giant octopus from bottom trawl surveys of the Aleutian Islands -- A hurdle-GAM model was used to predict the presence and absence of Pacific giant octopus and explained 71% of the variability in the training data, and 66% of the variability in the test data set. Sponge presence and bottom temperature were the most important variables explaining the distribution of Pacific giant octopus. The model correctly explained 8.4% of the deviance, and correctly classified 64% of the training data set and 60% of the test data set. The model predicted probable suitable habitat across the AI chain and highest near Amlia Island (Figure 247).

The second part of the hurdle model found bottom depth and geographic location influence the CPUE of Pacific giant octopus the most, and explained 6.5% of the deviance, and 7% of the training and test data sets. The model predicted probable suitable habitat across the AI (Figure 248).

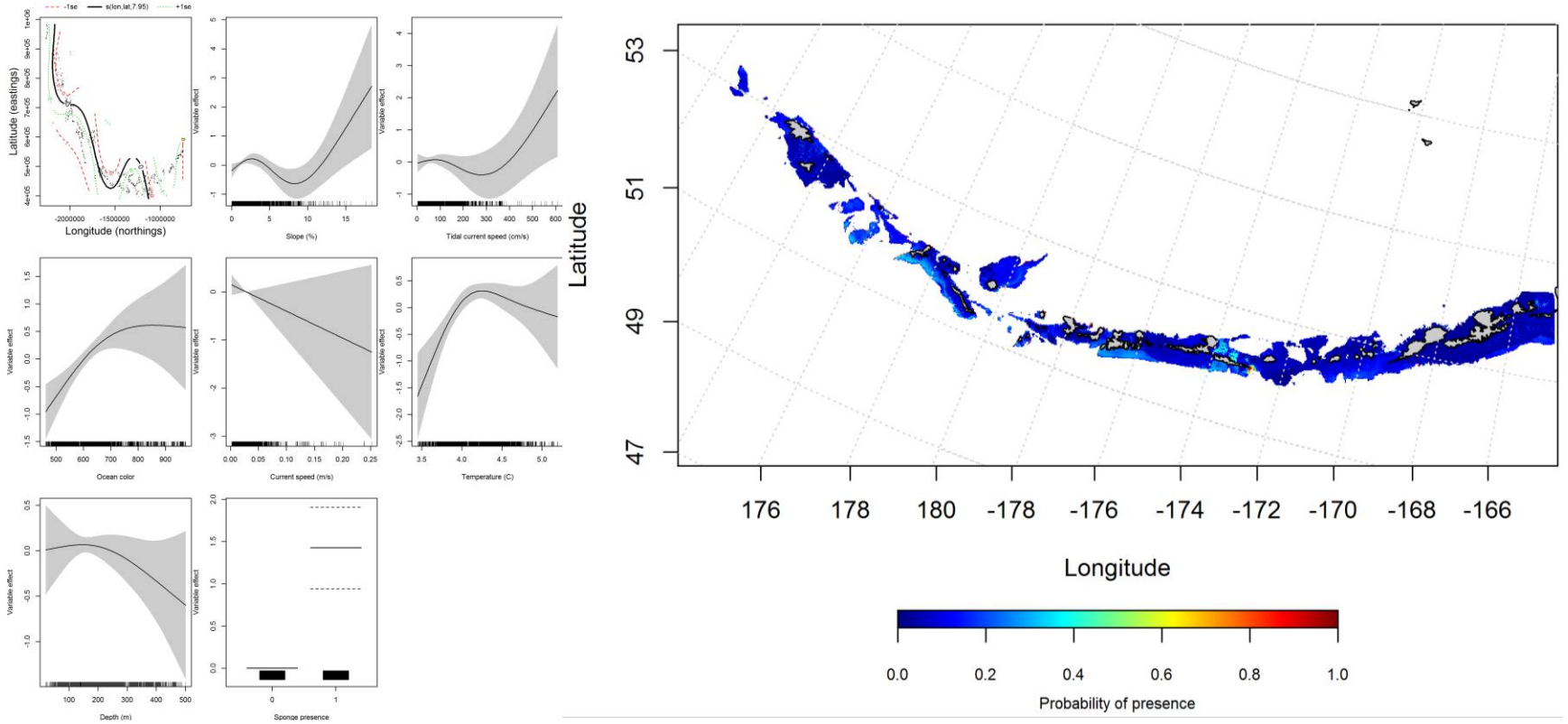

Figure 247. Best-fitting hurdle model effects of retained habitat variables on presence absence (PA) of Pacific giant octopus from summer bottom trawl surveys of the Aleutian Islands (left panel) alongside hurdle-predicted Pacific giant octopus PA (right panel).

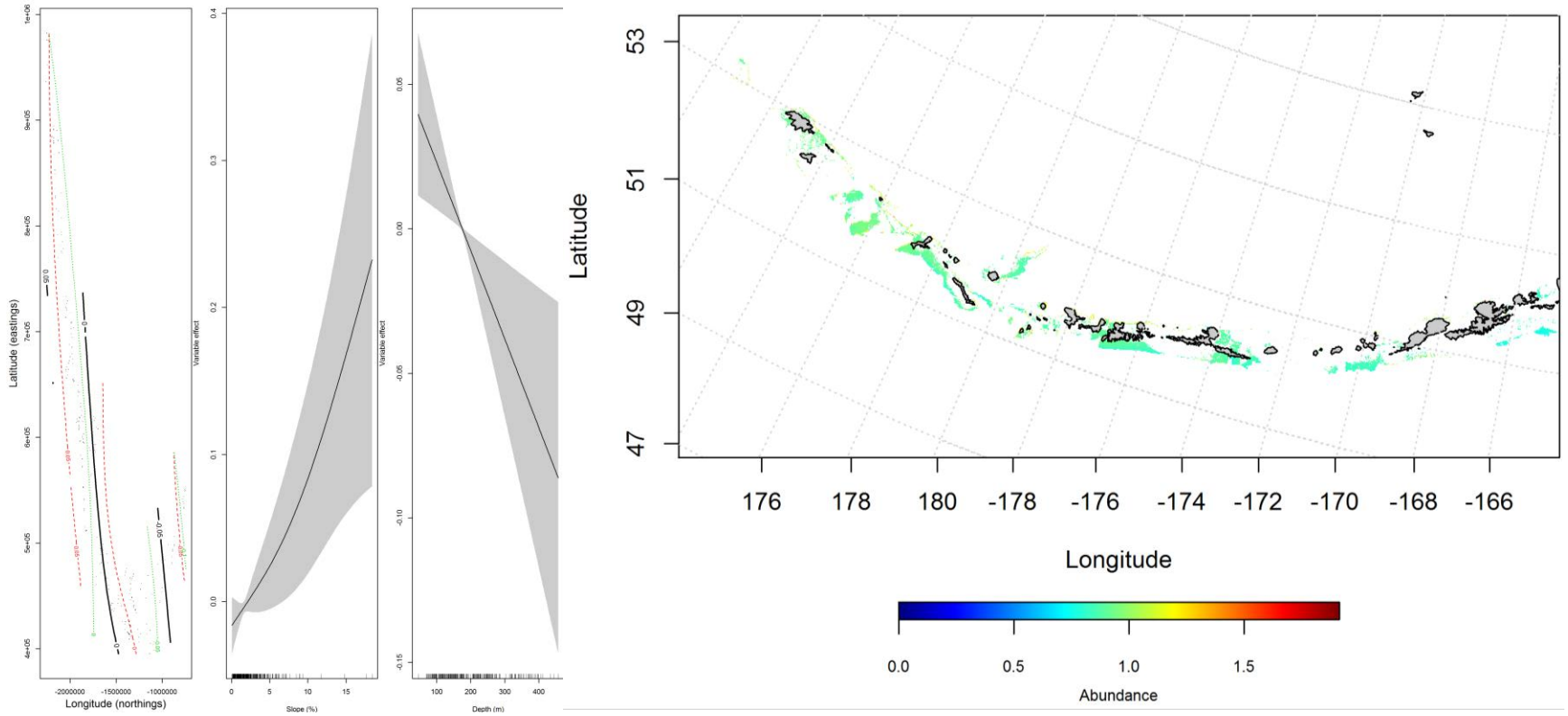

Figure 248. Best-fitting hurdle model effects of retained habitat variables on cpue of Pacific giant octopus from summer bottom trawl surveys of the Aleutian Islands (left panel) alongside hurdle-predicted Pacific giant octopus cpue (right panel).

Seasonal distribution of commercial fisheries catches of unidentified octopus species in the Aleutian Islands-- Distribution of unidentified octopus species in the Aleutian Islands in commercial fisheries catches was generally consistent throughout all seasons. In the fall, bottom depth, tidal current, ocean surface color, and current speed were the most important variables determining the distribution of unidentified octopus species (relative importance: 29.8%, 25.5%, 16.9%, and 15.8%, respectively). The AUC of the fall maxent model was 94% for the training data and 79% for the test data. The model correctly classified 89% of the training data and 7% of the test data. The model predicted probable suitable habitat of unidentified octopus species across that AI and highest near Akutan Island (Figure 249).

In the winter, surface color, bottom depth, and bottom temperature were the most important variables determining the distribution of unidentified octopus species (relative importance: 39.7%%, 33%, and 15.6%, respectively). The AUC of the winter maxent model was 94% for the training data and 84% for the test data. The model correctly classified 86% of the training data and 84% of the test data. The model predicted probable suitable habitat of unidentified octopus species across that AI and highest near Akutan, Atka, and Attu Islands (Figure 250).

In the spring, bottom depth, surface color, and tidal current were the most important variables determining the distribution of unidentified octopus species (relative importance: 44.7%, 27%, and 13%, respectively). The AUC of the spring maxent model was 93% for the training data and 84% for the test data. The model correctly classified 86% of the training data and 84% of the test data. The model predicted probable suitable habitat of unidentified octopus species across that AI and highest near Atka, Adak, and Attu Islands (Figure 251).

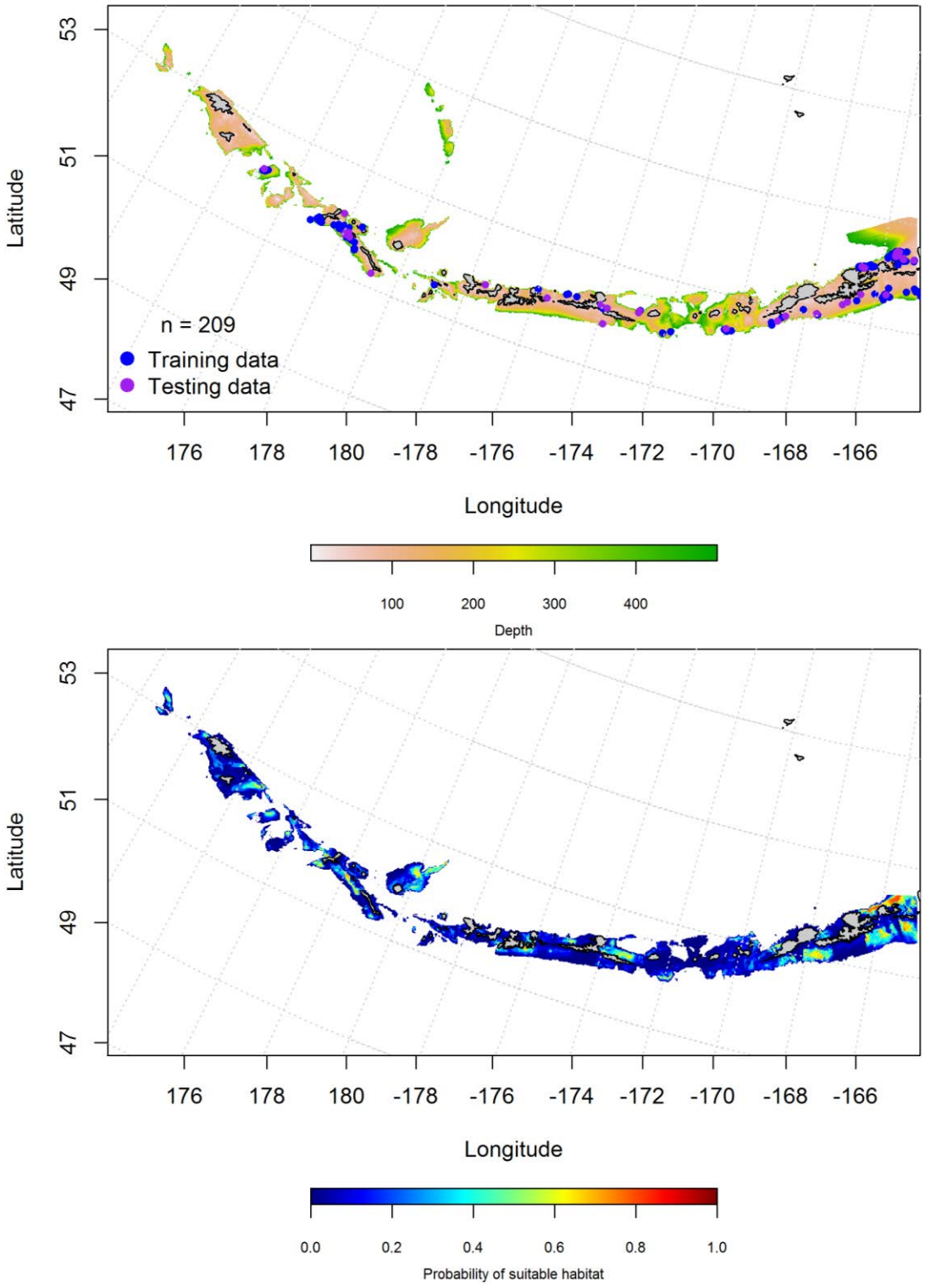

Figure 249. Locations of fall (September-November) commercial fisheries catches of unidentified octopus species (top panel). Blue points were used to train the maximum entropy model predicting the probability of suitable habitat supporting commercial fisheries of

unidentified octopus species (bottom panel) and the purple points were used to validate the model.

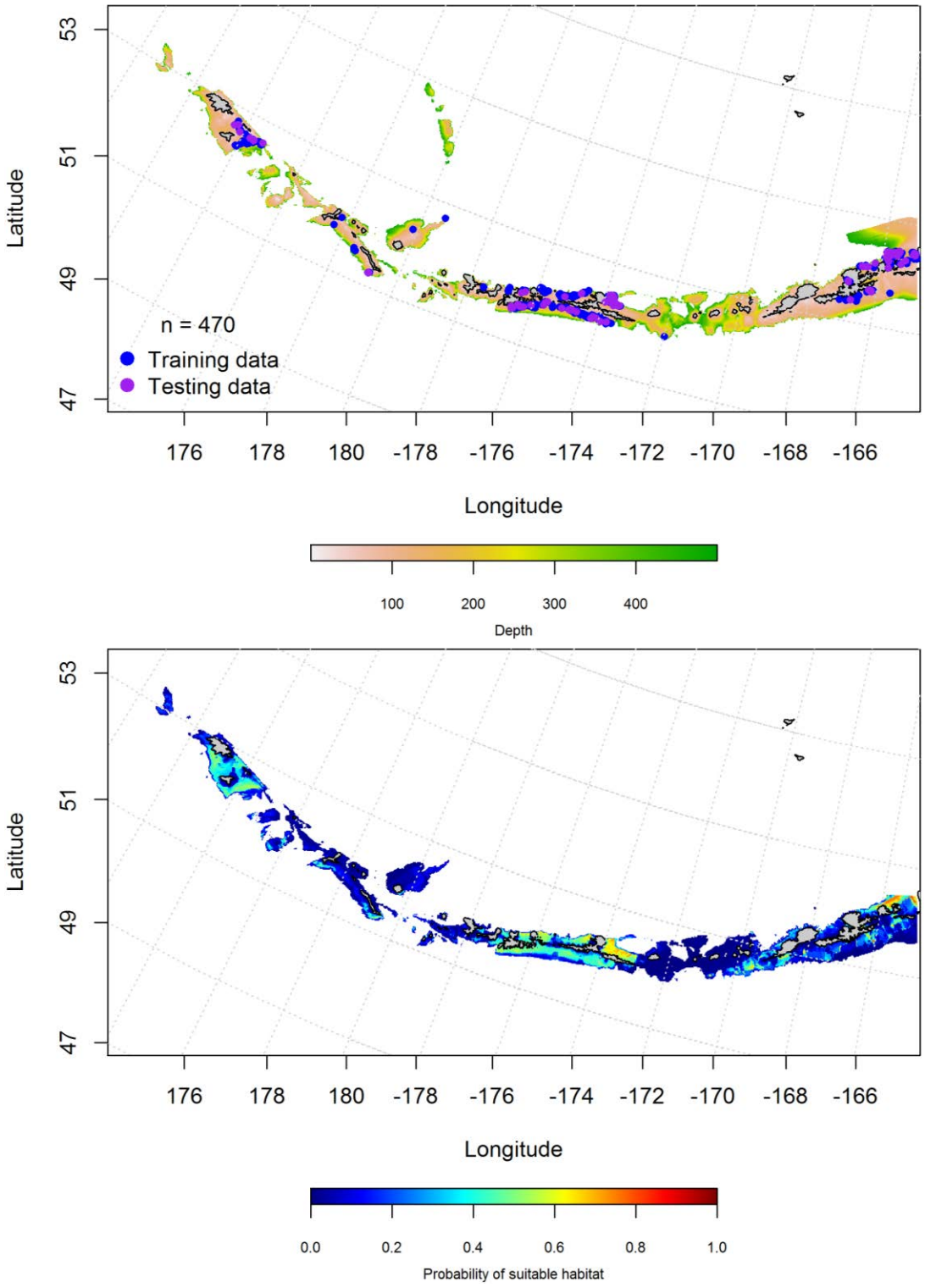

Figure 250. Locations of winter (December-February) commercial fisheries catches of unidentified octopus species (top panel). Blue points were used to train the maximum entropy model predicting the probability of suitable winter habitat supporting commercial fisheries of

unidentified octopus species (bottom panel) and the purple points were used to validate the model.

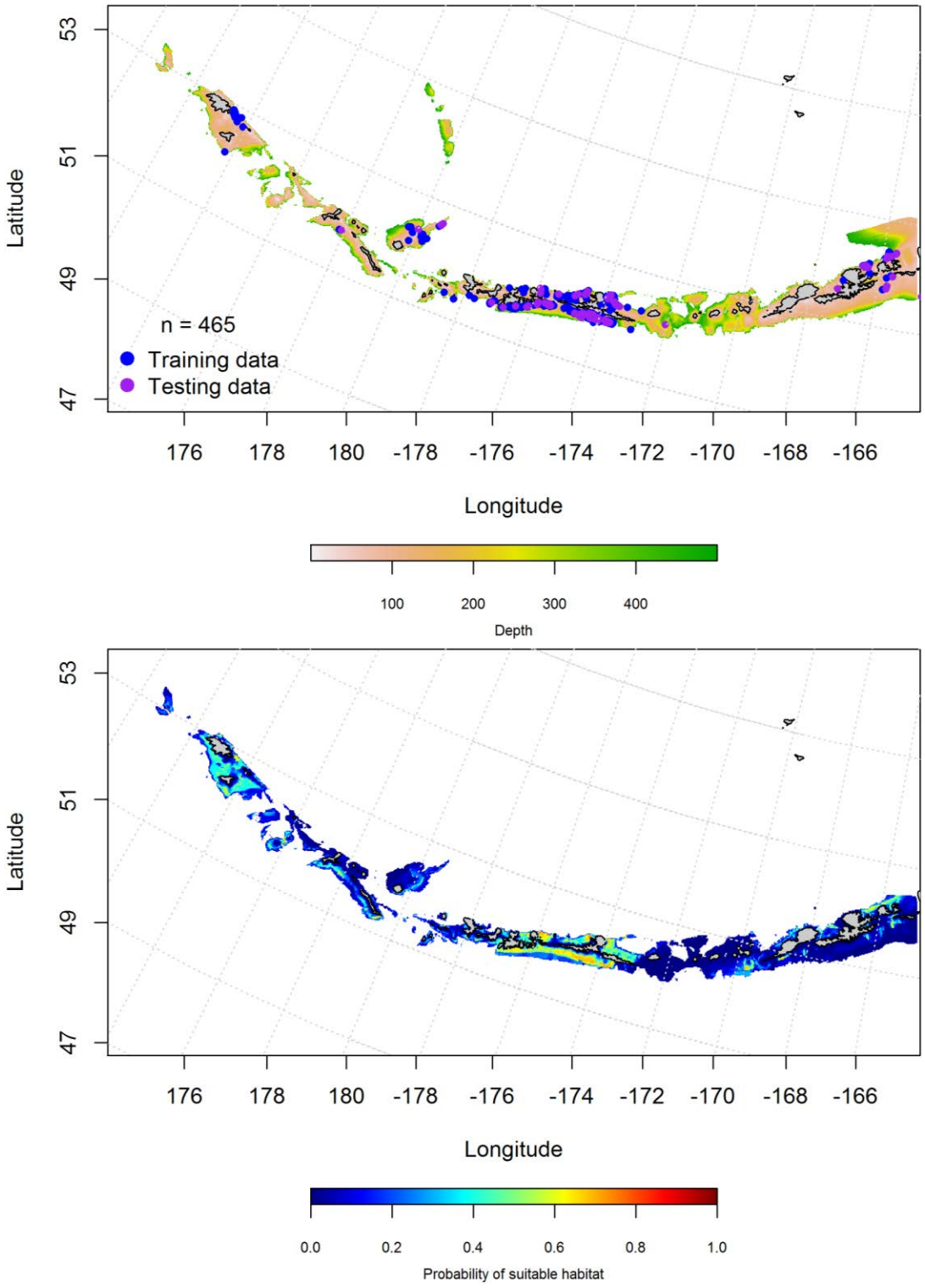

Figure 251. Locations of spring (March-May) commercial fisheries catches of unidentified octopus species (top panel). Blue points were used to train the maximum entropy model predicting the probability of suitable spring habitat supporting commercial fisheries of

unidentified octopus species (bottom panel) and the purple points were used to validate the model.

Aleutian Islands Pacific giant octopus Essential Fish Habitat Maps and Conclusions

-- Pacific giant octopus essential fish habitat predicted from summer bottom trawl surveys modeling is distributed across the central and western Aleutian Islands near Kiska Island and the ?? pass (Figure 252).

Pacific giant octopus essential fish habitat from commercial fisheries surveys was similar across seasons (Figure 253). Predicted EFH from the modeling is distributed across the central and eastern Aleutian Islands in the fall and winter, and more abundant in the western AI in the spring (Figure 253).

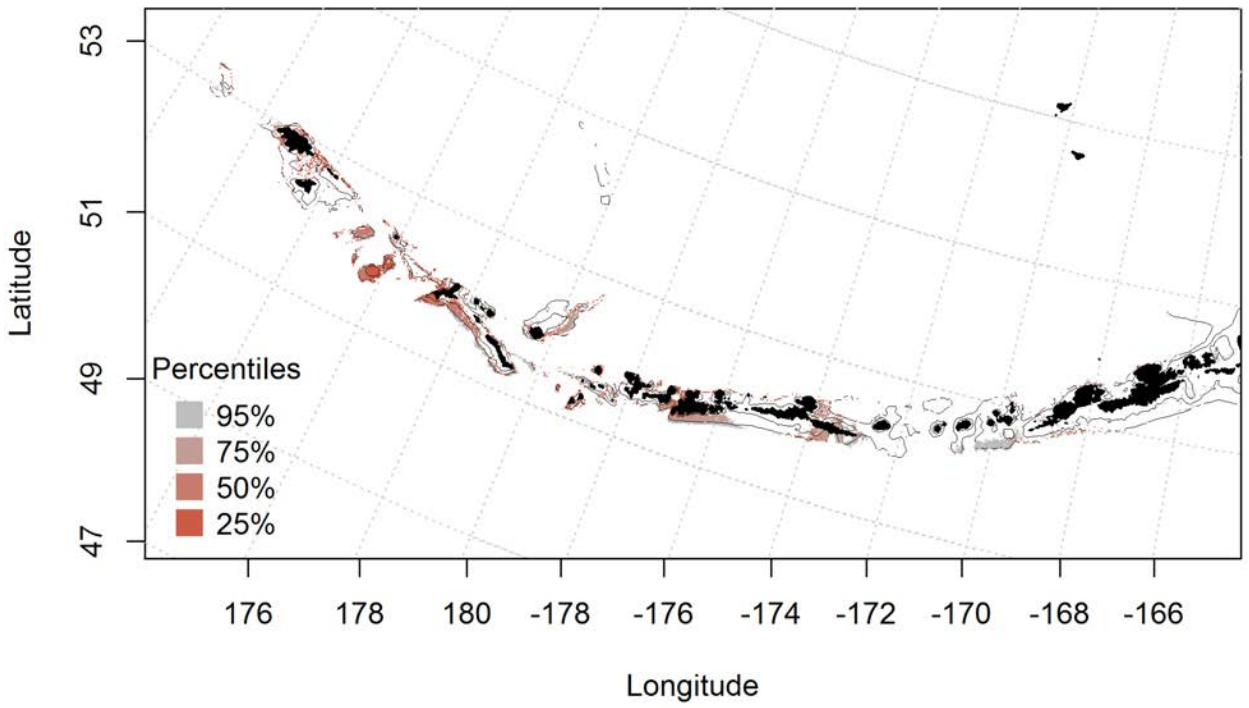

Figure 252. Predicted summer essential fish habitat for Pacific giant octopus from summertime bottom trawl surveys.

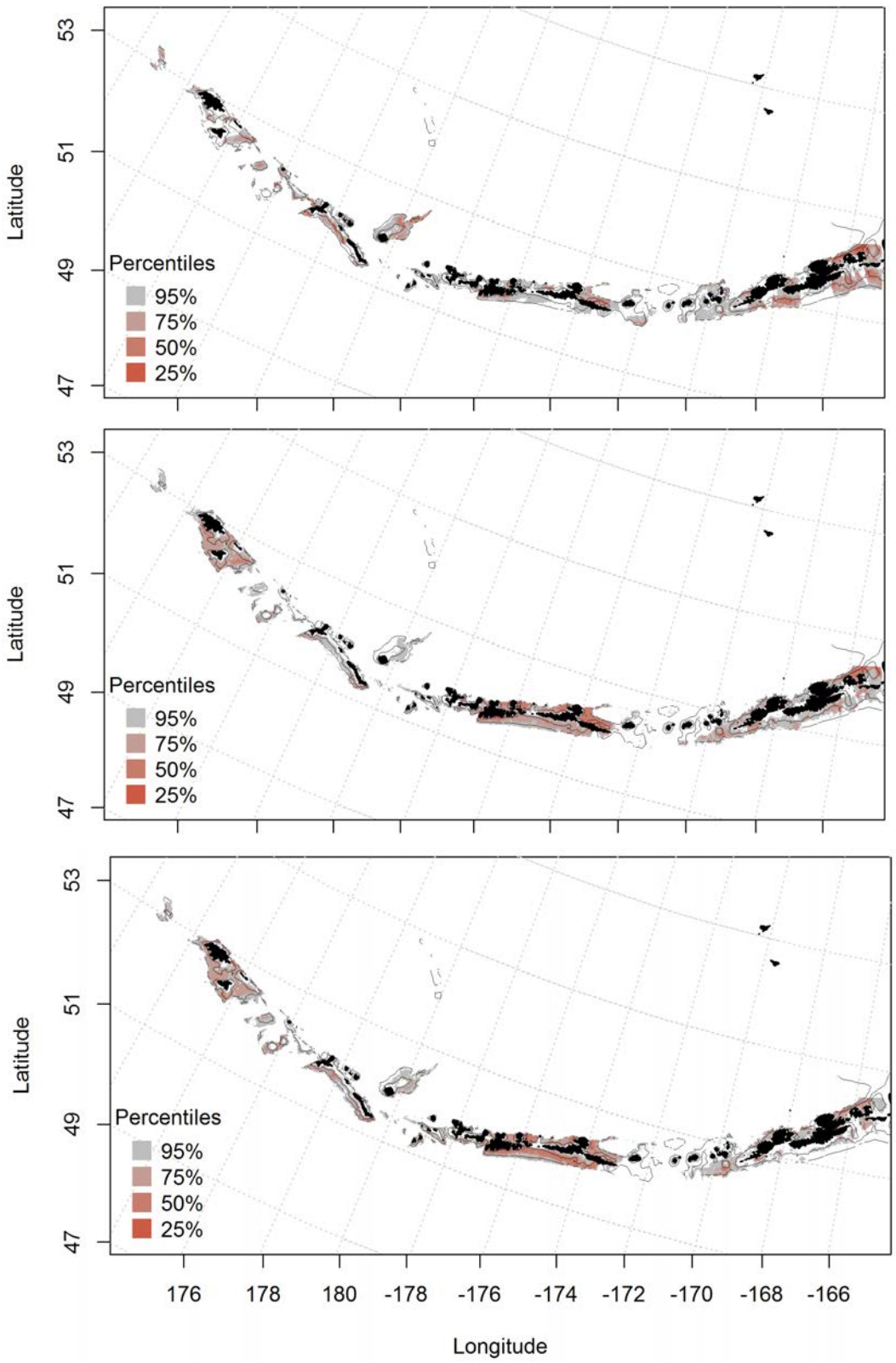

Figure 253. Essential fish habitat predicted for unidentified octopus species during fall (top panel), winter (middle panel) and spring (bottom panel) from summertime commercial catches.